Synthesis of Natural Abundant Butenolides and Analogues

Fakultät für Mathematik, Informatik, und Naturwissenschaften
Fachbereich Chemie, Institut für Pharmazie
der Universität Hamburg

Dissertation

Zur Erlangung des naturwissenschaftlichen Doktorgrades

vorgelegt von

Herrn Mathias Schacht

aus

Hamburg

Hamburg 2019

Die vorliegende Arbeit wurde in der Zeit von 20015 bis 2019 im Institut für Pharmazie der Universität Hamburg unter der Betreuung von Prof. Dr. Nina Schützenmeister angefertigt.

Gutachter der Dissertation

Erstgutachterin: Prof. Dr. Nina Schützenmeister

Zweitgutachter: Prof. Dr. Wolfgang Maison

Prüfungskommission

Vorsitz: Prof. Dr. Nina Schützenmeister

Stellv. Vorsitz: Prof. Dr. Ralph Holl

Dr. Thomas Hackl

Datum der Disputation: 06.09.2019

Danksagungen

Frau Prof. Dr. Nina Schützenmeister danke ich für die Begleitung innerhalb der letzten Jahre, die interessante Themenstellungen, den wissenschaftlichen Freiraum, welchen ich zuvor vergeblich gesucht habe, und für das Vertrauen mich 2015 aufzunehmen.

Mein weiterer Dank gilt Herrn Prof. Dr. Wolfgang Maison für die Übernahme des Zweitgutachtens.

Dem technischen Personal des NMR-Teams um Herrn Dr. Thomas Hackl, der MS-Abteilung von Frau Dr. Maria Riedner, sowie der Röntgenstrukturanalyse von Herrn Dr. Frank Hoffmann danke ich für die Hilfestellungen bei analytischen Problemen und der Vermessung unzähliger Proben. Hierbei möchte ich besonders Frau Claudia Wontorra danken, für die Durchführung und Organisation der zahlreichen Tieftemperaturmessungen. Ebenso danke ich Frau Isabelle Nevoigt für die Begutachtungen und Messungen der unzähligen Kristallansätze.

Außerdem möchte ich an der Stelle bei dem kompletten technischen Personal im Institut Pharmazie bedanken. Ohne den Einsatz von euch - Anette, Kathleen und Rainer - wären die letzten Jahre am Fachbereich so überhaupt möglich gewesen. Ich kann euch nicht genug danken.

Frau Prof. Dr. Gülsah Gabriel und Frau Dr. Stephanie Bertram danke ich für die Durchführung der antiviralen Assays. Ebenso möchte ich mich bei Herrn Prof. Dr. Peter Heisig und Phyllis Zimmermann für die Durchführung der antibakteriellen Testungen bedanken.

Für die tatkräftige Unterstützung bei experimentellen Arbeiten möchte ich mich bei Christoph Alberti, Svilena Draganova, David L. Prüss, Alexander Plukett, Dominique Kehlenbeck, Katja Scholz, Verena Schwarz, Christina Wolf und Jana Ketzel, die in den letzten Jahren Experimente für mich durchgeführt haben. Besonders die Bachelorarbeiten von Jessica De Vries, Vincent Mittag, Jasmin Janneschütz, Rodrigo Meißner und Djawid Mohammadi seien dabei hervorgehoben, die alle einen hervorragen Job gemacht haben. Danke für euren Einsatz und die hervorragenden Ergebnisse, die Ihr erzielt habt. Ich wünsche euch für euren Weg alles Gute und viel Erfolg.

Herzlichen Dank geht an Maik Assmann, Jacob Boehlich und Yodita Asfaha für das Korrekturlesen und konstruktive Kritik, trotz eigener Projekte und Verpflichtungen habt ihr euch die Zeit genommen meine Arbeit unter die Lupe zu nehmen.

Dem AKS – mit seinen aktiven wie ehemaligen Mitgliedern – danke ich für die entspannte Atmosphäre, Zusammenhalt und der stetigen Hilfsbereitschaft bei Fragestellungen jeglicher Art. Besonders möchte ich mich hier bei Maik, Jake, Jessi und Theresa bedanken für die Zeit mit euch im und außerhalb des Labors, sowie den wissenschaftlichen Exkursen nach Berlin auf die ORCHEM oder dem OC/PHA Symposium. An der Stelle möchte ich mich auch bei dem kompletten Arbeitskreis Maison bedanken nicht nur, dass ich auch eure Chemikalien und Geräte benutzen durfte, sondern ihr mich so nett hier im Institut für Pharmazie aufgenommen habt.

Natürlich geht auch hier ein Dank raus an meine ältesten Weggefährten Serge Kliewer und Malte Holzapfel vom Arbeitskreis Maison. Wir kennen uns seit 2009, haben zusammen angefangen und sind durch dick und dünn gegangen. Ihr seid maßgeblich daran beteiligt, dass ich mich nach dem Master zur Doktorarbeit motivieren konnte und ich wieder zurück in Hamburg bin. Danke Jungs.

Ein ganz besonderer Dank geht auch an dich Natalija. Danke, dass ich 2015 kennenlernen durfte und die wundervolle Zeit mit dir. Du hast mich immer unterstützt, mir geholfen nie den Blick fürs Wesentlich zu verlieren und auf dem richtigen Weg zu bleiben. Ich freue mich auf die Zukunft mit dir. Хвала ти што ме волиш онаквог какав јесам. Хвала ти што си мој партнер на овом путовању. Волим те.

Zu aller Letzt möchte ich mich bei meiner Familie bedanken, ihr habt mich bedingungslos unterstützt seit je her. Ohne euch wäre das alles überhaupt nicht möglich gewesen, ich hätte das damals nicht gedacht. Ihr habt nie aufgehört an mich zu glauben, auch wenn es manchmal hoffnungslos war. Ihr alle habt mir als Vorbilder immer wieder gezeigt was alles mit der richtigen Einstellung und der Unterstützung der Familie möglich ist. Ich kann euch nicht genug Danken für die Werkzeuge, die von euch erhalten habe seit der Kindheit, um diesen Pfad zu bestreiten. Ich liebe euch!

Für meine Eltern

„Kann ich nicht… gibt es nicht!“

Papa

Publicationlist

Parts of the dissertation were already published in following publications:

Articles

- Mathias Schacht, Gordon Jacob Boehlich, Jessica de Vries, Stephanie Bertram, Gülsah Gabriel, Phyllis Zimmermann, Peter Heisig, Nina Schützenmeister, Protecting-Group-Free Total Syntheses of Rubrolide R and S, *Eur. J. Org. Chem.* **2017**, 1745-1748. (DOI: 10.1002/ejoc.201700158)
- Mathias Schacht, Djawid Mohammadi, Nina Schützenmeister, Pd-Catalyzed Synthesis of *γ*-Keto Esters as Key Intermediates for the Synthesis of γ-Hydroxybutenolides, *Eur. J. Org. Chem.* **2019**, 2587-2591 (DOI: 10.1002/ejoc.201900023)

Poster

- Mathias Schacht, Gordon Jacob Boehlich, Jessica de Vries, Nina Schützenmeister, Protecting-Group-Free Total Syntheses of Rubrolide R and S, *20th ORCHEM*, **2016**, Weimar.
- Mathias Schacht, Gordon Jacob Boehlich, Jessica de Vries, Nina Schützenmeister, Protecting-Group-Free Total Syntheses of Rubrolide R and S, *DPhG Jahrestagung* **2016**, München.
- Mathias Schacht, Maik Assmann, Nina Schützenmeister, Total Syntheses of Rubrolide R and S and their derivatives, *DPhG Jahrestagung* **2017**, Saarbrücken.
- Mathias Schacht, Djawid Mohammadi, Nina Schützenmeister, γ-Ketoester as Key Intermediates for the Synthesis of *γ*-Hydroxybutenolides, *ORCHEM* **2018**, Berlin.
- Mathias Schacht, Djawid Mohammadi, Nina Schützenmeister, γ-Ketoester as Key Intermediates for the Synthesis of *γ*-Hydroxybutenolides, *DPhG Jahrestagung* **2018**, Hamburg.

Talks

- Auf Schatzsuche in der blauen Apotheke, *Tag der Pharmazie Symposium*, **2016**, Hamburg.
- Flash Talk - invited speaker, Protecting-Group-Free Total Syntheses of Rubrolide R and S, *20th ORCHEM*, **2016**, Weimar.
- Marine Naturstoffe als Leitstruktur für neuartige Antiinfektiva, *Tag der Pharmazie Symposium,* 2017, Hamburg.

Table of Content

Abbrevation

µ	micro
Å	Ångstrom (1 Å = $1 \cdot 10^{-10}$ m)
Ac	acetyl
aq.	aqueous
ABTS	2,2'-azino-bis(3-ethylbenzthiazoline-6-sulphonic acid)
ATR	attenuated total reflectance
BINAP	2,2′-bis(diphenyl-phosphino)-1,1′-binaphthyl
Boc	*tert*-butyloxycarbonyl
BTEAC	benzlyltriethyl-ammoniumchloride
c	concentration
calcd.	calculated
cat.	catalytic
conc.	concentrated
COSY	correlated spectroscopy
Cy	cyclohexyl
δ	chemical shift
d	dublett
dd	dublett of dublett
DBU	1,8-diazabicyclo-undecen-7-ene
DCM	dichlormethane
DIPEA	*N*,*N*-diisopropyl-ethylamine
DMC	dimethylcarbonate
DMF	dimethylformamide
DMSO	dimethyl sulfoxide
dppf	1,1'-bis(diphenyl-phosphino)ferrocene
DPPH	di-(phenyl)-(2,4,6-tri-nitrophenyl)iminoazanium
dppm	1,1-bis(diphenyl-phosphino)methane
dppp	1,3-bis(diphenyl-phosphino)propane
Dp	decomposition point
EDC	*N*-(3-dimethylamino-propyl)-*N*'-ethyl-δ-carbodiimide hydrochloride
EI	electron ionisation
equiv.	equivalent
ESI ionisation	electron spray
Et	ethyl
FA	formic acid
g	gram
GHS	globally harmonised system
h	hour
HCl	hydrochloric acid
HTIB	hydroxy(tosyloxy)-iodobenzene

HRMS	high resolution mass spectrometry
HMBC	heteronuclear multiple bond correlation
HSQC	heteronuclear single quantum coherence
Hz	hertz
IC_{50}	half maximal inhibitory concentration
*i*Pr	isopropyl
IR	infrared spectroscopy
J	coupling constant
lit.	literature
λ	wavelength
m	multiplet (NMR)
m	*meta*
M	molar concentration
m/*z*	mass per charge
Man	D-mannose
Me	Methyl
MeCN	acetonitrile
MeOH	methanol
MHz	mega hertz
min	minute
mmol	milli molar
Mp	melting point
MS	molecular sieve
M.W.	micro wave
n-BuLi	*n*-butyllithium
Neop	neopentylglycolato
nm	nanometer
NMR	nuclear magnetic resonance
NOESY	nuclear overhauser effect spectroscopy
o	*ortho*
o.n.	overnight
p	*para*
PTSA	*p*-toluenesulfonic acid
sat.	saturated
OSu	O-succinimidyl
PCy_3	triscyclohexyl-phosphane
PCy_3HBF4	Tricyclohexyl-phosphine tetra-fluoroborate
PE	petroleum ether
Ph	Phenyl
*p*HBA	*para*-hydroxybenz-aldehyde
Pip	Piperidine
Pin	pinacolato
ppm	parts per million
PTC	phase transfer catalyst
Py	pyridine
q	quartet (NMR)
R_f	retention factor
RB	rose bengal
r.t.	room temperature

s	singlet (NMR)
sat.	saturated
Sia	disiamyl
SIPr	1,3-bis(2,6-di*iso*-propylphenyl)-2-imidazolidinylidene
t	triplet (NMR)
TBAB	*n*-tetrabutyl-ammonium bromide
TBAI	*n*-tetrabutyl-ammonium iodide
TBS	*tert*-butyldimethylsilyl
TFA	trifluoro-acetate
TMEDA	tetramethylethylendiamin
TMS	trimethylsilyl
Tf	triflate
THF	tetrahydrofuran
Ts	tosylate
TLC	thin layer chromatography
UV	ultraviolet
$\tilde{\nu}$	wavenumber
v/*v*	volume per volume
Vis	visible
W	watt
Xantphos	4,5-Bis(diphenyl-phosphino)-9,9-dimethylxanthene

1. Introduction

Cancer, cardiovascular and infectious diseases are still the three main death causes worldwide.[1] The published WHO (World Health Organization) health report of 2018 estimated approximately 6.7 million deaths worldwide caused by infectious diseases such as HIV, haemorrhagic fever (e.g. ebola), malaria, leprosy. Noteworthy is the evolving number of new tuberculosis infections in the European region. Due to lack a of proper hygiene standards and insufficient applications of antiinfectives, resistant strains of bacterial and viral pathogens evolved over the last decades[1] causing an increased number of infections. In 2016, approximately 600000 new tuberculosis infections were registered of which 490000 were multidrug resistant against common antibiotics.[2] Infectious pathogens such as bacterial develop rapid novel resistances against antibiotics caused by the evolutionary pressure combined with high mutation rates [2]. This generates a growing number of multi-resistant bacteria and the loss of the antibiotic potency. That bears the issue that reserve antibiotics may lose their antibacterial activity before they are applied to disease treatment.[2]

Modern drug development and design should not only be focussed on the screening of known compounds. Moreover, the search of novel active candidates addressing alternative molecular targets should be considered. Nonetheless, this approach is cost-intensive and requires often synthetic analogues, bearing the potential of losing their biological activity due to required derivatization steps. On behalf of the emerging number of resistant strains the discovery and development of novel anti-infective drugs are urgently needed.

1.1. Marine natural products

Terrestrial microorganism and plants have been the traditional source for drug discovery. Known agents such as atropine, caffeine, camphor and ephedrine were originally isolated from terrestrial organisms and are applied in our everyday life and clinical use.[3,4] The successful pathway of natural product based drug development has resulted in significant reduction of epidemics and infectious diseases by vaccinations, chemotherapeutic and antibiotics.[5] Nowadays, approximately 60% of the approved drugs in clinical use are based on natural products and their derived structures.[5–7] These metabolites are structurally advanced molecules with well-defined orientations of functionalities enabling an efficient interaction with a biological target.[7] Besides their unique structure, their scaffolds serve as a promising starting point for the development of novel lead structures.[4,6]

The major issue of terrestrial natural product sources is the reisolation of known structures from several organisms.[5,7] Thus, the focus has shifted from traditional natural product

discovery to rational designed drugs. Therefore, combinatorial chemistry [8,9] established high throughput screening technologies (HTS).[10]

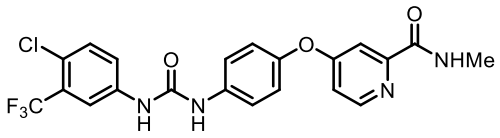

Sorafenib **1**

Figure 1: Chemical structure of sorafenib .

In 2005, the FDA approved soranfenib **1** (figure 1) for renal cancer therapy, which is so far the only commercialized drug designed by combinatorial chemistry and HTS.[11–14] Despite the rapid synthesis of novel chemical entities and establishment of huge substance libraries, this approach failed to deliver a significant amount of biologically active compounds due to lack of complexity and diversity of the chemical entities from high throughput screening.[14]

Therefore, novel natural product classes are urgently required, leading to the renaissance of the natural product derived drug development in order to challenge the emerging number of resistant pathogens. The discovery of novel scaffolds demands the acquirement of alternative sources of natural products.[15]

Marine ecosystems are unique from tropical waters to polar regions, where organisms have adapted to ecological demands with enormous biodiversity.[16] The coral reefs are unique ecosystems similar to tropical rainforest, which are characteristic for their limitations in space and nutrient supply. The evolutionary pressure resulted in the adaption to the environmental conditions and led to a variety of plants and animals. Moreover, the selection pressure caused several symbioses of microorganisms with animals and plants living in beneficial coexistence. Therefore, marine sponges contain large amounts of microorganisms in their tissue, which account for up to 40% of their biomass.[16] Limited space and the strong competitive pressure on the inhabitants require an effective defense system in order to survive in this environment. Sessile invertebrates possess a chemical defense mechanism by producing growth inhibiting or toxic metabolites. These biologically active compounds from marine origin are promising in terms of drug development.[16]

In 1951, bioactive substances of marine origin attracted interest by discovering two arabino- and ribopentosyl-nucleosides from a marine sponge.[3,17–19] The novel metabolites served as essential lead structure for the development of vidarabine **2** and cytorabine **3** (figure 2) which are effective in antiviral and anticancer therapies and are in clinical use for decades.[3]

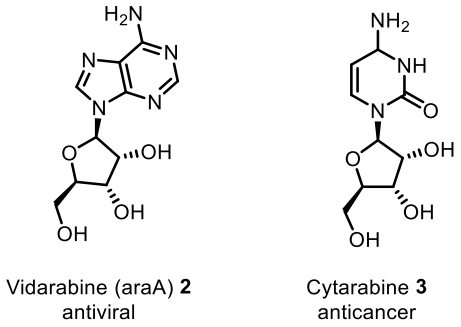

Figure 2: Chemical structures of Vidarabin **2** and Cytarabin **3**.

In 1970, the peptide *ω*-conotoxin MVIIC **4** (figure 3) was isolated from the tropical marine cone snail *conus magus*. This peptide is the first drug exclusively produced from marine organisms, which was approved by the FDA in 2004 as non-opioid analgesic for chronic pain. [3,20,21]

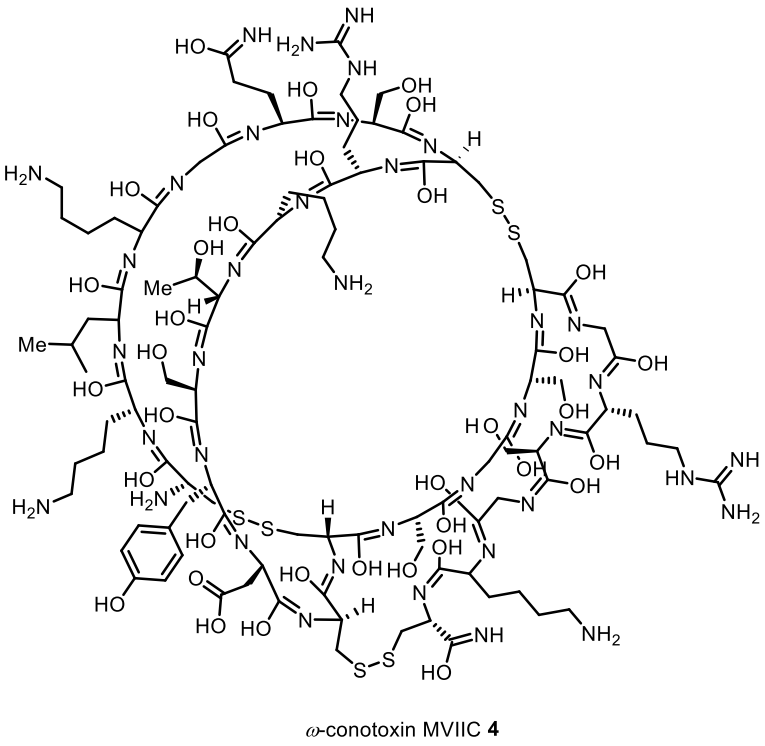

Figure 3: Chemical structure of *ω*-conotoxin MVIIC **4**.

A second milestone is the ecteinascidin-743 **5** (figure 4) isolated from the tropical sea squirt *Ecteinascidia turbinata* by *Rinehart* et al.[22] in 1984. This metabolite was approved in 2007 by the European Union for treating soft tissue sarcoma. Continuing efforts over the last decades led to the discovery of more potent bioactive compounds.[3,23]

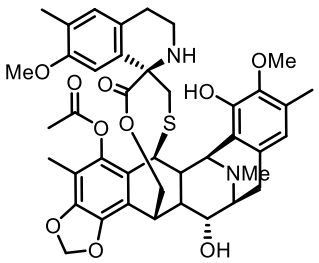

Ecteinascidin **5**

Figure 4: Structure of ecteinascidin-743 **5**.

The marine based drug development faces several challenges such as the acquisition of rare biomaterial in large quantities, which remains the major drawback in this field. Furthermore the cultivation of the marine sponges is demanding, due to the specific environmental conditions, isolation and characterization of the active metabolites.[3–5,7,14]

1.2. Rubrolides

Promising structure motifs are butenolides. This structural motif occurs frequently in several biological natural products, such as penicillic acid **6** [24], oleandrin **7** (cardiac glycoside)[25,26] or patulin **8** (mycotoxin) (figure 5).[27]

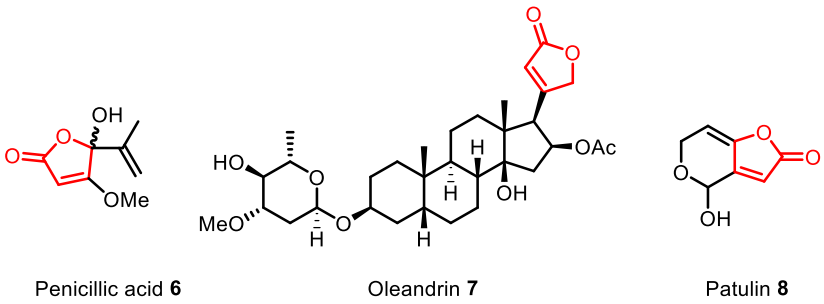

Figure 5: Butenolide containing natural products penicillic acid **6**, oleandrin **7** and patulin **8**.

Miao et al. isolated from the tunicate *Ritterella rubra* discovered the marine natural product class of rubrolides **9** in 1991. Over the last decades additional 19 representatives of this natural product class were isolated.[28]

A common structural feature of rubrolides **9** is the central butenolide and two *para*-hydroxyphenyl moieties with or without halogen atoms. These metabolites were often isolated together with the structural related cadiolides **10** and prunolides **11** (figure 6).

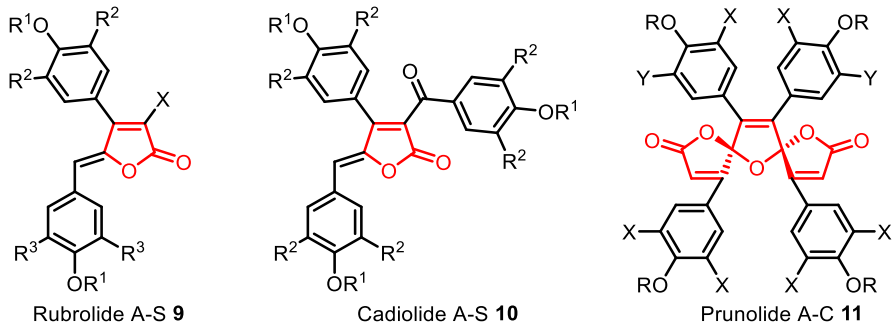

Figure 6: General chemical structures of rubrolides **9**, cadiolides **10** and prunolides **11**.

In vitro studies of rubrolides revealed the plethora of biological activities. Rubrolide B (table 1) has shown antibacterial activity against *S. aureus* and *B. subtilis* and inhibited protein phosphatase 1 and 2A. Both phosphatases are promising targets for the treatment of Parkinson and Alzheimer.[28] Furthermore, rubrolide F exhibited moderate antibiotic activity against *S. epidermidis* and *methicillin-resistant S. aureus* (MRSA).[29] The natural product class of rubrolides such as rubrolide I, K, L, and M also revealed cytotoxic properties against several cancer cell lines.[30,31] Motivated by the diversity of the biological activities of rubrolides and their potential as lead structures, further studies were performed. Since the

natural product class occurs with different halogenation pattern, *Ortega* et al. investigated the introduction of halogens. Rubrolides with chlorine substituents at the furanone core showed higher inhibition rates. Furthermore, *Perreira* et al. used rubrolides as substrates [31,32] for the synthesis of lactam-derived analogues, which displayed promising anticancer, antibiotic and antifouling activity. [31,32]

Table 1: Identified natural occurring rubrolides.

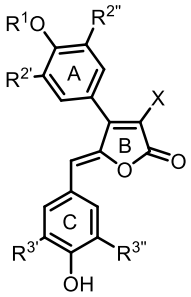

9

Rubrolide	X	R^1	$R^{2'}$	$R^{2''}$	$R^{3'}$	$R^{3''}$
A		-	Br	Br	Br	Br
B	Cl	-	Br	Br	Br	Br
C	-	-	-	-	Br	Br
D	-	-	Br	Br	-	-
E	-	-	-	-	-	-
F	-	Me	-	-	-	-
I	Cl	-		Br	Br	Br
J	-	-	-	Br	Br	Br
K	Cl	-	-	Br	Br	-
L	Cl	-	-	-	Br	Br
M	Cl	-	-	-	Br	-
N	Br/Cl	-	-	Cl	Br	-
O	Cl	-	Br	Br	Br	-
P	-	Me	Br	Br	-	-
Q	-	Me	Br	-	-	-

In 2014, *Zhu* et al. discovered two novel rubrolide species R **12** and S **13**. These were isolated from *Aspergillus terreus* with an unique prenyl and 2,2-dimethylchromane moiety at the *C*-ring instead of the frequently occurring halogenation (figure 7).[33,34]

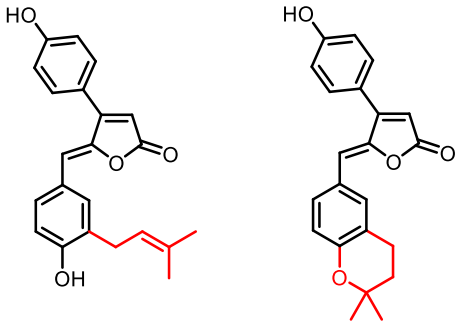

Figure 7: Structures of rubrolides R **12** and S **13**.

Both structures have shown activity against influenza virus (H1N1) and low cytotoxicity.[34] Rubrolide S **13** shows higher anti-viral activity (IC_{50} = 87.1 µmol/L) compared to the virostaticum ribavirin (IC_{50} = 118.8 µmol/L) while rubrolide R **12** shows lower activity (IC_{50} = 221.6 µmol/L). Rubrolide R **12** has also exhibited antioxidative activity against DPPH and ABTS.[34] Moreover, a significant reduction of the NO production was identified.[35] These attributes qualify this marine derived natural products as lead structure, and led to the development of validated synthetic protocols (scheme 1). Hereby two major synthetic approaches were established for the synthesis of rubrolides: de novo synthesis of the central (*5H*)furan-2-one and application of commercially available building blocks.

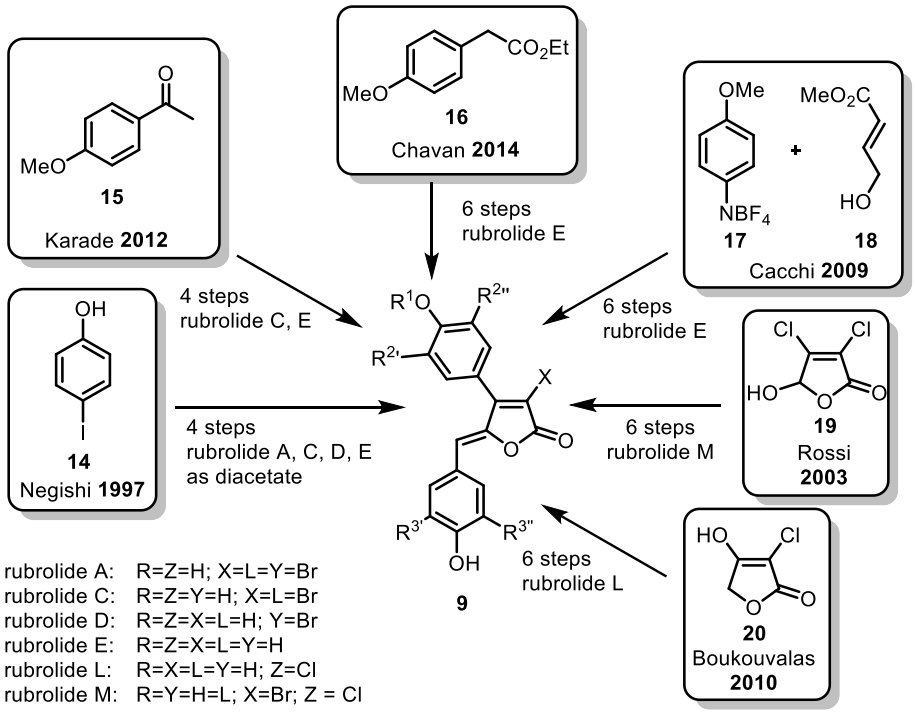

Scheme 1: Overview of literature known protocols for rubrolides **9**.

The first total synthesis of rubrolides was reported by *Kotora* and *Negishi* via a Pd-catalyzed *Sonogashira*/lactonization sequence with iodocinnamic acid **21** and aryl alkyne **22** yielding

the desired structures as diacetate.[36] This preceded by a *Sonogashira* cross-coupling of the aryl alkyne with the corresponding (*Z*)-*β*-alkynylcinnamon acid, followed by an in situ lactonization to generate the rubrolide diacetate **24** with *Z*/*E* ratio of 30:1 (scheme 2).

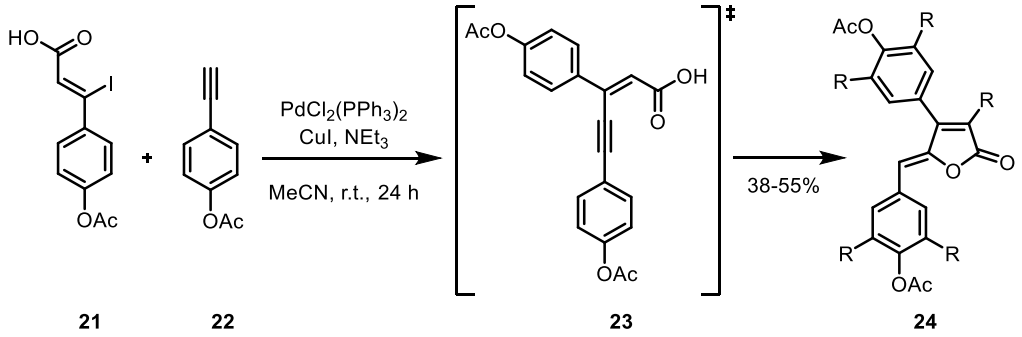

Scheme 2: Rubrolide synthesis via *Sonogashira*/lactonization sequence.

Another rubrolide synthesis approach considering a de novo furanone was reported by *Chavan* et al.[37] Starting from acetophenone **15**, the enol-ether is formed, which is epoxidatized with *m*CPBA and subsequent hydrolyzed resulting in *α*-hydroxyketone **25**. Finally, Reformatzki reaction with bromoethylacetate with subsequent lactonization led to formation of the central furanone **26** in sufficient yields. Aldol condensation with *para*-hydroxybenzaldehyde **27** and deprotection yielded rubrolide E **28** (scheme 3).[37]

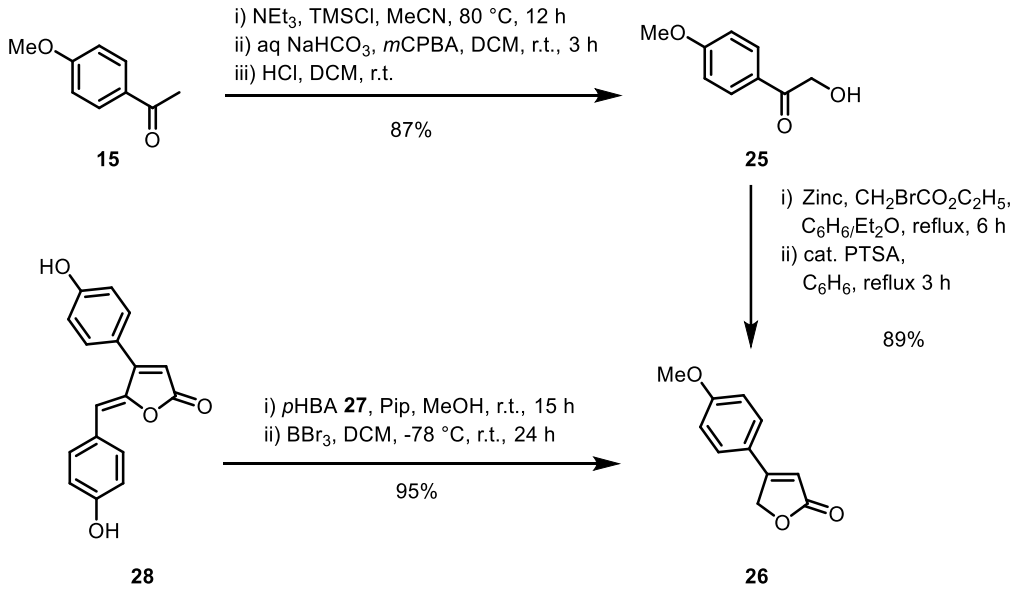

Scheme 3: Rubrolide synthesis with *de novo* furanone synthesis according to *Chavan* et al..

Alternatively, *Karade* et al. reported a de novo synthesis employing an intramolecular Wittig reaction as key step. This protocol considered the tosylation of acetophenone **15** and conversion with bromoacetic acid, followed by the intramolecular Wittig reaction (scheme 4).[38]

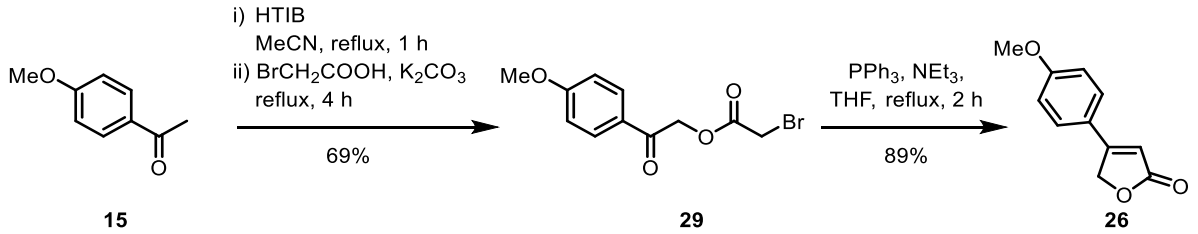

Scheme 4: De novo furanone synthesis by *Karade* et al..

Cacchi et al. established a cross-coupling lactonization sequence of aryldiazonium tetrafluoroborate **17** with *α*,*β*-unsaturated ester **18**. This approach considers in situ diazotation of an aniline **30** followed by a *Heck*-reaction/lactonization sequence to afford furanone, which was converted in an aldol condensation to rubrolide E **28** (scheme 5).[39]

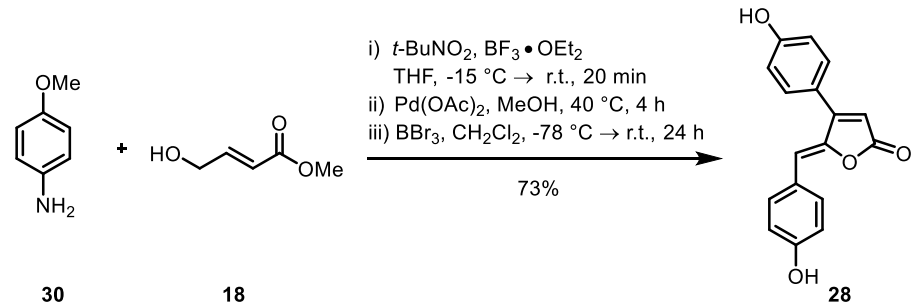

Scheme 5: Synthesis of rubrolide E **28** after *Cacchi* et al. via *Heck* reaction/lactonization sequence with subsequent aldol condensation.

Another approach applies commercially available building blocks, which already contain the desired butenolide motif. [40–43] *Rossi* et al. introduced mucochloric acid **19a** and mucobromic acid **19b** derived from (*5H)*furan-2-ones as building blocks **20a/b**, which were successfully applied in *Suzuki-Miyaura* and *Stille* cross-coupling protocols (Scheme).[31,44–46] Herefore, a silver(I)oxide mediated variant of the *Stille* coupling yielded regioselective monoarylation of the building block.[40] In analogy to *Stille* conditions, the *Suzuki* cross-coupling of **20a/b** and phenyl boronic acid **32** also provided regioselective coupling.[41] Among these mucochloric or mucobromic derived substrates, *Boukouvalas* et al. investigated the application of tetronic acid derived triflates **34** and tosylates **35**.[47] These alternative building blocks were also successfully applied in *Suzuki* cross-coupling reactions (scheme 6).

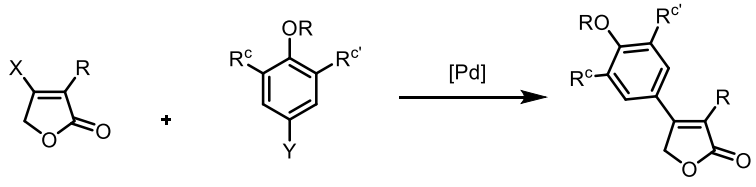

20a X = R = Cl
20b X = R = Br
33 X = Br, R = H, Me
34 X = OTf, R = Cl
35 X = OTs, R = Cl

31 Y = SnR_3
32 Y = $B(OH)_2$

Scheme 6: Literature known synthesis of arylfuran-2-one.[40,41,43,46–48]

Besides the total synthesis of rubrolide **9** of *Kotora* and *Negishi* [36], the introduction of the benzylidene moiety was obtained by vinylogous aldol condensation or Knoevenagel condensation. The latter conditions were successfully applied in the synthesis of rubrolide E **28**. Alternatively, a one pot vinylogous aldol condensation for the introduction of the benzylidene moiety was established by *Boukouvalas* et al.[48,49] The furanone **36** and aldehyde **39** were converted with TBSOTf and DIPEA to the *syn* **42a/b** and *anti* **42a/b** aldol products. Formation of the silyloxyfurane **38**, which serves as synthon **39**, enables a regioselective, nucleophilic attack of the *γ*-carbon at the electrophilic benzaldehyde **39**. This step is followed by the DBU-mediated condensation of water generating the double bond of the rubrolide scaffold (scheme 7**Scheme**).

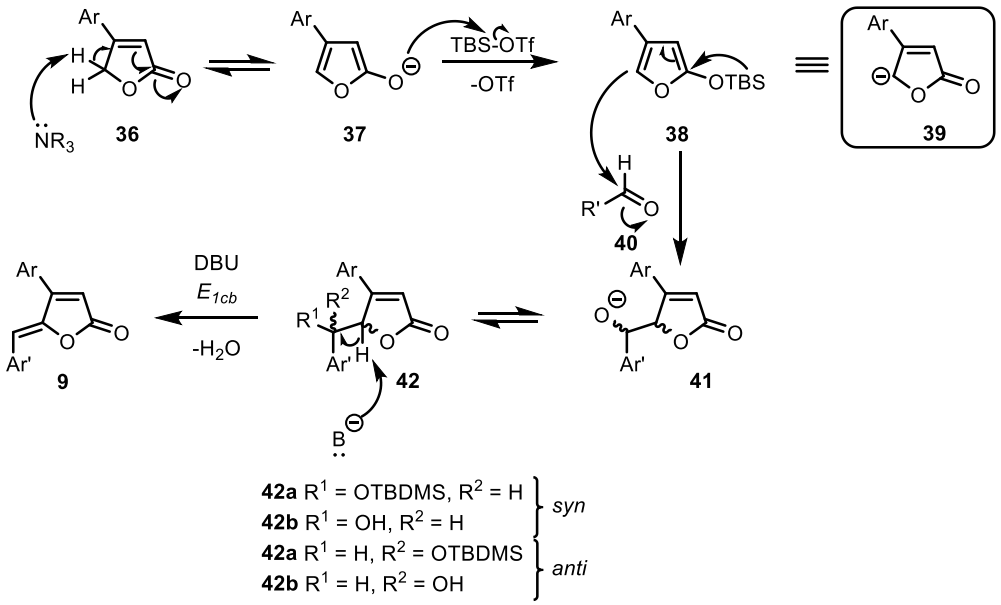

Scheme 7: Proposed mechanism of the vinylogous aldol.

Ongoing studies of *Downey* et al. on the aldol reaction with non-vinylogous substrates observed that a slight excess of the non-nucleophilic base compared to the silylating agent is beneficial for the reaction. The silylating reagent should induce the formation of the silylenolether, which is crucial for the activation of the vinylogues position for the aldol addition. They also investigated the role of the applied base showing that non-nucleophilic bases were beneficial for the formation of the silylenolether.[50–52] Furthermore, they hypothesized that strong bases cause a coordination of the silyl species or formation of a pentavalent silicium species.[53]

1.3. Prunolides

Prunolides are derived natural products with a unique tetraphenolic bisspiroketal scaffold. They have been firstly isolated from the Australian ascidian *Synoicum prunum* in 1998.[54] Prunolide A and prunolide C (table 2) showed in preclinical studies cytotoxic activity against HeLa cells at concentrations of 25 µM and 15 µM, respectively.[54] Furthermore, prunolide A displayed antiviral activity against the *Japanese encephalitis virus* (JEV). Due to the antiviral activity, this natural product class is an attractive synthetic target, since there is no established antiviral treatment for JEV infections.[33]

Table 2: Identified naturally occurring prunolides.

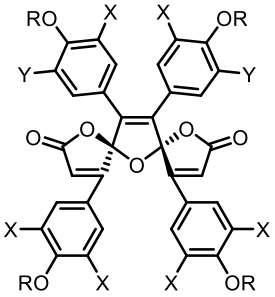

11

Prunolide	R	X	Y
A	H	Br	Br
B	H	Br	H
C	H	H	H

Although these metabolites showed excellent antiviral activity against JEV, only the method for the synthesis of the bisspiroketal scaffold was published so far.[55,56] The key step of the methodology is the $TiCl_4$ catalyzed dimerization of furan **44**, followed by singlet oxygen Diels-Alder reaction forming **47**, followed by the endoperoxide opening, generating the complex spirocyclic scaffold **48** (scheme 8).[56]

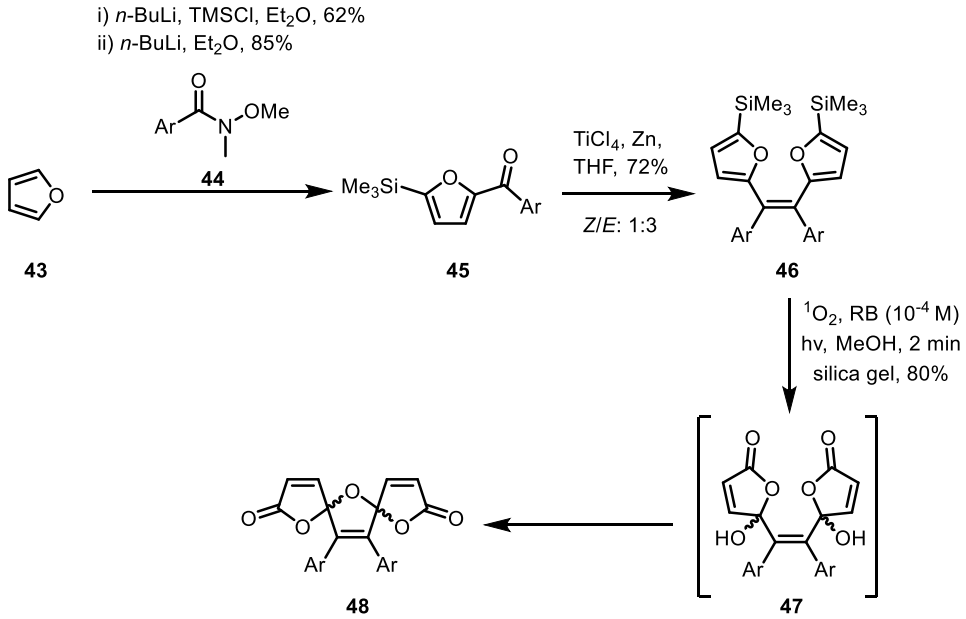

Scheme 8: Synthesis of the bisspiroketal scaffold by *Vassilikogiannakis* et al..

Vassilikogiannakis et al. described the synthesis of the spirocyclic core structure **48** via *Diels-Alder* with singlet oxygen and subsequent endoperoxide opening.[56] Hereby, a hydroxybutenolide **47** is formed as an intermediate prior to spirocyclization to form the spirocyclic compound **48** (scheme 8).

1.4. Hydroxybutenolide

The structural motif often occurs in natural products and received significant attention due to the wide plethora of biological activities such as anti-inflammatory[57–61], antitumor [62–65], antibiotic[[60,66–70]], antifungal[71–73] and antifouling activity.[74–77] Besides the naturally occurring *γ*-hydroxybutenolides, synthetic *γ*-hydroxybutenolides such as PD156707 **54** by *Doherty* et al. showed potent endothelin receptor type A antagonist activity (figure 8).[78,79]

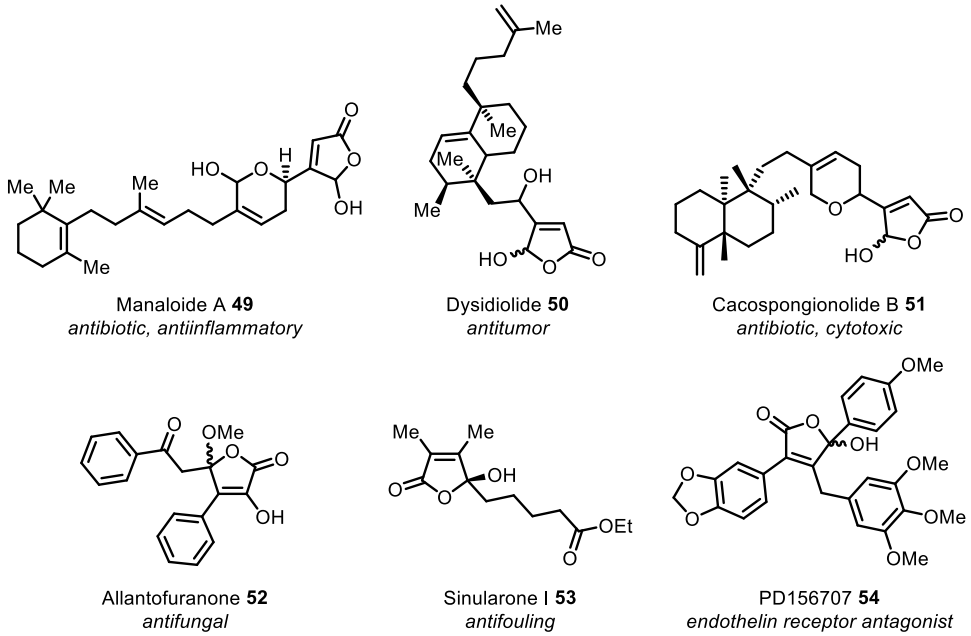

Figure 8: Biologically active *γ*-hydroxybutenolides **49-54**.

Conventional synthesis of this structural motif is achieved by a rose bengal mediated singlet oxygen photooxidation of 3-alkylfurans **55**. Formation of the endoperoxide **56** by *Diels-Alder* followed by base activated ring opening, generates the *γ*-hydroxybutenolide **57** (Scheme 9).[80]

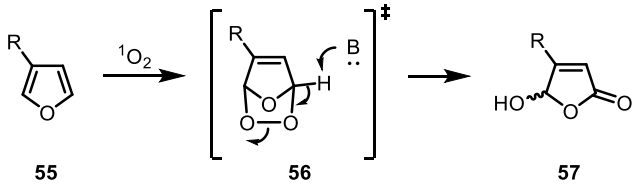

Scheme 9 *γ*-Hydroxybutenolide synthesis via photo-oxidation of 3-alkylfurans **55**.

Due to low yields and the limited substrate scope [81–84] alternative synthetic approaches of *γ*-hydroxybutenolides were established and reported, providing access to higher substituted structures. For this purpose, *Kim* et al. established a protocol for trisubsituted *γ*-hydroxybutenolides **58** using an indium mediated *Barbier* type reaction of *Baylis-Hillman* adducts **59** with an aldehyde **60** followed by lactonization/aerobic oxidation (scheme 10).[85,86]

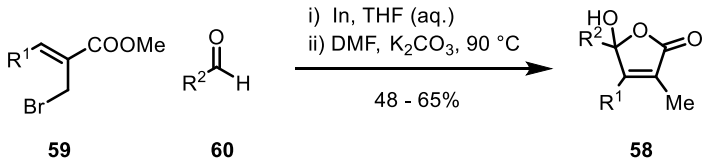

Scheme 10: Indium mediated *Barbier* type reaction with subsequent lactonization/aerobic oxidation for the synthesis of trisubstituted hydroxybutenolides.

This approach provides a higher substitution pattern compared to photooxidation of furan moieties under basic conditions.[84,87–90] Another synthetic approach for the synthesis of tetrasubstituted *γ*-hydroxybutenolides **61** was demonstrated by *Shishido* et al. via a ruthenium-catalyzed [2+2+1] oxo-*Pauson Khand* reaction of aldehydes **60** with alkynes **62** under CO-gas atmosphere and subsequent oxidation to afford the desired structures **61** (scheme 11).[91]

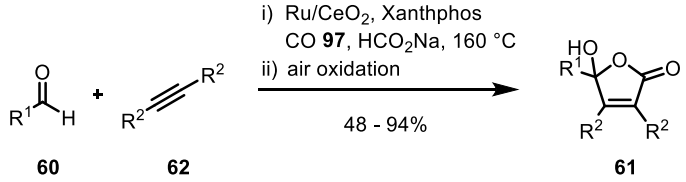

Scheme 11: Ruthenium-catalyzed [2+2+1] oxo-*Pauson Khand* reaction of aldehydes **60** with alkynes **62** under CO-atmosphere, followed by oxidation.

Furthermore, *Zhu* et al. described an efficient protocol of highly functionalized *γ*-hydroxybutenolides **61** formed via BF_3-catalyzed annulation of keto acids **63** with alkynes **62** (scheme 12).[92]

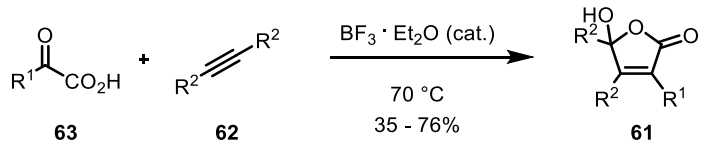

Scheme 12: BF_3-catalyzed annulation of keto acids **63** with alkyne **62**.

1.5. Suzuki-Miyaura cross-coupling reaction

The Suzuki-Miyaura cross-coupling reaction is one of the most relevant cross-coupling reactions besides *Stille*[93], *Kumada*[94], *Negishi*[95] and *Sonogashira-Hagihara*[96] coupling. It has has been discovered by *Miyaura* and *Suzuki* in 1979.[97,98],. In 2010, *R. Heck, E. Negishi* and *A. Suzuki* were rewarded for their contributions with the *Nobel Prize* for palladium catalyzed cross-coupling reactions. The *Suzuki-Miyuara* cross-coupling describes a palladium catalyzed reaction between organoboron compounds **64** and organic halides/pseudohalogenide **65** providing a convenient and efficient method for the formation of carbon-carbon bonds **66** (scheme 13).

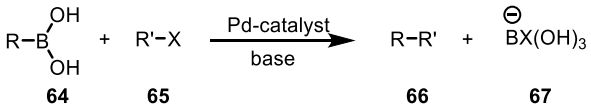

Scheme 13: General reaction overview of the *Suzuki* cross-coupling reaction.

The first reaction *Suzuki-Miyaura* cross-coupling, was the conversion of disiamylborane **68** with (*E*)-1-bromo-2-phenylethene **69** in the presence of 1.0 mol% $Pd(PPh_3)_4$ in THF with aqueous 2 M sodium hydroxide as base (scheme 14).[97,98]

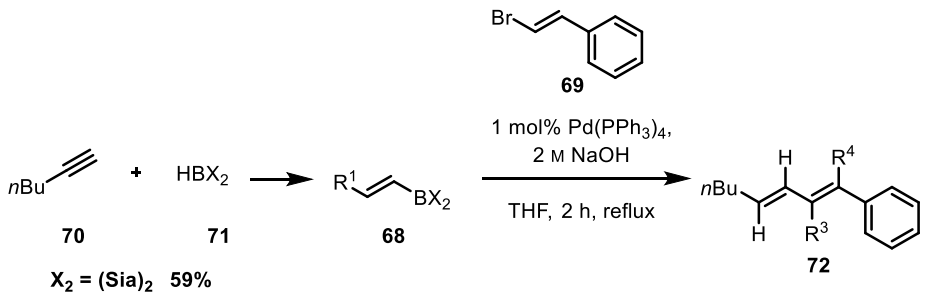

Scheme14: First reported *Suzuki-Miyaura* cross-coupling.

In 2016, *Thomas* and *Denmark* published new insights into the mechanism of this cross-coupling reaction (scheme 15).[99]

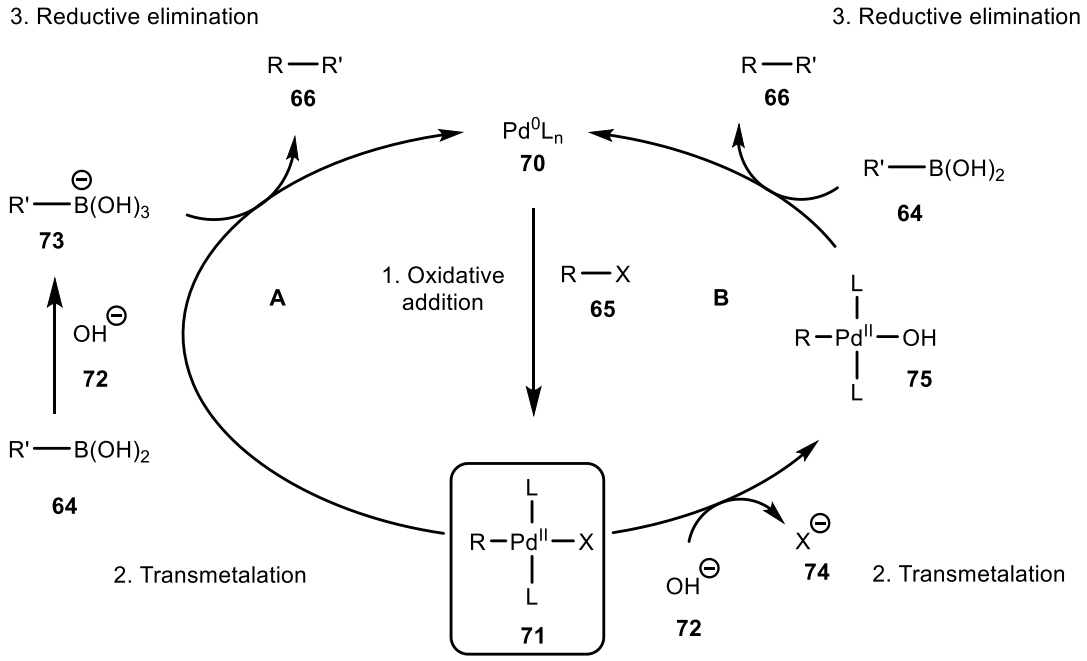

Scheme 15: Proposed mechanism of the *Suzuki* cross-coupling reaction.

To enter the catalytic cycle formation of the catalytic active 14 electron Pd^0 species **70** is crucial. The Pd^0 species **70** can be formed by in situ reduction of Pd(II) salts (such as $PdCl_2$, $Pd(OAc)_2$) by addition of phosphane ligands or the dissociation of weakly coordinating ligands (such as $Pd(PPh_3)_4$). [100–104] Furthermore, ligand free protocols were established [105,106] preventing two considerable side reaction such as phosphonium salt formation as well as aryl-aryl exchange between substrate and phosphine.[107,108] Besides the commonly use of Pd-catalysts, reactions with nickel or gold as catalyst have also been published with sufficient yields.[109-119]

The mechanism contains three major steps. In the first step, the oxidative addition takes place by addition of the aryl halide/pseudohalide **65** to the catalytic active Pd^0 species **70** forming a stable *trans*-*σ*-Pd^0 complex **71**. This step proceeds with retention of the alkenyl halides and inversion for allylic and benzylic halides. Oxidative addition of alkyl halides are rare due to the competing *β*-hydride elimination, which proceeds faster than the oxidative elimination. The oxidative addition is considered as rate determining step in the catalytic cycle. The reactivity of the substrate is highly dependent on the leaving group. This step is followed by a *cis*/*trans* isomerization forming the stable *trans*-σ-Pd^0 complex **71**.[120] The weaker the bond between the halide or pseudohalide and the carbon the more faster the oxidative additions to the Pd^0 species **70** proceeds.[121] The reactivity of this step decreases in following order of I > OTf > Br >>OTs > Cl.[122–124] Electron-withdrawing groups in conjugation to the leaving group enhance the reactivity compared to electron-donating groups, allowing organochlorides to participate in transition metal catalyzed cross-coupling reactions.[125–129] Two different mechanisms proposed for the stable *σ*-vinyl-Pd^{2+} complex **76**

for vinyl halides are possible. The first mechanism considers the formation of a three membered palladacycle **77**, which generates the σ-Pd^{2+}complex **76** by rearrangement (scheme 16).[130,131]

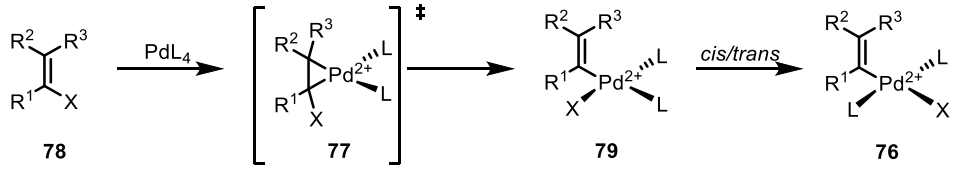

Scheme 16: Oxidative addition of vinyl halides **78** via three-membered palladacycle **77**.

The second proposed mechanism suggests a five coordinated transition state **80** from the oxidative addition of the organohalide to the Pd^0 species **70** (scheme 17).[131]

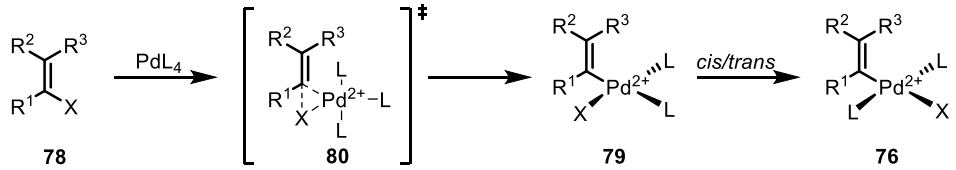

Scheme 17: Oxidative addition of vinyl halides **78** via a five coordinated transition state **80**.

Compared to alkenyl halides **78** the oxidative addition of aryl halides **81** similar to the nucleophilic aromatic substitution with cleavage of the leaving group as rate determining step (scheme 18).[131,132]

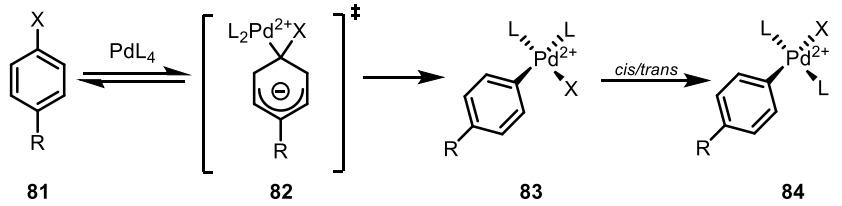

Scheme 18: Oxidative addition of aryl halide **81** via nucleophilic aromatic substitution pathway.

The second step of the *Suzuki-Miyaura* reaction is the transmetalation, where a ligand exchange between the palladium complex **71** and the boronic acid **64** takes place. The question is whether, as shown in *pathway A* (scheme 15, *pathway A*), the boronic acid **64** is firstly converted into boronate **73** by the base **72** or the palladium complex **71** is firstly activated by the base **72** (scheme 15, *pathway B*). Nonetheless, this step has not been fully clarified so far and both pathways are used in literature.[99] By means of rapid injection NMR spectroscopy and the nuclear *Overhauser* effect, *Thomas* and *Denmark* were able to identify three different palladium complexes **85-87** formed during transmetalation (figure 9).[99]

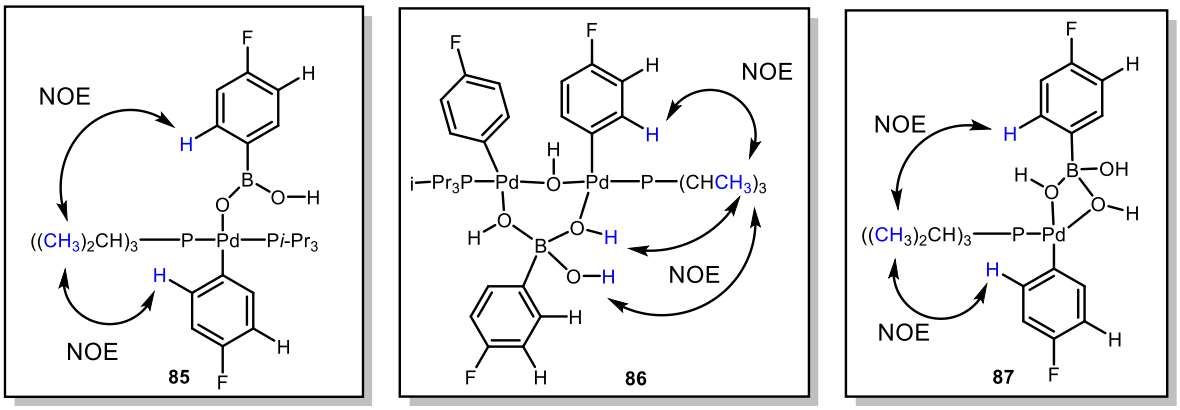

Figure 9: Palladium complexes **85-87** formed during the transmetalation step in the *Suzuki* cross-coupling reaction.

This study provided evidence that both suggested pathways can take place. In the final step, the *trans-cis* isomerization of **88** occurs, which is essential for reductive elimination. Hereby, the oxidation state of the palladium, as well as the coordination number is reduced.[133] Simultaneously the organic moieties form a carbon-carbon bond. The nature of the organic moieties influence the rate of the reductive elimination, which forms the order of reactivity: aryl-aryl > aryl-alkyl > propyl-propyl > ethyl-ethyl > methyl-methyl. Additional *π*-orbital interactions of aryl moieties are beneficial during the bond formation process.[120]

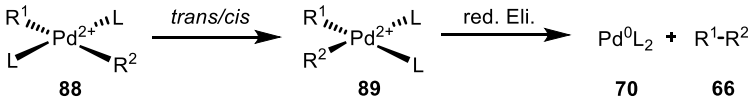

Scheme 19: Reductive elimination via *trans-cis* isomerisation under the formation of Pd^0 and the coupling product.

The catalytic cycle is completed by a reductive elimination forming the C-C bond while regenerating the Pd^0 catalyst **70** is regenerated. This step is also in both pathways (scheme 19).[134]

Over the last decades, the Pd-catalyzed *Suzuki-Miya*ura cross-coupling revolutionized modern organic chemistry and plays an essential role in the industrial production of agrochemicals and pharmaceuticals. Low toxicity and high stability of these building blocks as well as the high versatility are beneficial for big scale applications. Moreover this methodology is a powerful tool for the syntheses of biologically active natural products such as Nannocystin A **90** and (+)-Dynemicin **91** (scheme 20 and scheme 21).[135]

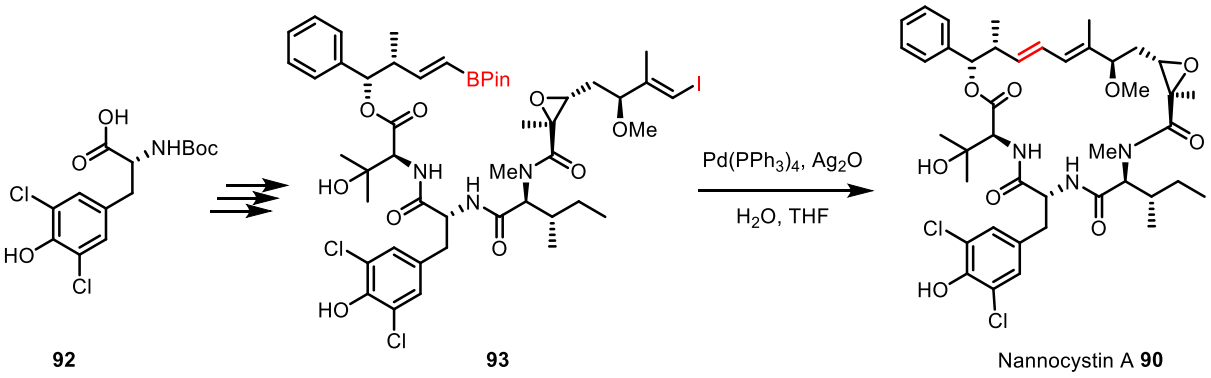

Scheme 20: Pd-catalyzed *Suzuki-Miyaura* cross-coupling as key step for the syntheses of nannocystin A **90**.

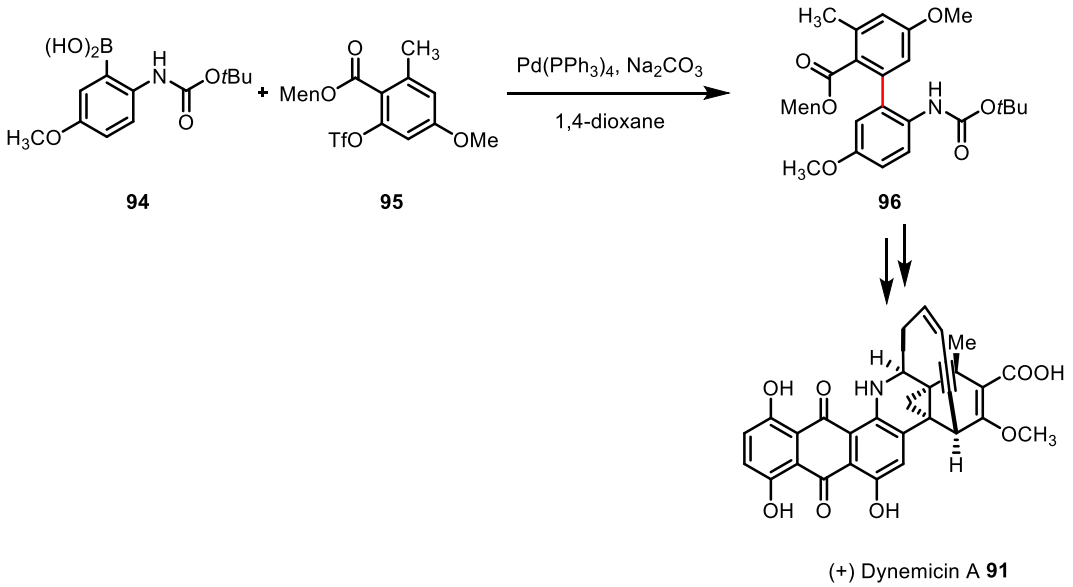

Scheme 21: Pd-catalyzed *Suzuki-Miyaura* cross-coupling as key step for the syntheses of (+) dynemicin **91**.

1.6. Carbonylative *Suzuki-Miyaura* cross-coupling

In 1991, *Miyaura* and *Suzuki* reported an efficient procedure for the synthesis of unsymmetrical ketones by coupling 9-alkyl-9-borabicyclo[3.3.1]nonane derivatives with vinyl iodides under CO-gas atmosphere.[136] The conventional way of common carbonylative cross-coupling considers gaseous CO-gas **97** as source (scheme 22).[98,137]

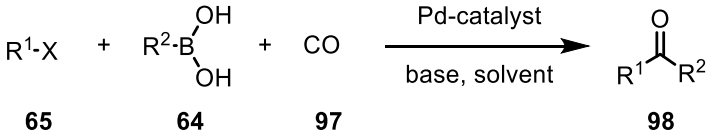

Scheme 22: General reaction of a Pd-catalyzed carbonylative *Suzuki-Miyaura* cross-coupling.

The catalytic cycle of the carbonylative *Suzuki-Miyaura* cross-coupling can be divided into six steps (scheme 23).[99,138] In contrast to the conventional *Suzuki-Miyaura* coupling, the CO-coordination (**B**) and insertion (**C**) take place after oxidative addition and prior to the transmetalation step.

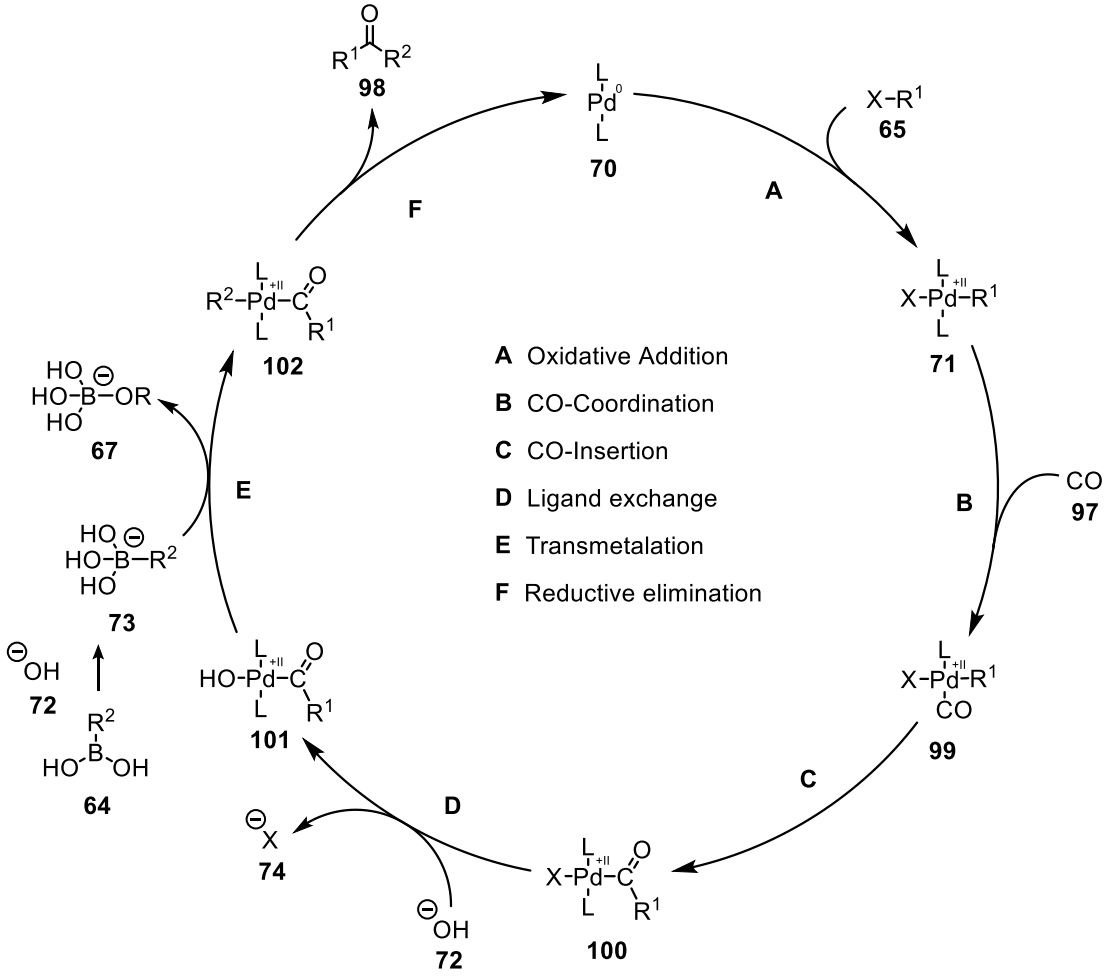

Scheme 23: Proposed catalytic cycle mechanism of the Pd-catalyzed carbonylative *Suzuki-Miyaura* cross-coupling.

The oxidative addition (**A**) of organohalide **65** or pseudohalogenide and the palladium(0) catalyst **70** generate the *trans*-*σ*-palladium(II) complex **71** by insertion into the carbon halide bond. This step is followed by coordination of CO **97** to the palladium (II) complex **99**, since carbon monoxide **97** is a strong *σ*-donor and *π*-acceptor. Subsequent CO-insertion (**C**) affords the acyl-palladium(II) complex **100.** Then, ligand exchange (**D**) leads to the formation of a HO-Pd-COR[1] **101** species. In analogy to the common *Suzuki-Miyaura* reaction, the transmetalation (**E**) is enhanced due to the highly polarized Pd-O bond of **101** and the nucleophilic borate **73**, which can be obtained by the reaction of the boronic acid **64** with base.[99,138] Finally, the desired product **98** is formed and the palladium(0) catalyst **70** is regenerated by reductive elimination (**F**).[120,137] Although the application of carbon monoxide for the carbonylative coupling is convenient and commonly used, major drawbacks such as flammable, colorless, odorless and toxic properties demand for less dangerous alternatives.

Alternatively, the CO gas **97** can be generated in situ from carbonyl sources such as derivatives of formic acid,[139] chloroform,[140] DMF[141] or metal carbonyls[142–149] avoiding the use of toxic and difficult to handle gaseous CO **97**.

Wu et al. reporting a gas free carbonylative Suzuki-Miyaura cross-coupling reaction for biaryl ketones 103 applied this substitution strategy. In situ carbon monoxide **97** was obtained by decomposition of acetic formic anhydride in presence of a base (scheme 24). [139]

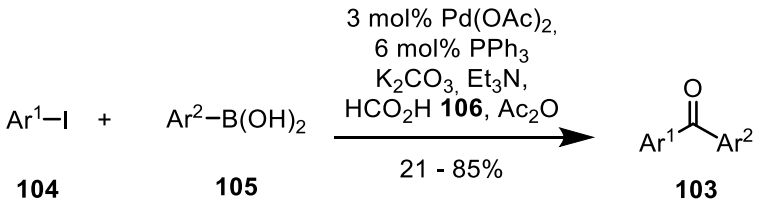

Scheme 24: Carbonylative cross-coupling of aryl iodide **104** and aryl boronic acid **105** with formic acid **106** as CO source.

Furthermore, *Jain* et al. reported the in situ generation of CO **97** from chloroform under basic conditions for the Pd-catalyzed carbonylative *Suzuki-Miyaura* reaction (scheme 25).[140]

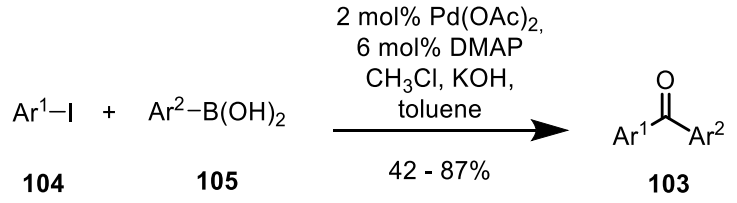

Scheme 25: Carbonylative cross-coupling of aryl iodide **104** and aryl boronic acid **105** with chloroform as CO source.

Lu et al. established a protocol forming CO gas in situ from DMF with $NiBr_2$·diglyme to yield diaryl ketone **106** (scheme 26).[141]

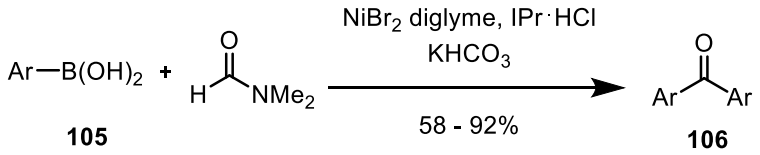

Scheme 26: Carbonylative cross-coupling of phenyl boronic acid **105** with DMF as CO source.

Among the solid CO sources, metal carbonyls, especially molybdeniumhexacarbonyl ($Mo(CO)_6$), has been widely used in a number of palladium-catalyzed carbonylation reacctions such as *Negishi* [147], *Sonogashira* [143], *Stille*. [150,151] *Kashani* et al. reported a versatile carbonylative *Suzuki-Miyaura* cross-coupling using $Mo(CO)_6$ **107** as CO-source and catalytic amounts of $Pd(OAc)_2$ for the synthesis of unsymmetrical ketones. Herein, electron-rich and electron-poor iodoarenes were converted successfully in good yields into the desired products with significant suppression of the conventional *Suzuki* cross-coupling product (scheme 27).[152]

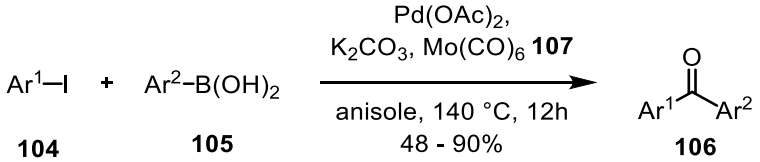

Scheme 1: Carbonylative cross-coupling of aryl iodide **104** and aryl boronic acid **105** with $Mo(CO)_6$ **107** as CO source.

Another example for the feasibility of $Mo(CO)_6$ **107** in carbonylative *Suzuki-Miyaura* cross-coupling was demonstrated by *Odell* et al.[149] Hereby a light induced cross-coupling of alkyl halides **108** and arylboronic acids **105** was established. This approach provided a LED promoted release of CO gas from $Mo(CO)_6$ **107**, as well as the alkyl radical formation of alkyl halides **108** at ambient temperatures (scheme 28).[149]

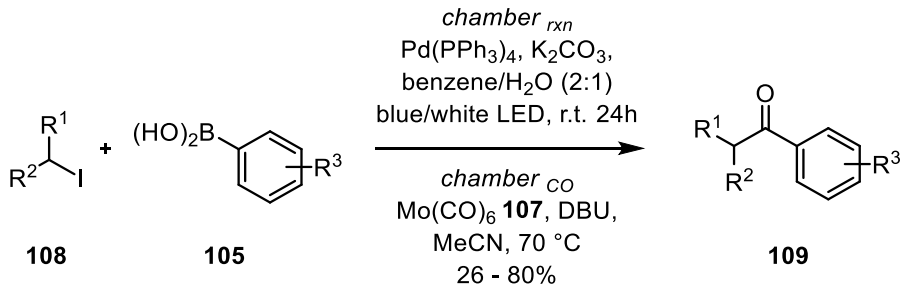

Scheme 28: Carbonylative cross-coupling of alkyl iodide **108** and aryl boronic acid **105** with $Mo(CO)_6$ **107** as CO source.

Alternatively, the acylative *Suzuki-Miyaura* cross-coupling enables the synthesis of ketones from boronic acids and carboxylic acid derivatives, instead of organohalides and toxic carbon monoxide. Several procedures report the successful use of acylchlorides[153–162] and amides.[163,164]Due to the simple access from corresponding carboxylic acids and their stability esters and amides moved into focus for acylative coupling methods. *Szostak* et al. and *Garg* et al. published acylative *Suzuki* couplings using amides. Major advantages of this variant are the utilization of bench stable substrates that are easy accessible from the corresponding carboxylic acid.

Szostak et al. described the application of twisted amides **110** with $Pd(OAc)_2/PCy_3$ as catalyst, providing the the acyl-palladium species **100** for further transmetalation.[163] *Gargs* approach used $Ni(cod)_2$/SIPr as catalyst to couple *Boc*-protected amides **111** with boronic acids **64**.[164] Both protocols afford the ketone **98** in good yields starting from the corresponding amide **110/111** (scheme 29).

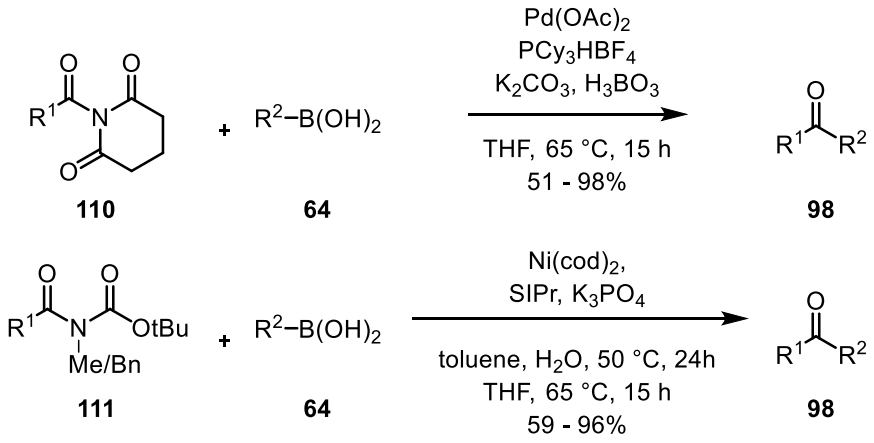

Scheme 29: Acylative *Suzuki-Miyaura* coupling of amides **110/111** with boronic acids **64**.

Beside the application of amides, *Yamamoto* et al. reported a cross-coupling of phenyl trifluoroacetate **112** with organoboron compounds **105** to yield trifluoromethylketones **113**.[165] In contrast to the previously reported procedures, this approach does not require the presence of base for the acylative coupling (scheme 30).

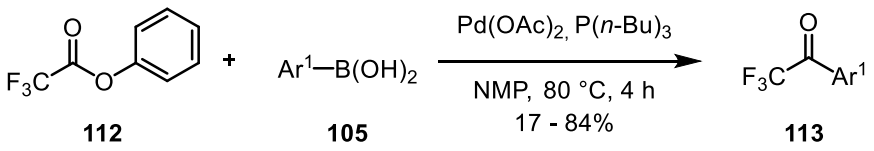

Scheme 30: Acylative *Suzuki-Miyaura* cross-coupling of phenyl-trifluoroacetate **112** with boronic acids **105**.

Chatani et al. reported a ketone synthesis by acylative *Suzuki-Miyaura* coupling of 2-pyridyl esters **114** with boronic acids **115**.[166] Similar to the approach of *Yamamoto*, the acylative coupling of pyridylester does not require additional base (scheme 31).[166]

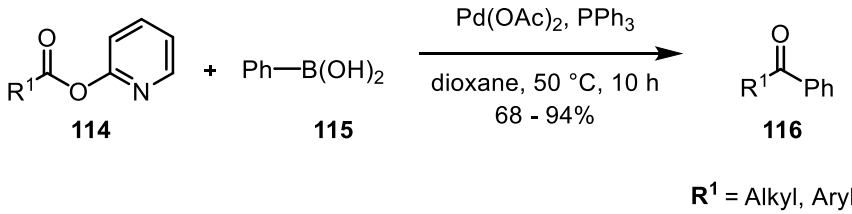

Scheme 31: Acylative *Suzuki-Miyaura* cross-coupling of 2-pyridylester **114** with phenylboronic acid **115**.

2. Aim

Due to the emerging number of resistant pathogens, modern anti-infective drug development requires active candidates addressing alternative molecular targets. For this purpose, marine derived natural products are a promising source for the discovery of novel lead structures. Rubrolides and the related natural product classes of the prunolides and cadiolides represent interesting lead structure with relatively low molecular weight.

Rubrolides were isolated in 1991 by *Miao* et al. from the tunicate *Ritterella rubra*.[28] Over the last decades 19 representatives of this natural product class were isolated. In 2014 *Zhu* et al. discovered two novel rubrolide species. Rubrolide R **12** and S **13** (figure 10) isolated from *Aspergillus terreus* OUCMDZ-1925, showing promising activity against influenza A inferior to Ribavirin.[34] Moreover, rubrolide S **13** has also shown activity against the tobacco mosaic virus.[33]

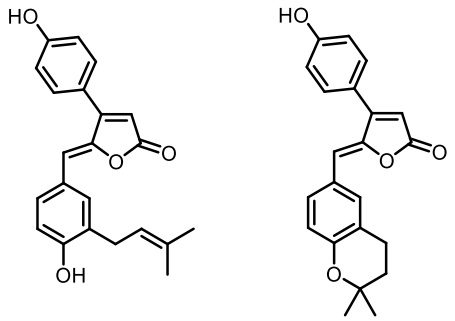

12 **13**

Figure 10: Structures of rubrolides R **12** and S **13**.

Aim of this work was the total synthesis of rubrolide R **12** and S **13** (figure 10) as novel anti-infectives, recently *Damodar* et al. reported the first total synthesis of these two natural compounds over eight steps and an overall yield of 27 - 35%.[35] Hereby, the synthetic aim is to establish a short and versatile synthesis with low step count avoiding toxic tin compounds to enable broader biological testing on the field of antiviral and antibiotic compounds.

Retrosynthetic analysis of rubrolide R **12** and S **13** revealed that these natural products can be synthesized from three major building blocks **26**, **116** and **117** (scheme 32) Both metabolites should be obtained by vinylogous aldol condensation of furanone **26** and benzaldehyde **116/117** followed by subsequent deprotection of the methylether. *Suzuki-Miyaura* cross-coupling should provide furanone building block I **26** starting from triflate **118** and methoxyphenylboronic acid **119**. The prenylated building block II **116** may be obtained via *Suzuki-Miyaura* cross-coupling of prenylbromide **120** and boronic acid **121**. Building block III can be synthesized by a literature known protocol of *Tripathi* et al.[167] from isoprene **122** and **27**.

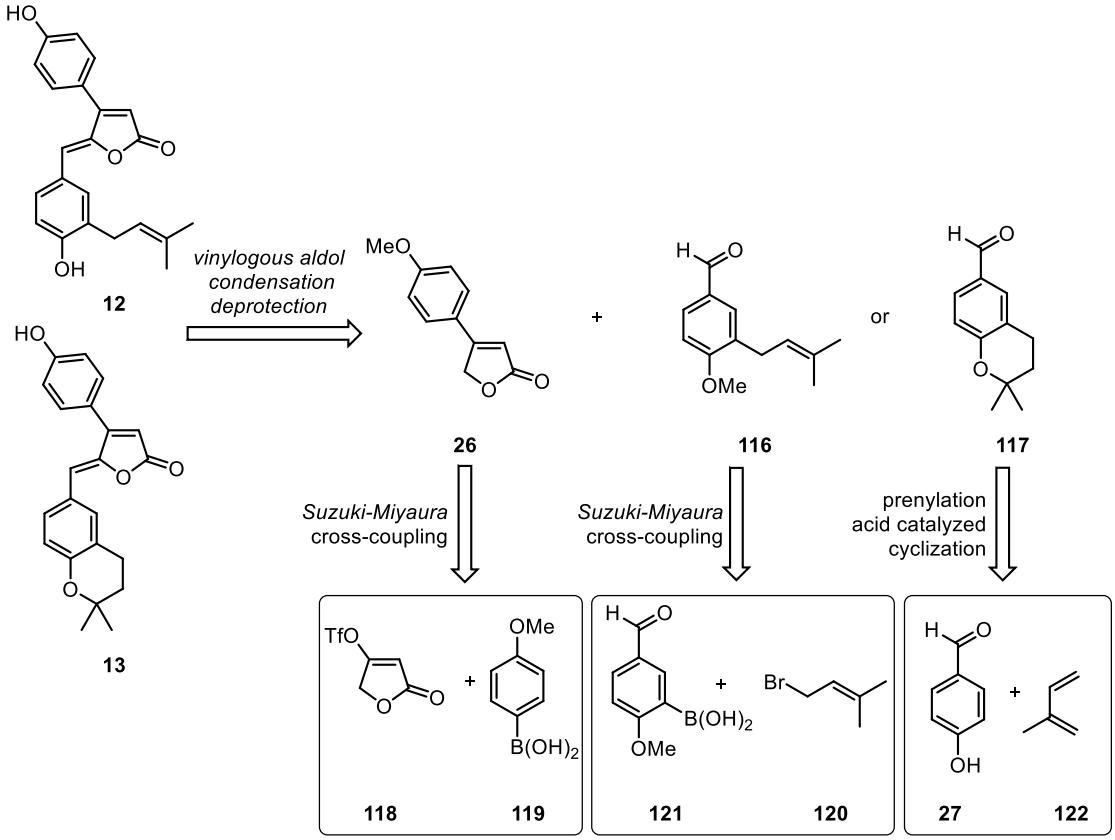

Scheme 32: Retrosynthetic analysis of rubrolide R **12** and S **13**.

Prunolides are a class of natural products occurring furanone derivatives, which have been isolated for the first time from the Australian ascidian *Synoicum prunum* in 1998 with an unique tetraphenolic bisspiroketal scaffold.[54] Biological testing of Prunolide A and C showed cytotoxic activity against HeLa cells at concentrations of 25 µM and 15 µM, respectively.[54] Additionally, Prunolide A revealed promising antiviral activity against the *Japanese encephalitis virus* (JEV).[33,54] This natural product class is an attractive synthetic target since there is no antiviral treatment for JEV infections.

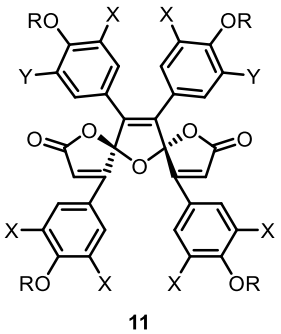

Figure 11: General scaffold of prunolides.

Despite the importance, no total synthesis of the prunolides (figure 11) was reported so far. Within this work, a new methodology for the total synthesis prunolide will be developed to generate novel antiviral compounds of this highly symmetric natural product class.

Starting from 4-iodoanisole **123** and trimethylsilylacetylene **124** a two-fold *Sonogashira* cross-coupling[168] should provide the bis(methoxyphenyl)acetylene **125** followed by subsequent *Z*-selective diborylation[169–171] to afford diboronic ester **126**. The required vinylic halogen **128** should be synthesized from the 4-methoxyacetophenone **15** via *Vilsmeier-Haack* formylation[172], *Pinnick* oxidation[173] and an esterification reaction sequence. With both building blocks **125** and **127**, the diketone-intermediate **128** should be obtained by carbonylative *Suzuki-Miyaura* cross-coupling. Finally, saponification of the carboxylic ester **128** and subsequent acid-catalyzed spirolactonization should provide the desired prunolide scaffold **130** (scheme 33).

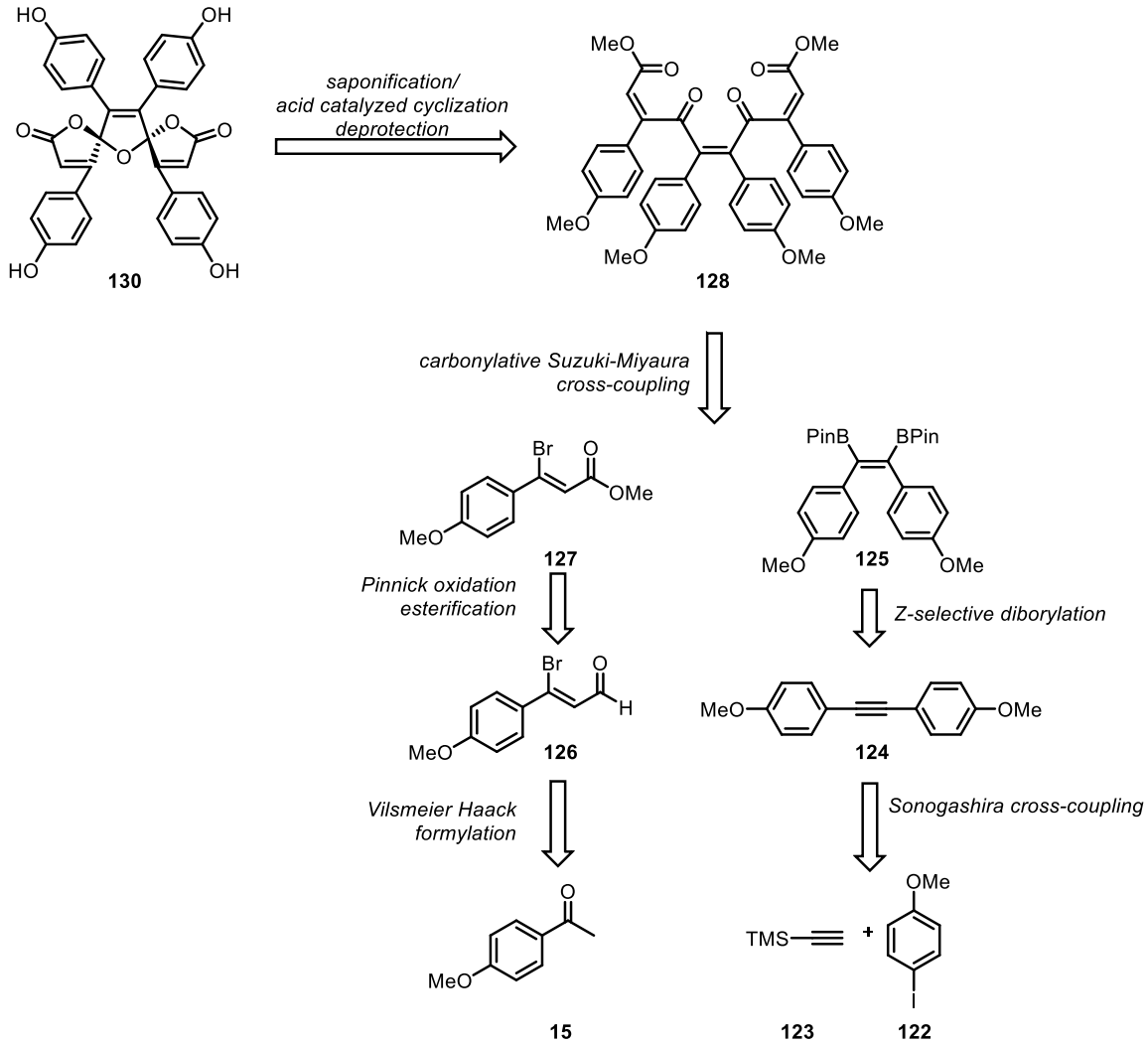

Scheme 33: Retrosynthetic analysis of the prunolide C **130** synthesis.

3. Results and Discussion

3.1. Rubrolide R 12 and S 13

3.1.1. Synthesis of building block I

Starting from commercially available tetronic acid **131**, a triflate leaving group was installed for the *Suzuki-Miyaura* cross-coupling. By a modified procedure of *Grigg* et al.[174] the desired triflate **118** was obtained in 87% yield (scheme 34).

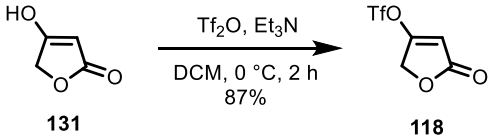

Scheme 34: Synthesis of 5-oxo-2,5-dihydrofuran-3-yl trifluoromethanesulfonate **118**.

For the next step, the Pd-catalyzed *Suzuki-Miyaura* cross-coupling of triflate **118** and methoxyphenylboronic acid **119**, various reaction conditions were screened to obtain building block I **26** (table 3).[175]

Table 3: Optimization of the Pd-catalyzed *Suzuki-Miyaura* cross-coupling between triflate **118** and methoxyphenylboronic acid **119**.

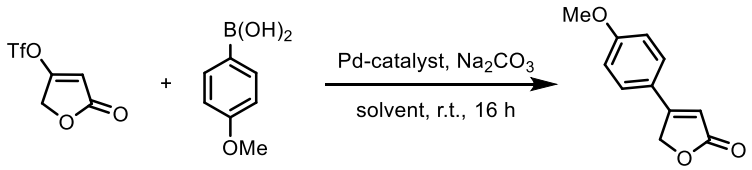

entry	catalyst	loading	ligand	loading	base (3.0 equiv.)	additive (5.0 mol%)	solvent	yield
1	$Pd(OAc)_2$	5.0 mol%	PCy_3	5.0 mol%	Na_2CO_3	BTEAC	Tol/H_2O (9:1)	36%
2	$Pd(OAc)_2$	5.0 mol%	PCy_3	5.0 mol%	Na_2CO_3	BTEAC	Tol/H_2O (2:1)	57%
3	$Pd(OAc)_2$	5.0 mol%	PCy_3	5.0 mol%	Na_2CO_3	BTEAC	Tol/H_2O (1:1)	32%
4	$Pd(OAc)_2$	5.0 mol%	PCy_3	5.0 mol%	Na_2CO_3	TBAB	Tol/H_2O (9:1)	38%
5	$Pd(PPh_3)_4$	5.0 mol%	-	-	Na_2CO_3	-	1,4-dioxane	60%
6	$Pd(PPP_3)_4$	2.5 mol%	-	-	Na_2CO_3	-	1,4-dioxane	67%
7	$Pd(PPh_3)_4$	1.0 mol%	-	-	Na_2CO_3	-	1,4-dioxane	78%
8	$Pd(PPh_3)_4$	5.0 mol%	-	-	Na_2CO_3	-	1,4-dioxane	92%[a]

[a] reaction performed at 60 °C.

Firstly, a protocol of *Boukouvalas* et al.[47] was applied with $Pd(OAc)_2$ as Pd-source, PCy_3 as ligand, sodium carbonate as base, BTEAC[41] as additive and a solvent mixture of toluene/water mixture (2:1) at room temperature (table 3, entry 2). Hereby, a moderate yield of 57% was obtained. Further variation of the toluene/water ratio caused significant reduction

in yield (table 3, entry 1 and 3). Substitution of the phase transfer catalyst to TBAB as well as performing the reaction in a 1:1 toluene/water mixture (table 3, entry 4) did not lead to higher yields. The cross-coupling reaction with $Pd(PPh_3)_4$ in 1,4-dioxane slightly increased the yield (table 3, entry 5). Stepwise reduction of the catalyst loading resulted in higher yields up to 78% (table 3**Table** , entry 5-7). Moreover, elevated reaction temperature of 60 °C with 5.0 mol% $Pd(PPh_3)_4$ provided the desired product in 92% yield (table 3, entry 8).

3.1.2. Synthesis of prenyl aldehyde 116

For the total synthesis of rubrolide R **12** the prenylated building block **116** is required. The reaction conditions for the introduction of the prenyl moiety by Pd-catalyzed *Suzuki-Miyaura* cross-coupling between boronic acid **121** and prenylbromide **120** was investigated. Therefore, the required boronic acid **121** was obtained according to scheme 35. In the first step, 3-bromo-4-hydroxybenzaldehyde **132** underwent a Williamson ether synthesis[176], followed by 1,3-dioxolane formation with ethylene glycol to afford **133** in 81% yield. Next, lithium–halogen exchange of **133** was performed and subsequent treatment with trimethyl borate and acidic hydrolysis of the 1,3-dioxolane **133** yielded the desired boronic acid **121** in a quantitative yield (scheme 35).[177]

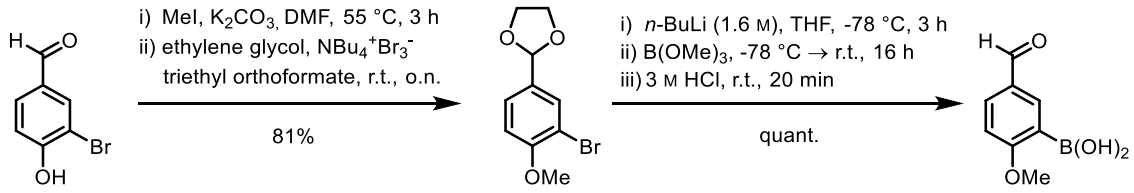

132 **133** **121**

Scheme 35: Synthesis of (5-formyl-2-methoxyphenyl)boronic acid **121**.

Afterwards, reaction conditions for the prenylation of **116** by Pd-catalyzed *Suzuki-Miyaura* cross-coupling were screened (table 4).

Table 4: Optimization of the Pd-catalyzed *Suzuki-Miyaura* cross-coupling

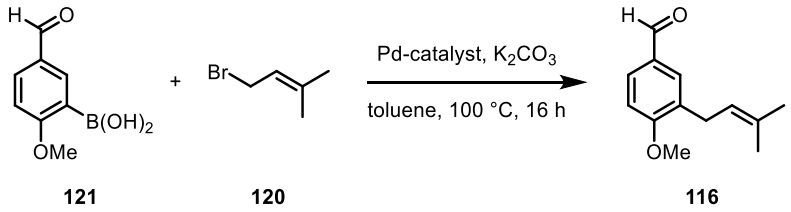

121 **120** **116**

entry	catalyst	loading	time	yield
1	$Pd(PPh_3)_4$	2.5 mol%	16 h	-
2	$Pd(PPh_3)_4$	5.0 mol%	16 h	-
3	Pd_2dba_3	2.5 mol%	16 h	33%
4	Pd_2dba_3	5.0 mol%	16 h	39%

a) *Reaction conditions* **120** (1.0 equiv.), **121** (1.2 equiv.), K_2CO_3 (5.0 equiv.), 100 °C, sealed tube.

As starting conditions $Pd(PPh_3)_4$ as precatalyst with Na_2CO_3 as base in toluene were chosen, which are literature known coupling conditions for aryl halogens with boronic acid **121**.[178–180] The *Suzuki-Miyaura* cross-coupling with 2.5 mol% and 5.0 mol% catalyst loading did not afford the prenylated benzaldehyde **116** (table 4, entry 1-2). Moreover, protodeboronation[181] of **121** was observed as major product. Performing the cross-coupling with Pd_2dba_3 instead (table 4, entry 3-4) yielded the prenylated building block was obtained in a yield of 39% (table 4, entry 4).

Alternatively, prenylation was conducted via lithium-halogen exchange of **133** and subsequent conversion with CuBr · DMS and prenyl bromide **120,** formed the desired building block **116** in a moderate yield of 31% (scheme 36).[182]

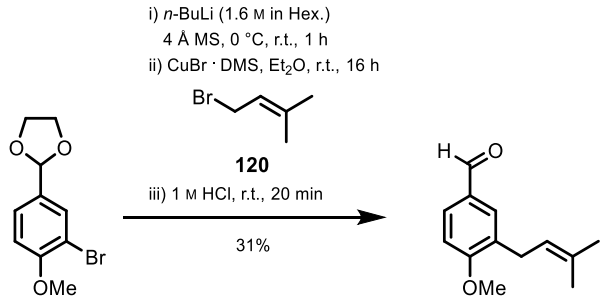

133 **116**

Scheme 36: Reaction scheme for the synthesis of methyl protected prenyl benzaldehyde **116**.

3.1.3. Synthesis of 2,2-dimethylchromane-6 carbaldehyde 117.

The required aldehyde for the synthesis of rubrolide S **13** was synthesized according to a protocol of *Tripathi* et al..[167] Prenylation of *p*-hydroxybenzaldehyde **27** with isoprene **122** and acid mediated cyclization afforded the 2,2-dimethylchromane-6-carbaldehyde **117** in a 52% yield (scheme 37).[183]

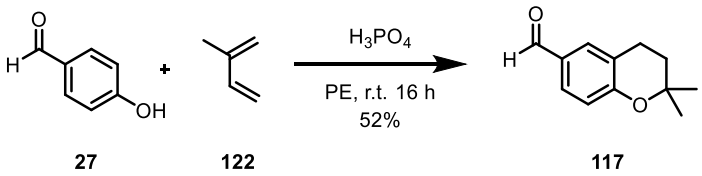

27 **122** **117**

Scheme 37: Synthesis of 2,2-dimethylchromane-6carbaldehyde **117**.

Additionally a suitable single crystal of 2,2-dimethylchromane-6-carbaldehyde **117** was isolated to verify the structure via single crystal X-ray analysis (figure 12).

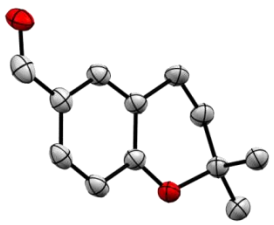

Figure 12: X-ray single crystal structure of 2,2-dimethylchromane-6carbaldehyde **117**. Thermal ellipsoids are shown at 50% probability level. Hydrogen atoms are omitted for clarity

3.1.4. Vinylogous aldol condensation of the twofold methyl protected rubrolide R 12 and S 13[175,177]

The one-pot vinylogous aldol condensation of **26**, **116** and **117** was the key step. 4-(4-methoxyphenyl)furan-2(5*H*)-one **26** was activated under basic conditions by silylation, followed by nucleophile attack of aldehyde **116/117** at room temperatur. Afterwards, DBU mediated condensation afforded methyl-protected rubrolide R **134** in a 56 % and protected rubrolide S **135** in 66 % yield (scheme 38).

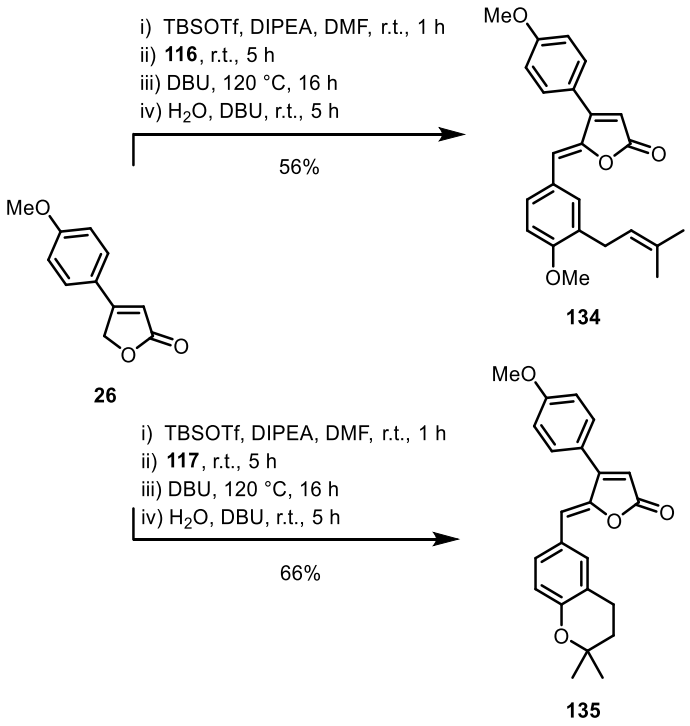

Scheme 38: Synthesis of twofold methyl protected rubrolide R **134** and S **135**.

In the final step, the cleavage of the methyl ether **134** und **135** was attempted. BBr_3 mediated deprotection did not afford the desired natural product **12** and **13**. For the methyl protected rubrolide R **134** cyclization of the prenyl moiety was observed instead (scheme 39). Similar outcome was observed for the methyl protected rubrolide S **135**. Also an alternative cleavage protocol using NaSEt in DMF[184] did not generate the desired structures.

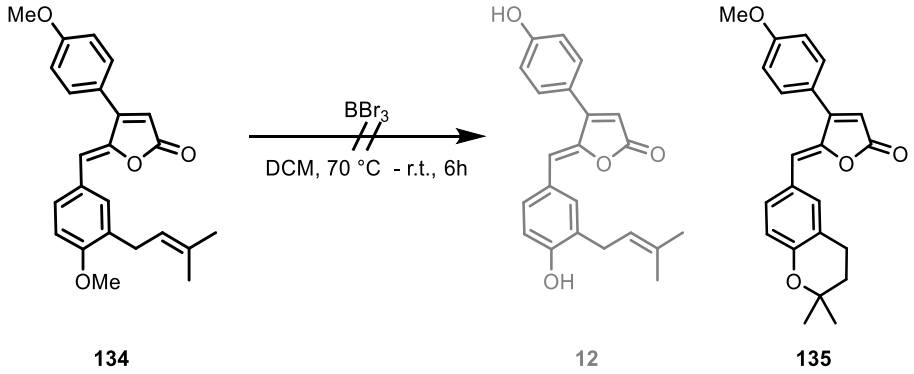

134 **12** **135**

Scheme 39: BBr_3 mediated methyl ether cleavage of **134** and **135**.

3.1.5. Protecting group free synthesis of rubrolide R 12 and S 13

To bypass the deprotection of the methylether, a protecting group free synthesis of rubrolide R **12** and S **13** was developed. Therefore, minor modifications of the building blocks I and II were required. Compared to literature known procedures, this synthetic strategy significantly shortens the general rubrolide synthesis.

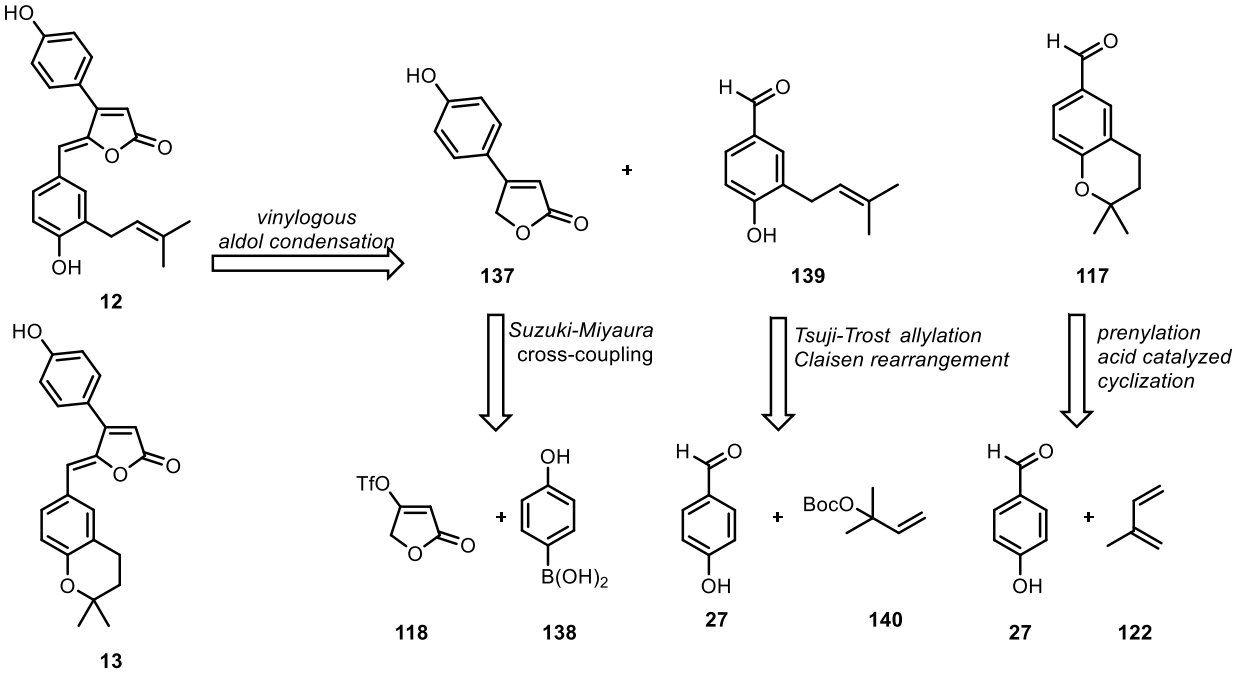

Scheme 40: Retrosynthetic analysis of the protecting group free synthesis of rubrolide R **12** and S **13**.

For this purpose, the central furanone synthesis should be performed by *Suzuki-Miyaura* cross-coupling with the previous described triflate **118** and 4-hydroxyphenylboronic acid **138** (scheme 40). The prenylated benzaldehyde **139** supposed to be prepared by *Tsuji-Trost* allylation with subsequent *Claisen*-rearrangement. Herein, the vinylogous aldol condensation is considered as final step of the total synthesis (scheme 40).

3.1.6. Protecting group free *Suzuki-Miyaura* cross-coupling[8,177]

The protecting group free *Suzuki-Miyaura* cross-coupling was conducted with commercially available 4-hydroxyphenylboronic acid **138** and triflate **118** as substrates using $Pd(PPh_3)_4$ or $PdCl_2(PPh_3)_2$ as precatalysts and Na_2CO_3 as base at 70 °C (table 5).[185]

Table 5: Optimization of the Pd-catalyzed *Suzuki-Miyaura* cross-coupling (1.0 equiv. **119**, 1.2 equiv. **138**, 3.0 equiv. Na_2CO_3, 70 °C).

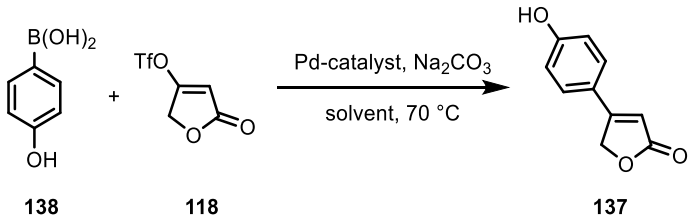

138 **118** **137**

entry	catalyst	loading	solvent	time	yield
1	$PdCl_2(PPh_3)_2$	5.0 mol%	1,4-dioxane	66 h	72%
2	$PdCl_2(PPh_3)_2$	2.5 mol%	1,4-dioxane	66 h	54%
3	$PdCl_2(PPh_3)_2$	1.0 mol%	1,4-dioxane	66 h	33%
4	$PdCl_2(PPh_3)_2$	5.0 mol%	1,4-dioxane	16 h	21%
5	$PdCl_2(PPh_3)_2$	2.5 mol%	1,4-dioxane	16 h	29%
6	$PdCl_2(PPh_3)_2$	1.0 mol%	1,4-dioxane	16 h	29%
7	$Pd(PPh_3)_4$	5.0 mol%	1,4-dioxane	66 h	72%
8	$Pd(PPh_3)_4$	2.5 mol%	1,4-dioxane	66 h	54%
9	$Pd(PPh_3)_4$	1.0 mol%	1,4-dioxane	66 h	33%
10	$Pd(PPh_3)_4$	5.0 mol%	1,4-dioxane	16 h	45%
11	$Pd(PPh_3)_4$	2.5 mol%	1,4-dioxane	16 h	68%
12	$Pd(PPh_3)_4$	1.0 mol%	1,4-dioxane	16 h	81%
13	$Pd(PPh_3)_4$	0.5 mol%	1,4-dioxane	16 h	95%
14	$Pd(PPh_3)_4$	1.0 mol%	toluene	16 h	81%
15	$Pd(PPh_3)_4$	1.0 mol%	2-MeTHF	16 h	69%

Reaction conditions: **119** (1.0 equiv.), 4-hydroxyphenylboronic acid **138** (1.2 equiv.), Na_2CO_3 (3.0 equiv.), 70 °C.

With 5.0 mol% $PdCl_2(PPh_3)_2$ as precatalyst and a reaction time of 66 h, a yield of 72% was achieved (table 5, entry 1). Stepwise decrease of the catalyst loading and reaction time (table 5, entry 2-6) resulted in significant lower yield of **137**. Further screening experiments investigated the application of $Pd(PPh_3)_4$ as precatalyst. By using 5.0 mol% of $Pd(PPh_3)_4$ and a reaction time of 66 h a yield of 72% was obtained (table 5, entry 7). In analogy to $PdCl_2(PPh_3)_2$, the stepwise reduction of the catalyst loading led to decreased yields (table 5, entry 8-9). On the contrary, with a reaction time of 16 h (table 5, entry 10-13) the opposite effect was observed. Continuous reduction of the catalyst loading increased the yield of **137** (table 5, entry 10-13) reaching an optimum with 0.5 mol% $Pd(PPh_3)_4$ and a yield of 95% (table 5, entry 13). Further solvent screening showed that there was only a slight difference between toluene and dioxane, whereas application of 2-MeTHF (table 5, entry 15) led to a decreased yield. [185]

3.1.7. Synthesis of 4-hydroxy-3-(3-methylbut-2-en-1-yl)benzaldehyde 139

Tsuji-Trost allylation of 4-hydroxybenzaldehyde **27** and subsequent Claisen rearrangement should provide the building block **139**. For this purpose, Boc-protected 2-methylbut-3-en-2-ol **140** was obtained via deprotonation of 2-methylbut-3-en-2-ol **142** with *n*-BuLi at 0 °C, followed by conversion with Boc_2O to yield **140** in 76% yield (scheme 41, method A).[186] **140** was also obtained by Lewis acid mediated Boc-protection of **142** with 88% yield (scheme 41, method B).[187]

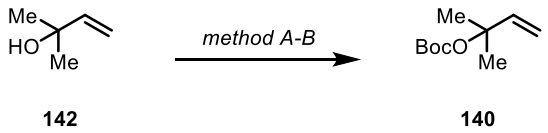

142 **140**

method A) i) THF, *n*-BuLi (1.6 M in Hex), 0 °C, 30 min ii) Boc_2O, r.t., 16 h, 76%
method B) $Zn(OAc)_2 \bullet H_2O$, Boc_2O, DCM, 50 °C, 7 d, 88%

Scheme 41: Synthesis of Boc-allyl ether **140**.

Afterwards, Pd-catalyzed *Tsuji-Trost* allylation of Boc-allyl ether **140** with 4-hydroxybenzaldehyde **27** afforded the desired product **141** in a yield of 79% (scheme 42).

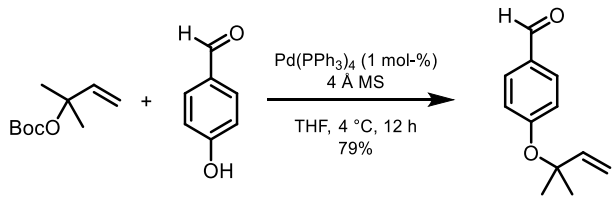

140 **27** **141**

Scheme 42: Synthesis of **141** via Pd-catalyzed *Tsuji-Trost* allylation

In analogy to the *Suzuki* reaction the palladium catalyzed *Tsuji-Trost* allylation starts with a Pd(0)-species **70**. Coordination of **143** forms the η^2-π-allyl complex **144** (**A**). Then, oxidative addition (**B**) forming the η^3-π-allyl complex **145** serving as electrophile for the next step. Depending on the nature of the nucleophile two distinct mechanistic pathways can take place. Hard nucleophiles (**146a**) attack the metal centre and therefore the stereo information of the π-allyl complex retains (**C**). Whereas soft nucleophiles (**146b**) attach directly to the allylic moiety inverting the stereo information in the π-allyl complex **145**. The allylation product **148** is finally obtained by reductive elimination (**D**), which leads to an inversion of the stereochemistry. Dissociation of the Pd(0)-species **70** liberates the product **146** and regenerates the active palladium catalyst **70** (scheme 43).[188,189]

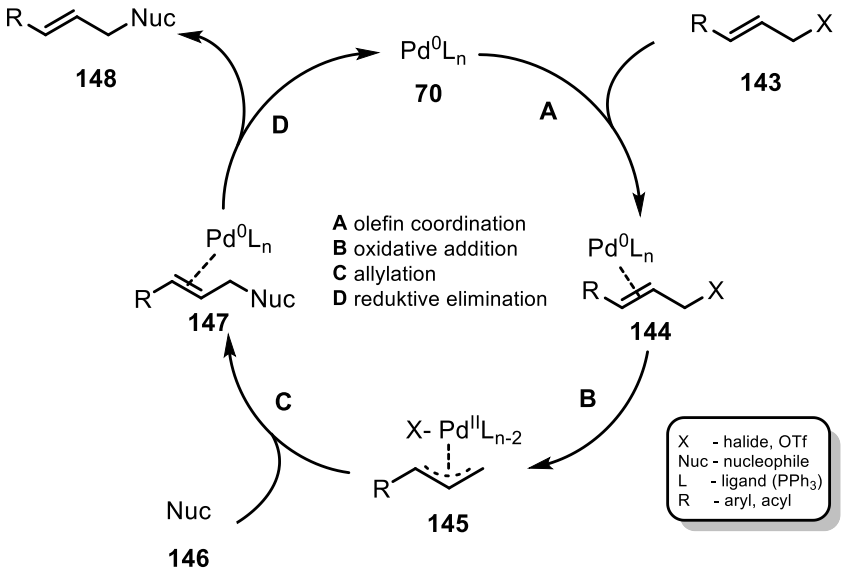

Scheme 43: Catalytic cycle of *Tsuji-Trost* allylation.

Prenyl building block **139** was obtained by microwave assisted Claisen-rearrangement at 180 °C in DMF for 45 min. Chromatographic purification provided the desired product **139** in 88% yield (scheme 44).[185]

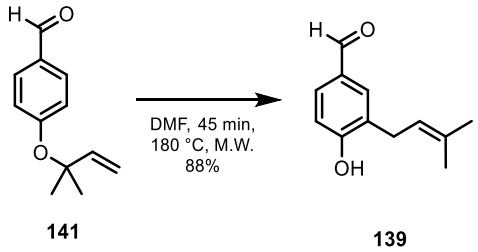

Scheme 44: Synthesis of **139** via microwave assisted Claisen rearrangement.

3.1.8. Synthesis of rubrolide R 12 and S 13 via vinylogous aldol condensation[175,177]

In the final step, the one-pot vinylogous aldol condensation between the key building blocks **137** and the benzaldehyde derivatives **117** and **139** was performed. The condensation afforded *E*/*Z* mixtures of both natural products. By proton NMR ratios of approximately 1:10 for rubrolide R **12** and 1:4 for rubrolide S **13** were identified. Standard separation methods such as crystallization, normal phase column chromatography and sublimation did not yield the pure *Z*-isomers **12** and **13**. Furthermore, the double bond readily isomerized under light exposure and Brønsted/Lewis acidic condition. For example, long exposure to silica induced double bond isomerization. Therefore, only purification via reversed-phase column chromatography yield rubrolide R **12** in 63% and rubrolide S **13** in 66% as pure *Z*-isomers (scheme 45).[185]

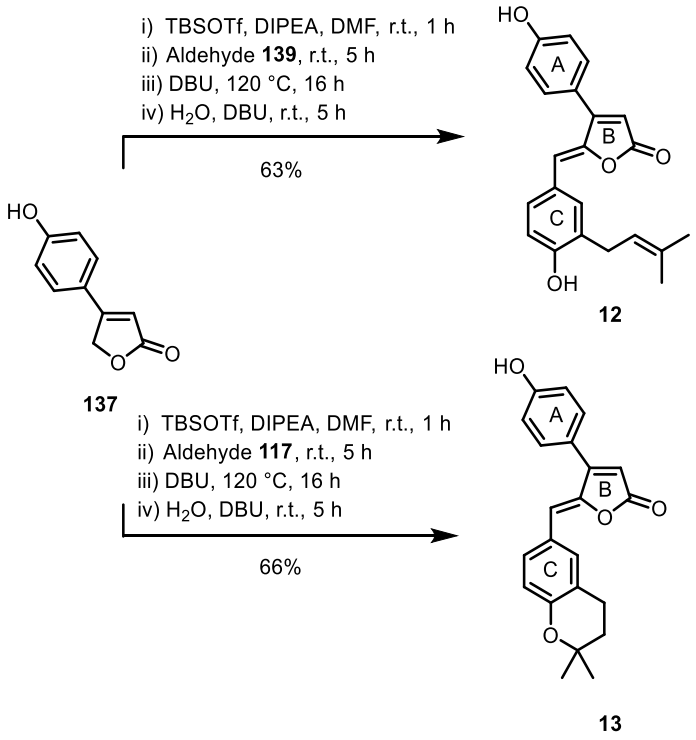

Scheme 45: Synthesis of rubrolide R **12** and S **13** via vinylogous aldol condensation.

Figure 13 displays the proton-NMR of rubrolide R **12**. Signals at 6.93 (d, *J* = 8.6 Hz, 2 H, 3'-H, 5-H) and 7.48 (d, *J* = 8.6 Hz, 2 H, 2'-H, 6'-H) correspond to the 1,4-disubstituted A-ring. While the singlet at 6.35 (s, 1H, 3-H) indicate the furanone ring B. Furthermore, signals at 6.86 (d, *J* = 8.4 Hz, 1 H, 5''-H), 7.54 (dd, *J* = 8.4 Hz, 2.1 Hz, 2 H, 6''-H) and 7.56 (d, *J* = 2.1 Hz, 1 H, 2''-H) indicate the 1,2,4-trisubstitued phenyl ring C. Signals at 3.22 (d, *J* = 7.4 Hz, 2 H, 1'''-H), 5.18 (m, 1 H, 2'''-H), 1.70 (s, 3 H, 4'''-H_3) and 1.69 (s, 3 H, 5'''-H_3) are characteristic for the protons of the prenyl chain. The characteristic signal at 6.28 (s, 1 H, 6-H) derived from the benzylidene protons confirms the successful formation of the rubrolide **12** by aldol condensation. In addition, the hydroxyl groups were observed at 9.99 (s, 1) and 10.07 (s, 1) ppm.

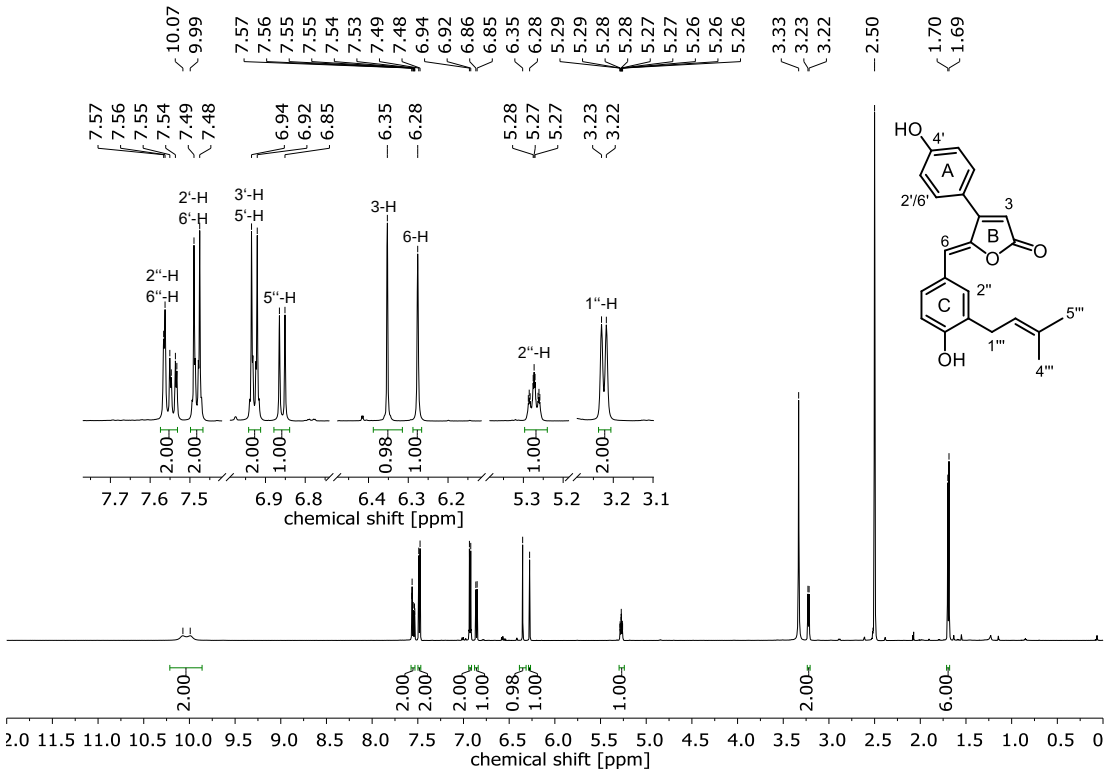

Figure 13: ^{1}H NMR spectrum (600 MHz, DMSO-d_6) of rubrolide R **12**.

Since the vinylogous aldol condensation generates the double bond in *E*- and *Z*-configuration NOESY spectra of **12** were acquired (figure 14).[14,190]

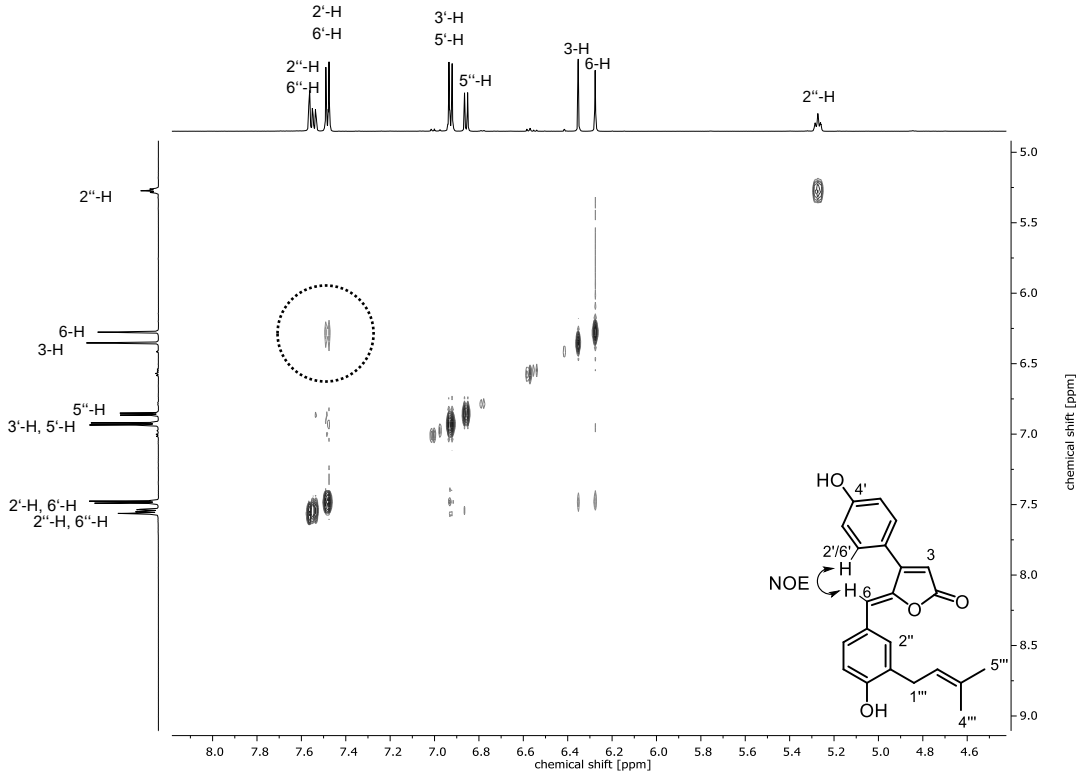

Figure 14: NOESY spectrum (600 MHz DMSO-d_6) of rubrolide R **12**.

The NOESY spectra (figure 14) verified the Z-configuration of the exocyclic double bond between C-5/C-6. NOE-signals between the aromatic proton 2'/6'-H and the benzylidene proton 6-H of **12** (figure 14) were detected. High-resolution ESI-MS indicated the successful synthesis of rubrolide R **12** with a measured *m*/*z* ratio of 349.1447 (M+H; ± 3.72 ppm).

Figure 15 displays the proton-NMR of rubrolide S **13**. In analogy to rubrolide S **13**, signals at 6.93 (d, *J* = 8.5 Hz, 2 H, 3'-H, 5-H) and 7.49 (d, *J* = 8.5 Hz, 2 H, 2'-H, 6'-H) correspond to the 1,4-disubstituted A-ring. The signal at 6.35 (s, 1 H, 3-H) corresponds to the furanone ring B. The characteristic signal of the benzylidene protons at 6.28 (s, 1 H, 6-H) confirm the successful formation of rubrolide S **13**. Furthermore, signals at 6.78 (d, *J* = 8.2 Hz, 1 H, 8''-H), and 7.60—7.56 (m, 2 H, 5''-H, 7''-H) indicate the 1,2,4-trisubstitued phenyl ring C. Characteristic signals at 1.78 (t, *J* = 6.7 Hz, 2 H, 3''-H_2) and 2.76 (t, *J* = 6.7 Hz, 2 H, 4''-H_2) correspond to methylene groups of the 2,2-dimethylchromane. In addition, the phenolic hydroxyl group was observed at 10.11 (s, 1).

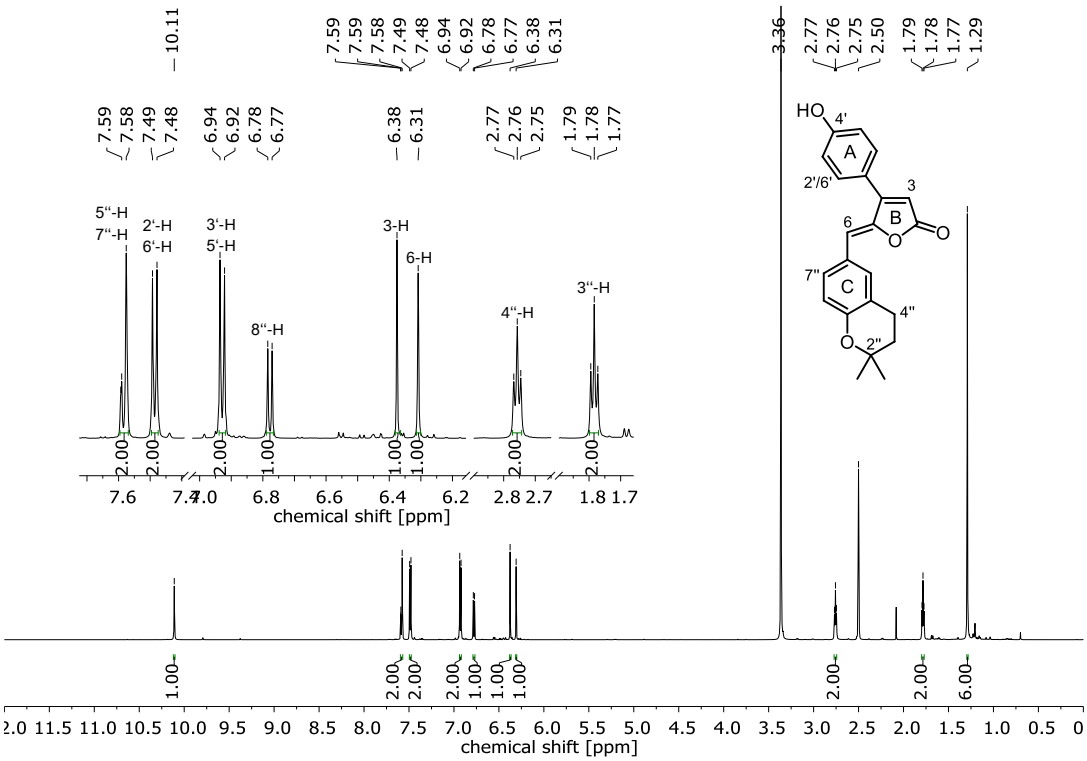

Figure15: ^{1}H NMR spectrum (600 MHz DMSO-d_6) of rubrolide S **13**.

Additional NOESY spectra of **13** (figure 16) verified the *Z*-configuration of the exocyclic double bond between C-5/C-6. NOE-signals between the aromatic proton 2'/6'-H and the benzylidene proton 6-H of **13** (figure 16) were detected.

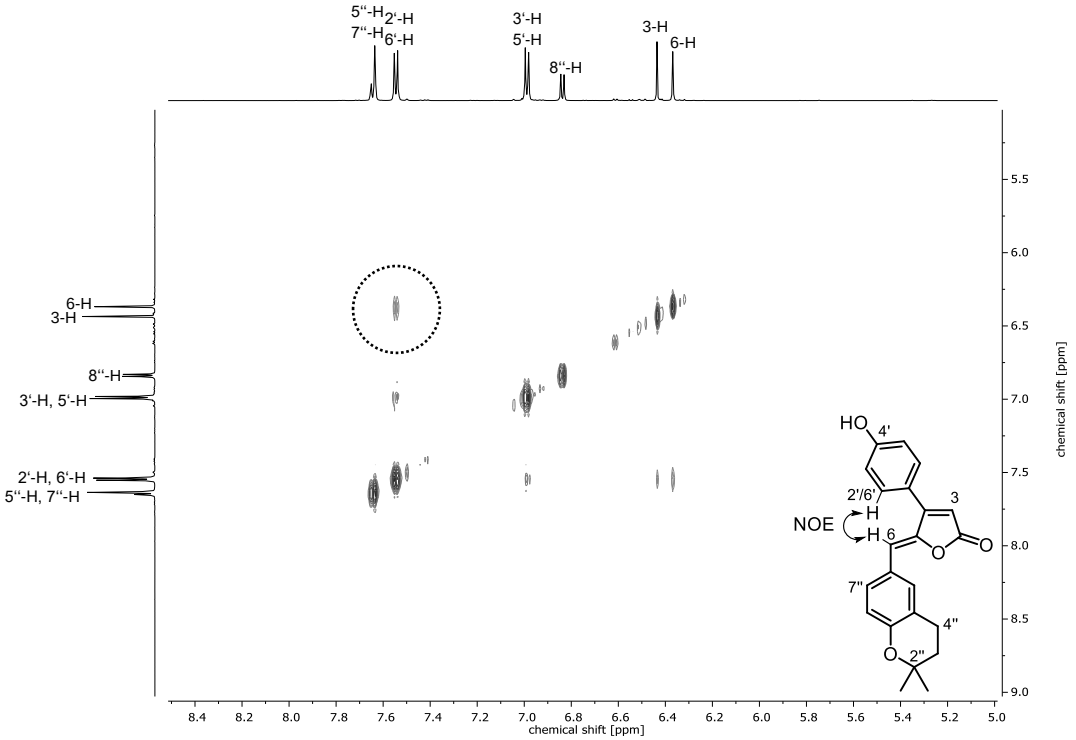

Figure 16: NOESY spectrum (600 MHz DMSO-d_6) of rubrolide S **13**.

Subsequent high-resolution ESI-MS with a measured *m*/*z* ratio of 349.1440 (M+H; ± 3.72 ppm) indicated the successful synthesis of rubrolide S **13**. Moreover, suitable crystals of rubrolide R **12** and rubrolide S **13** were collected to verify the absolute configuration of the *Z*-double bond geometry (figure 17).

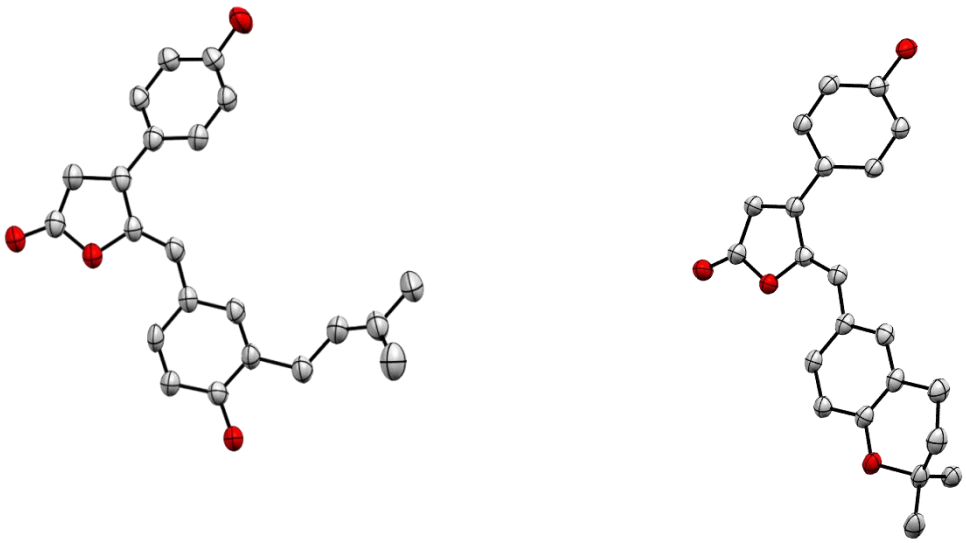

12 **13**

Figure 17: X-ray single crystal structure of rubrolide R **12** and S **13**. Thermal ellipsoids are shown at 50% probability level. Hydrogen atoms are omitted for clarity.

3.1.9. Derivatization of the rubrolide R and S

Since rubrolide R **12** and S **13** revealed in preclinical studies antiviral activity against *p*H1N1 and H3N2[34,185], further derivatization steps of the scaffold for structure-activity relationship studies (SAR-studies) were considered. The structure allows following derivatization opportunities (figure 18):

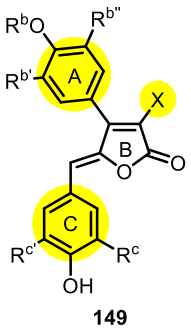

149

Figure 18: General rubrolide structure (positions of derivation highlighted in yellow).

- *Suzuki Miyaura* cross-coupling provides an easy access for the introduction of different aromatic moieties (**ring A**).
- Introduction of halogens to the central butenolide at C-3, since naturally occurring biologically active rubrolides B, K-L have a chloride or bromide at this position (**ring B**).
- Vinylogous aldol condensation enables the introduction of different aromatic systems at the C-5 position (**ring C**)

3.1.10. Rubrolide derivatization (ring B)

Manzanaro et al. investigated the influence of the halogenation pattern on rubrolide E **28** by chlorination of the furanone ring and bromination of the phenyl moieties. Hereby, greater inhibition of the human aldose reductase was discovered.[191] Additional studies revealed the enhancing effect of chloride on the inhibition compared to the non-chlorinated derivatives (figure 19).[191]

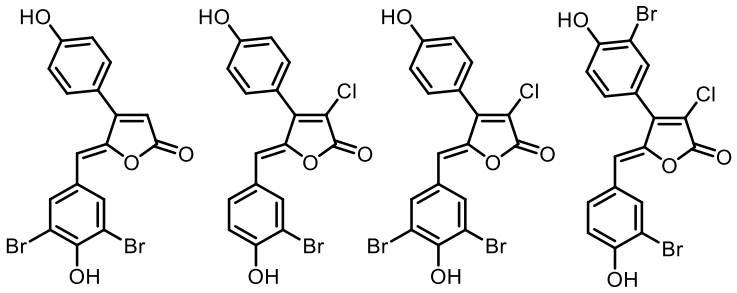

150 IC_{50} <57 µM | **151** IC_{50} 46.2 µM | **152** IC_{50} 0.8 µM | **153** IC_{50} 16.9µM

Figure 19: Halogenated rubrolide E derivative, IC_{50} values against HumanALR2.

Based on this approach the halogenation of rubrolide R **12** and S **13** by introduction of chlorine at the central lactone was investigated to improve biological activities (scheme 46).

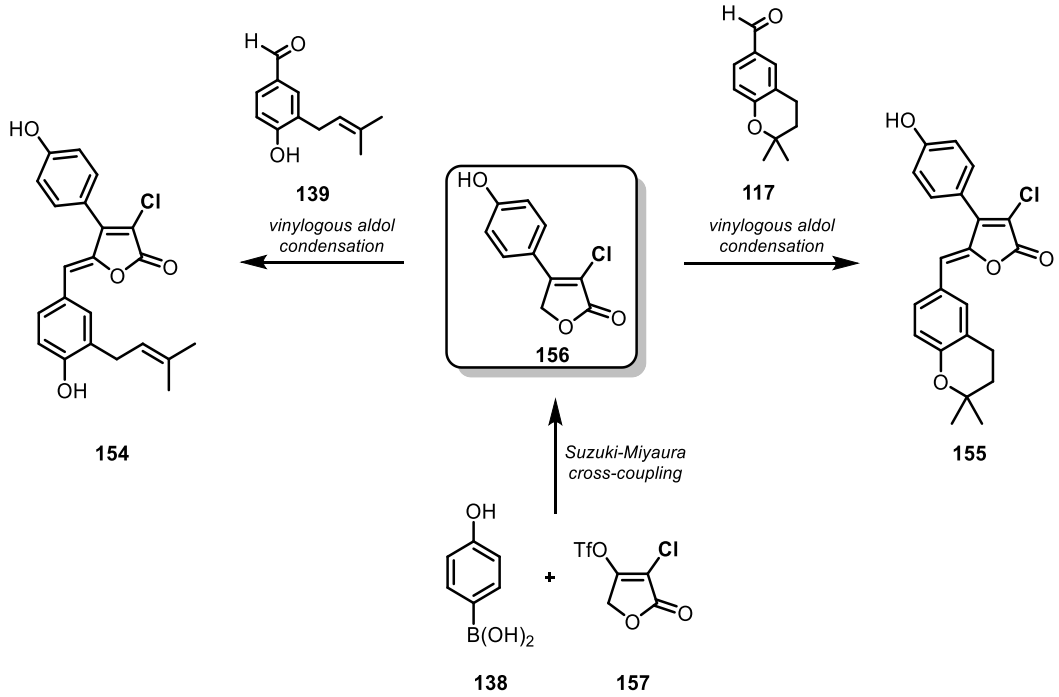

Scheme 46: Retrosynthetic analysis of the chlorinated rubrolide R **154** and S **155**.

In analogy to the previous described syntheses of rubrolide R **12** and S **13**, vinylogous aldol condensation and *Suzuki-Miyaura* cross-coupling as key steps should provide the chloro-derivatives (scheme 46). For this novel type of metabolite, 3-chlorotetronic acid **157** was converted into the required triflate **34** according to the protocol of *Grigg* et al (scheme 47).[174]

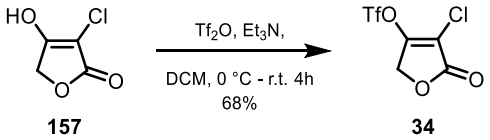

Scheme 47: Synthesis of *chloro*-triflate **34**.

In the following step, screening experiments for the introduction of the aromatic moiety by *Suzuki-Miyaura* cross-coupling on the *γ*-lactone **156** were performed (table 6).

Table 6: Optimization of the *Suzuki-Miyaura* coupling between **156** and hydroxyphenylboronic acid **138**.

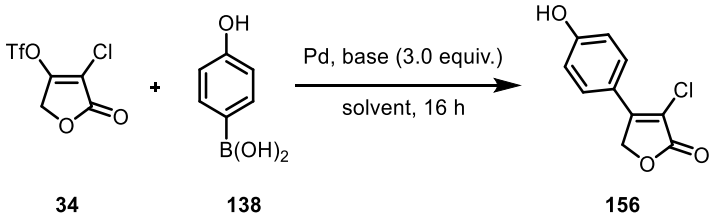

entry	[Pd]	loading	ligand	loading	base	solvent	T [°C]	yield
1	$Pd(PPh_3)_4$	4.0 mol%	-	-	Na_2CO_3	1,4-dioxane	70 °C	-
2	$Pd(OAc)_2$	5.0 mol%	PCy_3	5.0 mol%	Na_2CO_3	toluene/H_2O (1:1)	r.t.	-
3[a]	$Pd(PhCN)_2Cl_2$	5.0 mol%	PPh_3	10.0 mol%	CsF	toluene/H_2O (2:1)l	60 °C	-
4	$Pd(OAc)_2$	5.0 mol%	PCy_3	5.0 mol%	Na_2CO_3	dioxane	70 °C	17% (crude)
5	$Pd(OAc)_2$	5.0 mol%	PCy_3	5.0 mol%	Na_2CO_3	THF	70 °C	traces
6[b]	$Pd(OAc)_2$	5.0 mol%	PCy_3	5.0 mol%	Na_2CO_3	1,4-dioxane/H_2O (12:1)	r.t.	-
7[b]	$Pd(OAc)_2$	5.0 mol%	PCy_3	5.0 mol%	Na_2CO_3	1,4-dioxane	r.t.	-
8[b]	$Pd(OAc)_2$	5.0 mol%	PCy_3	5.0 mol%	Na_2CO_3	toluene/H_2O (12:1)	r.t.	-
9[b]	$Pd(OAc)_2$	5.0 mol%	PCy_3	5.0 mol%	K_3PO_4	toluene/H_2O (12:1)	r.t.	-

[a] 5.0 mol% TBAB additive [b] 5.0 mol% BTEAC.

Previously described *Suzuki-Miyaura* cross-coupling and literature known protocols[47,192] did not yield the desired product (table 6, entry 1-3). While performing the coupling with $Pd(OAc)_2/PCy_3$ as catalyst[193] at elevated temperatures in dioxane, a yield of 17% was obtained (table 6, entry 4). Besides the coupling of the desired building block, GC-MS analysis revealed also the formation of the biarylated product **158** and homocoupled product **159** (figure 20). Performing the cross-coupling in THF led to decreasing yields (table 6, entry 5). Furthermore, water and BTEAC[41,194] as additives (table 6, entry 6-9) were responsible for a decreasing formation of building block **156**.

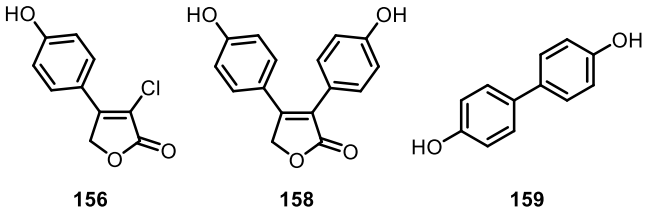

Figure 20: Reaction products of the conducted *Suzuki-Miyaura* coupling.

Due to undesired biarylation of **34** and homocoupling **159**, we further investigated the Pd-catalyzed cross-coupling of *chloro*-triflate **34** and 4-methoxyphenyl boronic acid **119** (table 7).

Table 7: Optimization of the *Suzuki-Miyaura* cross-coupling of *chloro*-triflate **34** and **119**.

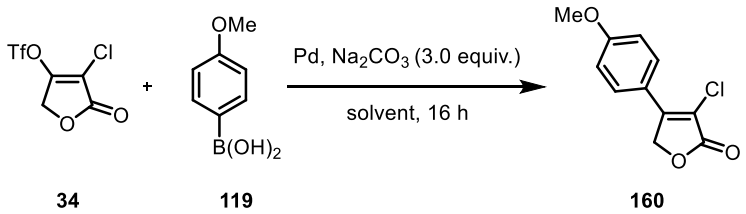

entry	[Pd]	loading	ligand	loading	additive	solvent	T [°C]	yield
1	$Pd(PPh_3)_4$	4.0 mol%	-		-	1,4-dioxane	70°C	-
2	$Pd(PPh_3)_4$	4.0 mol%	-	-	BTEAC	1,4-dioxane	70 °C	-
3	$Pd(PPh_3)_4$	4.0 mol%	-	-	BTEAC	1,4-dioxane/H_2O (12:1)	70 °C	-
4	$Pd(PPh_3)_4$	4.0 mol%	-	-	BTEAC	toluene	70 °C	-
5	$Pd(PPh_3)_4$	4.0 mol%	-	-	BTEAC	toluene/H_2O (12:1)	70 °C	-
6	$Pd(OAc)_2$	5.0 mol%	PCy_3	5.0 mol%	BTEAC	toluene/H_2O (1:1)	r.t.	-
7[47]	$Pd(OAc)_2$	5.0 mol%	PCy_3	5.0 mol%	BTEAC	toluene/H_2O (12:1)	r.t.	traces
8	$Pd(OAc)_2$	5.0 mol%	PCy_3	5.0 mol%	BTEAC	toluene/H_2O (12:1)	70 °C	78%
9	$Pd(OAc)_2$	5.0 mol%	PCy_3	5.0 mol%	BTEAC	1,4-dioxane	70 °C	-

The *Suzuki-Miyaura* cross-coupling in presence of $Pd(PPh_3)_4$ with varying solvent mixtures and TBEAC as additive did not provide furanone **160** (table 7, entry 1-4). In analogy to previous screenings, literature-known conditions by *Boukouvalas* et al. (table 7, entry 6)[47] did not afford the desired compound **160**. By carrying out the reaction in a toluene/water mixture (12:1 *v*/*v*) traces of **160** were isolated (table 7, entry 7). Elevating the reaction temperature to 70 °C an improved yield of 78% was obtained (table 7, entry 8). Whereas performing the reaction in dioxane (table 7, entry 9) no product was detected. In the following, BBr_3 mediated deprotection provided the 3-chloro-4-(4-hydroxyphenyl)furan-2(5*H*)one **156** in quantitative yield (scheme 48).[48]

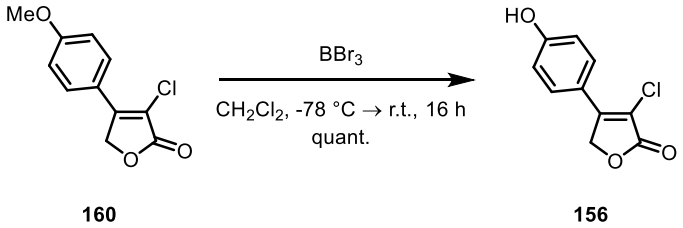

Scheme 48: BBr_3 mediated deprotection of *chloro*-furanone **156**.

3.1.11. Synthesis of *chloro*-rubrolide R 154 and S 155 via vinylogous aldol condensation

In analogy to the previously described syntheses of rubrolide R **12** and S **13**, a vinylogous aldol condensation should provide the *chloro*-derivatives **154** and **155**. While this protocol afforded *chloro*-rubrolide R **154** in a yield of 11%, these conditions were not applicable for the *chloro*-rubrolide S **155** (scheme 49).

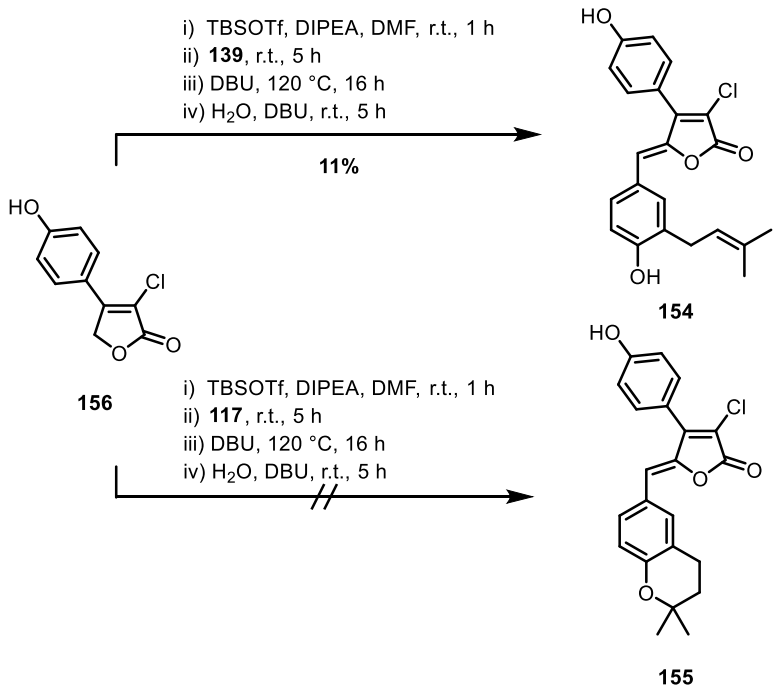

Scheme 49: Synthesis of *chloro*-rubrolide R **154** and S **155** analogue.

Additional NOESY correlation spectra verified the *Z*-geometry of the exocyclic double bond of the *chloro*-rubrolide R **154**. Proton NMR comparison of the rubrolide R **12** (figure 21, top) and the *chloro*-rubrolide R **154** (figure 21, down) revealed the introduction of the chloride at C-3 by the absence of the 3-H proton (~6.30 ppm). In addition to proton-NMR analysis, high-resolution ESI-MS confirmed the successful formation of *chloro*-rubrolide R **154**.

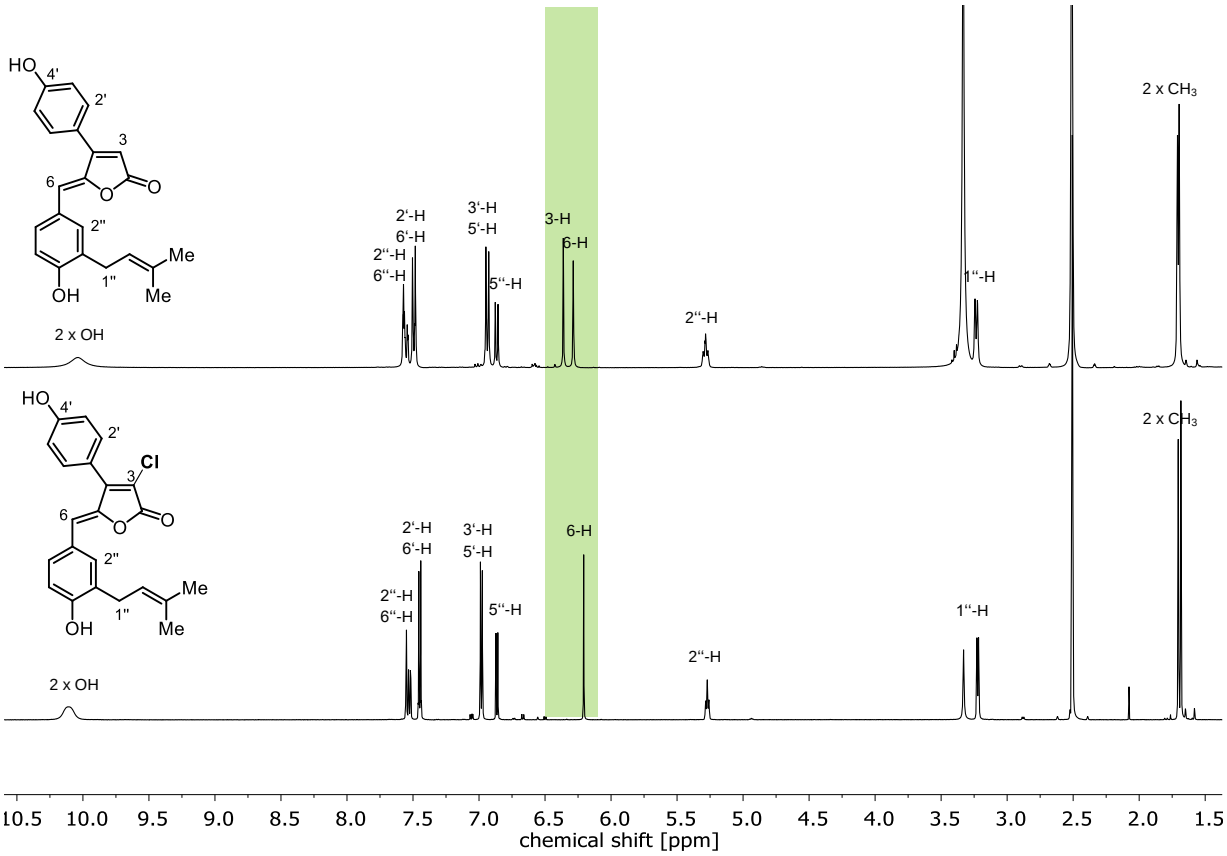

Figure 21: Stacked ^{1}H NMR (400 MHz, DMSO-d_6) of rubrolide R **12** (top) and the *chloro*-rubrolide R **154** (down).

3.1.12. Rubrolide derivatization (ring A)

In vitro studies of methyl-protected and non-methylated rubrolides against pathogenic bacteria (MRSA, *S. epidermidis*, *E. faecalis* and *E. coli*)[195] and several cancer cell lines (NCI- H460, MCF-7, and SF-268)[41] revealed significant higher antibiotic and cytotoxicity for non-methylated rubrolides due to different cell membrane permeability.[29,41]

In order to verify the vital role of the hydroxyl group on rubrolide R **12** and S **13**, the focus was on the functional group substitution of phenolic ring A. This should be conducted by *Suzuki-Miyaura* cross-coupling by using phenyl boronic acids with electron donating and electron withdrawing groups. Hereby, the substitution of the hydroxyl group by fluorine and *N*-Acetyl-group was considered, in order to provide further hydrogen bonding. Furthermore, the catechol motif should be investigated since enzymatic mediated oxidation modifies phenolic structures.[196,197] These derivatives should mimic the oxidized form, while still providing a hydrogen bonding donor combined with a better water solubility. In contrast to the electron donating functional groups, the installation of nitro groups should also be performed. The ability of withdrawing electrons and generating electron deficient sites may enable further interaction with biological nucleophiles such as enzymes and nucleic acids.[198]

3.1.13. Synthesis of boronic acid 161[199]

Preceding the *Suzuki Miyaura* cross-coupling for the catechol-derived rubrolide R **162** and S **163**, the corresponding phenylboronic acid was obtained in a three step synthesis. In the first step, 3-bromosalicylic aldehyde **164** was oxidized under *Dakin* conditions to the corresponding catechol **165**[200] which underwent subsequent TBS-protection. With the TBS-protected catechol **166** a lithium-halogen exchange was performed. Subsequent conversion with B(O*i*Pr)$_3$ and hydrolysis afforded the desired boronic acid **161** in an overall yield of 78% (scheme 50).

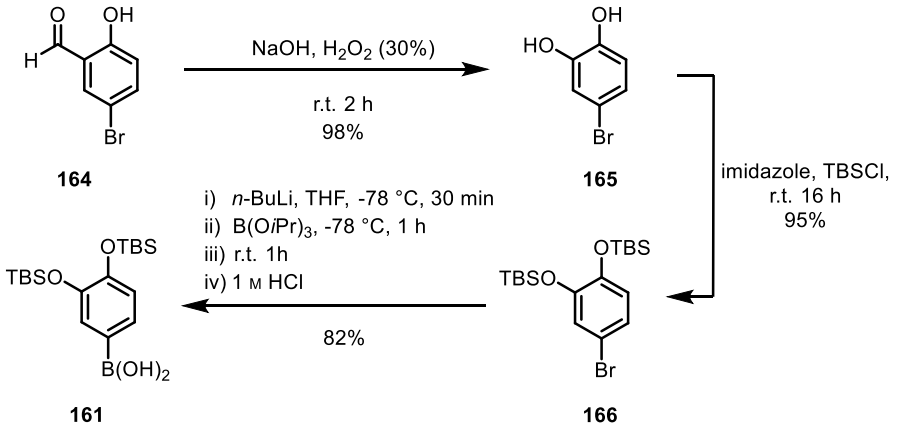

Scheme 50: Synthesis of the TBS-protected catechol boronic acid **161** via *Dakin* oxidation, TBS-protection, followed by lithiation and conversion with B(O*i*Pr)$_3$.

3.1.14. *Suzuki-Miyaura* cross-coupling with various functionalities[199]

For the derivatization of ring A the established Pd-catalyzed *Suzuki-Miyaura* protocol[185] was applied (table 8).

Table 8: Scope of the Pd-catalyzed *Suzuki-Miyaura* cross-coupling of triflate **118** and phenylboronic acids **161** and **167-169**.

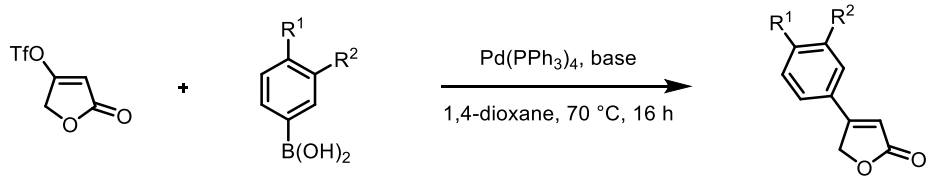

118

R^1 = OTBS	R^2 = OTBS	**161**
R^1 = NHAc	R^2 = H	**167**
R^1 = F	R^2 = H	**168**
R^1 = NO_2	R^2 = H	**169**

R^1 = OTBS	R^2 = OTBS	**170**
R^1 = NHAc	R^2 = H	**171**
R^1 = F	R^2 = H	**172**
R^1 = NO_2	R^2 = H	**173**

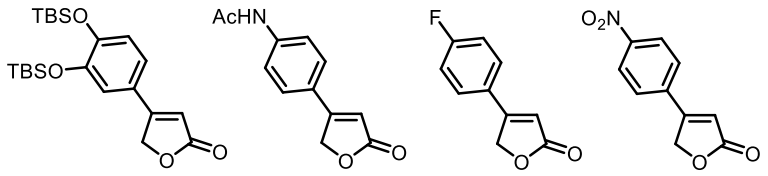

170 83% **171** 67% **172** 95% **173** 66%[a]

[a] 3.0 equiv. K_3PO_4 as base.

As shown in table 8, the triflate **118** and phenyl boronic acids **161/167-169** were coupled successfully in moderate to good yield. However, the cross-coupling of nitrophenylboronic acid **169** required the use of potassium phosphate to yield the desired furanone in 66% yield. Moreover, a suitable crystal of the TBS-protected catechol furanone **170** was isolated and analysed by single-crystal X-ray crystallography confirming the successful synthesis of the furanone building block **170** (figure 22).

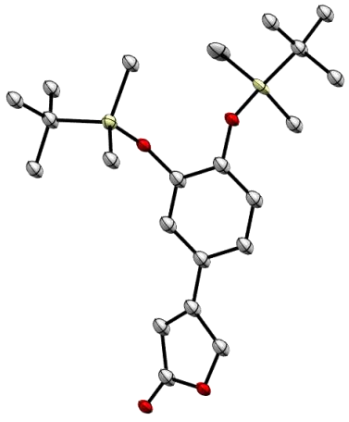

Figure 22: X-ray single crystal structure of *catechol*-furanone **170**. Thermal ellipsoids are shown at 50% probability level. Hydrogen atoms are omitted for clarity.

3.1.15. Synthesis of rubrolide derivatives 174-181 via vinylogous aldol condensation[199]

After the successful Suzuki-Miyaura coupling providing **170-173**, an one-pot vinylogous aldol condensation protocol[185] using benzaldehyde **117/139** and furanone **170-173** provided the novel rubrolide derivatives (table 9).

Table 9: Scope of the vinylogous aldol condensation of furanone **170-173** and aldehyde **117/139**.

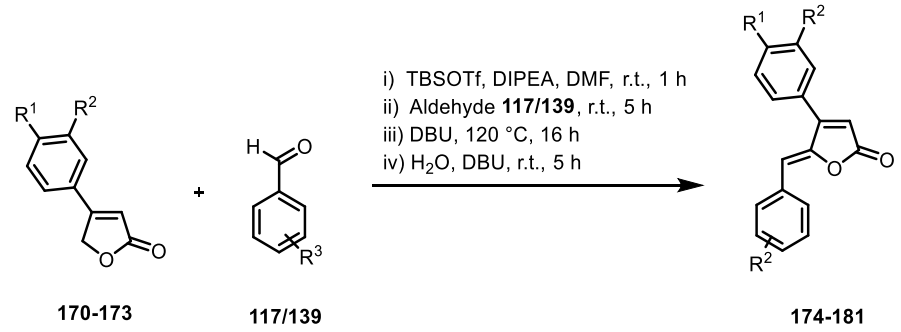

170-173 **117/139** **174-181**

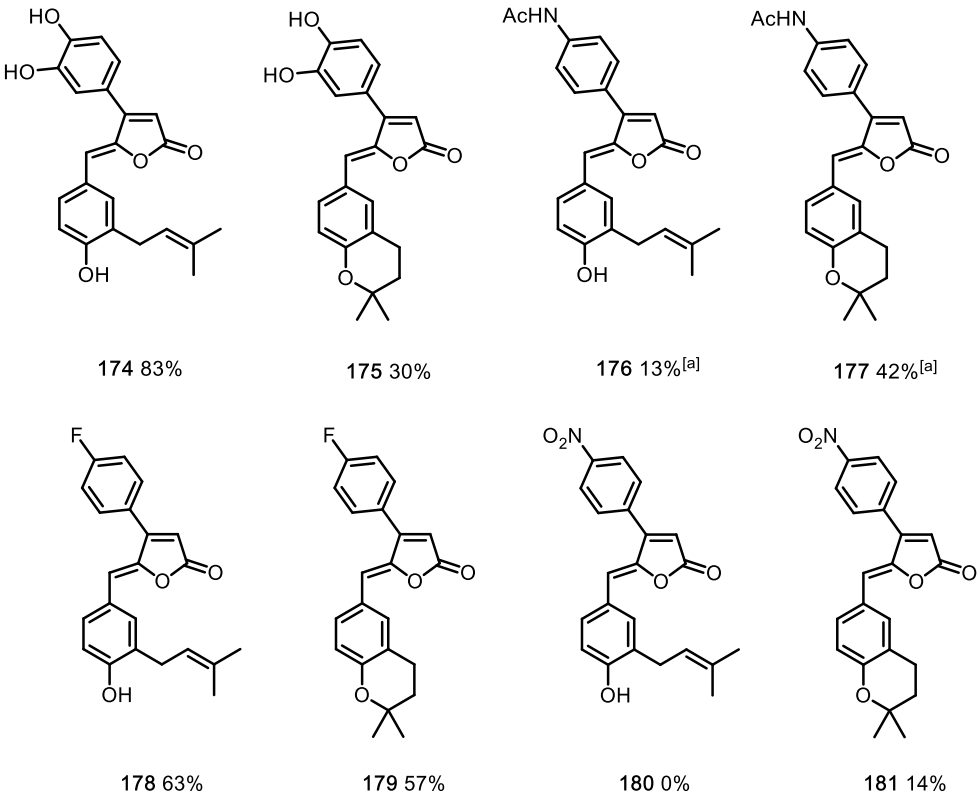

174 83% **175** 30% **176** 13%[a] **177** 42%[a]

178 63% **179** 57% **180** 0% **181** 14%

[a] dichloromethane was used as solvent.

The products **174-179** and **181** were obtained in moderate to good yields. Hereby, a solvent exchange in case of *N*-acetyl derivatives was necessary in order to obtain the corresponding rubrolide R **176** and S **177** structures. While the vinylogous aldol condensation of the nitrophenyl furanone **173** with the 2,2-dimethylchromane-6-carbaldehyde **117** afforded the

rubrolide S analogue **181** in only 14% yield, no successful coupling was obtained with the prenyl building block **139**. Neither toluene or dichloromethane as solvent did lead to an increased conversion. In analogy to **12** and **13**, the NOESY spectra of **174-179** and **181** verified the *Z*-configuration of the exocyclic double bond between C-5 and C-6. The structures of **174**, **175**, **178** and **179** were unambiguously determined by single-crystal X-ray crystallography (figure 23 and figure 24).

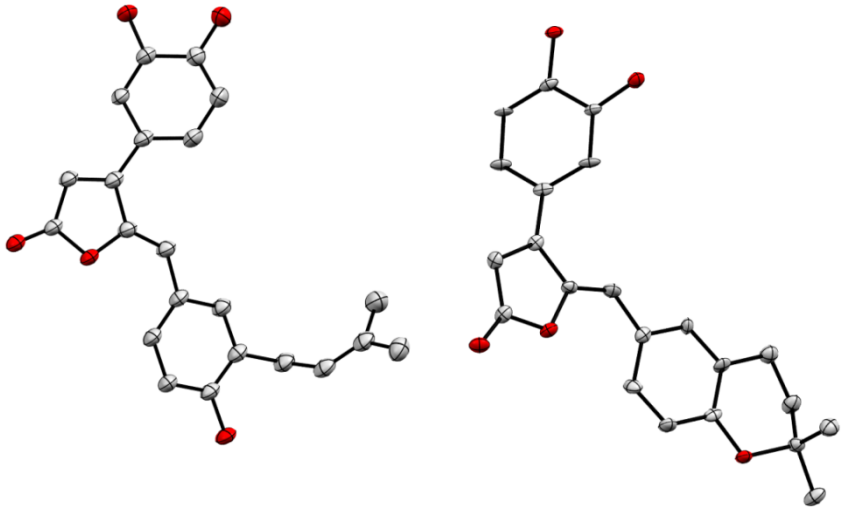

174 **175**

Figure 23: X-ray single crystal structures of catechol rubrolide R **174** and S **175**. Thermal ellipsoids are shown at 50% probability level. Hydrogen atoms are omitted for clarity.

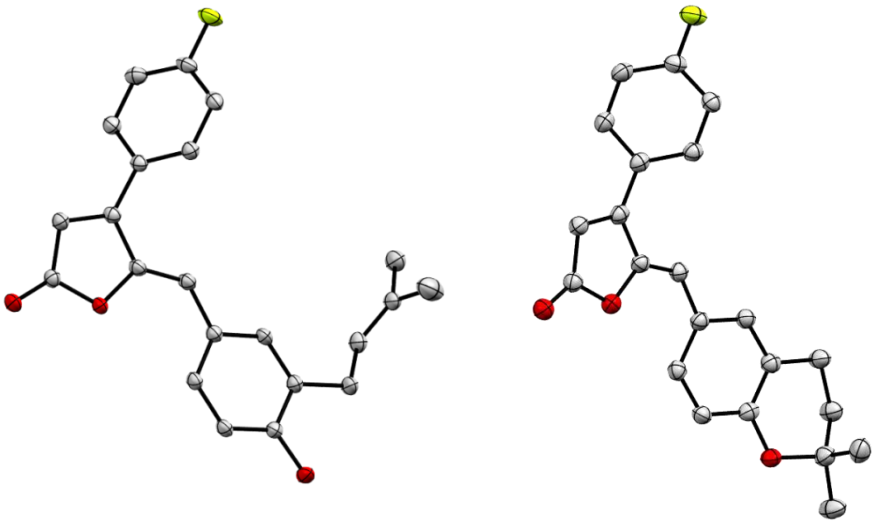

178 **179**

Figure 24: X-ray single crystal structures of *fluoro*-rubrolide R **178** and S **179**. Thermal ellipsoids are shown at 50% probability level. Hydrogen atoms are omitted for clarity.

3.1.16. Glycosylation of rubrolide S 13[201]

Although rubrolide R **12** and S **13** showed promising antiviral activities[34], their applicability is limited due to poor water solubility. In order to challenge this problem, the glycosylation of these compounds was investigated. Among increased water solubility these glyco-conjugates (figure 25) may be applied as prodrug-concept since the unprotected hydroxyl group is essential for the biological activity.[29,41]

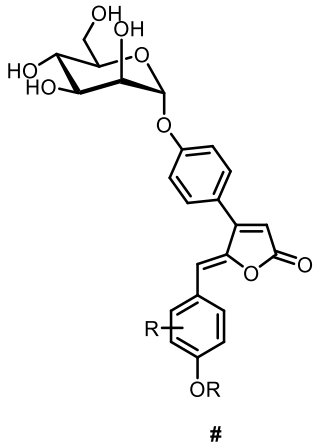

Figure 25: Mannosylated rubrolide S **182** analogue.

In this chapter the focus will be on mannosylation of rubrolide S **13**. The desired conjugate **182** should be obtained via *Koenigs-Knorr* glycosylation or *Schmidt* glycosylation from rubrolide S **13** and a suitable mannosyl-donor **183/184** and subsequent *Zemplén*-deacetylation (scheme 51).

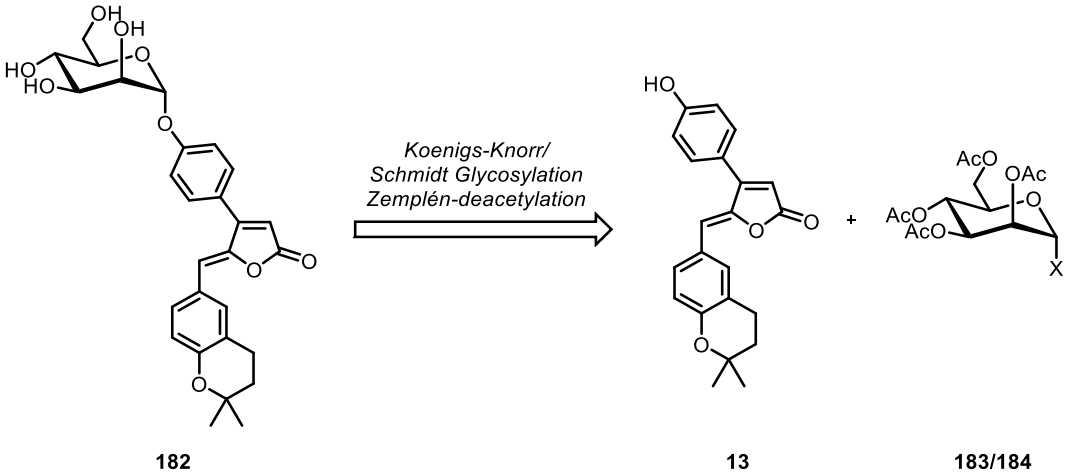

Scheme 51: Retrosynthetic analysis of the D-mannosyl-rubrolide S **182**.

3.1.17. Glycosyl donor synthesis

The required glycosyl donor **183** for the *Koenigs-Knorr* glycosylation and **184** for the *Schmidt* glycosylation should be obtained in two or three step synthesis (scheme 52).

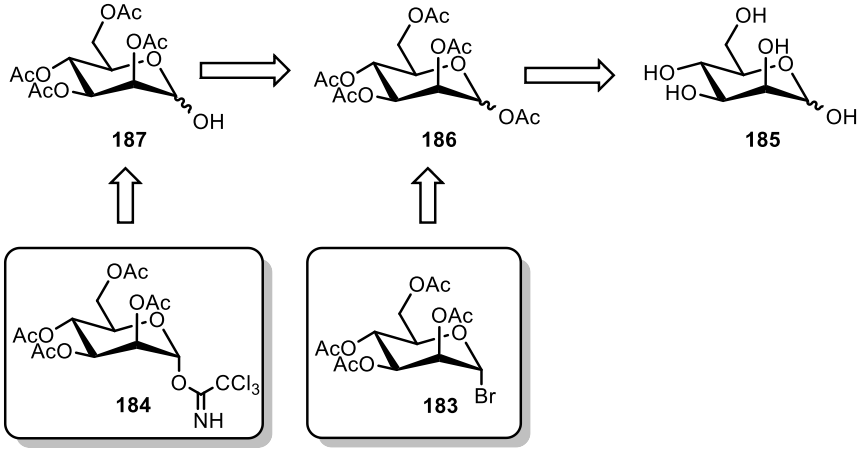

Scheme 52: Retrosynthesis of glycosyldonor **183** and **184**.

The peracetylated D-mannose **186** was synthesized according to a protocol of *Abbas* et al. (scheme 53) converting D-mannose **185** with acetic anhydride in pyridine in quantitative yield.[202] With the precursor **186** in hand, the glycosyl donor **183** was synthesized by conversion of peracetylated D-mannose **186** with hydrobromic acid in dichloromethane (scheme 53).

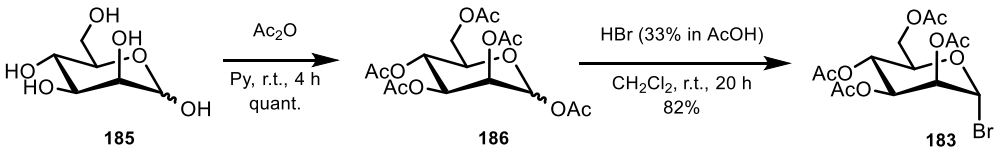

Scheme 53: Synthesis of the D-mannosyl bromide **183**.

For the glycosyl donor **184**, the peracetylated D-mannose **186** was selectively deprotected at the anomeric carbon **187** in 94% yield.[203] Afterwards, **187** was converted with trichloroacetonitrile under basic conditions to receive the desired trichloroacetimidate **184** in 63% yield (scheme 54).[204]

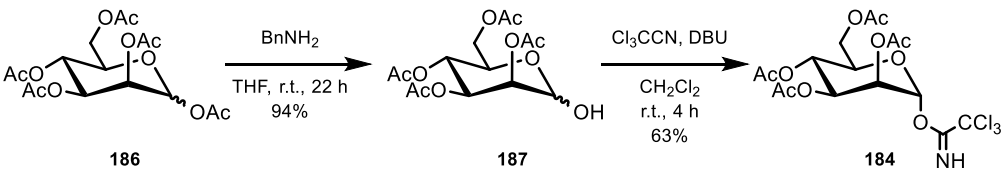

Scheme 54: Synthesis of D-mannosyl trichloracetimidate **184**.

3.1.18. Glycosylation of rubrolide S 13[201]

After observing low solubility of rubrolide R **12** and S **13** and their derivatives in biological tests the glycosylation of rubrolide S **182** might increase water solubility. The glycosylation between rubrolide S **13** and glycosyl donor was investigated via *Koenigs-Knorr*- and *Schmidt*-glycosylation (Scheme 55). With a modified procedure of *Ferse* et al.[205] coupling of glycosyl bromide **183** and rubrolide S **13** was mediated by Ag_2O and $AgCO_3$ under exclusion of light in dichloromethane affording the conjugate in 21% yield. Addition of drierite was beneficial for the formation of glycoside **188** leading to an improved yield of 70%. On the contrary, TMSOTf mediated *Schmidt*-glycosylation[206] did not yield the desired product **188**.

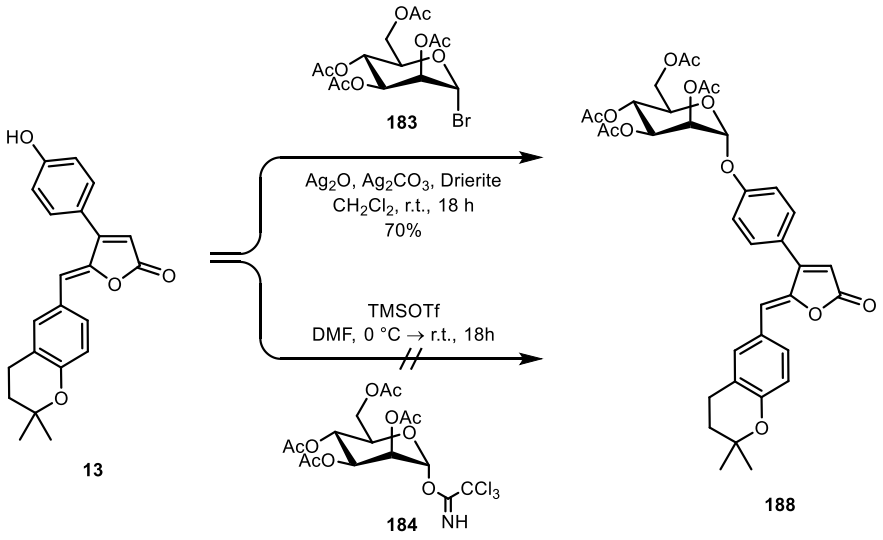

Scheme 55: Glycosylation of rubrolide S **13** under *Koenigs-Knorr* glycosylation and *Schmidt* glycosylation.

The mannosylated rubrolide S **188** was characterized via ^{1}H-NMR spectroscopy (figure 26), verifying the successful formation of the glycoside **188**. The characteristic doublet at 5.45 (d, *J* = 2.3 Hz, 1 H, 1'''-H) indicated the anomeric α-proton of **188**. Furthermore, signals between 3.75 and 5.25 ppm which correspond to the mannosyl moiety of **188**. The acetyl groups of the sugar moiety resonate as singlets between 1.89 and 2.15 ppm with an integral of 3 H each. Signals at 7.28 (d, *J* = 8.6 Hz, 2 H, 3'-H, 5-H) and 7.49 (d, *J* = 8.5 Hz, 2 H, 2'-H, 6'-H) correspond to the 1,4-disubstituted A-ring. Characteristic signals at 6.24 (s, 1 H, 3-H) correspond to furanone ring B of **188** and the signal at 6.28 ppm (s, 1 H, 6-H) corresponds to the benzylidene proton. Furthermore, signals at 6.74 (d, *J* = 8.2 Hz, 1 H, 8''-H), 7.53 (dd, *J* = 8.6 Hz, 2.1 Hz, 1 H, 7''-H) and 7.66 (d, *J* = 2.1 Hz, 1 H, 5''-H) indicate the 1,2,4-trisubstitued phenyl ring C. Signals at 1.78 (t, *J* = 6.7 Hz, 2 H, 3''-H_2) and 2.76 (t, *J* = 6.7 Hz, 2 H, 4''-H_2) correspond to methylene groups of the 2,2-dimethylchromane.

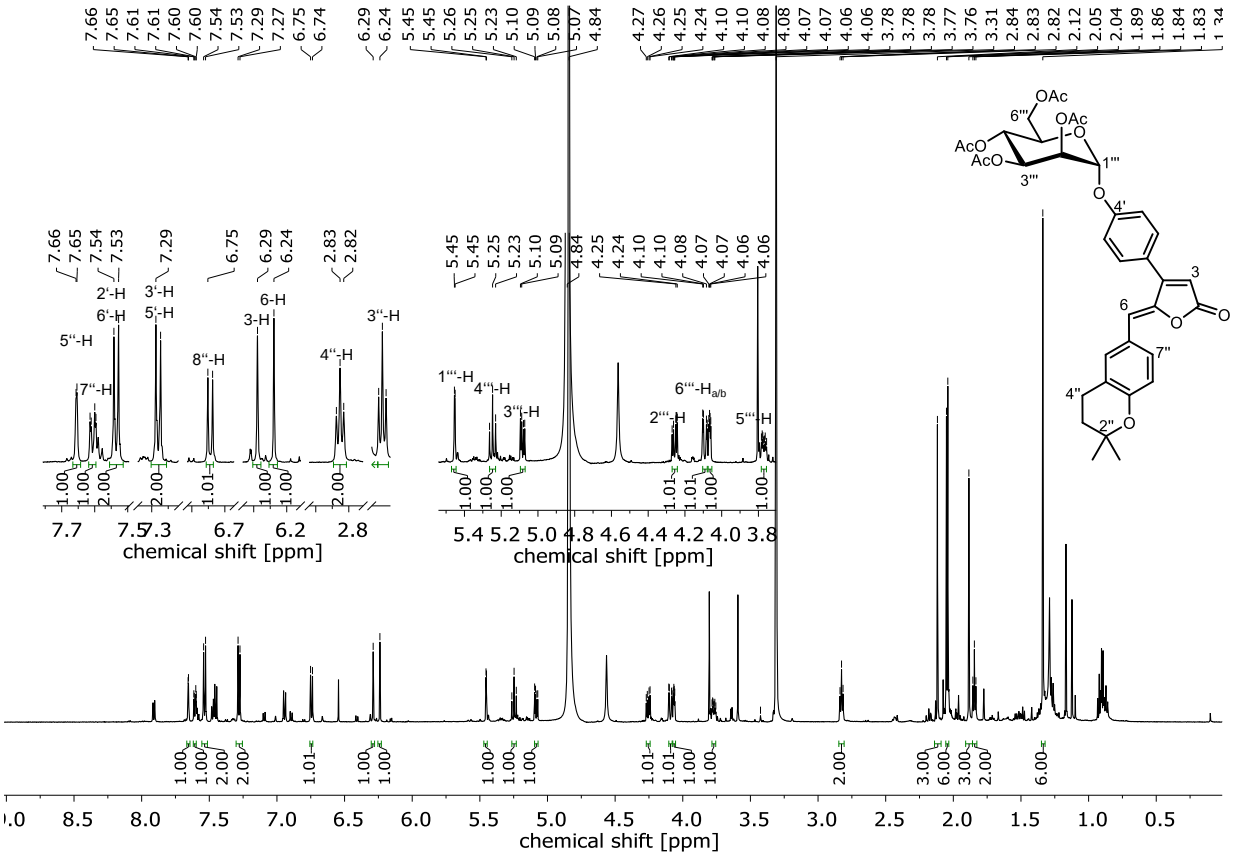

Figure 26: ^{1}H-NMR spectrum (600 MHz, MeOD-d_4) of (2,3,4,6-tetra-*O*-acetyl-*α*-D-mannosyl)oxy rubrolide S **188**.

In addition to ^{1}H-NMR analysis, high-resolution ESI-MS confirmed the formation of the glyco-conjugate. The measured *m/z* ratio of 679.2378 (± 0.001 ppm) represents the protonated mannosyl-rubrolide conjugate and a peak at 701.2190 the corresponding sodium adduct.

3.1.19. Deacetylation of 188[201]

After successful formation of glycoside **88**, deprotection of the carbohydrate moiety should be performed via *Zemplén*-deacetylation (scheme 56).[207] For this purpose, a solution of sodium methanolate (15 mol%) in anhydrous MeOH was used. However, subsequent NMR- and MS-analysis verified the cleavage of the glycosidic bond under *Zemplén* conditions.

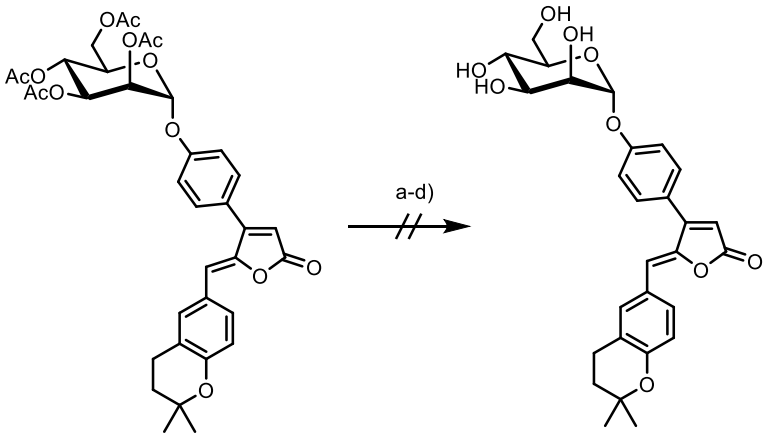

188 **182**

reaction condition a) NaOMe/MeOH, r.t., 16 h
reaction condition b) MeOH, Et_3N, r.t., 24 h
reaction condition c) Drierite, TsOH, DCM, MeOH (9:1), r.t. - 40 °C, 12 h
reaction conditon d) lipase AS Amano, 25mM Citrate Buffer pH = 5.0, DMSO, 40 °C, 3 h
reaction condition e) PLE , 25mM Citrate Buffer pH = 5.0, DMSO, 40 °C, 3 h

Scheme 56: Deacetylation of 2,3,4,6-tetra-*O*-acetyl-*α*-D-mannosyl)oxy rubrolide S **188**.

Deacetylation by MeOH/Et_3N[208] or *Lewis* acidic TsOH[209,210] induced the cleavage of the glycosidic bond. Among chemically mediated cleavage protocols, the enzymatic deacetylation of carbohydrates providing mild reaction conditions was investigated. For this purpose, the protocol of *Baba* et al. with lipase AS Amano in citrate buffered medium (pH = 5.0) was tested. Despite the milder reaction conditions[211] cleavage of the glycosidic bond was again observed. Moreover, the application of porcine liver esterase (PLE) led to as well cleavage of the carbohydrate.

3.2. Prunolides

3.2.1. Synthesis of bisboron building block 189 and 190

According to a protocol of *Plunkett* et al.[168] the twofold Pd-catalyzed *Sonogashira* cross-coupling was used to construct the internal alkyne (table 10).

Table 10: Pd-catalyzed *Sonogashira* reaction of **189** and **190**.

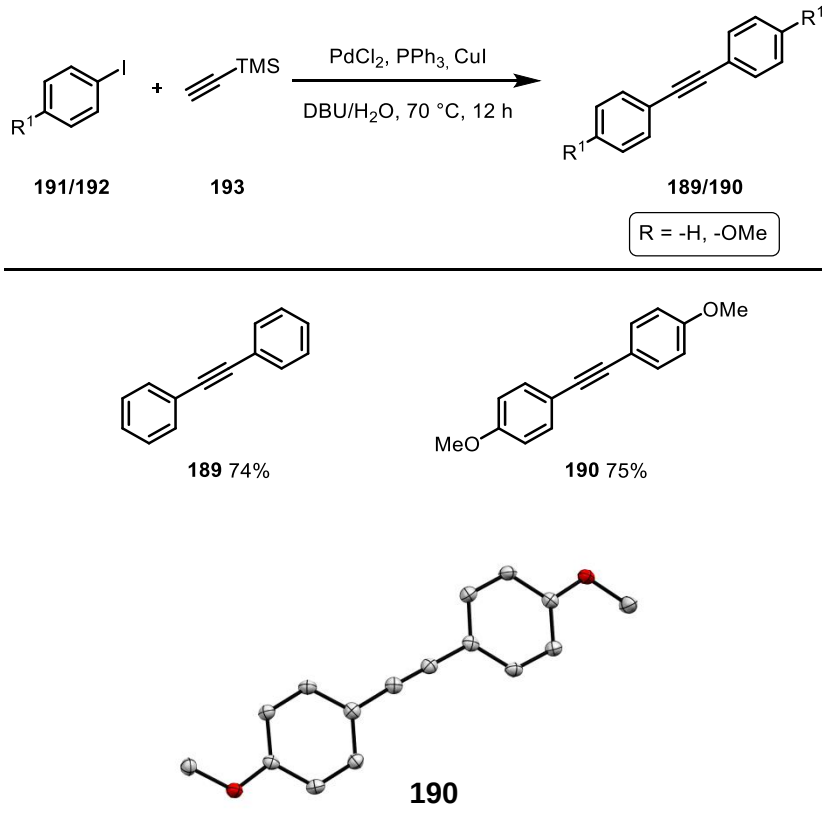

Figure 27: X-ray single crystal structure **190**. Thermal ellipsoids are shown at 50% probability level. Hydrogen atoms are omitted for clarity.

The twofold cross-coupling was tested with iodobenzene **191** affording the diphenylacetylene **189** in 74% yield. In addition, these conditions were applied for the 4-iodoanisole **192**, achieving a yield of 75%. Moreover, a suitable crystal of **190** was isolated to verify the successful synthesis of the internal alkyne **190** (figure 27).

In order to obtain building block **125** the literature known Pt-catalyzed *Z*-selective bisborylation of *Suzuki* et al. **190** was realized.[170] The catalytic cycle of this reaction requires the Pt(0)-species **194**, which undergoes an oxidative addition **A** into the B-B bond of **195**, generating the bis(boryl)-platinum(II) intermediate **196** (scheme 57). This step is followed by migratory insertion **B** of the alkyne **190** into the B-Pt bond by providing the alkenyl-boryl platinum(II) intermediate **197**.

By reductive elimination **C** of **197** product **125** is formed regenerating the Pd-catalyst **194**, which again can enter the catalytic cycle.[170]

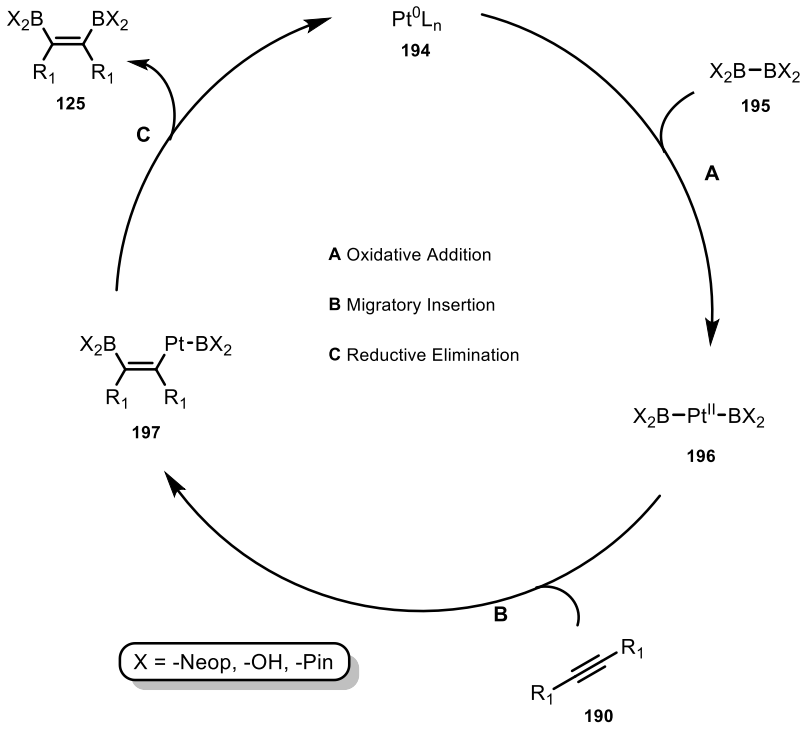

Scheme 57: Catalytic cycle for the Pt-catalyzed diboration of alkyne **190**.

In order to optimize the diboration of **190**, following screening experiment was conducted with $Pt(PPh_3)_4$ as suitable catalyst (table 11).

Table 11: Optimization of Pt-catalyzed *Z*-selective bisborylation of **190**.

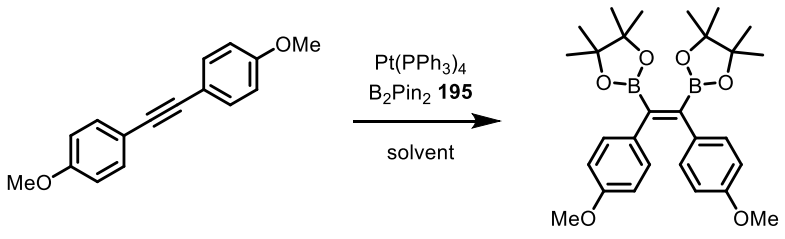

190 **125**

entry	t	T [°C]	loading	solvent	yield
1	19 h	120 °C	10.0 mol%	1,4-dioxane	74%
2	34 h	120 °C	5.0 mol%	1,4-dioxane	69%
3	17 h	120 °C	1.0 mol%	1,4-dioxane	61%
4	24 h	80 °C	0.2 mol%	DMF	85%
5	48 h	80 °C	0.2 mol%	DMF	89%
6[b]	6 h	80 °C	2.0 mol%	DMF	69%

a) *Reaction conditions:* diphenylacetylene **190** (1.0 equiv.), B_2Pin_2 (1.1 equiv.), $Pt(PPh_3)_4$, solvent b) application of microwave irradiation.

With 10.0 mol% $Pt(PPh_3)_4$ in dioxane at 120 °C a yield of 74% was obtained (table 11, entry 1). Stepwise reduction of the catalyst loading (table 11, entry 2-3) resulted in decreasing yield. Furthermore, using DMF as solvent and a reduced catalyst loading to 0.2 mol% at 80 °C (table 11, entry 4) a significant increase of the yield of 85% was detected. Under the optimized conditions and prolonged reaction time of 48 h an enhanced yield of 89% was achieved. Additional optimization steps by microwave assisted heating with reduced reaction time did not increase the yields any further (table 11, entry 6).

After optimization of the reaction conditions, the diboron-sources **198** and **199** were investigated. While B_2Pin_2 **195**, B_2Neop_2 **198** were employed successfully under the established conditions (table 12) tetrahydroxydiboron **199** did not lead to **203** or **204** (table 12).

Table 12: Pt-catalyzed bisborylation with different diboron sources **195, 198, 199**.

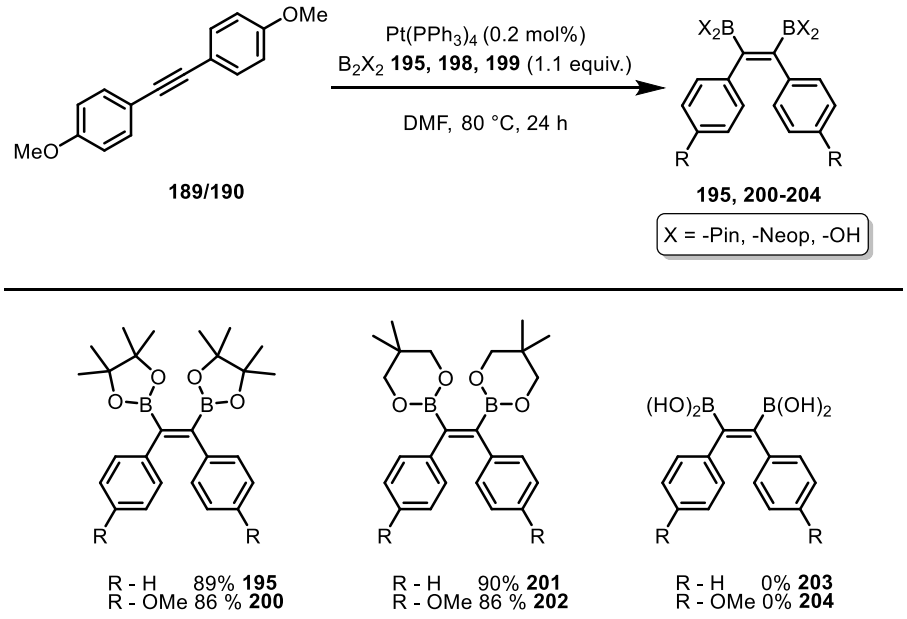

3.2.2. Synthesis of building block 127

The synthesis of the vinyl halide **127** starts with the formation of the aldehyde **126** by *Vilsmeier Haak* reaction. In this reaction, 4-methoxyacetophenone **15** was converted with PBr_3 and *N*,*N*-dimethylformamide generating the desired aldehyde **126** in 54% yield (scheme 58).[172,212]

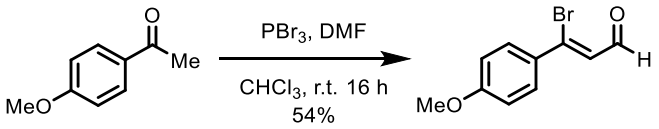

15 **126**

Scheme 58: Synthesis of (2*Z*)-3-bromo-3-(4-methoxyphenyl)prop-2-enal **126** by *Vilsmeier Haack* formylation.

Afterwards, *Pinnick* oxidation of aldehyde **126** in 80% yield to acrylic acid **206** and subsequent esterification provided the desired building block **127** (scheme 59).[173,212]

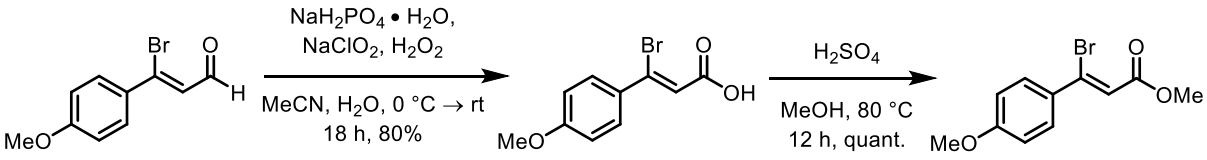

126 **205** **127**

Scheme 59: *Pinnick* oxidation of aldehyde **126** with subsequent acid catalyzed esterification.

Application of other scavengers like DMSO[213] and 2-methyl-2-butene[214,215] did not yield carboxylic acid **205**. Acid catalyzed esterification in methanol afforded the desired building block **127** in a quantitative yield (scheme 59).

Alternatively, Vanadium catalyzed oxidative esterification of the aldehyde **126** directly to vinyl bromide **127** may provide the product reducting the number of synthetic steps (scheme 60).[216–218]

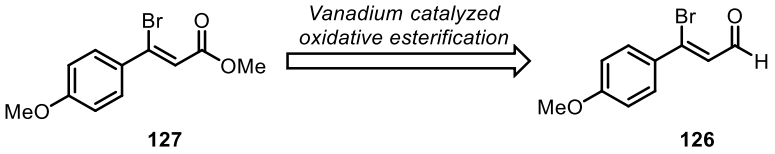

127 **126**

Scheme 60: Retrosynthetic analysis of (2*Z*)-3-bromo-3-(4-methoxyphenyl)prop-2-enoate **127**.

Patel et al. and *Thakur* et al.[216–218] demonstrated the conversion of several aldehydes to the corresponding carboxylic acid under mild conditions. *Thakur* et al. described this type of mechanism (scheme 61). Peracid **207** resulted from addition of VO(IV)(acac)$_2$ **206** to H_2O_2 (step A)[218] and subsequent formation of the peroxo vanadium(V) species **208**. The reactive species **208** deprotonates the methanol generating a methanolate, which further reacts with the carbonyl carbon of the aldehyde **126** affording the methyl ester **127** (scheme 61).[216]

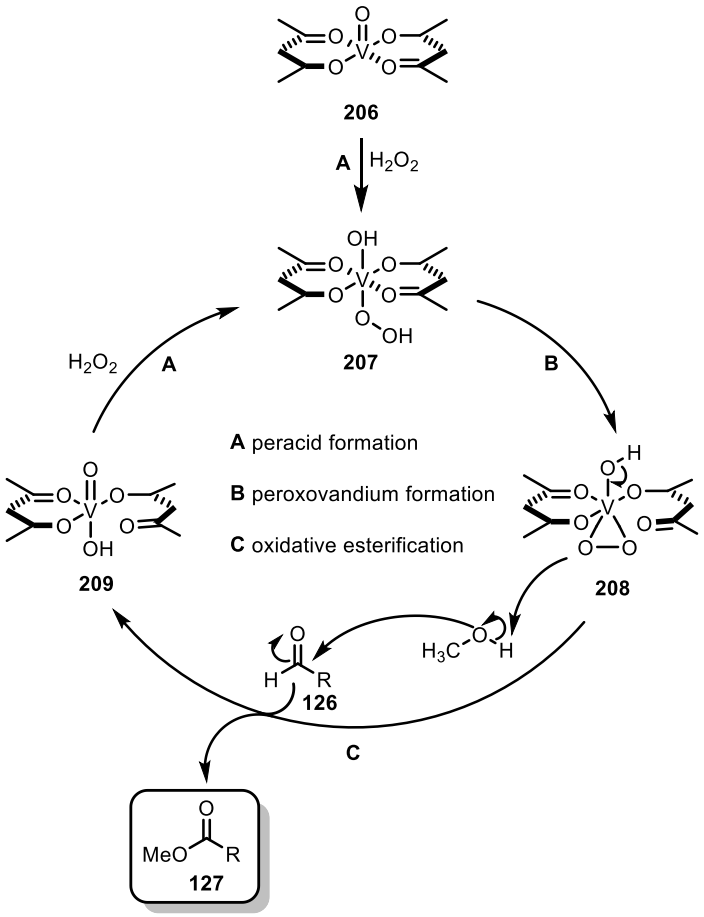

Scheme 61: Proposed mechanism of the oxidative esterification reaction for the formation of **127**.

$VO(acac)_2$ was chosen as suitable catalyst in the presence of hydrogen peroxide in methanol to generate vinyl bromide **127**.[216] Herefore, several conditions were tested (table 13).

Table 13: Optimization of the vanadium catalyzed oxidative esterification of aldehyde **126**.

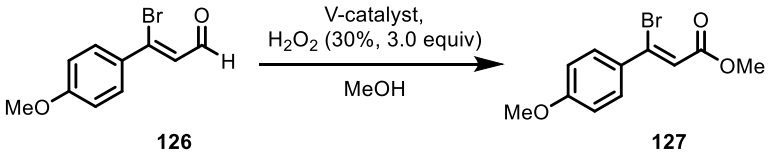

entry	catalyst	loading	additives 1.1 (equiv.)	solvent	T	time	yield[b]
1	$VO(acac)_2$	1.0 mol%	-	MeOH	r.t.	16 h	3%
2	$VO(acac)_2$	0.5 mol%	-	MeOH	r.t.	16 h	4%
3	$VO(acac)_2$	0.1 mol%	-	MeOH	r.t.	16 h	5%
4	$VO(acac)_2$	0.1 mol%	-	MeOH	0 °C	2 h	22%
5	$VO(acac)_2$	0.1 mol%	$NaH_2PO_4 \cdot H_2O$	MeOH	0 °C	2 h	-
6	V_2O_5	0.1 mol%	-	MeOH	0 °C	2 h	14%

a) *Reaction condition:* **126** (1.0 equiv.), catalyst, H_2O_2 (30%, 3.0 equiv.), MeOH b) isolated yield.

By varying the catalyst loadings (table 13, entry 1, 2, 3) at room temperature, low yields were obtained. Besides the formation of the desired acrylic ester **127** dominantly elimination of HBr to the alkyne occurred since the α-proton of **127** is prone to deprotonation. Therefore, a reduction of the reaction time and temperature were conducted in order to avoid the undesired side reaction. With a catalyst loading of 0.1 mol% and a reaction time of 2 h (table 13, entry 4) the desired building block **127** was obtained in 22% yield. Furthermore, by changing the catalyst to V_2O_5 (table 13, entry 6) a lower yield of 14% was achieved. Despite the successful formation of **127**, the elimination product was formed. By performing the reaction in a NaH_2PO_4-buffered solvent mixture in analogy to the *Pinnick* conditions (table 13, entry 5) no conversion of the substrate was observed.

3.2.3. Synthesis of vinyl tosylates210-212

The synthesis of easier accessible and bench stable vinyl tosylates **211** were investigated, which were successfully applied in literature reported *Suzuki-Miyaura* cross-coupling reactions.[219–224] Hereby, building block **211** can be afforded by a two-step synthesis via an aldol addition of acetophenone **15** with dimethycarbonate **215**, followed by subsequent enolization and tosylation (scheme 62).

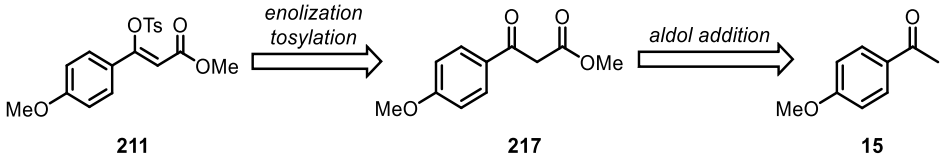

211 **217** **15**

Scheme 62: Synthesis of the vinyl tosylate **211** via aldol addition with subsequent enolization/tosylation sequence.

The functionalized *β*-keto ester **211** was synthesized by aldol addition of *para*-substituted acetophenone **15** and dimethyl carbonate **215** (scheme 62).[225] For this purpose, sodium hydride was used for the deprotonation of the *α*-CH acidic proton of **15** followed by addition of dimethyl carbonate **215**. Furthermore, 4-fluoro-acetophenone **214** and acetophenone **213** were successfully converted. Proton-NMR and GC-MS reaction control revealed a clean complete conversion to the *β*-ketoester **216-218** and were used in the next step without further purification. Then, the vinyl tosylates **210-212** were obtained by a modified procedure of *Tanabe* et al. by enolization and subsequent tosylation.[221] TMEDA abstracted the *α*-CH acidic proton to generate the enolate. In the presence of lithium chloride, coordination of the oxygen atoms of the *β*-ketoester **216-218** provided the (*Z*)-configuration of the double bond. The desired vinyl tosylates **210-212** were received in good yields between 60-82%. This protocol allowed the implication of several acetonephenons **15, 213** and **214** with either

electron donating or withdrawing functional groups. Furthermore, the desired building blocks were obtained by recrystallization as the only purification step (table 14).[138,226]

Table 14: Synthesis of the (*Z*)-vinyl tosylates **210-212**.

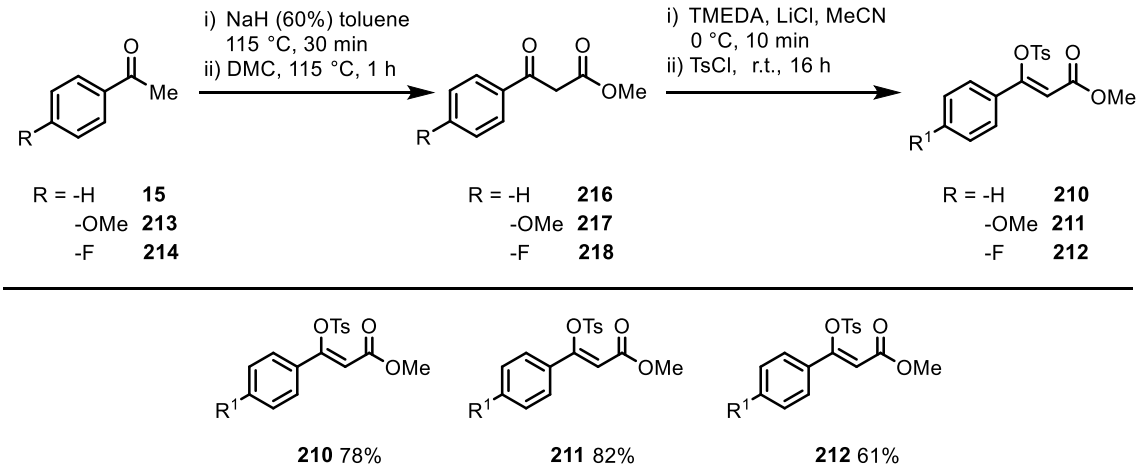

Additionally, suitable crystals of **210-212** were obtained for single crystal structure analysis and accurately determination of the relative double bond configuration of **210-212** (figure 28).[138]

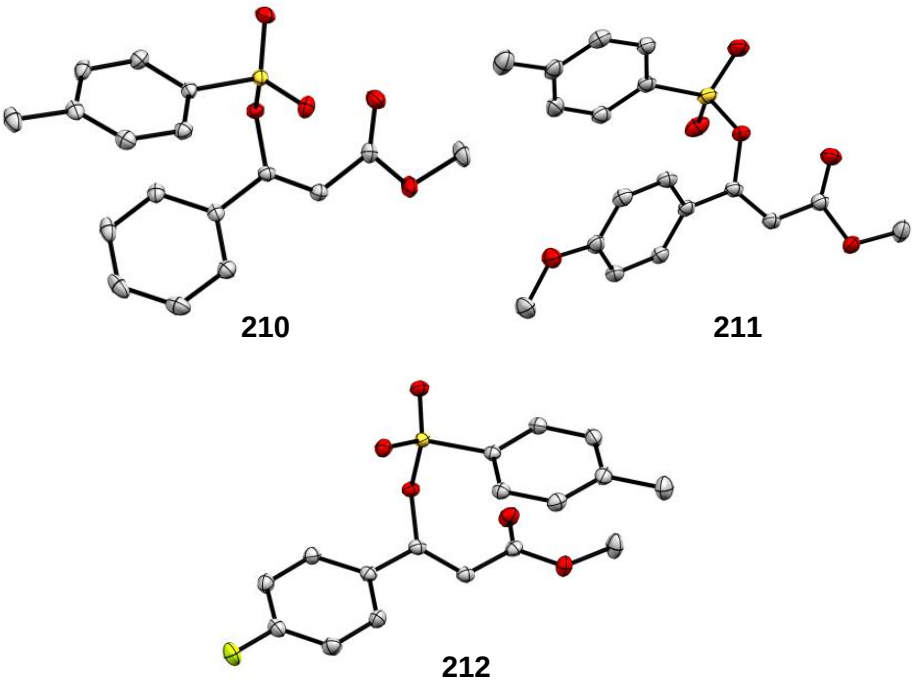

Figure 28: X-ray single crystal structure of the vinyl tosylates **210-212**. Thermal ellipsoids are shown at 50% probability level. Hydrogen atoms are omitted for clarity.

3.2.4. Carbonylative *Suzuki-Miyaura* cross-coupling

With the vinyl building blocks **127/211** and **125** in hand, the carbonylative *Suzuki-Miyaura* cross-coupling with 3.0 bar carbon monoxide was further investigated (table 15).

Table 15: Carbonylative *Suzuki-Miyaura* cross-coupling with carbon monoxide (3.0 bar)

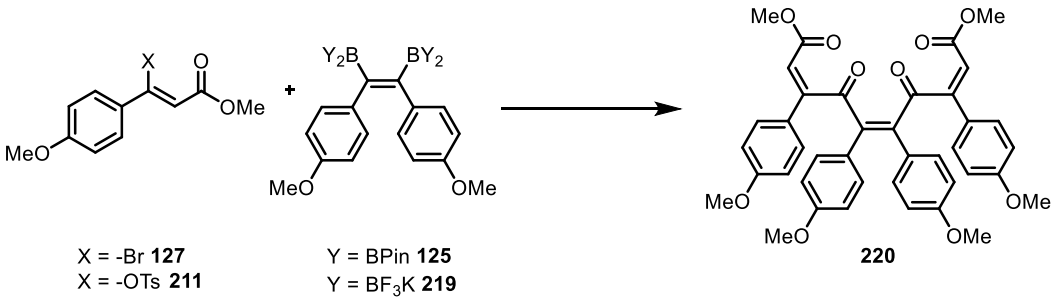

X = -Br **127**
X = -OTs **211**

Y = BPin **125**
Y = BF_3K **219**

220

entry	catalyst	loading	ligand	loading	base	X	Y	Solvent	yield
1	$Pd(TFA)_2$	16.0 mol%	PCy_3	32.0 mol%	K_2CO_3	Tos	BF_3K	THF	-
2	$Pd(TFA)_2$	16.0 mol%	PCy_3	32.0 mol%	K_2CO_3	Tos	BF_3K	Toluene	-
3	$Pd(TFA)_2$	16.0 mol%	PCy_3	32.0 mol%	K_2CO_3	Br	BF_3K	Toluene	-
4	$Pd(PPh_3)_4$	16.0 mol%	-	-	K_2CO_3	Tos	BF_3K	Toluene	-
5	$Pd(TFA)_2$	16.0 mol%	PCy_3	32.0 mol%	K_2CO_3	Tos	BF_3K	Toluene	-
6	NiCl(naphthyl) $(PPh_3)_2$	10.0 mol%	PCy_3	20.0 mol%	K_3PO_4	Tos	BPin	THF	-
7	NiPincer	10.0 mol%	-	-	K_3PO_4	Tos	BPin	Toluene	-
8	NiCl(naphthyl) $(PPh_3)_2$	10.0 mol%	PCy_3	20.0 mol%	K_3PO_4	Tos	BPin	THF	-
9	$Pd(PPh_3)_4$	16.0 mol%	-	-	K_2CO_3	Tos	BF_3K	THF	-
10	$Pd(PPh_3)_4$	16.0 mol%	-	-	K_2CO_3	Tos	BF_3K	THF	-
11	$Pd(PPh_3)_4$	16.0 mol%	-	-	K_3PO_4	Tos	BF_3K	Toluene	-
12	$Pd(PPh_3)_4$	16.0 mol%	-	-	KF	Tos	BF_3K	Toluene	-
13	$Pd(PPh_3)_4$	16.0 mol%	-	-	KOH	Tos	BF_3K	Toluene	-
14	$Pd(PPh_3)_4$	16.0 mol%	-	-	KF	Tos	Pin	Toluene	-

a) *Reaction conditions*: catalyst, ligand, base (6.0 equiv.), vinyl building block **127/211** (2.0 equiv.), boronic ester/ boronate/ **125/219** (1.0 equiv.) solvent, 80 °C, 16 h.

Under the applied conditions with altering catalyst loadings, catalyst and solvent mixtures no conversion was observed (table 15). Also the in situ formation of the corresponding BF_3K salt, which is more reactive than the boronic ester[227,228], did not yield the desired product (table 15, entry 1-5, 9-13. For this purpose a protocol of *Wu* et el.[139] was conducted by generating carbon monoxide via decomposition of acetic formic anhydride in the presence of base (table 16).

Table 16: Carbonylative *Suzuki-Miyaura* cross-coupling with in situ carbon monoxide generation.

entry	catalyst	loading	ligand	Loading	FA/Ac_2O	X	Y	solvent	yield
1	$Pd(OAc)_2$	3.0 mol%	PPh_3	6.0 mol%	2.0 equiv.	Br	Pin	toluene	-
2	$Pd(OAc)_2$	3.0 mol%	PPh_3	6.0 mol%	10.0 equiv.	Br	BPin	toluene	-
3	$Pd(OAc)_2$	3.0 mol%	PPh_3	6.0 mol%	10.0 equiv.	Br	BPin	toluene	-
4	$Pd(OAc)_2$	3.0 mol%	PPh_3	6.0 mol%	20.0 equiv.	Br	BPin	toluene	-
5	$Pd(TFA)_2$	8.0 mol%	PCy_3	16.0 mol%	10.0 equiv.	Tos	BF_3K	toluene	-
6	$Pd(TFA)_2$	16.0 mol%	PCy_3	32.0 mol%	10.0 equiv.	Tos	BF_3K	toluene	-
7	$Pd(TFA)_2$	16.0 mol%	PCy_3	32.0 mol%	30.0 equiv.	Tos	BF_3K	THF	-
8	$Pd(TFA)_2$	16.0 mol%	PCy_3	32.0 mol%	30.0 equiv.	Tos	BF_3K	THF	-
9	$Pd(TFA)_2$	16.0 mol%	PCy_3	32.0 mol%	30.0 equiv.	Tos	BF_3K	THF	-
10	$Pd(PPh_3)_4$	16.0 mol%	-	-	30.0 equiv.	Tos	BF_3K	THF	-
11	$Pd_2(dba)_3$	16.0 mol%	-		30.0 equiv.	Tos	BF_3K	THF	-

a) *Reaction conditions*: catalyst, ligand, K_2CO_3 (6.0 equiv.), FA/Ac_2O, vinyl building block **127/211** (2.0 equiv.), boronate/boronic ester **125/219** (1.0 equiv.), solvent, 80 °C, 16 h.

In analogy to previous screenings, these attempts did not result in the desired coupling. Instead, an inseparable and unidentifiable mixture of products was obtained (table 16).

3.2.5. Acylative *Suzuki-Miyaura* cross-coupling

Based on previously obtained screening results, the acylative *Suzuki-Miyaura* cross-coupling reaction with succinimdyl esters was studied (scheme 63). This approach was supposed to afford the ketone without formation of the conventional *Suzuki-Miyaura* product. Although active esters are essential compounds for peptide coupling reactions, their application in acylative cross-coupling reactions were reported previously.[163,165,166,229]

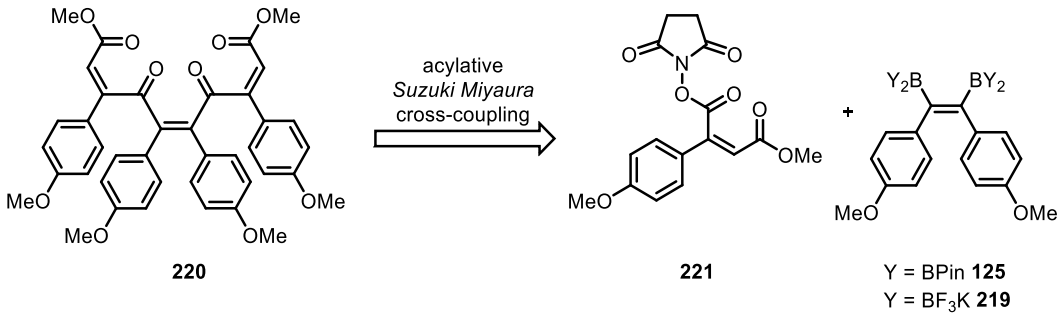

Scheme 63: Acylative *Suzuki-Miyaura* cross-coupling.

To validate the utility of succinimidyl-esters in acylative cross-coupling reactions, coupling of acetyl-OSu **222** with 4-methoxyphenylboronic acid **119** has been chosen as test reaction. Acetyl-OSu **222** was prepared by a protocol of *Jacobsen* et al. in a yield of 87% (scheme 64).[230]

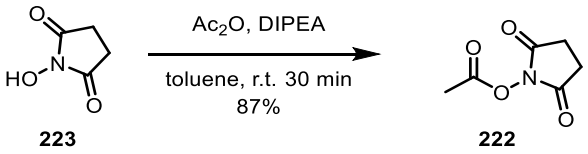

223 222

Scheme 64: Synthesis of AcOSu **222**.

First attempts of coupling **222** with 4-methoxyphenylboronic acid **119** were conducted with $Pd(OAc)_2$ as precatalyst, different ligands, K_2CO_3 as base and toluene as solvent at 80 °C (table 17).

Table 17: Ligand screening.

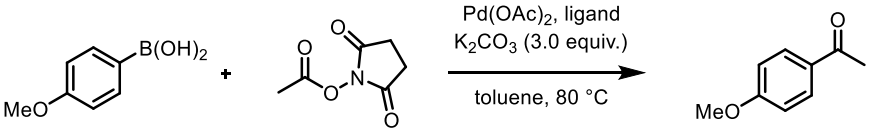

119 222 15

entry	ligand	t	yield[b]
1	PPh_3	19.5 h	traces
2	PCy_3	19.5 h	42%
3	P(*n*-Bu)$_3$	14.5 h	-
4	dppp	14.5 h	-
5	dppf	14.5 h	traces
6	Xantphos	14.5 h	-

a) *Reaction conditions*: **119** (1.2 equiv.), $Pd(OAc)_2$ (10.0 mol%), ligand (20.0 mol%), K_2CO_3 (3.0 equiv.), toluene, 80 °C. b) isolated yield.

Application of dppp, Xantphos or P(*n*-Bu)$_3$ (table 17, entry 3, 4, 6) as ligands did not afford the desired product. With PPh_3 and dppf (table 17, entry 1, 5) only traces of the desired product **15** were obtained, while use of PCy_3 (table 17, entry 2) led to product formation in moderate yield of 42%. Besides the product formation, homocoupling of the boronic acid **119** was observed. In following screening experiments, the impact of solvent and base in product formation was investigated (table 18).

Table 18: Base and solvent screening.

entry	base	t	Solvent	yield[b]
1	K_2CO_3	19.5 h	toluene	42%
2	K_2CO_3	19.5 h	1,4-dioxane	52%
3	Na_2CO_3	25 h	1,4-dioxane	18%
4	Cs_2CO_3	25 h	1,4-dioxane	10%
5	KF	1 h	1,4-dioxane	33%
6	Et_3N	25 h	1,4-dioxane	40%
7	Pyridine	3 h	1,4-dioxane	-
8	NaOAc × 3 H_2O	3 h	1,4-dioxane	-
9	KOAc	1 h	1,4-dioxane	45%
10	K_2HPO_4	16 h	1,4-dioxane	18%
11	K_3PO_4	25 h	1,4-dioxane	57%
12	K_3PO_4	70h	THF	20%

a) *Reaction conditions*: **119** (1.2 equiv.), $Pd(OAc)_2$ (10.0 mol%), ligand (20.0 mol%), K_2CO_3 (3.0 equiv.), toluene, 80 °C. b) isolated yield.

By performing the acylative cross-coupling in 1,4-dioxane (table 18, entry 2) a yield of 52% was obtained. Furthermore, base screening (table 18, entry 2-11) demonstrated that K_3PO_4 (table 18, entry 11) afforded the best yield with 57%. Therefore, K_3PO_4 as base and 1,4-dioxane were applied in further screening experiments. Continuing studies were carried out with different catalysts (table 19).

Table 19: Metal source screening results.

entry	catalyst	ligand	Base	T	t	solvent	yield[b]
1	$Pd(OAc)_2$	PCy_3	K_3PO_4	80 °C	25 h	1,4-dioxane	57%
2	$Pd(PPh_3)_4$	-	K_3PO_4	80 °C	23 h	1,4-dioxane	traces
3	$PdCl_2(PPh_3)_2$	-	K_3PO_4	80 °C	23 h	1,4-dioxane	traces
4	$PdCl_2$	PCy_3	K_3PO_4	80 °C	23 h	1,4-dioxane	traces
5	$Pd(OTs)_2(MeCN)_2$	PCy_3	K_3PO_4	80 °C	16 h	1,4-dioxane	traces
6	Pd_2dba_3	PCy_3	K_3PO_4	80 °C	16 h	1,4-dioxane	traces
7	$NiCl_2$	PCy_3	K_3PO_4	100 °C	16 h	1,4-dioxane	-

a) *Reaction conditions*: **119** (1.2 equiv.), $Pd(OAc)_2$ (10.0 mol%), ligand (20.0 mol%), K_2CO_3 (3.0 equiv.), toluene, 80 °C. b) isolated yield.

Most of the applied palladium catalysts (table 19, entry 2-6) did not provide the coupling product. Only $Pd(OAc)_2/PCy_3$ as catalyst system (table 19, entry 1) provided **15** in a sufficient yield of 57%. Although the adverse outcome was expected for entry 2 and 3, entry 3-4 (table 19) with PCy_3 as ligand supposed to generate the catalytically active $Pd(PCy_3)_2$ species. This indicates that $Pd(PCy_3)_2$ may not be the catalytic active species in this process. *Amatore* and *Jutand* reported the formation of $[Pd(PPh_3)_2OAc]^-$ which was catalytically active

in Heck reactions[231]. It is suggested that the complex $[Pd(PCy_3)_2OAc]^-$ acts here as the catalytically active species. All components were evaluated in control experiments, where in each procedure one component was left out (table 20).

Table 20: Control experiments of the carbonylative cross-coupling.

entry	$Pd(OAc)_2$	PCy_3	K_3PO_4	yield[b]
1	10.0 mol%	20.0 mol%		traces
2	10.0 mol%		3.0 equiv.	-
3		20.0 mol%	3.0 equiv.	-

a) *Reaction conditions*: OSu-ester **222** (1.0 equiv.), boronic acid **119** (1.3 equiv.), 80 °C, 1,4-dioxane, b) isolated yield

The control experiment demonstrated that all reaction components ($Pd(OAc)_2$, PCy_3 and K_3PO_4), are essential for a successful cross-coupling. Without K_3PO_4 only traces of **15** were obtained. Furthermore, the OSu-ester was stable under this condition (table 20, entry 1). As expected by conducting the carbonylative cross-coupling in the absence of $Pd(OAc)_2$ or PCy_3 no product formation was observed. Moreover, due to moderate yields caused by homocoupling of the boronic acid **119** further reactions were carried out under inert atmosphere with increased amount of boronic acid **119** (2.0 equiv). Additionally, temperature screening was carried out under the optimized conditions (table 21).

Table 21: Temperature screening results under inert atmosphere.

entry	T	t	yield[b]
1	r.t.	16 h	traces
2	50 °C	2 h	26%
3	80 °C	3 h	69%
4	100 °C	2 h	69%

a) *Reaction conditions*: $Pd(OAc)_2$ (10.0 mol%), PCy_3 (20.0 mol%), AcOSu **222** (1.0 equiv.), boronic acid **119** (2.0 equiv.), K_3PO_4 (3.0 equiv.), 80 °C, 1,4-dioxane, b) isolated yield.

Performing the reaction under inert gas atmosphere (table 21, entry 3) led to reproducible results with yields up to 69% of **15**. While carrying out the reaction at room temperature (table 21, entry 1) only traces of **15** were isolated. The reaction proceeded best at high temperatures. The same yield of 69% was obtained at 80 °C and 100 °C. (table 21, entry 3 & 4). In order to investigate the feasibility of this reaction, phenylboronic acid **105** was coupled with benzoyl-OSu **224** (table 22).

Table 22: Pd-catalyzed acylative *Suzuki* coupling of benzoylOSu-ester **224** and phenylboronic acid **105/119**.

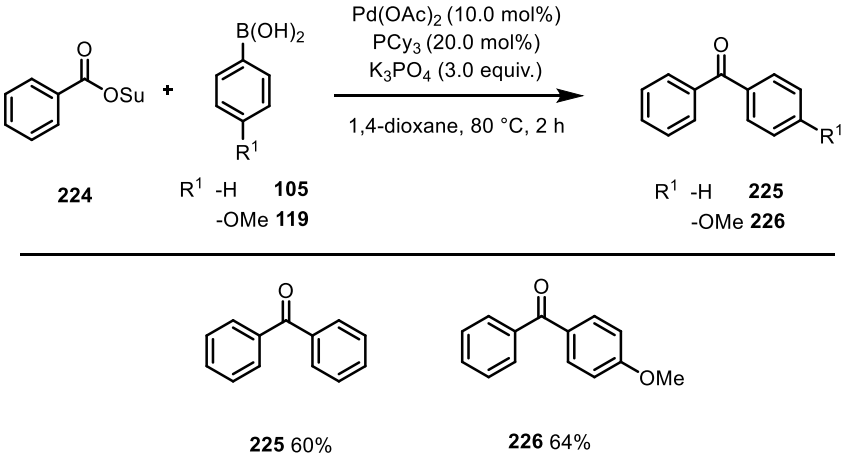

In both cases the benzophenones **225** and **226** were obtained in sufficient yields of 60% (**225**) and 64% (**226**), respectively (table 22). This indicates that other substrates are also suitable for this reaction type. Encouraged by this result, this reaction type was studied for the prunolide building block. For this purpose, the succinimidyl-ester synthesis **221** of vinyl bromide **127** with formyl-OSu **227** should be proceeded by a protocol of *Levacher* et al.[232] Herefore, formyl-OSu **227** was obtained in quantitative yields from esterification of formic acid **228** with hydroxysuccinimide **223** in acetic anhydride (scheme 65).[232]

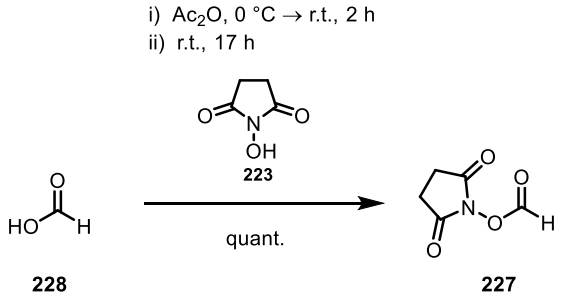

Scheme 65: Synthesis of formyl-OSu **227**.

Afterwards, the Pd-catalyzed carbonylation of vinyl bromide **127** and with formyl-OSu **227** was performed (scheme 66).

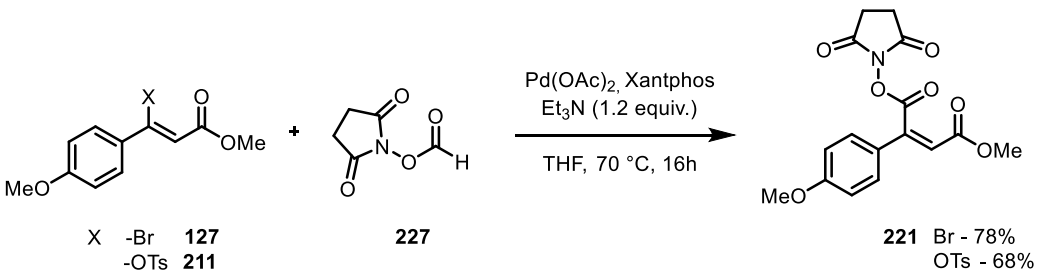

Scheme 66: Pd-catalyzed carbonylation of vinyl bromide **127** and vinyl tosylate **211** with **227**

In the presence of $Pd(OAc)_2$ (3.0 mol%), Xantphos (6.0 mol%), Et_3N (1.2 equiv.) and formyl-OSu **227** (1.2 equiv.) the carbonylated product **221** was obtained in 78% yield. Moreover, the corresponding vinyl tosylate **211** also provided the active ester **221** in a good yield of 68% (scheme 66). With the OSu-ester **221** in hand, the acylative *Suzuki-Miyaura* cross-coupling was further investigated (table 23).

Table 23: Acylative *Suzuki-Miyaura* optimization of vinyl active ester **221** with diboronic species.

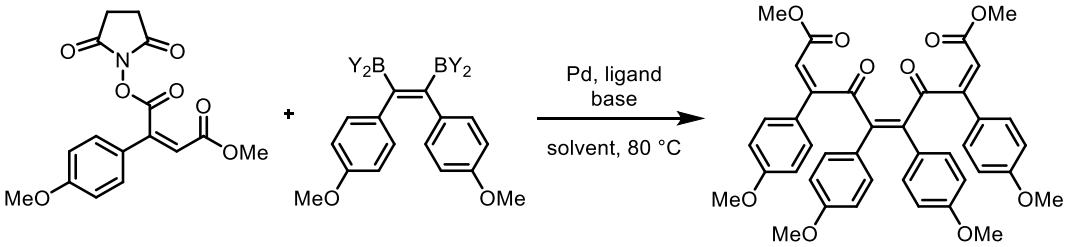

221 Y = BPin **125** Y = BF_3K **219** **220**

entry	catalyst	loading	ligand	loading	Y	base	solvent	Yield
1	$Pd(OAc)_2$	3.0 mol%	PCy_3	7.0 mol%	BPin	Na_2CO_3	THF	-
2	$Pd(OAc)_2$	3.0 mol%	PPh_3	7.0 mol%	BPin	Na_2CO_3	THF	-
3	$Pd(OAc)_2$	3.0 mol%	PCy_3	7.0 mol%	BPin	Na_2CO_3	THF/H_2O 9.1	-
4	$Pd(OAc)_2$	6.0 mol%	PCy_3	14.0 mol%	BPin	Na_2CO_3	THF	-
5	$Pd(OAc)_2$	6.0 mol%	dppf	7.0 mol%	BPin	Na_2CO_3	THF	-
6	$NiCl_2$dppf	10.0 mol%	-	-	BPin	Na_2CO_3	THF	-
7	$NiCl_2$dppp	10.0 mol%	-	-	BPin	Na_2CO_3	THF	-
8	Pd_2dba_3	10.0 mol%	SIPr	20.0 mol%	BPin	K_3PO_4	THF	-
9	$Pd(OAc)_2$	4.0 mol%	PCy_3	8.0 mol%	BF_3K	K_3PO_4	1,4-dioxane/ H_2O 9:1	-
10	$Pd(OAc)_2$	20.0 mol%	PCy_3	40.0 mol%	BF_3K	K_3PO_4	1,4-dioxane	-
11	$Pd(OAc)_2$	20.0 mol%	PCy_3	40.0 mol%	BF_3K	K_3PO_4	1,4-dioxane/ H_2O 9:1	-
12	$Pd(OAc)_2$	20.0 mol%	PCy_3	40.0 mol%	BF_3K	K_3PO_4	THF	-
13	$Pd(OAc)_2$	20.0 mol%	PCy_3	40.0 mol%	BF_3K	K_3PO_4	THF/H_2O 9:1	-

Unfortunately, no conversion was observed under optimized and literature known conditions (table 23).[233–235] Besides the bispinacolborane **125** and the corresponding BF_3K salt **219** did not yield the desired product (table 23, entry 9-13). Although succinimidyl active esters are prone to hydrolysis the OSu-active ester **221** was completely reisolated in most cases.

3.2.6. Carbonylative *Suzuki-Miyaura* cross-coupling with $Mo(CO)_6$ 229 as CO-source

Due to previous screenings, a different method needed to be developed. Because of the complexity of the diboronic substrate a simplified model system for the Pd-catalyzed carbonylative *Suzuki-Miyaura* cross-coupling was required. For this purpose $Mo(CO)_6$ **229** was applied as solid and safe carbon monoxide source. It was successfully applied in various cross-coupling reactions so far.[142–149] In order to verify the feasibility of the vinyl building blocks **210-212** for carbonylative cross-coupling reactions structurally less complex phenyl boronic acids **105, 119, 168, 230-234** were applied. Furthermore, with *γ*-ketoester **235-258** the acid catalyzed ketalization of the *γ*-keto acid was also investigated, which is also the final step of the prunolide synthesis (scheme 67).

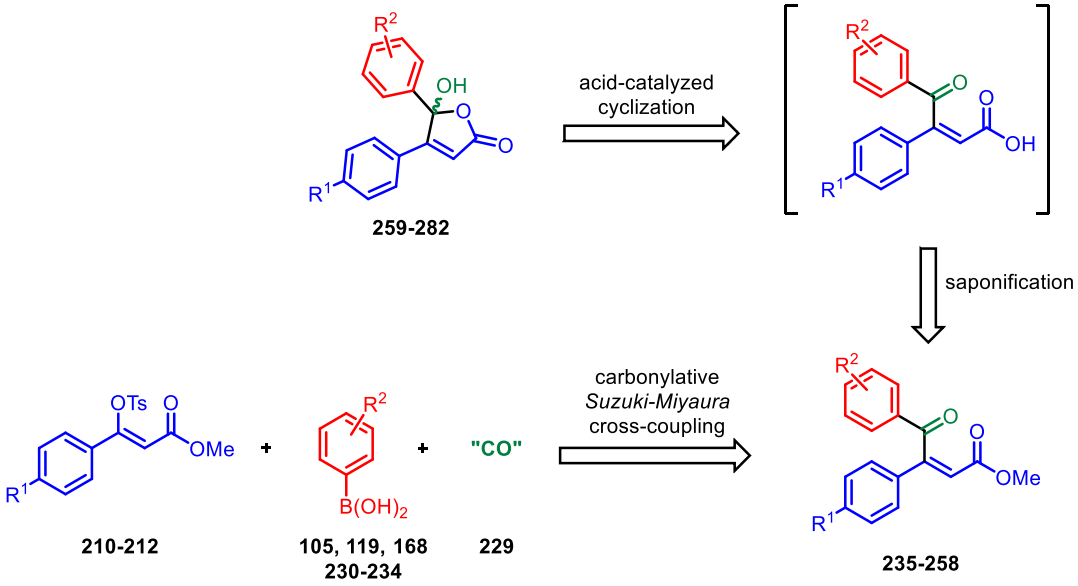

Scheme 67: Synthesis of *γ*-hydroxybutenolides **259-282** by $Mo(CO)_6$ **229** mediated carbonylative *Suzuki-Miyaura* of an vinyl tosylate **210-212** and phenylboronic acid **105**, **119**, **168**, **230-234** with subsequent one-pot saponification/cyclisation.

First, the viability of the model reaction with $Mo(CO)_6$ **229** was investigated. Herefore, vinyl tosylates **211** (1.0 equiv.) and phenylboronic acid **105** (2.0 equiv.) were treated with $Pd(OAc)_2$ (4.0 mol%), various ligands in presence of K_2CO_3 (3.0 equiv.) and $Mo(CO)_6$ **229** (2.0 equiv.) in anisole at 100 °C (table 24).

Table 24: Ligand screening results on the formation of **236**.

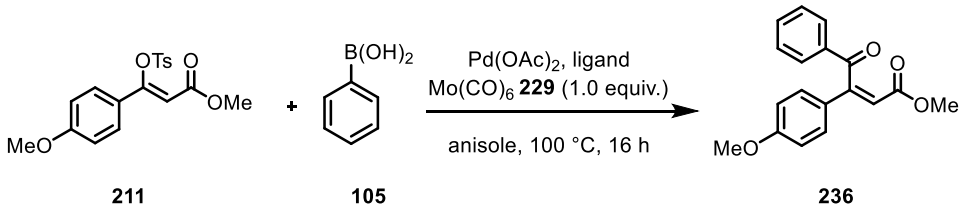

211 105 236

entry	ligand	loading	yield[b]
1	P(*n*-Bu)$_3$	8.0 mol%	30%
2	PPh_3	8.0 mol%	54%
3	PCy_3	8.0 mol%	60%
4	P(*p*-anisyl)$_3$	8.0 mol%	-
5	SIPr	4.0 mol%	55%
6	dppm	4.0 mol%	traces
7	dppp	4.0 mol%	10%
8	dppf	4.0 mol%	-
9	Xantphos	4.0 mol%	traces
10	*rac*-BINAP	4.0 mol%	-

Reaction conditions: vinyl tosylate **211** (1.0 equiv.), phenylboronic acid **105** (2.0 equiv.), $Pd(OAc)_2$ (4.0 mol%), ligand (4.0-8.0 mol%), $Mo(CO)_6$ **229** (1.0 equiv.), K_2CO_3 (3.0 equiv.), 100 °C, anisole. b) isolated yield.

A selected range of mono- and bidentate ligands were chosen in order to evaluate the influence of the ligand on the carbonylative cross-coupling. Firstly, the use of stabilizing bidentate ligands was tested, which are crucial for reported palladium catalyzed carbonylative cross-coupling. [143,236–240] Then, dppf and *rac*-BINAP were tested (table 24, entry 8 & 10) and the desired coupling product could not be detected. Further screenings of bidentate ligands using dppm, dppp and Xantphos (table 24, entry 6, 7 & 9) afforded traces of the desired product **236**. However, the experiments with monodentate ligands such as PPh_3, PCy_3 and SIPr (table 24, entry 2, 3 & 5) afforded the desired product **236** in moderate yields between 54-60%.

Figure 29 displays the proton-NMR of **236**. Signals at 7.42–7.45 (m, 4 H, 3'-H, 5'-H, 3''-H, 5''-H), 7.54 (t, J = 7.4 Hz, 1 H, 4''-H), and 7.95 (d, J = 7.8 Hz, 2 H, 2''-H, 6''-H) correspond to the introduced phenyl ring by carbonylative cross-coupling. Further aromatic signals at 7.42–7.45 (m, 4 H, 3'-H, 5'-H, 3''-H, 5''-H) and 6.87 (d, J = 8.9 Hz, 2 H, 2'-H, 6'-H) indicate the 1,4-disubstituted phenyl ring of **236**. Moreover, the signal at 6.43 (s, 1 H, 2-H) correspond to the vinyl proton. In addition, the methyl ether was observed at 3.79 (s, 3 H, OCH_3) and the methyl ester was observed at 3.61 (s, 3 H, CO_2CH_3)

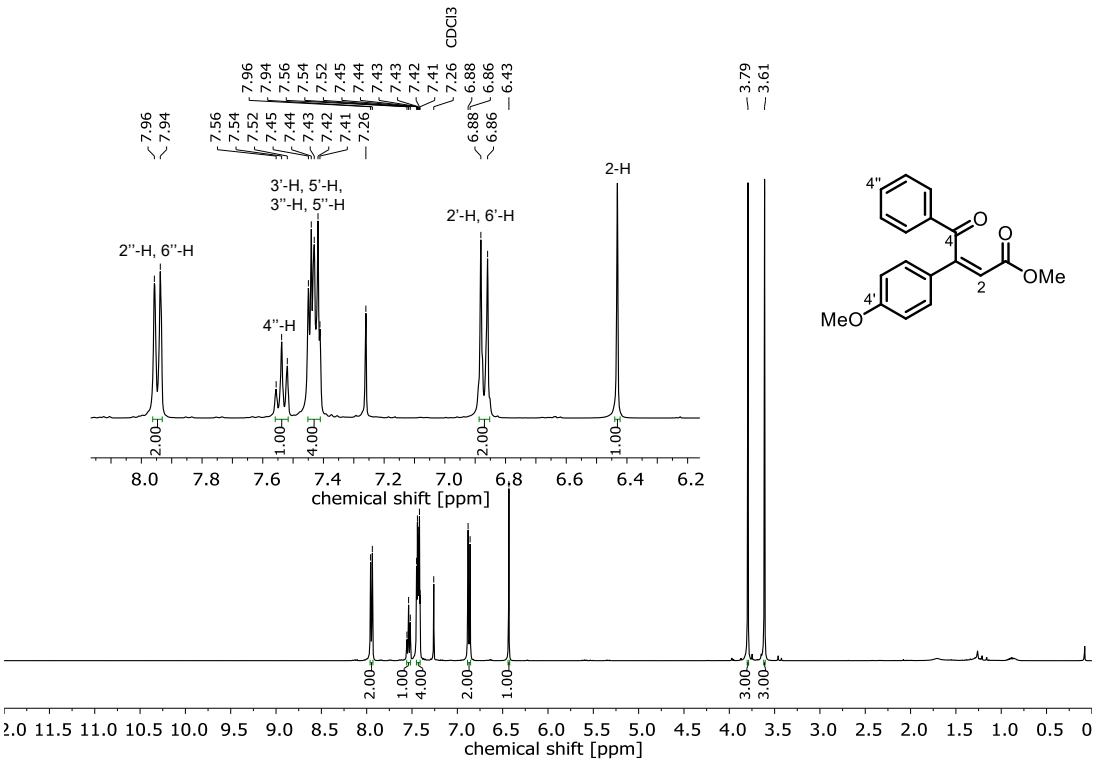

Figure 29: ^{1}H-NMR spectrum (400 MHz, $CDCl_3$, 300 K) of **236**.

Subsequent carbon NMR analysis (figure 30) verified the successful formation of **236** with the characteristic signal at 197.1 ppm (C-4) indicating the presence of a ketone. Additionally, IR-spectrum with two characteristic carbonyl bands at 1712 and 1673 cm^{-1} confirm also successful product formation.

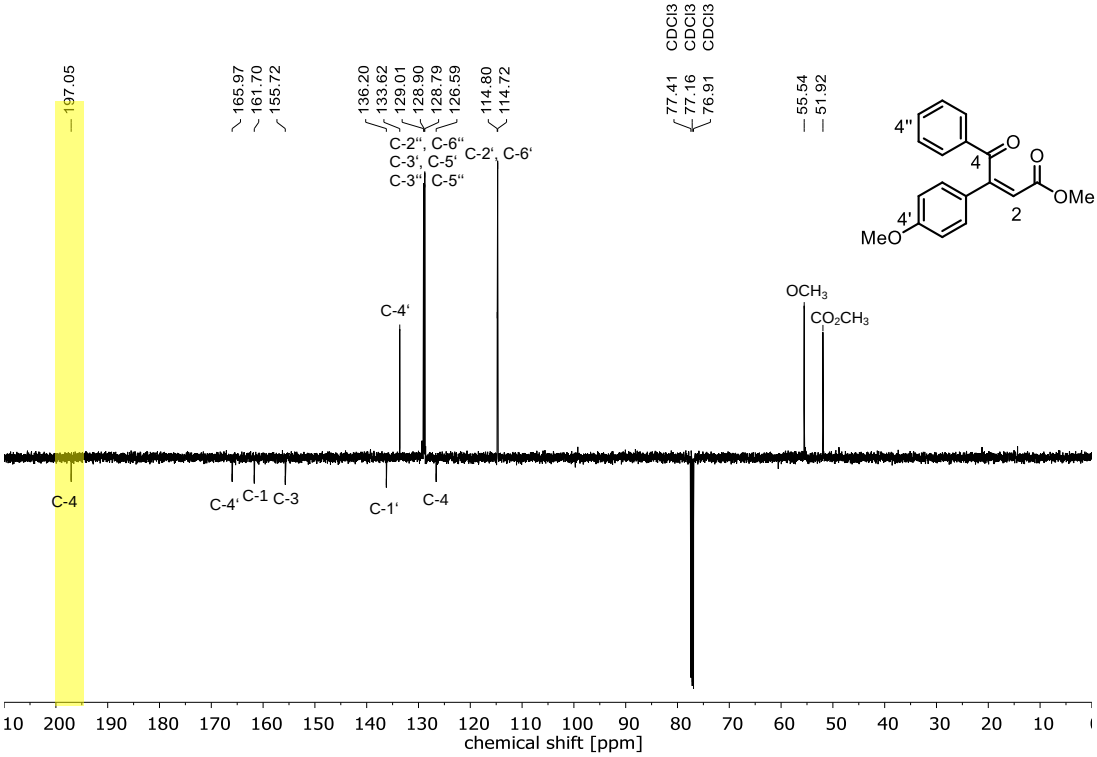

Figure 30: DEPTQ spectrum (126 MHz, $CDCl_3$, 296 K) of **236**.

GC-MS reaction control also verified the formation of the conventional *Suzuki-Miyaura* cross-coupling as competing side reaction. Detosylation of the vinyl building block **211** and homocoupling of boronic acid **105** were identified as major side reactions. In order to reduce the competing non-carbonylative coupling, the Pd-source was replaced by $Pd(TFA)_2$, which was successfully applied in several carbonylative cross-coupling reactions (table 25).[241–243]

Table 25: Ligand screening results with $Pd(TFA)_2$ as metal source.

entry	ligand	loading	yield[b]
1	PPh_3	8.0 mol%	12%
2	PCy_3	8.0 mol%	53%
3	SIPr	4.0 mol%	27%

Reaction conditions: vinyl tosylate **211** (1.0 equiv.) phenylboronic acid **105** (2.0 equiv.), $Pd(TFA)_2$ (4.0 mol%), ligand (4.0/8.0 mol%), $Mo(CO)_6$ **229** (1.0 equiv.), K_2CO_3 (3.0 equiv.), 100 °C, anisole, b) isolated yield.

$Pd(TFA)_2$ with PCy_3 as ligand (table 25, entry 2) revealed satisfying yields with significant reduction of the non-carbonylative cross-coupling. A solvent screen followed to evaluate the effect on the carbonylative cross-coupling (table 26).

Table 26: Solvent screening.

entry	solvent	yield[b]
1	toluene	66%
2	xylene	58%
3	1,4-dicholobenzene	56%
4	fluorobenzene	46%
5	CpOMe	37%
6	Bu_2O	45%
7	CyOMe	27%
8	1,4-dioxane	12%
9	THF	7%
10	DMF	-
11	DMAc	-

Reaction conditions: vinyl tosylate **211** (1.0 equiv.), phenylboronic acid **105** (2.0 equiv.), $Pd(TFA)_2$ (4.0 mol%), PCy_3 (8.0 mol%), $Mo(CO)_6$ **229** (1.0 equiv.), K_2CO_3 (3.0 equiv.), 100 °C, solvent b) isolated yield.

By performing the reaction in DMF and DMAc (table 26, entry 10 & 11) no product formation **236** was detected. While ethers (table 26, entry 5-9) gave the desired product in low to moderate yields less polar aromatic solvents were the most promising (table 26, entry 1-4). Toluene afforded the desired product in 66% yield (table 26, entry 1). Encouraged by the use of the $Pd(TFA)_2$ as precatalyst and PCy_3 as ligand the equivalents of $Mo(CO)_6$ were further increased in order to provide a higher carbon monoxide concentration and to minimize the non-carbonylative cross-coupling. For this purpose the carbonylative cross-coupling with $Pd(TFA)_2/PCy_3$ was performed in aromatic solvents with 2.0 equiv. of $Mo(CO)_6$ **229** (table 27).

Table 27: Solvent screening with 2.0 equiv. $Mo(CO)_6$.

entry	solvent	yield[b]
1	toluene	72%
2	xylene	63%
3	1,4 dichorobenzene	56%
4	fluorobenzene	46%
5	anisole	54%

Reaction conditions: vinyl tosylate **211** (1.0 equiv.), phenylboronic acid **105** (2.0 equiv.), $Pd(TFA)_2$ (4.0 mol%), PCy_3 (8.0 mol%), $Mo(CO)_6$ **229** (2.0 equiv.), K_2CO_3 (3.0 equiv.), 100 °C, solvent b) isolated yield.

Among the tested solvents toluene (table 27, entry 1) again provided the highest yield of 72%. Minor improvement was detected in xylene, 1,4-dichlorobenzene, fluorobenzene and anisole (table 27, entry 2-5). In the following, the effect of the base on the model reaction was studied (table 28).

Table 28: Base screening.

entry	base	yield[b]
1	Na_2CO_3	11%
2	K_2CO_3	72%
3	Cs_2CO_3	-
4	NaOAc	traces
5	KOAc	traces
6	KF	50%
7	CsF	-
8	K_3PO_4	45%
9	NaOH	30%
10	KOH	43%

Reaction conditions: vinyl tosylate **211** (1.0 equiv.), phenylboronic acid **105** (2.0 equiv.), $Pd(TFA)_2$ (4.0 mol%), PCy_3 (8.0 mol%), $Mo(CO)_6$ (2.0 equiv.), base (3.0 equiv.), 100 °C, toluene, b) isolated yield.

Lower yields were obtained with caesium and sodium bases (table 28, entry 1, 3-5, 7, 9). Use of K_2CO_3 led to the most promising results. Other potassium bases (table 28, entry 6, 8 & 10) afforded moderate yields of **236**. Potassium may play an important role in the carbonylative cross-coupling. To sum up, all reactions components were evaluated in following control experiments. For this purpose, each procedure was carried out by leaving out one component (table 29, entry 1-4).

Table 29: Control experiments of the carbonylative cross-coupling.

entry	$Pd(TFA)_2$	PCy_3	K_2CO_3	$Mo(CO)_6$ **229**	yield[b]
1	4.0 mol%	8.0 mol%	3.0 equiv.		-
2	4.0 mol%	8.0 mol%		2.0 equiv.	traces
3	4.0 mol%		3.0 equiv.	2.0 equiv.	-
4		8.0 mol%	3.0 equiv.	2.0 equiv.	-

Reaction conditions: vinyl tosylate (1.0 equiv.), phenylboronic acid (2.0 equiv.), $Pd(TFA)_2$ (4.0 mol%), PCy_3 (8.0 mol%), $Mo(CO)_6$ (2.0 equiv.), base (3.0 equiv.), 100 °C, toluene, b) isolated yield.

These experiments revealed that all reaction components ($Pd(TFA)_2$, PCy_3, K_2CO_3, and $Mo(CO)_6$ **229** were essential for the formation of **236** (table 29). When the reaction was performed in absence of K_2CO_3 (table 29, entry 2-3) only traces of the carbonylated product were obtained. Furthermore, in the absence of $Pd(TFA)_2$ or $Mo(CO)_6$ (table 29, entry 1 & 4) no formation of **236** was observed.

Additionally, the efficiency of $Mo(CO)_6$ **229** as CO-source was compared to the use of carbon monoxide gas (3.0 bar). Proton NMR comparison of the crude reactions demonstrated clean formation of **236** by using of $Mo(CO)_6$ **229** (figure 31, - top blue), while the reaction with 3.0 bar CO-gas revealed more side reactions (figure 31, buttom - red).

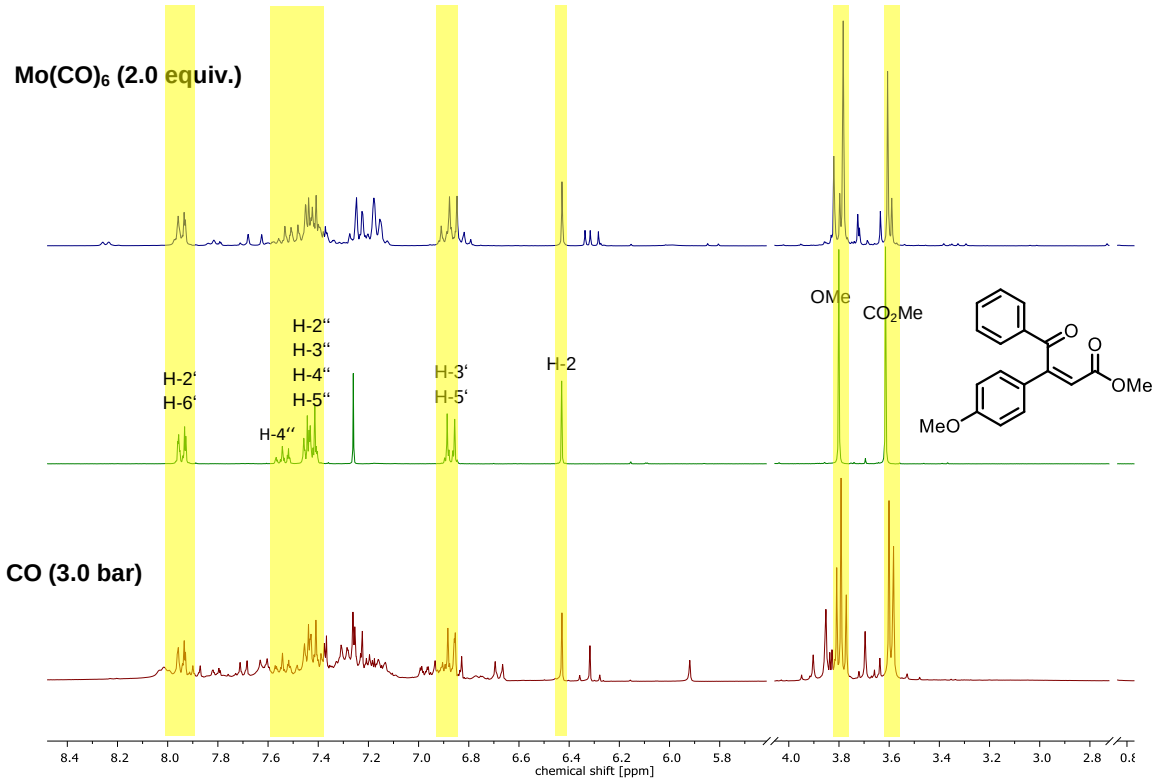

Figure 31: ^{1}H-NMR (300 MHz, $CDCl_3$-*d*, 25 °C; blue: $Mo(CO)_6$ **229** - carbonylative *Suzuki-Miyaura* cross-coupling; green: reference spectra; red: carbon monoxide (3.0 bar) carbonylative *Suzuki-Miyaura* cross-coupling.

Based on the optimized reaction conditions, the scope of the carbonylative cross-coupling was examined. For this purpose, vinyl tosylates **210-212** and boronic acids **105, 119, 169, 230-234** were employed bearing either electron donating or electron withdrawing groups (table 30).[138,226]

Table 30: Scope of the $Mo(CO)_6$ **229**-mediated reaction of vinyl tosylate **210-212** with boronic acids **105, 119, 168, 230-234**. [a,b]

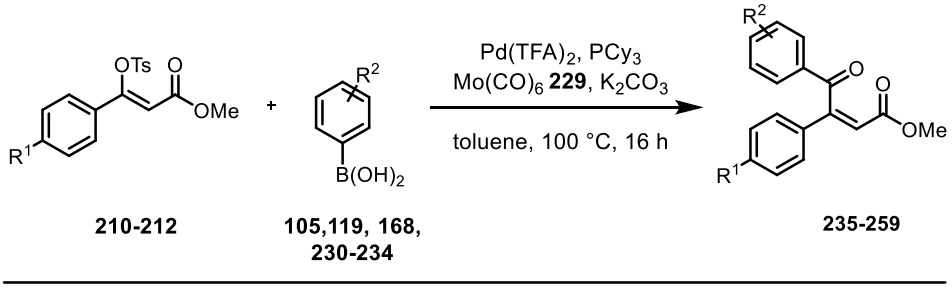

210-212 | **105,119, 168, 230-234** | **235-259**

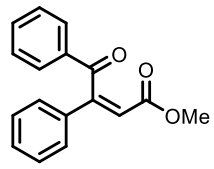

235, 27%[a]
M.W. 15%[b]

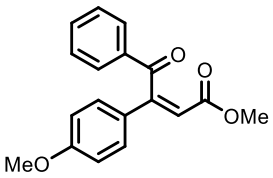

236, 72%[a]
M.W. 55%[b]

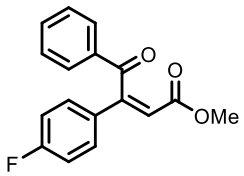

237, 72%
M.W. 55%[b]

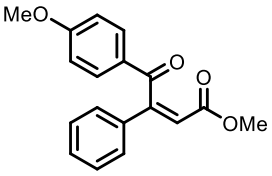

238, 33%[a]
M.W. 68%[b]

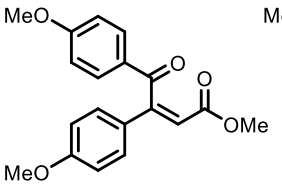

239, 54%[a]
M.W. 63%[b]

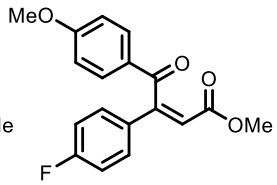

240, 44%[a]
M.W. 49%[b]

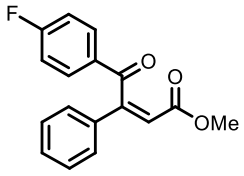

241, 79%[a]
M.W. 25%[b]

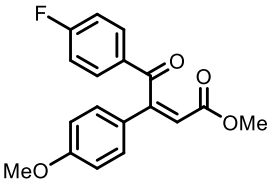

242 66%[a]
M.W. 55%[b]

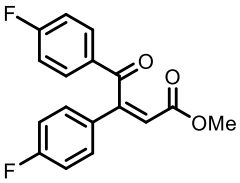

243, 66%[a]
M.W. 63%

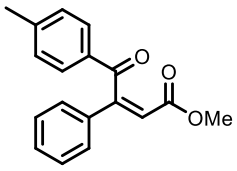

244, 45%[a]
M.W. 15%[b]

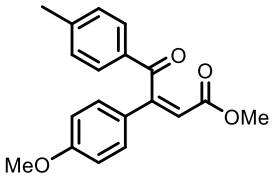

245, 67%[a]
M.W. 64%[b]

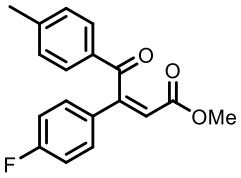

246, 43%[a]
M.W. 33%[b]

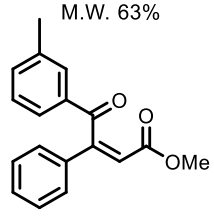

247, 12%[a]
M.W. 54%[b]

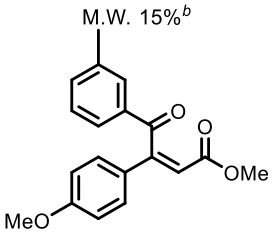

248, 30%[a]
M.W. 80%[b]

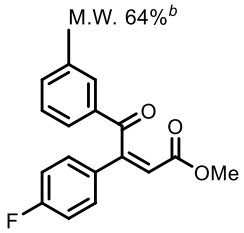

249, 24%[a]
M.W. 67%[b]

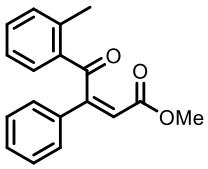

250, 0%[a]
M.W. 10%[b]

a) *Reaction conditions A*: vinyl tosylates **210-212**, boronic acid **105, 119, 168, 230-234** (2.0 equiv.), $Pd(TFA)_2$ (4.0 mol%), PCy_3 (8.0 mol%), $Mo(CO)_6$ **229** (2.0 equiv.), K_2CO_3 (3.0 equiv.), 100 °C, 16 h, toluene; b) *Reaction conditions B*: vinyl tosylates **210-212**, boronic acid **105, 119, 168, 230-234** (2.0 equiv.), $Pd(TFA)_2$ (4.0 mol%), PCy_3 (8.0 mol%), $Mo(CO)_6$ **229** (2.0 equiv.), base (3.0 equiv.), 100 °C, 1 h, M.W., toluene.

Table 30 (continued): Scope of the $Mo(CO)_6$ **229**-mediated reaction of vinyl tosylate **210-212** with boronic acids **105, 119, 168, 230-234**. [a,b]

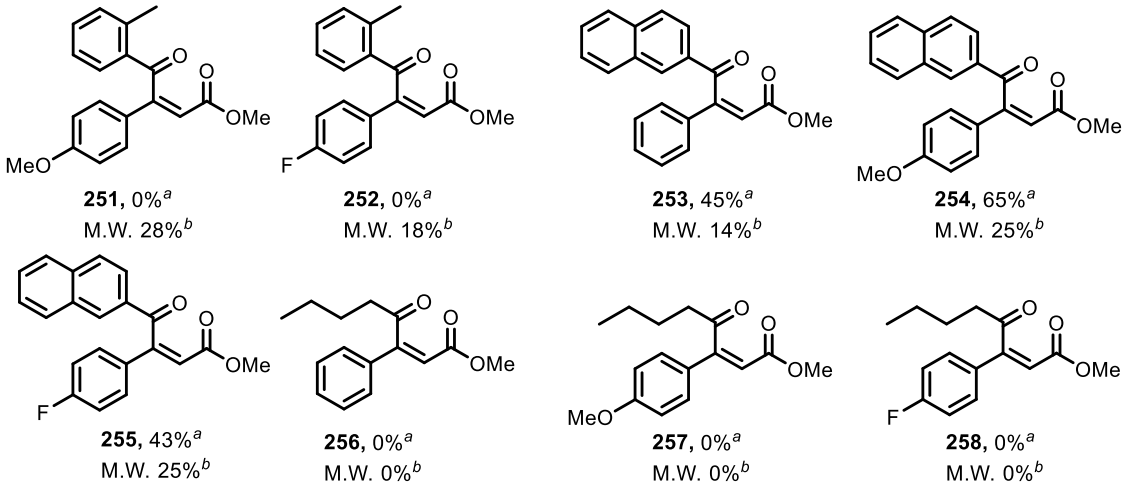

251, 0%[a] M.W. 28%[b]

252, 0%[a] M.W. 18%[b]

253, 45%[a] M.W. 14%[b]

254, 65%[a] M.W. 25%[b]

255, 43%[a] M.W. 25%[b]

256, 0%[a] M.W. 0%[b]

257, 0%[a] M.W. 0%[b]

258, 0%[a] M.W. 0%[b]

a) *Reaction conditions A*: vinyl tosylates **210-212**, boronic acid **105, 119, 168, 230-234** (2.0 equiv.), $Pd(TFA)_2$ (4.0 mol%), PCy_3 (8.0 mol%), $Mo(CO)_6$ **229** (2.0 equiv.), K_2CO_3 (3.0 equiv.), 100 °C, 16 h, toluene; b) *Reaction conditions B*: vinyl tosylates **210-212**, boronic acid **105, 119, 168, 230-234** (2.0 equiv.), $Pd(TFA)_2$ (4.0 mol%), PCy_3 (8.0 mol%), $Mo(CO)_6$ **229** (2.0 equiv.), base (3.0 equiv.), 100 °C, 1 h, M.W., toluene.

Electron-donating and electron-withdrawing functionalities on tosylates **210-212** and boronic acids **105, 119, 168, 230** and **233** were coupled in a carbonylative manner with moderate to good yields. Furthermore, *meta*-, and *ortho* functionalized aryl boronic acids **231** & **232** were coupled. Due to the steric hindrance of *m*-tolylboronic acid **231** lower yields of **247-249** between 12-30% were achieved, while the application of *o*-tolylboronic acids **232** and butylboronic acid **234** did not afford the desired structures **250-252, 256-258** (table 30).

Further optimization steps were carried out under microwave irradiation. The studies revealed higher yields for *m*-tolyl boronic acid **231** with an increase of 50% for **247-249**. Moreover, microwave irradiation was beneficial for *o-tolyl* boronic acid **232** to generate **250-252**. Butylboronic acid **234** did not provide the desired coupling product **253-255** either under conventional nor under microwave assisted reaction conditions. In addition, suitable crystals of **242** and **244** were collected and the structures determined by single-crystal structure analysis (figure 32).

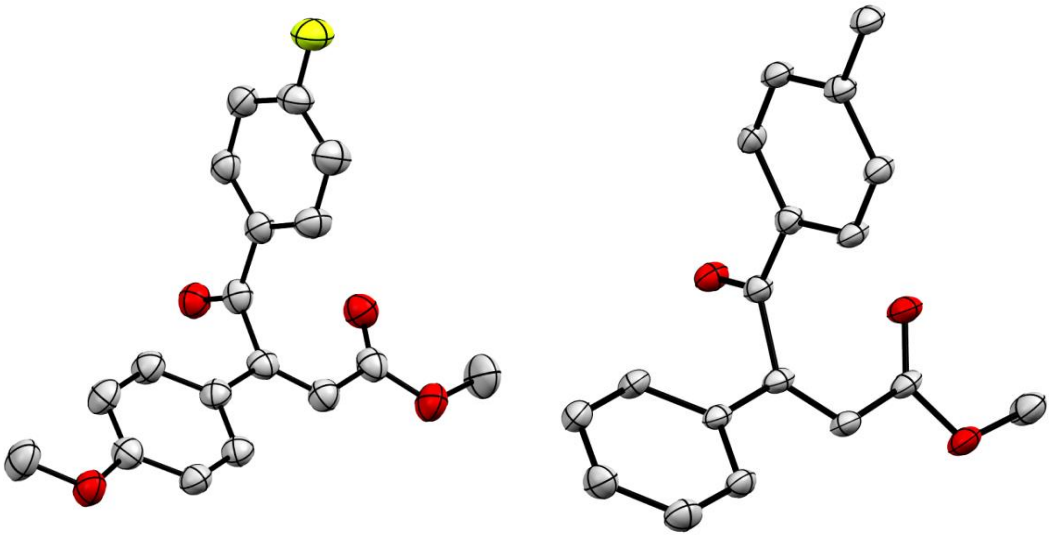

242 **244**

Figure 32: Single crystal structure of the *γ*-ketoesters **242** and **244**. Thermal ellipsoids are shown at 50% probability level. Hydrogen atoms are omitted for clarity.

With the *γ*-ketoester **225-255** as key intermediate in hand the last step of the *γ*-hydroxybutenolide synthesis was conducted by one-pot saponification/cyclisation sequence yielding the desired *γ*-hydroxybutenolide **259-279** in good yields (table 31).[138,226]

Table 31: Scope of the one-pot saponification/acid catalyzed cyclization reaction.

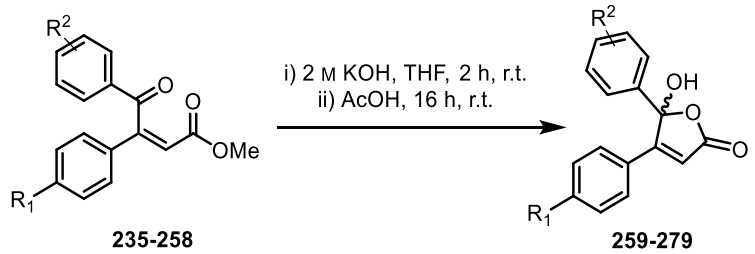

235-258 **259-279**

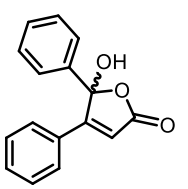

259, 98%

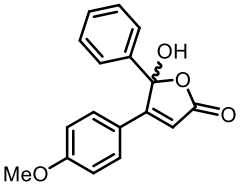

260, 71%

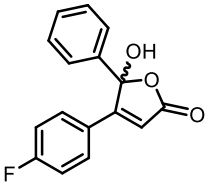

261, 95%

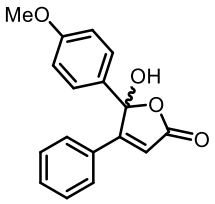

262, 71%

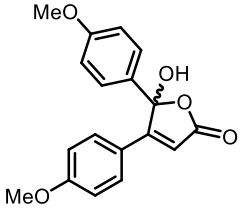

263, 78%

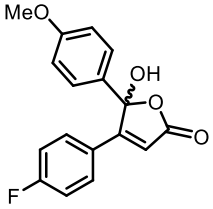

264, 58%

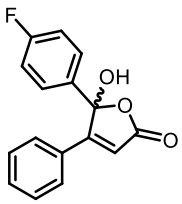

265, 85%

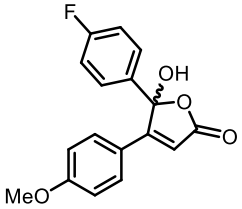

266, 70%

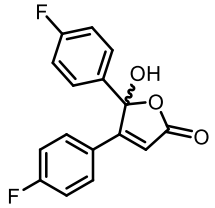

267, 86%

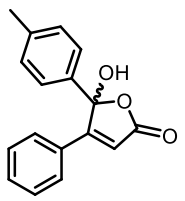

268, 64%

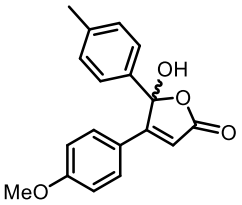

269, 66%

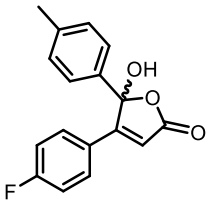

270, 97%

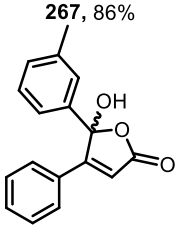

271, 83%

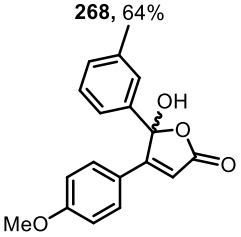

272, 76%

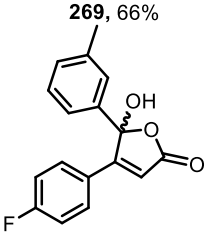

273, 48%

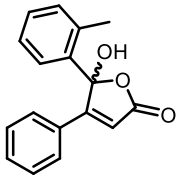

274, 81%

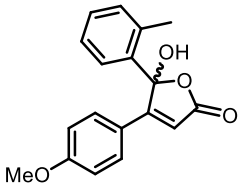

275, 93%

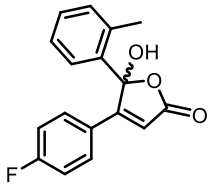

276, 58%

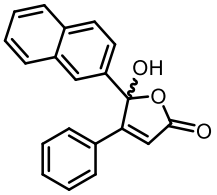

277, 54%

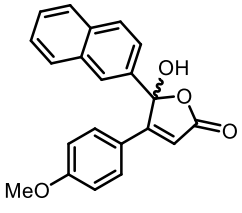

278, 75%

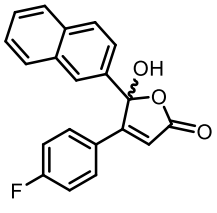

279, 77%

The hydroxybutenolides **259-279** revealed in solution a dynamic equilibrium between the cyclized butenolide **283** and the open chained tautomer **284** (scheme 68).

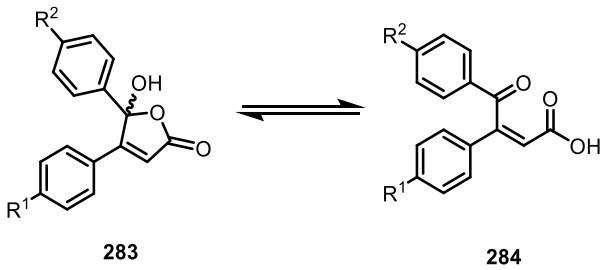

Scheme 68: Tautomerization of *γ*-hydroxybutenolide **283** and **284**.

The equilibrium was confirmed by carbon NMR analysis at room temperature and 223K. While conducting the carbon NMR at room temperature signals of quaternary carbons such as the signal of the hemiketal carbon (C-5) were not detected (figure 33, top). By proceeding experiments at 223 °K characteristic signals for the hemiketal at ~106 ppm were observed (figure 33).[138]

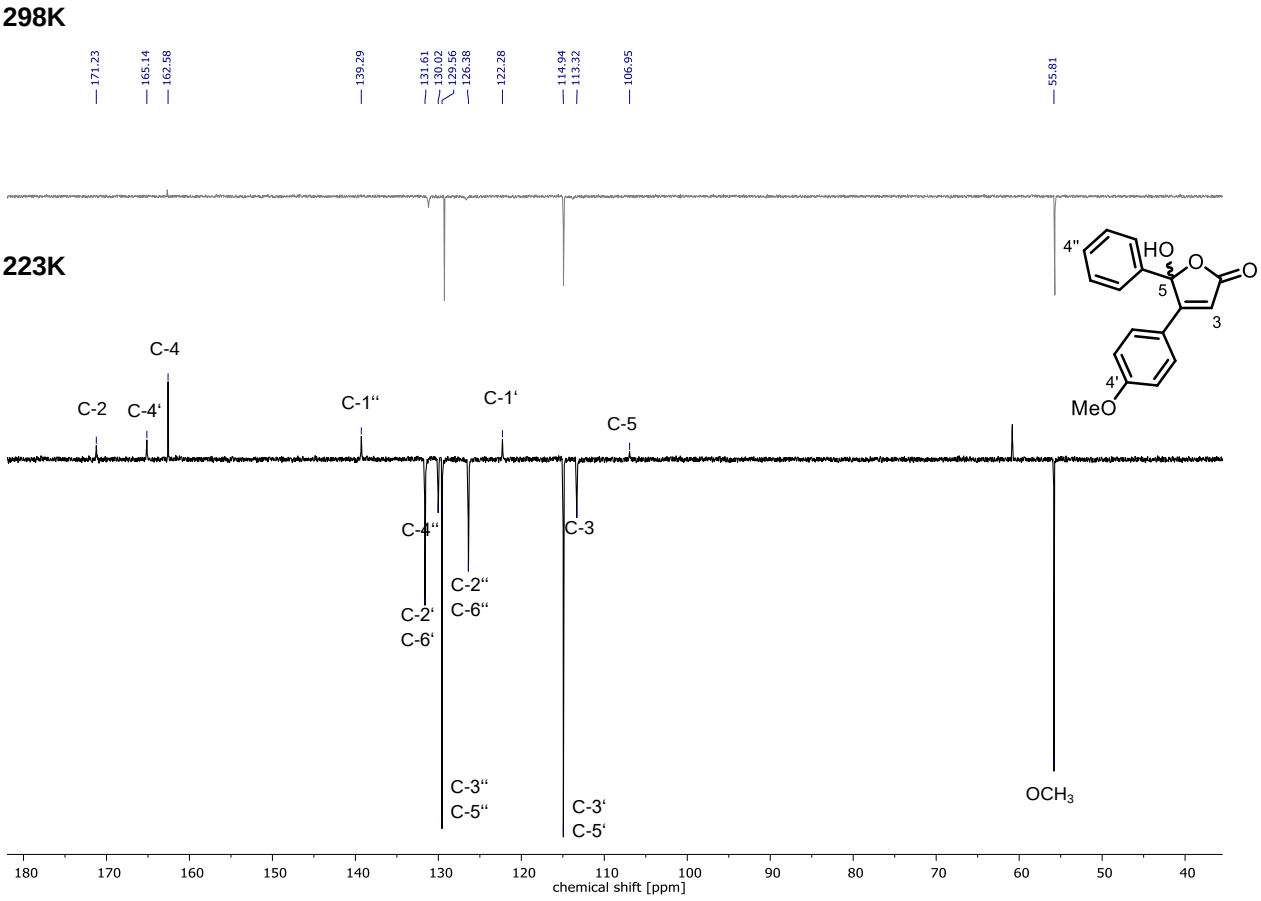

Figure 33: Stacked DEPTQ spectra (101 MHz, acetone-d_6, 298K – top, grey; 223K – down, black) of **260**

Furthermore, single crystals of the open tautomer of **260** were received, which were examined by single crystal structure analysis (figure 34). This implicated the dynamic equilibrium between the open and closed form of the hydroxybutenolide in solution.

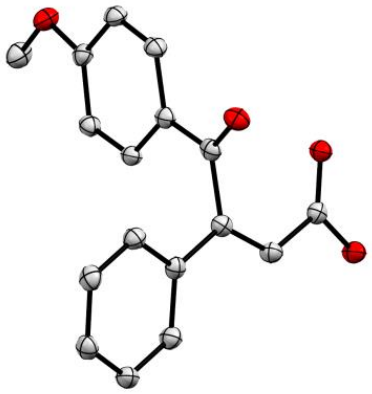

Figure 34: X-ray single-crystal structure of the open tautomer of **260**. Thermal ellipsoids are shown at 50% probability level. Hydrogen atoms are omitted for clarity.

After analyzing the reactivity of vinyl tosylates **210-212** and $Mo(CO)_6$ **229** as solid carbon monoxide source, the two-fold carbonylative *Suzuki-Miyaura* cross-coupling with diboronic building blocks **125, 202, 219** under the optimized conditions were studied (table 32).

Table 32: Screening of the two-fold carbonylative *Suzuki-Miyaura* cross-coupling.

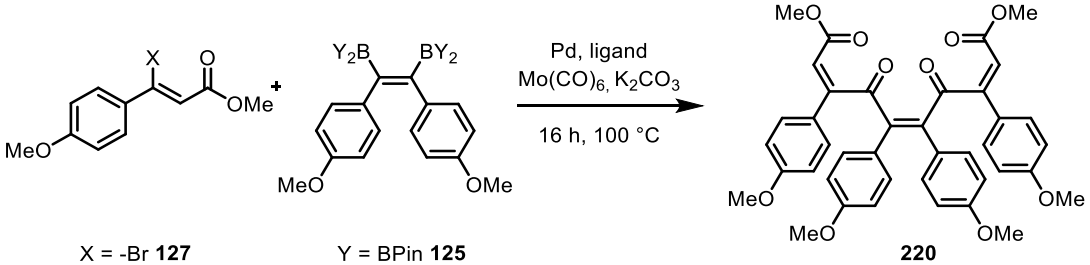

X = -Br **127**
X = -OTs **211**

Y = BPin **125**
Y = BF_3K **219**
Y = BNeop **202**

220

entry	catalyst	loading	ligand	loading	$Mo(CO)_6$ **229**	X	Y	solvent	yield
1	$Pd(TFA)_2$	4.0 mol%	PCy_3	8.0 mol%	2.0 equiv.	Tos	BPin	THF	-
2	$Pd(TFA)_2$	4.0 mol%	PCy_3	8.0 mol%	2.0 equiv.	Tos	BPin	toluene	-
3	$Pd(TFA)_2$	16.0 mol%	PCy_3	32.0 mol%	4.0 equiv.	Tos	BPin	THF	-
4	$Pd(TFA)_2$	16.0 mol%	PCy_3	32.0 mol%	4.0 equiv.	Tos	BPin	toluene	-
5	$Pd(TFA)_2$	16.0 mol%	PCy_3	32.0 mol%	6.0 equiv.	Tos	BPin	THF	-
6	$Pd(TFA)_2$	16.0 mol%	PCy_3	32.0 mol%	6.0 equiv.	Tos	BPin	toluene	-
7	$Pd(PPh_3)_4$	16.0 mol%	PCy_3	32.0 mol%	6.0 equiv.	Tos	BPin	THF	-
8	$Pd_2(dba)_3$	16.0 mol%	PCy_3	32.0 mol%	6.0 equiv.	Tos	BPin	toluene	-
9	$Pd(PPh_3)_4$	16.0 mol%	-	-	6.0 equiv.	Tos	BF_3K	toluene	-
10	$Pd(PPh_3)_4$	16.0 mol%	-	-	6.0 equiv.	Tos	BF_3K	toluene	-
13	$Pd(PPh_3)_4$	16.0 mol%	SPhos	32.0 mol%	6.0 equiv.	Tos	BF_3K	toluene	-
14	$Pd(PPh_3)_4$	16.0 mol%	JohnPhos	32.0 mol%	6.0 equiv.	Tos	BF_3K	toluene	-
15	$Pd(PPh_3)_4$	16.0 mol%	P(*p*-tolyl)$_3$	32.0 mol%	6.0 equiv.	Tos	BF_3K	toluene	-
16	$Pd(PPh_3)_4$	16.0 mol%	PCy_3	32.0 mol%	6.0 equiv.	Tos	BF_3K	toluene	-
17	$Pd(PPh_3)_4$	16.0 mol%	SIPr	32.0 mol%	6.0 equiv.	Tos	BF_3K	toluene	-
18	$Pd(PPh_3)_4$	16.0 mol%	dppf	32.0 mol%	6.0 equiv.	Tos	BF_3K	toluene	-
19	$Pd(PPh_3)_4$	16.0 mol%	dppb	32.0 mol%	6.0 equiv.	Tos	BF_3K	toluene	-
20	$Pd(PPh_3)_4$	16.0 mol%	dppp	32.0 mol%	6.0 equiv.	Tos	BF_3K	toluene	-
21	$Pd(PPh_3)_4$	16.0 mol%	dppe	32.0 mol%	6.0 equiv.	Tos	BF_3K	toluene	-
21	$Pd(PPh_3)_4$	16.0 mol%	Xantphos	32.0 mol%	6.0 equiv.	Tos	BF_3K	toluene	-
24	$Pd(PPh_3)_4$	16.0 mol%	-	16.0 mol%	6.0 equiv.	Tos	BNeop	toluene	-
25	$Pd(PPh_3)_4$	16.0 mol%	Xantphos	16.0 mol%	6.0 equiv.	Tos	BNeop	toluene	-
26	NiCl(naphthyl) $(PPh_3)_2$	16.0 mol%	PPh_3	32.0 mol%	6.0 equiv.	Br	BNeop	toluene	-
27	NiCl(naphthyl) $(PPh_3)_2$	16.0 mol%	PCy_3	32.0 mol%	6.0 equiv.	Br	BNeop	toluene	-

Nonetheless, these attempts resulted in an inseparable mixture of products (table 32). Drawback of this approach is the formation of undesired side products resulting from detosylation **285**, homocoupling **286** and protodeborylation of **125, 202** and **219**. These side products were identified by ESI- and GC-MS analysis (figure 35). Also exchanging the vinyl tosylate **211** to the corresponding vinyl bromide **129** did not improve the reaction outcome. Despite the major side reactions, traces of the *Suzuki* reaction product **289**, the carbonylated *Suzuki* product **290** and the protodeborylated adducts **287** and **289** were identified by ESI-MS analysis (figure 35). This indicates that the reactivity of the diboronic sources **125, 202** and **219** was not sufficient for the two-fold *Suzuki-Miyaura* cross-coupling reaction.

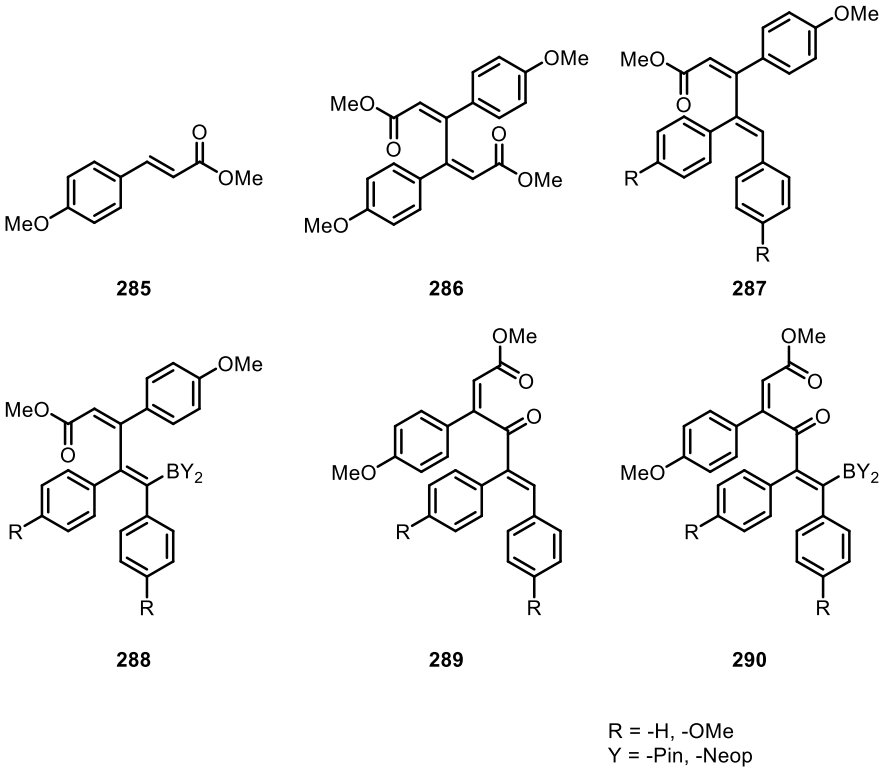

Figure 35: Identified side products in the carbonylative *Suzuki-Miyaura* cross-coupling.

3.3. Biological data

3.3.1. Antibiotic studies

Since various isolated rubrolides from natural tissue showed biological activity, the pure rubrolide R **12** and S **13** were tested against strains of *Escherichia coli*, *Pseudomonas aeruginosa*, *Enterococcus faecalis* and *Staphylococcus aureus* to investigate their antibacterial activity.The preliminary agar droplet experiments performed by *Heisig* et al. indicated growth inhibition of gram-negative *E. coli* (figure 36 and figure 37, left) and in a weak growth inhibition for *Pseudomonas aeruginosa* (figure 36 and figure 37, right). Both novel rubrolide structures were applied in concentrations of 100 µg/µL in DMSO and Rifampicin served as a positive control**.** However, these observations could not be confirmed either by additional agar diffusion nor by serial dilution tests.[185]

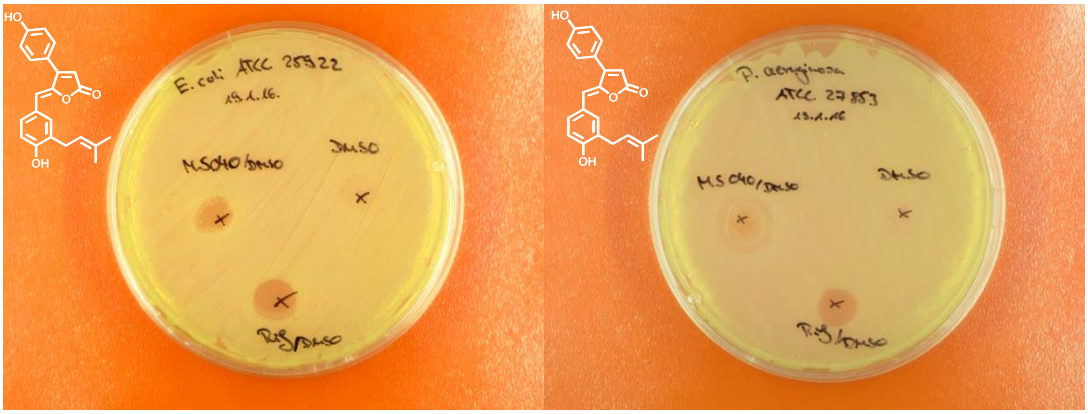

Figure 36: Agar droplet method using gram negative *E. coli* (left) and *P.aeruginosa* (right) as bacterial strain with DMSO as negative control, Rifampicin, as positive control (second row, middle). Rubrolide R **12** (MS040, first row, left), showed moderate antibacterial activity against *E. coli* and low activity against *P. aeruginosa*. The experiments were conducted by P. Zimmermann.[185]

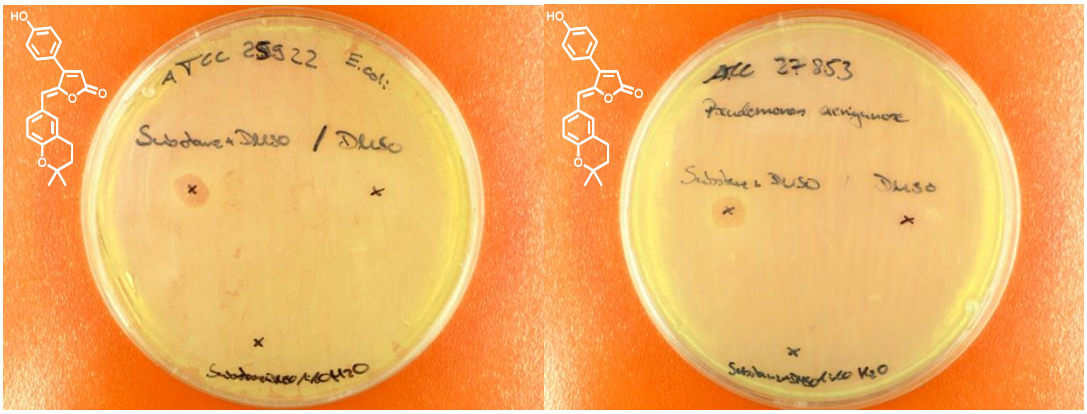

Figure 37 Agar droplet method using gram negative *E. coli* (plate, left) *and P.aeruginosa* (plate, right) as bacterial strain with DMSO (first row, right) as negative control, Rifampicin, and a 1:10 substance/water dilution (second row, middle). Rubrolide S **13** (first row, left) showed moderate antibacterial activity against *E. coli* and low activity against *P. aeruginosa*. The experiments were conducted by P. Zimmermann [185]

Furthermore, rubrolide R and S derivatives **174-181** exhibiting substitution of the upper phenyl ring A, were ineffective against the bacterial strains *Escherichia coli*, *Pseudomonas aeruginosa*, *Enterococcus faecalis* and *Staphylococcus aureus.* These results indicated the necessity of the hydroxyl group at phenyl ring B for the biological activity.

The *chloro*-rubrolide R **162** was also tested against the mentioned bacterial strains above. The preliminary test revealed significant growth inhibition for the gram-positive *Staphylococcus aureus* (figure 38) at concentrations of 100 µg/µL in DMSO with Rifampicin as a positive control.

Figure 38: Agar droplet method using gram positive *S. aureus* as bacterial strain with DMSO as negative control, Rifampicin, as positive control. Rubrolide R **13** (MS096, second row, left), *chloro*-rubrolide R **162** (first row left) showed moderate antibacterial activity. The experiments were conducted by P. Zimmermann.

3.3.2. Antiviral studies

effects against several cancer cell lines (K562, A549, HL-60, HeLa & HCT-116) and antiviral activity against influenza virus (A/Puerto Rico/8/34 (H1N1), PR/8) with superior activity compared to ribavirin.[34]

In cooperation with *Gabriel* et al. the antiviral activities of rubolide R and S were evaluated by applying the *E/Z*-mixtures and the Z-isomers, respectively. Hereby, MDCK cells were infected with H3N2 or *p*H1N1 influenza viruses and co-treated with ribavirin or rubrolide R **12** and S **13**. The viral titer of infected and PBS (Ctr1) or DMSO (Ctr2) treated cells served as a negative control. Rubrolide R **12** and S **13** as *E/Z*-mixtures showed a weak inhibition of H3N2 and no inhibition of *p*H1N1 virus replication (figure 39, A and C). In contrast, the *Z*-isomers of rubrolide R **12** and S **13** displayed significant inhibition of H3N2 and *p*H1N1 virus replication in a concentration dependent manner compared to the controls (figure 39, B and D). The rubrolide R **12** were more potent against H3N2 (figure 39, A and B) compared to *p*H1N1

(figure 39, C and D) virus replication. Treatment of viral cells with ribavirin, which is a guanosine analogue and inhibits viral RNA synthesis, resulted in no significant inhibition of the influenza virus replication (figure 39). These data demonstrated that the *Z*-isomers of rubrolide R **12** and S **13** inhibit the influenza virus replication of H3 and H1 subtypes more efficiently than the *E/Z*-mixtures.[185]

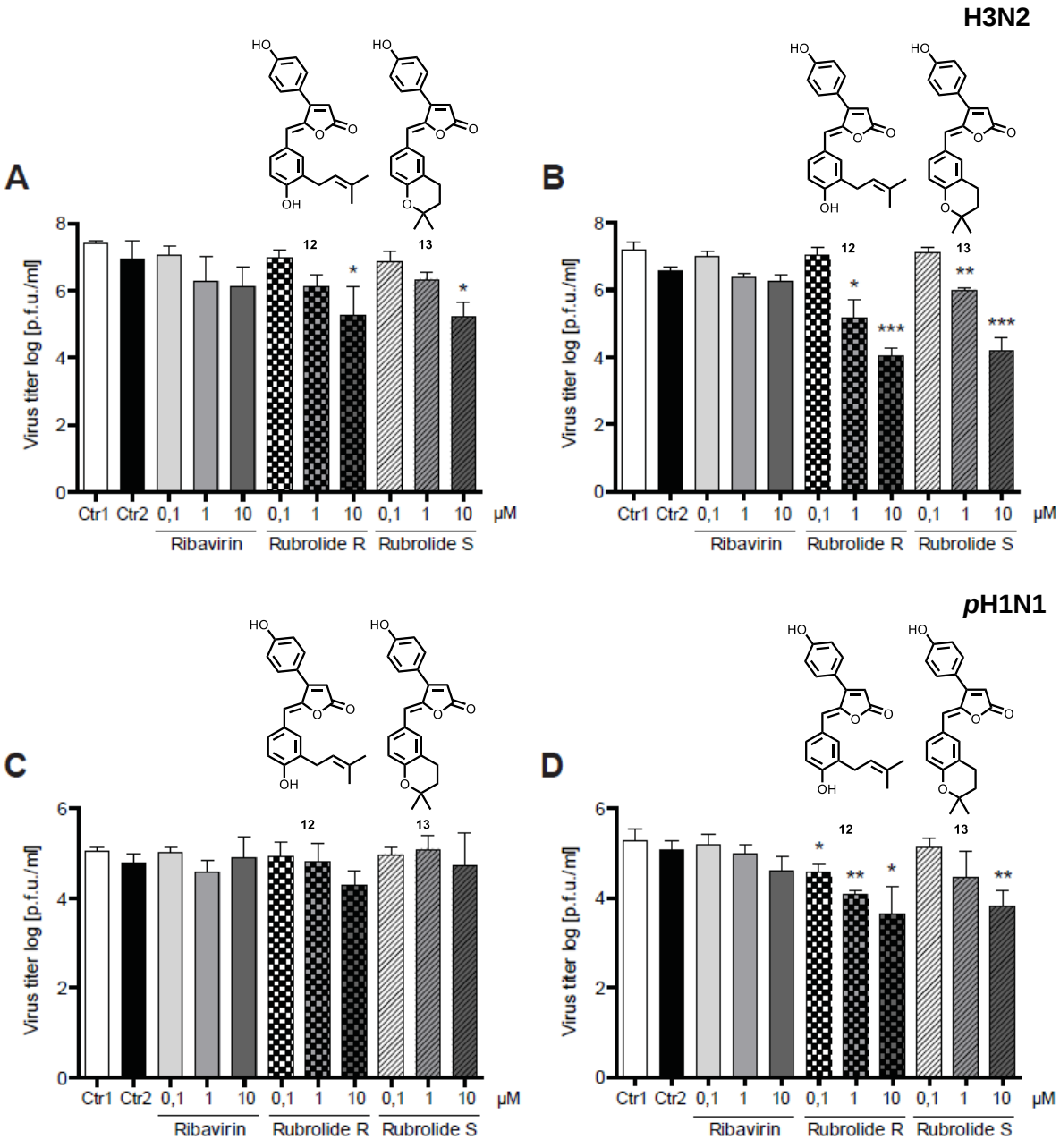

Figure 39: Antiviral effect of rubrolide R 1 and S 2 on influenza virus replication. MDCK cells were infected with either H3N2 (A and B) or pH1N1 (C and D) influenza viruses and co-treated with either an *E*/*Z*-mixtures (A and C) or the *Z*-isomers (B and D) of rubrolide R **12** and S **13**.[185]

Since rubrolide R **12** and S **13** demonstrated antiviral activity against *p*H1N1 and subtype H3N2 (figure 39) the rubrolide derivatives were further tested. Preliminary experiments revealed the high cytotoxicity of catechol-, fluoro- and nitro rubrolide derivatives. Therefore, only the *N*-Acetyl rubrolide structures **176**/**177** (figure 40 and figure 41, entry 2 & 3) and the peracetylmannosy rubrolide S **188** (Figure 40 and Figure 41, entry 4) were assayed against H3N2 and *p*H1N1 (Figure 40 and Figure 41) showing no significant antiviral activity. This confirmed the crucial role of the free hydroxyl group for the biological activity.

Furthermore, the antiviral activity of *chloro*-rubrolide R **154** was investigated for both influenza types. The antiviral tests revealed an improved reduction of the virus titer compared to the non-chlorinated Rubrolide R **12** and S **13**. Hereby, the *chloro*-rubrolide R **154** was more effective against *p*H1N1 (Figure 41) compared to H3N2 (Figure 40).

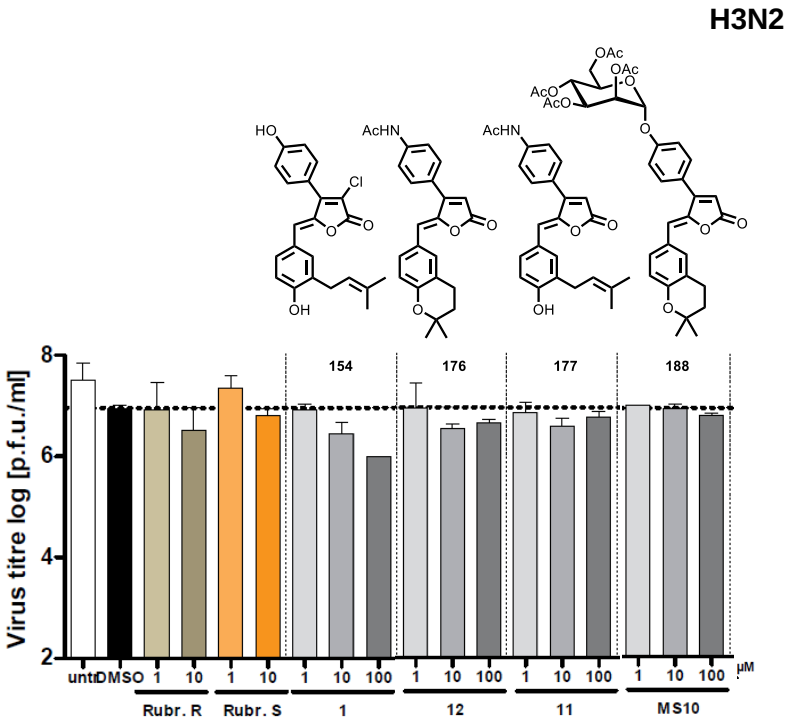

Figure 40: Antiviral effect of rubrolide derivatives on influenza virus replication. MDCK cells were infected with H3N2 influenza virus and preincubated with the *Z*-isomer of the rubrolides (p.f.u.=plaque-forming unit).

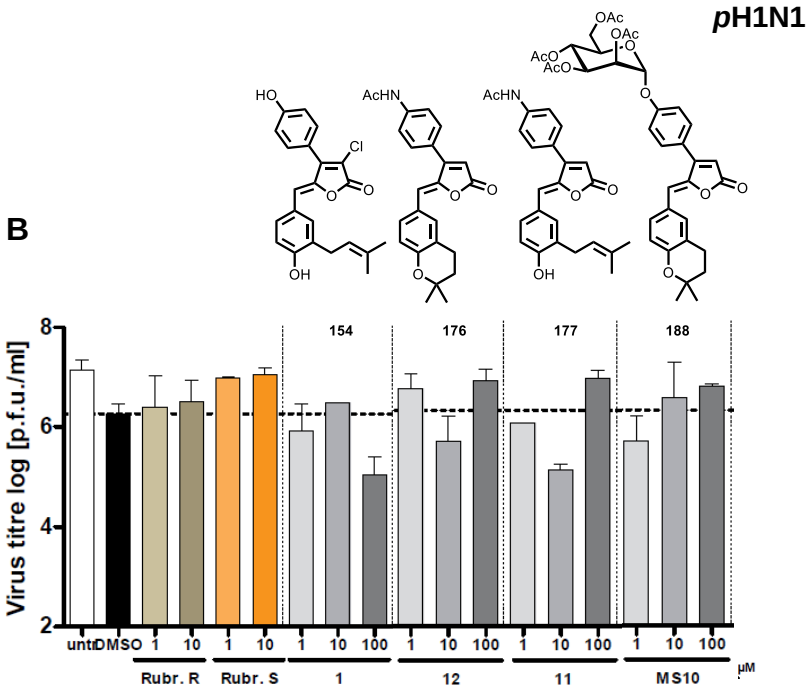

Figure 41: Antiviral effect of rubrolide derivatives on influenza virus replication. MDCK cells were infected with *p*H1N1 influenza virus and preincubated with the *Z*-isomer of the rubrolides (p.f.u.=plaque-forming unit).

The introduction of chlorine to the scaffold improved the lipophilicity resulting in a better permeability through the cell membrane and therefore in a higher bioavailability compared to rubrolide R **12** and S **13.** This might be the reason for the relatively higher antiviral activity of **154**.[5,244]

Moreover, the additional chlorine and its steric demand could hinder the free rotation of the upper phenyl ring around the carbon-carbon bond. Minimization studies by MM2 calculations displayed a higher dihedral angle of $\varphi = 32.9°$ (figure 42, right) for the *chloro*-derivative **154** compared to the rubrolide R **12** with $\varphi = 22.6°$ (figure 42, left). Inducing a twisted orientation of the phenyl moiety on **154** could lead to a fixation of the active conformation and increase the antiviral activity. A similar effect was observed for diclofenac, whereby chlorine substituents fixed the active conformation of the molecule and increased its activity compared to fenoprofen.[244]

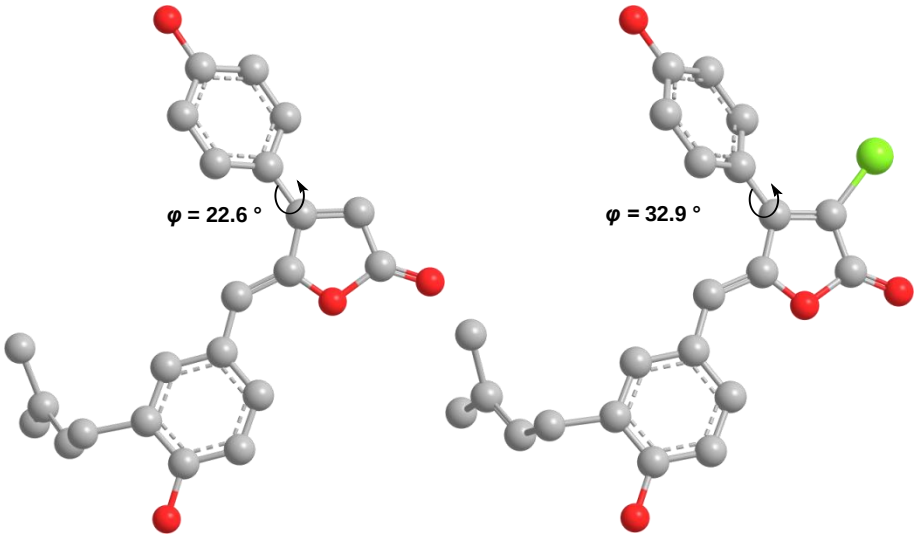

12 **154**

Figure 42: Minimized structures of rubrolide R **12** and the *chloro*-derivative **154** obtained by MM2 calculation showing a dihedral angle of the phenyl moiety to the γ-lactone at rubrolide R **12** φ = 22.6° and for *chloro*-rubrolide R **154** φ = 32.9°.

4. Conclusion

Aim of this work was the synthesis of both natural products rubrolide R **12** and S **13** for biological evaluation. For this purpose a protecting group free total synthesis of **12** and **13** was established. A highly efficient Pd-catalyzed *Suzuki-Miyaura* protocol was established to provide the central butenolide **137**. Starting from triflate **118** and hydroxyphenylboronic acid **138** the desired building block **137** was synthesized in 95% yield after crystallization. After vinylogous aldol condensation of **137** with aldehyde **117**/**139** Rubrolide R **12** and S **13** were obtained in a 54-56% yield over three steps (scheme 69). Moreover, NOESY spectra and X-ray crystal structure analysis verified the *Z*-configuration of the exocyclic double bond of **12** and **13**. Antiviral studies showed significant inhibition of virus replication of a seasonal influenza virus (H3N2) and the pandemic swine influenza (*p*H1N1) superior to ribavirin. Preliminary biological test revealed low antibiotic activity against gram-negative *E. coli* and *P. aeruginosa.*

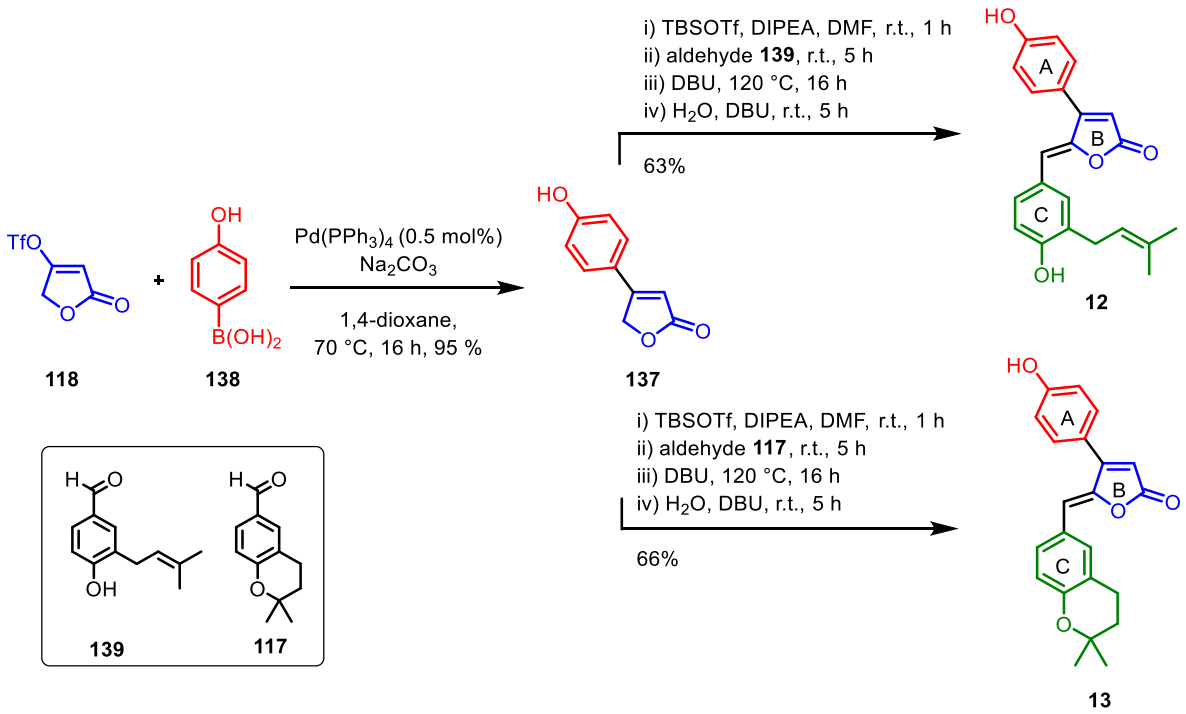

Scheme 69: Protecting group free total syntheses of rubrolide R **12** and S **13**.

Derivatization steps of the aromatic A-ring for structure-activity relation were conducted to verify the vital role of the hydroxyl functions. Hereby, derivatives with a catechol-, fluoro-, *N*-acetyl-, and nitro-substitution on the aromatic A-ring were successfully synthesized using the established protocol (scheme 70). The derivatives showed lower activity in antibacterial and antiviral tests. This indicated the necessity of the free hydroxyl group at phenyl ring B for the biological activity. Further derivatization steps considered the introduction of a chlorine

substituent at the central butenolide scaffold. To our delight *chloro*-rubrolide R **154** demonstrated growth inhibition of gram-positive *S. aureus* and higher antiviral activity against H3N2 and *p*H1N1 compared to the non-chlorinated origin **12**.

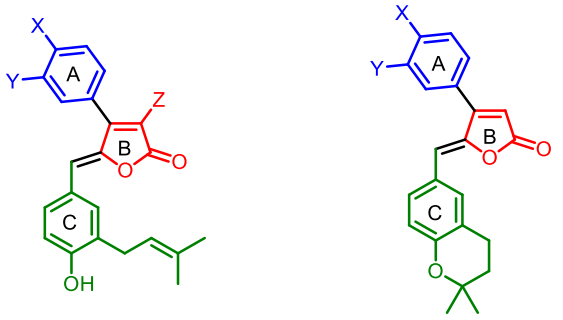

X = -OH, Y = -OH, Z = -H **174** 83%
X = -NHAc, Y = -H, Z = -H **176** 67%
X = -F, Y = -H #, Z = -H **178** 63%
X = -OH, Y = -H #, Z = Cl **154** 17%

X = -OH, Y = -OH **175** 30%
X = -NHAc, Y = -H **177** 42%
X = -F, Y = -H **179** 57%
X = $-NO_2$, Y = -H **181** 14%

Scheme 70: Tested rubrolide R and S derivatives.

After observing low solubility of rubrolide R **12** and S **13** and their derivatives in biological tests, glycosylation of rubrolide S **188** was investigated in order to increase water solubility. *Koenigs-Knorr* glycosylation provided the peracetylated mannosyl-rubrolide S **188** in yields up to 70%. Chemical and enzymatic deacetylation steps induced the cleavage of the glycosidic bond, respectively. Nonetheless, antiviral studies of **188** demonstrated as expected no significant activity against H3N2 and *p*H1N1.

To conclude, this thesis provided the short and protecting-group-free syntheses rubrolides R **12** and S **13** and their derivatives. Both rubrolides showed inhibition of virus replication of a seasonal influenza virus (H3N2) and the pandemic swine influenza (*p*H1N1) from 2009. By introduction of chlorine to the B-ring an increased antiviral activity against both strains was observed. Further derivatization steps of the hydroxyl function, revealed the necessity for the biological activity.

Furthermore, first steps towards the total synthesis of prunolides were investigated with a two fold carbonylative *Suzuki-Miyaura* cross-coupling and saponification/acid mediated cyclization sequence to provide the prunolide scaffold. Herein, the vinyl bromide **127** and diboronic ester **125** were considered as suitable building blocks. Starting from 4-iodoinsole **192** and trimethylsilylacetylene **193**, alkyne **190** was obtained and converted into the corresponding diboronic esters **125** and **202** *via* Pt-catalyzed diborylation. Optimization steps allowed a significant reduced catalyst loading of 0.2 mol%, affording the desired building blocks **125** and **202** in up to 90%. The vinyl bromide **127** was obtained by a *Vilsmeyer Haak*/*Pinnick oxidation*/esterification sequence with a 43% yield over three steps. Alternatively, Vanadium catalyzed oxidative esterification of the aldehyde **128** provided the

vinyl bromide **127** in 22% yield enabling the reduction of the synthetic steps. In addition, the corresponding vinyl tosylate **211** as alternative substrate was obtained in an 82% yield over two steps after recrystallization. The two-fold carbonylative *Suzuki-Miyaura* cross-coupling with **125** and **127** under the use of 3.0 bar CO-gas and in situ generation of carbon monoxide did not afford the desired product. In following studies the acylative coupling was considered for the prunolide synthesis. Herein, preliminary screenings demonstrated the successful coupling of succinimidyl active ester of benzoic acid **224** with phenylboronic acids **105** and **119** in an acylative manner. According to a protocol of *Levacher* et al. vinyl active ester **221** was obtained from the vinyl bromide **127** and tosylate **211**. Nonetheless, screenings of the vinyl active ester and the diboronic ester did not generate the desired structure.

A simplified model reaction for the carbonylative *Suzuki-Miyaura* cross-coupling was used to proof the feasibility of the novel methodology of this reaction type. Coupling of vinyl building block **211**with phenylboronic acids **105** was achieved. For this purpose an effective and robust $Pd(TFA)_2/PCy_3$ catalyst was established for coupling of vinyl tosylates **210-212** and various aryl boronic acids **105**, **119**, **168**, **230-234** with $Mo(CO)_6$ **229** as carbon monoxide source. Carbon-NMR and additional single crystal structure analysis verified the successful formation of the *γ*-ketoester **242** and **244**. In analogy to the proposed prunolide synthesis, these structures served as intermediate for the synthesis of *γ*-hydroxybutenolide **259-279** motif *via* saponification/cyclization sequence in moderate to good yields (scheme 71).

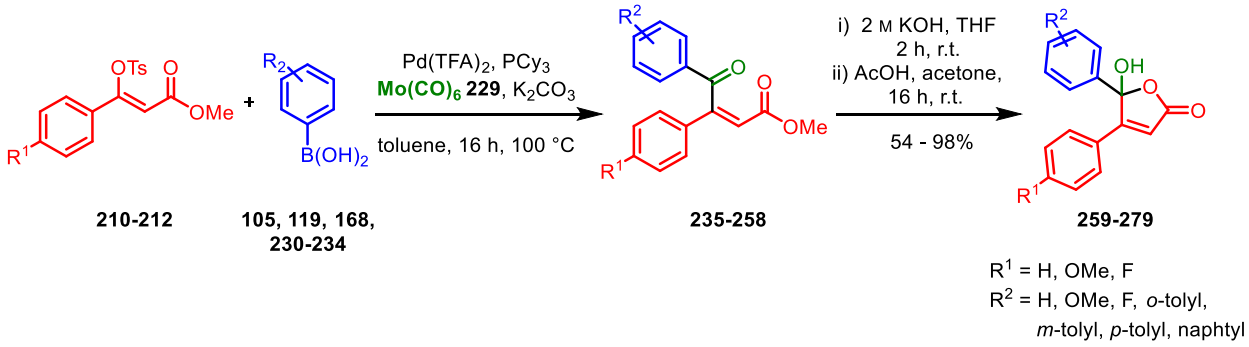

Scheme 71: Synthesis of hydroxybutenolides **259-279** *via* carbonylative *Suzuki-Miyaura* cross-coupling followed by a saponification/acid mediated cyclization.

Although the vinyl building blocks **210-212** showed sufficient conversion with various boronic acids **105**, **119**, **168**, **230-233** the application of the diboronic ester **125** and **202** resulted in an inseparable mixture of products. This indicates that the reactivity of the diboronic sources was not sufficient for the twofold *Suzuki-Miyaura* cross-coupling.

Although the prunolide scaffold was not obtained, a robust and safe Pd-catalyzed reaction has been developed for the first reported carbonylative Suzuki–Miyaura cross-coupling of vinyl tosylates **210-212** with aryl boronic acids **105**, **119**, **168**, **230-233** with $Mo(CO)_6$ **229** as

solid carbon monoxide source. By avoiding CO gas this method provides a modular, very robust and safe protocol for the preparation of varieties of *γ*-ketoesters **235-255**. These compounds were highly valuable key intermediates for the synthesis of *γ*-hydroxybutenolides **259-279** via a saponification/acid mediated cyclization sequence.

5. Zusammenfassung

Ziel der Arbeit war die Synthese von Rubrolide R **12** und S **13** zur biologische Evaluierung. Hierfür wurde eine effiziente schutzgruppenfreie Totalsynthese unter Erhalt beider Naturstoffe entwickelt. In einer Pd-katalysierten *Suzuki-Miyaura* Kreuzkupplung erfolgte die Darstellung des zentralen Butenolidbausteins **137**. Ausgehend von Triflat **118** und der Hydroxyphenyl-boronsäure **138** wurde dieser essentielle Baustein in einer Ausbeute von 95% nach Kristallisation erhalten. Anschließend wurden Rubrolide R **12** und S **13** mittels vinyloger Aldolkondensation in einer Gesamtausbeute von 54% bzw. 56% über drei Syntheseschritte erhalten (Schema 72). NOESY Spektren und zusätzliche Röntgenkristallstrukturen verifizierten die Z-Konfiguration beider Naturstoffe. Rubrolide R **12** und S **13** zeigten eine signifikante Inhibition der Virusreplikation des saisonalen Influenzavirus H3N2 und pandemischen Schweinegrippevirus *p*H1N1, welche dem Standard Ribavirin überlegen waren. In vorläufigen biologischen Untersuchungen konnte eine schwache antibiotische Aktivität gegenüber gram-negative *E.coli* und *P. aeruginosa* Bakterienstämme beobachtet werden.

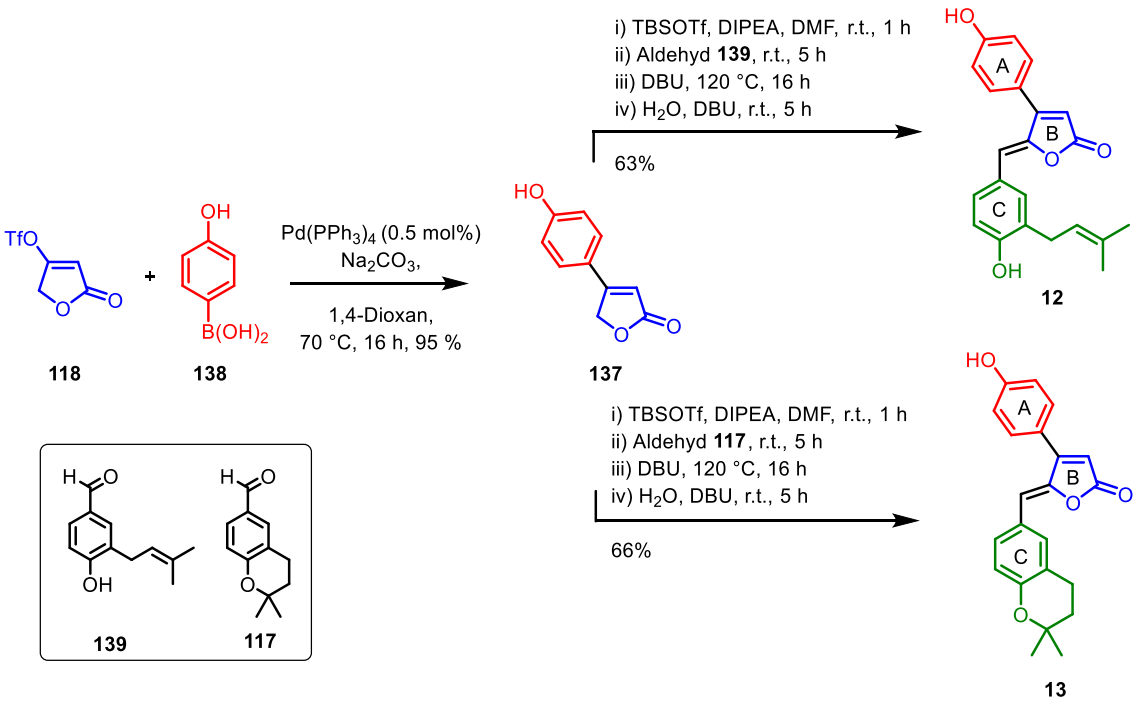

Schema 72: Schutzgruppenfreie Totalsynthese von Rubrolide R **12** und S **13**.

In anschließenden Untersuchungen wurden zur Verifizierung der Rolle der Hydroxyfunktion für die biologische Aktivität, Derivatisierungsschritte am aromatischen A-Ring für die Struktur-Aktivitäts-Beziehung durchgeführt. Dazu erfolgte die Synthese von Catechol-, Fluor-, *N*-Acetyl- und Nitroderivate von Rubrolid R und S **174-181** (Abbildung 74). Anschließende antibakterielle und antivirale Untersuchungen bestätigten die Notwendigkeit der

Hydroxylgruppe am aromatischen A-Ring. Des Weiteren wurde basierend auf den Untersuchungen von *Manzanaro* et al. die Chlorierung am zentralen Furanon B-Ring untersucht. Hierbei zeigte sich, dass *chloro*-Rubrolid R **154** eine antibiotische Aktivität gegenüber gram-positivem *S. aureus* und eine höhere antivirale Aktivität gegenüber H3N2 und *p*H1N1, verglichen zum Rubrolid R **12** besitzt.

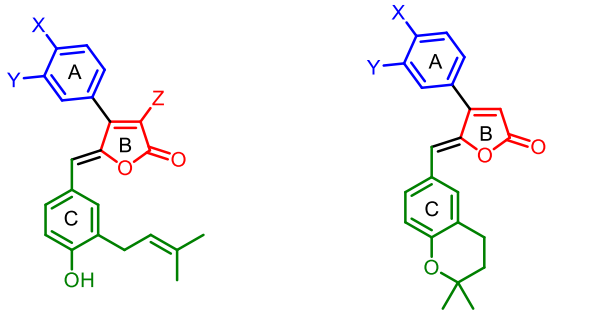

X = -OH, Y = -OH, Z = -H **174** 83%
X = -NHAc, Y = Z = H **176** 67%
X = -F, Y = -H #, Z = -H **178** 63%
X = -OH, Y = -H #, Z = Cl **154** 17%

X = -OH, Y = -OH **175** 30%
X = -NHAc, Y = -H **177** 42%
X = -F, Y = -H **179** 57%
X = -NO_2, Y = -H **181** 14%

Abbildung 74: Rubrolide R und S Derivate **174-181**.

Zusätzlich wurde die Glykosilierung von Rubrolid S **13** untersucht, um eine verbesserte Wasserlöslichkeit zu erreichen. Mittels *Koenigs-Knorr* Glykosilierung wurde das peracetylierte mannosyl-Rubrolid S Konjugat **188** in 70% Ausbeute synthetisiert. Anschließende Deacetylierungsschritte unter chemischen und enzymatischen Bedingungen führte ausschließlich zur Spaltung der glykosidischen Bindung. Antivirale Untersuchungen des peracetylierten Glykokonjugates zeigten keine signifikante Aktivität gegenüber H3N2 und H1N1.

Im Rahmen dieser Arbeit wurde eine kurze und schutzgruppenfreie Synthesezur Darstellung von Rubrolid R 12 und S **13** und deren Derivate entwickelt. Beide Naturstoffe zeigten in antiviralen Tests eine signifikante Inhibierung der Virusreplikation des saisonalen Influenzavirus (H3N2) und der pandemischen Schweinegrippe (*p*H1N1). Durch die Einführung von Chlor-Substituenten am Butenolidgrundgerüst konnte eine erhöhte antivirale Aktivität gegenüber beiden Stämmen beobachtet werden. Zudem wurde durch Derivatisierungdes aromatischen A-Ringes die Relevanz der phenolischen Hydroxygruppen für die biologische Aktivität weiter verdeutlicht.

Des Weiteren wurde die Totalsynthese von Prunoliden untersucht, wobei eine zweifache carbonylierende *Suzuki-Miyaura* Kreuzkupplung mit einer anschließenden Hydrolyse gefolgt von einersauer induzierten Zyklisierung als Schlüsselschritte vorgesehen waren. Hierbei wurden das Vinylbromid **127** und der Diboronsäureester **125** als geeignete Bausteine

verwendet. Ausgehend von 4-Iodanisol **192** und Trimethylsilylacetylen **193**, wurde das Alkin **190** via zweifacher *Sonogashira* Kreuzkupplung erhalten. Abschließend wurde mittels Pt-katalysierter Diborylierung der Diboronsäureester **125** synthetisiert. Optimierung der Reaktion ermöglichte die Durchführung mit signifikant reduzierter Katalysatorbeladung von 0.2 mol-%, wobei die Bausteine **125** und **202** in Ausbeuten von 90% erhalten wurde.

Das Vinylbromid **127** wurde über eine *Vilsmeyer Haak/Pinnick* Oxidation/Veresterung Reaktionssequenz in einer Gesamtausbeute von 43% erhalten. Alternativ ermöglichte eine Vanadium-katalysierte oxidative Veresterung des Aldehyds **128** die Darstellung von Baustein **127** über eine verkürzte Syntheseroute in einer Ausbeute von 22%. Im Rahmen der Arbeit erfolgte zusätzlich die Darstellung des korrespondierenden Vinyltosylates **211** in einer Ausbeute von 82% über zwei Schritte nach Umkristallisation. Die zweifache carbonylierenden *Suzuki-Miyaura* Kreuzkupplung von **127/211** und **125** mit 3.0 bar oder in situ erzeugtem Kohlenstoffmonoxid führte nicht zur Darstellung des gewünschten Diketons **220**. Aus diesem Grund wurde die acylierende Kreuzkupplung für die Prunolidesynthese untersucht. Hierfür wurde in vorausgehenden Untersuchungen Succinimidyl Aktivester der Benzoesäure **224** mit diversen Boronsäuren **105** und **119** zum Keton umgesetzt. Nachdem erfolgreich die Anwendbarkeit von Succinimidyl Aktivester für acylierende *Suzuki-Miyaura* Reaktionen untersucht worden war, erfolgte anschließend die Darstellung des Vinylaktivesters nach einem modifizierten Protokoll von *Levacher* et al. Jedoch konnte mit diesem Baustein **127**/**211** und dem Diboronsäureester **125/202** nicht das gewünschte Diketon **220** synthetisiert werden.

Die Durchführbarkeit der carbonylierenden *Suzuki-Miyaura* Kreuzkupplung wurde zunächst an einer vereinfachten Modellreaktion untersucht. Hierbei wurde Phenylboronsäure **105** und Vinyltosylat **211** als geeignete Testsubstrate ausgewählt, da diese bisher in carbonylierenden Kreuzkupplungen nicht untersucht worden sind. Nach ausgiebiger Optimierung konnte ihm Rahmen des Projektes ein effektives und robustes $Pd(TFA)_2/PCy_3$ Katalysatorsystem etabliert werden, wobei $Mo(CO)_6$ als geeignete Kohlenstoffmonoxidquelle verwendet wurde. In fortlaufenden Untersuchungen konnten verschiedene Vinyltosylate **210-212** mit einer Reihe von Arylboronsäuren **105**, **119**, **168**, **230**-**233** erfolgreich zum Keton umgesetzt werden. ^{13}C-NMR Untersuchungen und zusätzliche Röntgenkristallstruktur Analysen konnten die Synthese des *γ*-Ketoester **236** bestätigen. In Analogie zur Prunolidsysnthese dienten die *γ*-Ketoester **235-255** als Schlüsselintermediate zur Darstellung von *γ*-Hydroxybutenolide **259-279** via Hydrolyse und sauer vermittelter Zyklisierung in guten Ausbeuten (Schema 75).

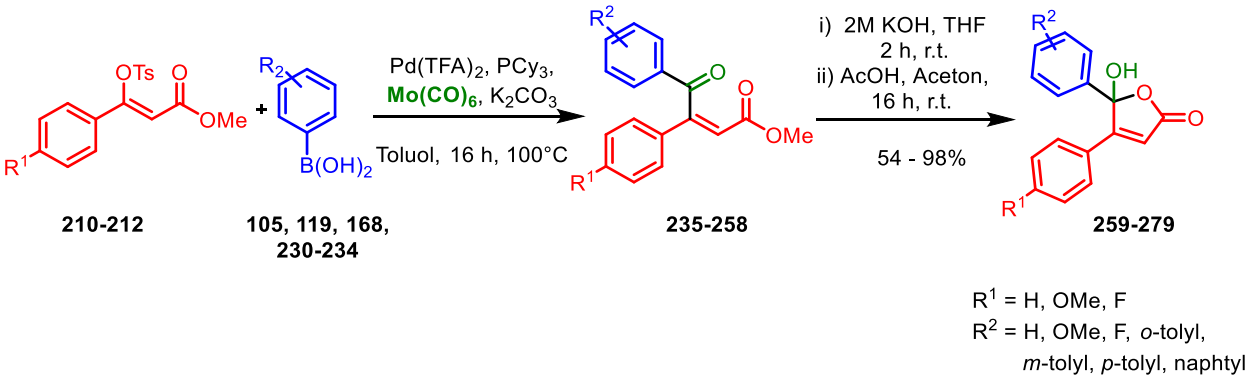

Schema 75: Synthese von γ-Hydroxybutenoliden **259-279** via carbonylierender *Suzuki-Miyaura* Kreuzkupplung gefolgt von Hydrolyse/sauer vermittelten Zyklisierung.

Zwar konnte in vorausgehenden Untersuchungen der Vinylbaustein **210-212** erfolgreich mit unterschiedlichen Boronsäuren umgesetzt werden, jedoch führte die Reaktion mit dem Diboronsäureestern **125/202** zu einem undefinierbaren Produktgemisch. Dies impliziert, dass die Reaktivität der Diboronsäureester für die carbonylierende *Suzuki-Miyaura*-Kreuzkupplung nicht ausreichend war.

Obwohl das Prunolid-Gerüst nicht erhalten wurde, konnte eine effiziente und robuste Pd-katalysierte carbonylative Suzuki-Miyaura-Kreuzkupplung entwickelt werden. Hierbei konnten erstmals Vinyltosylate **210-212** mit verschiedenen Arylboronsäuren **105**, **119**, **168**, **230-233** mit $Mo(CO)_6$ **229** als Kohlenstoffmonoxidquelle zum γ-Ketoester **235-255** gekuppelt werden. Die Verwendung von $Mo(CO)_6$ ermöglicht eine sicheres, modulares und sehr robustes Syntheseprotokoll von γ-Ketoestern **235-255**. Diese Verbindungen sind als wertvolle Schlüsselverbindungen für die Synthese von γ-Hydroxybutenoliden **259-279**.

6. Experimental Part

6.1. General Information

All reactions requiring anhydrous condition were performed under argon atmosphere. Reactions carried out at 0 °C employed an ice bath and reactions carried out at –78 °C a liquid nitrogen/acetone bath. Microwave reactions were performed in a *Biotage*® Initiator+ Microwave System. Tf_2O and NaH were stored under argon atmosphere. All commercially purchased chemicals were used without further purification, unless otherwise noted. Infrared spectra were obtained from neat solids or liquids on a *Jasco* FT/IR-4100 with an ATR PRO470-H unit. Melting points were determined in open capillary tubes and are uncorrected. High resolution mass spectra were measured with an Agilent 6224 ESI-TOF. ^{1}H-NMR and ^{13}C-NMR spectra were recorded on a Bruker Fourier 300MHz, *Bruker* AVANCE I 400 or *Bruker* AVANCE III HD 600 MHz instrument. As internal standards, the residual proton signals of deuterated solvent δ ^{1}H/^{13}C (solvent) = 2.05 / 29.84, 206.26 (acetone); 7.26 / 77.16 ($CDCl_3$); 2.50 / 39.52 (DMSO); 3.31 / 49.00 (methanol) and are tabulated as follows: chemical shift, multiplicity (s = singlet, d = doublet, t = triplet q = quartet, m = multiplet) and coupling constant(s), number of protons. Reactions were monitored by thin layer chromatography on silica-coated aluminum plates (*Macherey-Nagel*, DC Kieselgel Alugram® Xtra SIL G/UV254, layer thickness 0.2 mm). Low and non-fluorescent compounds were visualized with a Hannessian staining (5.0 g ceric sulfate, 25 g ammonium molybdate, 50 mL sulfuric acid and 450 mL water) or permanganate solution (3.0 g potassium permanganate, 20 g potassium carbonate, 5 mL 5% sodium hydroxide solution and 300 mL water). Flash chromatography was performed using silica 60 (particle size 0.040-0.063 nm, 230-400 mesh, *Macherey-Nagel*) at room temperature.

6.2. General procedures

6.2.1. General procedure 1: Pd-catalyzed *Suzuki-Miyaura* coupling[185]

A solution of 5-oxo-2,5-dihydrofuran-3-yltrifluoromethane sulfonate **131** (1.00 equiv.), arylboronic acid **119, 138, 166-169** (3.00 equiv.) and Na_2CO_3 (3.00 equiv.) were dissolved in 1,4-dioxane (0.500 mol/L) and degassed with argon for 10 min. Afterwards, $Pd(PPh_3)_4$ (0.5–6.0 mol%) was added to the solution and stirred for 16 h at 70 °C. The reaction was cooled to room temperature, filtered through celite® and the solvent was removed in vacuum. The crude product was purified by recrystallization from chloroform or column chromatography (silica gel, PE/EtOAc).

6.2.2. General procedure 2: Pd-catalyzed *Suzuki-Miyaura* coupling II.

A solution of 5-oxo-2,5-dihydrofuran-3-yltrifluoromethane sulfonate **131** (1.00 equiv.), arylboronic acid **119, 138, 166-169** (3.00 equiv.) and K_3PO_4 (3.00 equiv.) were dissolved in 1,4-dioxane (0.500 mol/L) and degassed with argon for 10 min. Afterwards, $Pd(PPh_3)_4$ (0.5–6.0 mol%) was added to the solution and stirred for 16 h at 70 °C. The reaction was cooled to room temperature, filtered through celite® and the solvent was removed in vacuum. The crude product was purified by column chromatography (silica gel, PE/EtOAc).

6.2.3. General procedure 3: *β*-Ketoester synthesis 216-218

A solution of sodium hydride (2.50 equiv.) and dimethylcarbonate **215** (2.50 equiv.) in toluene (3.80 mol/L) was stirred for 30 min at 115 °C. Then, acetophenone **215, 13, 214** (1.00 equiv.) in toluene (3.00 mol/L) was added to the solution and stirred for 1 h at 115 °C. Afterwards, the mixture was cooled to room temperature and neutralized with $AcOH/H_2O$ (1:1). The mixture was extracted three times with EtOAc. The combined organic layers were dried over $MgSO_4$, filtered and the solvent was removed in vacuum. The product **216-218** was used without further purification.

6.2.4. General procedure 4: (*Z*)-Enol tosylation of β-ketoester 235-255 [138]

The *β*-ketoester **216-218** (1.00 equiv.), TMEDA (1.50 equiv.) and LiCl (1.50 equiv.) were dissolved in MeCN (0.70 mol/L) and cooled to 0 °C. Afterwards, TsCl (1.50 equiv.) in MeCN (1.60 mol/L) was added to the solution and stirred for 16 h at room temperature. Water (130 equiv.) was added to the reaction and the extracted three times with EtOAc. The combined organic layers were dried over $MgSO_4$, filtered and the solvent was removed in vacuum. The crude product **210-212** was purified by recrystallization from PE/EtOAc.

6.2.5. General procedure 5: Pd-catalyzed carbonylative *Suzuki-Miyaura* cross-coupling with $Mo(CO)_6$[138]

A mixture of vinytosylate **210-212** (1.00 equiv.), boronic acid **105, 119, 168, 230-234** (2.00 equiv.) and potassium carbonate (3.00 equiv.) was dissolved in toluene (0.150 mol/L) and degassed with argon for 5 min. Afterwards, $Pd(TFA)_2$ (4.0 mol%), PCy_3 (8.0 mol%) and $Mo(CO)_6$ **229** (2.00 equiv.) were added to the solution and stirred for 16 h at 100 °C. The reaction was cooled to room temperature, filtered through celite® and the solvent was removed in vacuum. The crude product was purified by column chromatography (silica gel, PE/EtOAc) to yield the *γ*-ketoester **235-258**.

6.2.6. General procedure 6: Pd-catalyzed carbonylative *Suzuki-Miyaura* cross-coupling with $Mo(CO)_6$ under microwave irradiation [138]

A mixture of vinyltosylate **210-212** (1.00 equiv.), boronic acid **105, 119, 168, 230-234** (2.00 equiv.) and potassium carbonate (3.00 equiv.) was dissolved in toluene (0.150 mol/L) and degassed with argon for 5 min. Afterwards, $Pd(TFA)_2$ (4.0 mol%), PCy_3 (8.0 mol%) and $Mo(CO)_6$ **229** (2.00 equiv.) were added to the solution and stirred for 1 h at 100 °C under microwave irradiation. The reaction was cooled to room temperature, filtered through celite® and the solvent was removed in vacuum. The crude product was purified by column chromatography (silica gel, PE/EtOAc) to yield the *γ*-ketoester **235-255**.

6.2.7. General procedure 7: Synthesis of 5-hydroxybutenolides[138]

The *γ*-ketoester **235-252** and KOH (2 M in H_2O, 3.00 equiv.) were dissolved in THF (0.200 mol/L) and stirred at room temperature overnight. Afterwards, the solution was neutralized with AcOH and the solvent was removed in vacuum. Then, AcOH (0.100 mL) was added and stirred until full conversion (TLC control). The solvent was removed under reduced pressure and coevaporated with toluene. The crude product was purified by reversed phase column chromatography (RP-C_{18} silica gel, MeCN/H_2O + 0.1% FA) to yield the *γ*-hydroxy-butenolide **259-282**.

6.3. Synthetic procedures

6.3.1. Starting material synthesis of furanones for rubrolide synthesis

5-Oxo-2,5-dihydrofuran-3-yl-trifluoromethanesulfonate 118[185]

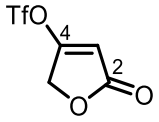

118

Prepared using a modified protocol originally reported by *Grigg* et al.[174] Under argon atmosphere tetronic acid **131** (500 mg, 4.99 mmol, 1.00 equiv.) was dissolved in anhydrous CH_2Cl_2 (30.0 mL) and the solution was cooled to 0 °C. Then, NEt_3 (820 µL, 5.90 mmol, 1.20 equiv.) and Tf_2O (1.00 mL, 5.94 mmol, 1.20 equiv.) were added at 0 °C and the mixture was stirred for 2 h. Afterwards, the reaction was diluted with CH_2Cl_2 (20.0 mL) and the organic layer was washed with water (3 × 100 mL). The organic layer was dried over $MgSO_4$, filtered and the solvent was removed in vacuum. The crude product was purified by Kugelrohr-distillation to yield triflate **118** (1.00 g, 4.33 mmol, 87%) as colorless oil.

Bp: 140 °C (9.3×10^{-2} mbar).

UV (CH_2Cl_2): λ_{max} (nm) = 225, 296.

IR (ATR): 3141, 1784, 1649, 1213, 1125, 1047, 930, 808, 765, 601, 522 cm^{-1}.

^{1}H-NMR (400 MHz, $CDCl_3$): δ = 6.07 (t, J = 1.8 Hz, 1 H, 3-H), 4.89 (d, J = 1.8 Hz, 2 H, 5-H_2).

^{13}C-NMR (101 MHz, $CDCl_3$): δ = 168.9 (C-4), 166.9 (C-2), 118.6 (q, J_{CF} = 322 Hz, -CF_3), 104.7 (C-3), 67.6 (C-5).

$C_5H_3F_3O_5S$ (232.13 g/mol).

5-Oxo-2,5-dihydrofuran-3-yl-trifluoromethanesulfonate 34

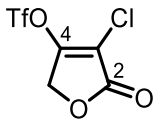

34

Prepared using a modified protocol originally reported by *Grigg* et al.[174] Under argon atmosphere *chloro*-tetronic acid **157** (1.12 g, 8.33 mmol, 1.00 equiv.) was dissolved in anhydrous CH_2Cl_2 (20.0 mL) and the solution was cooled to 0 °C. Then, NEt_3 (1.74 mL, 12.5 mmol, 1.50 equiv.) and Tf_2O (2.10 mL, 12.5 mmol, 1.50 equiv.) were added at 0 °C and the mixture was stirred for 4 h. Afterwards, the reaction was diluted with CH_2Cl_2 (100.0 mL) and the organic layer was washed with water (4 × 100 mL) and brine (100 mL). The organic

layer was dried over $MgSO_4$, filtered and the solvent was removed in vacuum. The crude product was purified by Kugelrohr-distillation to yield the triflate **34** (1.51 g, 5.67 mmol, 68%) as colorless oil.

Bp: 132 °C (9.3×10^{-2} mbar).

UV (CH_2Cl_2): λ_{max} (nm) = 229.

IR (ATR): 1789, 1677, 1437, 1358, 1291, 1219, 1128, 1046, 1022, 994, 799, 759, 723, 616, 592 cm^{-1}.

^{1}H-NMR (400 MHz, $CDCl_3$): δ = 5.05 (s, 2 H, 5-H_2).

^{13}C-NMR (101 MHz, $CDCl_3$): δ = 164.4 (C-2), 159.1 (C-4), 118.5 (q, J_{CF} = 119 Hz), 112.1 (C-3), 66.8 (C-5).

$C_5H_2ClF_3O_5S$ (266.57 g/mol).

4-Bromo-1,2-benzenediol 165

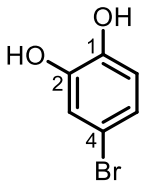

165

Prepared using a protocol originally reported by *Zhao* et al.[200] To a stirred suspension of 5-bromo-2-hydroxybenzaldehyde **164** (6.00 g, 29.8 mmol, 1.00 equiv.) in aq. NaOH (1.00 M in H_2O, 34.0 mL) H_2O_2 (30% in H_2O, 3.04 mL, 3.38 g, 29.8 mmol, 1.00 equiv.) was added dropwise at room temperature and stirred for 2 h. Afterwards, the mixture was acidified with H_2SO_4 (96%, 1.00 mL), neutralized with sat. aq. $NaHCO_3$ solution and extracted with Et_2O (3 × 50 mL). The combined organic layers were washed with H_2O (50 mL), dried over $MgSO_4$, filtered and the solvent was removed in vacuum. The desired product **165** (5.54 g, 29.3 mmol, 98%) was obtained as orange solid.

TLC: R_f = 0.38 (PE/EtOAc 4:1 *v/v*).

Mp: 78 °C (*lit.:* 86 °C[200])

UV ($CHCl_3$): λ_{max} (nm) = 238, 285.

IR (ATR): 2362, 2341, 1828, 1696, 1588, 1504, 1338, 1234, 1110, 1045, 886, 801, 797, 575, 505 cm^{-1}.

^{1}H-NMR (500 MHz, DMSO-d_6): δ (ppm) = 9.27 (s, 2 H, 2 × OH), 6.86 (d, J = 2.4 Hz, 1 H, 5-H), 6.75 (dd, J = 8.5, 2.4 Hz, 1 H, 3-H), 6.67 (d, J = 8.5 Hz, 1 H, 6-H).

^{13}C-NMR (101 MHz, DMSO-d_6): δ (ppm) = 146.7 (C-2), 145.0 (C-1), 121.7 (C-3), 118.2 (C-5), 117.2 (C-6), 109.6 (C-4).

MS (ESI) for $[C_6H_5BrO_2 + H]^+$ calcd.: 188.9546
found:188.9523.

$C_6H_5BrO_2$ (189.01 g/mol).

4-Bromo-1,2-bis[[(1,1-dimethylethyl)dimethyl-silyl]oxy]-benzene 166

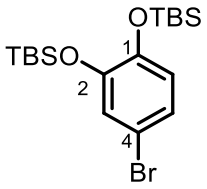

166

Under argon atmosphere 4-bromo-1,2-benzenediol **165** (1.63 g, 8.62 mmol, 1.00 equiv.) and imidazole (1.41 g, 20.7 mmol, 2.40 equiv.) were dissolved in anhydrous CH_2Cl_2 (30.0 mL) at room temperature. A suspension of TBSCl (3.12 g, 20.7 mmol, 2.40 equiv.) in anhydrous CH_2Cl_2 (20 mL) was added dropwise to the reaction mixture and stirred at room temperature for 16 h. The reaction mixture was filtered through a silica plug (EtOAc) and the solvent was removed in vacuum to yield the TBS protected catechol **166** (3.41 g, 8.17 mmol, 95%) as pale yellow oil.

TLC: R_f = 0.85 (PE/EtOAc 40:1 *v/v*).

UV ($CHCl_3$): λ_{max} (nm) = 239, 283.

IR (ATR): 2960, 2361, 1740, 1491, 1399, 1287, 1214, 1206, 1123, 938, 892, 823, 781, 750, 670 cm^{-1}.

^{1}H-NMR (600 MHz, $CDCl_3$): δ (ppm) = 6.95–6.90 (m, 2 H, 3-H, 5-H), 6.69 (d, J = 8.5 Hz, 1 H, 6-H), 0.99, 0.97 (2 × s, 18 H, 2 × ($C(CH_3)_3$), 0.20, 0.18 (2 × s, 2 × 6 H, 2 × Si-CH_3).

^{13}C-NMR (101 MHz, $CDCl_3$): δ (ppm) = 148.0 (C-2), 146.6 (C-1), 124.4 (2 C, C-3, C-5), 122.3 (C-6), 112.9 (C-4), 26.0 (6 C, 2 × 3 C, ($C(\underline{C}H_3)_3$), 18.6 (2 C, ($\underline{C}(CH_3)_3$), –4.0 (4 C, 4 × Si-CH_3).

MS (ESI) for $[C_{18}H_{33}BrO_2Si_2 + H]^+$ calcd: 417.1281
found: 417.1251.

$C_{18}H_{33}BrO_2Si_2$ (417.53 g/mol).

[3,4-Bis[[(1,1-dimethylethyl)dimethylsilyl]oxy]phenyl]boronic acid 161

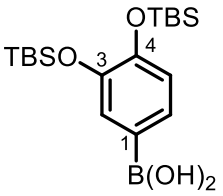

161

A solution of 4-bromo-1,2-bis{[(1,1-dimethylethyl)dimethylsilyl]oxy}benzene **166** (3.00 g, 7.19 mmol, 1.00 equiv.) in anhydrous THF (20.0 mL) was cooled to –78 °C, followed by dropwise addition of *n*-BuLi (1.6 M in *n*-hexane, 5.40 mL, 8.62 mmol, 1.20 equiv.) and stirred for 30 min. Afterwards, B(O*i*Pr)$_3$ (3.65 mL, 2.97 g, 15.8 mmol, 2.20 equiv.) was added dropwise and stirred at –78 °C for 1 h and for an additional 1 h at room temperature. After addition of aq. HCl (1 M, 60.0 mL) and EtOAc (100 mL), the aqueous layer was extracted with EtOAc (3 × 50 mL) and the combined organic layers were washed with brine (100 mL), dried over $MgSO_4$, filtered and the solvent was removed in vacuum. The crude product was purified by column chromatography (silica gel, CH_2Cl_2/MeOH 50:1) to yield the boronic acid **161** (2.25 g, 5.88 mmol, 82%) as light yellow liquid.

TLC: $\mathbf{R_f}$ = 0.26 (CH_2Cl_2/MeOH 50:1 *v/v*).

UV ($CHCl_3$): λ_{max} (nm) = 239, 283.

IR (ATR): 3449, 3012, 2363, 2333, 1735, 1476, 1464, 1399, 1346, 1231, 1204, 1034, 889, 835, 754 cm^{-1}.

^{1}H-NMR (500 MHz, DMSO-d_6): δ (ppm) = 7.30–7.26 (m, 2 H, 2-H, 6-H), 6.80 (d, J = 7.8 Hz, 1 H, 5-H), 0.96, 0.94 (2 × s, 2 × 9 H, 2 × (C(CH$_3$)$_3$), 0.18, 0.17 (2 × s, 2 × 6 H, 4 × Si-CH$_3$).

^{13}C-NMR (101 MHz, DMSO-d_6): δ (ppm) = 148.0 (C-3), 145.3 (C-4), 128.1 (2 C, C-2, C-6), 126.7 (C-5), 119.9 (C-1), 25.7 (6 C, 2 × 3 C, (C(<u>C</u>H$_3$)$_3$), 18.1 (2 C, (<u>C</u>(CH$_3$)$_3$), –4.2 (4 C, 4 × Si-CH$_3$).

MS (ESI) for $[C_{18}H_{35}BO_4Si_2 + H]^+$ calcd.: 383.2239
found: 383.2107.

$C_{18}H_{35}BO_4Si_2$ (382.45 g/mol).

4-(4-Methoxyphenyl)furan-2(5*H*)-one) 26

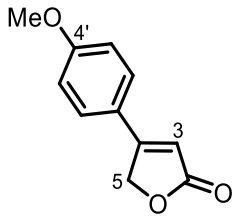

26

Following general procedure 1 the *Suzuki-Miyaura* cross-coupling was performed using 5-oxo-2,5-dihydrofuran-3-yltrifluoromethane sulfonate **118** (1.00 g, 4.30 mmol, 1.00 equiv.), 4-methoxyphenylboronic acid **119** (786 mg, 5.17 mmol, 1.20 equiv.), Na_2CO_3 (1.37 g, 12.9 mmol, 3.00 equiv.) and $Pd(PPh_3)_4$ (249 mg, 215 µmol, 5.0 mol%). The crude product was purified by column chromatography (silica gel, PE/EtOAc 4:1 → 2:1) to yield the desired product **26** (756 mg, 3.97 mmol, 92%).

TLC: $\mathbf{R_f}$ (PE/EtOAc 1:1 *v/v*) = 0.57.

Mp: 122 °C (*lit*: 120 °C[245]).

UV (CH_2Cl_2): λ_{max} (nm) = 227, 298.

IR (ATR): 3115, 3033, 2976, 2940, 2837, 1727, 1620, 1604, 1511, 1260, 1161, 830, 812 cm^{-1}.

^{1}H NMR (300 MHz, DMSO-d_6): δ (ppm) = 7.45 (d, J = 9.0 Hz, 2 H, 3'-H, 5'-H), 6.96 (d, J = 9.0 Hz, 2 H, 2'-H, 6'-H), 6.22 (t, J = 1.7 Hz, 1 H, 3-H), 5.18 (d, J = 1.7 Hz, 2 H, 5-H_2), 3.86 (s, 3 H, OCH_3).

^{13}C NMR (101 MHz, DMSO-d_6) δ (ppm) = 174.4 (C-2), 163.7 (C-4'), 162.5 (C-4), 128.3 (2 C, C-2', C-6'), 122.4 (C-1'), 114.8 (2 C, C-3', C-5'), 110.7 (C-3), 71.1 (C-5), 55.6 (OCH_3).

HRMS (ESI) for $[C_{11}H_{10}O_3+Na]^+$ calcd.: 213.0522
found: 213.0534.

$C_{11}H_{10}O_3$ (190.20 g/mol).

4-(4-Hydroxyphenyl)furan-2(5*H*)-one) 137[185]

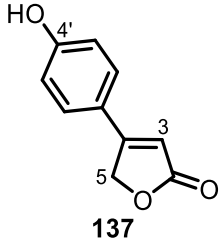

137

Method A:

Following general procedure 1 the *Suzuki-Miyaura* cross-coupling was performed using 5-oxo-2,5-dihydrofuran-3-yltrifluoromethane sulfonate **119** (503 mg, 2.17 mmol, 1.00 equiv.), 4-hydroxyphenylboronic acid **138** (359 mg, 2.60 mmol, 1.20 equiv.), Na_2CO_3 (689 mg, 6.50 mmol, 3.00 equiv.) and $Pd(PPh_3)_4$ (12.5 mg, 10.8 µmol, 0.5 mol%). The crude product was purified by recrystallization from chloroform to yield the product **137** (364 mg, 2.07 mmol, 95%) as pale yellow solid.

Method B:

To a solution of4-(4-methoxyphenyl)furan-2(5*H*)-one **26** (200 mg, 1.05 mmol, 1.00 equiv.) in CH_2Cl_2 (10.0 mL) was added dropwise BBr_3 (300 µL, 789 mg, 3.15 mmol, 3.0 equiv.) at -78 °C. The solution was allowed to warm to room temperature and stirred for 24 h. The reaction mixture was the poured into sat. NH_4Cl-solution (50 mL) and the aqueous layer was extracted with EtOAc (2 × 50 mL). The combined organic layers were washed with brine (50 mL), dried over $MgSO_4$, filtered and the solvent was removed in vacuum to yield 4-(4-hydroxyphenyl)furan-2(5*H*)-one **137** (154 g, 874 µmol, 83 %) as a pale yellow solid.

TLC: R_f (PE/EtOAc 1:1 *v/v*) = 0.37.

Mp: 235 °C (*lit*: 262.5 °C[246]).

UV (CH_2Cl_2): λ_{max} (nm) = 273, 310.

IR (ATR): 3216, 2360, 1699, 1584, 1517, 1331, 1276, 1173, 905, 823 cm^{-1}.

^{1}H NMR (500 MHz, DMSO-d_6): δ (ppm) = 10.20 (s, 1 H, OH), 7.56 (d, J = 8.7 Hz, 2 H, 2'-H, 6'-H), 6.86 (d, J = 8.7 Hz, 2 H, 3'-H, 5'-H), 6.46 (t, J = 1.7 Hz, 1 H, 3-H), 5.30 (d, J = 1.7 Hz, 2 H, 5-H_2).

^{13}C NMR (101 MHz, DMSO-d_6) δ (ppm) = 174.2 (C-2), 165.0 (C-4), 160.6 (C-4'), 129.0 (2 C, C-2', C-6'), 120.7 (C-1'), 115.8 (2 C, C-3', C-5'), 108.8 (C-3), 70.9 (C-5).

HRMS (ESI) for $[C_{10}H_8O_3+Na]^+$ calcd.:199.0371
found:199.0370.

$C_{10}H_8O_3$ (176.17 g/mol).

4-(3,4-bis((*tert*-butyldimethylsilyl)oxy)phenyl)furan-2(5*H*)-one 170

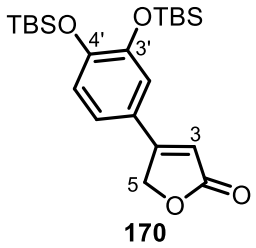

170

Following general procedure 1 the *Suzuki-Miyaura* cross-coupling was performed using 5-oxo-2,5-dihydrofuran-3-yltrifluoromethane sulfonate **118** (150 mg, 646 µmol, 1.00 equiv.), 3,4-bis[[(1,1-dimethylethyl)dimethylsilyl]oxy]phenyl]boronic acid **161** (321 mg, 840 µmol, 1.30 equiv.), Na_2CO_3 (206 mg, 1.94 mmol, 3.00 equiv.) and $Pd(PPh_3)_4$ (30.0 mg, 26.0 µmol, 4.0 mol%). Purification by column chromatography (silica gel, PE/EtOAc 10:1) yielded **170** (226 mg, 536 µmol, 83%) as pale yellow solid.

TLC: R_f (PE/EtOAc 10:1 *v/v*) = 0.38.

Mp: 181 °C.

UV (CH_2Cl_2): λ_{max} (nm) = 273, 310.

IR (ATR): 2958, 2859, 2385, 1794, 1732, 1617, 1502, 1430, 1256, 1157, 1045, 895, 840, 781, 747 cm^{-1}.

^{1}H NMR (500 MHz, DMSO-d_6): δ (ppm) = 7.00–6.97 (m, 2 H, 3-H, 6'-H), 6.90–6.87 (m, 1 H, 5'-H), 6.18 (t, J = 1.4 Hz, 1 H, 2'-H), 5.15 (d, J = 1.5 Hz, 2 H, 5-H_2), 1.00 (s, 9 H, $C(CH_3)_3$), 0.99 (s, 9 H, $C(CH_3)_3$), 0.24–0.21 (m, 12 H, 4 × Si-CH_3).

^{13}C NMR (101 MHz, DMSO-d_6) δ (ppm) = 174.4 (C-2), 163.8 (C-4), 150.9 (C-3'), 147.8 (C-4'), 123.2 (C-1'), 121.6 (C-6'), 120.4 (C-5'), 119.3 (C-2'), 111.0 (C-3), 71.1 (C-5), 26.0 (6 C, 2 × ($C\underline{C}H_3)_3$), 18.7 (2 C, ($\underline{C}(CH_3)_3$), –3.9 (4 C, 4 × Si-CH_3).

HRMS (ESI) for $[C_{22}H_{36}O_4Si_2 + H]^+$ calcd.: 421.2225
found: 421.2208.

$C_{22}H_{36}O_4Si_2$ (420.70 g/mol).

4-(4-fluorophenyl)furan-2(5*H*)-one 172

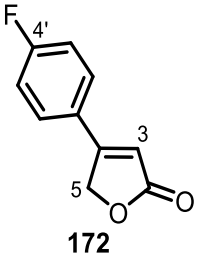

172

Following general procedure 1 the *Suzuki-Miyaura* coupling was performed using 5-oxo-2,5-dihydrofuran-3-yltrifluoromethane sulfonate **118** (300 mg, 1.29 mmol, 1.00 equiv.), 4-fluorophenylboronic acid **168** (235 mg, 1.68 mmol, 1.30 equiv.), Na_2CO_3 (1025 mg, 6.50 mmol, 3.00 equiv.) and $Pd(PPh_3)_4$ (59.7 mg, 51.7 µmol, 4.0 mol%). Purification by column chromatography (silica gel, PE/EtOAc 4:1 → 1:1) yielded **172** (219 mg, 1.23 mmol, 95%) as beige amorphous powder.

TLC: R_f (PE/EtOAc 1:1 *v/v*) = 0.37.

Mp: 161-162 °C. (*lit*: 144 °C [247])

UV ($CHCl_3$): λ_{max} (nm) = 272.

IR (ATR): 1702, 1621, 1598, 1509 1418, 1321, 1224, 1159, 1045, 990, 890, 836, 816, 807, 705 cm^{-1}.

^{1}H NMR (400 MHz, $CDCl_3$): δ (ppm) = 7.52 (dd, *J* = 8.8, 5.5 Hz, 2 H, 2'-H, 6'-H), 7.17 (t, *J* = 8.8 Hz, 2 H, 3'-H, 5'-H), 6.33 (t, *J* = 1.6 Hz, 1 H, 3-H), 5.20 (d, *J* = 1.6 Hz, 2 H, 5-H_2).

^{13}C NMR (101 MHz, DMSO-d_6) δ (ppm) = 173.7 (C-2), 164.8 (d, *J* = 253 Hz, C-4'), 162.7 (C-4), 128.8 (d, *J* = 8.8 Hz, 2 C, C-2', C-6'), 126.2 (d, *J* = 3.6 Hz, C-1'), 116.8 (d, *J* = 22.2 Hz, 2 C, C-3', C-5'), 113.0 (C-3), 71.6 (C-5).

HRMS (ESI) for [$C_{10}H_7FO_2$+H] calcd.:179.0503
found: 179.0515.

$C_{10}H_7FO_2$ (178.16 g/mol).

N-(4-(5-Oxo-2,5-dihydrofuran-3-yl)phenyl)acetamide 171

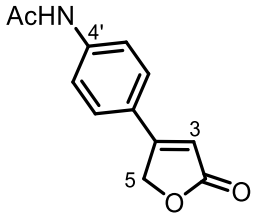

171

Following general procedure 1 the *Suzuki-Miyaura* cross-coupling was performed using 5-oxo-2,5-dihydrofuran-3-yltrifluoromethane sulfonate **118** (250 mg, 1.08 mmol, 1.00 equiv.), 4-acetamidophenylboronic acid **167** (212 mg, 1.19 mmol, 1.20 equiv.), Na_2CO_3 (342 mg, 3.23 mmol, 3.00 equiv.) and $Pd(PPh_3)_4$ (49.8 mg, 4.31 µmol, 4.0 mol%). Purification by column chromatography (silica gel, CH_2Cl_2/MeOH 40:1) yielded **171** (156 mg, 719 µmol, 67%) as colorless powder.

TLC: R_f (CH_2Cl_2/MeOH 1:1 *v/v*) = 0.30.

Mp: 200 °C.

UV (CH_2Cl_2): λ_{max} (nm) = 231, 306.

IR (ATR): 2362, 2341, 1728, 1698, 1684, 1596, 1533, 1405, 1372, 1318, 1281, 1232, 1179, 1042, 955 cm^{-1}.

^{1}H NMR (400 MHz, DMSO-d_6): δ (ppm) = 10.23 (s, 1 H, NH), 7.73–7.62 (m, 4 H, 2'-H, 3'-H, 5'-H, 6'-H), 6.58 (t, J = 1.5 Hz, 1 H, 3-H) 5.33 (d, J = 1.8 Hz, 2 H, 5-H_2), 2.07 (s, 3 H, CH_3CONH).

^{13}C NMR (151 MHz, DMSO-d_6): δ (ppm) = 174.0 (CH_3C=ONH), 168.8 (C-2), 164.5 (C-4'), 142.3 (C-4), 128.0 (2 C, C-2', C-6'), 124.1 (C-1'), 118.7 (2 C, C-3', C-5'), 110.5 (C-3), 71.0 (C-5), 24.2 (CH_3C=ONH).

HRMS (ESI) for $[C_{11}H_{11}NO_3+H]^+$ calcd.: 218.0812
found: 218.0843.

$C_{12}H_{11}NO_3$ (217.22 g/mol).

4-(4-Nitrophenyl)furan-2(5*H*)-one 173

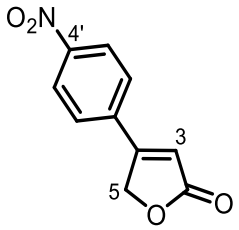

173

Following general procedure 2 the *Suzuki-Miyaura* cross-coupling was performed by using 5-oxo-2,5-dihydrofuran-3-yltrifluoromethane sulfonate **118** (108 mg, 469 µmol, 1.00 equiv.), 4-nitrophenylboronic acid **169** (93.3 mg, 559 µmol, 1.20 equiv.), potassium phosphate (275 mg, 1.30 mmol, 2.77 equiv.) and $Pd(PPh_3)_4$ (5.20 mg, 4.50 µmol, 0.96 mol%). Purification by column chromatography (silica gel, PE/EtOAc 9:1 → 1:1) yielded **173** (63.5 mg, 310 µmol, 66%) as beige amorphous powder.

TLC: R_f (PE/EtOAc 1:1 *v/v*) = 0.32.

Mp: 251 °C.

UV (CH_2Cl_2): λ_{max} (nm) = 226, 292.

IR (ATR): 1797, 1743, 1593, 1514, 1451, 1342, 1316, 1286, 1260, 1167, 1108, 1045, 994, 892, 846 cm^{-1}.

^{1}H NMR (400 MHz, $CDCl_3$) δ (ppm) = 8.35 (d, J = 8.9 Hz, 2 H, 2'-H, 6'-H), 7.69 (d, J = 8.9 Hz, 2 H, 3'-H, 5'-H), 6.56 (t, J = 1.9 Hz, 1 H, 3-H), 5.27 (d, J = 1.9 Hz, 2 H, 5-H_2).

^{13}C NMR (101 MHz, DMSO-d_6) δ (ppm) = 173.2 (C-2), 162.5 (C-4), 148.8 (C-4'), 135.6 (C-1'), 128.4 (2 C, C-2', C-6'), 124.1 (2 C, C-3', C-5'), 116.2 (C-3), 71.2 (C-5).

HRMS (ESI) for $[C_{10}H_7NO_4+H]^+$ calcd.: 206.0448
found: 206.0443.

$C_{10}H_7NO_4$ (205.17 g/mol).

3-Chloro-4-(4-methoxyphenyl)furan-2(*5H*)-one 160

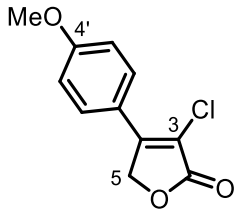

160

A mixture of triflate **34** (502 mg, 1.88 mmol, 1.00 equiv.), 4-methylphenylboronic acid **119** (430 mg, 2.83 mmol, 1.51 equiv.), Na_2CO_3 (600 mg, 5.66 mmol, 3.01 equiv.) and $BnEt_3NCl$ (21.4 mg, 94.0 µmol, 5.0 mol%) were dissolved in a toluene/water mixture (12:1 *v*/*v*) and degassed with argon for 10 min. Afterwards, $Pd(OAc)_2$ (21.8 mg, 97.1 µmol, 5.0 mol%) and PCy_3 (52.6 mg, 188 µmol, 10.0 mol%) were added to the solution and stirred for 16 h at room temperature. The solvent was removed in vacuum and the crude product was purified by column chromatography (silica gel, PE/CH_2Cl_2 9:1 → 100% CH_2Cl_2 *v*/*v*). The title compound **160** was obtained as colourless solid (330 mg, 1.47 mmol, 78%)

TLC: R_f (PE/CH_2Cl_2 1:1 *v/v*) = 0.29.

Mp: 185 °C.

UV (CH_2Cl_2): λ_{max} (nm) = 229, 307.

IR (ATR): 2957, 2920, 2842, 2360, 2336, 1603, 1469, 1466, 1436, 1273, 1246, 1182, 1039, 822, 550 cm^{-1}.

^{1}H-NMR (500 MHz, $CDCl_3$,): δ (ppm) = 7.80 (d, J = 9.0 Hz, 2 H, 2'-H, 6'-H), 7.02 (d, J = 9.0 Hz, 2 H, 3'-H, 5'-H), 5.20 (s, 2 H, 5-H_2), 3.89 (s, 3 H, OCH_3).

^{13}C-NMR (126 MHz, $CDCl_3$): δ (ppm) = 169.2 (C-2), 162.4 (C-4'), 151.4 (C-4), 129.2 (2 C, C-2', C-6'), 121.4 (C-1'), 114.8 (2 C, C-3', C-5'), 100.1 (C-3), 70.1 (C-5), 55.7 (OCH_3).

HRMS (ESI) for $[C_{11}H_9ClO_3+H]^+$ calcd.: 225.0318
found: 225.0308.

$C_{11}H_9ClO_3$ (224.64 g/mol).

3-Chloro-4-(4-hydroxyphenyl)furan-2(*5H*)-one 156

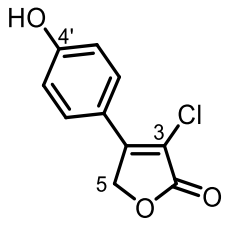

156

A solution of 3-chloro-4-(4-methoxyphenyl)furan-2(*5H*)-one **160** (89.1 mg, 397 µmol, 1.00 equiv.) in CH_2Cl_2 (4.0 mL) was cooled to -78 °C, followed by the dropwise addition of BBr_3 (45.0 µL, 0.475 mmol, 1.20 equiv.). After complete addition the mixture was allowed to stir for 16 h at room temperature. Afterwards, the solution was diluted with water (30.0 mL) and extracted with EtOAc (3 x 50 mL). The combined organic extracts were washed with water (50 mL) and brine (50 mL), dried over $MgSO_4$, filtered and the solvent was removed in vacuum.The title compound **156** was obtained as colorless solid (76.1 mg, 361 µmol, 91%).

TLC: R_f (PE/EtOAc 1:1 *v/v*) = 0.58.

Mp: 262 °C.

UV (CH_2Cl_2): λ_{max} (nm) = 288, 301.

IR (ATR): 3267, 1726, 1604, 1580, 1509, 1330, 1274, 1182, 1065, 1049, 1014, 753, 741 cm^{-1}.

^{1}H-NMR (500 MHz, DMSO-d_6): δ (ppm) = 10.40 (s, 1 H, OH), 7.78 (d, J = 8.8 Hz, 2 H, 2'-H, 6'-H), 6.95 (d, J = 8.8 Hz, 2 H, 3'-H, 5'-H), 5.42 (s, 2 H, 5-H_2).

^{13}C-NMR (126 MHz, $CDCl_3$): δ (ppm) = 169.2 (C-2), 160.7 (C-4'), 153.4 (C-4), 129.6 (2 C, C-2', C-6'), 119.4 (C-1'), 115.0 (C-3), 116.0 (2 C, C-3', C-5'), 70.4 (C-5).

HRMS (ESI) for $[C_{10}H_7ClO_3+H]^+$ calcd.: 211.0156
found: 211.0168.

$C_{10}H_7ClO_3$ (210.61 g/mol).

6.3.2. Starting material synthesis of aldehydes for rubrolide synthesi

2-(3-bromo-4-methoxyphenyl)-1,3-dioxolane 133

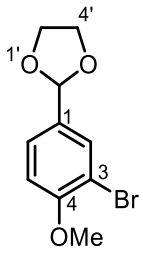

133

The compound was prepared using a modified protocol originally reported by *Gopinath* et al.[176]. To a solution of 3-bromo-4-hydroxybenzaldehyde **132** (506.0 mg, 2.52 mmol, 1.00 equiv.) and K_2CO_3 (765 mg, 5.54 mmol, 2.20 equiv.) in abs. DMF (10.0 mL) methyliodide (344 µL, 786 mg, 5.54 mmol, 2.20 equiv.) was added dropwise at room temperature. The reaction mixture was warmed to 55 °C and stirred for 3 h. The solution was cooled to room temperature and diluted with EtOAc (50.0 mL). The organic phase was washed with sat. $NaHCO_3$ solution (2 × 50 mL), dried over $MgSO_4$ and filtered. The solvent was removed in vacuum to yield the crude methyl ether (557 mg, 2.59 mmol, 98%) as light yellow oil, which can be used for the next step without further purification.

The crude methyl ether (506.0 mg, 2.52 mmol, 1.00 equiv.) was suspended in toluene (30.0 mL), ethylene glycol (563 µL, 625 mg, 10.1 mmol, 4.00 equiv.) and PTSA (23.9 mg, 126 µmol, 5.0 mol%) was added. The reaction mixture was stirred at 140 °C for 16 h using a Dean-Stark trap. Then, the mixture was diluted in EtOAc (100 mL) and washed with sat. $NaHCO_3$ solution (2 × 50 mL), water (2 × 50 mL) and brine (50 mL). The organic extracts were dried over $MgSO_4$, filtered and the solvent was removed in vacuum. The crude product was purified by column chromatography (silica gel, PE/EtOAc 6:1 → 2:1) to yield the acetal **133** (654 mg, 2.52 mmol, quant.) as pale yellow oil.

TLC: R_f (PE/EtOAc 3:1 *v/v*) = 0.28.

UV (CH_2Cl_2): λ_{max} (nm) = 249, 259.

IR (ATR): 2928, 2841, 1685, 1598, 1496, 1254, 1115, 1025, 813, 640 cm^{-1}.

^{1}H-NMR (400 MHz, MeOD-d_4) δ (ppm) = 7.61 (d, J = 2.0 Hz, 1 H, 2-H), 7.39 (dd, J = 8.5, 2.0 Hz, 1 H, 6-H), 7.02 (d, J = 8.5 Hz, 1 H, 5-H), 5.67 (s, 1 H, 2'-H), 4.13–4.05 (m, 2 H, 4'-H_a, 5'-H_a), 4.03–3.95 (m, 2 H, 4'-H_b, 5'-H_b), 3.88 (s, 3 H, OCH_3).

^{13}C-NMR (101 MHz, MeOD-d_4) δ (ppm) = 158.0 (C-3), 133.1 (C-1), 132.5 (C-2), 128.4 (C-6), 112.8 (C-5), 112.2 (C-4), 104.0 (C-2'), 66.3 (2 C, C-4', C-5'), 56.7 (OCH_3).

HRMS (ESI) for $[C_{10}H_{16}O_2+H]^+$ calcd.: 258.9964
found: 258.9950.

$C_{10}H_{11}BrO_3$ (259.10 g/mol).

(5-Formyl-2-methoxyphenyl)boronic acid 121

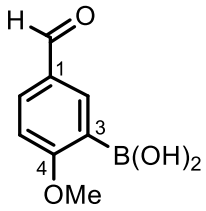

121

The compound was prepared using a modified protocol originally reported by *Speicher* et al..[180] A solution of 2-(3-bromo-4-methoxyphenyl)-1,3-dioxolane **133** (524 mg, 1.91 mmol, 1.0 equiv.) in THF (10.0 mL) was cooled to -78 °C. Then, *n*-BuLi (1.6 M in *n*-hexane, 1.47 mL, 2.00 mmol, 1.25 equiv.) was added and stirred for 3 h at -78 °C. Afterwards, $B(OMe)_3$ (290 mg, 270 µL, 2.39 mmol, 1.25 equiv.) was added. The mixture was allowed to warm to room temperature and stirred for 16 h. Aq. HCl (3 M, 10.0 mL) was added to the solution, stirred for additional 20 min and extracted with Et_2O (2 × 200 mL). The combined organic extracts were dried over $MgSO_4$, filtered, and the solvent was removed under reduced pressure. The title compound **121** was obtained as beige amorphous solid (1.90 mmol, quant.)

TLC: R_f (PE/EtOAc 2:1 *v/v*) = 0.12.

^{1}H-NMR (300 MHz, $CDCl_3$) δ (ppm) = 9.88 (s, 1 H, CHO), 8.05 (d, *J* = 2.2 Hz, 1 H, 6-H), 7.94 (s, 2 H, $B(OH)_2$), 7.93 (dd, *J* = 8.6, 2.2 Hz, 1 H, 5-H), 7.16 (d, *J* = 8.6 Hz, 1 H, 2-H), 3.89 (s, 3 H, OCH_3).

^{13}C-NMR (75 MHz, $CDCl_3$) δ (ppm) = 191.6 (CHO), 167.9 (C-2), 136.9 (C-6), 133.7 (C-3, C-4), 129.1 (C-5), 110.8 (C-1), 55.9 (OCH_3).

$C_8H_9BO_4$ (179.97 g/mol).

4-methoxy-3-(3-methylbut-2-en-1-yl)benzaldehyde 116

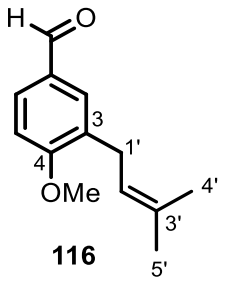

116

Method A

Prepared using a modified protocol originally reported by *Maiti* et al.[182] To a solution of bromide **132** (480 mg, 1.85 mmol, 1.00 equiv.) in Et_2O (5.00 mL) were added molecular sieves (4 Å, 800 mg) and the mixture was cooled to 0 °C. A solution of *n*-BuLi (1.6 M in *n*-hexane 1.40 mL, 2.32 mmol, 1.25 equiv.) was added dropwise and the reaction mixture was warmed to room temperature and allowed to stir for 30 min. Afterwards, CuBr × DMS (194 mg, 965 µmol, 0.56 equiv.) was added and the mixture was stirred for 1 h at room temperature. Then, prenylbromide **120** (300 µL 345 mg, 2.32 mmol, 1.25 equiv.) was added to the solution and stirred for 16 h at room temperature. Afterwards, sat. aq. NH_4Cl (10 mL) solution and aq. HCl (1 M, 10.0 mL) were added to the mixture and stirred for 20 min at room temperature. The solution was diluted with Et_2O (20 mL) and filtered. The filtrate was washed with aq. acetic acid (20%, 25 mL), dried over $MgSO_4$, filtered and the solvent was removed in vacuum. The crude product was purified by column chromatography (silica gel, PE/EtOAc 12:1 → 8:1) to yield the prenylated compound **116** (119 mg, 581 µmol, 31%) as yellow oil.

Method B

A mixture of prenylbromide **120** (50.0 mg, 336 µmol, 1.00 equiv.), boronic acid **121** (75.0 mg, 417 µmol, 1.24 equiv.) and K_2CO_3 (140 mg, 1.01 mmol; 3.00 equiv.) was dissolved in toluene (1.50 mL) and degassed with argon for 5 min. Afterwards, $Pd_2(dba)_3$ (11.3 mg, 12.3 µmol, 4.4 mol%) was added to the solution and stirred for 17 h at 110 °C. The reaction was cooled to room temperature, filtered through celite® and the solvent was removed in vacuum. The crude product was purified by column chromatography (silica gel, PE/EtOAc 12:1 → 8:1) to yield the prenylated benzaldehyde **116** (26.8 mg, 131 µmol, 39%) yellow oil.

TLC: R_f (PE/EtOAc 8:1 *v/v*) = 0.36.

UV (CH_2Cl_2): λ_{max} (nm) = 249, 259.

IR (ATR): 2928, 2841, 1685, 1598, 1496, 1254, 1115, 1025, 813, 640 cm^{-1}.

^{1}H-NMR (300 MHz, $CDCl_3$) δ (ppm) = 9.86 (s, 1 H, CHO), 7.72 (dd, *J* = 8.4, 2.2 Hz, 1 H, 6-H), 7.68 (d, *J* = 2.2 Hz, 1 H, 2-H), 6.94 (d, *J* = 8.4 Hz, 1 H, 5-H), 5.30 (m, 1 H, 2'-H), 3.92 (s, 3 H, OCH_3), 3.34 (d, *J* = 7.4 Hz, 2 H, 1'-H_2), 1.71, 1.76 (2 × s, 4'-H_3, 5'-H_3).

^{13}C-NMR (101 MHz, $CDCl_3$) δ (ppm) = 191.7 (CHO), 162.5 (C-4), 133.9 (C-3'), 131.5 (C-2), 131.0 (C-6), 130.7 (C-3), 130.0 (C-1), 121.7 (C-2'), 110.3 (C-5), 56.1 (OCH_3), 28.6 (C-1'), 26.2, 18.2 (2 C, C-4', C-5').

MS (ESI) for $[C_{13}H_{16}O_2+H]^+$ calcd.: 205.1223
found: 205.1197.

$C_{13}H_{16}O_2$ (204.27 g/mol).

***Tert*-butyl-1,1-dimethylallyl carbonate 140**

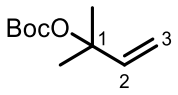

140

Method A:

The compound **140** was prepared by a procedure of *Carreira* et al.[186] A solution of 2-methylbut-3-en-2-ol **142** (5.20 mL, 50.1 mmol, 1.00 equiv.) in THF (90.0 mL) was cooled to 0 °C and *n*-BuLi (1.6 M in *n*-hexane, 31.3 mL, 50.1 mmol, 1.00 equiv.) was added dropwise. The reaction was stirred at 0 °C for 30 min. Afterwards, Boc_2O (12.0 g, 55.1 mmol, 1.10 equiv.) was added and stirred for 16 h at room temperature. The reaction mixture was washed with sat. aq. $NaHCO_3$ solution (150 mL), H_2O (50 mL) and brine (150 mL), dried over $MgSO_4$, filtered and the solvent was removed in vacuum. The allyl carbonate **140** (7.10 g, 38.1 mmol, 76%) was obtained as pale yellow oil.

Method B:

The compound was prepared using a modified protocol originally reported by *Bartoli* et al.[187] A solution of 2-methylbut-3-en-2-ol **142** (500 µL, 4.83 mmol, 1.00 equiv.), Boc_2O (1.16 g, 5.30 mmol, 1.10 equiv.) and $Zn(OAc)_2 \times H_2O$ (106 mg, 482 µmol, 10.0 mol%) in CH_2Cl_2 (90.0 mL) was stirred for 7 d at 60 °C in a sealed tube. Afterwards, the mixture was cooled to room temperature and the solvent removed in vacuum. The crude product was purified by column chromatography (silica gel, PE/EtOAc 9:1 → 4:1) to yield the desired product **140** (791 mg, 4.25 mmol, 88%) as colorless oil.

TLC: R_f = 0.80 (PE/EtOAc 20:1 v/v).

IR (ATR): 3607, 3019, 2975, 2362, 2336, 1735, 1478, 1366, 1283, 1253, 1119, 915, 841, 795, 748 cm^{-1}.

^{1}H-NMR (400 MHz, $CDCl_3$): δ (ppm) = 6.06 (dd, J = 17.5, 10.9 Hz, 1 H, 2-H), 5.14 (d, J = 17.5 Hz, 1 H, 3-H_A), 5.06 (d, J = 10.9 Hz, 1 H, 3-H_B), 1.49 (s, 6 H, 2 × CH_3), 1.42 (s, 9 H, $C(CH_3)_3$).

^{13}C-NMR (126 MHz, $CDCl_3$): δ (ppm) = 152.1 (C=O), 142.5 (C-2), 113.2 (C-3), 81.6 (C-1), 81.5 ($C(CH_3)_3$), 28.0 (3 C, $C(CH_3)_3$), 26.6 (2 C, 2 x C-1-CH_3).

MS (ESI) for $[C_{10}H_{18}O_3]^+$ calcd.: 186.1256
found: 186.1312.

$C_{10}H_{18}O_3$ (186.25 g/mol).

4-[(2-Methylbut-3-en-2-yl)oxy]benzaldehyde 141

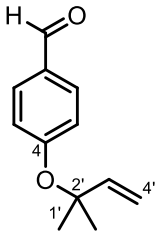

141

The compound was prepared using a modified protocol originally reported by *Schmidt* et al.[248] A solution of 4-hydroxybenzaldehyde **27** (310 mg, 2.54 mmol, 1.00 equiv.) and *Boc*-protected 2-methylbut-3-en-2-ol **140** (1.65 g, 8.89 mmol, 3.50 equiv.) in abs. THF (6.0 mL) were added molecular sieves (4 Å, 2.0 g). The reaction mixture was saturated with argon by evacuating and flooding with argon three times. $Pd(PPh_3)_4$ (29.3 mg, 2.50 µmol, 1.0 mol%) was added and the mixture stirred at 4 °C for 12 h. The reaction mixture was diluted in EtOAc (5.0 mL), filtered through a syringe filter and the solvent was removed in vacuum. The crude product was purified by column chromatography (silica gel, PE/EtOAc 19:1 → 13:1) to yield allyl ether **141** (382 mg, 2.01 mmol, 79%) as colorless oil.

TLC: R_f (PE/EtOAc 9:1 *v/v*) = 0.51.

UV (CH_2Cl_2): λ_{max} (nm) = 251, 297.

IR (ATR): 2981, 1737, 1686, 1598, 1504, 1365, 1249, 1157, 1127, 942, 906, 835, 698, 617 cm^{-1}.

^{1}H-NMR (500 MHz, $CDCl_3$) δ (ppm) = 9.87 (s, 1 H, CHO), 7.75 (d, J = 8.8 Hz, 2 H, 2-H, 6-H), 7.08 (d, J = 8.8 Hz, 2 H, 3-H, 5-H), 6.14 (dd, J = 17.7, 10.9 Hz, 1 H, 2'-H), 5.18–5.26 (m, 2 H, 3'-H), 1.54 (s, 6 H, 2 × CH_3).

^{13}C-NMR (101 MHz, $CDCl_3$) δ (ppm) = 191.3 (CHO), 182.6 (C-4), 144.2 (C-3'), 131.7 (2 C, C-2, C-6), 120.0 (2 C, C-3, C-5), 114.6 (C-4'), 81.1 (C-2'), 27.7 (2 C, 2 × C-2'-CH_3).

MS (ESI) for $[C_{12}H_{14}O_2+H]^+$ calcd.: 191.1066
found:191.1011.

$C_{12}H_{14}O_2$ (190.24 g/mol).

4-Hydroxy-3-(3-methylbut-2-en-1-yl)benzaldehyde 139[185]

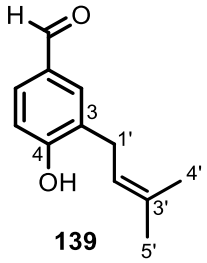

139

The compound was prepared using a modified protocol originally reported by *Schmidt* et al. [248] A solution of 4-[(2-methylbut-2-en-2-yl)oxy]benzaldehyde **141** (131 mg, 690 µmol, 1.00 equiv.) in DMF (3.0 mL) was heated to 180 °C under microwave irradiation for 45 min. Afterwards, the solvent was removed in vacuum. The crude product was purified by column chromatography (silica gel, PE/EtOAc 20:1 → 4:1) to yield the prenylated benzaldehyde **139** (115 mg, 604 µmol, 88%) as pale yellow solid.

TLC: R_f (PE/EtOAc 9:1 *v/v*) = 0.13.

Mp: 61 °C (lit.: 58-61 °C[249]).

UV (CH_2Cl_2): λ_{max} (nm) = 272, 287.

IR (ATR): 3228, 2959, 2821, 2742, 1661, 1579, 1504, 1284, 1230, 1087, 967, 815, 633 cm^{-1}.

^{1}H NMR (500 MHz, DMSO-d_6,): δ (ppm) = 10.57 (s, 1 H, OH), 9.77 (s, 1 H, CHO), 7.57–7.62 (m, 2 H, 2-H, 6-H), 6.95 (d, J = 8.2 Hz, 1 H, 5-H) , 5.29 (m, 1 H, 2'-H) , 3.27 (d, J = 7.3 Hz, 2 H, 1'-H_2), 1.71, 1.67 (2 × s, 2 × 3 H, 4'-H_3, 5'-H_3).

^{13}C NMR (126 MHz, DMSO-d_6): δ (ppm) = 191.1 (CHO), 161.1 (C-4), 132.2 (C-2), 130.6 (C-1), 130.1 (C-3'), 128.4 (C-6), 128.3 (C-3), 121.8 (C-2'), 115.0 (C-5), 27.7 (C-1'), 25.5, 17.6 (2 C, C-4', C-5').

HRMS (ESI) for $[C_{12}H_{14}O_2+H]^+$ calcd.: 191.1066
found: 191.1050.

$C_{12}H_{14}O_2$ (190.24 g/mol).

2,2-Dimethylchromane-6-carboxaldehyde 117

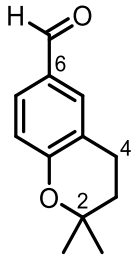

117

The compound was prepared using a modified protocol originally reported by *Tripathi* et al.[167,183] A solution of 4-hydroxybenzaldehyde **27** (2.00 g, 16.4 mmol, 1.00 equiv.) in PE (20.0 mL) and isoprene (3.30 mL, 2.24 g, 32.9 mmol, 2.00 equiv.) was added dropwise to the reaction mixture at room temperature. Afterwards, aq. H_3PO_4 (85%, 2.00 mL, 2.90 g, 29.6 mmol, 1.81 equiv.) was added dropwise and the reaction mixture was stirred at room temperature for 16 h. The mixture was poured into a mixture of ice and solid $NaHCO_3$. Then, the aqueous layer was extracted with EtOAc (3 × 100 mL) and the combined organic layers were dried over Na_2SO_4, filtered and the solvent was removed in vacuum to yield the aldehyde **117** (1.62 g, 8.52 mmol, 52%) as colorless oil.

TLC: R_f = 0.47 (PE/EtOAc 5:1 *v/v*).

UV ($CHCl_3$): λ_{max} (nm) = 294.

IR (ATR): 2972, 2358, 1814, 1740, 1686, 1601, 1575, 1491, 1372, 1265, 1231, 1116, 944, 819, 761 cm^{-1}.

^{1}H-NMR (400 MHz, $CDCl_3$): *δ* (ppm) = 9.83 (s, 1 H, CHO), 7.60–7.65 (m, 2 H, 5-H, 7-H), 6.87 (d, *J* = 9.0 Hz, 1 H, 8-H), 2.84 (t, *J* = 6.8 Hz, 2 H, 3-H_2), 1.85 (t, *J* = 6.8 Hz, 2 H, 4-H_2), 1.37 (s, 6 H, 2 × CH_3).

^{13}C-NMR (101 MHz, $CDCl_3$): *δ* (ppm) = 191.2 (CHO), 160.0 (C-8a), 132.1 (C-7), 129.8 (C-6), 129.2 (C-5), 121.6 (C-4a), 118.1 (C-8), 76.0 (C-2), 32.5 (C-3), 27.1 (2 C, 2 × C-2-CH_3), 22.4 (C-4) ppm

HRMS (ESI) for $[C_{12}H_{14}O_2+H]^+$ calcd.: 190.0994
found: 191.1004.

$C_{12}H_{14}O_2$ (190.24 g/mol).

6.3.3. Rubrolide synthesis via aldolcondensation

Methyl protected rubrolide R 134

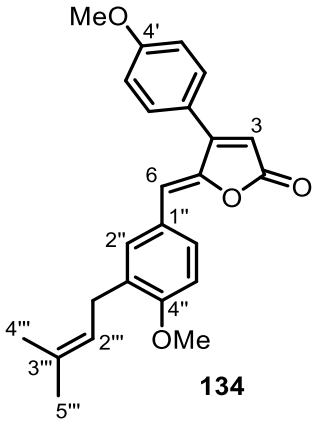

134

To a solution of 4-(4-methoxyphenyl)furan-2(5*H*)-one **26** (40.0 mg, 210 µmol, 1.00 equiv.) in toluene (10.0 mL) were added molecular sieves (4 Å, 800 mg). Afterwards, TBSOTf (100 µL, 115 mg, 420 µmol, 2.00 equiv.), 4-methoxy-3-(3-methylbut-2-en-1-yl)benzaldehyde **116** (58.7 mg, 287 µmol, 1.36 equiv.) and DIPEA (100 µL, 81.5 mg, 630 µmol, 3.00 equiv.) were added to the mixture and stirred for 1 h at room temperature. Then, DBU (80.0 µL, 64.0 mg, 420 µmol, 2.00 equiv.) was added, warmed to 110 °C and stirred for 16 h. The mixture was cooled to room temperature, diluted with Et_2O (70 mL), washed with aq. HCl (1 M, 50 mL), sat. aq. $NaHCO_3$ solution (50 mL), water (50 mL), and brine (50 mL). The organic layer was dried over $MgSO_4$, filtered and the solvent was removed in vacuum. The crude product was purified by column chromatography (silica gel, PE/EtOAc 12:1) to yield the twofold methyl protected rubrolide R **134** (74.5 mg, 198 µmol, 94%) as yellow solid.

TLC: R_f (PE/EtOAc 9:1 *v/v*) = 0.16.

Mp: 113 °C.

UV (CH_2Cl_2): λ_{max} (nm) = 249, 362.

IR (ATR): 2929, 2342, 1744, 1609, 1497, 1247, 1179, 1025, 828, 676, 596 cm^{-1}.

^{1}H-NMR (300 MHz, $CDCl_3$) δ (ppm) = 7.78 (dd, J = 8.6, 2.3 Hz, 1 H, 6''-H), 7.50–7.43(m, 3 H, 2''-H, 3'-H, 5'-H), 7.04 (d, J = 8.8 Hz, 2 H, 2'-H, 6'-H), 6.87 (d, J = 8.6 Hz, 1 H, 5''-H), 6.14 (s, 1 H, 3-H), 6.08 (d, J = 0.8 Hz, 1 H, 6-H), 5.31–5.24 (m, 1 H, 2''-H), 3.89 (s, 3 H, OCH_3), 3.88 (s, 3 H, OCH_3), 3.31 (d, J = 7.3 Hz, 2 H, 1'''-H), 1.75, 1.72 (2 × s, 2 × 3 H, 4-H_3, 5-H_3).

^{13}C-NMR (101 MHz, $CDCl_3$) δ (ppm) = 170.0 (C-2), 169.2 (C-4), 161.5 (C-4'), 158.4 (C-4''), 147.7 (C-5), 132.2 (2 C, C-2'', C-3''), 130.6 (C-6''), 130.2 (C-3'''), 130.0 (2 C, C-2', C-6'),

125.8 (C-1''), 123.3 (C-1'), 122.0 (C-2'''), 114.5 (2 C, C-3', C-5'), 114.2 (C-3), 112.2 (C-6), 110.5 (C-5''), 55.6 (2 C, 2 × OCH_3), 28.4 (C-1'''), 25.9, 17.9 (2 C, C-4''', C-5''').

HRMS (ESI): for $[C_{24}H_{24}O_4+H]^+$ calcd.: 377.1747

found: 377.1748.

$C_{24}H_{24}O_4$ (776.45 g/mol).

Rubrolide R 12[185]

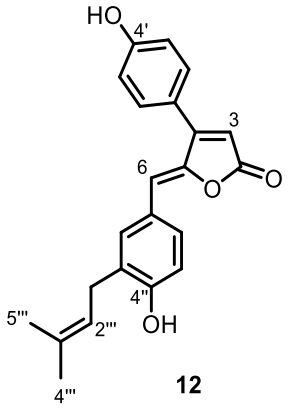

12

To a solution of furanone **137** (55.0 mg, 312 µmol, 1.00 equiv.) in DMF (2.00 mL) was added dropwise TBSOTf (329 µL, 378 mg, 1.43 mmol, 4.58 equiv.) and DIPEA (245 µL, 214 mg, 1.66 mmol, 5.32 equiv.) at room temperature. The solution was stirred at room temperature for 1 h. Then, a solution of aldehyde **139** (77.2 mg, 406 µmol, 1.30 equiv.) in DMF (1.00 mL) was added and the reaction mixture was stirred at room temperature for further 5 h. Afterwards, DBU (55.9 µL, 57.0 mg, 375 µmol, 1.20 equiv.) was added and the reaction mixture was warmed to 120 °C and stirred for 12 h. The mixture was cooled to room temperature and water (1.00 mL, 1.00 g, 55.5 mmol, 178 equiv.) and further DBU (100 µL, 102 mg, 669 µmol, 2.14 equiv.) were added and the solution was stirred for 16 h at room temperature. The reaction mixture was then poured into ethyl acetate (50 mL) and washed with 3 M aq. hydrochloric acid (50 mL), sat. aq. $NaHCO_3$-solution (50 mL), and brine (50 mL). The organic layer was dried over $MgSO_4$, filtered and the solvent was removed in vacuum. Purification by column chromatography (silica gel, PE/EtOAc 4:1 → 2:1) yielded an *E*/*Z* mixture (ratio = ~ 1:10 (*E*/*Z*) determined by ^{1}H-NMR) of **12**, which was further purified by reversed phase column chromatography (RP-C_{18} H_2O/MeCN 9:1→4:1) to yield rubrolide R **12** (68.1 mg, 196 µmol, 63%) as yellow amorphous powder.

TLC: R_f (PE/EtOAc 1:1 *v/v*) = 0.32.

Mp: 178 °C.

UV (CH_2Cl_2): λ_{max} (nm) = 250, 369.

IR (ATR): 3302, 2374, 2119, 1599, 1505, 1435, 1358, 1279, 1229, 1091, 826, 653 cm^{-1}.

^{1}H NMR (600 MHz, DMSO-d_6): δ (ppm) = 10.07 (s, 1 H, OH), 9.99 (s, 1 H, OH), 7.56 (d, *J* = 2.1 Hz, 1 H, 2''-H), 7.54 (dd, *J* = 8.4 Hz, 2.1 Hz, 1 H, 6''-H), 7.48 (d, *J* = 8.6 Hz, 2 H, 2'-H, 6'-H), 6.93 (d, *J* = 8.6 Hz, 2 H, 3'-H, 5'-H), 6.86 (d, *J* = 8.4 Hz, 1 H, 5''-H), 6.35 (s, 1 H, 3-H), 6.28 (s, 1 H, 6-H), 5.27 (m, 1 H, 2'''-H), 3.23 (d, *J* = 7.4 Hz, 2 H, 1'''-H_2), 1.70, 1.69 (2 × s, 2 × 3 H, 4'''-H, 5'''-H).

^{13}C NMR (151 MHz, DMSO-d_6): δ (ppm) = 168.7 (C-2), 159.7 (C-4'), 158.1 (C-4), 156.5 (C-4''), 145.2 (C-5), 132.4 (C-2''), 131.8 (C-3'''), 130.4 (2 C, C-2',C-6'), 130.0 (C-6''), 128.0 (C-3''), 124.2 (C-1''), 122.4 (C-2'''), 120.7 (C-1'), 115.9 (2 C, C-3', C-5'), 115.3 (C-5''), 113.7 (C-6), 110.7 (C-3), 27.9 (C-1'''), 25.5, 17.7 (2 C, C-4''', C-5''').

HRMS (ESI): for $[C_{22}H_{20}O_4+H]^+$ calcd.: 349.1434
found: 349.1447.

$C_{22}H_{20}O_4$ (348.40 g/mol).

Catechol-rubrolide R 174

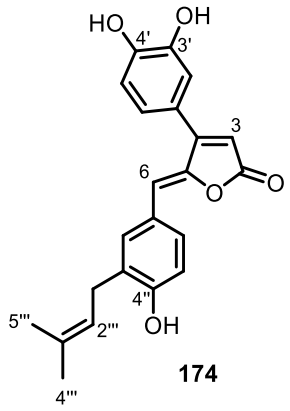

174

To a solution of furanone **137** (100 mg, 238 µmol, 1.00 equiv.) in DMF (2.00 mL) was added dropwise TBSOTf (170 µL, 196 mg, 0,740 mmol, 3.11 equiv.) and DIPEA (122 mg, 160 µL, 0.944 mmol, 3.97 equiv.) at room temperature. The solution was stirred at room temperature for 1 h. Then, a solution of aldehyde **139** (58.8 mg, 0.309 mmol, 1.30 equiv.) in DMF (1.00 mL) was added and the reaction mixture was stirred at room temperature for further 5 h. Afterwards, DBU (46.6 µL, 43.5 mg, 286 µmol, 1.20 equiv.) was added and the reaction mixture was warmed to 120 °C and stirred for 12 h. The mixture was cooled to room temperature and water (1.00 mL, 1.00 g, 55.5 mmol, 233 equiv.) and further DBU (100 µL, 102 mg, 669 µmol, 2.80 equiv.) were added and the solution was stirred for 16 h at room temperature. The reaction mixture was then poured into ethyl acetate (50 mL) and washed with 3 M aq. hydrochloric acid (50 mL), sat. aq. $NaHCO_3$-solution (50 mL), and brine (50 mL). The organic layer was dried over $MgSO_4$, filtered and the solvent was removed in vacuum.

Purification by column chromatography (silica gel, PE/EtOAc 4:1 → 2:1) yielded an *E*/*Z* mixture of **174**, which was further purified by reversed phase column chromatography (RP-C_{18} H_2O/MeCN 9:1→4:1) to yield **174** (72.0 mg, 198 µmol, 83%) as yellow amorphous powder.

TLC: R_f (CH_2Cl_2/MeOH 20:1 *v/v*) = 0.34.

Mp: 225 °C.

UV (CH_2Cl_2): λ_{max} (nm) = 257, 371.

IR (ATR): 3720, 3163, 3015, 2826, 2358, 1739, 1660, 1574, 1394, 1347, 1232, 1086, 886, 813, 632 cm^{-1}.

^{1}H-NMR (400 MHz, DMSO-d_6): δ (ppm) = 9.98–9.34 (3 × s, 3 H, 3 × OH), 7.56–7.51 (m, 2 H, 2''-H, 5''-H), 7.00 (d, *J* = 1.9 Hz, 1 H, 6''-H), 6.94 (dd, *J* = 8.1, 1.9 Hz, 1 H, 6'-H), 6.91–6.84 (m, 2 H, 2'-H, 5'-H), 6.29 (s, 1 H, 3-H), 6.27 (s, 1 H, 6-H), 5.31–5.23 (m, 1 H, 2'''-H), 3.23 (d, *J* = 7.2 Hz, 2 H, 1'''-H_2), 1.70, 1.69 (2 × s, 2 × 3 H, 4'''-H_3, 5'''-H_3).

^{13}C NMR (101 MHz, DMSO-d_6,): δ = 168.7 (C-2), 158.3 (C-4), 156.5 (C-4''), 148.0 (C-3'), 145.6 (C-4'), 145.3 (C-5), 132.3 (C-2''), 131.8 (C-3'''), 130.0 (C-6''), 128.1 (C-3''), 124.2 (C-1''), 122.4 (C-6'), 121.1 (C-1'), 120.5 (C-2'''), 116.0, 115.8 (2 C, C-2', C-5'), 115.4 (C-5''), 113.6 (C-3), 110.5 (C-6), 27.9 (C-1'''), 25.5, 17.7 (2 C, C-4''', C-5''').

HRMS (ESI): for $[C_{22}H_{20}O_5+H]^+$ calcd.: 365.1389
found: 365.1389.

$C_{22}H_{20}O_5$ (364.40 g/mol).

Fluoro-rubrolide R 178

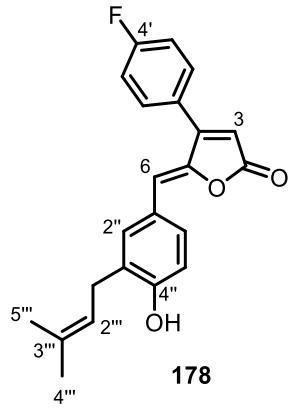

178

To a solution of furanone **172** (100.0 mg, 561 µmol, 1.00 equiv.) in toluene (5.00 mL) was added dropwise TBSOTf (290 µL, 331 mg, 1.24 mmol, 2.20 equiv.) and DIPEA (287 µL, 218 mg, 1.68 mmol, 3.00 equiv.) at room temperature. The solution was stirred at room temperature for 1 h. Then, a solution of aldehyde **139** (139 mg, 731 µmol, 1.30 equiv.) in

toluene (2.00 mL) was added and the reaction mixture was stirred at room temperature for further 5 h. Afterwards, DBU (101 µL, 103 mg, 673 µmol, 1.20 equiv.) was added and the reaction mixture was warmed to 120 °C and stirred for 12 h. The mixture was cooled to room temperature and water (2.00 mL, 1.00 g, 111 mmol, 198 equiv.) and further DBU (234 µL, 239 mg, 1.57 mmol, 2.80 equiv.) were added and the solution was stirred for 16 h at room temperature. The reaction mixture was then poured into ethyl acetate (100 mL) and washed with 3 M aq. hydrochloric acid (50 mL), sat. aq. $NaHCO_3$-solution (50 mL), and brine (50 mL). The organic layer was dried over $MgSO_4$, filtered and the solvent was removed in vacuum. Purification by column chromatography (silica gel, PE/EtOAc 20:1 → 1:1) yielded an *E*/*Z* mixture of **178**, which was further purified by reversed phase column chromatography (RP-C_{18} H_2O/MeCN 9:1→1:1) to yield **178** (123 mg, 351 µmol, 63%) as yellow amorphous powder.

TLC: R_f (PE/EtOAc 4:1 *v/v*) = 0.44.

Mp: 212.6 °C.

UV (CH_2Cl_2): λ_{max} (nm) = 259, 378.

IR (ATR): 3332, 2987, 2972, 2901, 1730, 1600, 1501, 1433, 1407, 1276, 1232, 1160, 1076, 1066, 831 cm^{-1}.

^{1}H-NMR (600 MHz, DMSO-d_6): δ (ppm) = 10.01 (s, 1 H, OH), 7.69 (dd, *J* = 8.9, 5.5 Hz, 2 H, 3'-H, 5'-H), 7.57 (d, *J* = 2.1 Hz, 1 H, 2''-H), 7.55 (dd, *J* = 8.4, 2.2 Hz, 1 H, 6''-H), 7.41 (t, *J* = 8.9 Hz, 2 H, 2'-H, 6'-H), 6.86 (d, *J* = 8.4 Hz,1 H, 5''-H), 6.51 (s, 1 H, 3-H), 6.23 (s, 1 H, 6-H), 5.30–5.25 (m, 1 H, 2'''-H), 3.22 (d, *J* = 7.3 Hz, 2 H, 1'''-H_2) 1.70, 1.68 (2 × s, 2 × 3 H, 4'''-H_3, 5'''-H_3).

^{13}C-NMR (151 MHz, DMSO-d_6): δ (ppm) = 168.3 (C-2), 163.3 (d, *J* = 248 Hz, C-4'), 156.9 (C-4), 156.7 (C-4''), 144.9 (C-5), 132.5 (C-2''), 131.8 (C-3'''), 131.1 (d, *J* = 8.7 Hz, 2 C, C-2', C-6'), 130.1 (C-3''), 128.1 (C-6''), 126.5 (d, *J* = 3.1Hz, C-1'), 124.1 (C-1''), 122.3 (C-2'''), 116.1 (d, *J* = 21.8 Hz, 2 C, C-3', C-5'), 115.4 (C-5''), 114.0 (C-6), 112.9 (C-3), 27.9 (C-1'''), 25.5, 17.7 (2 C, C-4''', C-5''').

HRMS (ESI): for $[C_{22}H_{19}FO_3+H]^+$ calcd.: 351.1396
found: 351.1398.

$C_{22}H_{19}FO_3$ (350.39 g/mol).

NHAc-rubrolide R 176

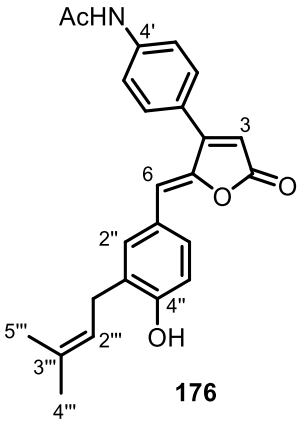

176

To a solution of furanone **171** (120 mg, 552 µmol, 1.00 equiv.) in DMF (5.00 mL) was added dropwise TBSOTf (520 µL, 599 mg, 2.27 mmol, 4.11 equiv.) and DIPEA (210 µL, 283 mg, 2.19 mmol, 3.97 equiv.) at room temperature. The solution was stirred at room temperature for 1 h. Then, a solution of aldehyde **139** (139 mg, 731 µmol, 1.30 equiv.) in DMF (2.00 mL) was added and the reaction mixture was stirred at room temperature for further 5 h. Afterwards, DBU (99.0 µL, 101 mg, 662 µmol, 1.20 equiv.) was added and the reaction mixture was warmed to 120 °C and stirred for 12 h. The mixture was cooled to room temperature and water (2.00 mL, 2.00 g, 111 mmol, 201 equiv.) and further DBU (230 µL, 235 mg, 1.55 mmol, 2.80 equiv.) were added and the solution was stirred for 16 h at room temperature. The reaction mixture was then poured into ethyl acetate (100 mL) and washed with 3 M aq. hydrochloric acid (50 mL), sat. aq. $NaHCO_3$-solution (50 mL), and brine (50 mL). The organic layer was dried over $MgSO_4$, filtered and the solvent was removed in vacuum. Purification by column chromatography (silica gel, PE/EtOAc 4:1 → 2:1) yielded an *E*/*Z* mixture of **176**, which was further purified by reversed phase column chromatography (RP-C_{18} H_2O/MeCN 9:1→4:1) to yield **176** (28.0 mg, 71.9 µmol, 13%) as yellow amorphous powder.

TLC: R_f (PE/EtOAc 1:1 *v/v*) = 0.11.

Mp: 200 °C.

UV (CH_2Cl_2): λ_{max} (nm) = 250, 268.

IR (ATR): 2980, 2889, 2363, 2340, 1716, 1589, 1496, 1375, 1315, 1280, 1254,1232, 948, 821 cm^{-1}.

^{1}H NMR (600 MHz, DMSO-d_6,): δ (ppm) = 10.22 (s, 1 H, $CH_3CO\underline{NH}$), 9.99 (s, 1 H, OH), 7.76 (d, *J* = 8.6 Hz, 2 H, 3'-H, 5'-H), 7.60–7.57 (m, 3 H, 2'-H, 6'-H, 2''-H), 7.55 (dd, *J* = 8.4, 2.2 Hz, 1 H, 6''-H), 6.86 (d, 8.4 Hz, 1 H, 5''-H), 6.43 (s, 1 H, 3-H), 6.29 (s, 1 H, 6-H), 5.29–5.26 (m, 1 H, 2'''-H), 3.23 (d, *J* = 7.3 Hz, 2 H, 1'''-H_2), 2.09 (CH_3), 1.70, 1.69 (2 × s, 2 × 3 H, 4'''-H_3, 5'''-H_3).

^{13}C NMR (151 MHz, DMSO-d_6,: δ (ppm) = 168.7 (CH_3CONH), 168.6 (C-2), 157.6 (C-4), 156.6 (C-4''), 145.0 (C-5), 141.36 (C-4'), 132.5 (C-2''), 131.8 (C-3'''), 130.1 (C-6''), 129.4 (2 C, C-2', C-6'), 128.1 (C-3''), 124.4 (C-1'), 124.2 (C-1''), 122.4 (C-2'''), 119.0 (2 C, C-3', C-5'), 115.4 (C-5''), 113.9 (C-6), 111.6 (C-3), 27.9 (C-1'''), 25.5 (CH_3CONH-), 24.1, 17.7 (2 C, C-4''', C-5''').

HRMS (ESI): for $[C_{24}H_{23}NO_4+H]^+$ calcd.: 390.1700
found: 390.1716.

$C_{24}H_{23}NO_4$ (389.45 g/mol).

Rubrolide S 13[185]

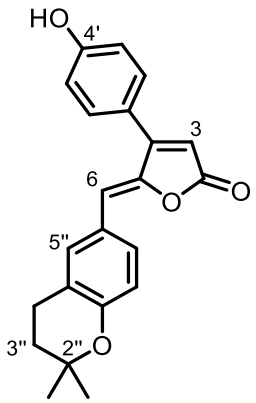

13

To a solution of furanone **137** (100 mg, 567 µmol, 1.00 equiv.) in DMF (5.00 mL) was added TBSOTf (400 µL, 460 mg, 1.74 mmol, 3.07 equiv.) dropwise at room temperature. DIPEA (390 µL, 289 mg, 2.24 mmol, 3.95 equiv.) was added and the solution was stirred at room temperature for 1 h. Then, a solution of aldehyde **117** (164 mg, 862 µmol, 1.52 equiv.) in DMF (1.00 mL) was added and the reaction mixture was stirred at room temperature for further 2 h. Then DBU (170 µL, 173 mg, 1.14 mmol, 2.00 equiv.) was added and the reaction mixture was warmed to 120 °C and stirred for 5 h. The mixture was cooled to room temperature and water (2.00 mL, 2.00 g, 111 mmol, 196 equiv.) and DBU (100 µL, 102 mg, 669 µmol, 1.18 equiv.) were added and the solution was stirred for 16 h at room temperature. The reaction mixture was then poured into ethyl acetate (50 mL) and washed with 3 M aq. hydrochloric acid (50 mL), sat. aq. $NaHCO_3$- solution (50 mL), water (50 mL) and brine (50 mL). The organic layer was dried over $MgSO_4$, filtered and the solvent was removed in vacuum. Purification by column chromatography (silica gel, PE/EtOAc 4:1 → 2:1) yielded an *E*/*Z* mixture (ratio = ~ 1:4 (*E*/*Z*) determined by ^{1}H-NMR) of **13,** which was further purified by reversed phase column chromatography (RP-C_{18} H_2O/MeCN 9:1→4:1) to yield rubrolide S **13** (130 mg, 373 µmol, 66%) as yellow amorphous powder.

TLC: R_f (PE/EtOAc 2:1 *v/v*) = 0.44.

Mp: 204 °C.

UV (CH_2Cl_2): λ_{max} (nm) = 225, 258, 380.

IR (ATR): 3278, 2976, 2931, 2851, 1710, 1606, 1568, 1494, 1345, 1236, 1172, 1119, 1115, 931, 822 cm^{-1}.

^{1}H-NMR (600 MHz, DMSO-d_6): δ (ppm) = 10.11 (s, 1 H, OH), 7.60–7.56 (m, 2 H, 5''-H, 7''-H), 7.49 (d, *J* = 8.5 Hz, 2 H, 2'-H, 6'-H), 6.93 (d, *J* = 8.5 Hz, 2 H, 3'-H, 5'-H), 6.78 (d, *J* = 8.2 Hz, 1 H, 8''-H), 6.38 (s, 1 H, 3-H), 6.31 (s, 1 H, 6-H), 2.76 (t, *J* = 6.7 Hz, 2 H, 4''-H_2), 1.78 (t, *J* = 6.7 Hz, 2 H, 3''-H_2), 1.29 (s, 2 × 3 H, 2 × C-2''-CH_3).

^{13}C-NMR (151 MHz, DMSO-d_6): δ (ppm) = 168.6 (C-2), 159.8 (C-4'), 158.0 (C-4), 154.9 (C-8a''), 145.6 (C-5), 132.5 (C-5''), 130.4 (2 C, C-2', C-6'), 130.1 (C-7''), 124.8 (C-6''), 121.4 (C-4a''), 120.6 (C-1'), 117.4 (C-8''), 115.9 (2 C, C-3', C-5'), 113.3 (C-6), 111.0 (C-3), 75.0 (C-2''), 31.9 (C-3''), 26.6 (2 × C, C-2''-CH_3), 21.8 (C-4'').

HRMS (ESI): for $[C_{22}H_{20}O_4+H]^+$ calcd.: 349.1362
found: 349.1400.

$C_{22}H_{20}O_4$ (348.40 g/mol).

Catechol-rubrolide S 175

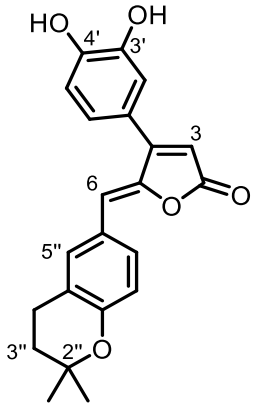

175

To a solution of furanone **170** (70.0 mg, 166 µmol, 1.00 equiv.) in DMF (2.00 mL) was added TBSOTf (120 µL, 135 mg, 499 µmol, 3.00 equiv.) dropwise at room temperature. DIPEA (110 µL, 86.0 mg, 666 µmol, 4.00 equiv.) was added and the solution was stirred at room temperature for 1 h. Then, a solution of aldehyde **117** (41.2 mg, 216 µmol, 1.30 equiv.) in DMF (500 µL) was added and the reaction mixture was stirred at room temperature for further 5 h. Then DBU (29.7 µL, 30.3 mg, 199 µmol, 1.20 equiv.) was added and the reaction mixture was warmed to 120 °C and stirred for 5 h. The mixture was cooled to room temperature and

water (1.00 mL, 1.00 g, 55.5 mmol, 334 equiv.) and DBU (44.5 µL, 45.4 mg, 298 µmol, 2.10 equiv.) were added and the solution was stirred for 16 h at room temperature. The reaction mixture was then poured into ethyl acetate (50 mL) and washed with 3 M aq. hydrochloric acid (50 mL), sat. aq. $NaHCO_3$- solution (50 mL), water (50 mL) and brine (50 mL). The organic layer was dried over $MgSO_4$, filtered and the solvent was removed in vacuum. Purification by column chromatography (silica gel, PE/EtOAc 4:1 → 2:1) yielded an *E*/*Z* mixture of **175,** which was further purified by reversed phase column chromatography (RP-C_{18} H_2O/MeCN 9:1→4:1) to yield rubrolide S **175** (18.0 mg, 49.4 µmol, 30%) as yellow amorphous powder.

TLC: R_f (CH_2Cl_2/MeOH 20:1 *v/v*) = 0.59.

Mp: 205 °C.

UV (CH_2Cl_2): λ_{max} (nm) = 259, 379.

IR (ATR): 3732, 3176, 2958, 2360, 1805, 1718, 1591, 1344, 1281, 1230, 1117, 898, 813, 776, 630 cm^{-1}.

^{1}H-NMR (400 MHz, DMSO-d_6): δ (ppm) = 9.41 (s, 2 H, 2 × OH), 7.57–7.50 (m, 2 H, 5''-H, 7''-H), 7.01 (d, *J* = 2.1 Hz, 1 H, 2'-H), 6.95 (dd, *J* = 8.1, 2.1 Hz, 1 H, 6'-H), 6.89 (d, *J* = 8.1 Hz, 1 H, 5'-H), 6.79 (d, *J* = 9.2 Hz, 1 H, 8''-H), 6.33 (s, 1 H, 3-H), 6.32 (s, 1 H, 6-H), 2.77 (t, *J* = 6.7 Hz, 2 H, 3''-H_2), 1.79 (t, *J* = 6.7 Hz, 2 H, 4''-H_2), 1.30 (s, 3 × 3 H, 2 × 2''-CH_3).

^{13}C NMR (151 MHz, DMSO-d_6): δ (ppm) = 168.6 (C-2), 158.3 (C-4), 154.9 (C-8a''), 148.1 (C-5), 145.7 (2 C, C-3', C-4'), 132.4 (C-5''), 130.0 (C-7''), 124.8 (C-6''), 121.4 (C-1'), 121.0 (C-4a''), 117.4 (C-6'), 116.0 (2 C, C-2', C-5'), 113.2 (C-8'''), 110.8 (C-3), 99.5 (C-6), 75.1 (C-2''), 31.9 (C-3''), 26.6 (2 C, 2 × C-2''-CH_3), 21.7 (C-4'').

HRMS (ESI): for $[C_{22}H_{20}O_5+H]^+$ calcd.: 365.1384
found: 365.1365.

$C_{22}H_{20}O_5$ (364.40 g/mol).

Fluoro-rubrolide S 179

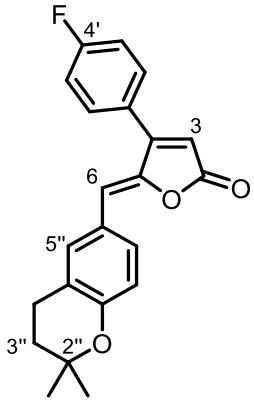

179

To a solution of furanone **172** (100 mg, 0.561 µmol, 1.00 equiv.) in DMF (5.00 mL) was added TBSOTf (331 mg, 290 µL, 1.24 mmol, 2.20 equiv.) dropwise at room temperature. DIPEA (220 mg, 290 µL, 1.68 mmol, 3.00 equiv.) was added and the solution was stirred at room temperature for 1 h. Then, a solution of aldehyde **117** (139 mg, 731 µmol, 1.29 equiv.) in DMF (2.00 mL) was added and the reaction mixture was stirred at room temperature for further 5 h. Then DBU (100 µL, 103 mg, 673 µmol, 1.20 equiv.) was added and the reaction mixture was warmed to 120 °C and stirred for 5 h. The mixture was cooled to room temperature and water (2.00 mL, 2.00 g, 111 mmol, 198 equiv.) and DBU (176 µL, 179 mg, 1.18 mmol, 2.10 equiv.) were added and the solution was stirred for 16 h at room temperature. The reaction mixture was then poured into ethyl acetate (100 mL) and washed with 3 M aq. hydrochloric acid (50 mL), sat. aq. $NaHCO_3$- solution (50 mL), water (50 mL) and brine (50 mL). The organic layer was dried over $MgSO_4$, filtered and the solvent was removed in vacuum. Purification by column chromatography (silica gel, PE/EtOAc 20:1 → 1:1) yielded an *E*/*Z* mixture of **179,** which was further purified by reversed phase column chromatography (RP-C_{18} H_2O/MeCN 9:1→4:1) to yield rubrolide S **179** (124 mg, 353 µmol, 63%) as yellow amorphous powder.

TLC: R_f (PE/EtOAc 4:1 *v/v*) = 0.47.

Mp: 159 °C.

UV (CH_2Cl_2): λ_{max} (nm) = 261, 387.

IR (ATR): 1739, 1608, 1568, 1498, 1425, 1381, 1344, 1263, 1158, 1083, 925, 854, 817, 676, 647 cm^{-1}.

^{1}H NMR (600 MHz, DMSO-d_6): δ (ppm) = 7.70 (dd, J = 8.8, 5.5 Hz, 2 H, 2'-H, 6'-H), 7.61–7.58 (m, 2 H, 5''-H, 7''-H), 7.41 (t, J = 8.9 Hz, 2 H, 3'-H, 5'-H), 6.79 (d, J = 8.4 Hz, 1 H, 8''-H), 6.55 (s, 1 H, 3-H), 6.27 (s, 1 H, 6-H), 2.77 (t, J = 6.7 Hz, 2 H, 3'''-H_2), 1.79 (t, J = 6.7 Hz, 2 H, 4'''-H_2), 1.30 (s, 2 × 3 H, 2 x C-2''-CH_3).

^{13}C NMR (151 MHz, DMSO-d_6): δ (ppm) = 168.3 (C-2), 163.3 (d, J = 249 Hz, C-4'), 156.9 (C-4), 155.0 (C-8a''), 145.3 (C-5), 132.6 (C-5''), 131.2 (d, J = 8.8 Hz, 2 C, C-3', C-5'), 130.1 (C-7''), 126.4 (d, J = 3.2 Hz, C-1'), 124.6 (C-6''), 121.4 (C-4a''), 117.4 (C-8''), 116.1 (d, J = 21.7 Hz, 2 C, C-2', C-6'), 113.5 (C-6), 113.3 (C-3), 75.1 (C-2''), 31.9 (C-3''), 26.6 (2 C, 2 × C-2''-CH_3), 21.7 (C-4'').

HRMS (ESI): for $[C_{22}H_{19}FO_3+H]^+$ calcd.: 351.1391
found: 351.1398.

$C_{22}H_{19}FO_3$ (350.39 g/mol).

NHAc-rubrolide S 177

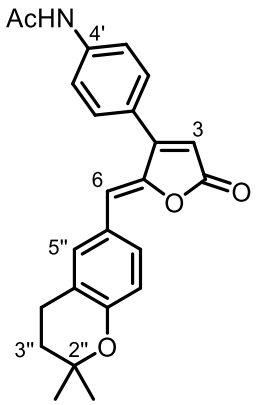

177

To a solution of furanone **171** (120 mg, 552 µmol, 1.00 equiv.) in DMF (5.00 mL) was added TBSOTf (520 µL, 599 mg, 2.27 mmol, 4.11 equiv.) dropwise at room temperature. DIPEA (210µL, 283 mg, 2.19 mmol, 3.97 equiv.) was added and the solution was stirred at room temperature for 1 h. Then, a solution of aldehyde **117** (159 mg, 836 µmol, 1.51 equiv.) in DMF (2.00 mL) was added and the reaction mixture was stirred at room temperature for further 5 h. Then DBU (98.9 µL, 101 mg, 662 µmol, 1.20 equiv.) was added and the reaction mixture was warmed to 120 °C and stirred for 5 h. The mixture was cooled to room temperature and water (2.00 mL, 2.00 g, 111 mmol, 201 equiv.) and DBU (173 µL, 177 mg, 1.16 mmol, 2.10 equiv.) were added and the solution was stirred for 16 h at room temperature. The reaction mixture was then poured into ethyl acetate (100 mL) and washed with 3 M aq. hydrochloric acid (50 mL), sat. aq. $NaHCO_3$- solution (50 mL), water (50 mL) and brine (50 mL). The organic layer was dried over $MgSO_4$, filtered and the solvent was removed in vacuum. Purification by column chromatography (silica gel, PE/EtOAc 4:1 → 2:1) yielded an *E*/*Z* mixture of **177,** which was further purified by reversed phase column chromatography (RP-C_{18} H_2O/MeCN 9:1→4:1) to yield rubrolide S **177** (90.9 mg, 232 µmol, 42%) as yellow amorphous powder.

TLC: R_f (PE/EtOAc 2:1 *v/v*) = 0.36.

Dp: 223 °C.

UV (CH_2Cl_2): λ_{max} (nm) = 251, 383.

IR (ATR): 1743, 1697, 1597, 1564, 1523, 1496, 1425, 1344, 1319, 1296, 1262, 1236, 1151, 1090, 947 cm^{-1}.

^{1}H NMR (600 MHz, DMSO-d_6): δ (ppm) = 10.23 (s, 1 H, $CH_3CO\underline{NH}$), 7.77 (d, *J* = 8.6 Hz, 2 H, 3'-H, 5'-H), 7.62–7.58 (m, 4 H, H-2', H-6', H-5'', H-7''), 6.79 (d, *J* = 9.2 Hz, 1 H, H-8''), 6.47 (s, 1 H, 3-H), 6.34 (s, 1 H, 6-H), 2.77 (t, *J* = 6.9 Hz, 2 H, 3''-H_2), 2.09 (s, 3 H, CH_3), 1.79 (t, *J* = 6.9 Hz, 2 H, 4''-H_2), 1.30 (s, 2 × 3 H, 2 × C-2''-CH_3).

^{13}C NMR (151 MHz, DMSO-d_6): δ (ppm) = 168.8 ($CH_3\underline{CO}$NH), 168.5 (C-2), 157.6 (C-4), 155.0 (C-8a''), 145.4 (C-5), 141.4 (C-4'), 132.6 (C-5''), 130.1 (C-7''), 129.5 (2 C, C-2', C-6'), 124.8 (C-6''), 124.3 (C-1'), 121.4 (C-4a''), 119.0 (2 C, C-3', C-5'), 117.4 (C-8''), 113.5 (C-6), 111.9 (C-3), 75.1 (C-2''), 31.9 (C-3''), 26.6 (2 C, 2 × C-2''-CH_3), 24.1 ($\underline{CH_3}$CONH), 21.7 (C-4'').

HRMS (ESI): for $[C_{24}H_{23}NO_4+H]^+$ calcd.: 390.1700
found: 390.1719.

$C_{24}H_{23}NO_5$ (389.45 g/mol).

Nitro-rubrolide S 181

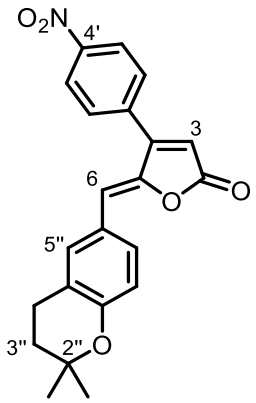

181

To a solution of furanone **173** (100 mg, 487 µmol, 1.00 equiv.) in DMF (4.00 mL) was added TBSOTf (400 µL, 460 mg, 1.74 mmol, 3.57 equiv.) dropwise at room temperature. DIPEA (390 µL, 289 mg, 2.24 mmol, 4.60 equiv.) was added and the solution was stirred at room temperature for 1 h. Then, a solution of aldehyde **117** (164 mg, 862 µmol, 1.77 equiv.) in DMF (2.00 mL) was added and the reaction mixture was stirred at room temperature for further 5 h. Then DBU (87.2 µL, 89.0 mg, 584 µmol, 1.20 equiv.) was added and the reaction mixture was

warmed to 120 °C and stirred for 5 h. The mixture was cooled to room temperature and water (2.00 mL, 2.00 g, 111 mmol, 228 equiv.) and DBU (153 µL, 156 mg, 1.02 mmol, 2.10 equiv.) were added and the solution was stirred for 16 h at room temperature. The reaction mixture was then poured into ethyl acetate (100 mL) and washed with 3 M aq. hydrochloric acid (50 mL), sat. aq. $NaHCO_3$- solution (50 mL), water (50 mL) and brine (50 mL). The organic layer was dried over $MgSO_4$, filtered and the solvent was removed in vacuum. Purification by column chromatography (silica gel, PE/EtOAc 4:1 → 2:1) yielded an *E*/*Z* mixture of **181,** which was further purified by reversed phase column chromatography (RP-C_{18} H_2O/MeCN 9:1→4:1) to yield rubrolide S **181** (25.7 mg, 68.1 µmol, 14%) as yellow amorphous powder.

TLC: R_f (PE/EtOAc 5:1 *v/v*) = 0.44.

Mp: 136 °C**.**

UV (CH_2Cl_2): λ_{max} (nm) = 277, 322, 439.

IR (ATR): 1733, 1604, 1499, 1345, 1295, 1253, 1197, 1186, 1172, 1107, 1086, 1022, 958, 926, 811 cm^{-1}.

^{1}H NMR (600 MHz, DMSO-d_6): δ (ppm) = 8.38 (d, *J* = 8.8 Hz, 2 H, 2'-H, 6'-H), 7.91 (d, *J* = 8.8 Hz, 2 H, 3'-H, 5'-H), 7.62–7.59 (m, 2 H, 5''-H, 7''-H), 6.80 (d, *J* = 8.4 Hz, 1 H, 8''-H), 6.72 (s, 1 H, 3-H), 6.29 (s, 1 H, 6-H), 2.77 (t, *J* = 6.7 Hz, 2 H, 3''-H), 1.80 (t, *J* = 6.7 Hz, 2 H, 4''-H), 1.30 (s, 2 × 3 H, 2 × C-2''-CH_3).

^{13}C NMR (151 MHz, DMSO-d_6): δ (ppm) = 168.0 (C-2), 155.7 (C-4), 155.2 (C-8a''), 148.4 (C-4'), 144.9 (C-5), 136.2 (C-1'), 132.7 (C-5''), 130.3 (2 C, C-3', C-5'), 130.2 (C-7''), 124.5 (C-6''), 124.0 (2 C, C-2', C-6'), 121.5 (C-4a''), 117.5 (C-8''), 114.9 (C-3), 113.9 (C-6), 75.2 (C-2''), 31.9 (C-3''), 26.6 (2 C, 2 × C-2''-CH_3), 21.7 (C-4'').

HRMS (ESI): for $[C_{22}H_{19}NO_5+H]^+$ calcd.: 378.1336
found: 378.1342.

$C_{22}H_{19}NO_5$ (377.40 g/mol).

Chloro rubrolide R 154

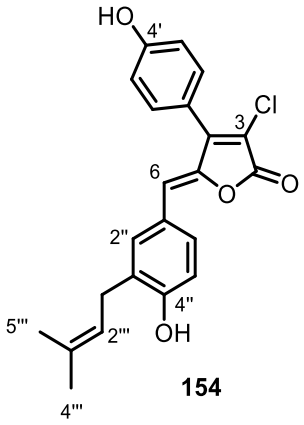

154

To a solution of furanone **156** (30.0 mg, 142 µmol, 1.00 equiv.) in DMF (1.50 mL) was added dropwise TBSOTf (150 µL, 173 mg, 653 µmol, 4.60 equiv.) and DIPEA (112 µL, 83.0 mg, 642 mmol, 4.52 equiv.) at room temperature. The solution was stirred at room temperature for 1 h. Then, a solution of aldehyde **139** (35.2 mg, 185 µmol, 1.30 equiv.) in DMF (500 µL) was added and the reaction mixture was stirred at room temperature for further 5 h. Afterwards, DBU (25.4 µL, 25.9 mg, 170 µmol, 1.20 equiv.) was added and the reaction mixture was warmed to 120 °C and stirred for 12 h. The mixture was cooled to room temperature and water (1.00 mL, 1.00 g, 55.5 mmol, 391 equiv.) and further DBU (59.3 µL, 60.5 mg, 398 µmol, 2.80 equiv.) were added and the solution was stirred for 16 h at room temperature. The reaction mixture was then poured into ethyl acetate (50 mL) and washed with 3 M aq. hydrochloric acid (50 mL), sat. aq. $NaHCO_3$-solution (50 mL), and brine (50 mL). The organic layer was dried over $MgSO_4$, filtered and the solvent was removed in vacuum. Purification by column chromatography (silica gel, PE/EtOAc 4:1 → 1:1) yielded an *E*/*Z* mixture of **154**, which was further purified by reversed phase column chromatography (RP-C_{18} H_2O/MeCN 9:1→4:1) to yield **154** (5.98 mg, 15.6 µmol, 11%) as yellow amorphous powder.

TLC: R_f (PE/EtOAc 2:1 *v/v*) = 0.26.

Mp: 210 °C.

UV (CH_2Cl_2:) λ_{max} (nm) = 228, 256, 373.

IR (ATR): 1727, 1599, 1507, 1501, 1432, 1342, 1265, 1172, 1106, 1029, 838, 818, 757, 530, 523 cm^{-1}.

^{1}H NMR (600 MHz, DMSO-d_6,): δ (ppm) = 10.10 (s, 2 H, 2 × OH), 7.55 (d, J = 2.1 Hz, 1 H, 2''-H), 7.52 (dd, J = 8.5, 2.1 Hz, 1 H, 6''-H), 7.44 (d, J = 8.7 Hz, 2 H, 2'-H, 6'-H), 6.98 (d, J = 8.7 Hz, 2 H, 3'-H, 5'-H), 6.86 (d, J = 8.5 Hz, 1 H, 5''-H), 6.20 (s, 1 H, 6-H), 5.29–5.24 (m, 1 H, 2'''-H), 3.22 (d, J = 7.3 Hz, 2 H, 1'''-H_2), 1.70, 1.68 (2 × s, 2 × 3 H, 4'''-H_3, 5'''-H_3).

^{13}C NMR (151 MHz, DMSO-d_6,: δ (ppm) = 164.2 (C-2), 159.6 (C-4'), 156.6 (C-4''), 150.0 (C-4), 143.6 (C-5), 132.6 (C-2''), 131.9 (C-3'''), 130.9 (2 C, C-2', C-6'), 130.3 (C-6''), 128.2 (C-3''), 123.8 (C-1''), 122.3 (C-2'''), 118.1 (C-1'), 115.8 (2 × C, C-3'. C-5'), 115.4 (C-5''), 115.1 (C-6), 114.1 (C-3), 27.8 (C-1'''), 25.5, 17.7 (2 C, C-4''', C-5''').

HRMS (ESI): for $[C_{22}H_{19}ClO_4+H]^+$ calcd.: 383.1045
found: 383.1047.

$C_{22}H_{19}ClO_4$ (382.84 g/mol).

Per(OAc)-D-mannosyl-rubrolide S 188

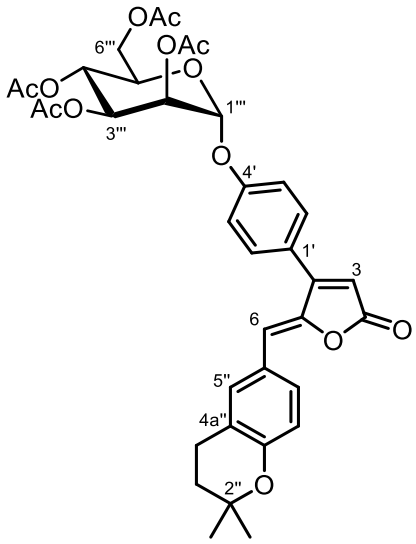

188

Under exclusion of light 1-bromo-2,3,4,6-tetra-*O*-acetyl-*α*-D-mannopyranose **183** (11.6 mg, 28.2 µmol, 1.05 equiv.), rubrolide S **13** (9.30 mg, 26.7 µmol, 1.00 equiv.) and Drierite® (22.5 mg, 64.6 mmol, 2.40 equiv.) were dissolved in CH_2Cl_2 (500 µL) and stirred for 40 min under argon atmosphere. To the solution Ag_2O (26.2 mg, 113 µmol, 3.97 equiv.) and Ag_2CO_3 (5.30 mg, 19.2 µmol, 0.69 equiv.) were added. The suspension was stirred for 19 h at room temperature. After filtration through celite® the solvent was removed in vacuum. The crude product was purified by column chromatography (silica gel, PE/EtOAc, 0% → 100% EtOAc) to yield **188** (12.7 mg, 18.7 µmol, 70%) as a yellow solid.

TLC: R_f = 0.24 (PE/EtOAc 2:1 *v*:*v*).

UV (MeCN) λ_{max} (nm) = 343.

IR (ATR): 3364, 2925, 2855, 2363, 1740, 1608, 1495, 1370, 1121, 1047, 1032, 824, 640 cm^{-1}.

^{1}H-NMR (600 MHz, MeOD-d_4): δ (ppm) = 7.66 (d, J = 1.6 Hz, 1 H, 5''-H), 7.53 (dd, J = 8.6, 2.1 Hz, 1 H, 7''-H), 7.53 (d, J = 8.5 Hz, 2 H, 2'-H, 6'-H), 7.28 (d, J = 8.5 Hz, 2 H, 3'-H, 5'-H), 6.74 (d, J = 8.6 Hz, 1 H, 8''-H), 6.29 (s, 1 H, 6-H), 6.24 (s, 1 H, 3-H), 5.45 (d, J = 2.3 Hz, 1 H, 1'''-H), 5.25 (t, J = 9.9 Hz, 1 H, 4'''-H), 5.08 (dd, J = 9.9, 4.4 Hz, 1 H, 3'''-H), 4.26 (dd, J = 12.2, 4.4 Hz, 1 H, 2'''-H), 4.09 (dd, J = 12.2, 2.4 Hz, 1 H, 6'''-H_a), 4.06 (dd, J = 4.0, 2.4 Hz 1 H, 6'''-H_b), 3.77–3.75 (m, 1 H, 5'''-H), 2.83 (t, J = 6.7 Hz, 2 H, 4''-H_2), 2.12, 2.05, 2.04, 1.89 (s, 4 × 3 H, 4 × (CO)$\underline{CH_3}$), 1.83 (t, J = 6.7 Hz, 2 H, 3''-H_2), 1.35 (s, 2 × 3 H, 2 × C-2''-CH_3).

^{13}C-NMR (126 MHz, $CDCl_3$) δ (ppm) = 169.6 (4 C, 4 × $\underline{CO}CH_3$), 169.5 (C-2), 158.1 (C-4), 155.8 (C-8a''), 154.7 (C-4'), 146.2 (C-5), 132.6 (C-5''), 130.9 (C-7''), 129.8 (C-2', C-6'), 124.5 (C-6''), 124.5 (C-4a''), 122.9 (C-3', C-5'), 121.6 (C-1'), 118.0 (C-8''), 114.7 (C-3), 112.9 (C-6), 97.4 (C-1'''), 76.0 (C-2'''), 75.3 (C-2''), 71.8 (C-5'''), 70.3 (C-3'''), 65.5 (C-4'')', 62.6 (C-6'''), 32.8 (C-4''), 27.1 (2 C, 2 × CH_3), 24.3 (CO$\underline{CH_3}$), 22.6 (C-3''), 20.9 (2 C, 2 × CO$\underline{CH_3}$), 20.8 (CO$\underline{CH_3}$).

HRMS (ESI): for $[C_{36}H_{38}O_{13}+H]^+$ calcd.: 679.2385

found: 679.2384.

$C_{36}H_{38}O_{13}$ (678.69 g/mol).

6.3.4. Starting material synthesis for prunolide synthesis

1,2-Diphenylethylene 189[168]

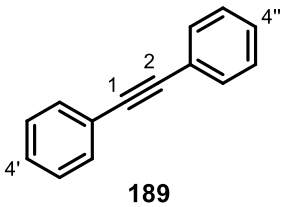

189

A solution of iodobenzene **191** (3.00 g, 12.8 mmol, 1.98 equiv.), trimethylsilylacetylene **193** (1.60 mL, 1.10 g, 6.46 mmol, 1.00 equiv.) and water (120 µL, 120 mg, 6.66 mmol, 1.03 equiv.) in DBU (12.0 mL) was degassed with argon for 5 min. Afterwards, $PdCl_2$ (56.8 mg, 320 µmol, 5 mol%) and PPh_3 (168 mg, 641 µmol. 9.9 mol%) were added and stirred for 12 h at 70 °C. After cooling to room temperature the solvent removed in vacuum. The crude product was purified by column chromatography (silica gel, PE/EtOAc 9:1 *v*/*v*). Diphenylethylene **189** (852 mg, 4.78 mmol, 74%) was obtained in a yield of as colorless solid.

TLC: R_f = 0.72 (PE/EtOAc 19:1 *v/v*).

UV (CH_2Cl_2) λ_{max} (nm) = 224, 280, 296.

Mp: 69 °C (*lit*.: 68-70 °C[250])

IR (ATR): 2321, 1599, 1493, 1442, 916, 753, 687, 665, 534, 506 cm^{-1}.

^{1}H-NMR (500 MHz, $CDCl_3$): δ (ppm) = 7.61–7.52 (m, 4 H, 2'-H, 6'-H, 2''-H, 6''-H), 7.42–7.31 (m, 6 H, 3'-H, 4'-H, 5'-H, 3''-H, 4''-H, 5''-H).

^{13}C-NMR (126 MHz, $CDCl_3$): δ (ppm) = 132.8 (4 C, C-2', C-6', C-2'', C-6''), 128.5 (4 C, C-3', C-5', C-3'', C-5''), 128.4 (2 C, C-4', C-4''), 123.4 (2 C, C-1', C-1''), 89.5 (2 C, C-1, C-2).

$C_{14}H_{10}$ (178.23 g/mol).

1,2-Bis(4-methoxyphenyl)ethyne 190[168]

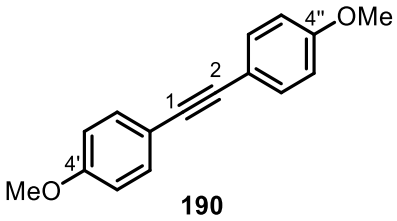

190

A solution of *p*-Iodoanisole **192** (3.00 g, 12.8 mmol, 1.98 equiv.), trimethylsilylacetylene **193** (920 µL, 635 g, 6.46 mmol, 1.00 equiv.) and water (120 µL, 120 mg, 6.66 mmol, 1.03 equiv.) in DBU (12.0 mL) at room temperature was degassed with argon for 5 min. Afterwards, $PdCl_2$ (56.8 mg, 0.320 mmol, 5.0 mol%) and PPh_3 (168 mg, 0.641 mmol. 10.0 mol%) were added to the reaction and stirred for 12 h at 70 °C. After cooling to room temperature the solvent was removed in vacuum. The crude product was purified by column chromatography (silica gel, Pe/EtOAc 9:1 *v/v*). **190** was obtained as colorless solid (1.16 g, 4.85 mmol, 75 %).

TLC: R_f = 0:18 (PE/EtOAc 8:1 *v/v*).

UV (CH_2Cl_2) λ_{max} (nm) = 294, 312.

Mp: 148 °C (lit.: 147-148 °C[251]).

IR (ATR): 1605, 1506, 1458, 1442, 1284, 1244, 1195, 1169, 1106, 1025, 956, 819, 747, 715, 587 cm^{-1}.

^{1}H-NMR (500 MHz, $CDCl_3$): δ (ppm) = 7.45 (d, J = 8.9 Hz, 4 H, 2'-H, 6'-H, 2''-H, 6''-H), 6.87 (d, J = 8.9 Hz, 4 H, 3'-H, 5'-H, 3''-H, 5''-H), 3.82 (s, 2 × 3 H, 2 × OCH_3).

^{13}C-NMR (126 MHz, $CDCl_3$): δ (ppm) = 159.5 (2 C, C-4', C-4''), 133.0 (4 C, C-2', C-6', C-2'', C-6''), 115.9 (2 C, C-1', C-1''), 114.1 (4 C, C-3', C-5', C-3'', C-5''), 88.1 (2 C, C-1, C-2), 55.4 (2 C, 2 × OCH_3).

$C_{16}H_{14}O_2$ (238.29 g/mol).

(*Z*)-1,2-Diphenyl-1,2-bis(4,4,5,5-tetramethyl-1,3,2-dioxaborolan-2-yl)ethane 200

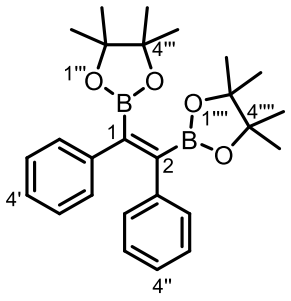

200

A solution of 1,2-diphenylethyne **189** (2.00 g, 11.2 mmol, 1.00 equiv.) and B_2Pin_2 **196** (3.13 g, 12.3 mmol, 1.10 equiv.) in DMF (10.0 mL) was degassed with argon for 5 min. Afterwards $Pt(PPh_3)_4$ (25.9 mg, 20.8 µmol, 0.2 mol%) was added and stirred for 18 h at 80 °C. The reaction mixture was cooled to room temperature and the solvent was removed in vacuum. The crude product was purified by recrystallization from (PE/EtOAc 9:1). The desired product **200** (3.50 mg, 8.10 mmol, 72%) was obtained as colorless solid.

Mp: 105 °C.

^{1}H-NMR (300 MHz, $CDCl_3$): δ (ppm) = 7.10–7.01 (m, 6 H, 3'-H, 4'-H, 5'-H, 3''-H, 4''-H, 5''-H), 6.97–6.91 (m, 4 H, 2'-H, 6'-H, 2''-H, 6''-H, 1.32 (s, 8 × 3 H, 8 × CH_3).

^{13}C-NMR (101 MHz, $CDCl_3$): δ (ppm) = 141.4 (2 C, C-1', C-1''), 129.4 (4 C, C-3', C-5', C-3'', C-5''), 127.5, (4 C, C-2', C-6', C-2'', C-6''), 125.9 (2 C, C-4', C-4''.), 84.2 (6 C, C-1, C-2, C-4''', C-5''', C-4'''', C-5''''), 25.0 (8 C, 2 × C-4'''-CH_3, 2 × C-5'''-CH_3, 2 × C-4''''-CH_3, 2 × C-5''''-CH_3).

MS (ESI): for $[C_{26}H_{34}B_2O_4+H]^+$ calcd.: 423.2721
found: 433.2793.

$C_{26}H_{34}B_2O_4$ (432.17 g/mol).

(*Z*)-1,2-Bis(4-methoxyphenyl)-1,2-bis(4,4,5,5-tetramethyl-1,3,2-dioxaborolan-2-yl)ethane 125

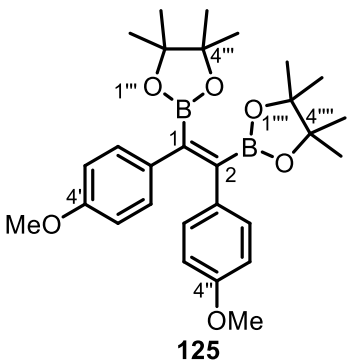

125

A solution of 1,2-bis(4-methoxyphenyl)ethyne **190** (1.00 g, 4.20 mmol, 1.00 equiv.) and B_2Pin_2 **196** (1.17 g, 4.61 µmol, 1.10 eq.) in DMF (20.0 mL) was degassed with argon for 10 min. Afterwards, $Pt(PPh_3)_4$ (10.8 mg, 8.68 µmol, 0.2 mol%) was added and stirred for 48 h at 80 °C. The reaction mixture was cooled to room temperature and the solvent removed in vacuum. The crude product was purified by recrystallization from (PE/EtOAc). The desired product **125** (1.86 g, 3.78 mmol, 90%) was obtained as colorless solid.

^{1}H-NMR (300 MHz, $CDCl_3$): *δ* (ppm) = 6.88 (d, *J* = 8.8 Hz, 4 H, 3'-H, 5'-H, 3-H'', 5-H''), 6.63 (d, *J* = 8.8 Hz, 4 H, 2'-H, 6'-H, 2''-H, 6''-H), 3.71 (s, 2 × 3 H, 2 × OCH_3), 1.32 (s, 8 × 3 H, 8 × CH_3).

^{13}C-NMR (101 MHz, $CDCl_3$): *δ* (ppm) = 157.7 (2 C, C-4', C-4''), 133.9 (2 C, C-1', C-1''), 130.7 (4 C, C-2', C-6', C-2'', C-6''), 113.1 (4 C, C-3', C-5', C-3'', C-5''), 84.1 (6 C, C-1, C-2, C-4''', C-5''', C-4'''', C-5''''), 55.1 (2 C, 2 × OCH_3), 25.0 (8 C, 2 × C-4'''-CH_3, 2 × C-5'''-CH_3, 2 × C-4''''-CH_3, 2 × C-5''''-CH_3).

HRMS (ESI): for $[C_{28}H_{38}B_2O_6+K]^+$ calcd.: 493.2933
found: 493.2924.

$C_{28}H_{38}B_2O_6$ (492.23 g/mol).

(*Z*)-1,2-Bis(5,5-dimethyl-1,3,2-dioxaborinan-2-yl)-1,2-diphenyl-ethene 200

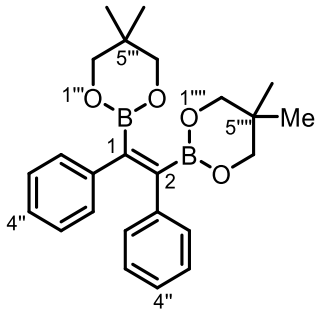

200

A solution of diphenylethyne **189** (1.00 g, 5.61 mmol, 1.00 equiv.) and B_2Neop_2 **198** (1.39 g, 6.17 mmol, 1.10 equiv.) in DMF (10.0 mL) was degassed with argon for 5 min. Then, $Pt(PPh_3)_4$ (14.0 mg, 11.3 µmol, 0.2 mol%) was added and stirred for 24 h at 80 °C. The reaction mixture was cooled to room temperature and the solvent was removed in vacuum. The crude product was purified by sublimation. The desired product **200** (2.04 g, 5.04 mmol, 90%) was obtained as colorless solid.

Mp: 156 °C.

UV (CH_2Cl_2) λ_{max} (nm) = 280, 298.

IR (ATR): 1599, 1476, 1441, 1397, 1290, 1214, 1139, 1069, 1037, 915, 813, 753, 686, 586, 535 cm^{-1}.

^{1}H-NMR (600 MHz, $CDCl_3$): δ (ppm) = 7.55–7.52 (m, 4 H, 2'-H, 6'-H, 2'-H, 6'-H), 7.36–7.32 (m, 6 H, 3'-H, 4'-H, 5'-H, 3''-H, 4''-H, 5''-H), 3.60 (s, 8 H, 4 × 2 H, 4'''-H, 6'''-H, 4''''-H, 6''''-H), 0.95 (s, 4 × 3 H, 2 × C-5'''-CH_3, 2 × C-5''''-CH_3).

^{13}C-NMR (151 MHz, $CDCl_3$): δ (ppm) = 131.7 (4 C, C-2', C-6', C-2'', C-6''), 128.5 (4 C, C-3', C-5', C-3'', C-5''), 128.4 (2 C, C-4', C-4''), 123.4 (2 C, C-1', C-1''), 89.5 (2 C, C-1, C-2), 71.6 (4 C, C-4''', C-5''', C-4'''', C-5''''), 31.8 (2 C, C-5''', C-5''''), 22.2 (4 C, 2 × C-5'''-CH_3, 2 × C-5''''-CH_3).

$C_{24}H_{30}B_2O_4$ (404.12 g/mol).

(*Z*)-1,2-Bis(5,5-dimethyl-1,3,2-dioxaborinan-2-yl)-1,2-bis(4-methoxyphenyl)-ethene 202

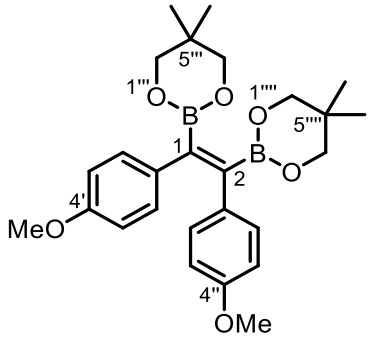

202

A solution of 1,2-bis(4-methoxyphenyl)ethyne **190** (794 g, 3.33 mmol, 1.00 equiv.) and B_2Neop_2 **198** (931 mg, 3.67 µmol, 1.10 equiv.) in DMF (5.00 mL) was degassed with argon for 5 min. Then, $Pt(PPh_3)_4$ (7.70. mg, 6.19 µmol, 0.2 mol%) was added and stirred for 20 h at 80 °C. The reaction mixture was cooled to room temperature and the solvent removed in vacuum. The crude product was purified by sublimation. The desired product **202** (1.33 g, 2.86 mmol, 86%) was obtained as colorless solid.

Mp: 174 °C.

UV (CH_2Cl_2): λ_{max} (nm) = 280, 298.

IR (ATR): 2969, 1605, 1509, 1475, 1396, 1286, 1238, 1142, 1025, 833, 683, 529 cm^{-1}.

^{1}H-NMR (300 MHz, $CDCl_3$): δ (ppm) = 7.44 (d, *J* = 8.9 Hz, 4 H, 3-H, 5-H, 3'-H, 5'-H), 6.96 (d, *J* = 8.9 Hz, 4 H, 2'-H, 6'-H, 2''-H, 6''-H), 3.83 (s, 2 × 3 H, 2 × OCH_3), 3.52 (s, 4 × 2 H, 4'''-H, 6'''-H, 4''''-H, 6''''-H), 0.92 (s, 4 × 3 H, 2 × 5'''-H-CH_3, 2 × 5''''-H-CH_3).

^{13}C-NMR (75 MHz, $CDCl_3$): δ (ppm) = 159.3 (2 C, C-4', C-4''), 132.7 (4 C, C-2', C-6', C-2'', C-6''), 114.6 (2 C, C-1', C-1''), 114.3 (4 C, C-3', C-5', C-3'', C-5''), 88.0 (2 C, C-1, C-2), 70.2 (4 C, C-4''', C-5''', C-4'''', C-5''''), 55.3 (2 C, 2 × OCH_3), 31.1 (2 C, C-5''', C-5''''), 21.5 (4 C, 2 × C-5'''-CH_3, 2 × C-5''''-CH_3).

MS (ESI): for $[C_{26}H_{34}B_2O_6+K]^+$ calcd.: 503.2173
found: 503.2135.

$C_{26}H_{34}B_2O_6$ (464.17 g/mol).

(2*Z*)-3-bromo-3-(4-methoxyphenyl)propen-2-enal 128

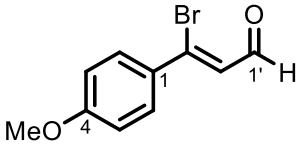

128

The compound was prepared using a modified protocol originally reported by *Gupton* et al.[212] To a solution of DMF (4.60 mL, 4.40 g, 59.9 mmol, 3.00 equiv.) in $CHCl_3$ (20.0 mL) was added dropwise PBr_3 (5.10 mL, 14.6 g, 53.9 mmol, 2.70 equiv.) at 0 °C over 20 min. The reaction mixture was stirred for 1 h at room temperature. Afterwards, acetanisol **15** (3.00 g, 20.0 mmol, 1.00 equiv.) was added and stirred at room temperature for 16 h. Then, ice water was added and neutralized with K_2CO_3 to pH ~ 8. The mixture was extracted with Et_2O (3 × 50 mL) and the organic phase was washed with brine (100 mL), dried over $MgSO_4$, filtered and the solvent was removed in vacuum. The crude product was purified by column chromatography (silica gel, PE/EtOAc 9:1 → 4:1) to yield aldehyde **128** (2.60 g, 10.8 mmol, 54%) as light yellow solid.

TLC: R_f (PE/EtOAc 9:1 *v/v*) = 0.37.

Mp: 42.5 °C (*lit*: 43.5-45.0 °C[212])

UV (CH_2Cl_2): λ_{max} (nm) = 326.

IR (ATR): 2842, 2022, 1658, 1597, 1505, 1255, 1173, 1123, 1019, 831, 809, 569 cm^{-1}.

^{1}H-NMR (300 MHz, DMSO-d_6) δ (ppm) = 9.94 (d, *J* = 6.5 Hz, 1 H, 3'-H), 7.85 (d, *J* = 8.9 Hz, 2 H, 2-H, 6-H) , 7.06 (d, *J* = 8.9 Hz, 2 H, 3-H, 5-H), 7.02 (d, *J* = 6.5 Hz, 1 H, 2'-H), 3.84 (s, 3 H, CH_3)

^{13}C-NMR (101 MHz, $CDCl_3$) δ (ppm) = 194.0 (C-1'), 162.7 (C-4), 145.2 (C-3'), 130.0 (2 C, C-2, C-6), 129.6 (C-1), 125.7 (C-2'), 114.3 (2 C, C-3, C-5), 55.7 (CH_3).

MS (ESI): for $[C_{10}H_{10}BrO_2+H]^+$ calcd.: 240.9858
found: 240.9884

$C_{10}H_9BrO_2$ (241.08 g/mol).

(*Z*)-3-bromo-3-(4-methoxyphenyl)acrylic acid 129

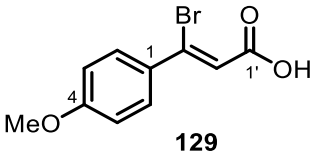

129

To a mixture of aldehyde **128** (1.00 g, 4.15 mmol, 1.00 equiv.) in MeCN/water mixture (6.50 mL, 2.5:1 *v*/*v*) was added $NaH_2PO_4 \times H_2O$ (805 mg, 5.83 mmol, 1.41 equiv.) and cooled to 0 °C. Following, H_2O_2 (30%, 450 µL, 495 mg, 4.31 mmol, 1.04 equiv.) was added and stirred for 10 min. Afterwards, $NaClO_2$ (528 mg, 5.84 mmol, 1.41 equiv.) in water (1.00 mL) was added to the mixture and stirred for 20 h at room temperature. Then, Na_2SO_3 (100 mg) was added and acidified with aq. HCl (1 M) to pH = 1. The mixture was extracted with EtOAc (3 × 150 mL). The combined oganic phases were washed with sat. $NaHCO_3$ solution (100 mL), water (100 mL) and brine (50 mL), dried over $MgSO_4$, filtered and the solvent removed in vaccuum. The crude product was purified by column chromatography (RP-C_{18}, H_2O/MeCN, 9:1 →1:1 *v*/*v*) to yield acid **129** (863 mg, 3.36 mmol, 81%) as colorless solid.

TLC: R_f (EtOAc *v*/*v*) = 0.49.

Mp: 146 °C.

UV (CH_2Cl_2) λ_{max} (nm) = 226, 302.

IR (ATR): 1679, 1580, 1502, 1460, 1420, 1320, 1287, 1259, 1175, 1126, 1023, 983, 908, 830, 557 cm^{-1}.

^{1}H-NMR (400 MHz, DMSO-d_6): δ (ppm) = 12.72 (bs, 1 H, CO_2H), 7.66 (d, J = 7.5 Hz, 2 H, 2-H, 6-H), 7.00 (d, J = 7.5 Hz, 2 H, 3-H, 5-H), 6.84 (s, 1 H, 2-H), 3.81 (s, 3 H, OCH_3).

^{13}C-NMR (101 MHz, $CDCl_3$): δ (ppm) = 165.5 (C-3'), 161.0 (C-4), 134.1 (C-1'), 130.4 (C-1'), 129.6 (2 C, C-2, C-6), 119.9 (C-2'), 114.0 (2 C, C-3, C-5), 55.5 (OCH_3).

MS (ESI): for $[C_{10}H_9BrO_3\text{-}H]^-$ calcd.: 254.9662
found: 254.9651

$C_{10}H_9BrO_3$ (257.08 g/mol).

Methyl-(2*Z*)-3-bromo-3-(4-methoxyphenyl)prop-2-enoate 127

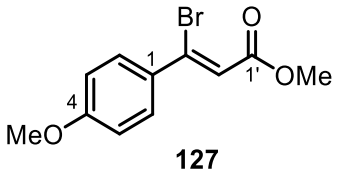

127

Method A:

To a mixture of acrylic acid **129** (1.23 g, 4.52 mmol, 1.0 equiv.) in methanol (12.0 mL), five drops of H_2SO_4 (95%) were added. The mixture was stirred for 16 h at 70 °C. Afterwards, the solvent was removed in vacuum. The crude product was purified via column chromatography (silica gel, PE/EtOAc 50:1 → 4:1 *v*/*v*). The desired compound **127** (1.22 g, 4.50 mmol, quant.) was obtained as beige solid.

Method B:

To a solution of $VO(acac)_2$ (1.10 mg, 4.00 µmol, 4.00 mol%) in H_2O_2 (210 µL, 242 mg, 2.49 mmol, 3.00 equiv.) was added the solution of aldehyde **128** (200 mg, 0.830 mmol, 1.00 equiv.) in methanol (800 µL) at to 0 °C.The reaction was stirred for 2 h at 0 °C. The crude product was purified twice by column chromatography (silica gel, PE/EtOAc 9:1 → 3:1) to yield the compound **127** (48.6 mg, 0.179 mmol, 22%) as colorless solid.

TLC: R_f (PE/EtOAc 9:1 *v*/*v*) = 0.22.

Mp: 37–39 °C

UV (CH_2Cl_2): λ_{max} (nm) = 297.

IR (ATR): 2953, 1760, 1672, 1597, 1511, 1422, 1319, 1257, 1170, 1024, 978, 842, 709, 567 cm^{-1}.

^{1}H-NMR (300 MHz, DMSO-d_6) δ (ppm) = 7.98 (d, *J* = 8.9 Hz, 2 H, 2-H, 6-H), 6.97 (d, *J* = 8.9 Hz, 2 H, 3-H, 5-H), 5.64 (s, 1 H, 2'-H), 3.89 (s, 3 H, CO_2CH_3), 3.83 (s, 3 H, OCH_3)

^{13}C-NMR (101 MHz, $CDCl_3$) δ (ppm) = 186.7 (C-1), 166.0 (C-1'), 164.6 (C-1'), 131.9 (2 C, C-2, C-6), 126.2 (C-4), 114.3 (2 C, C-3, C-5), 55.8 (OCH_3), 54.1 (CO_2CH_3), 45.9 (C-2').

HRMS (ESI): for $[C_{11}H_{11}BrO_3+K]^-$ calcd.: 308.9596
found: 308.9683.

$C_{11}H_{11}BrO_3$ (271.11 g/mol).

Methyl-benzoylacetate 216[138]

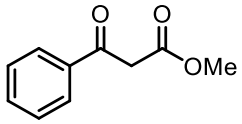

216

Following general procedure 3 the aldol addition was performed using acetophenone **213** (4.80 mL, 4.94 g, 41.1 mmol, 1.00 equiv.), NaH (60% mineral oil suspension, 4.06 g, 101 mmol, 2.46 equiv.) and dimethylcarbonate **215** (8.70 mL, 9.31 g, 103 mmol, 2.51 equiv.). The crude product **216** was used without further purification.

TLC: R_f = 0.42 (PE/EtOAc 8:1 *v/v*).

$C_{10}H_{10}O_3$ (178.19 g/mol).

Methyl-4-methoxybenzoylacetate 217[138]

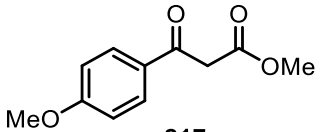

217

Following general procedure 3 the aldol addition was performed using 4-methoxy-acetophenone **15** (5.13 g, 30.9 mmol, 1.00 equiv.), NaH (60% mineral oil suspension, 3.27 g, 75.0 mmol, 2.43 equiv.) and dimethylcarbonate **215** (6.40 mL, 6.85 g, 76.0 mmol, 2.46 equiv.). The crude product **217** was used without further purification.

TLC: R_f = 0.49 (PE/EtOAc 4:1 *v/v*).

$C_{11}H_{12}O_4$ (208.21 g/mol).

Methyl-4-fluorobenzoylacetate 218[138]

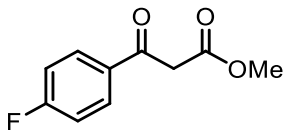

218

Following general procedure 3, the aldol addition was obtained by 4-fluoroacetophenone **214** (4.50 mL, 5.09 g, 36.8 mmol, 1.00 equiv.), NaH (60% mineral oil suspension, 3.71 g, 93.0 mmol, 2.53 equiv.) and dimethylcarbonate **215** (7.70 mL, 8.24 g, 91.5 mmol, 2.49 equiv.). The crude product **218** was used without further purification.

TLC: R_f = 0.44 (PE/EtOAc 4:1 *v/v*).

$C_{10}H_9FO_3$ (196.18 g/mol).

Methyl-(*Z*)-3-phenyl-3-(tosyloxy) acrylate 210[138]

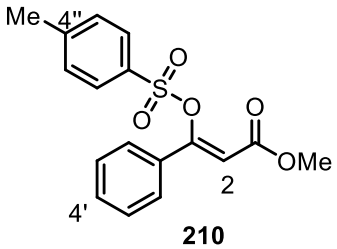

210

Following general procedure 4 tosylation was obtained by use of **216** (7.42 g, 41.6 mmol, 1.00 equiv.), TMEDA (9.50 mL, 7.32 g, 63.0 mmol, 1.51 equiv.), LiCl (2.65 g, 62.5 mmol, 1.50 equiv.) and TsCl (12.2 g, 64.0 mmol, 1.54 equiv.). The desired product **210** (10.8 g, 32.5 mmol, 78%) was obtained as colorless solid over two steps.

TLC: R_f = 0.44 (PE/EtOAc 4:1 *v/v*)

UV ($CHCl_3$): λ_{max} (nm) = 237, 268.

Mp: 105.5 °C (lit.: 103 – 105 °C[221]).

IR (ATR): 3410, 2946, 1727, 1642, 1375, 1260, 1181, 1151, 1035, 715, 670 cm^{-1}.

^{1}H-NMR (500 MHz, $CDCl_3$): δ (ppm) = 7.72 (d, *J* = 8.2 Hz, 2 H, 2''-H, 6''-H), 7.42 (d, *J* = 7.3 Hz, 2 H, 3'-H, 5'-H), 7.36 (t, *J* = 7.3 Hz, 1 H, 4'-H), 7.27–7.24 (m, 2 H, 2'-H, 6'-H), 7.23 (d, *J* = 8.2 Hz, 2 H, 3''-H, 5''-H), 6.12 (s, 1 H, 2-H), 3.70 (s, 3 H, CO_2CH_3), 2.41 (s, 3 H, CH_3).

^{13}C-NMR (126 MHz, $CDCl_3$): δ (ppm) = 163.9 (C-1), 155.7 (C-3), 145.3 (C-4''), 133.4 (C-1''), 133.0 (C-1'), 130.9 (C-4'), 129.5 (2 C, C-3'', C-5''), 128.5 (2 C, C-2'', C-6''), 128.5 (2 C, C-2', C-6'), 126.9 (2 C, C-3', C-5'), 110.4 (C-2), 51.7 (CO_2CH_3), 21.7 (CH_3).

HRMS (ESI): for $[C_{17}H_{16}O_5S + Na]^+$ calcd.: 355.0611
found: 355.0599.

$C_{17}H_{16}O_5S$ (332.37 g/mol).

Methyl-(*Z*)-3-(4-methoxyphenyl)-3-(tosyloxy) acrylate 211[138]

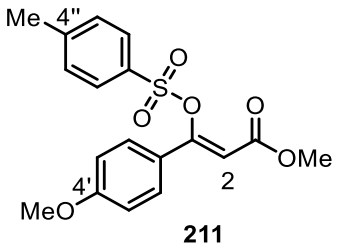

211

Following general procedure 4 tosylation was obtained by use of **217** (6.27 g, 30.1 mmol, 1.00 equiv.), TMEDA (8.00 mL, 6.16 g, 53.0 mmol, 1.76 equiv.), LiCl (2.28 g, 53.8 mmol, 1.78 equiv.) and TsCl (10.0 g, 52.5 mmol, 1.74 equiv.). The desired product **211** (8.93 g, 24.7 mmol, 82%) was obtained as colorless solid over two steps.

TLC: R_f = 0.30 (PE/EtOAc 4:1 *v/v*).

UV ($CHCl_3$): λ_{max} (nm) = 237, 299.

Mp: 91.0 °C.

IR (ATR): 1727, 1601, 1512, 1378, 1254, 1175, 1155, 1038, 848, 764, 669 cm^{-1}.

^{1}H-NMR (500 MHz, $CDCl_3$): δ (ppm) = 7.73 (d, *J* = 8.2 Hz, 2 H, 2''-H, 6''-H), 7.36 (d, *J* = 8.9 Hz, 2 H, 3'-H, 5'-H), 7.24 (d, *J* = 8.2 Hz, 2 H, 3''-H, 5''-H), 6.76 (d, *J* = 8.9 Hz, 2 H, 2'-H, 6'-H), 6.01 (s, 1 H, 2-H), 3.78 (s, 3 H, OCH_3), 3.65 (s, 3 H, CO_2CH_3), 2.40 (s, 3 H, CH_3).

^{13}C-NMR (126 MHz, $CDCl_3$): δ (ppm) = 164.1 (C-1), 161.9 (C-4'), 155.8 (C-3), 145.3 (C-4''), 133.6 (C-1''), 129.6 (2 C, C-3'', C-5''), 128.7 (2 C, C-3', C-5'), 128.6 (2 C, C-2'', C-6''), 125.7 (C-1'), 114.0 (2 C, C-2', C-6'), 108.2 (C-2), 55.5 (OCH_3), 51.6 (CO_2CH_3), 21.7 (CH_3).

HRMS (ESI): for $[C_{18}H_{18}O_6+Na]^+$ calcd.: 385.0716
found: 385.0701.

$C_{18}H_{18}O_6S$ (362.40 g/mol).

Methyl-(*Z*)-3-(4-fluorophenyl)-3-(tosyloxy) acrylate 212[138]

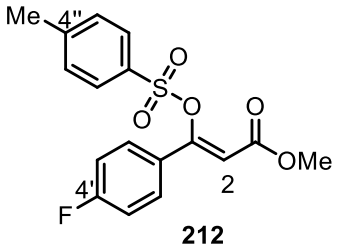

212

Following general procedure 4 tosylation was performed using **218** (7.10 g, 36.2 mmol, 1.00 equiv.), TMEDA (8.50 mL, 6.55 g, 56.4 mmol, 1.56 equiv.), LiCl (2.34 g, 55.2 mmol, 1.52 equiv.) and TsCl (10.4 g, 54.6 mmol, 1.51 equiv.). The desired product **212** (7.67 g, 21.9 mmol, 61%) was obtained as colorless solid over two steps.

TLC: R_f = 0.44 (PE/EtOAc 4:1 *v/v*).

Mp: 93.2 °C.

UV ($CHCl_3$): λ_{max} (nm) = 237, 269.

IR (ATR): 1731, 1651, 1371, 1201, 1179, 1029, 838, 806, 764 cm^{-1}.

^{1}H-NMR (500 MHz, $CDCl_3$): δ (ppm) = 7.73 (d, J = 8.2 Hz, 2 H, 2''-H, 6''-H), 7.43 (dd, J = 8.8, 5.2 Hz, 2 H, 2'-H, 6'-H), 7.26 (d J = 8.2 Hz, 2 H, 3''-H, 5''-H), 6.96 (t, J = 8.8 Hz, 2 H, 3'-H, 5'-H), 6.06 (s, 1 H, 2-H), 3.69 (s, 3 H, CO_2CH_3), 2.42 (s, 3 H, CH_3).

^{13}C-NMR (126 MHz, $CDCl_3$): δ (ppm) = 164.3 (d, J = 253 Hz, C-4'), 163.8 (C-1), 154.8 (C-3), 145.6 (C-4''), 133.5 (C-1''), 129.7 (2 C, C-3'', C-5''), 129.5 (d, J = 8.8 Hz, 2 C, C-2', C-6'), 129.4 (d, J = 3.2 Hz, C-1'), 128.6 (2 ×, C-2'', C-6''), 115.9 (d, J = 22.1 Hz, 2 C, C-3', C-5'), 110.4 (C-2), 51.9 (CO_2CH_3), 21.8 (CH_3).

HRMS (ESI): for $[C_{17}H_{15}FO_5S + Na]^+$ calcd.: 373.0516
found: 373.0539.

$C_{17}H_{15}FO_5S$ (350.36 g/mol).

6.3.5. Acylative Suzuki-Miyaura cross-coupling

2,5-Dioxopyrrolidin-1-yl acetate 222

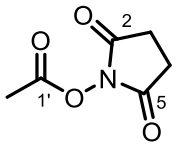

222

The compound was prepared using a modified protocol originally reported by *Jacobson* et al.[230] To a solution of HOSu **223** (2.88 g, 25.0 mmol, 1.00 equiv.) in THF (20.0 mL) were added Ac_2O (2.67 mL, 2.88 g), 28.2 mmol, 1.13 equiv.) and Et_3N (2.67 g, 3.67 mL, 26.3 mmol, 1.05 equiv.) and stirred for 30 min at room temperature. Afterwards, PE (20.0 mL) was added and the obtained precipitate was collected by filtration. The desired product **222** (3.42 g, 21.8 mmol, 87%) was obtained as colorless powder.

^{1}H-NMR (400 MHz, $CDCl_3$): δ (ppm) = 2.84 (s, 2 × H, 4-H_2, 5-H_2), 2.34 (s, 3 H, 2'-H_3).

^{13}C-NMR (101 MHz, $CDCl_3$): δ (ppm) = 169.3 (2 C, C-2, C-5), 165.7 (C-1'), 25.7 (C-2'), 17.7 (2 C, C-3, C-4).

$C_6H_7NO_4$ (157.13 g/mol).

2,5-Dioxopyrrolidin-1-yl benzoate 224

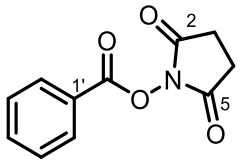

224

To a solution of benzoic acid (500 mg, 4.09 mmol, 1.00 equiv.) and HOSu **223** (518 mg, 4.50 mmol, 1.10 equiv.) in DMF (5.00 mL) was added EDC × HCl (863 mg, 4.50 mmol, 1.10 equiv.) and stirred for 15 min. Water (20.0 mL) was added and the precipitate was collected by filtration**.** The desired product **224** (775 mg, 3.54 mmol, 87%) was obtained as colorless powder.

^{1}H-NMR (400 MHz, $CDCl_3$): δ (ppm) = 8.14 (m, 2 H, 2'-H, 6'-H), 7.68 (m, 1 H, 4'-H), 7.53 (m, 2 H, 3'-H, 5'-H), 2.91 (s, 2 × 2 H, 3-H_2, 4-H_2).

^{13}C-NMR (101 MHz, $CDCl_3$): δ (ppm) = 169.4 (C-2, C-5), 162.0 (C=O), 135.1 (C-4'), 130.7 (2 C, C-2', C-6'), 129.0 (2 C, C-3', C-5'), 125.2 (C-1), 25.8 (2 C, C-3, C-4).

$C_{11}H_9NO_4$ (219.20 g/mol).

Benzophenone 225

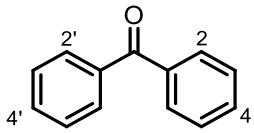

225

A mixture of K_3PO_4 (291 mg, 1.37 mmol, 3.00 equiv.) and PCy_3 (25.6 mg, 91.3 µmol, 20.0 mol%) was evacuated and purged with argon three times. Then 1,4-dioxane (10.0 mL) was added and the reaction mixture was degassed with argon for 5 min. Afterwards, 2,5-dioxopyrrolidin-1-yl benzoate **224** (100 mg, 456 µmol, 1.00 equiv.), phenylboronic acid **105** (111 mg, 913 µmol, 2.00 equiv.) and $Pd(OAc)_2$ (10.2 mg, 45.6 µmol, 10.0 mol%) were added. The reaction mixture was stirred for 2 h at 80 °C. The suspension was cooled to room temperature, filtered through celite® and the solvent was removed in vacuum. The product was purified by column chromatography (silica gel, PE/EtOAc 19:1 → 1:9 *v*/*v*) to yield benzophenone **225** (50.0 mg, 274 µmol, 60% (determined by ^{1}H-NMR)) as yellow amorphous solid.

^{1}H-NMR (400 MHz, $CDCl_3$): δ (ppm) = 7.84–7.76 (m, 4 H, 2-H, 2'-H, 6-H, 6'-H), 7.63–7.56 (m, 2 H, 4-H, 4'-H), 7.51–7.44 (m, 4 H, 3-H, 3'-H, 5-H, 5'-H).

^{13}C-NMR (151 MHz, $CDCl_3$): δ (ppm) = 196.9 (C-5), 137.7 (2 C, C-1, C-1'), 132.5 (2 C, C-4, C-4'), 130.2 (4 C, C-2, C-2', C-6, C-6'), 128.4 (4 C, C-3, C-3', C-5, C-5').

MS (ESI): for $[C_{13}H_{10}O+H]^+$ calcd.: 183.0804
found: 183.0894

$C_{13}H_{10}O$ (182.22 g/mol).

4-Methoxybenzophenone 226

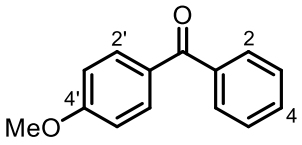

226

A mixture of K_3PO_4 (291 mg, 1.37 mmol, 3.00 equiv.) and PCy_3 (25.6 mg, 91.3 µmol, 20.0 mol%) was evacuated and purged with argon three times. Then 1,4-dioxane (10.0 mL) was added and the reaction mixture was degassed with argon for 5 min. Afterwards, 2,5-dioxopyrrolidin-1-yl benzoate **224** (100 mg, 456 µmol, 1.00 equiv.), 4-methoxyphenylboronic acid **119** (139 mg, 913 µmol, 2.00 equiv.) and $Pd(OAc)_2$ (10.2 mg, 45.6 µmol, 10.0 mol%) were added. The reaction mixture was stirred for 2 h at 80 °C. The suspension was cooled to room temperature, filtered through celite® and the solvent was removed in vacuum. The product was purified by column chromatography (silica gel, PE/EtOAc 19:1 → 1:9 *v*/*v*) to yield 4-methoxyacetophenone **226** (62.0 mg, 292 µmol, 64%, determined by ^{1}H-NMR) s colorless crystalline solid.

^{1}H-NMR (400 MHz, $CDCl_3$): δ (ppm) = 7.83 (d, J = 8.9 Hz, 2 H, 2'-H, 6'-H), 7.79–7.70 (m, 2 H, 2-H, 6-H), 7.59–7.53 (m, 1 H, 4-H), 7.50–7.43 (m, 2 H, 3-H, 5-H), 6.96 (d, J = 8.9 Hz, 2 H, 3'-H, 5'-H), 3.89 (s, 3 H, OCH_3).

^{13}C-NMR (151 MHz, $CDCl_3$): δ (ppm) = 195.7 (C=O), 163.3 (C-4'), 138.4 (C-1), 132.7 (2 C, C-2', C-6'), 132.0 (C-4), 130.3 (C-1'), 129.8 (2 C, C-2, C-6), 128.3 (2 C, C-3, C-5), 113.7 (C-3', C-5'), 55.6 (OCH_3).

MS (ESI): for $[C_{14}H_{12}O_2+H]^+$ calcd.: 213.0916
found: 213.0997.

$C_{14}H_{12}O_2$ (212.24 g/mol).

1-(2,5-dioxopyrrolidin-1-yl) 4-methyl 2-(4-methoxyphenyl)maleate 221

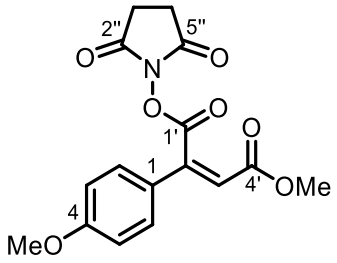

221

To a solution of vinyl bromide **127** (208.9 mg, 771 µmol, 1.00 equiv.) and **227** (221 mg, 1.54 mmol, 2.00 equiv.) in THF (4.00 mL) was degassed with argon for 5 min. Afterwards, $Pd(OAc)_2$ (5.20 mg, 23.2 µmol, 3.0 mol%) and Xantphos (11.1 mg, 19.2 mmol, 2.5 mol%) were added to the solution an heated to 70 °C. After 5 min, Et_3N (129 µL, 925 µmol, 1.20 equiv.) was added to the solution and stirred for 16 h at 70 °C. The reaction was cooled to room temperature and the solvent was removed in vacuum. The crude product was purified via column chromatography (Pe/EtOAc 9:1 → 100% EtOAc *v*/*v*). The desired product **221** (201 mg, 604 µmol, 78%) was obtained as beige solid

TLC: R_f (PE/EtOAc 9:1 *v*/*v*) = 0.10.

Mp: 133–135 °C.

UV (CH_2Cl_2): λ_{max} (nm) = 230, 316.

IR (ATR): 2349, 1787, 1740, 1594, 1434, 1345, 1267, 1200, 1171, 1092, 1047, 1005, 969, 834, 649 cm^{-1}.

^{1}H-NMR (600 MHz, $CDCl_3$) δ (ppm) = 7.70 (d, *J* = 8.9 Hz, 2 H, 3-H, 5-H), 6.96 (d, *J* = 8.9 Hz, 2 H, 2-H, 6-H), 6.44 (s, 1 H, 3'-H), 3.84 (s, 6 H, 2 × 3 H, OCH_3, CO_2CH_3), 2.90 (s, 2 × 2 H, 3''-H_2, 4''-H_2).

^{13}C-NMR (101 MHz, $CDCl_3$) δ (ppm) = 168.9 (2 C, C-2'', C-4''), 164.8 (C-4'), 163.4 (C-1'), 162.2 (C-4), 143.0 (C-1), 129.1 (2 C, C-2, C-6), 124.5 (C-2'), 118.2 (C-3'), 114.8 (2 C, C-3, C-5), 55.6 (OCH_3), 52.6 (CO_2CH_3), 25.9 (2 C, C-3'', C-4'').

HRMS (ESI): for $[C_{16}H_{15}NO_7+Na]^+$ calcd.: 356.0741
found: 356.0740.

$C_{16}H_{15}NO_7$ (333.30 g/mol).

6.3.6. *γ*-Ketoester synthesis via pd-catalyzed Suzuki-Miyaura cross-coupling[138]

Methyl-(Z)-4-oxo-3,4-diphenylbut-2-enoate 235[138]

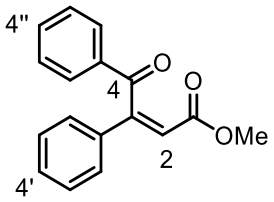

235

Following general procedure 5, the carbonylative *Suzuki-Miyaura* cross-coupling was performed using vinyltosylate **210** (111 mg, 334 µmol, 1.00 equiv.), phenylboronic acid **105** (78.3 mg, 642 µmol, 1.92 equiv.), K_2CO_3 (156 mg, 1.13 mmol, 3.38 equiv.), $Pd(TFA)_2$ (5.00 mg, 15.0 µmol, 4.5 mol%), PCy_3 (7.10 mg, 25.3 µmol, 7.6 mol%) and $Mo(CO)_6$ **229** (164 mg, 621 µmol, 1.86 equiv.). The desired product **235** (23.6 mg, 88.6 µmol, 27%) was obtained as yellow oil.

TLC: R_f = 0.40 (PE/EtOAc 6:1 *v/v*).

UV ($CHCl_3$): λ_{max} (nm) = 256.

IR (ATR): 2979, 2888, 1712, 1669, 1618, 1448, 1350, 1278, 1216, 1192, 1171, 948, 698, 687, 589 cm^{-1}.

^{1}H-NMR (400 MHz, $CDCl_3$): *δ* (ppm) = 7.95 (d, *J* = 8.1 Hz, 2 H, 2''-H, 6''-H), 7.58–7.33 (m, 8 H, 2'-H, 3'-H, 4'-H, 5'-H, 6'-H, 3''-H, 4''-H, 5''-H), 6.51 (s, 1 H, 2-H), 3.63 (s, 3 H, CO_2CH_3).

^{13}C-NMR (101 MHz, $CDCl_3$): *δ* (ppm) = 196.6 (C-4), 165.7 (C-1), 156.2 (C-3), 136.1 (C-1''), 134.3 (C-1'), 133.7 (C-4''), 130.7 (C-4'), 129.3 (2 C, C-2', C-6'), 129.1 (2 C, C-3'', C-5''), 128.9 (2 C, C-2'', C-6''), 127.1 (2 C, C-3', C-5'), 117.4 (C-2), 52.0 (CO_2CH_3).

HRMS (ESI): for $[C_{16}H_{11}O_2]^+$ calcd.: 235.0754
found: 235.0715.

$C_{17}H_{14}O_3$ (266.30 g/mol).

Methyl-(Z)-3-(4-methoxyphenyl)-4-oxo-4-phenylbut-2-enoate 236[138]

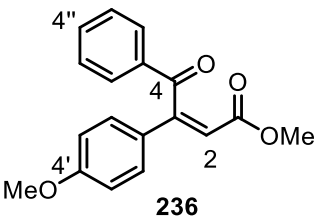

236

Following general procedure 5 the carbonylative *Suzuki-Miyaura* cross-coupling was performed using vinyltosylate **211** (100 mg, 276 µmol, 1.00 equiv.), phenylboronic acid **105** (72.6 mg, 595 µmol, 2.16 equiv.), K_2CO_3 (185 mg, 1.34 mmol, 4.86 equiv.), $Pd(TFA)_2$ (4.60 mg, 13.8 µmol, 5.0 mol%), PCy_3 (7.30 mg, 26.0 µmol, 9.4 mol%) and $Mo(CO)_6$ **229** (163 mg, 617 µmol, 2.24 equiv.). The desired product **236** (59.0 mg, 199 µmol, 72%) was obtained as yellow oil.

TLC: R_f = 0.30 (PE/EtOAc 5:1 *v/v*).

UV ($CHCl_3$): λ_{max} (nm) = 241, 310.

IR (ATR): 3060, 2979, 2889, 1712, 1673, 1595, 1511, 1352, 1283, 1255, 1165, 1027, 949, 832, 689 cm^{-1}.

^{1}H-NMR (400 MHz, $CDCl_3$): δ (ppm) = 7.95 (d, *J* = 7.8 Hz, 2 H, 2''-H, 6''-H), 7.54 (t, *J* = 7.4 Hz, 1 H, 4''-H), 7.45–7.41 (m, 4 H, 3'-H, 5'-H, 3''-H, 5''-H), 6.87 (d, *J* = 8.9 Hz, 2 H, 2'-H, 6'-H), 6.43 (s, 1 H, 2-H), 3.79 (s, 3 H, OCH_3), 3.61 (s, 3 H, CO_2CH_3).

^{13}C-NMR (126 MHz, $CDCl_3$): δ (ppm) = 197.1 (C-4), 166.0 (C-1), 161.7 (C-4'), 155.7 (C-3), 136.2 (C-1''), 133.6 (C-4''), 129.0 (2 C, C-2'', C-6''), 128.9 (2 C, C-3', C-5'), 128.8 (2 C, C-3'', C-5''), 126.6 (C-1'), 114.8 (2 C, C-2', C-6'), 114.7 (C-2), 55.5 (OCH_3), 51.9 (CO_2CH_3).

HRMS (ESI): for $[C_{17}H_{13}O_3]^+$ calcd.: 265.0859
found: 265.0859.

$C_{18}H_{16}O_4$ (296.32 g/mol)

Methyl-(*Z*)-3-(4-fluorophenyl)-4-oxo-4-phenylbut-2-enoate 237[138]

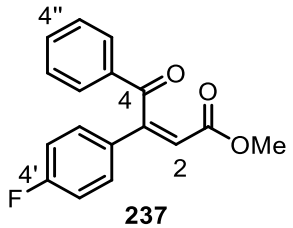

237

Following general procedure 5 the carbonylative *Suzuki-Miyaura* cross-coupling performed by using vinyltosylate **212** (105 mg, 300 µmol, 1.00 equiv.), phenylboronic acid **105** (87.0 mg, 714 µmol, 2.38 equiv.), K_2CO_3 (126 mg, 912 mmol, 3.04 equiv.), $Pd(TFA)_2$ (6.50 mg, 19.5 µmol, 6.5 mol%), PCy_3 (8.00 mg, 28.5 µmol, 9.5 mol%) and $Mo(CO)_6$ **229** (161 mg, 610 µmol, 2.03 equiv.). The desired product **237** (61.4 mg, 216 µmol, 72%) was obtained as colorless oil.

TLC: R_f = 0.30 (PE/EtOAc 6:1 *v/v*).

UV ($CHCl_3$): λ_{max} (nm) = 254.

IR (ATR): 1715, 1674, 1598, 1508, 1449, 1436, 1348, 1280, 1217, 1194, 1003, 949, 847, 689, 513 cm^{-1}.

^{1}H-NMR (400 MHz, $CDCl_3$): δ (ppm) = 7.93 (dd, J = 8.6, 1.4 Hz, 2 H, 2''-H, 6''-H), 7.56 (t, J = 7.4 Hz, 1 H, 4''-H), 7.51–7.42 (m, 4 H, 2'-H, 6'-H, 3''-H, 5''-H), 7.06 (t, J = 8.6 Hz, 2 H, 3'-H, 5'-H), 6.46 (s, 1 H, 2-H), 3.63 (s, 3 H, CO_2CH_3).

^{13}C-NMR (101 MHz, $CDCl_3$): δ (ppm) = 196.4 (C-4), 165.6 (C-1), 164.3 (d, J = 252 Hz, C-4'), 155.0 (C-3), 135.9 (C-1''), 133.8 (C-4''), 130.5 (d, J = 3.4 Hz, C-1'), 129.2 (2 C, C-3'', C-5''), 129.1 (2 C, C-2'', C-6''), 129.0 (d, J = 8.7 Hz, 2 C, C-3', C-5'), 117.3 (C-2), 116.5 (d, J = 21.9 Hz, 2 C, C-2', C-6'), 52.1 (CO_2CH_3).

HRMS (ESI): for $[C_{16}H_{10}FO_2]^+$ calcd.: 253.0665
found: 253.0676

$C_{17}H_{13}FO_3$ (284.29 g/mol).

Methyl-(*Z*)-4-(4-methoxyphenyl)-4-oxo-3-phenylbut-2-enoate 238[138]

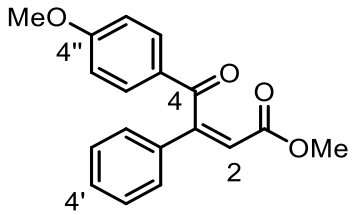

238

Following general procedure 5 the carbonylative *Suzuki-Miyaura* cross-coupling was performed using vinyltosylate **210** (103 mg, 310 µmol, 1.00 equiv.), 4-methoxyphenylboronic acid **119** (93.3 mg, 614 µmol, 1.98 equiv.), K_2CO_3 (126 mg, 912 mmol, 2.94 equiv.), $Pd(TFA)_2$ (4.10 mg, 12.3 µmol, 4.0 mol%), PCy_3 (7.20 mg, 25.7 µmol, 8.3 mol%) and $Mo(CO)_6$ **229** (163 mg, 617 µmol, 1.99 equiv.). The desired product **238** (62.5 mg, 211 µmol, 68%) was obtained as yellow oil.

TLC: R_f = 0.20 (PE/EtOAc 6:1 *v/v*).

UV ($CHCl_3$): λ_{max} (nm) = 282.

IR (ATR): 2850, 1710, 1662, 1599, 1573, 1452, 1424, 1352, 1257, 1165, 1011, 947, 846, 778, 588 cm^{-1}.

^{1}H-NMR (400 MHz, $CDCl_3$): δ (ppm) = 7.92 (d, J = 9.0 Hz, 2 H, 2''-H, 6''-H), 7.49 (dd, J = 7.9, 1.8 Hz, 2 H, 2'-H, 6'-H), 7.40–7.35 (m, 3 H, 4'-H, 3'-H, 5'-H), 6.91 (d, J = 9.0 Hz, 2 H, 3''-H, 5''-H), 6.48 (s, 1 H, 2-H), 3.84 (s, 3 H, OCH_3), 3.64 (s, 3 H, CO_2CH_3).

^{13}C-NMR (126 MHz, $CDCl_3$): δ (ppm) = 195.2 (C-4), 165.7 (C-1), 164.0 (C-4''), 156.3 (C-3), 134.5 (C-1'), 131.4 (2 C, C-2'', C-6''), 130.6 (C-4'), 129.4 (C-1''), 129.2 (2 C, C-3', C-5'), 127.1 (2 C, C-2', C-6'), 117.0 (C-2), 114.2 (2 C, C-3'', C-5''), 55.6 (OCH_3), 52.0 (CO_2CH_3).

HRMS (ESI): for $[C_{17}H_{13}O_3]^+$ calcd.: 265.0888
found: 265.0859.

$C_{18}H_{16}O_4$ (296.32 g/mol).

Methyl-(*Z*)-3,4-di-(4-methoxyphenyl)-4-oxobut-2-enoate 239[138]

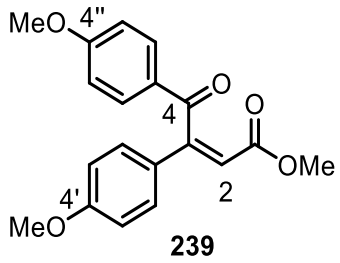

239

Following general procedure 5 the carbonylative *Suzuki-Miyaura* cross-coupling was performed using vinyltosylate **211** (501 mg, 1.38 mmol, 1.00 equiv.), 4-methoxyphenylboronic acid **119** (421 mg, 2.77 mmol, 2.01 equiv.), K_2CO_3 (571 mg, 4.13 mmol, 2.99 equiv.), $Pd(TFA)_2$ (19.2 mg, 57.8 µmol, 4.2 mol%), PCy_3 (32.1 mg, 114 µmol, 8.3 mol%) and $Mo(CO)_6$ **229** (722 mg, 2.73 mmol, 1.98 equiv.). The desired product **239** (285 mg, 873 µmol, 63%) was obtained as yellow oil.

TLC: R_f = 0.10 (PE/EtOAc 10:1 *v/v*).

UV ($CHCl_3$): λ_{max} (nm) = 290.

IR (ATR): 2979, 2841, 1712, 1663, 1595, 1573, 1510, 1284, 1254, 1228, 1159, 1026, 948, 832, 793 cm^{-1}.

^{1}H-NMR (400 MHz, $CDCl_3$): δ (ppm) = 7.91 (d, J = 8.6 Hz, 2 H, 2''-H, 6''-H), 7.43 (d, J = 8.7 Hz, 2 H, 2'-H, 6'-H), 6.91 (d, J = 8.6 Hz, 2 H, 3''-H, 5''-H), 6.86 (d, J = 8.7 Hz, 2 H, 3'-H, 5'-H), 6.40 (s, 1 H, 2-H), 3.84 (s, 3 H, -OCH_3), 3.80 (s, 3 H, OCH_3), 3.62 (s, 3 H, CO_2CH_3).

^{13}C-NMR (101 MHz, $CDCl_3$): δ (ppm) = 195.5 (C-4), 165.8 (C-1), 163.8 (C-4''), 161.5 (C-4'), 155.7 (C-3), 131.2 (2 C, C-2'', C-6''), 129.3 (C-1''), 128.6 (2 C, C-2', C-6'), 126.7 (C-1'), 114.5 (2 C, C-3', C-5'), 114.3 (C-2), 114.1 (2 C, C-3'', C-5''), 55.8 (OCH_3), 55.4 (OCH_3), 51.7 (CO_2CH_3).

HRMS (ESI): for $[C_{18}H_{15}O_4]^+$ calcd.: 295.0965
found: 295.0963.

$C_{19}H_{18}O_5$ (326.35 g/mol).

Methyl-(*Z*)-3-(4-fluorophenyl)-4-(4-methoxyphenyl)-4-oxobut-2-enoate 240[138]

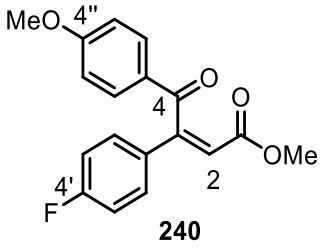

240

Following general procedure 6 the carbonylative *Suzuki-Miyaura* cross-coupling was performed by using vinyltosylate **212** (106 mg, 303 µmol, 1.00 equiv.), 4-methoxyphenylboronic acid **119** (112 mg, 737 µmol, 2.43 equiv.), K_2CO_3 (132 mg, 955 µmol, 3.15 equiv.), $Pd(TFA)_2$ (3.90 mg, 11.7 µmol, 3.9 mol%), PCy_3 (9.20 mg, 32.8 µmol, 10.8 mol%) and $Mo(CO)_6$ **229** (143 mg, 542 µmol, 1.79 equiv.). The desired product **240** (46.8 mg, 149 µmol, 49%) was obtained as colorless oil.

TLC: R_f = 0.40 (PE/EtOAc 4:1 *v/v*).

UV ($CHCl_3$): λ_{max} (nm) = 283.

IR (ATR): 3658, 2979, 2888, 1716, 1663, 1383, 1350, 1258, 1227, 1159, 949, 836, 565, 523 cm^{-1}.

^{1}H-NMR (400 MHz, $CDCl_3$): *δ* (ppm) = 7.90 (d, *J* = 8.9 Hz, 2 H, 2''-H, 6''-H), 7.48 (dd, *J* = 8.8, 5.2 Hz, 2 H, 2'-H, 6'-H), 7.05 (t, *J* = 8.8 Hz, 2 H, 3'-H, 5'-H), 6.92 (d, *J* = 8.9 Hz, 2 H, 3''-H, 5''-H), 6.43 (s, 1 H, 2-H), 3.84 (s, 3 H, OCH_3), 3.63 (s, 3 H, CO_2CH_3).

^{13}C-NMR (101 MHz, $CDCl_3$): *δ* (ppm) = 195.0 (C-4), 165.4 (C-1), 164.1 (d, *J* = 252 Hz, C-4'), 164.1 (C-4''), 155.1 (C-3), 131.4 (2 C, C-2'', C-6''), 130.7 (d, *J* = 3.4 Hz, C-1'), 129.2 (C-1''), 129.1 (d, *J* = 8.6 Hz, 2 C, C-2', C-6'), 116.9 (d, *J* = 1.7 Hz, C-2), 116.4 (d, *J* = 22.0 Hz, 2 C, C-3', C-5'), 114.3 (2 C, C-3'', C-5''), 55.6 (OCH_3), 52.0 (CO_2CH_3).

HRMS (ESI): for $[C_{17}H_{12}FO_3]^+$ calcd.: 283.0765
found: 283.0762.

$C_{18}H_{15}FO_4$ (314.31 g/mol).

Methyl-(Z)-4-(4-fluorophenyl)-4-oxo-3-phenylbut-2-enoate 241[138]

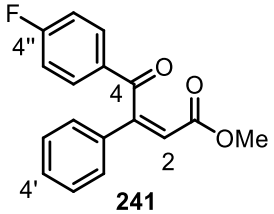

241

Following general procedure 5, the carbonylative *Suzuki-Miyaura* cross-coupling was obtained by vinyltosylate **210** (99.3 mg, 299 µmol, 1.00 equiv.), 4-fluorophenylboronic acid **168** (83.4 mg, 596 µmol, 1.99 equiv.), K_2CO_3 (122 mg, 883 µmol, 2.95 equiv.), $Pd(TFA)_2$ (4.20 mg, 12.6 µmol, 4.21 mol%), PCy_3 (6.80 mg, 24.3 µmol, 8.13 mol%) and $Mo(CO)_6$ **229** (160 mg, 606 µmol, 2.03 equiv.). The desired product **241** (67.2 mg, 236 µmol, 79%) was obtained as yellow oil.

TLC: R_f = 0.44 (PE/EtOAc 4:1 *v/v*).

UV ($CHCl_3$): λ_{max} (nm) = 260.

IR (ATR): 2979, 1711, 1667, 1622, 1595, 1447, 1430, 1348, 1280, 1172, 1003, 948, 871, 771, 698 cm^{-1}.

^{1}H-NMR (400 MHz, $CDCl_3$): δ (ppm) = 7.97 (dd, *J* = 8.8, 5.4 Hz, 2 H, 2''-H, 6''-H), 7.48 (dd, *J* = 8.0, 1.7 Hz, 2 H, 2'-H, 6'-H), 7.41–7.37 (m, 3 H, 3'-H, 4'-H, 5'-H), 7.11 (t, *J* = 8.8 Hz, 2 H, 3''-H, 5''-H), 6.51 (s, 1 H, 2-H), 3.65 (s, 3 H, CO_2CH_3).

^{13}C-NMR (126 MHz, $CDCl_3$): δ (ppm) = 195.0 (C-4), 166.5 (d, *J* = 256 Hz, C-4''), 165.7 (C-1), 155.9 (C-3), 134.0 (C-1'), 132.7 (d, *J* = 2.6 Hz, C-1''), 131.7 (d, *J* = 9.5 Hz, 2 C, C-2'', C-6''), 130.8 (C-4'), 129.4 (2 C, C-2', C-6'), 127.0 (2 C, C-3', C-5'), 117.4 (C-2), 116.2 (d, *J* = 22.1 Hz, 2 C, C-3'', C-5''), 50.1 (CO_2CH_3).

HRMS (ESI): for $[C_{16}H_{10}FO_2]^+$ calcd.: 253.0659
found: 253.0670.

$C_{17}H_{13}FO_3$ (284.29 g/mol).

Methyl-(*Z*)-4-(4-fluorophenyl)-3-(4-methoxyphenyl)-4-oxobut-2-enoate 242[138]

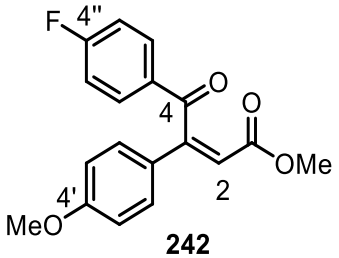

242

Following general procedure 5, the carbonylative *Suzuki-Miyaura* cross-coupling was performed using vinyltosylate **211** (98.3 mg, 271 µmol, 1.00 equiv.), 4-fluorophenylboronic acid **168** (79.6 mg, 569 µmol, 2.10 equiv.), K_2CO_3 (143 mg, 1.03 mmol, 3.80 equiv.), $Pd(TFA)_2$ (3.50 mg, 10.5 µmol, 3.9 mol%), PCy_3 (6.30 mg, 22.5 µmol, 8.3 mol%) and $Mo(CO)_6$ **229** (145 mg, 550 µmol, 2.03 equiv.). The desired product **242** (56.2 mg, 179 µmol, 66%) was obtained as colorless oil.

TLC: R_f = 0.14 (PE/EtOAc 10:1 *v/v*).

UV ($CHCl_3$): λ_{max} (nm) = 239, 311.

IR (ATR): 3659, 2979, 2888, 1709, 1666, 1593, 1504, 1384, 1347, 1253, 1227, 1152, 948, 842, 567 cm^{-1}.

^{1}H-NMR (400 MHz, $CDCl_3$): δ (ppm) = 7.96 (dd, J = 8.7, 5.4 Hz, 2 H, 2''-H, 6''-H), 7.41 (d, J = 8.9 Hz, 2 H, 2'-H, 6'-H), 7.10 (t, J = 8.7 Hz, 2 H, 3''-H, 5''-H), 6.88 (d, J = 8.9 Hz, 2 H, 3'-H, 5'-H), 6.42 (s, 1 H, 2-H), 3.80 (s, 3 H, OCH_3), 3.63 (s, 3 H, CO_2CH_3).

^{13}C-NMR (101 MHz, $CDCl_3$): δ (ppm) = 195.5 (C-4), 166.1 (d, J = 255 Hz, C-4''), 166.0 (C-1), 161.8 (C-4'), 155.4 (C-3), 132.8 (d, J = 3.0 Hz, C-1''), 131.6 (d, J = 9.5 Hz, 2 C, C-2'', C-6''), 128.8 (2 C, C-2', C-6'), 126.4 (C-1'), 116.1 (d, J = 22.1 Hz, 2 C, C-3'', C-5''), 114.9 (C-2), 114.8 (2 C, C-3', C-5'), 55.6 (OCH_3), 52.0 (CO_2CH_3).

HRMS (ESI): for $[C_{17}H_{12}FO_3]^+$ calcd.: 283.0765
found: 283.0781.

$C_{18}H_{15}FO_4$ (314.31 g/mol).

Methyl-(*Z*)-3,4-di(4-fluorophenyl)-4-oxobut-2-enoate 243[138]

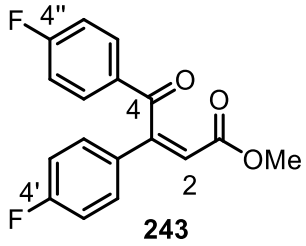

243

Following general procedure 5 the carbonylative *Suzuki-Miyaura* cross-coupling was performed using vinyltosylate **212** (102 mg, 291 µmol, 1.00 equiv.), 4-fluorophenylboronic acid **168** (86.6 mg, 623 µmol, 2.14 equiv.), K_2CO_3 (124 mg, 897 µmol, 3.1 equiv.), $Pd(TFA)_2$ (3.40 mg, 10.2 µmol, 3.5 mol%), PCy_3 (6.60 mg, 23.5 µmol, 8.1 mol%) and $Mo(CO)_6$ **229** (147 mg, 557 µmol, 1.91 equiv.). The desired product **243** (58.0 mg, 192 µmol, 66%) was obtained as yellow oil.

TLC: R_f = 0.28 (PE/EtOAc 10:1 *v/v*).

UV ($CHCl_3$): λ_{max} (nm) = 257.

IR (ATR): 3077, 1713, 1669, 1595, 1506, 1347, 1279, 1226, 1196, 945, 845, 805, 564, 512 cm^{-1}.

^{1}H-NMR (400 MHz, $CDCl_3$): δ (ppm) = 7.95 (dd, J = 8.7, 5.4 Hz, 2 H, 2''-H, 6''-H), 7.47 (dd, J = 8.7, 5.3 Hz, 2 H, 2'-H, 6'-H), 7.11 (t, J = 8.7 Hz, 2 H, 3''-H, 5''-H), 7.06 (t, J = 8.7 Hz, 2 H, 3'-H, 5'-H), 6.45 (s, 1 H, 2-H), 3.64 (s, 3 H, CO_2CH_3).

^{13}C-NMR (101 MHz, $CDCl_3$): δ (ppm) = 194.8 (C-4), 166.1 (d, J = 256 Hz, C-4''), 165.6 (C-1), 164.0 (d, J = 253 Hz, C-4'), 154.6 (C-3), 132.5 (d, J = 2.8 Hz, C-1''), 131.6 (d, J = 9.5 Hz, 2 C, C-2'', C-6''), 130.2 (d, J = 3.4 Hz, C-1'), 129.1 (d, J = 8.7 Hz, 2 C, C-2', C-6'), 117.3 (C-2) 116.6 (d, J = 22.0 Hz, 2 C, C-3'', C-5''), 116.2 (d, J = 22.1 Hz, 2 C, C-3', C-5'), 52.1 (CO_2CH_3).

HRMS (ESI): for $[C_{16}H_9F_2O_2]^+$ calcd.: 271.0565
found: 271.0577.

$C_{17}H_{12}F_2O_3$ (302.28 g/mol).

Methyl-(*Z*)-4-oxo-3-phenyl-4-(*p*-tolyl)but-2-enoate 244[138]

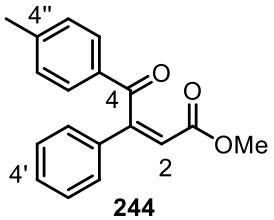

244

Following general procedure 5 the carbonylative *Suzuki-Miyaura* cross-coupling was performed using vinyltosylate **210** (101 mg, 304 µmol, 1.00 equiv.), 4-tolylboronic acid **230** (82.1 mg, 604 µmol, 1.99 equiv.), K_2CO_3 (125 mg, 904 µmol, 2.98 equiv.), $Pd(TFA)_2$ (4.0 mg, 12.0 µmol, 4.0 mol%), PCy_3 (6.80 mg, 24.2 µmol, 8.0 mol%) and $Mo(CO)_6$ **229** (167 mg, 632 µmol, 2.08 equiv.). The desired product **244** (38.3 mg, 137 µmol, 45%) was obtained as colorless solid.

TLC: R_f = 0.41 (PE/EtOAc 6:1 *v/v*).

Mp: 148.9 °C.

UV ($CHCl_3$): λ_{max} (nm) = 263.

IR (ATR): 1709, 1665, 1604, 1429, 1349, 1280, 1221, 1193, 1172, 1005, 947, 870, 772, 692, 553 cm^{-1}.

^{1}H-NMR (600 MHz, acetone-d_6): δ (ppm) = 7.83 (d, J = 8.1 Hz, 2 H, 2''-H, 6''-H), 7.57 (dd, J = 7.8, 1.7 Hz, 2 H, 2'-H, 6'-H), 7.47–7.41 (m, 3 H, 3'-H, 4'-H, 5'-H), 7.30 (d, J = 8.1 Hz, 2 H, 3''-H, 5''-H), 6.61 (s, 1 H, 2-H), 3.59 (s, 3 H, CO_2CH_3), 2.38 (s, 3 H, CH_3).

^{13}C-NMR (101 MHz, acetone-d_6): δ (ppm) = 195.9 (C-4), 166.0 (C-1), 156.8 (C-3), 145.1 (C-4''), 135.5 (C-1'), 134.8 (C-1''), 131.3 (C-4'), 130.4 (2 C, C-3', C-5'), 130.2 (2 C, C-3'', C-5''), 129.9 (2 C, C-2'', C-6''), 128.0 (2 C, C-2', C-6') 117.9 (C-2), 51.9 (CO_2CH_3), 21.8 (CH_3).

HRMS (ESI): for $[C_{18}H_{16}O_3+Na]^+$ calcd.: 303.0992
found: 303.0983.

$C_{18}H_{16}O_3$ (280.32 g/mol).

Methyl-(*Z*)-3-(4-methoxyphenyl)-4-oxo-4-(*p*-tolyl)but-2-enoate 245[138]

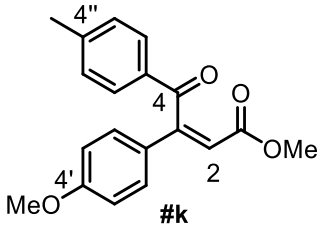

#k

Following general procedure 5 the carbonylative *Suzuki-Miyaura* cross-coupling was performed using vinyltosylate **211** (109 mg, 301 µmol, 1.00 equiv.), 4-tolylboronic acid **230** (83.5 mg, 614 µmol, 2.04 equiv.), K_2CO_3 (124 mg, 897 µmol, 2.98 equiv.), $Pd(TFA)_2$ (4.2 mg, 12.6 µmol, 4.2 mol%), PCy_3 (6.80 mg, 24.2 µmol, 8.1 mol%) and $Mo(CO)_6$ **229** (159 mg, 602 µmol, 2.00 equiv.). The desired product **245** (62.7 mg, 202 µmol, 67%) was obtained as colorless solid.

TLC: R_f = 0.33 (PE/EtOAc 6:1 *v/v*).

Mp: 118.2 °C.

UV ($CHCl_3$): λ_{max} (nm) = 264, 310.

IR (ATR): 1713, 1660, 1602, 1509, 1349, 1294, 1255, 1224, 1193, 1170, 1025, 947, 838, 672, 570 cm^{-1}.

^{1}H-NMR (600 MHz, $CDCl_3$): δ (ppm) = 7.85 (d, *J* = 8.1 Hz, 2 H, 2''-H, 6''-H), 7.43 (d, *J* = 8.9 Hz, 2 H, 2'-H, 6'-H), 7.23 (d, *J* = 8.1 Hz, 2 H, 3''-H, 5''-H), 6.86 (d, *J* = 8.9 Hz, 2 H, 3'-H, 5'-H), 6.42 (s, 1 H, 2-H), 3.78 (s, 3 H, OCH_3), 3.61 (s, 3 H, CO_2CH_3), 2.38 (s, 3 H, CH_3).

^{13}C-NMR (150 MHz, $CDCl_3$): δ (ppm) = 196.6 (C-4), 165.9 (C-1), 161.6 (C-4'), 155.8 (C-3), 144.5 (C-4''), 133.8 (C-1'') 129.6 (2 C, C-3'', C-5''), 129.0 (2 C, C-2'', C-6''), 128.7 (2 C, C-2', C-6'), 126.7 (C-1'), 114.6 (2 C, C-3', C-5'), 114.5 (C-2), 55.5 (OCH_3), 51.8 (CO_2CH_3), 21.8 (CH_3).

HRMS (ESI): for $[C_{18}H_{15}O_3]^+$ calcd.: 279.1016
found: 279.0999.

$C_{19}H_{18}O_4$ (310.35 g/mol).

Methyl-(*Z*)-3-(4-fluorophenyl)-4-oxo-4-(*p*-tolyl)but-2-enoate 246[138]

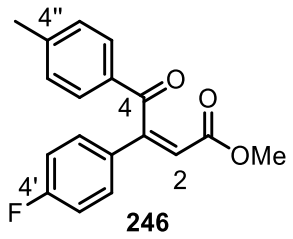

246

Following general procedure 5 the carbonylative *Suzuki-Miyaura* cross-coupling was performed using vinyltosylate **212** (103 mg, 291 µmol, 1.00 equiv.), 4-tolylboronic acid **230** (82.4 mg, 606 µmol, 2.00 equiv.), K_2CO_3 (127 mg, 920 µmol, 3.04 equiv.), $Pd(TFA)_2$ (4.2 mg, 12.6 µmol, 4.3 mol%), PCy_3 (6.80 mg, 24.2 µmol, 8.0 mol%) and $Mo(CO)_6$ **229** (163 mg, 617 µmol, 2.04 equiv.). The desired product **246** (37.3 mg, 125 µmol, 43%) was obtained as colorless solid.

TLC: R_f = 0.32 (PE/EtOAc 6:1 *v/v*).

Mp: 110.8 °C.

UV ($CHCl_3$): λ_{max} (nm) = 266.

IR (ATR): 2970, 1714, 1665, 1603, 1508, 1435, 1348, 1191, 1167, 1043, 946, 842, 673, 567, 515 cm^{-1}.

^{1}H-NMR (400 MHz, $CDCl_3$): δ (ppm) = 7.83 (d, *J* = 8.2 Hz, 2 H, 2''-H, 6''-H); 7.48 (dd, *J* = 8.8, 5.2 Hz, 2 H, 2'-H, 6'-H), 7.24 (d, *J* = 8.2 Hz, 2 H, 3''-H, 5''-H), 7.05 (t, *J* = 8.8 Hz, 2 H, 3'-H, 5'-H), 6.44 (s, 1 H, 2-H), 3.64 (s, 3 H, CO_2CH_3), 2.39 (s, 3 H, CH_3).

^{13}C-NMR (101 MHz, $CDCl_3$): δ (ppm) = 196.1 (C-4), 165.6 (C-1), 164.1 (d, *J* = 252 Hz, C-4'), 155.1 (C-3), 144.8 (C-4''), 133.5 (C-1''), 130.6 (d, *J* = 3.4 Hz, C-1'), 129.7 (2 C, C-2'', C-6''), 129.2 (d, *J* = 8.6 Hz, 2 C, C-2', C-6'), 129.1 (2 C, C-3'', C-5''), 117.0 (d, *J* = 1.7 Hz, C-2), 116.4 (d, *J* = 21.9 Hz, 2 C, C-3', C-5'), 52.0 (CO_2CH_3), 21.9 (CH_3).

HRMS (ESI): for $[C_{17}H_{12}FO_2]^+$ calcd.: 267.0816
found: 267.0811.

$C_{18}H_{15}FO_3$ (298.31 g/mol).

Methyl-(*Z*)-4-oxo-3-phenyl-4-(*m*-tolyl)but-2-enoate 247[138]

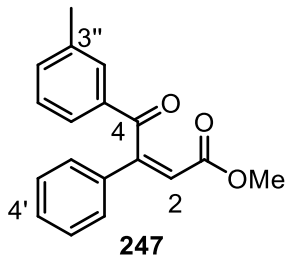

247

Following general procedure 6 the microwave assisted carbonylative *Suzuki-Miyaura-Miyaura* cross-coupling was performed using vinyltosylate **210** (101 mg, 304 µmol, 1.00 equiv.), 3-tolylboronic acid **231** (82.0 mg, 603 µmol, 1.98 equiv.), K_2CO_3 (125 mg, 904 µmol, 2.97 equiv.), $Pd(TFA)_2$ (4.5 mg, 13.5 µmol, 4.4 mol%), PCy_3 (7.1 mg, 25.3 µmol, 8.3 mol%) and $Mo(CO)_6$ **229** (161 mg, 610 µmol, 2.01 equiv.). The desired product **247** (45.7 mg, 163 µmol, 54%) was obtained as colorless solid.

TLC: R_f = 0.30 (PE/EtOAc 9:1 *v/v*).

UV (CH_2Cl_2): λ_{max} (nm) = 260.

IR (ATR): 1717, 1674, 1619, 1558, 1541, 1522, 1455, 1435, 1351, 1282, 1173, 686 cm^{-1}.

^{1}H-NMR (400 MHz, $CDCl_3$): δ (ppm) = 7.81 (s, 1 H, 2''-H), 7.70 (d, J = 7.5 Hz, 1 H, 6''-H), 7.49 (dd, J = 7.9, 1.7 Hz, 2 H, 2'-H, 6'-H), 7.40–7.35 (m, 4 H, 3'-H, 4'-H, 5'-H, 4''-H), 7.31 (t, J = 7.5 Hz, 1 H, 5''-H), 6.51 (s, 1 H, 2-H), 3.64 (s, 3 H, CO_2CH_3), 2.38 (s, 3 H, CH_3).

^{13}C-NMR (101 MHz, $CDCl_3$): δ (ppm) = 196.8 (C-4), 165.7 (C-1), 156.3 (C-3), 138.8 (C-3''), 136.1 (C-1''), 134.6 (C-4'), 134.4 (C-1'), 130.6 (C-5''), 129.3 (2 C, C-3', C-5'), 129.2 (C-4''), 128.2 (C-2''), 127.1 (2 C, C-2', C-6'), 126.6 (C-6''), 117.2 (C-2), 52.0 (CO_2CH_3), 21.5 (CH_3).

HRMS (ESI): for $[C_{17}H_{13}O_2]^+$ calcd.: 249.0910
found: 249.0913.

$C_{18}H_{16}O_3$ (280.32 g/mol).

Methyl-(*Z*)-3-(4-methoxyphenyl)-4-oxo-4-(*m*-tolyl)but-2-enoate 248[138]

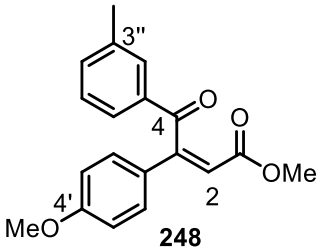

248

Following general procedure 6 the microwave assisted carbonylative *Suzuki-Miyaura-Miyaura* cross-coupling was performed using vinyltosylate **248** (110 mg, 304 µmol, 1.00 equiv.), 3-tolylboronic acid **231** (82.3 mg, 605 µmol, 1.99 equiv.), K_2CO_3 (126 mg, 912 µmol, 3.00 equiv.), $Pd(TFA)_2$ (4.1 mg, 12.3 µmol, 4.1 mol%), PCy_3 (6.9 mg, 24.6 µmol, 8.1 mol%) and $Mo(CO)_6$ **229** (160.7 mg, 609 µmol, 2.00 equiv.). The desired product **248** (75.0 mg, 242 µmol, 80%) was obtained as colorless solid.

TLC: R_f = 0.24 (PE/EtOAc 9:1 *v/v*).

UV (CH_2Cl_2): λ_{max} (nm) = 224, 303.

IR (ATR): 2954, 1714, 1672, 1598, 1512, 1460, 1435, 1352, 1288, 1258, 1169, 1031, 959, 834, 672 cm^{-1}.

^{1}H-NMR (300 MHz, $CDCl_3$): δ (ppm) = 7.80 (s, 1 H, 2''-H), 7.70 (d, J = 7.4 Hz, 1 H, 6''-H), 7.43 (d, J = 9.0 Hz, 2 H, 2'-H, 6'-H), 7.38–7.28 (m, 2 H, 4''-H, 5''-H), 6.87 (d, J = 9.0 Hz, 2 H, 3'-H, 5'-H), 6.42 (s, 1 H, 2-H), 3.79 (s, 3 H, -OCH_3), 3.62 (s, 3 H, CO_2CH_3), 2.37 (s, 3 H, CH_3).

^{13}C-NMR (101 MHz, $CDCl_3$): δ (ppm) = 197.2 (C-4), 166.0 (C-1), 161.7 (C-4'), 155.9 (C-3), 138.7 (C-3''), 136.2 (C-1''), 134.5 (C-5''), 129.2 (C-2''), 128.8 (3 C, C-2', C-6', C-4''), 126.7 (C-1'), 126.5 (C-6''), 114.6 (3 C, C-2, C-3', C-5'), 55.6 (OCH_3), 51.8 (CO_2CH_3), 21.5 (CH_3).

HRMS (ESI): for $[C_{18}H_{15}O_5]^+$ calcd.: 279.1020
found: 279.1016.

$C_{19}H_{18}O_4$ (310.43 g/mol).

Methyl-(*Z*)-3-(4-fluorophenyl)-4-oxo-4-(*m*-tolyl)but-2-enoate 249[138]

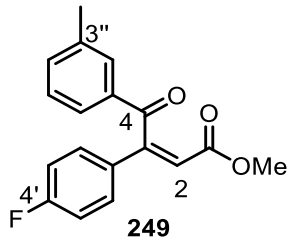

249

Following general procedure 6 the microwave assisted carbonylative *Suzuki-Miyaura-Miyaura* cross-coupling was performed using vinyltosylate **212** (106 mg, 300 µmol, 1.00 equiv.), 3-tolylboronic acid **231** (84.1 mg, 623 µmol, 2.08 equiv.), K_2CO_3 (127 mg, 919 µmol, 3.06 equiv.), $Pd(TFA)_2$ (4.3 mg, 12.9 µmol, 4.3 mol%), PCy_3 (7.0 mg, 25.0 µmol, 8.3 mol%) and $Mo(CO)_6$ **229** (160 mg, 606 µmol, 2.02 equiv.). The desired product **249** (60.4 mg, 202 µmol, 67%) was obtained as colorless solid.

TLC: R_f = 0.37 (PE/EtOAc 9:1 *v/v*).

UV (CH_2Cl_2): λ_{max} (nm) = 260.

IR (ATR): 1717, 1670, 1508, 1435, 1381, 1348, 1281, 1238, 1163, 958, 750, 673, 652 cm^{-1}.

^{1}H-NMR (300 MHz, $CDCl_3$): δ (ppm) = 7.79 (s, 1 H, 2''-H), 7.69 (d, J = 7.4 Hz, 1 H, 6''-H), 7.48 (dd, J = 8.8, 5.2 Hz, 2 H, 2'-H, 6'-H), 7.39–7.29 (m, 2 H, 4''-H, 5''-H), 7.06 (t, J = 8.8 Hz, 2 H, 3'-H, 5'-H), 6.45 (s, 1 H, 2-H), 3.63 (s, 3 H, CO_2CH_3), 2.38 (s, 3 H, CH_3).

^{13}C-NMR (101 MHz, $CDCl_3$): δ (ppm) = 196.6 (C-4), 165.5 (C-1), 164.3 (d, J = 252 Hz, C-4'), 155.1 (C-3), 138.9 (C-3''), 135.9 (C-1''), 134.7 (C-5''), 130.6 (d, J = 3.5 Hz, C-1'), 129.2

(C-2''), 129.2 (d, *J* = 8.8 Hz, 2 C, C-2', C-6'), 128.8 (C-4''), 126.5 (C-6''), 117.1 (d, *J* = 1.7 Hz, C-2), 116.5 (d, *J* = 22.0 Hz, 2 C, C-3', C-5'), 52.1 ($CO_2\underline{CH_3}$), 21.5 (CH_3).

HRMS (ESI): for $[C_{17}H_{12}FO_2]^+$ calcd.: 267.0816
found: 267.0817.

$C_{18}H_{15}FO_3$ (298.31 g/mol).

Methyl-(*Z*)-4-oxo-3-phenyl-4-(*o*-tolyl)but-2-enoate 250[138]

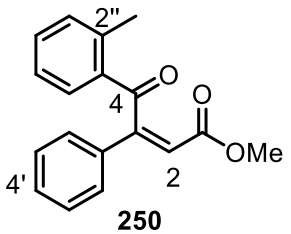

250

Following general procedure 6 the microwave assisted carbonylative *Suzuki-Miyaura-Miyaura* cross-coupling was performed using vinyltosylate **210** (405 mg, 1.22 mmol, 1.00 equiv.), 2-tolylboronic acid **232** (325 mg, 2.39 mmol, 1.96 equiv.), K_2CO_3 (499 mg, 3.61 mmol, 2.96 equiv.), $Pd(TFA)_2$ (15.9 mg, 47.8 µmol, 3.9 mol%), PCy_3 (27.4 mg, 97.7 µmol, 8.0 mol%) and $Mo(CO)_6$ **229** (640 mg, 2.42 mmol, 1.99 equiv.). The desired product **250** (35.5 mg, 127 µmol, 10%) was obtained as colorless solid.

TLC: R_f = 0.27 (PE/EtOAc 9:1 *v/v*).

UV (CH_2Cl_2): λ_{max} (nm) = 254.

IR (ATR): 1716, 1671, 1542, 1508, 1489, 1460, 1377, 1350, 1261, 1174, 1085, 942, 671 cm^{-1}.

^{1}H-NMR (400 MHz, $CDCl_3$): δ (ppm) = 7.59 (dd, *J* = 7.8, 1.2 Hz, 1 H, 6''-H), 7.52 (dd, *J* = 7.7, 1.0 Hz, 2 H, 2'-H, 6'-H), 7.42–7.36 (m, 4 H, 3'-H, 4'-H, 5'-H, 4''-H), 7.30 (d, *J* = 7.6 Hz, 1 H, 3''-H), 7.15 (t, *J* = 7.6 H, 1 H, 5''-H), 6.43 (s, 1 H, 2-H), 3.63 (s, 3 H, CO_2CH_3), 2.80 (s, 3 H, CH_3).

^{13}C-NMR (101 MHz, $CDCl_3$): δ (ppm) = 198.1 (C-4), 165.8 (C-1), 157.5 (C-3), 141.1 (C-2''), 134.9 (C-1''), 134.9 (C-1'), 132.6 (C-3'') 132.5 (C-4''), 132.1 (C-6''), 130.5 (C-4'), 129.3 (2 C, C-3', C-5'), 127.1 (2 C, C-2', C-6'), 125.8 (C-5''), 116.7 (C-2), 51.9 ($CO_2\underline{CH_3}$), 22.3 (CH_3).

HRMS (ESI): for $[C_{17}H_{13}O_2]^+$ calcd.: 249.0910
found: 249.0915.

$C_{18}H_{16}O_3$ (280.32 g/mol).

Methyl-(*Z*)-3-(4-methoxyphenyl)-4-oxo-4-(*o*-tolyl)but-2-enoate 251[138]

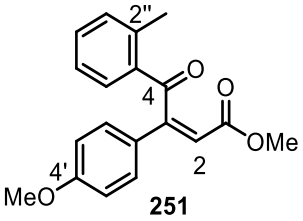

251

Following general procedure 5 the microwave assisted carbonylative *Suzuki-Miyaura-Miyaura* cross-coupling was performed using vinyltosylate **211** (440 mg, 1.21 mmol, 1.00 equiv.), 2-tolylboronic acid **232** (329 mg, 2.42 mmol, 2.00 equiv.), K_2CO_3 (506 mg, 3.66 mmol, 3.03 equiv.), $Pd(TFA)_2$ (16.1 mg, 48.4 µmol, 4.0 mol%), PCy_3 (28.0 mg, 99.9 µmol, 8.3 mol%) and $Mo(CO)_6$ **229** (644 mg, 2.44 mmol, 2.02 equiv.). The desired product **251** (106 mg, 342 µmol, 28%) was obtained as colorless solid.

TLC: R_f = 0.23 (PE/EtOAc 9:1 *v/v*).

UV (CH_2Cl_2): λ_{max} (nm) = 237, 304.

IR (ATR): 2979, 1712, 1670, 1596, 1512, 1460, 1434, 1350, 1257, 1169, 1036, 944, 833, 674 cm^{-1}.

^{1}H-NMR (300 MHz, $CDCl_3$): δ (ppm) = 7.58 (dd, *J* = 7.6, 1.0 Hz, 1 H, 6''-H), 7.45 (d, *J* = 9.0 Hz, 2 H, 2'-H, 6'-H), 7.37 (dt, *J* = 7.6, 1.3 Hz, 1H, 4''-H), 7.30 (d, *J* = 7.6 Hz, 1 H, 3''-H), 7.14 (dt, *J* = 7.6, 1.0 Hz, 1 H, 5''-H), 6.89 (d, *J* = 9.0 Hz, 2 H, 3'-H, 5'-H), 6.36 (s, 1H, 2-H), 3.81 (s, 3 H, $-OCH_3$), 3.62 (s, 3 H, $-CO_2CH_3$), 2.81 (s, 3 H, $-CH_3$).

^{13}C-NMR (151 MHz, $CDCl_3$): δ (ppm) = 198.4 (C-4), 165.9 (C-4'), 161.5 (C-1), 156.9 (C-3), 140.9 (C-2''), 134.8 (C-1''), 132.4 (C-4''), 132.3 (C-3''), 132.0 (C-6''), 128.6 (2 C, C-2', C-6'), 127.1 (C-1'), 125.6 (C-5''), 114.6 (2 C, C-3', C-5'), 114.0 (C-2), 55.4 ($-OCH_3$), 51.7 ($-CO_2CH_3$), 22.2 ($-CH_3$).

HRMS (ESI): for $[C_{18}H_{15}O_3]^+$ calcd.: 279.1016
found: 279.1018.

$C_{19}H_{18}FO_4$ (298.31 g/mol).

Methyl (*Z*)-3-(4-fluorophenyl)-4-oxo-4-(*o*-tolyl)but-2-enoate 252[138]

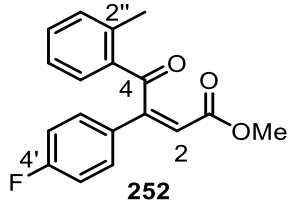

252

Following general procedure 5 the microwave assisted carbonylative *Suzuki-Miyaura-Miyaura* cross-coupling was performed using vinyltosylate **212** (423 mg, 1.21 mmol,

1.00 equiv.), 2-tolylboronic acid **232** (324 mg, 2.38 mmol, 1.97 equiv.), K_2CO_3 (501 mg, 3.63 mmol, 3.00 equiv.), $Pd(TFA)_2$ (17.1 mg, 51.4 µmol, 4.2 mol%), PCy_3 (28.2 mg, 101 µmol, 8.3 mol%) and $Mo(CO)_6$ **229** (637 mg, 2.41 mmol, 1.99 equiv.). The desired product **252** (63.7 mg, 210 µmol, 18%) was obtained as colorless solid.

TLC: R_f = 0.36 (PE/EtOAc 9:1 *v/v*).

UV (CH_2Cl_2): λ_{max} (nm) = 253.

IR (ATR): 1717, 1673, 1600, 1509, 1461, 1378, 1348, 1261, 1173, 1094, 1019, 801, 675, 657 cm^{-1}.

^{1}H-NMR (400 MHz, $CDCl_3$): *δ* (ppm) = 7.56 (dd, *J* = 7.8, 1.4 Hz, 1 H, 6''-H), 7.51 (dd, *J* = 8.8, 5.3 Hz, 2 H, 2'-H, 6'-H), 7.39 (dt, *J* = 7.4, 1.2 Hz, 1H, 4''-H), 7.31 (d, *J* = 7.4 Hz, 1H, 3''-H), 7.18–7.13 (m, 1H, 5''-H), 7.07 (t, *J* = 8.8 Hz, 2 H, 3'-H, 5'-H), 6.38 (s, 1 H, 2-H), 3.63 (s, 3 H, CO_2CH_3), 2.80 (s, 3 H, CH_3).

^{13}C-NMR (101 MHz, $CDCl_3$): *δ* (ppm) = 197.9 (C-4), 165.6 (C-1), 164.1 (d, *J* = 252 Hz, C-4'), 156.2 (C-3), 141.2 (C-2''), 134.7 (C-1''), 132.7 (C-4''), 132.6 (C-3''), 132.0 (C-6''), 131.1 (d, *J* = 3.4 Hz, C-1'), 129.1 (d, *J* = 8.6 Hz, 2 C, C-2', C-6'), 125.8 (C-5''), 116.6 (C-2), 116.5 (d, *J* = 21.8 Hz, 2 C, C-3', C-5'), 52.0 (CO_2CH_3), 22.3 (CH_3).

HRMS (ESI): for $[C_{17}H_{12}FO_2]^+$ calcd.: 267.0816
found: 267.0819.

$C_{18}H_{15}FO_3$ (298.31 g/mol).

Methyl-(*Z*)-4-(naphthalen-2-yl)-4-oxo-3-phenylbut-2-enoate 253[138]

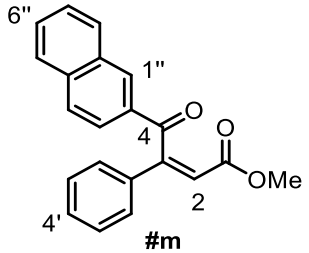

#m

Following general procedure 5 the carbonylative *Suzuki-Miyaura* cross-coupling was performed using vinyltosylate **210** (102 mg, 306 µmol, 1.00 equiv.), 2-naphthylboronic acid **233** (105 mg, 623 µmol, 2.04 equiv.), K_2CO_3 (128 mg, 926 µmol, 3.03 equiv.), $Pd(TFA)_2$ (4.10 mg, 12.3 µmol, 3.9 mol%), PCy_3 (6.80 mg, 24.3 µmol, 7.9 mol%) and $Mo(CO)_6$ **229** (161 mg, 610 µmol, 1.99 equiv.). The desired product **253** (43.7 mg, 138 µmol, 45%) was obtained as colorless oil.

TLC: R_f = 0.44 (PE/EtOAc 6:1 *v/v*).

UV ($CHCl_3$): λ_{max} (nm) = 254, 286.

IR (ATR): 1736, 1618, 1358, 1346, 1250, 1217; 1177, 1124; 933, 859, 818, 770, 757, 685, 645 cm^{-1}.

^{1}H-NMR (500 MHz, $CDCl_3$): δ (ppm) = 8.38 (s, 1 H, 1''-H), 8.12 (dd, *J* = 8.6, 1.7 Hz, 1 H, 3''-H), 7.92 (d, *J* = 8.6 H, 1 H, 4''-H), 7.89 (d, *J* = 8.3 Hz, 1 H, 8''-H), 7.86 (d, *J* = 8.3 Hz, 1 H, 5''-H), 7.61–7.57 (m, 1 H, 7''-H), 7.57–7.54 (m, 2 H, 2'-H, 6'-H), 7.53–7.49 (m, 1 H, 6''-H), 7.42–7.35 (m, 3 H, 3'-H, 4'-H, 5'-H), 6.60 (s, 1 H, 2-H), 3.61 (s, 3 H, CO_2CH_3).

^{13}C-NMR (126 MHz, $CDCl_3$): δ (ppm) = 196.6 (C-4), 165.7 (C-1), 156.2 (C-3), 136.1 (C-2''), 134.4 (C-1''), 133.7 (C-8a''), 132.7 (C-4a''), 131.4 (C-1''), 130.7 (C-4'), 129.9 (C-8''), 129.3 (2 C, C-3', C-5'), 129.0 (C-4''), 128.8 (C-7''), 128.0 (C-5''), 127.2 (2 C, C-2', C-6'), 126.9 (C-6''), 124.1 (C-3''), 117.4 (C-2), 52.1 (CO_2CH_3).

HRMS (ESI): for $[C_{20}H_{13}O_2]^+$ calcd.: 285.0910
found: 285.0898.

$C_{21}H_{16}O_3$ (316.36 g/mol).

Methyl-(*Z*)-3-(4-methoxyphenyl)-4-(naphthalen-2-yl)-4-oxobut-2-enoate 254[138]

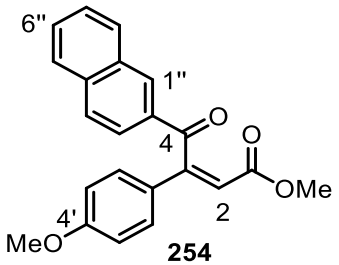

254

Following general procedure 5 the carbonylative *Suzuki-Miyaura* cross-coupling was performed using vinyltosylate **211** (110 mg, 304 µmol, 1.00 equiv.), 2-naphthylboronic acid **233** (105 mg, 611 µmol, 2.01 equiv.), K_2CO_3 (125 mg, 905 µmol, 2.98 equiv.), $Pd(TFA)_2$ (4.10 mg, 12.3 µmol, 4.1 mol%), PCy_3 (6.90 mg, 24.6 µmol, 8.1 mol%) and $Mo(CO)_6$ **229** (161 mg, 610 µmol, 269.01 equiv.). The desired product **254** (69.0 mg, 199 µmol, 65%) was obtained as colorless oil.

TLC: R_f = 0.27 (PE/EtOAc 6:1 *v/v*).

UV ($CHCl_3$): λ_{max} (nm) = 254, 298.

IR (ATR): 1712, 1668, 1624, 1511, 1462, 1435, 1358, 1346, 1286, 1255, 1165, 1122, 1028, 932, 795 cm^{-1}.

^{1}H-NMR (500 MHz, $CDCl_3$): δ (ppm) = 8.37 (s, 1 H, 1''-H), 8.11 (dd, *J* = 8.6, 1.6 Hz, 1 H, 3''-H), 7.92–7.84 (m, 3 H, 4''-H, 5''-H, 8''-H), 7.60–7.55 (m, 1 H, 7''-H) 7.52–7.49 (m, 1 H, 6''-H),

7.49 (d, *J* = 9.0 Hz, 2 H, 2'-H, 6'-H), 6.88 (d, *J* = 9.0 Hz, 2 H, 3'-H, 5'-H), 6.51 (s, 1 H, 2-H), 3.79 (s, 3 H, OCH_3), 3.60 (s, 3 H, CO_2CH_3).

^{13}C-NMR (126 MHz, $CDCl_3$): *δ* (ppm) = 197.1 (C-4), 166.0 (C-1), 161.7 (C-4'), 155.7 (C-3), 136.0 (C-2''), 133.7 (C-8a''), 132.7 (C-4a''), 131.3 (C-1''), 129.9 (C-8''), 128.9 (C-4''), 128.9 (2 C, C-2', C-6'), 128.8 (C-7''), 128.0 (C-5''), 126.8 (C-6''), 126.7 (C-1'), 124.1 (C-3''), 114.8 (C-2), 114.7 (2 C, C-3', C-5'), 55.5 (OCH_3), 51.9 (CO_2CH_3).

HRMS (ESI): for $[C_{21}H_{15}O_3]^+$ calcd.: 315.1016
found: 315.1010.

$C_{22}H_{18}O_4$ (346.38 g/mol).

Methyl-(*Z*)-3-(4-fluorophenyl)-4-(naphthalen-2-yl)-4-oxobut-2-enoate 255[138]

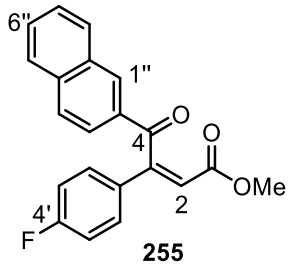

255

Following general procedure 5 the carbonylative *Suzuki-Miyaura* cross-coupling was performed using vinyltosylate **212** (107 mg, 305 µmol, 1.00 equiv.), 2-naphthylboronic acid 233 (611 mg, 611 µmol, 2.00 equiv.), K_2CO_3 (125 mg, 905 µmol, 2.97 equiv.), $Pd(TFA)_2$ (4.10 mg, 12.3 µmol, 4.0 mol%), PCy_3 (6.80 mg, 24.3 µmol, 8.0 mol%) and $Mo(CO)_6$**229** (158 mg, 598 µmol, 1.96 equiv.). The desired product **255** (43.8 mg, 131 µmol, 43%) was obtained as colorless oil.

TLC: R_f = 0.46 (PE/EtOAc 6:1 *v/v*).

UV ($CHCl_3$): λ_{max} (nm) = 254, 288.

IR (ATR): 1712, 1668, 1624, 1511, 1463, 1435, 1358, 1286, 1255, 1166, 1122, 1030, 932, 796, 760 cm^{-1}.

^{1}H-NMR (400 MHz, $CDCl_3$): *δ* (ppm) = 8.35 (s, 1H, 1''-H), 8.11 (dd, *J* = 8.6, 1.7 Hz, 1 H, 3''-H), 7.92 (d, *J* = 8.6 Hz, 1 H, 4''-H), 7.89 (d, *J* = 8.6 Hz, 1 H, 8''-H), 7.87 (d, *J* = 8.6 Hz, 1 H, 5''-H), 7.61–7.57 (m, 1 H, 7''-H), 7.54 (dd, *J* = 9.0, 8.8 Hz, 2 H, 2'-H, 6'-H), 7.54–7.50 (m, 1 H, 6''-H), 7.07 (t, *J* = 8.8 Hz, 2 H, 3'-H, 5'-H), 6.54 (s, 1 H, 2-H), 3.61 (s, 3 H, CO_2CH_3).

^{13}C-NMR (101 MHz, $CDCl_3$): *δ* (ppm) = 196.5 (C-4), 165.4 (C-1), 164.5 (d, *J* = 252 Hz, C-4'), 155.2 (C-3), 136.4 (C-2''), 133.5 (C-8a''), 132.7 (C-4a''), 131.4 (C-1''), 130.6 (d, *J* = 3.5 Hz, C-1'), 129.9 (C-8''), 129.3 (d, *J* = 8.6 Hz, 2 C, C-2', C-6'), 129-1 (C-4''), 128.9 (C-7''), 128.0

(C-5''), 127.0 (C-6''), 124.0 (C-3''), 117.3 (d, *J* = 1.7 Hz, C-2), 116.5 (d, *J* = 22.0 Hz, 2 C, C-3', C-5'), 52.1 ($CO_2\underline{CH_3}$).

HRMS (ESI): for $[C_{20}H_{12}FO_2]^+$ calcd.: 303.0816
found: 303.0823.

$C_{21}H_{15}FO_3$ (334.35 g/mol).

6.3.7. γ-Hydroxybutenolide synthesis via saponification/acid mediated cyclization sequence

5-Hydroxy-4,5-diphenylfuran-2(5*H*)-one 259[138]

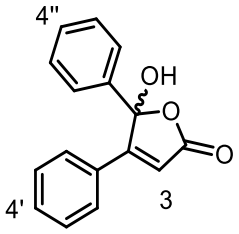

259

Following general procedure 7 saponification and cyclisation were obtained by using **235** (23.6 mg, 88.6 µmol, 1.00 equiv.) and aq. KOH (2 M, 133 µL, 266 µmol, 3.00 equiv.). The desired product **259** (21.8 mg, 86.4 µmol, 98%) was obtained as yellow oil.

TLC: R_f = 0.58 (PE/EtOAc 2:1 *v/v*).

UV ($CHCl_3$): λ_{max} (nm) = 278.

IR (ATR): 2979, 2888, 1735, 1461, 1384, 1252, 1152, 1074, 955, 685 cm^{-1}.

^{1}H-NMR (600 MHz, acetone-d_6): δ (ppm) = 7.74 (d, *J* = 7.2 Hz, 2 H, 2''-H, 6''-H), 7.66 (d, *J* = 6.1 Hz, 2 H, 2'-H, 6'-H), 7.42–7.36 (m, 6 H, 3'-H, 4'-H, 5'-H, 3''-H, 4''-H, 5''-H), 6.73 (s, 1 H, 3-H).

^{13}C-NMR (151 MHz, acetone-d_6): δ (ppm) = 170.7 (C-2), 165,0 (C-4), 138.7 (C-1'), 131.8 (C-4''), 129.8 (C-4'), 129.6 (C-1''), 129.4 (2 C, C-3'', C-5''), 129.3 (2 C, C-3', C-5'), 129.3 (2 C, C-2'', C-6''), 126.1 (2 C, C-2', C-6'), 115.7 (C-3), 107.0 (C-5).

HRMS (ESI): for $[C_{16}H_{11}O_2]^+$ calcd.: 235.0754
found: 235.0771.

$C_{16}H_{12}O_3$ (252.27 g/mol).

5-Hydroxy-4-(4-methoxyphenyl)-5-phenylfuran-2(5*H*)-one 260[138]

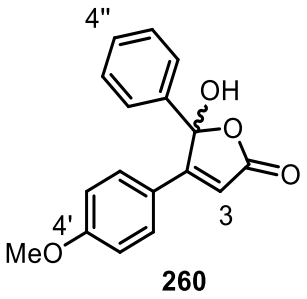

260

Following general procedure 7 saponification and cyclisation were performed using **236** (40.6 mg, 137 µmol, 1.00 equiv.) and aq. KOH (2 M, 206 µL, 438 mg, 411 µmol, 3.00 equiv.). The desired product **260** (27.6 mg, 97.8 µmol, 71%) was obtained as yellow oil.

TLC: R_f = 0.26 (PE/EtOAc 2:1 *v/v*).

UV ($CHCl_3$): λ_{max} (nm) = 312.

IR (ATR): 2360, 2340, 1732, 1689, 1595, 1511, 1254, 1162, 836, 770, 688 cm^{-1}.

^{1}H-NMR (400 MHz, acetone-d_6): δ (ppm) = 7.70 (d, J = 8.9 Hz, 2 H, 2'-H, 6'-H), 7.64 (d, J = 5.9 Hz, 2 H, 2''-H, 6''-H), 7.44–7.36 3 H, 3''-H, 4''-H, 5''-H), 6.91 (d, J = 8.9 Hz, 2 H, 3'-H, 5'-H), 6.60 (s, 1 H, 3-H), 3.80 (s, 3 H, OCH_3).

^{13}C-NMR (101 MHz, acetone-d_6): δ (ppm) = 170.2 (C-2), 164.1 (C-4'), 161.5 (C-4), 138.2 (C-1''), 130.6 (2 C, C-2', C-6'), 129.0 (C-4''), 128.5 (2 C, C-3'', C-5''), 125.3 (2 C, C-2'', C-6''), 121.2 (C-1'), 113.9 (2 C, C-3', C-5'), 112.3 (C-3), 105.9 (C-5), 54.7 (OCH_3).

HRMS (ESI): for $[C_{17}H_{13}O_3]^+$ calcd.: 265.0859
found: 265.0849.

$C_{17}H_{14}O_4$ (282.30 g/mol).

4-(4-Fluoroyphenyl)-5-hydroxy-5-phenylfuran-2(5*H*)-one 261[138]

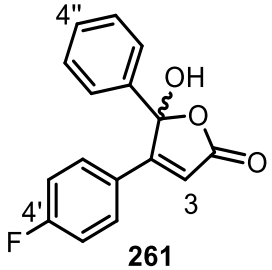

261

Following general procedure 7 saponification and cyclisation were performed by using **237** (18.0 mg, 63.3 µmol, 1.00 equiv.) and aq. KOH (2 M, 90.0 µL, 201 mg, 190 µmol, 3.00 equiv.). The desired product **261** (16.2 mg, 59.9 µmol, 95%) was obtained as yellow oil.

TLC: R_f = 0.34 (PE/EtOAc 2:1 *v/v*).

UV ($CHCl_3$): λ_{max} (nm) = 280.

IR (ATR): 2980, 2361, 1735, 1601, 1508, 1223, 1161, 956, 835, 696, 578, 504 cm^{-1}.

^{1}H-NMR (600 MHz, acetone-d_6): δ (ppm) = 7.82 (dd, J = 8.8, 5.5 Hz, 2 H, 2'-H, 6'-H), 7.65 (d, J = 5.8 Hz, 2 H, 2''-H, 6''-H), 7.40–7.43 (m, 3 H, 3''-H, 4''-H, 5''-H), 7.16 (t, J = 8.8 Hz, 2 H, 3'-H, 5'-H), 6.72 (s, 1 H, 3-H).

^{13}C-NMR (151 MHz, acetone-d_6,): δ (ppm) = 170.2 (C-2), 164.4 (C-4), 164.3 (d, J = 254 Hz, C-4'), 136.6 (C-1''), 130.8 (d, J = 8.8 Hz, 2 C, C-2', C-6'), 129.7 (C-4''), 128.8 (2 C, C-3'', C-5''), 125.6 (2 C, C-2'', C-6''), 125.0 (d, J = 3.4 Hz, C-1'),116.7 (d, J = 21.9 Hz, 2 C, C-3', C-5'), 114.7 (C-3), 106.6 (C-5).

HRMS (ESI): for $[C_{16}H_{10}FO_2]^+$ calcd.: 253.0659
found: 253.0665.

$C_{16}H_{11}FO_3$ (270.26 g/mol).

5-Hydroxy-5-(4-methoxyphenyl)-4-phenylfuran-2(5*H*)-one 262[138]

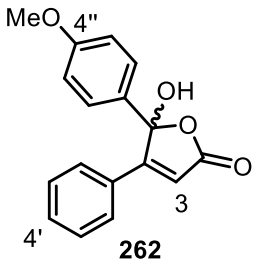

262

Following general procedure 7 saponification and cyclisation were performed using **238** (45.6 mg, 154 µmol, 1.00 equiv.) and aq. KOH (2 M, 230 µL, 489 mg, 462 µmol, 3.00 equiv.). The desired product **262** (30.9 mg, 109 µmol, 71%) was obtained as yellow oil.

TLC: R_f = 0.30 (PE/EtOAc 2:1 *v/v*).

UV ($CHCl_3$): λ_{max} (nm) = 280.

IR (ATR): 2979, 2888, 2360, 2339, 1727, 1600, 1510, 1457, 1384, 1254, 1156, 1074, 955, 828 cm^{-1}.

^{1}H-NMR (600 MHz, acetone-d_6): δ (ppm) = 7.79–7.57 (m, 4 H, 2'-H, 6'-H, 2''-H, 6''-H), 7.43–7.38 (m, 3 H, 3'-H, 4'-H, 5'-H), 6.96 (d, J = 8.7 Hz, 2 H, 3''-H, 5''-H), 6.65 (s, 1 H, 3-H), 3.82 (s, 3 H, OCH_3).

^{13}C-NMR (101 MHz, acetone-d_6): δ (ppm) = 170.0 (C-2), 164.2 (C-4), 159.9 (C-4''), 131.0 (C-4'), 129.7, (C-1''), 129.6 (C-1'), 128.7 (2 C, C-3', C-5'), 126.9 (4 C, C-2', C-6', C-2'', C-6''), 114.9 (C-3), 114.2 (2 C, C-3'', C-5''), 107.0 (C-5), 55.2 (-OCH_3).

HRMS (ESI): for $[C_{17}H_{13}O_3]^+$ calcd.: 265.0859
found: 265.0860.

$C_{17}H_{14}O_4$ (282.30 g/mol).

5-Hydroxy-4,5-di-(methoxyphenyl)-furan-2(5*H*)-one 263[138]

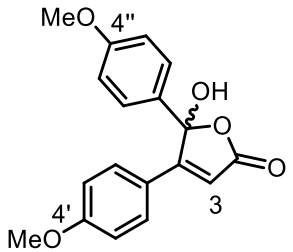

263

Following general procedure 7 saponification and cyclisation were performed by using **239** (43.4 mg, 133 µmol, 1.00 equiv.) and aq. KOH (2 M, 190 µL, 403 mg, 359 µmol, 2.70 equiv.). The desired product **263** (32.6 mg, 104 µmol, 78%) was obtained as yellow oil.

TLC: R_f = 0.20 (PE/EtOAc 2:1 *v/v*).

UV ($CHCl_3$): λ_{max} (nm) = 297.

IR (ATR): 2935, 2840, 2360, 2341, 1727, 1596, 1511, 1254, 1166, 1024, 832 cm^{-1}.

^{1}H-NMR (600 MHz, acetone-d_6): δ (ppm) = 7.72–7.57 (m, 4 H, 2'-H, 6'-H, 2''-H, 6''-H), 6.96–6.92 (m, 4 H, 3'-H, 5'-H, 3''-H, 5''-H), 6.54 (s, 1 H, 3-H), 3.81 (s, 6 H, 2 × OCH_3).

^{13}C-NMR (101 MHz, acetone-d_6): δ (ppm) = 170.9 (C-2), 164.7 (C-4'), 162.2 (C-4''), 160.5 (C-4), 131.3 (C-1''), 130.8 (C-1'), 127.5 (2 C, C-3', C-5'), 122.0 (2 C, C-3'', C-5''), 114.6 (2 C, C-2'', C-6''), 114.2 (2 C, C-2', C-6'), 112.9 (C-3), 106.8 (C-5), 55.5 (2 × OCH_3).

HRMS (ESI): for $[C_{18}H_{15}O_4]^+$ calcd.: 295.0965
found: 295.0961.

$C_{18}H_{16}O_5$ (312.32 g/mol).

4-(4-Fluorophenyl)-5-hydroxy-5-(4-methoxyphenyl)-furan-2(5*H*)-one 264[138]

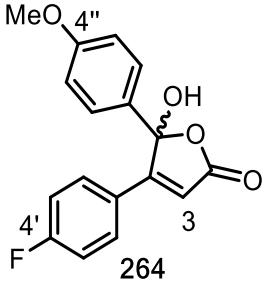

264

Following general procedure 7 saponification and cyclisation were performed by using **240** (37.4 mg, 119 µmol, 1.00 equiv.) and aq. KOH (2 M, 180 µL, 378 g, 357 µmol, 3.00 equiv.). The desired product **264** (20.7 mg, 69.0 µmol, 58%) was obtained as yellow oil.

TLC: R_f = 0.20 (PE/EtOAc 2:1 *v/v*).

UV ($CHCl_3$): λ_{max} (nm) = 282.

IR (ATR): 3065, 2361, 1690, 1660, 1596, 1507, 1421, 1205, 1164, 1024, 838, 583, 527, 508 cm^{-1}.

^{1}H-NMR (600 MHz, acetone-d_6): δ (ppm) = 7.75 (dd, *J* = 8.8, 5.4 Hz, 2 H, 2'-H, 6'-H), 7.67 (d, *J* = 8.5 Hz, 2 H, 2''-H, 6''-H), 7.17 (t, *J* = 8.8 Hz, 2 H, 3'-H, 5'-H), 6.96 (d, *J* = 8.5 Hz, 2 H, 3''-H, 5''-H), 6.64 (s, 1 H, 3-H), 3.82 (s, 3 H, -OCH_3).

^{13}C-NMR (151 MHz, acetone-d_6): δ (ppm) = 170.5 (C-2), 164.4 (d, *J* = 250 Hz, C-4'), 163.7 (C-4''), 160.6 (C-4), 131.9 (d, *J* = 8.7 Hz, 2 C, C-2', C-6'), 130.2 (C-1''), 127.6 (2 C, C-2'', C-6''), 126.4 (d, *J* = 2.9 Hz, C-1'), 116.5 (d, *J* = 22.1 Hz, 2 C, C-3', C-5'), 115.5 (C-3), 114.3 (2 C, C-3'', C-5''), 106.9 (C-5), 55.2 (-OCH_3).

HRMS (ESI): for $[C_{17}H_{12}FO_3]^+$ calcd.: 283.0765
found: 283.0786.

$C_{17}H_{13}FO_4$ (300.29 g/mol).

5-(4-Fluorophenyl)-5-hydroxy-4-phenylfuran-2(5*H*)-one 265[138]

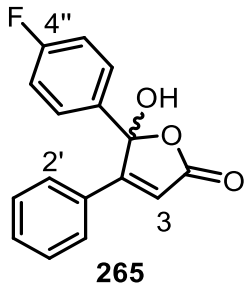

265

Following general procedure 7 saponification and cyclisation were performed by using **241** (51.4 mg, 181 µmol, 1.00 equiv.) and aq. KOH (2 M, 282 µL, 543 µmol, 3.00 equiv.). The desired product **265** (41.6 mg, 154 µmol, 85%) was obtained as yellow oil.

TLC: R_f = 0.54 (PE/EtOAc 2:1 *v/v*).

UV ($CHCl_3$): λ_{max} (nm) = 280.

IR (ATR): 1734, 1602, 1508, 1452, 1415, 1223, 1162, 1020, 955, 874, 835, 777, 733, 578, 546 cm^{-1}.

^{1}H-NMR (600 MHz, acetone-d_6): δ (ppm) = 7.75–7.69 (m, 4 H, 2'-H, 6'-H, 2''-H, 6''-H), 7.44–7.37 (m, 3 H, 3'-H, 4'-H, 5'-H), 7.17 (t, J = 8.9 Hz, 2 H, 3''-H, 5''-H), 6.73 (s, 1H, 3-H).

^{13}C NMR (101 MHz, acetone-d_6) δ (ppm) = 169.8 (C-2), 163.8 (d, J = 250 Hz, C-4''), 163.1 (C-4), 137.7 (C-1'), 131.2 (d, J = 8.8 Hz, 2 C, C-2'', C-6''), 129.2 (C-4'), 128.6 (2 C, C-3', C-5'), 125.6 (d, J = 2.2 Hz ,C-1''), 125.4 (2 C, C-2', C-6'), 115.8 (d, J = 21.9 Hz, 2 C, C-3'', C-5''), 114.9 (C-3), 106.0 (C-5).

HRMS (ESI): for $[C_{16}H_{10}FO_2]^+$ calcd.: 253.0659
found: 253.0666.

$C_{16}H_{11}FO_3$ (270.26 g/mol).

5-(4-Fluorophenyl)-5-hydroxy-4-(4-methoxyphenyl)-furan-2(5*H*)-one 266[138]

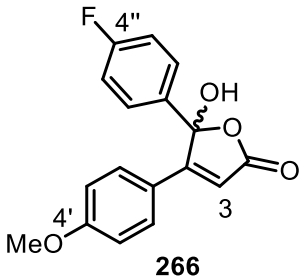

266

Following general procedure 7 saponification and cyclisation were performed by using **242** (34.7 mg, 110 µmol, 1.00 equiv.) and aq. KOH (2 M, 170 µL, 351 mg, 331 µmol, 3.00 equiv.). The desired product **266** (23.0 mg, 76.6 µmol, 70%) was obtained as yellow oil.

TLC: R_f = 0.48 (PE/EtOAc 2:1 *v/v*).

UV ($CHCl_3$): λ_{max} (nm) = 312.

IR (ATR): 2362, 2154, 1728, 1601, 1567, 1511, 1427, 1262, 1228, 1176, 1019, 952, 827, 588, 538 cm^{-1}.

^{1}H-NMR (600 MHz, acetone-d_6): δ (ppm) = 7.75–7.64 (m, 4 H, 2'-H, 6'-H, 2''-H, 6''-H), 7.16 (t, J = 8.9 Hz, 2 H, 3''-H, 5''-H), 6.93 (d, J = 9.0 Hz, 2 H, 3'-H, 5'-H), 6.60 (s, 1 H, 3-H), 3.81 (s, 3 H, OCH_3).

^{13}C-NMR (101 MHz, acetone-d_6): δ (ppm) = 170.0 (C-2), 162.6 (d, J = 244 Hz, C-4''), 161.6 (C-4'), 161.4 (C-4), 134.6 (d, J = 2.4 Hz, C-1''), 130.6 (2 C, C-2', C-6'), 127.8 (d, J = 8.6 Hz, 2 C, C-2'', C-6''), 121.1 (C-1'), 115.3 (d, J = 21.8 Hz, 2 C, C-3'', C-5''), 114.0 (2 C, C-3', C-5'), 112.4 (C-3), 105.4 (C-5), 54.8 (OCH_3)**.**

HRMS (ESI): for $[C_{17}H_{12}FO_3]^+$ calcd.: 283.0765
found: 283.0781.

$C_{17}H_{13}FO_4$ (300.29 g/mol).

4,5-Di-(4-fluorophenyl)-5-hydroxyfuran-2(5*H*)-one 267[138]

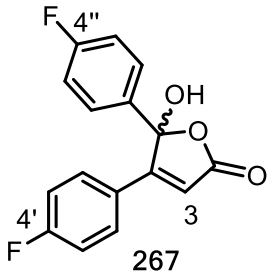

267

Following general procedure 7 saponification and cyclisation were performed by using **243** (46.2 mg, 153 µmol, 1.00 equiv.) and aq. KOH (2 M, 230 µL, 486 mg, 459 µmol, 3.00 equiv.). The desired product **267** (38.0 mg, 132 µmol, 86%) was obtained as yellow oil.

TLC: R_f = 0.52 (PE/EtOAc 2:1 *v/v*).

UV ($CHCl_3$): λ_{max} (nm) = 277.

IR (ATR): 2361, 2339, 1736, 1599, 1507, 1225, 1158, 834, 577, 541, 516 cm^{-1}.

^{1}H-NMR (600 MHz, acetone-d_6): δ (ppm) = 7.81 (dd, *J* = 7.9, 6.0 Hz, 2 H, 2''-H, 6''-H), 7.76–7.64 (m, 2 H, 2'-H, 6'-H), 7.20–7.14 (m, 4 H, 3'-H, 5'-H, 3''-H, 5''-H), 6.73 (s, 1 H, 3-H).

^{13}C NMR (101 MHz, acetone-d_6): δ (ppm) = 169.8 (C-2), 163.7 (d, *J* = 251 Hz, C-4'), 162.7 (d, *J* = 247 Hz, C-4''), 162.7 (C-4), 137.7 (d, *J* = 2.8 Hz, C-1''), 131.2 (d, *J* = 8.8 Hz, 2 C, C-2', C-6'), 127.9 (d, *J* = 8.7 Hz, 2 C, C-2'', C-6''), 125.4 (d, *J* = 3.2 Hz, C-1'), 116.0 (d, *J* = 21.9 Hz, 2 C, C-3', C-5'), 115.4 (d, *J* = 21.9 Hz, 2 C, C-3'', C-5''), 114.9 (C-3), 106.0 (C-5).

HRMS (ESI): for $[C_{16}H_9F_2O_2]^+$ calcd.: 271.0565
found: 271.0571.

$C_{16}H_{10}F_2O_3$ (288.25 g/mol).

5-Hydroxy-4-phenyl-5-(*p*-tolyl)furan-2(*5H*)-one 268[138]

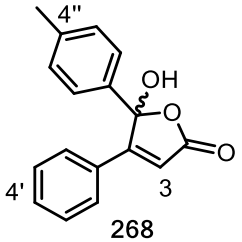

268

Following general procedure 7 saponification and cyclisation were performed by using **244** (13.7 mg, 48.9 µmol, 1.00 equiv.) and aq KOH (2 M, 74 µL, 147 µmol, 3.00 equiv.). The desired product **268** (8.34 mg, 31.3 µmol, 64%) was obtained as yellow oil.

TLC: R_f = 0.45 (PE/EtOAc 1:1 *v/v*).

UV ($CHCl_3$): λ_{max} (nm) = 274.

IR (ATR): 1737, 1672, 1606, 1220, 1176, 1114, 957, 874, 822, 770, 747, 689, 647, 580, 538 cm^{-1}.

^{1}H-NMR (400 MHz, acetone-d_6): δ (ppm) = 7.76–7.69 (m, 2 H, 2'-H, 6'-H), 7.56 (d, J = 7.9 Hz, 2 H, 2''-H, 6''-H), 7.43–7.36 (m, 3 H, 3'-H, 4'-H, 5'-H), 7.22 (d, J = 7.9 Hz, 2 H, 3''-H, 5''-H), 6.69 (s, 1 H, 3-H), 2.14 (s, 3 H, CH_3).

^{13}C-NMR (151 MHz, acetone-d_6): δ (ppm) = 171.1 (C-2), 165.4 (C-4), 142.5 (C-4''),139.8 (C-1'), 136.2 (C-1''), 132.1 (C-4'), 130.2 (2 C, C-3'', C-5''), 130.1 (C-1'), 129.8 (2 C, C-3', C-5'), 129.7 (2 C, C-2', C-6'), 126.5 (2 C, C-2'', C-6''), 116.0 (C-3), 107.4 (C-5), 21.3 (CH_3).

HRMS (ESI): for $[C_{17}H_{13}O_2]^+$ calcd.: 249.0909
found: 249.0910.

$C_{17}H_{14}O_3$ (266.30 g/mol).

5-Hydroxy-4-(4-methoxyphenyl)-5-(*p*-tolyl)furan-2(*5H*)-one 269[138]

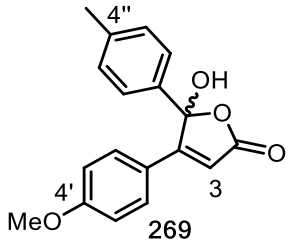

269

Following general procedure 7 saponification and cyclisation were performed by using **245** (35.9 mg, 116 µmol, 1.00 equiv.) and aq. KOH (2 M, 174 µL, 348 µmol, 3.00 equiv.). The desired product **269** (22.6 mg, 76.3 µmol, 66%) was obtained as yellow oil.

TLC: R_f = 0.49 (PE/EtOAc 1:1 *v/v*).

UV ($CHCl_3$): λ_{max} (nm) = 275.

IR (ATR): 1736, 1670, 1603, 1508, 1414, 1223, 1162, 1017, 957, 878, 836, 822, 713, 538, 510 cm^{-1}.

^{1}H-NMR (600 MHz, acetone-d_6): δ (ppm) = 7.69 (d, J = 9.0 Hz, 2 H, 2'-H, 6'-H), 7.53 (d, J = 8.0 Hz, 2 H, 2''-H, 6''-H), 7.21 (d, J = 8.0 Hz, 2 H, 3''-H, 5''-H), 6.91 (d, J = 9.0 Hz, 2 H, 3'-H, 5'-H) 6.56 (s, 1H, 3-H), 3.80 (s, 3 H, OCH_3), 2.31 (s, 3 H, CH_3).

^{13}C-NMR (151 MHz, acetone-d_6): δ (ppm) = 170.9 (C-2), 164.9 (C-4), 162.3 (C-4'), 139.4 (C-4''), 136.1(C-1''), 131.3 (2 C, C-2', C-6'), 129.8 (2 C, C-3'', C-5''), 126.0 (2 C, C-2'', C-6''), 122.4 (C-1'), 114.6 (2 C, C-3', C-5'), 112.9 (C-3), 106.0 (C-5, HMBC), 55.5 (OCH_3), 21.0 (CH_3).

HRMS (ESI): for $[C_{18}H_{15}O_3]^+$ calcd.: 279.1016
found: 279.1012.

$C_{18}H_{16}O_4$ (296.32 g/mol).

4-(4-Fluorophenyl)-5-hydroxy-5-(*p*-tolyl)furan-2(*5H*)-one 270[138]

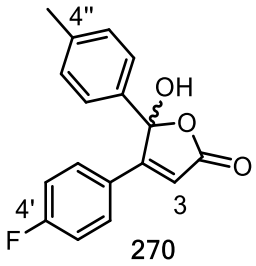

270

Following general procedure 7 saponification and cyclisation were performed by using **246** (12.6 mg, 42.3 µmol, 1.00 equiv.) and aq. KOH (2 M, 64.0 µL, 127 µmol, 3.00 equiv.). The desired product **270** (11.7 mg, 41.2 µmol, 97%) was obtained as yellow oil.

TLC: R_f = 0.61 (PE/EtOAc 1:1 *v/v*).

UV (MeCN): λ_{max} (nm) = 308.

IR (ATR): 1731, 1604, 1513, 1263, 1233, 1177, 1020, 951, 824, 798, 742, 677, 655, 590, 537 cm^{-1}.

^{1}H-NMR (600 MHz, acetone-d_6): δ (ppm) = 7.79 (dd, *J* = 8.9, 5.4 Hz, 2 H, 2'-H, 6'-H), 7.55 (d, *J* = 8.1 Hz, 2 H, 2''-H, 6''-H), 7.22 (d, *J* = 8.1 Hz, 2 H, 3''-H, 5''-H), 7.16 (t, *J* = 8.9 Hz, 2 H, 3'-H, 5'-H), 6.68 (s, 1 H, 3-H), 2.32 (s, 3 H, CH_3).

^{13}C-NMR (101 MHz, acetone-d_6): δ (ppm) = 169.9 (C-2), 163.8 (d, *J* = 251 Hz, C-4'), 163.4 (C-4), 138.9 (C-4''), 134.9 (C-1''), 131.2 (d, *J* = 7.7 Hz, 2 C, C-2', C-6'), 129.2 (2 C, C-2'', C-6''), 125.6 (C-1'), 125.4 (2 C, C-3'', C-5''), 115.8 (d, *J* = 22.4 Hz, 2 C, C-3', C-5'), 114.8 (C-3), 106.2 (C-5), 20.3 (CH_3).

HRMS (ESI): for $[C_{17}H_{12}FO_2]^+$ calcd.: 267.0816
found: 267.0810.

$C_{17}H_{13}FO_3$ (284.29 g/mol).

5-Hydroxy-4-phenyl-5-(*p*-tolyl)furan-2(*5H*)-one 271[138]

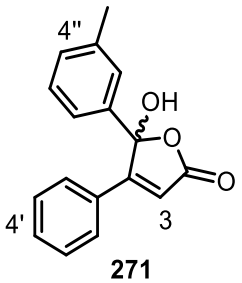

271

Following general procedure 7 saponification and cyclisation were performed by using **247** (45.7 mg, 163 µmol, 1.00 equiv.) and aq. KOH (2 M, 245 µL, 489 µmol, 3.00 equiv.). The desired product **271** (35.9 mg, 135 µmol, 83%) was obtained as colorless oil.

TLC: R_f = 0.43 (PE/EtOAc 2:1 *v/v*).

UV (CH_2Cl_2): λ_{max} (nm) = 280.

IR (ATR): 1718, 1604, 1508, 1256, 1228, 1165, 957, 877, 848, 789, 736, 699, 685, 581cm^{-1}.

^{1}H-NMR (400 MHz, acetone-d_6): δ (ppm) = 7.77–7.72 (m, 2 H, 2'-H, 6'-H), 7.49 (s, 1 H, 2''-H), 7.46 (d, *J* = 7.5 Hz,1 H, 6''-H) ,7.42–7.35 (m, 3 H, 4'-H, 5'-H, 6'-H), 7.28 (t, *J* = 7.5 Hz, 1 H, 5''-H), 7.21 (d, *J* = 7.5 Hz, 1 H, 4''-H), 6.73 (s, 1 H, 3-H), 2.32 (s, 3 H, -CH_3).

^{13}C-NMR (151 MHz, acetone-d_6): δ (ppm) = 170.7 (C-2), 164.9 (C-4), 138.8 (C-3''), 138.5 (C-1''), 131.8 (C-4'), 130.4 (C-4''), 129.5 (C-1'), 129.4 (2 C, C-2', C-6'), 129.3 (C-5''), 129.2 (2 C, C-3', C-5'), 126.5 (C-2''), 123.2 (C-6''), 115.7 (C-3), 106.9 (C-5), 21.2 (CH_3).

HRMS (ESI): for $[C_{17}H_{13}O_2]^+$ calcd.: 249.0909
found: 249.0909.

$C_{17}H_{14}O_3$ (266.30 g/mol).

5-Hydroxy-4-(4-methoxyphenyl)-5-(*p*-tolyl)furan-2(*5H*)-one 272[138]

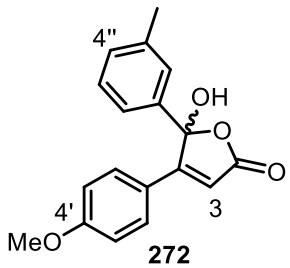

272

Following general procedure 7 saponification and cyclisation were performed by using **248** (75.0 mg, 242 µmol, 1.00 equiv.) and aq. KOH (2 M, 363 µL, 726 µmol, 3.00 equiv.). The desired product **272** (54.5 mg, 184 µmol, 76%) was obtained as yellow oil.

TLC: R_f = 0.38 (PE/EtOAc 2:1 *v/v*).

Mp: 215 °C

UV (CH_2Cl_2): λ_{max} (nm) = 230, 314.

IR (ATR): 1734, 1603, 1512, 1263, 1230, 1174, 1022, 953, 829, 791, 740, 677, 588 cm^{-1}.

^{1}H-NMR (400 MHz, acetone-d_6): δ (ppm) = 7.70 (d, *J* = 9.0 Hz, 2 H, 2'-H, 6'-H), 7.46 (s, 1 H, 2''-H), 7.44 (d, *J* = 7.5 Hz, 1 H, 6''-H), 7.28 (t, *J* = 7.5 Hz, 1 H, 5''-H), 7.19 (d, *J* = 7.5 Hz, 1 H, 4''-H), 6.91 (d, *J* = 9.0 Hz, 2 H, 3'-H, 5'-H), 6.59 (s, 1 H, 3-H), 3.80 (s, 3 H, -OCH_3), 2.32 (s, 3 H, -CH_3).

^{13}C-NMR (151 MHz, acetone-d_6): δ (ppm) = 171.2 (C-2), 165.7 (C-4), 162.6 (C-4'), 139.3 (C-1''), 139.1 (C-3''), 131.6 (2 C, C-2', C-6'), 130.8 (C-4''), 129.5 (C-5''), 126.9 (C-2''), 123.6 (C-6''), 122.5 (C-1''), 115.0 (2 C, C-3', C-5'), 113.5 (C-3), 100.9 (C-5), 55.9 (-OCH_3), 21.6 (-CH_3).

HRMS (ESI): for $[C_{18}H_{15}O_3]^+$ calcd.: 279.1016
found: 279.1005.

$C_{18}H_{16}O_4$ (296.32 g/mol).

4-(4-Fluorophenyl)-5-hydroxy-5-(*p*-tolyl)furan-2(*5H*)-one 273[138]

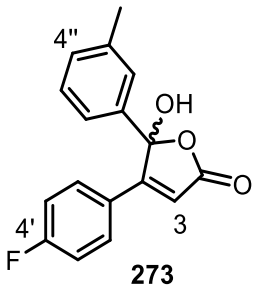

273

Following general procedure 7 saponification and cyclisation were performed by using **249** (60.4 mg, 202 µmol, 1.00 equiv.) and aq. KOH (2 M, 304 µL, 607 µmol, 3.00 equiv.). The desired product **273** (27.4 mg, 96.4 µmol, 48%) was obtained as yellow oil.

TLC: R_f = 0.44 (PE/EtOAc 2:1 *v/v*).

Mp: 117 °C

UV (CH_2Cl_2): λ_{max} (nm) = 278.

IR (ATR): 1712, 1615, 1271, 1183, 959, 856, 841, 797, 771, 731, 684, 647, 559, 517 cm^{-1}.

^{1}H-NMR (400 MHz, acetone-d_6): δ (ppm) = 7.78 (dd, *J* = 9.0, 5.4 Hz, 2 H, 2'-H, 6'-H), 7.44 (s, 1 H, 2''-H), 7.41 (d, *J* = 7.5 Hz, 1 H, 6''-H), 7.25 (t, *J* = 7.5 Hz, 1 H, 5''-H), 7.17 (d,

J = 7.5 Hz, 1 H, 4''-H), 7.12 (t, *J* = 9.0 Hz, 2 H, 3'-H, 5'-H), 6.68 (s, 1 H, 3-H), 2.28 (s, 3 H, -CH_3).

^{13}C-NMR (101 MHz, acetone-d_6): δ (ppm) = 170.5 (C-2) ,164.4 (d, *J* = 251 Hz, C-4'), 163.2 (C-4), 138.9 (C-3'') ,138.3 (C-1''), 131.9 (d, *J* = 8.6 Hz, 2 C, C-2', C-6'), 130.6 (C-4''), 129.2 (C-5''), 126.6 (C-2''), 126.3 (C-1'), 123.2 (C-6''), 116.5 (d, *J* = 21.9 Hz, 2 C, C-3', C-5'), 115.6 (C-3), 106.5 (C-5), 21.2 (-CH_3).

HRMS (ESI): for $[C_{17}H_{12}FO_2]^+$ calcd.: 267.0816
found: 267.0813.

$C_{17}H_{13}FO_3$ (284.29 g/mol).

5-Hydroxy-4-phenyl-5-(*p*-tolyl)furan-2(*5H*)-one 274[138]

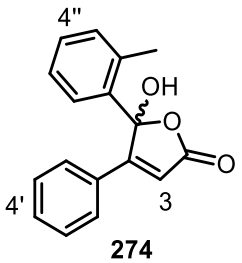

274

Following general procedure 7 saponification and cyclisation were performed by using **250** (35.5 mg, 127 µmol, 1.00 equiv.) and aq. KOH (2 M, 191 µL, 381 µmol, 3.00 equiv.). The desired product **274** (27.5 mg, 103 µmol, 81%) was obtained as yellow oil.

TLC: R_f = 0.43 (PE/EtOAc 2:1 *v/v*).

Mp: 194 °C

UV (CH_2Cl_2): λ_{max} (nm) = 280.

IR (ATR): 1673, 1602, 1448, 1421, 1342, 1282, 1214, 917, 869, 770, 741, 709, 598 cm^{-1}.

^{1}H-NMR (400 MHz, acetone-d_6): δ (ppm) = 7.75–7.66 (m, 3 H, 2'-H, 6'-H, 6''-H), 7.45–7.40, (m, 3 H, 3'-H, 4'-H, 5'-H), 7.35–7.30 (m, 1 H, 4''-H), 7.28–7.23 (m, 1 H, 3''-H), 7.21 (t, *J* = 7.5 Hz, 1 H, 5''-H), 6.69 (s, 1 H, 3-H), 2.54 (s, 3 H, -OCH_3).

^{13}C-NMR (151 MHz, acetone-d_6): δ (ppm) = 171.3 (C-2), 165.5 (C-4), 137.6 (C-1''), 136.5 (C-2''), 133.2 (C-3''), 132.3 (C-4''), 130.5 (C-1'), 130.4 (C-4'), 129.9 (2 C, C-3', C-5'), 129.6 (2 C, C-2', C-6'), 128.6 (C-6''), 127.0 (C-5''), 117.1 (C-3), 107.8 (C-5), 21.1 (-CH_3).

HRMS (ESI): for $[C_{17}H_{13}O_2]^+$ calcd.: 249.0909
found: 249.0910.

$C_{17}H_{14}O_3$ (266.30 g/mol).

5-Hydroxy-4-(4-methoxyphenyl)-5-(*p*-tolyl)furan-2(*5H*)-one 275[138]

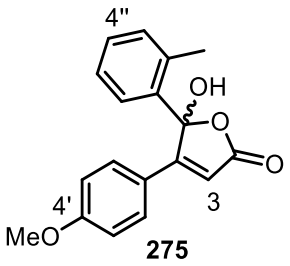

275

Following general procedure 7 saponification and cyclisation were performed by using **251** (106 mg, 342 µmol, 1.00 equiv.) and aq. KOH (2 M, 512 µL, 1.02 mmol, 3.00 equiv.). The desired product **275** (94.2 mg, 318 µmol, 93%) was obtained as yellow oil.

TLC: R_f = 0.30 (PE/EtOAc 2:1 *v/v*).

Mp: 196 °C

UV (CH_2Cl_2): λ_{max} (nm) = 232, 314.

IR (ATR): 1669, 1584, 1516, 1263, 1211, 1191, 1025, 866, 832, 772, 747, 595, 552, 505 cm^{-1}.

^{1}H-NMR (600 MHz, acetone-d_6): δ (ppm) = 7.80–7.59 (m, 3 H, 2'-H, 6'-H, 6''-H), 7.35–7.27 (m, 1 H, 4'-H), 7.25–7.17 (m, 2 H, 3''-H, 5''-H), 6.95 (d, *J* = 8.8 Hz, 2 H, 3'-H, 5'-H), 6.58 (s, 1 H, 3-H), 3.81 (s, 3 H, OCH_3), 2.05 (s, 3 H, CH_3).

^{13}C-NMR (151 MHz, acetone-d_6): δ (ppm) = 171.1 (C-2), 165.0 (C-4), 162.3 (C-4'), 137.2 (C-1''), 136.5 (C-2''), 132.8 (C-3''), 131.2 (2 C, C-2', C-6'), 129.9 (C-4''), 128.1 (C-6''), 126.5 (C-5''), 122.4 (C-1'), 114.6 (2 C, C-3', C-5'), 113.9 (C-3), 107.1 (C-5), 55.5 (OCH_3), 20.8 (CH_3).

HRMS (ESI): for $[C_{18}H_{15}O_3]^+$ calcd.: 279.1016
found: 279.1015.

$C_{18}H_{16}O_4$ (296.32 g/mol).

4-(4-Fluorophenyl)-5-hydroxy-5-(*p*-tolyl)furan-2(*5H*)-one 276[138]

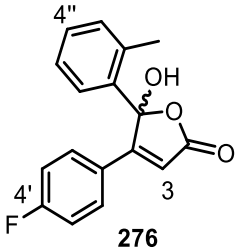

276

Following general procedure 7 saponification and cyclisation were performed by using **252** (62.7 mg, 210 µmol, 1.00 equiv.) and aq. KOH (2 M, 315 µL, 630 µmol, 3.00 equiv.). The desired product **276** (34.7 mg, 122 µmol, 58%) was obtained as yellow oil.

TLC: R_f = 0.38 (PE/EtOAc 2:1 *v/v*).

Mp: 186 °C

UV (CH_2Cl_2): λ_{max} (nm) = 282.

IR (ATR): 1673, 1592, 1507, 1433, 1283, 1245, 1209, 1160, 962, 916, 838, 770, 738, 586 cm^{-1}.

^{1}H-NMR (400 MHz, acetone-d_6): δ (ppm) = 7.81–7.73 (m, 2 H, 2'-H, 6'-H), 7.69 (d, *J* = 7.8 Hz, 1 H, 6''-H), 7.36–7.31 (m, 1 H, 4''-H), 7.25–7.17 (m, 4 H, 3'-H, 5'-H, 3''-H, 5''-H), 6.68 (s, 1 H, 3-H), 2.51 (s, 3 H, CH_3).

^{13}C-NMR (101 MHz, acetone-d_6): δ (ppm) = 170.8 (C-2), 164.5 (d, *J* = 251 Hz, C-4'), 163.9 (C-4), 137. 2 (C-1''), 135.9 (C-2''), 132.9 (C-3''), 131.8 (d, *J* = 8.8 Hz, 2 C, C-2', C-6'), 130.0 (C-6''), 128.2 (C-4''), 126.7 (C-1'), 126.6 (C-5''), 116.6 (d, *J* = 22.4 Hz, 2 C, C-3', C-5'), 116.6 (C-3), 107.6 (C-5), 20.7 (CH_3)

HRMS (ESI): for $[C_{17}H_{12}FO_2]^+$ calcd.: 267.0816
found: 267.0819.

$C_{17}H_{13}FO_3$ (284.29 g/mol).

5-Hydroxy-5-(naphthalen-2-yl)-4-phenylfuran-2(*5H*)-one 277[138]

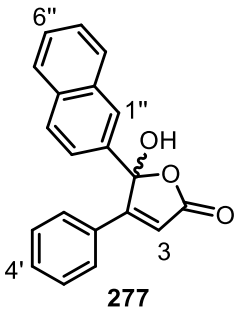

277

Following general procedure 7 saponification and cyclisation were performed by using **253** (18.5 mg, 58.5 µmol, 1.00 equiv.) and aq. KOH (2 M, 88.0 µL, 176 µmol, 3.00 equiv.). The desired product **277** (9.6 mg, 31.6 µmol, 54%) was obtained as colorless oil.

TLC: R_f = 0.23 (PE/EtOAc 1:1 *v/v*).

UV ($CHCl_3$): λ_{max} (nm) = 255, 280.

IR (ATR): 1736, 1618, 1358, 1250, 1217, 1177, 1124, 1023, 986, 939, 859, 819, 770, 757, 684 cm^{-1}.

^{1}H-NMR (600 MHz, acetone-d_6): δ (ppm) = 8.33 (s, 1 H, 1''-H), 8.01–7.96 (m, 1 H, 8''-H); 7.94–7.88 (m, 2 H, 4''-H, 5''-H), 7.82–7.76 (m, 2 H, 2'-H, 6'-H), 7.67 (d, 1 H, J = 8.1 Hz, 3''-H), 7.57–7.52 (m, 2 H, 6''-H, 7''-H), 7.40–7.33 (m, 3 H, 3'-H, 4'-H, 5'-H), 6.80 (s, 1 H, 3-H).

^{13}C NMR (101 MHz, acetone-d_6) δ (ppm) = 170.0 (C-2), 164.2 (C-4), 135.3 (C-2''), 133.2 (C-4a''), 132.8 (C-8a''), 131.1 (C-4'), 128.9 (C-1'), 128.7 (2 C, C-2', C-6'), 128.6 (C-5'',C-8''), 128.4 (2 C, C-3', C-5'), 127.5 (C-4''), 126.9 (C-7''), 126.6 (C-6''), 125.0 (C-1''), 122.8 (C-3''), 115.2 (C-3), 106.2 (C-5).

HRMS (ESI): for $[C_{20}H_{13}O_2]^+$ calcd.: 285.0914
found: 285.0912.

$C_{20}H_{14}O_3$ (302.33 g/mol).

5-Hydroxy-4-(4-methoxyphenyl)-5-(naphthalen-2-yl)furan-2(*5H*)-one 278[138]

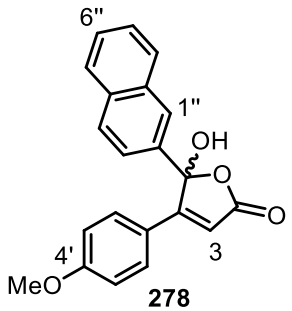

278

Following general procedure 7 saponification and cyclisation were performed by using **254** (58.7 mg, 170 µmol, 1.00 equiv.) and aq. KOH (2 M, 255 µL, 510 µmol, 3.00 equiv.). The desired product **278** (42.5 mg, 128 µmol, 75%) was obtained as colorless oil.

TLC: R_f = 0.27 (PE/EtOAc 1:1 *v/v*).

UV ($CHCl_3$): λ_{max} (nm) = 241, 255, 312.

IR (ATR): 1732, 1600, 1510, 1256, 1219, 1176, 1122, 1024, 938, 861, 833, 755, 735, 588, 542 cm^{-1}.

^{1}H-NMR (600 MHz, acetone-d_6): δ (ppm) = 8.32 (s, 1 H, 1''-H), 8.00–7.95 (m, 1 H, 8''-H); 7.94–7.87 (m, 2 H, 4''-H, 5''-H), 7.75 (d, *J* = 9.0 Hz, 2 H, 2'-H, 6'-H), 7.63 (d, *J* = 8.4 Hz, 1 H, 3''-H), 7.57–7.50 (m, 2 H, 6''-H, 7''-H), 7.40–7.33 (d, *J* = 9.0 Hz, 2 H, 3'-H, 5'-H), 6.67 (s, 1 H, 3-H), 3.75 (s, 3 H, OCH_3).

^{13}C-NMR (101 MHz, acetone-d_6) δ (ppm)= 170.3 (C-2), 164.0 (C-4), 161.6 (C-4'), 135.8 (C-2''), 133.2 (C-4a''), 132.8 (C-8a''), 130.6 (2 C, C-2', C-6'), 128.5 (C-8''), 128.4 (C-5''), 127.6 (C-4''), 126.9 (C-7''), 126.5 (C-6''), 124.9 (C-1''), 122.8 (C-3''), 121.2 (C-1'), 113.9 (2 C, C-3', C-5'), 112.5 (C-3), 106.8 (C-5), 54.7 (OCH_3).

HRMS (ESI): for $[C_{21}H_{15}O_3]^+$ calcd.: 315.1016
found: 315.1007.

$C_{21}H_{16}O_4$ (332.36 g/mol).

4-(4-Fluorophenyl)-5-hydroxy-5-(naphthalen-2-yl)furan-2(*5H*)-one 279[138]

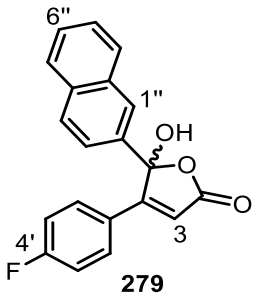

279

Following general procedure 7 saponification and cyclisation were performed by using **255** (25.5 mg, 76.3 µmol, 1.00 equiv.) and aq. KOH (2 M, 115 µL, 229 µmol, 3.00 equiv.). The desired product **279** (18.9 mg, 59.0 µmol, 77%) was obtained as colorless oil.

TLC: R_f = 0.29 (PE/EtOAc 1:1 *v/v*).

UV ($CHCl_3$): λ_{max} (nm) = 255, 281.

IR (ATR): 1737, 1600, 1508, 1178, 1162, 1125, 1027, 939, 878, 864, 838, 818, 755, 736, 578 cm^{-1}.

^{1}H-NMR (600 MHz, acetone-d_6): δ (ppm) = 8.32 (s, 1 H, 1''-H), 8.01–7.96 (m, 1 H, 8''-H); 7.94–7.89 (m, 2 H, 4''-H, 5''-H), 7.86 (dd, *J* = 9.0, 5.4 Hz, 2 H, 2'-H, 6'-H), 7.64 (d, *J* = 8.4 Hz, 1 H, 3''-H), 7.57–7.52 (m, 2 H, 6''-H, 7''-H), 7.13 (t, *J* = 9.0 Hz, 2 H, 3'-H, 5'-H), 6.67 (s, 1 H, 3-H).

^{13}C-NMR (101 MHz, acetone-d_6) δ (ppm) = 170.0 (C-2), 163.8 (d, *J* = 251 Hz, C-4'), 163.0 (C-4), 135.1 (C-2''), 133.2 (C-4a''), 132.8 (C-8a''), 131.2 (d, *J* = 8.4 Hz, 2 C, C-2', C-6'), 128.5 (C-8''), 128.4 (C-5''), 127.5 (C-4''), 126.9 (C-7''), 126.6 (C-6''), 125.5 (d, *J* = 3.1 Hz, C-1'), 125.1 (C-1''), 122.7 (C-3''), 115.8 (d, *J* = 22.0 Hz, 2 C, C-3', C-5'), 115.6 (C-3), 106.6 (C-5).

HRMS (ESI): for $[C_{20}H_{12}FO_2]^+$ calcd.: 303.0816
found: 303.0827.

$C_{20}H_{13}FO_3$ (320.22 g/mol).

7. Appendix

7.1. Crystal structures

Crystal structure of 117

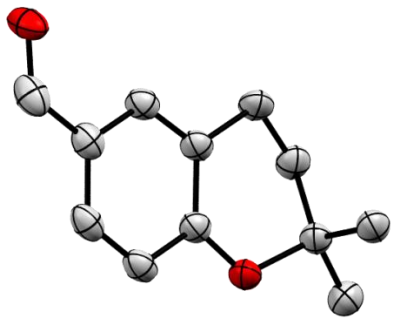

Figure 43: X-ray single crystal structure of **117**. Thermal ellipsoids are shown at 50% probability level. Hydrogen atoms are not shown for clarity)

Compound	**117**	*Z*	4
		Wavelength/Å	1.54184
Formula	$C_{12}H_{14}O_2$	Radiation type	CuKα
$D_{calc.}$/ g cm^{-3}	1.220	Θ_{min}/°	9.56
μ/mm^{-1}	0.655	Θ_{max}/°	154.8
Formula Weight	190.23	Measured Refl.	17746
Colour	colorless	Independent Refl.	2166
Shape	Block	Reflections Used	15580
Size/mm^3	0.28 × 0.15 × 0.10	R_{int}	0.0494
T/K	100(2)	Parameters	134
Crystal System	Monoclinic	Restraints	4
Space Group	$P2_1/n$	Largest Peak	0.66
a/Å	6.0513(3)	Deepest Hole	-0.21
b/Å	13.1405(8)	GooF	1.071
c/Å	13.1792(7)	wR_2 (all data)	0.1619
α/°	90	wR_2	0.1548
β/°	98.733(5)	R_1 (all data)	0.0624
γ/°	90	R_1	0.0582
V/Å^3	1035.82(10)		

These data are deposited at the Cambridge Crystallographic Data Centre and can be obtained via www.ccdc.cam.ac.uk/data_requested /cif (CCDC 1879231).

Crystal structure of 161

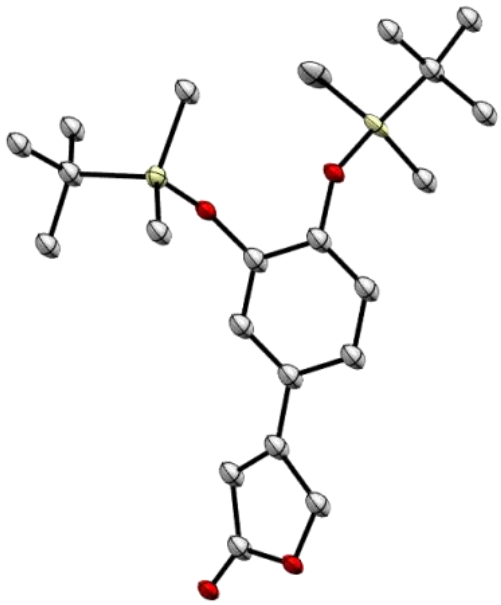

Figure 44: X-ray single crystal structure of **161**. Thermal ellipsoids are shown at 50% probability level. Hydrogen atoms are not shown for clarity).

Compound	**161**	*Z*	10
Formula	$C_{17.6}H_{29.2}O_{3.2}Si_{1.6}$	Wavelength/Å	1.54184
$D_{calc.}$/ g cm^{-3}	1.143	Radiation type	CuK_α
μ/mm^{-1}	1.497	Θ_{min}/°	6.99
Formula Weight	336.95	Θ_{max}/°	69.992
Colour	colorless	Measured Refl.	14665
Shape	plate	Independent Refl.	4232
Size/mm^3	0.22×0.15×0.08	Reflections with I > 2(I)	3795
T/K	293(1)	R_{int}	0.0675
Crystal System	triclinic	Parameters	437
Space Group	*P*-1	Restraints	0
a/Å	13.9071(8)	Largest Peak	0.41
b/Å	11.8476(6)	Deepest Hole	-0.41
c/Å	29.6999(19)	GooF	1.052
α/°	90	wR_2 (all data)	0.1809
β/°	90.631(6)	wR_2	0.1719
γ/°	90	R_1 (all data)	0.0884
V/Å^3	4893.2(5)	R_1	0.0755

Crystal structure of 12

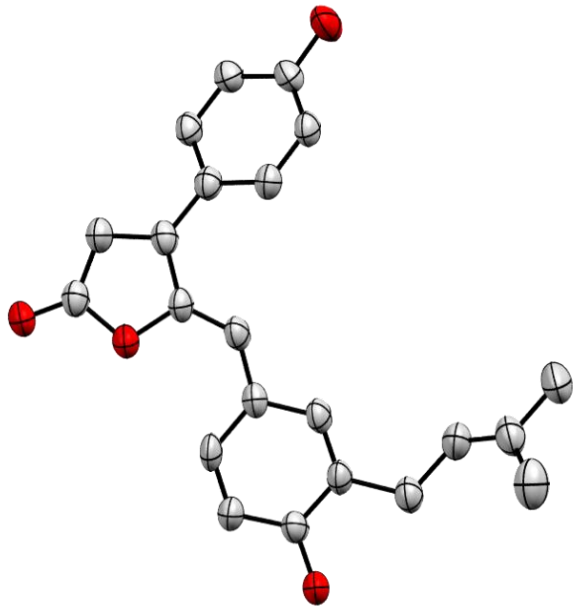

Figure 45 X-ray single crystal structure of **12**. Thermal ellipsoids are shown at 50% probability level. Hydrogen atoms are not shown for clarity)

Compound	**12**	*Z*	4
		Z'	2
Formula	$C_{22}H_{21}O_{4.5}$	Wavelength/Å	1.54184
$D_{calc.}$/ g cm^{-3}	1.335	Radiation type	CuK_α
μ/mm^{-1}	0.756	Θ_{min}/°	3.336
Formula Weight	357.39	Θ_{max}/°	62.971
Colour	yellow	Measured Refl.	20743
Shape	plate	Independent Refl.	5587
Size/mm^3	0.30×0.28×0.10	Reflections with I > 2(I)	2733
T/K	99.97(10)	R_{int}	0.0927
Crystal System	triclinic	Parameters	489
Space Group	*P*-1	Restraints	0
a/Å	9.3494(12)	Largest Peak	0.352
b/Å	13.283(2)	Deepest Hole	-0.258
c/Å	14.3527(11)	GooF	1.003
α/°	85.790(10)	wR_2 (all data)	0.2710
β/°	89.724(8)	wR_2	0.2096
γ/°	89.677(13)	R_1 (all data)	0.1635
V/Å^3	1777.5(4)	R_1	0.0842

These data are deposited at the Cambridge Crystallographic Data Centre and can be obtained via www.ccdc.cam.ac.uk/data_requested /cif (CCDC 1879226).

Crystal structure of 13

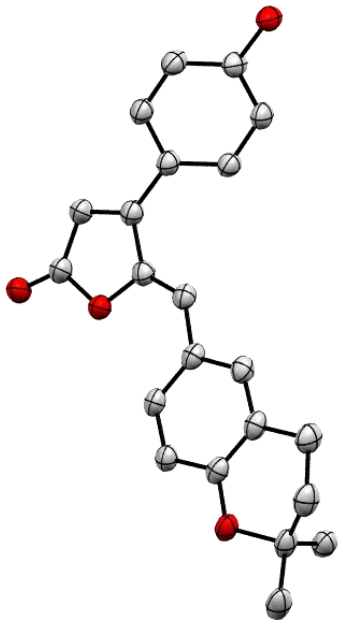

Figure 46: X-ray single crystal structure of **13**. Thermal ellipsoids are shown at 50% probability level. Hydrogen atoms are not shown for clarity)

Compound	**13**	*Z'*	1
Formula	$C_{22}H_{20}O_4$	Wavelength/Å	1.54184
$D_{calc.}$/ g cm^{-3}	1.332	Radiation type	CuK_α
μ/mm^{-1}	0.738	Θ_{min}/°	3.691
Formula Weight	348.38	Θ_{max}/°	76.722
Colour	clear yellow	Measured Refl.	49936
Shape	block	Independent Refl.	3615
Size/mm^3	0.20×0.12×0.10	Reflections Used	3230
T/K	100	R_{int}	0.0503
Crystal System	monoclinic	Parameters	238
Space Group	$P2_1/c$	Restraints	0
a/Å	12.19278(18)	Largest Peak	0.206
b/Å	17.7030(3)	Deepest Hole	-0.204
c/Å	8.19280(18)	GooF	1.055
α/°	90.0	wR_2 (all data)	0.1041
β/°	100.8077(18)	wR_2	0.1002
γ/°	90.0	R_1 (all data)	0.0535
V/Å^3	1737.04(5)	R_1	0.0475
Z	4		

These data are deposited at the Cambridge Crystallographic Data Centre and can be obtained via www.ccdc.cam.ac.uk/data_requested /cif (CCDC 1530345).

Crystal structure of 174

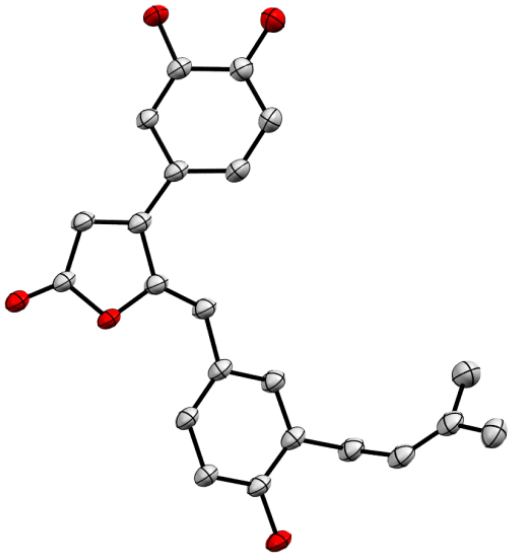

Figure 47: X-ray single crystal structure of **174**. Thermal ellipsoids are shown at 50% probability level. Hydrogen atoms are not shown for clarity)

Compound	**174**	*Z*	8
		Z'	2
Formula	$C_{22}H_{20}O_5$	Wavelength/Å	1.54184
$D_{calc.}$/ g cm^{-3}	1.323	Radiation type	CuK_α
μ/mm^{-1}	0.768	Θ_{min}/°	4.481
Formula Weight	364.38	Θ_{max}/°	77.334
Colour	orange	Measured Refl.	76726
Shape	plate	Independent Refl.	7667
Size/mm^3	0.24×0.15×0.03	Reflections Used	6092
T/K	99.97(12)	R_{int}	0.0727
Crystal System	monoclinic	Parameters	508
Space Group	$P2_1/c$	Restraints	0
a/Å	14.3885(5)	Largest Peak	0.351
b/Å	9.6575(3)	Deepest Hole	-0.331
c/Å	26.3454(8)	GooF	1.041
α/°	90	wR_2 (all data)	0.1516
β/°	91.803(3)	wR_2	0.1355
γ/°	90	R_1 (all data)	0.0655
V/Å^3	3659.1(2)	R_1	0.0510

These data are deposited at the Cambridge Crystallographic Data Centre and can be obtained via www.ccdc.cam.ac.uk/data_requested /cif (CCDC 1879229).

Crystal structure of 175

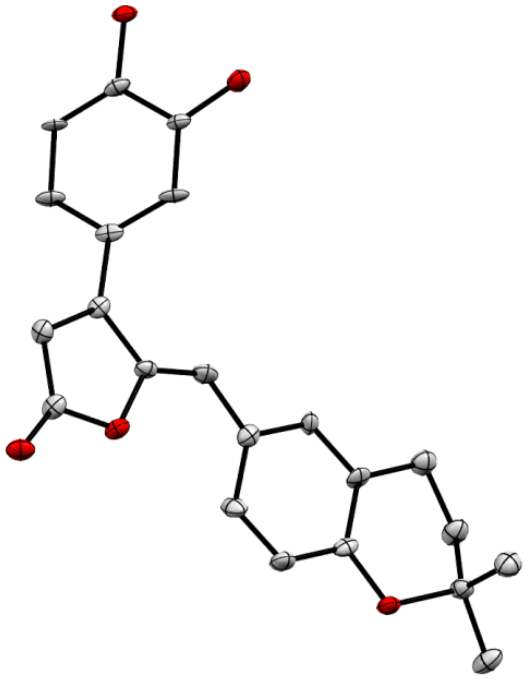

Figure 48: X-ray single crystal structure of **175**. Thermal ellipsoids are shown at 50% probability level. Hydrogen atoms are not shown for clarity)

Compound	**175**	*Z*	8
		Wavelength/Å	1.54184
Formula	$C_{23}H_{24}O_6$	Radiation type	CuK_α
$D_{calc.}$/ g cm^{-3}	1.401	Θ_{min}/°	6.95
μ/mm^{-1}	0.768	Θ_{max}/°	76.753
Formula Weight	396.42	Measured Refl.	77811
Colour	yellow	Independent Refl.	15609
Shape	needle	Reflections Used	14540
Size/mm^3	0.28×0.02×0.032	R_{int}	0.0727
T/K	99.9(3)	Parameters	1069
Crystal System	Triclinic	Restraints	0
Space Group	*P*-1	Largest Peak	0.46
a/Å	13.4626 (6)	Deepest Hole	-0.45
b/Å	15.5829 (5)	GooF	1.080
c/Å	18.9629 (5)	wR_2 (all data)	0.3333
α/°	89.951 (3)	wR_2	0. 2873
β/°	81.223(3)	R_1 (all data)	0.1856
γ/°	73.139 (4)	R_1	0.1082
V/Å^3	3758.6(2)		

Crystal structure of 178

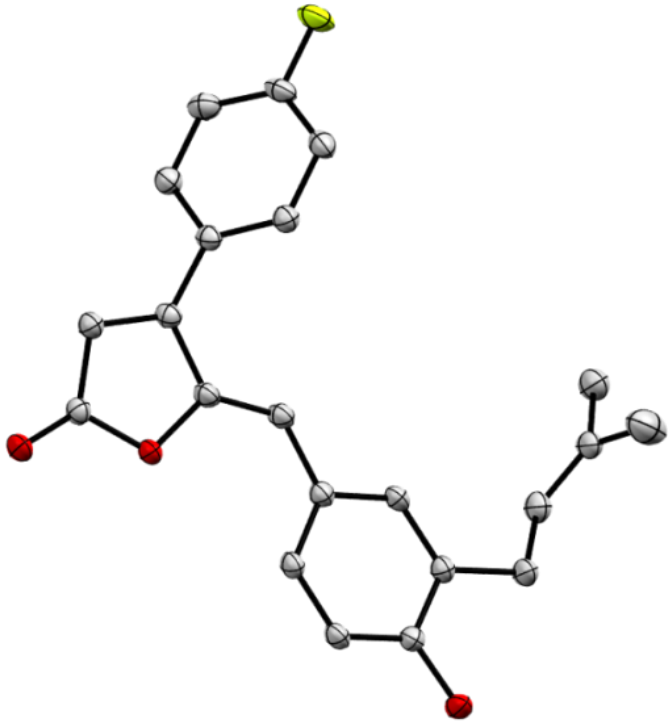

Figure 49: X-ray single crystal structure of MS-FRS **178**. Thermal ellipsoids are shown at 50% probability level. Hydrogen atoms are not shown for clarity)

Compound	**178**	*Z*	2
		Z'	1
Formula	$C_{22}H_{19}FO_3$	Wavelength/Å	1.54184
$D_{calc.}$/ g cm^{-3}	1.3437	Radiation type	Cu K_α
μ/mm^{-1}	0.785	Θ_{min}/°	3.89
Formula Weight	350.39	Θ_{max}/°	76.37
Colour	yellow	Measured Refl.	14523
Shape	plate	Independent Refl.	3583
Size/mm^3	0.24×0.05×0.02	Reflections Used	3279
T/K	100.4(7)	R_{int}	0.0219
Crystal System	triclinic	Parameters	238
Space Group	*P*-1	Restraints	0
a/Å	7.4466(4)	Largest Peak	0.4939
b/Å	10.2453(6)	Deepest Hole	-0.2942
c/Å	12.1572(7)	GooF	1.0595
α/°	74.094(5)	wR_2 (all data)	0.1120
β/°	76.154(5)	wR_2	0.1079
γ/°	87.078(5)	R_1 (all data)	0.0450
V/Å^3	865.97(9)	R_1	0.0415

These data are deposited at the Cambridge Crystallographic Data Centre and can be obtained via www.ccdc.cam.ac.uk/data_requested /cif (CCDC 1879230).

Crystal structure of 179

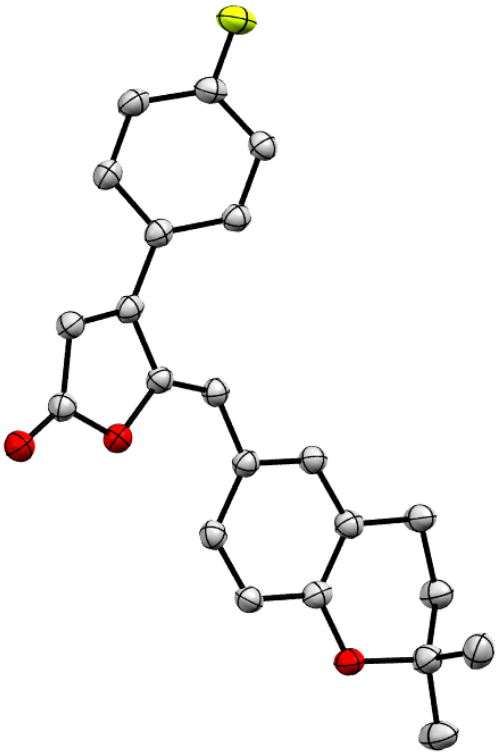

Figure 50: X-ray single crystal structure of **179**. Thermal ellipsoids are shown at 50% probability level. Hydrogen atoms are not shown) for clarity

Compound	**179**	*Z*	12
Formula	$C_{29.33}H_{25.33}F_{1.33}O_4$	Wavelength/Å	1.54184
$D_{calc.}$/ g cm^{-3}	1.335	Radiation type	Cu K_α
μ/mm^{-1}	0.780	Θ_{min}/°	7.038
Formula Weight	467.16	Θ_{max}/°	77.141
Colour	yellow	Measured Refl.	168500
Shape	plate	Independent Refl.	14599
Size/mm^3	0.32×0.22×0.05	Reflections Used	13653
T/K	99.98(11)	R_{int}	0.0884
Crystal System	monoclinic	Parameters	946
Space Group	$P112_1/a$	Restraints	0
a/Å	7.83085(13)	Largest Peak	0.25
b/Å	32.7280(5)	Deepest Hole	-0.48
c/Å	27.2050(4)	GooF	1.078
α/°	90	wR_2 (all data)	0.1515
β/°	90	wR_2	0.1442
γ/°	90	R_1 (all data)	0.0581
V/Å^3	6972.31(19)	R_1	0.0526

These data are deposited at The Cambridge Crystallographic Data Centre and can be obtained via www.ccdc.cam.ac.uk/data_request/cif (CCDC 1915475).

Crystal structure of 190

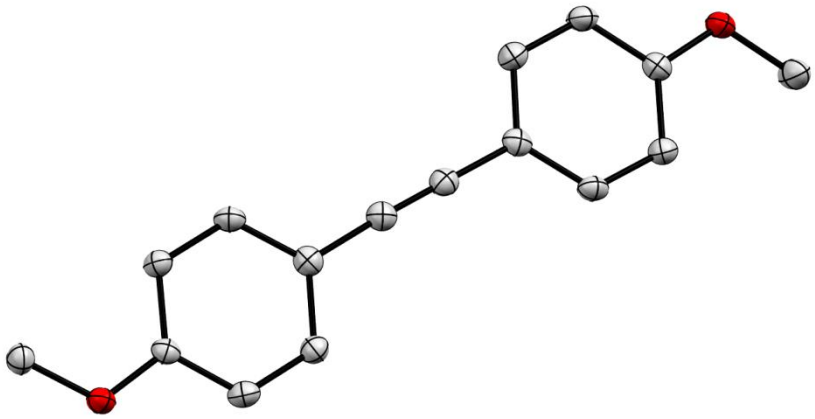

Figure 51: X-ray single crystal structure of **190**. Thermal ellipsoids are shown at 50% probability level. (Hydrogen atoms are not shown for clarity).

Compound	**190**	*Z*	2
Formula	$C_{32}H_{32}O_4$	Wavelength/Å	1.54184
$D_{calc.}$/ g cm^{-3}	1.248	Radiation type	CuK_a
μ/mm^{-1}	0.643	Θ_{min}/°	7.92
Formula Weight	480.57	Θ_{max}/°	152.51
Color	colorless	Measured Refl.	28919
Shape	block	Independent Refl.	5293
Size/mm^3	0.12×012×0.15	Reflections with I > 2(I)	4964
T/K	100K	R_{int}	0.0293
Crystal System	Monoclinic	Parameters	392
Space Group	$P2_1$	Restraints	1
a/Å	11.31512(11)	Largest Peak	0.24
b/Å	7.40726(5)	Deepest Hole	-0.56
c/Å	15.46629(12)	GooF	1.224
α/°	90	wR_2 (all data)	0.1295
β/°	99.99.4280(8)	wR_2	0.1285
γ/°	90	R_1 (all data)	0.0373
V/Å^3	1278.782(18)	R_1	0.0365

Crystal structure of 210

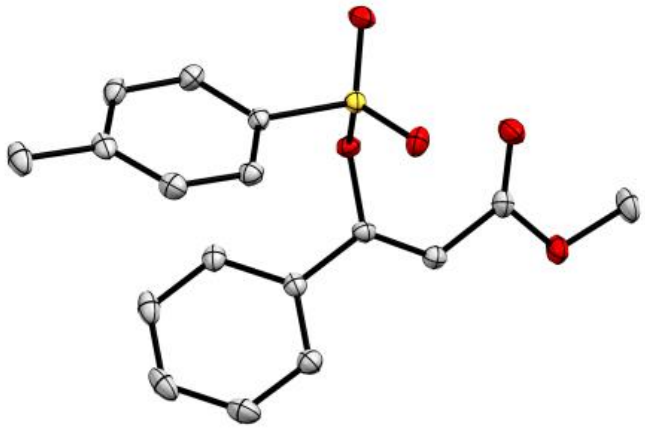

Figure 52: X-ray single crystal structure of **210**. Thermal ellipsoids are shown at 50% probability level. (Hydrogen atoms are not shown for clarity).

Compound	**210**	*Z'*	1
Formula	$C_{17}H_{16}O_5S$	Wavelength/Å	1.54184
$D_{calc.}$/ g cm^{-3}	1.424	Radiation type	CuK_α
μ/mm^{-1}	2.071	Θ_{min}/°	4.624
Formula Weight	332.36	Θ_{max}/°	76.455
Color	clear colorless	Measured Refl.	29048
Shape	plate	Independent Refl.	3234
Size/mm^3	0.24×0.22×0.10	Reflections with I > 2(I)	3204
T/K	99.97(13)	R_{int}	0.0225
Crystal System	triclinic	Parameters	210
Space Group	*P*-1	Restraints	0
*a*α/Å	8.2907(3)	Largest Peak	0.352
b/Å	9.8538(3)	Deepest Hole	-0.587
c/Å	9.8676(2)	GooF	1.039
α/°	84.679(2)	wR_2 (all data)	0.0801
β/°	82.236(2)	wR_2	0.0800
γ/°	76.532(3)	R_1 (all data)	0.0295
V/Å^3	775.21(4)	R_1	0.0294

These data are deposited at The Cambridge Crystallographic Data Centre and can be obtained via www.ccdc.cam.ac.uk/data_request/cif (CCDC 1879218).

Crystal structure of 211

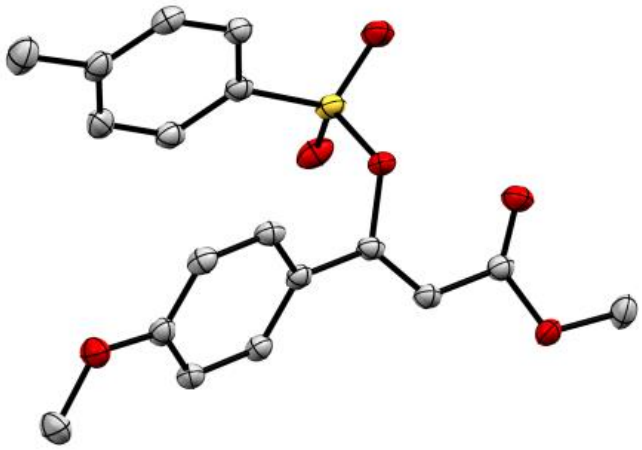

Figure 53: X-ray single crystal structure of **211**. Thermal ellipsoids are shown at 50% probability level. (Hydrogen atoms are not shown for clarity).

Compound	**211**	*Z*	2
Formula	$C_{18}H_{18}O_6S$	*Z'*	1
$D_{calc.}$/ g cm^{-3}	1.347	Wavelength/Å	1.54184
μ/mm^{-1}	1.886	Radiation type	CuK_α
Formula Weight	362.38	Θ_{min}/°	3.924
Color	clear colorless	Θ_{max}/°	76.469
Shape	plate	Measured Refl.	16071
Size/mm^3	0.28×0.20×0.03	Independent Refl.	3703
T/K	100.1(3)	Reflections with I > 2(I)	3350
Crystal System	triclinic	R_{int}	0.0348
Flack Parameter	*P*-1	Parameters	229
Hooft Parameter	7.0545(3)	Restraints	0
Space Group	11.2620(5)	Largest Peak	0.269
/Å	11.8291(5)	Deepest Hole	-0.429
/Å	73.461(4)	GooF	1.045
c/Å	82.726(3)	wR_2 (all data)	0.1047
α/°	86.534(3)	wR_2	0.0999
β/°	893.37(7)	R_1 (all data)	0.0415
γ/°	86.534(3)	R_1	0.0373
V/Å^3	893.37(7)		

These data are deposited at The Cambridge Crystallographic Data Centre and can be obtained via www.ccdc.cam.ac.uk/data_request/cif (CCDC 1879218).

Crystal structure of 212

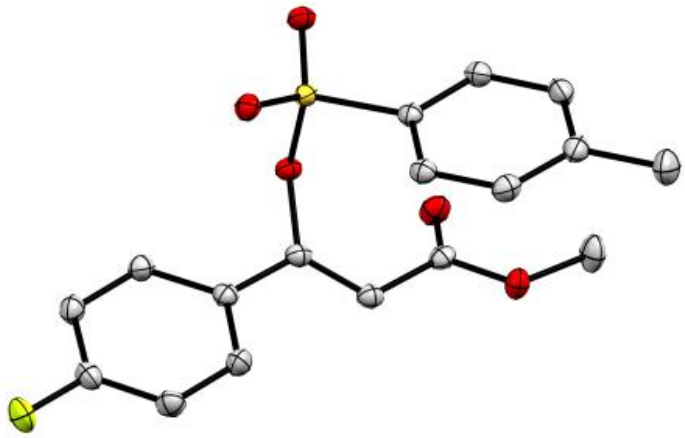

Figure 54: X-ray single crystal structure of **212**. Thermal ellipsoids are shown at 50% probability level. (Hydrogen atoms are not shown for clarity).

Compound	**212**	*Z'*	1
Formula	$C_{17}H_{15}FO_5S$	Wavelength/Å	1.54184
$D_{calc.}$/ g cm^{-3}	1.489	Radiation type	CuK_a
μ/mm^{-1}	2.182	Θ_{min}/°	3.780
Formula Weight	350.35	Θ_{max}/°	76.561
Color	colorless	Measured Refl.	28881
Shape	block	Independent Refl.	3262
Size/mm^3	0.30×0.28×0.20	Reflections with I > 2(I)	3137
T/K	100.01(10)	R_{int}	0.0276
Crystal System	monoclinic	Parameters	219
Space Group	$P2_1/n$	Restraints	0
a/Å	13.14250(10)	Largest Peak	0.342
b/Å	7.24870(10)	Deepest Hole	-0.411
c/Å	17.0728(2)	GooF	1.051
α/°	90	wR_2 (all data)	0.0847
β/°	106.0900(10)	wR_2	0.0839
γ/°	90	R_1 (all data)	0.0311
V/Å^3	1562.75(3)	R_1	0.0302
Z	4		

These data are deposited at The Cambridge Crystallographic Data Centre and can be obtained via www.ccdc.cam.ac.uk/data_request/cif (CCDC 1879221).

Crystal structure of 244

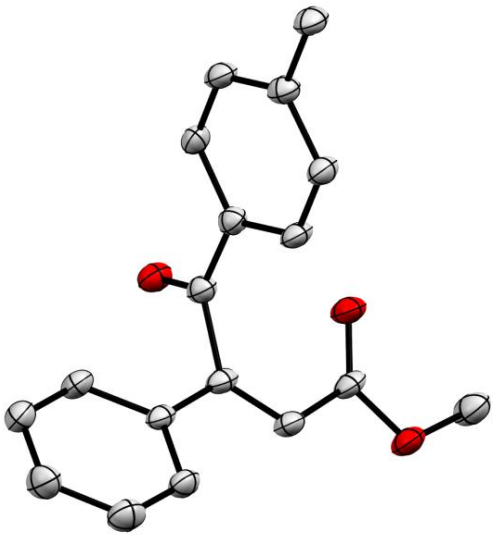

Figure 55: X-ray single crystal structure of **244**. Thermal ellipsoids are shown at 50% probability level. (Hydrogen atoms are not shown for clarity).

Compound	244	*Z*	8
Formula	$C_{36}H_{32}O_6$	*Z'*	0.5
$D_{calc.}$/ g cm^{-3}	1.286	Wavelength/Å	1.54184
μ/mm^{-1}	0.702	Radiation type	CuK_a
Formula Weight	560.61	Θ_{min}/°	4.983
Color	clear colorless	Θ_{max}/°	86.334
Shape	plate	Measured Refl.	29776
Size/mm^3	0.20×0.08×0.04	Independent Refl.	3069
T/K	99.9(2)	Reflections with I > 2(I)	2947
Crystal System	orthorhombic	R_{int}	0.1120
Flack Parameter	-0.20(11)	Parameters	192
Hooft Parameter	-0.14(7)	Restraints	1
Space Group	*Fdd*2	Largest Peak	0.559
a/Å	35.5043(8)	Deepest Hole	-0.470
b/Å	20.3635(5)	GooF	1.082
c/Å	8.0122(2)	wR_2 (all data)	0.2160
α/°	90	wR_2	0.2042
β/°	90	R_1 (all data)	0.0793
γ/°	90	R_1	0.0756
V/Å^3	5792.8(2)		

These data are deposited at The Cambridge Crystallographic Data Centre and can be obtained via www.ccdc.cam.ac.uk/data_request/cif (CCDC 1879217).

Crystal structure of 242

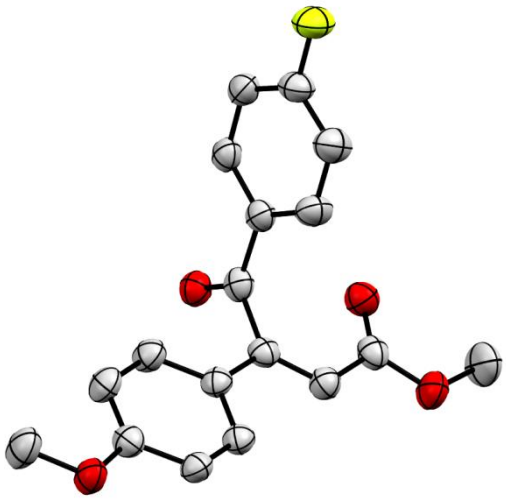

Figure 56: X-ray single crystal structure of **242**. Thermal ellipsoids are shown at 50% probability level. (Hydrogen atoms are not shown for clarity).

Compound	**242**	*Z*	4
Formula	$C_{72}H_{61}F_4O_{16}$	Wavelength/Å	1.54184
$D_{calc.}$/ g cm^{-3}	1.368	Radiation type	CuKα
μ/mm^{-1}	0.875	Θ_{min}/°	6.392
Formula Weight	1258.20	Θ_{max}/°	145.652
Color	colorless	Measured Refl.	97745
Shape	needle	Independent Refl.	11798
Size/mm^3	0.02x0.02x0.32	Reflections with I > 2(I)	11798
T/K	100 K	R_{int}	0.1238
Crystal System	Monoclinic	Parameters	837
Space Group	$P2_1/n$	Restraints	0
a/Å	14.5430(5)	Largest Peak	0.38
b/Å	17.6544(5)	Deepest Hole	-0.32
c/Å	24.7504(10)	GooF	1.034
α/°	90	wR_2 (all data)	0.2355
β/°	105.929(4)	wR_2	0.2105
γ/°	90	R_1 (all data)	0.1109
V/Å^3	6110.6(4)	R_1	0.0788

Crystal structure of the open tautomer of 260

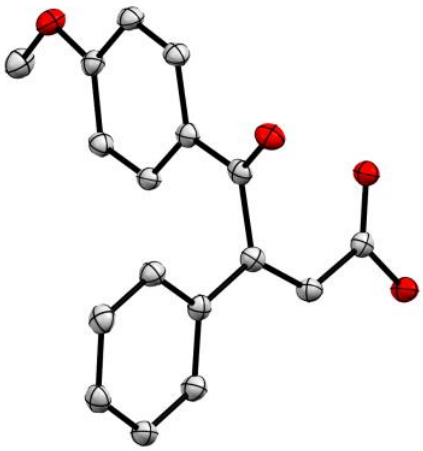

Figure 57: X-ray single crystal structure of the open tautomer of **260**. Thermal ellipsoids are shown at 50% probability level. (Hydrogen atoms are not shown for clarity).

Compound	**260**	*Z*	2
Formula	$C_{17}H_{14}O_4$	Wavelength/Å	1.54184
$D_{calc.}$/ g cm^{-3}	1.408	Radiation type	CuK_a
μ/mm^{-1}	0.827	Θ_{min}/°	5.109
Formula Weight	282.28	Θ_{max}/°	75.938
Color	colorless	Measured Refl.	11185
Shape	block	Independent Refl.	2750
Size/mm^3	0.2×0.12×0.08	Reflections with I > 2(I)	2544
T/K	99.97(11)	R_{int}	0.0203
Crystal System	triclinic	Parameters	192
Space Group	*P-1*	Restraints	0
a/Å	8.6273(6)	Largest Peak	0.24
b/Å	9.1807(6)	Deepest Hole	-0.23
c/Å	9.5517(7)	GooF	1.036
α/°	71.136(7)	wR_2 (all data)	0.0938
β/°	70.021(7)	wR_2	0.0977
γ/°	76.095(6)	R_1 (all data)	0.0365
V/Å^3	665.61(9)	R_1	0.0756

These data are deposited at The Cambridge Crystallographic Data Centre and can be obtained via www.ccdc.cam.ac.uk/data_request/cif (CCDC 1884165).

7.2. NMR Spectra

5-Oxo-2,5-dihydrofuran-3-yl trifluoromethanesulfonate 118

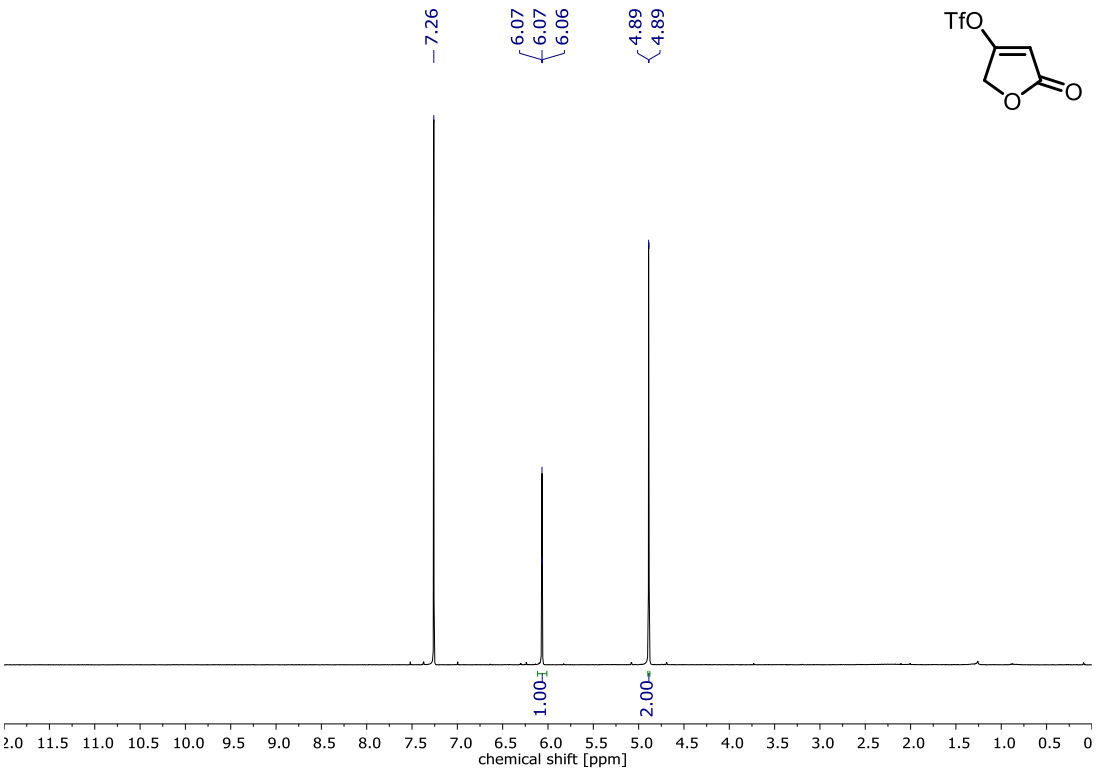

Figure 58: ^{1}H-NMR spectrum (400 MHz, $CDCl_3$-*d,* 300 K) of triflate **118**.

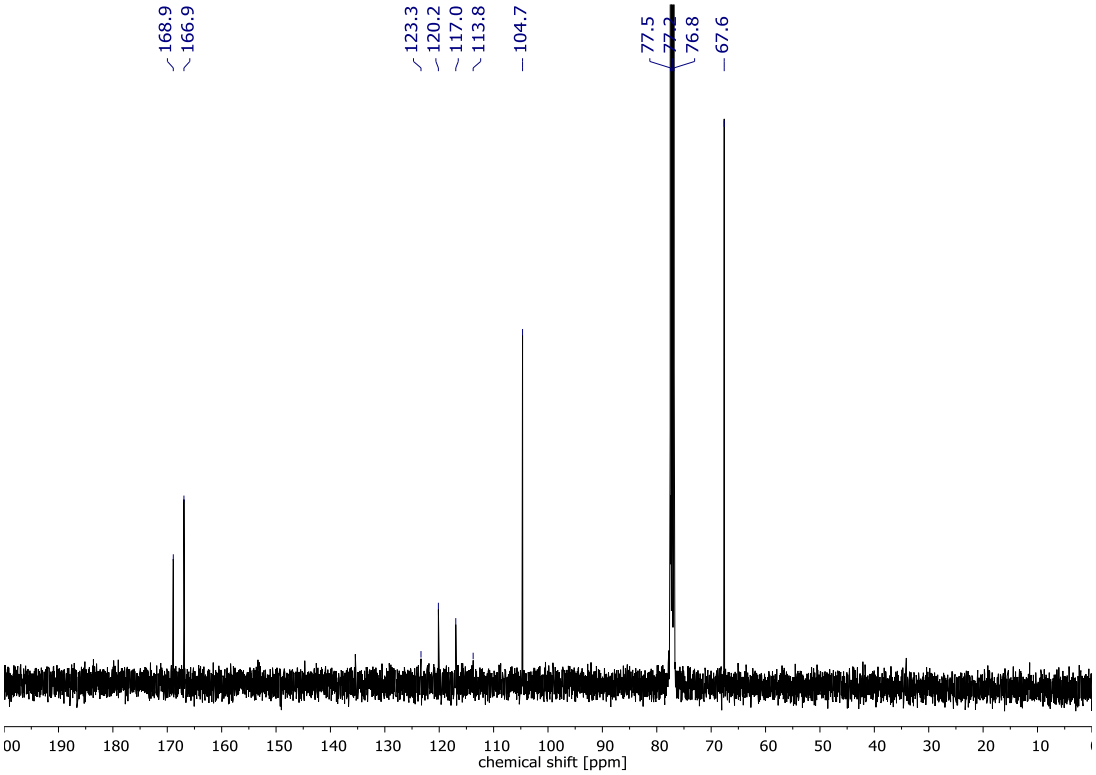

Figure 59: ^{13}C-NMR spectrum (101 MHz, $CDCl_3$-*d*, 298 K) of triflate **188**.

5-Oxo-2,5-dihydrofuran-3-yl-trifluoromethanesulfonate 34

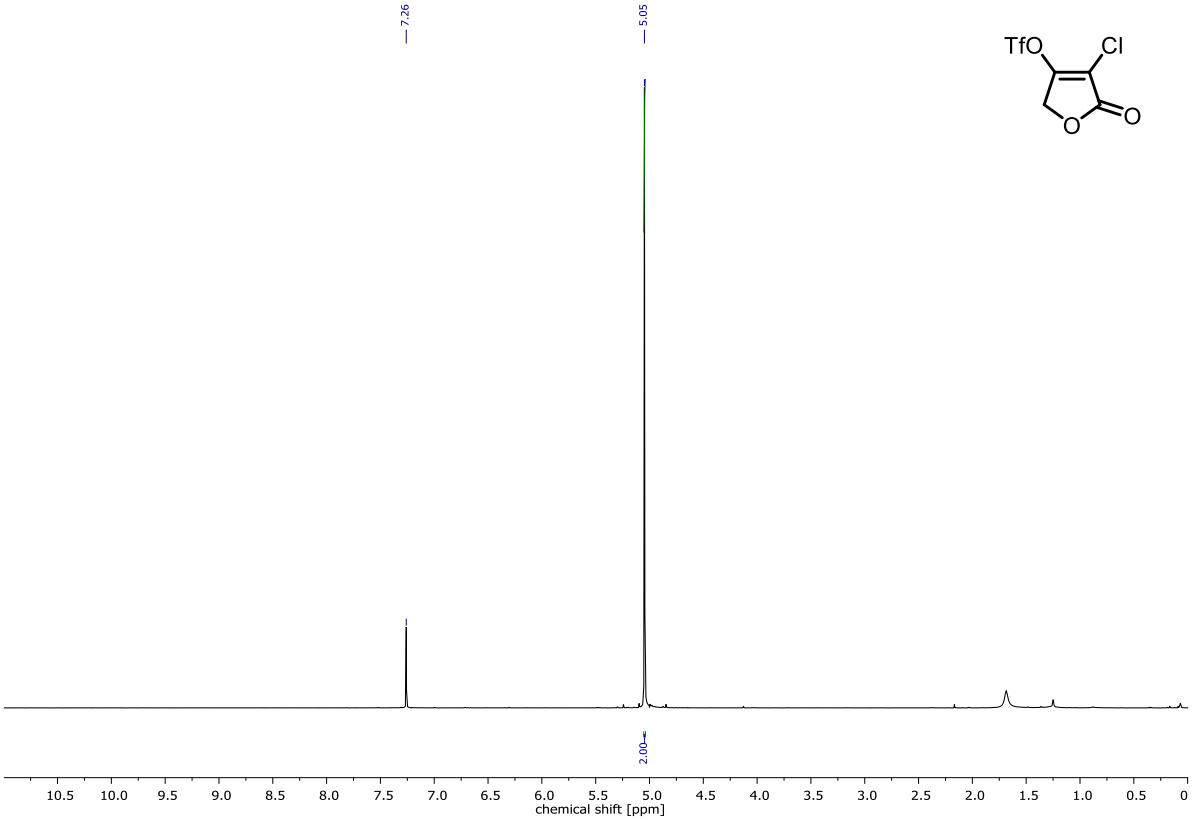

Figure 60: ^{1}H-NMR spectrum (400 MHz, $CDCl_3$-*d,* 298 K) of *chloro*-triflate **34**.

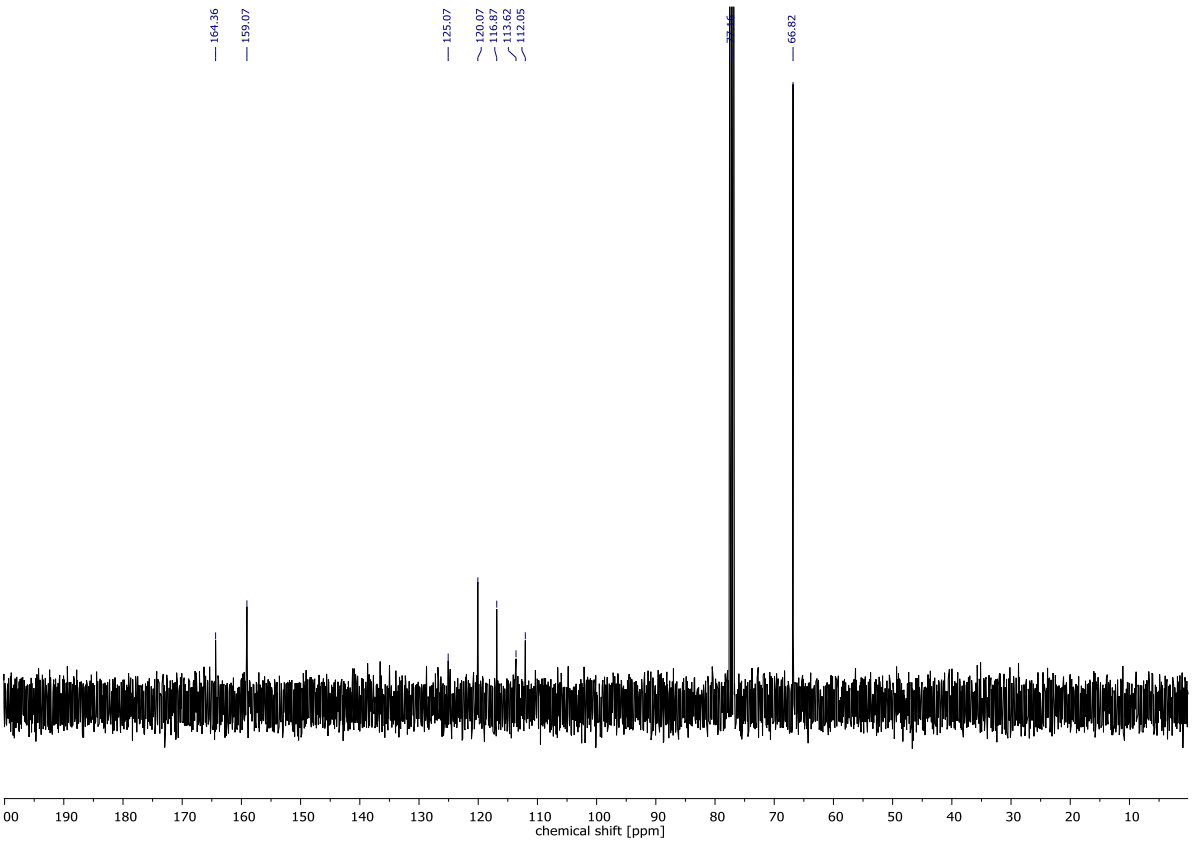

Figure 61: ^{13}C-NMR spectrum (101 MHz, CDCl3-d, 298 K) of *chloro*-triflate **34**.

4-Bromobenzene-1,2-diol 165

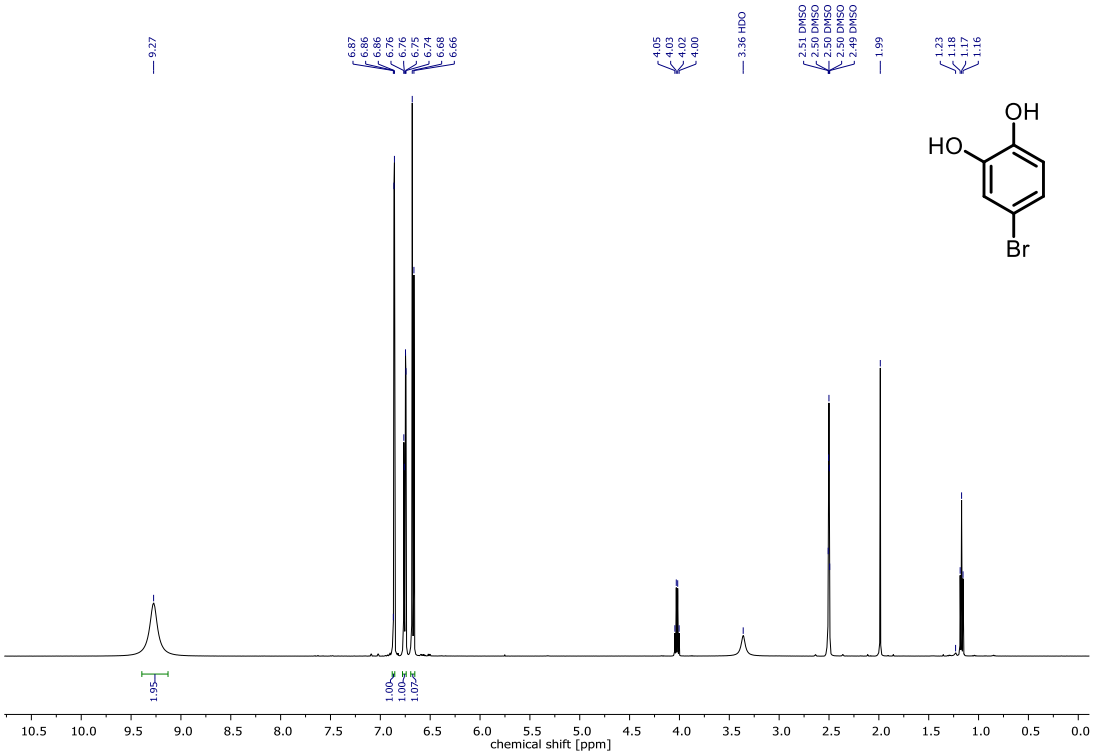

Figure 62: ^{1}H-NMR spectrum (500 MHz, $CDCl_3$-*d,* 296 K) of **165**.

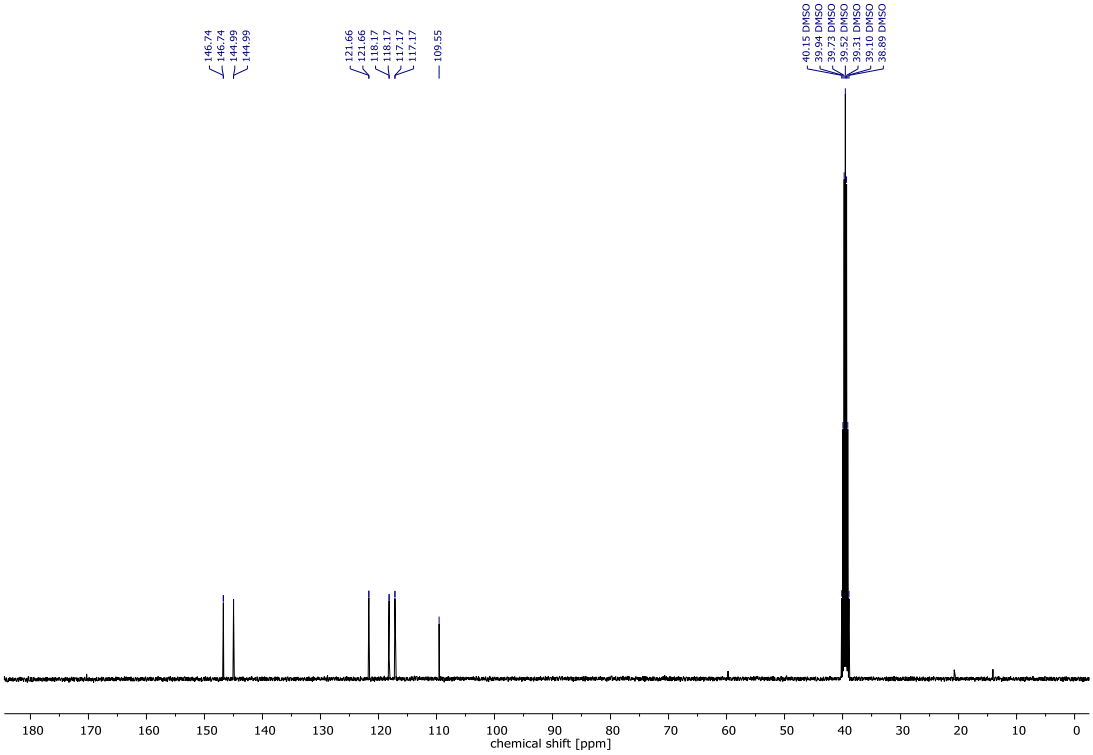

Figure 63: ^{13}C-NMR spectrum (101 MHz, $CDCl_3$-*d,* 298 K) of **165**.

((4-Bromo-1,2-phenylene)bis(oxy))bis(*tert*-butyldimethylsilane) 166

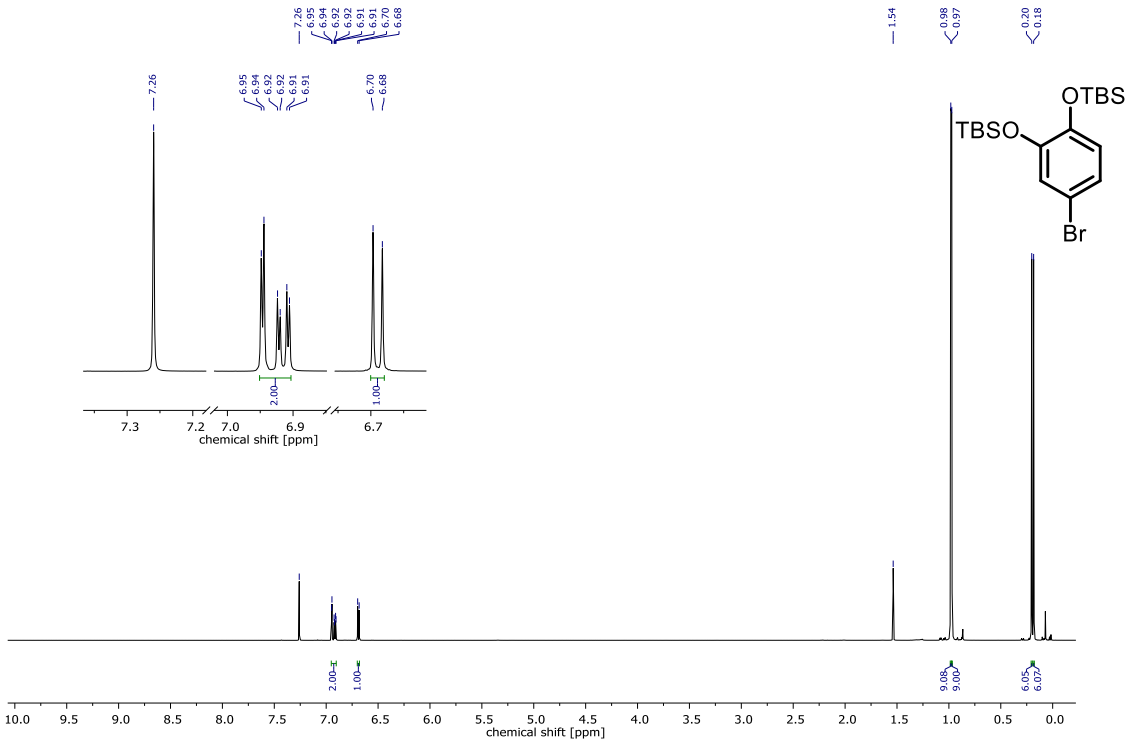

Figure 64: ^{1}H-NMR spectrum (600 MHz, $CDCl_3$-*d,* 300 K) of **166**.

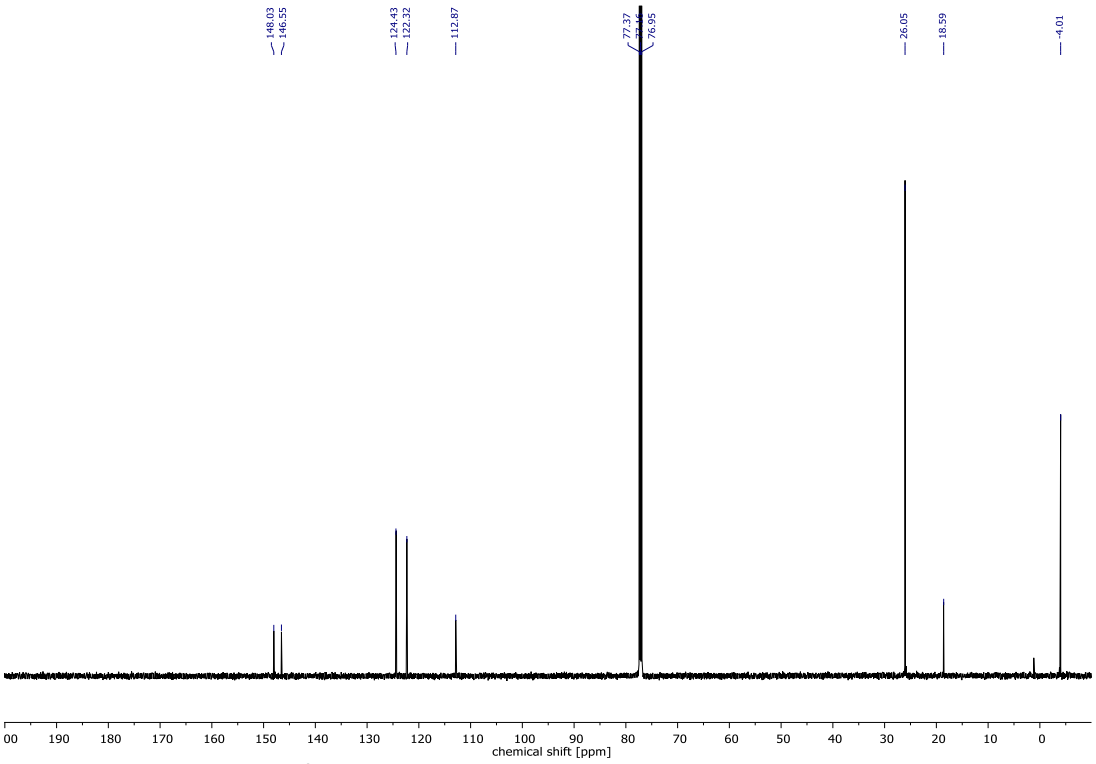

Figure 65: ^{13}C-NMR spectrum (126 MHz, $CDCl_3$-*d,* 300 K) of **166**.

(3,4-Bis((*tert*-butyldimethylsilyl)oxy)phenyl)boronic acid 161

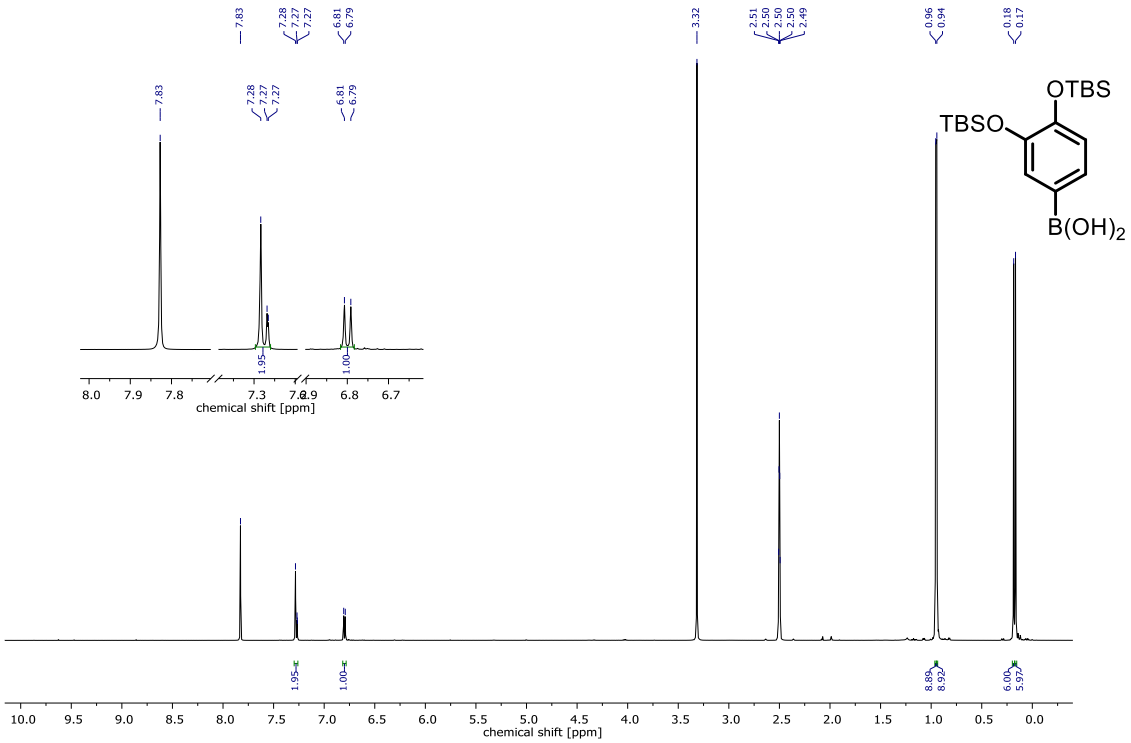

Figure 66: ^{1}H-NMR spectrum (500 MHz, DMSO-d_6, 299 K) of **161**.

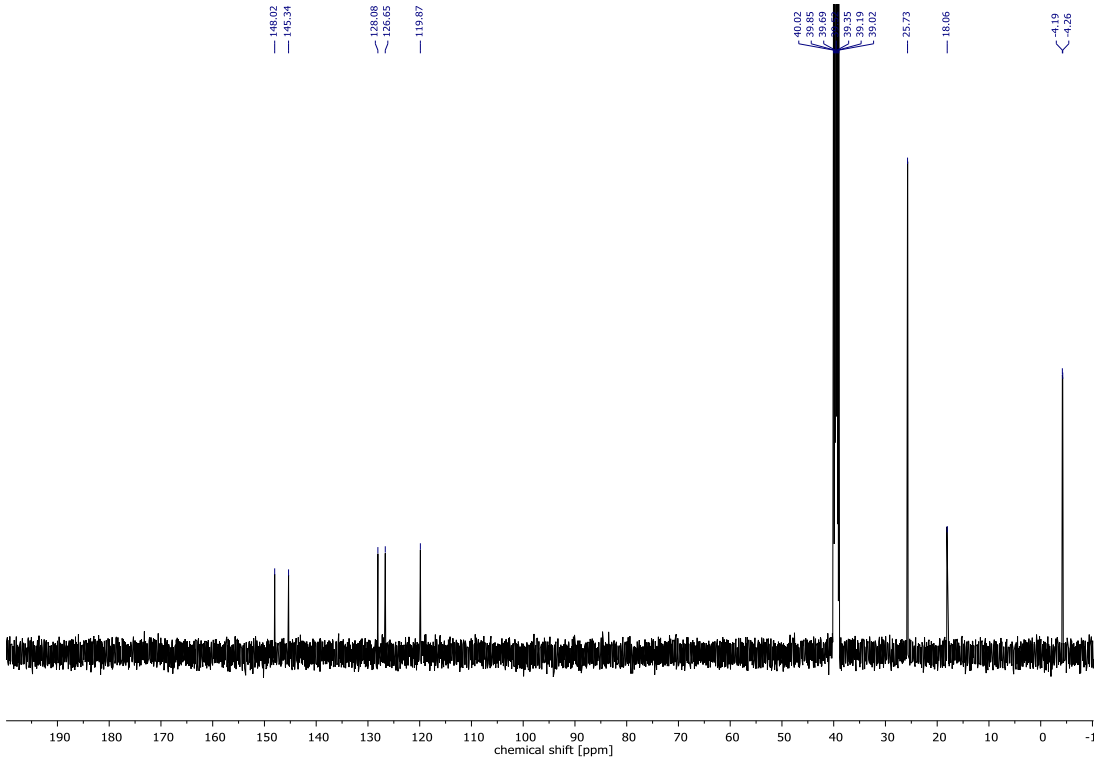

Figure 67: ^{13}C-NMR spectrum (126 MHz, DMSO-d_6, 300 K) of **161**.

Tert-butyl (2-methylbut-3-en-2-yl) carbonate 140

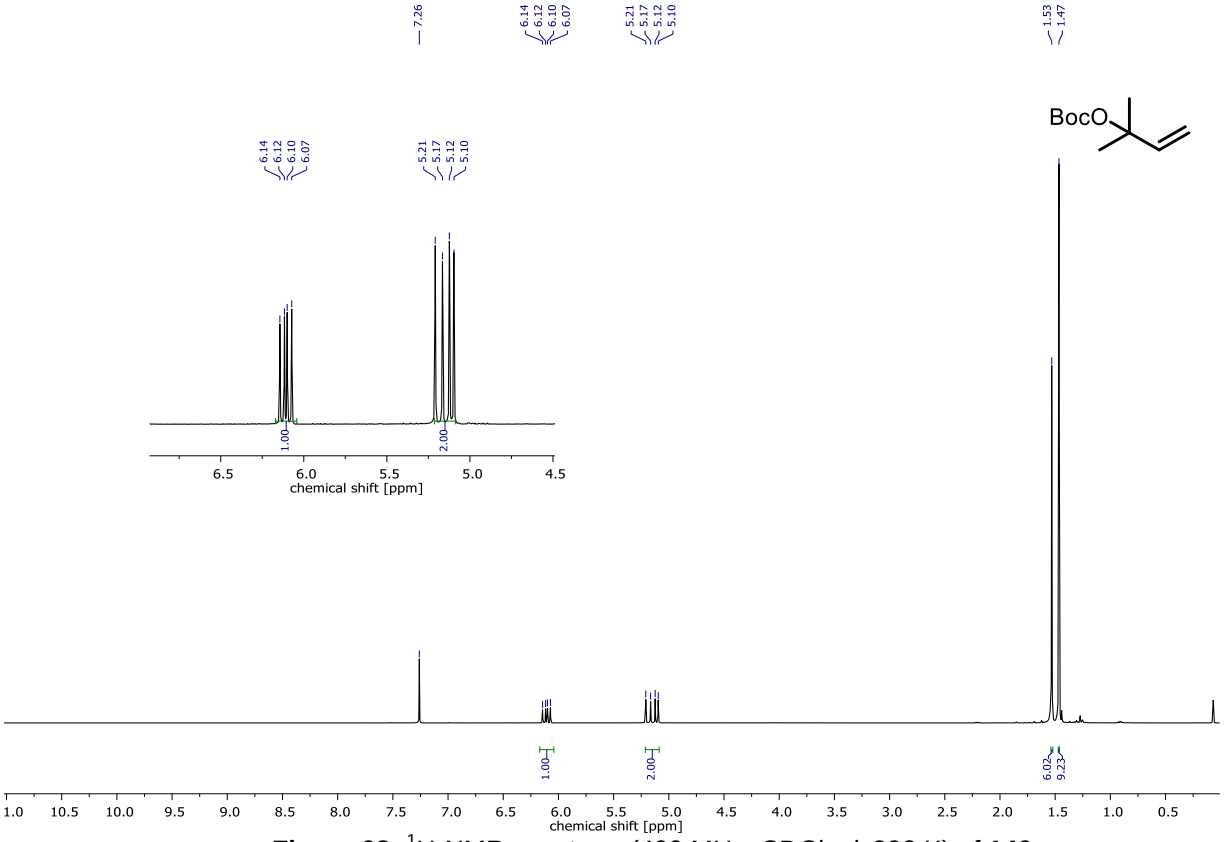

Figure 68: ^{1}H-NMR spectrum (400 MHz, $CDCl_3$-*d,* 298 K) of **140**.

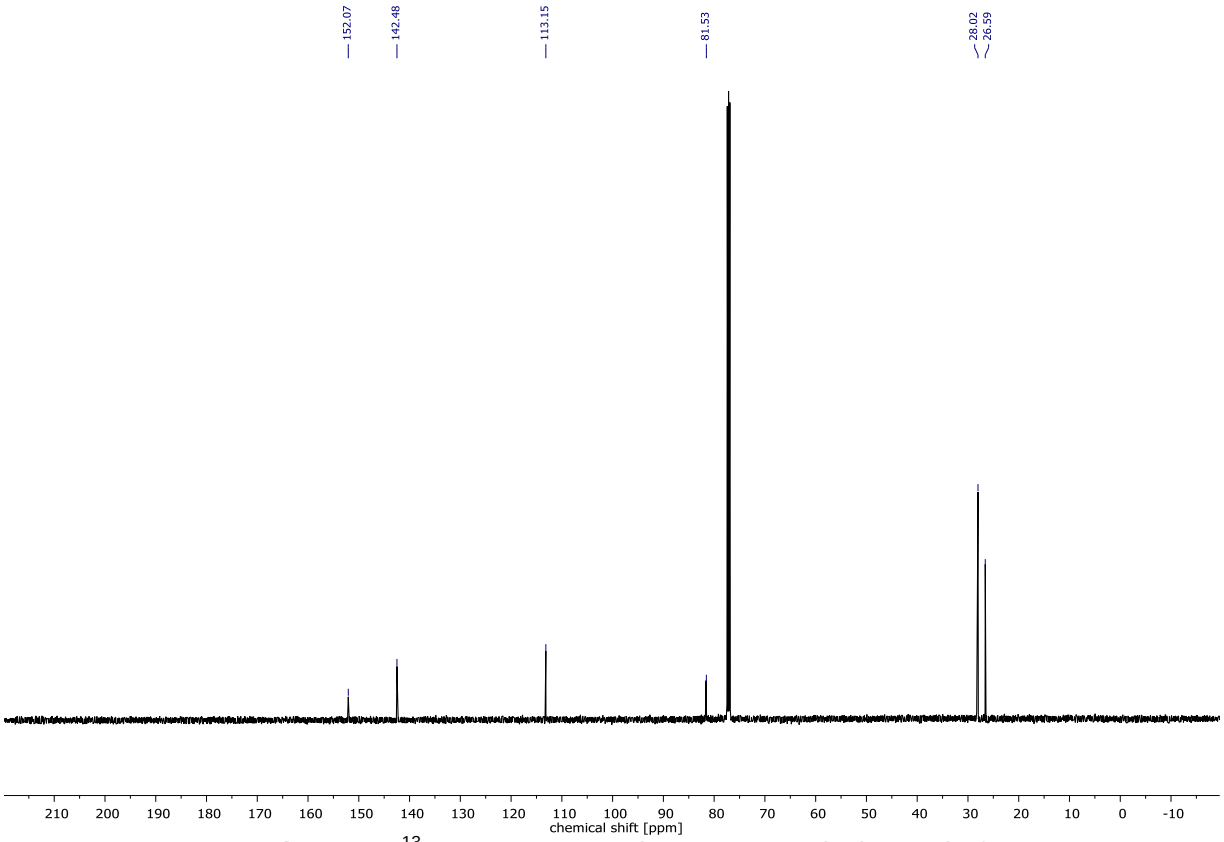

Figure 69: ^{13}C-NMR spectrum (500 MHz, $CDCl_3$-*d,* 299 K) of **140**.

4-((2-Methylbut-3-en-2-yl)oxy)benzaldehyde 141

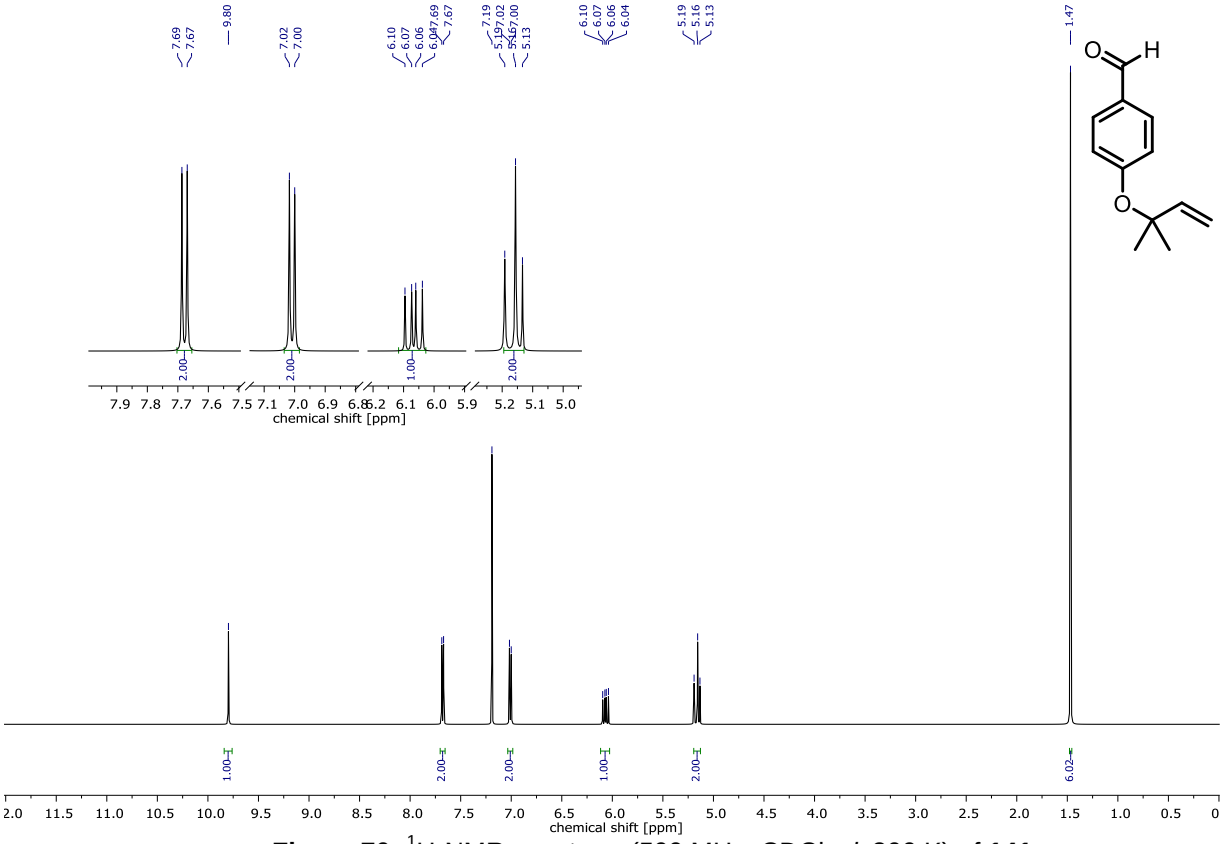

Figure 70: ^{1}H-NMR spectrum (500 MHz, $CDCl_3$-*d,* 300 K) of **141**.

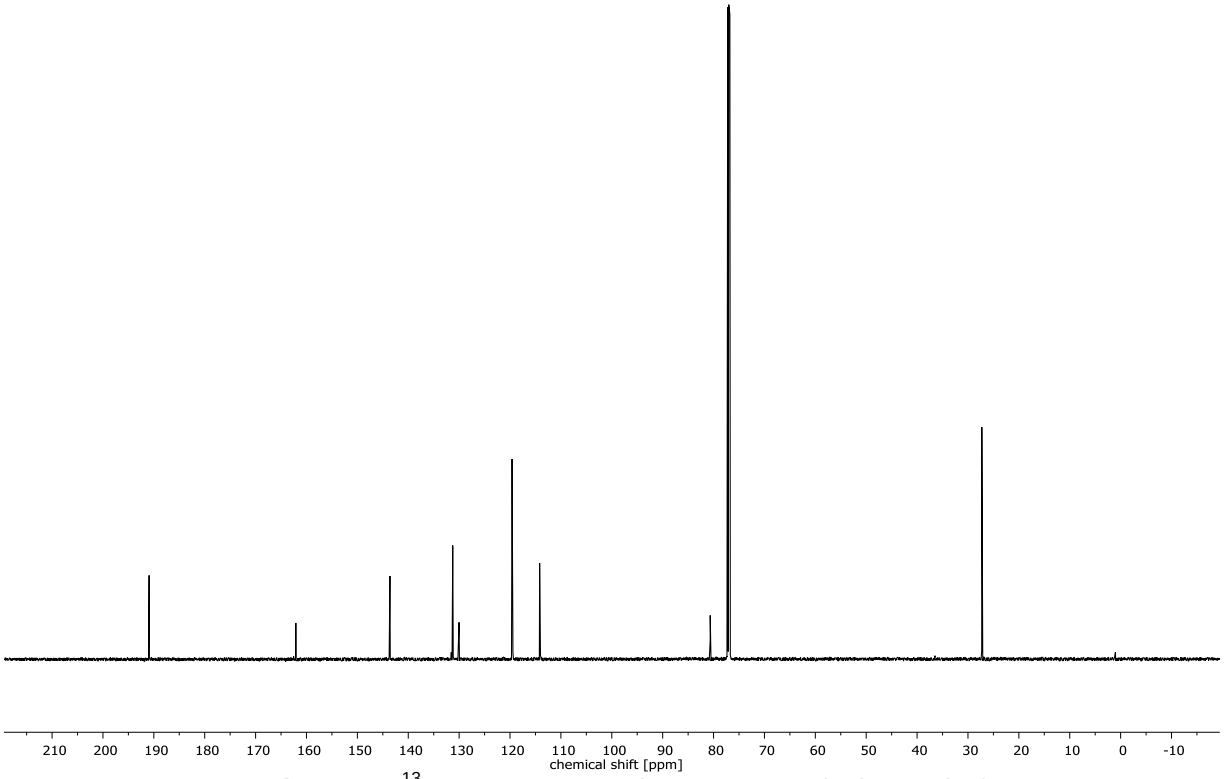

Figure 71: ^{13}C-NMR spectrum (150 MHz, $CDCl_3$-*d,* 300 K) of **141**.

4-Hydroxy-3-(3-methylbut-2-en-1-yl)benzaldehyde 139

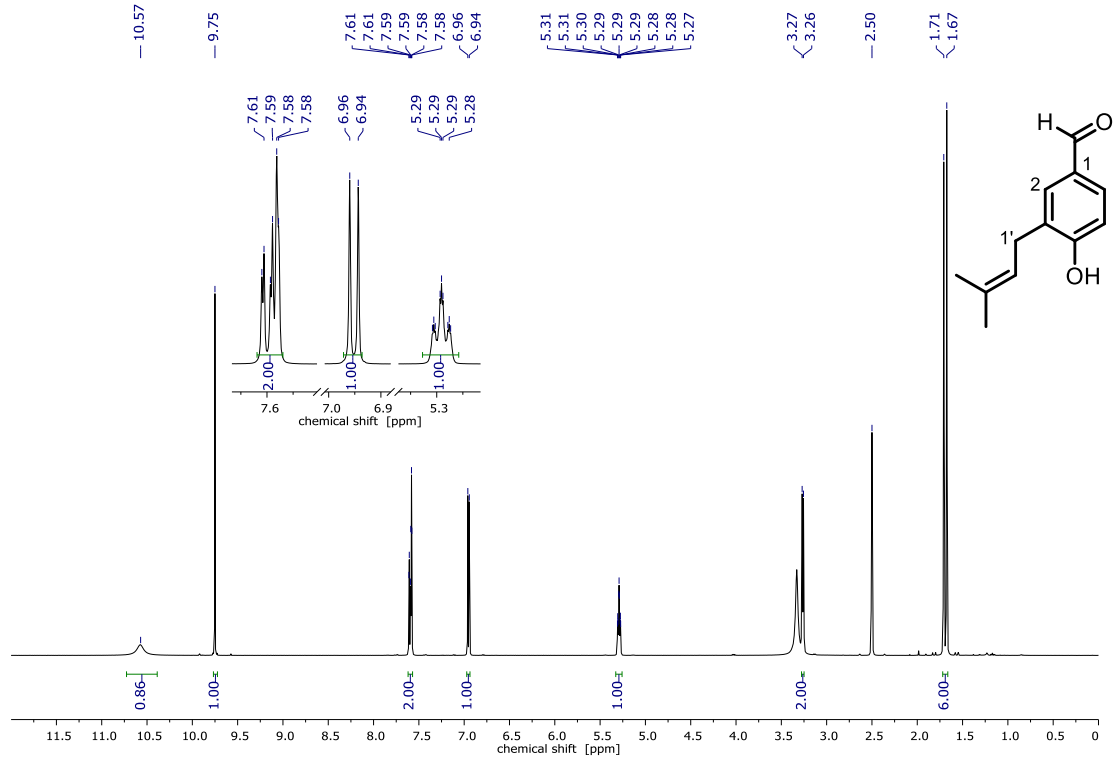

Figure 72: ^{1}H-NMR spectrum (500 MHz, DMSO-d_6, 300 K) of **139**.

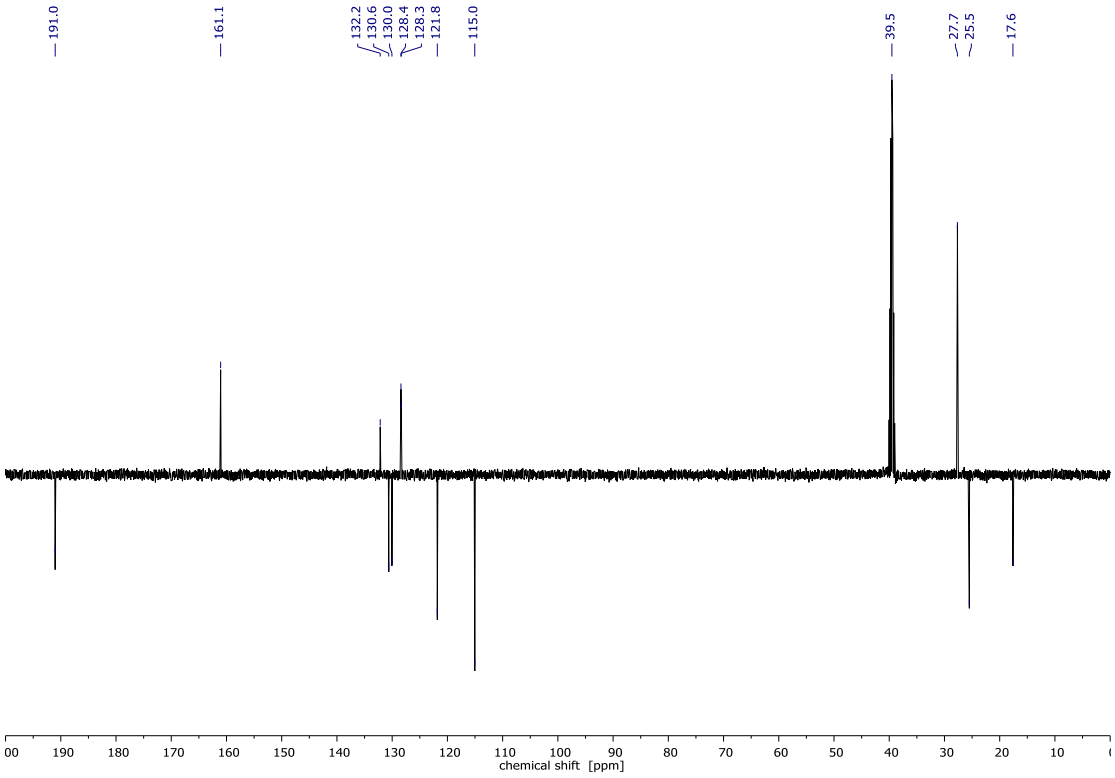

Figure 73: DEPTQ-NMR spectrum (126 MHz, DMSO-d_6, 300 K) of **139**.

2,2-Dimethylchromane-6-carbaldehyde 117

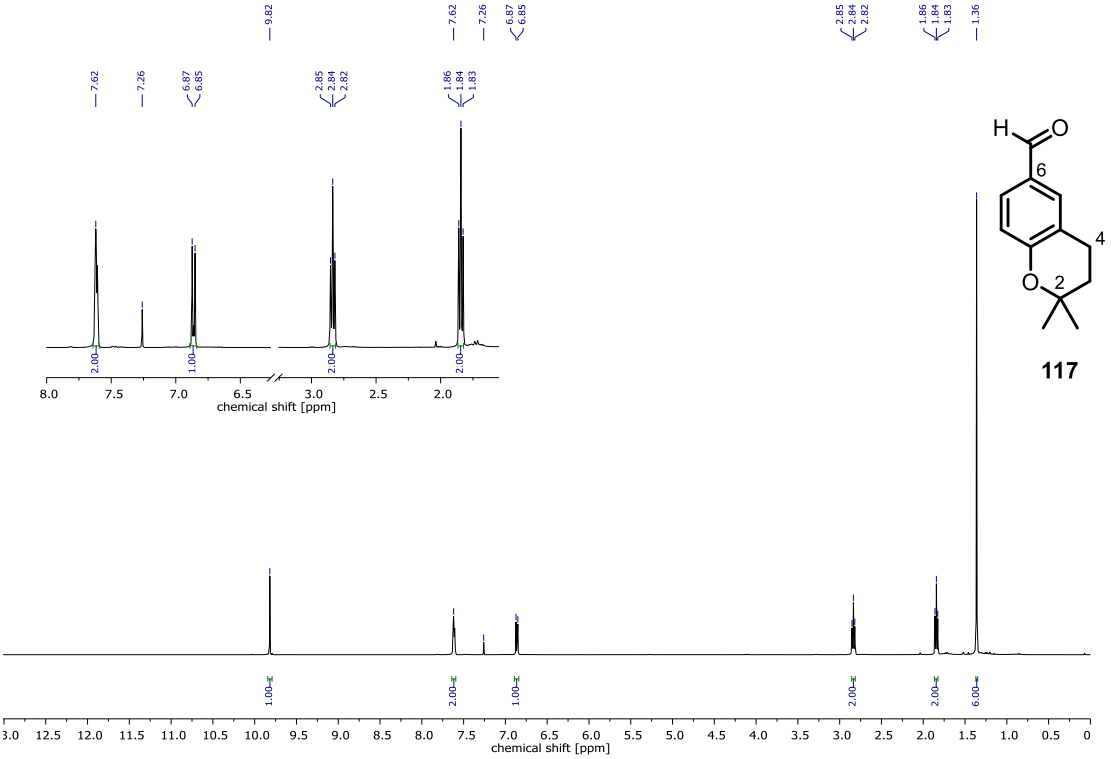

Figure 74: ^{1}H-NMR spectrum (400 MHz, $CDCl_3$-*d*, 298 K) of **117**.

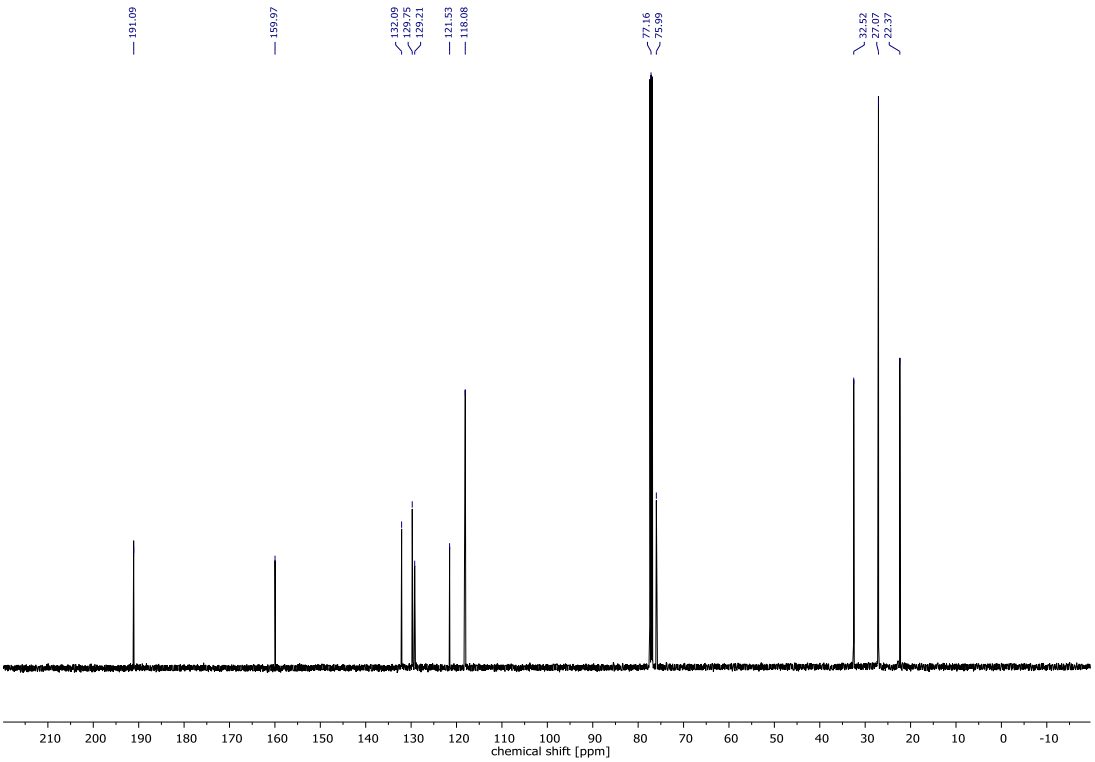

Figure 75: ^{13}C-NMR spectrum (126 MHz, $CDCl_3$-*d*, 299 K) of **117**.

4-(4-Methoxyphenyl)furan-2(5*H*)-one 26

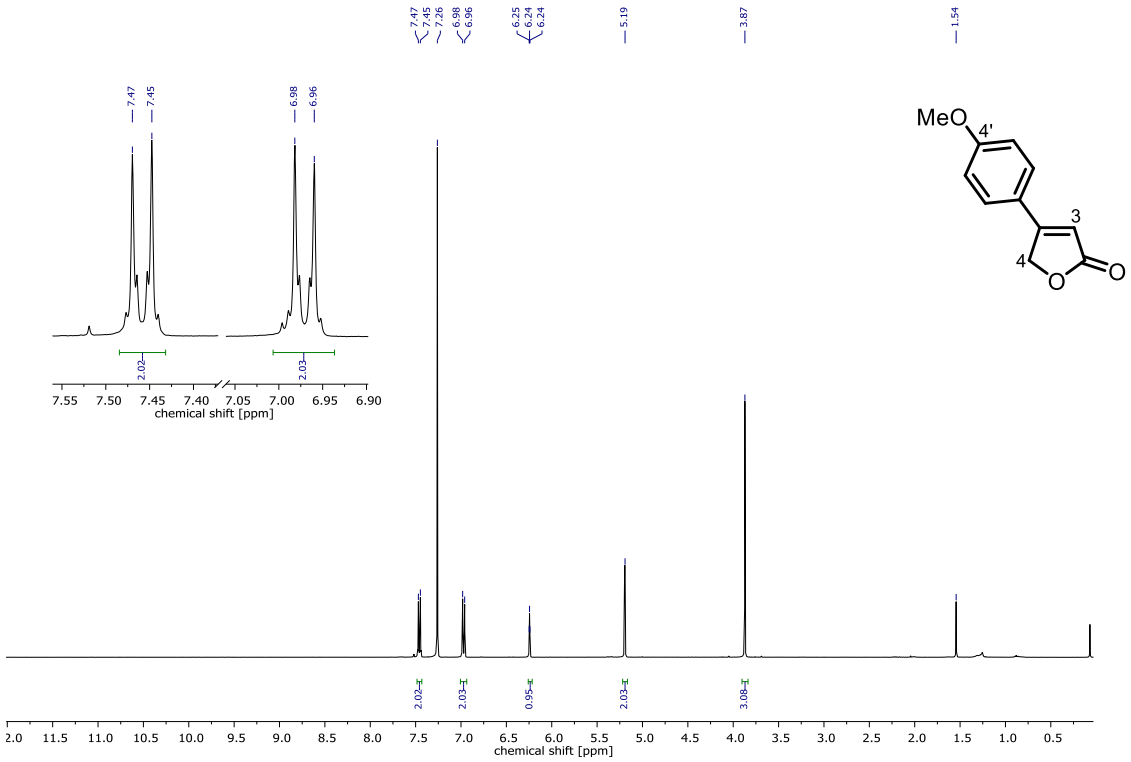

Figure 76: ^{1}H-NMR spectrum (400 MHz, $CDCl_3$-*d*, 298 K) of **26**.

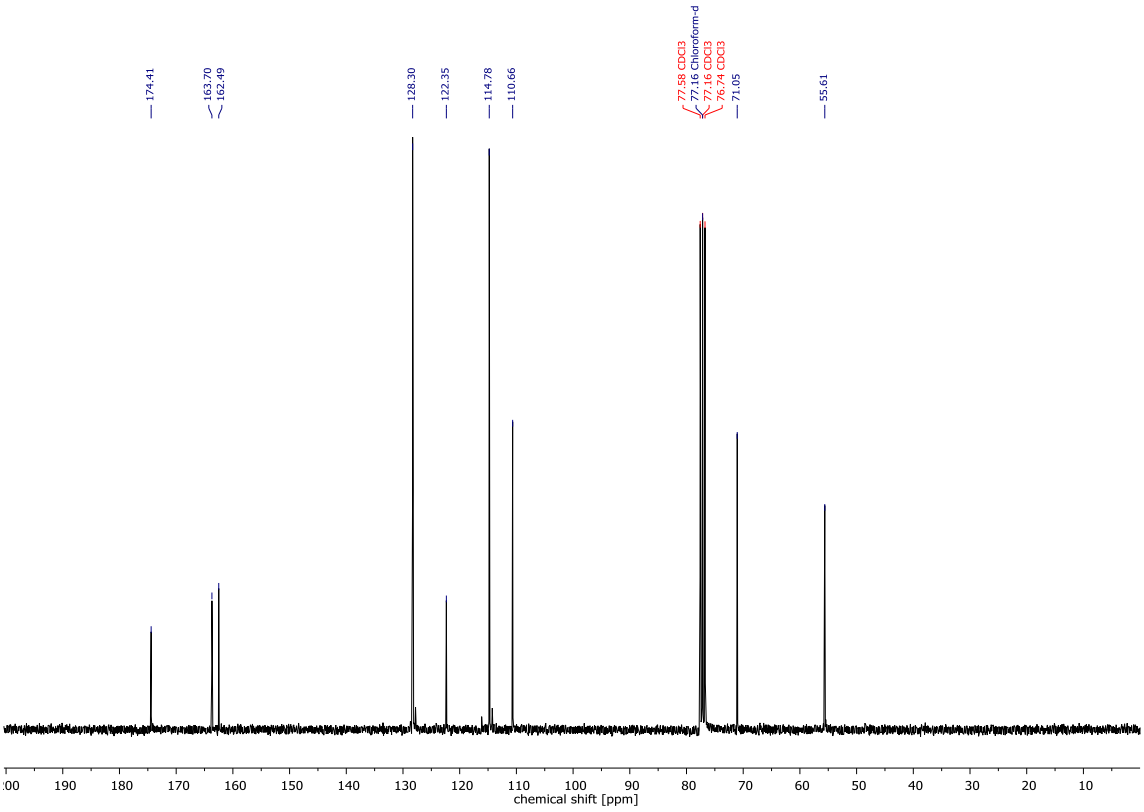

Figure 77: ^{13}C-NMR spectrum (76 MHz, $CDCl_3$-*d*, 299 K) of **26**.

4-(4-Hydroxyphenyl)furan-2(*5H*)-one 137

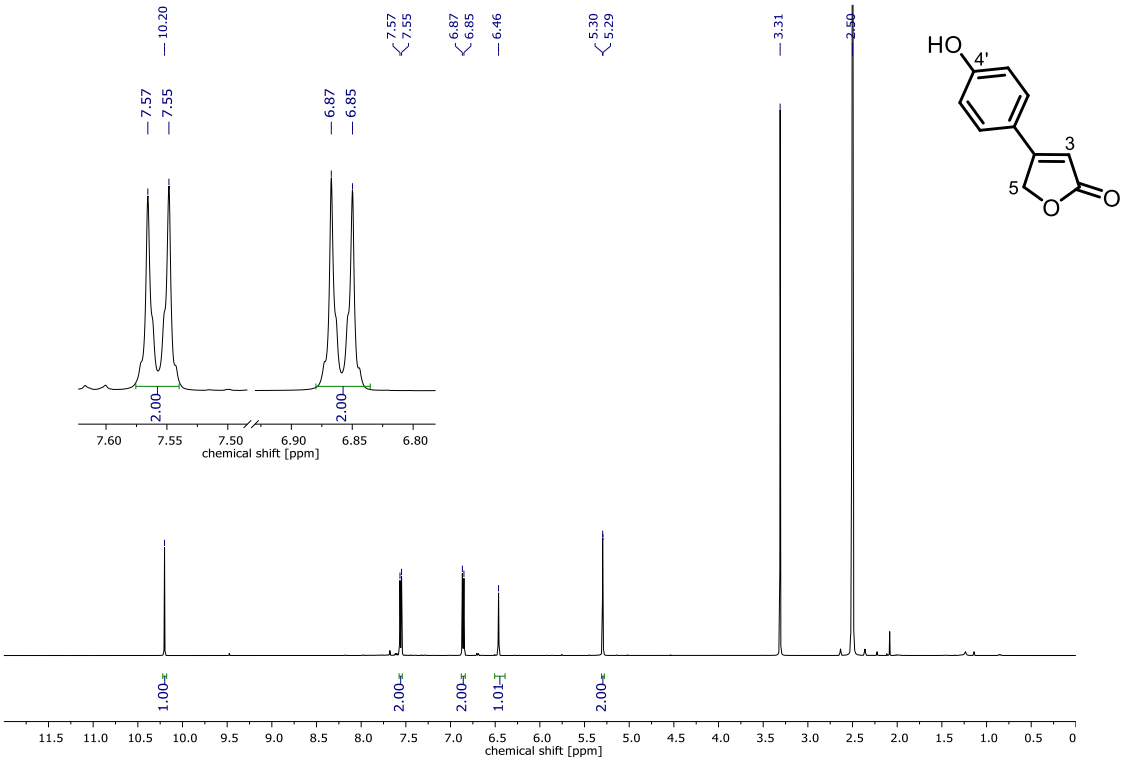

Figure 78: ^{1}H-NMR spectrum (500 MHz, DMSO-d_6, 298 K) of **137**.

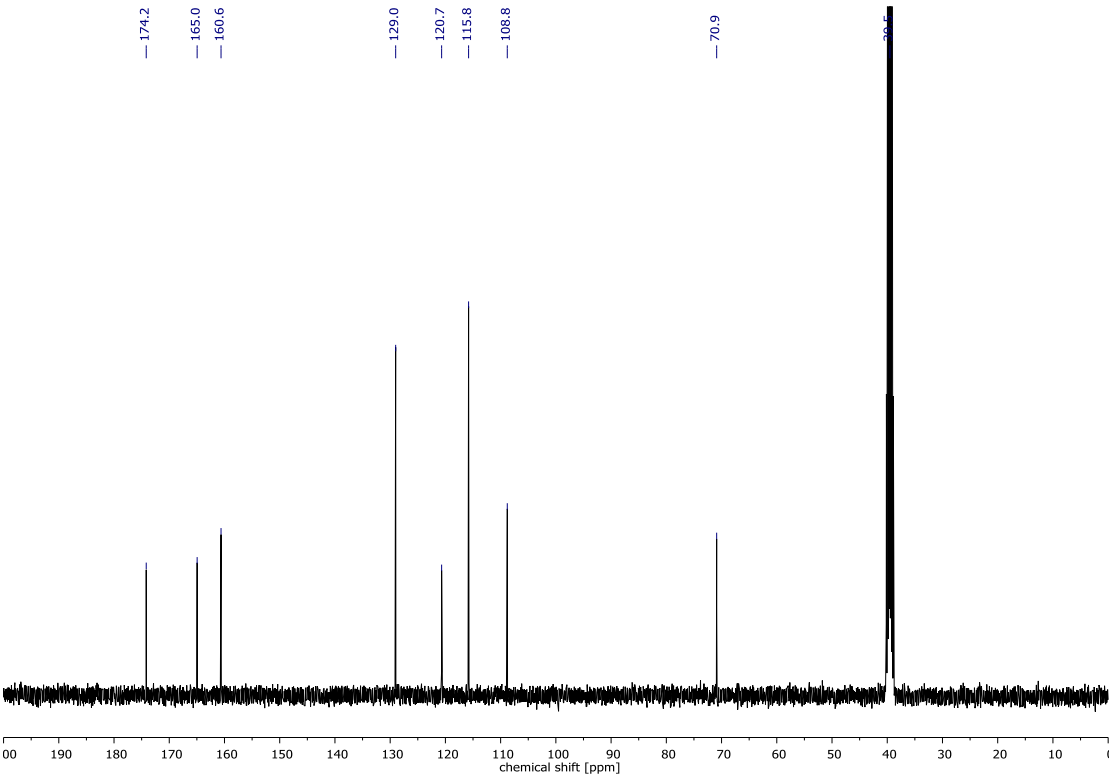

Figure 79: ^{13}C-NMR spectrum (101 MHz, DMSO-d_6, 298 K) of **137**.

4-(3,4-Bis((*tert*-butyldimethylsilyl)oxy)phenyl)furan-2(*5H*)-one 161

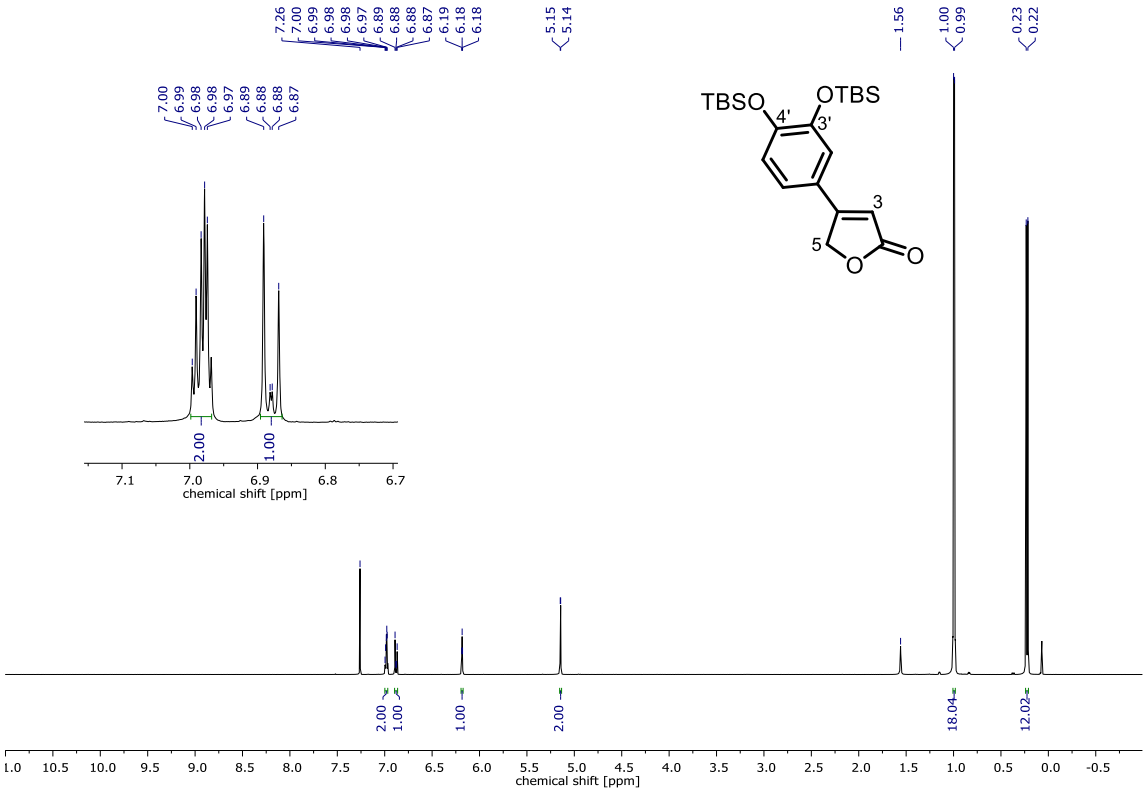

Figure 80: ^{1}H-NMR spectrum (400 MHz, $CDCl_3$-*d*, 298 K) of **161**.

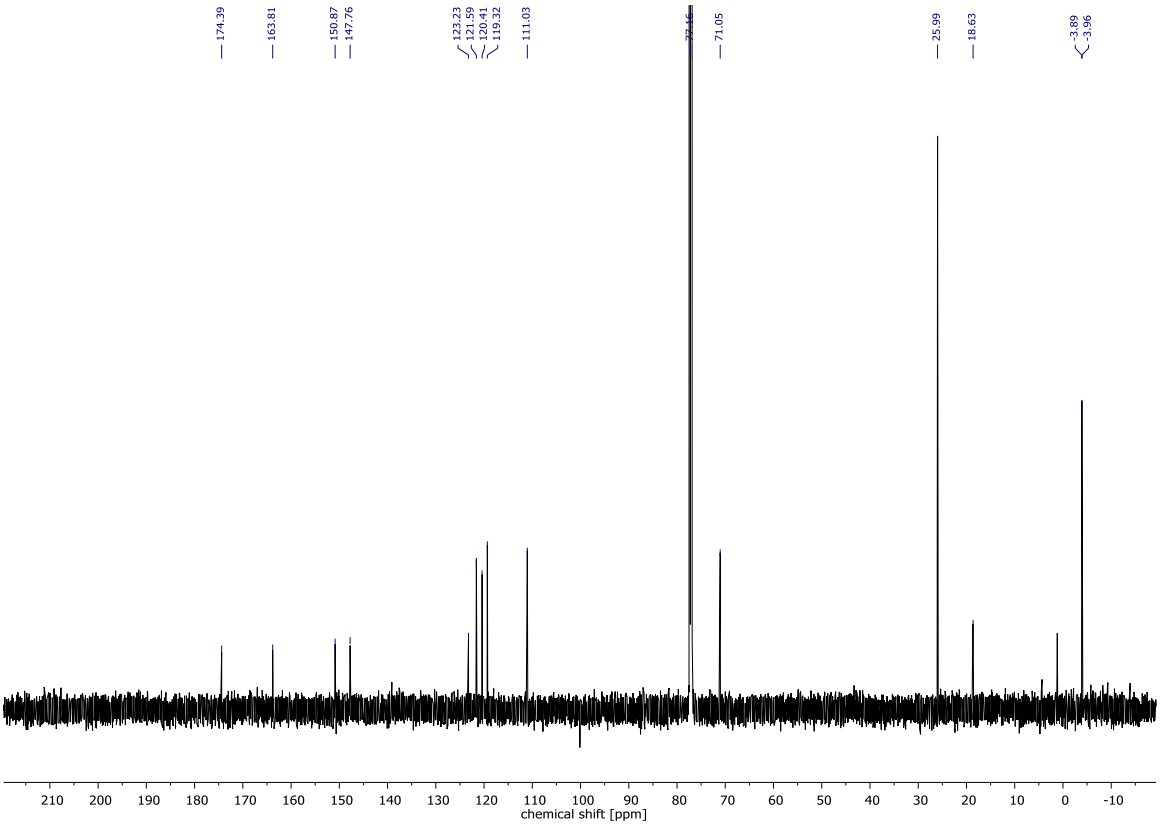

Figure 81: ^{13}C-NMR spectrum (151 MHz, $CDCl_3$-*d*, 300 K) of **161**.

N-(4-(5-Oxo-2,5-dihydrofuran-3-yl)phenyl)acetamide 171

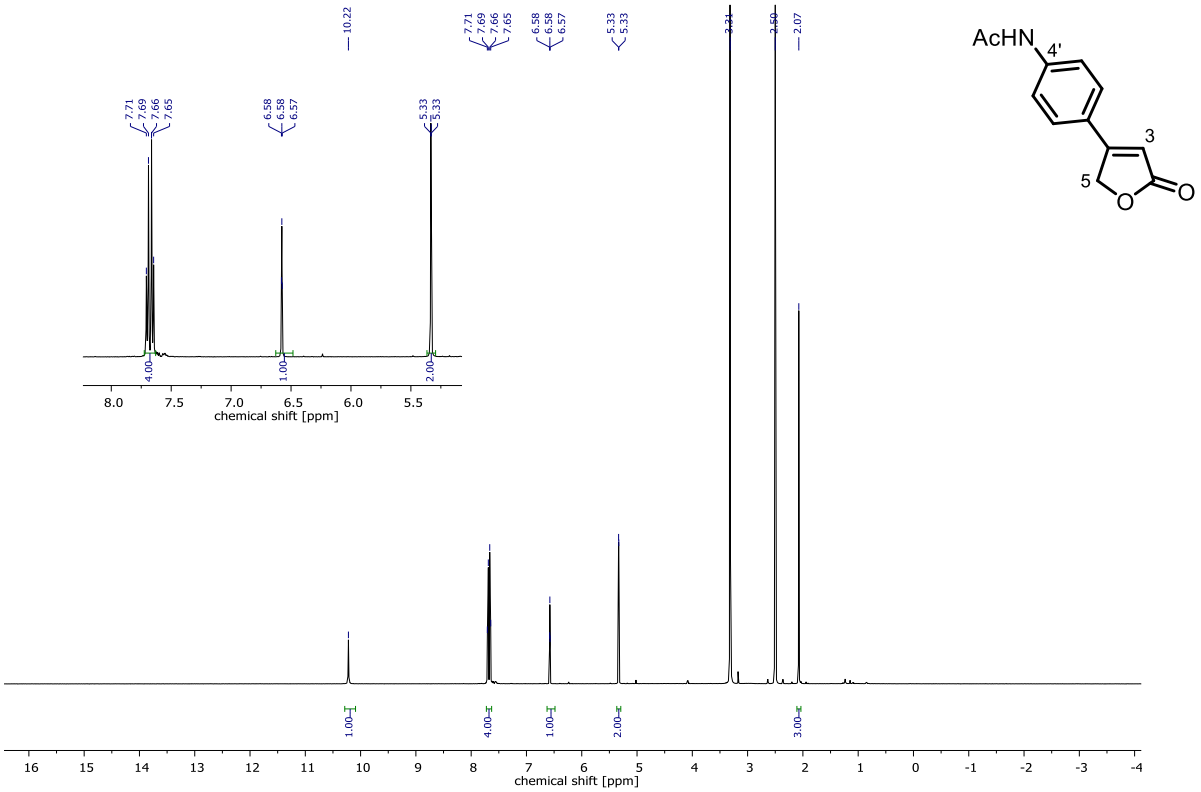

Figure 82: ^{1}H-NMR spectrum (500 MHz, DMSO-d_6, 300 K) of **171**.

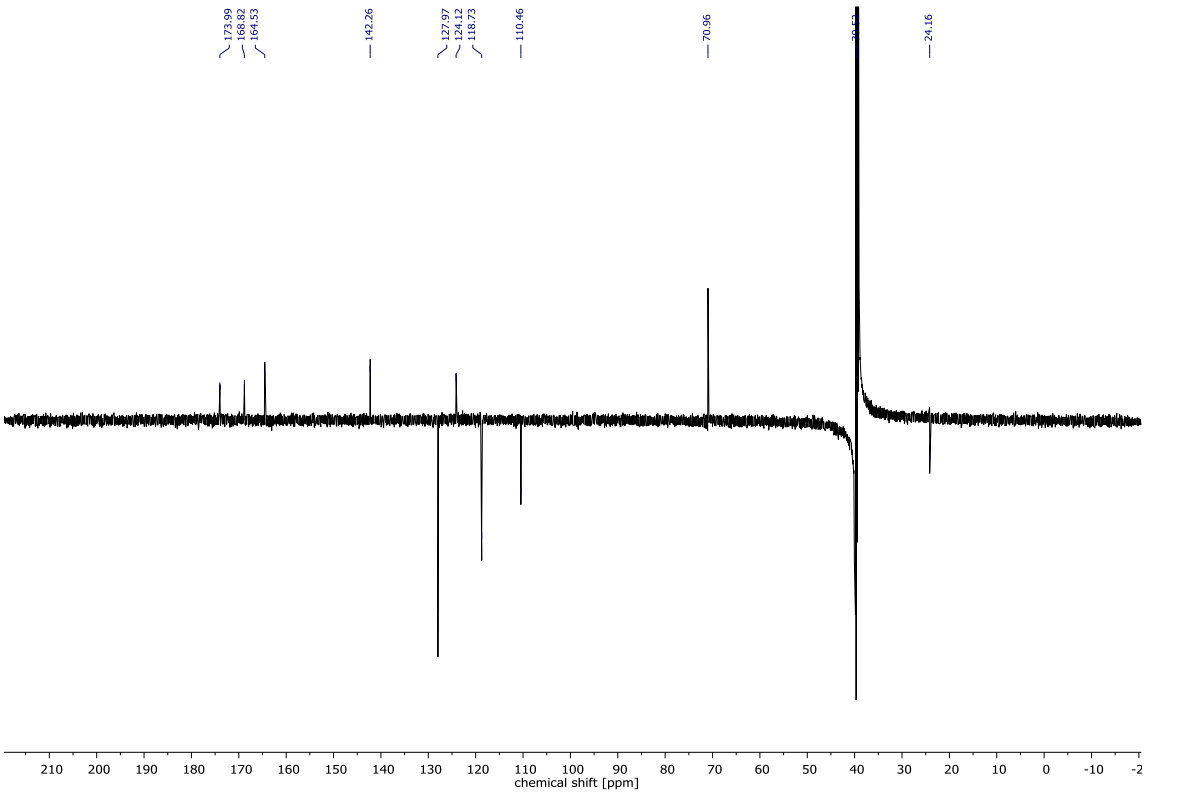

Figure 83: DEPTQ-NMR spectrum (151 MHz, DMSO-d_6, 298 K) of **171**.

4-(4-Fluorophenyl)furan-2(*5H*)-one 172

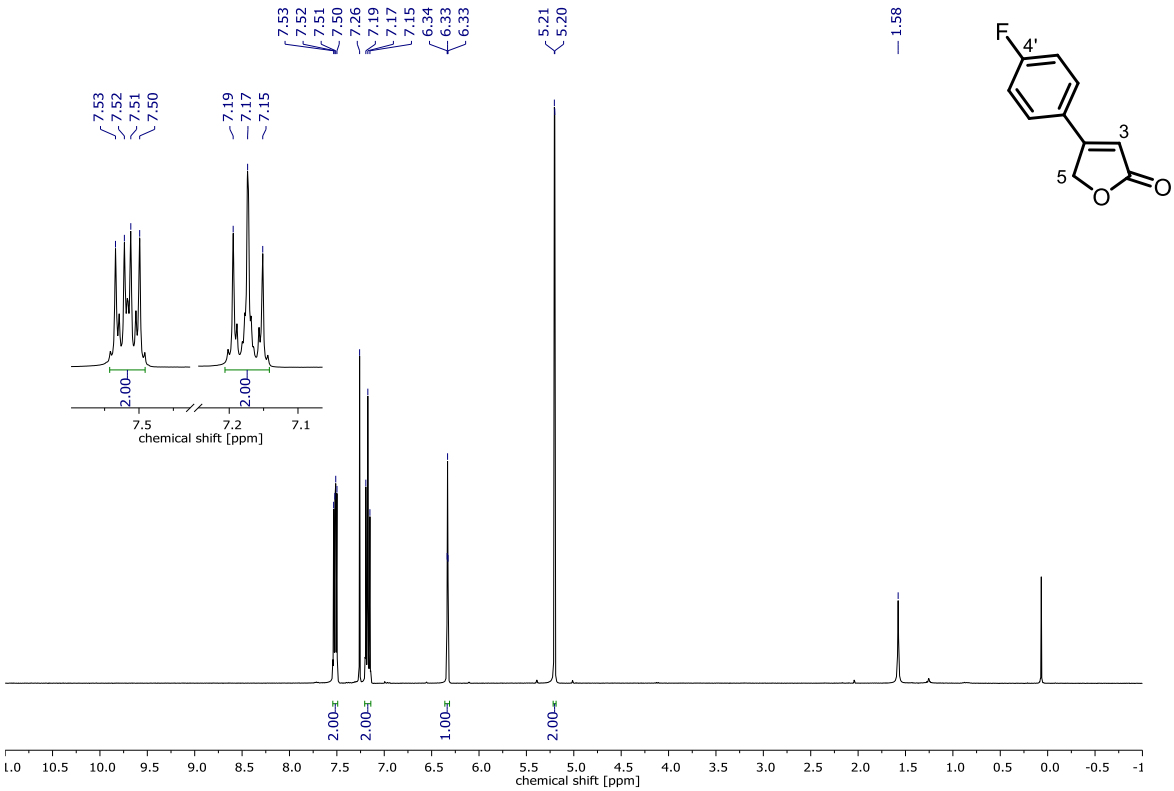

Figure 84: ^{1}H-NMR spectrum (400 MHz, $CDCl_3$-*d*, 298 K) of **172**.

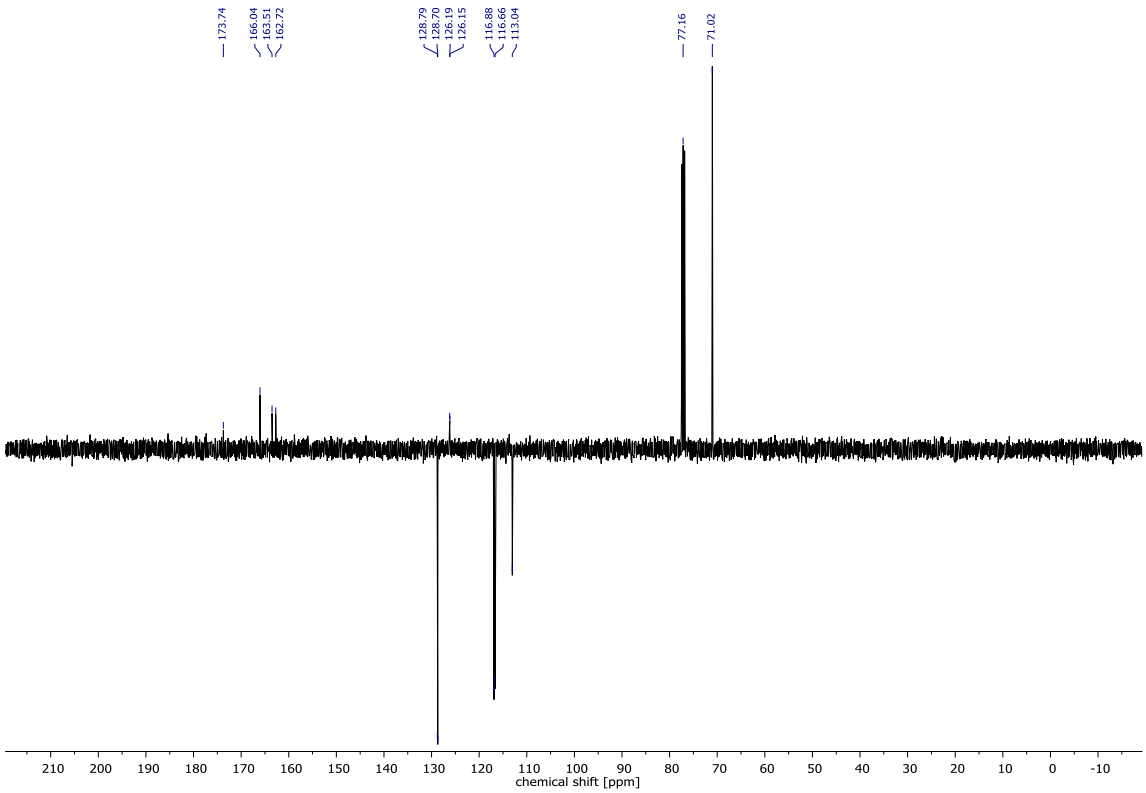

Figure 85: DEPTQ-NMR spectrum (101 MHz, $CDCl_3$-*d*, 300 K) of **172**.

4-(4-Nitrophenyl)furan-2(*5H*)-one 173

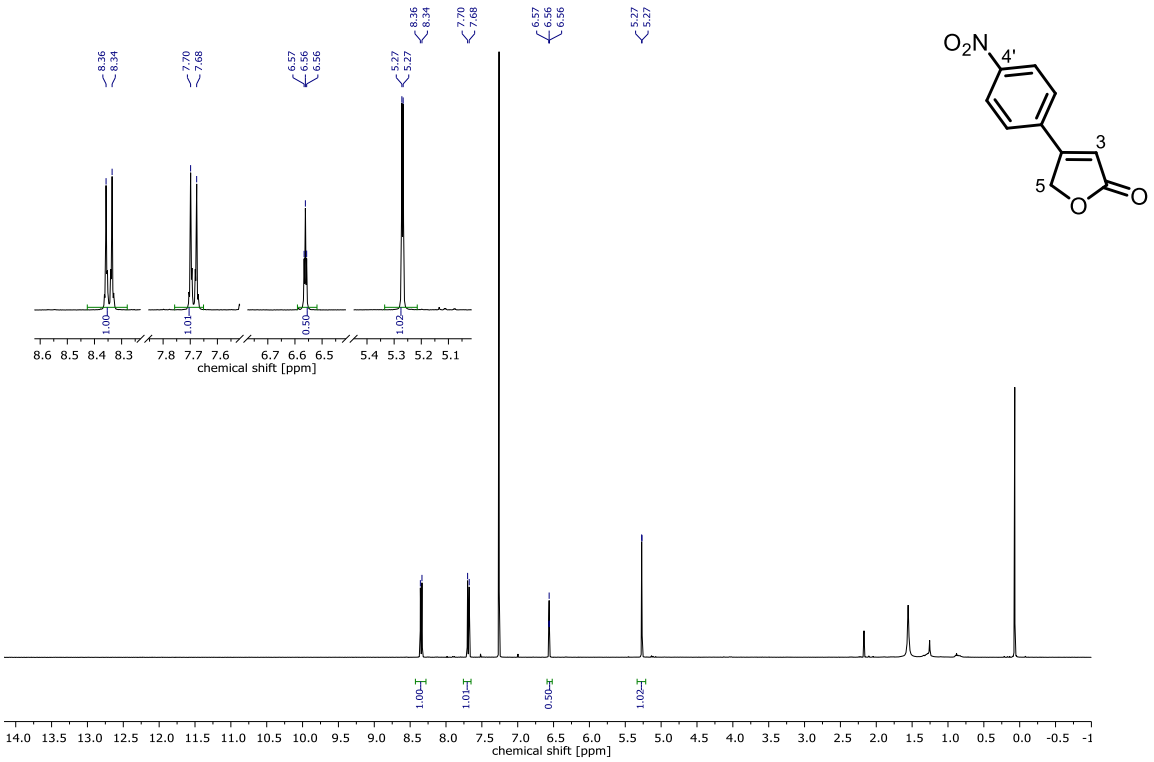

Figure 86: ^{1}H-NMR spectrum (400 MHz, $CDCl_3$-*d*, 298 K) of **173**.

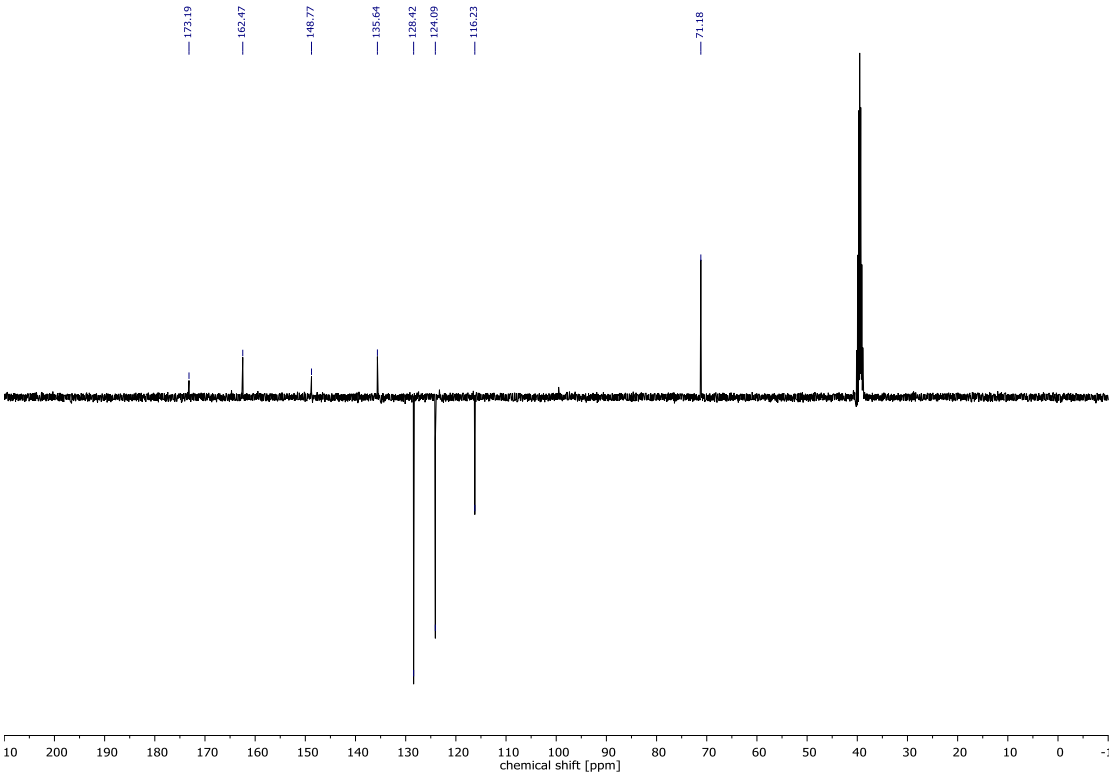

Figure 87: ^{13}C-NMR spectrum (101 MHz, $CDCl_3$-*d*, 296 K) of **173**.

3-Chloro-4-(4-methoxyphenyl)furan-2(*5H*)-one 160

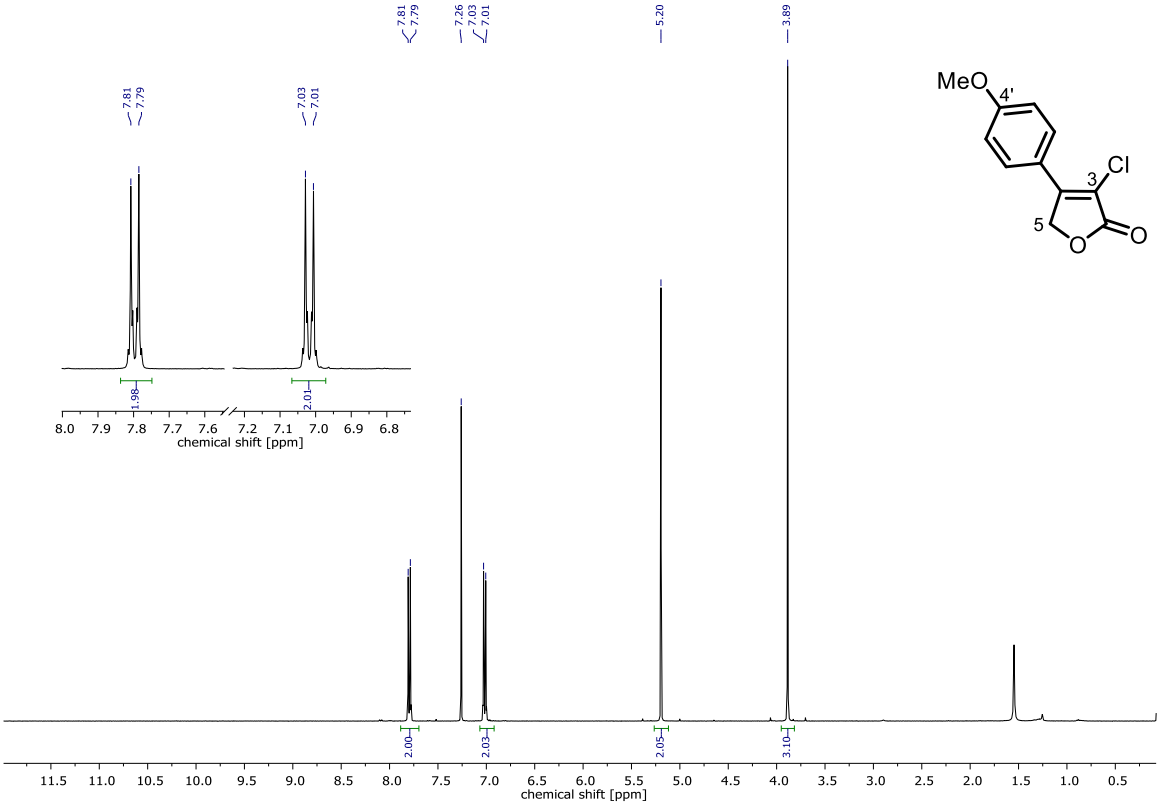

Figure 88: ^{1}H-NMR spectrum (400 MHz, $CDCl_3$-*d*, 300 K) of **160**.

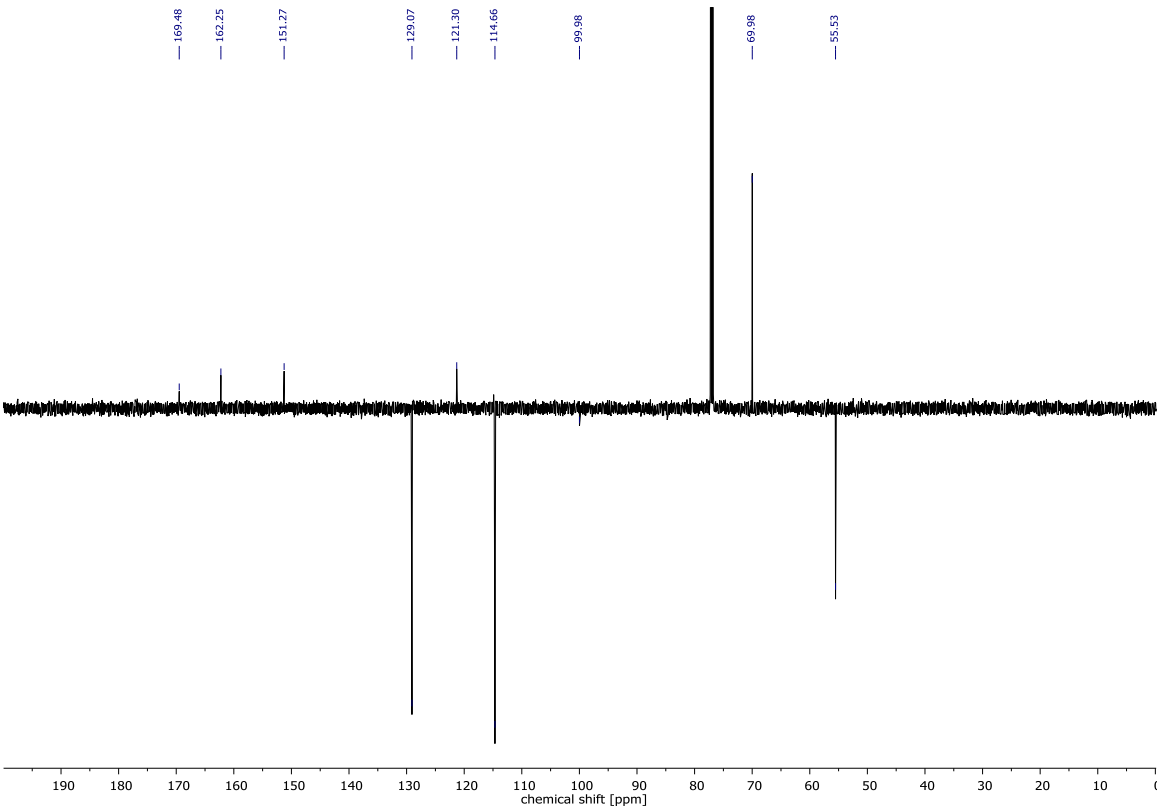

Figure 89: DEPTQ-NMR spectrum (151 MHz, $CDCl_3$-*d*, 298 K) of **160**.

3-Chloro-4-(4-hydroxyphenyl)furan-2(*5H*)-one 156

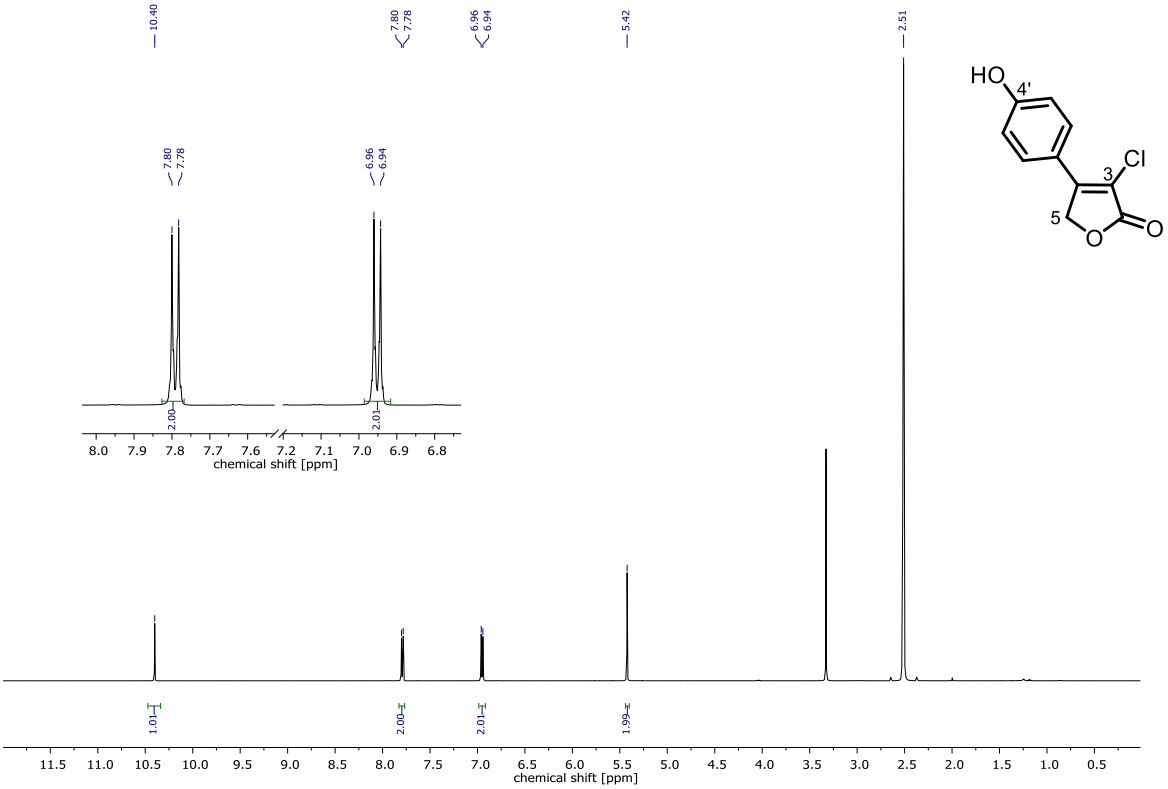

Figure 90: ^{1}H-NMR spectrum (500 MHz, DMSO-$d_{6,}$ 298 K) of **156**.

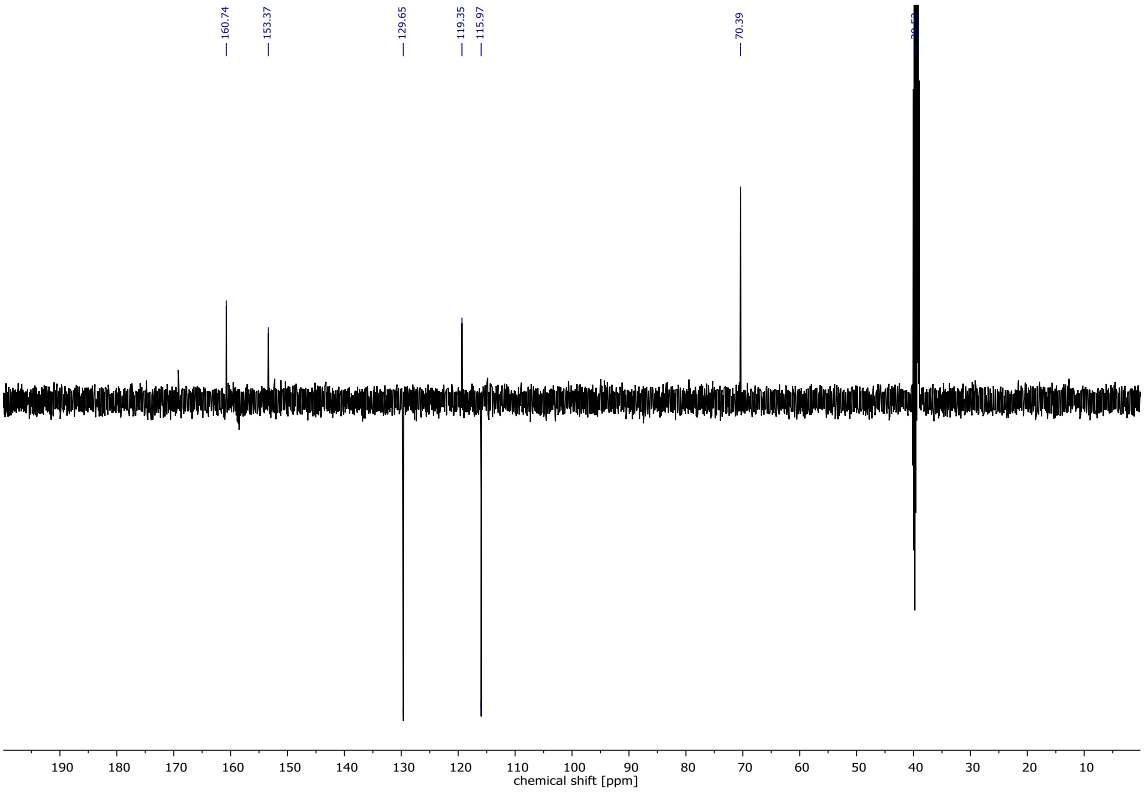

Figure 91: ^{1}H-NMR spectrum (126 MHz, DMSO-$d_{6,}$ 298 K) of **156**.

2-(3-Bromo-4-methoxyphenyl)-1,3-dioxolane 133

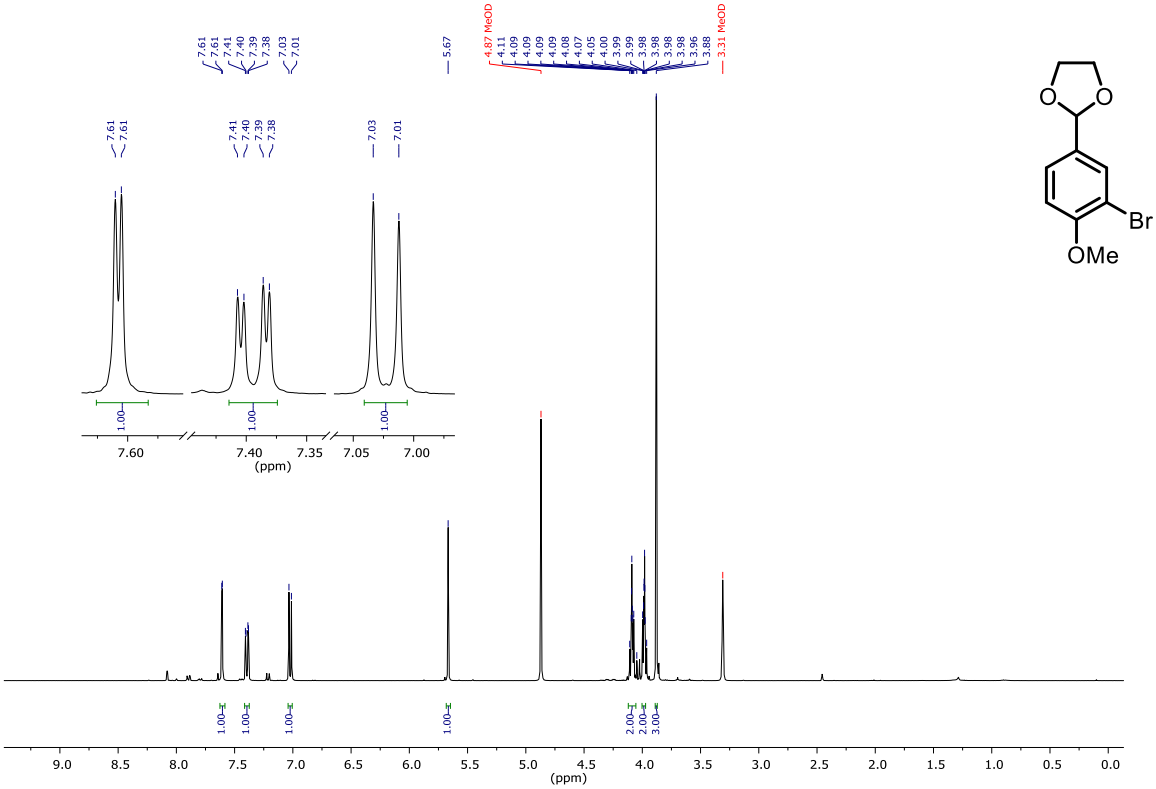

Figure 12: ^{1}H-NMR spectrum (400 MHz, methanol-d_4, 296 K) of **133**.

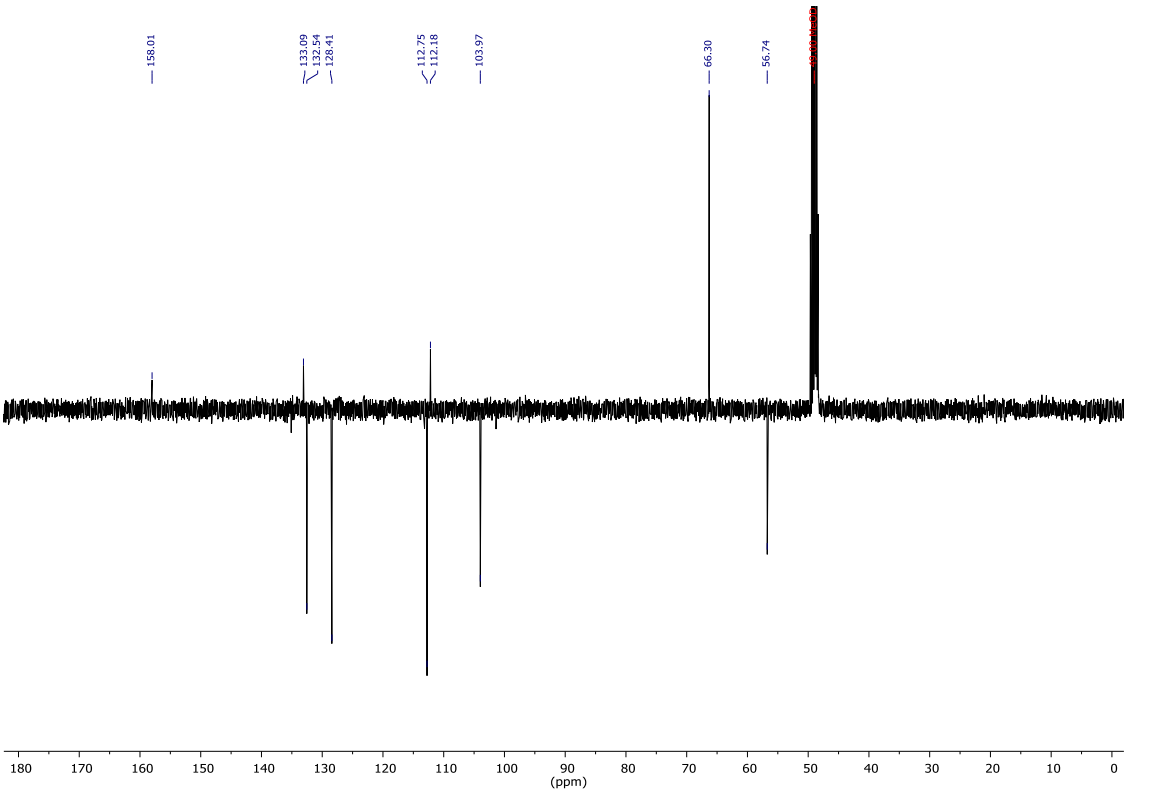

Figure 23: DEPTQ-NMR spectrum (101 MHz, methanol-d_4, 296 K) of **133**.

4-Methoxy-3-(3-methylbut-2-en-1-yl)benzaldehyde 116

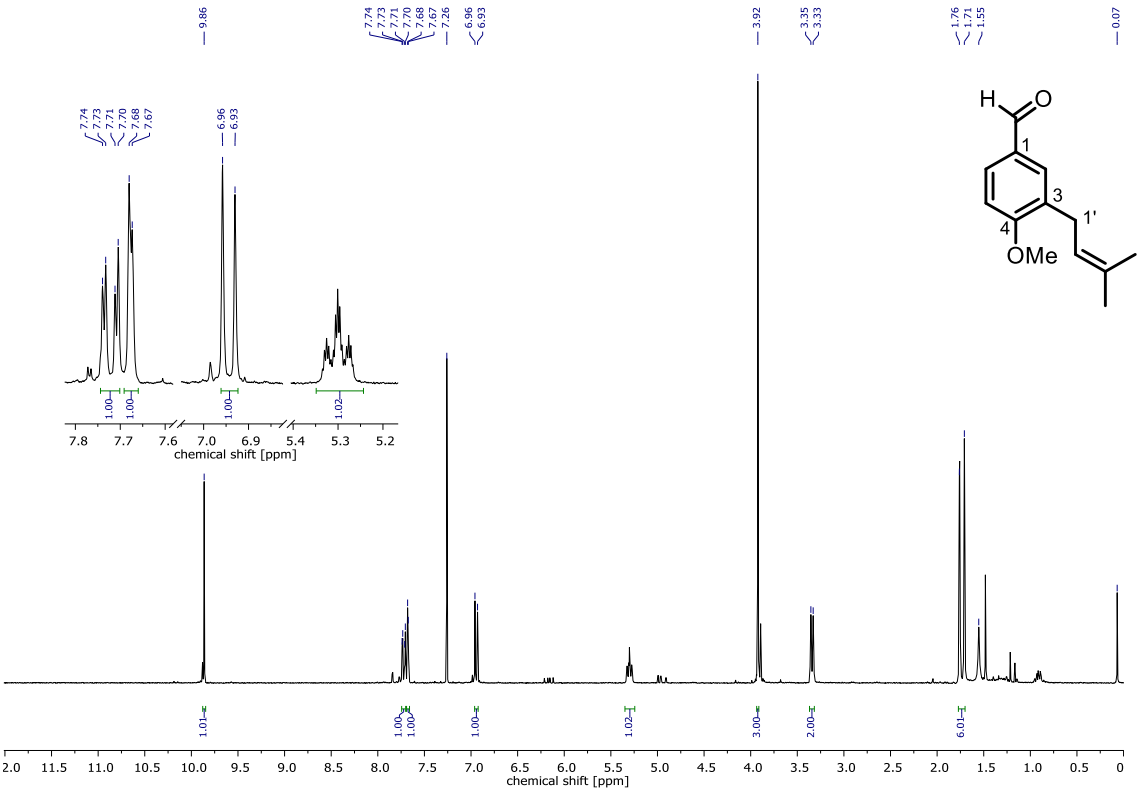

Figure 34: ^{1}H-NMR spectrum (300 MHz, $CDCl_3$-*d*, 298 K) of **116**.

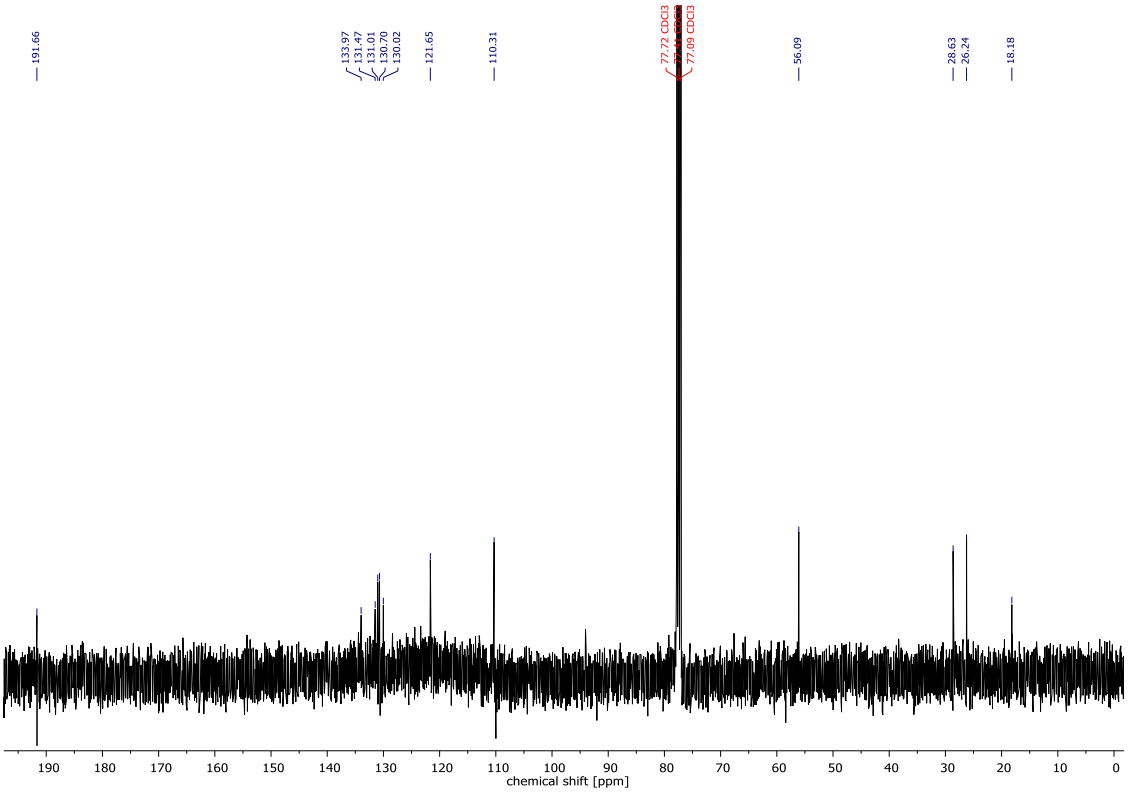

Figure 45: ^{1}H-NMR spectrum (101 MHz, $CDCl_3$-*d*, 298 K) of **116**.

(5-Formyl-2-methoxyphenyl)boronic acid121

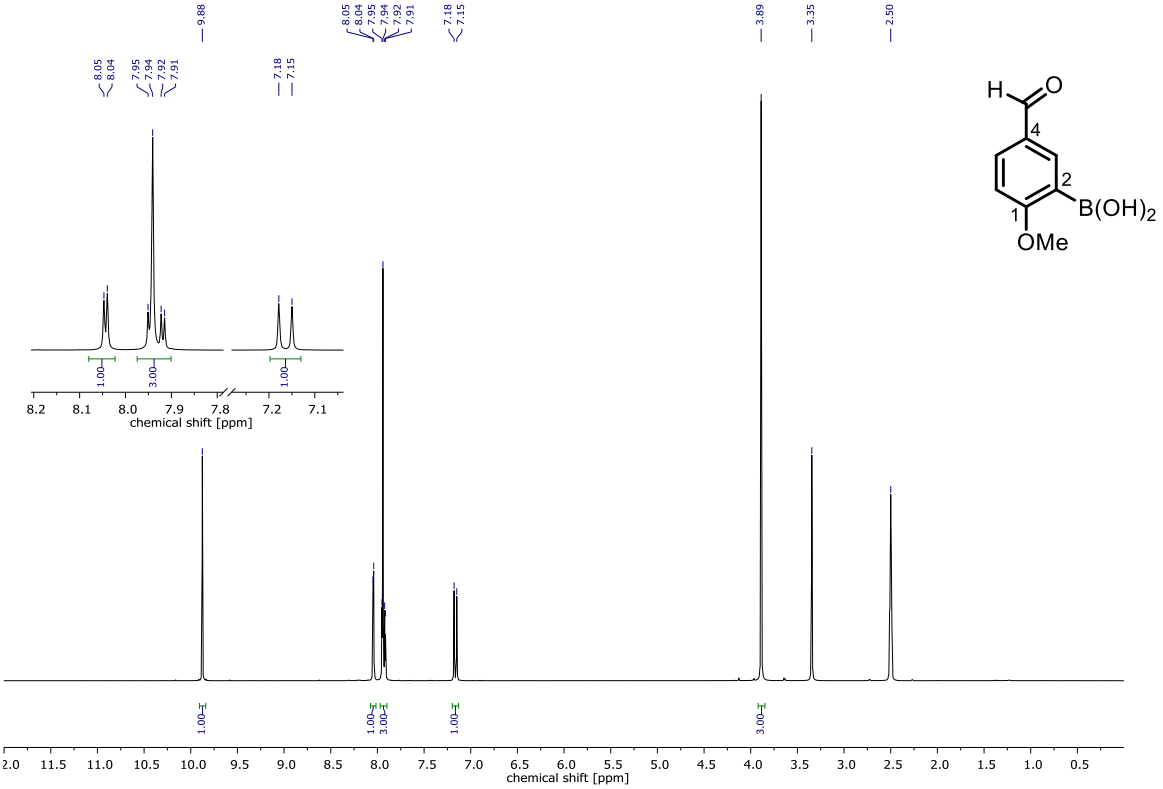

Figure 56: ^{1}H-NMR spectrum (300 MHz, DMSO-d_6, 296 K) of **121**.

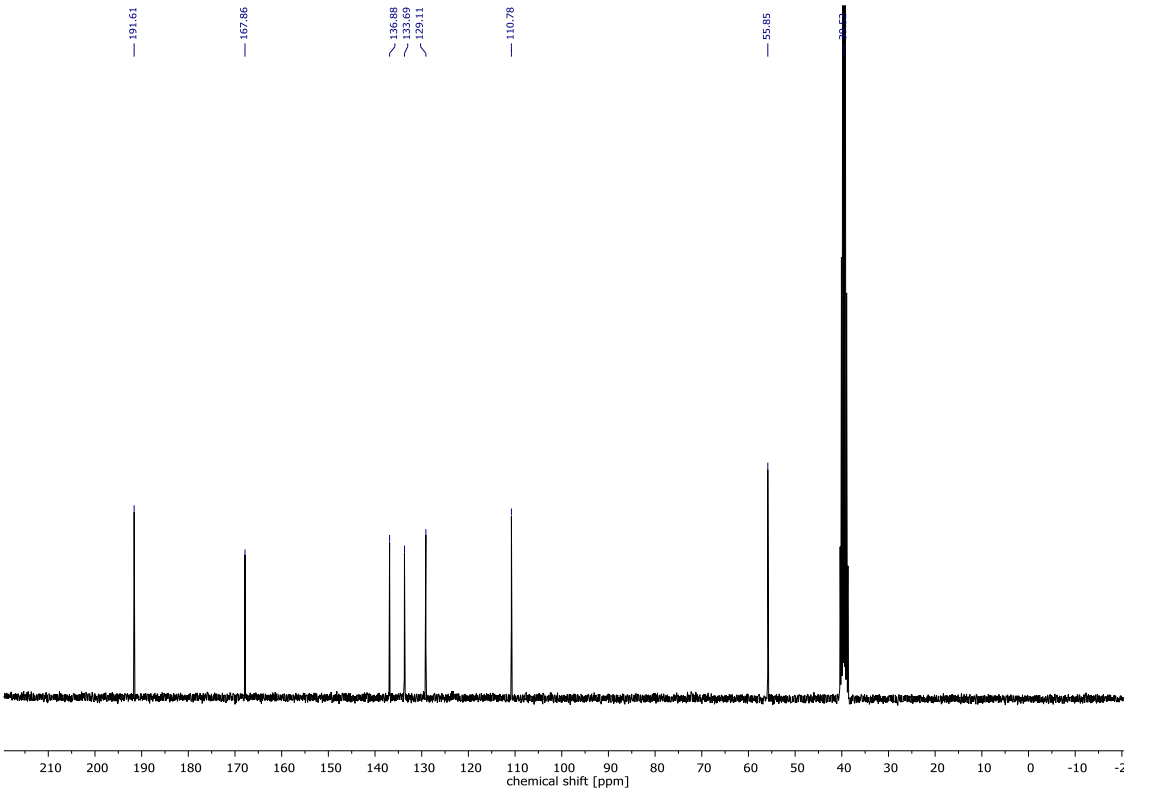

Figure 67: ^{13}C-NMR spectrum (76 MHz, DMSO-d_6, 297 K) of **121**.

Methyl-protected rubrolide R 134

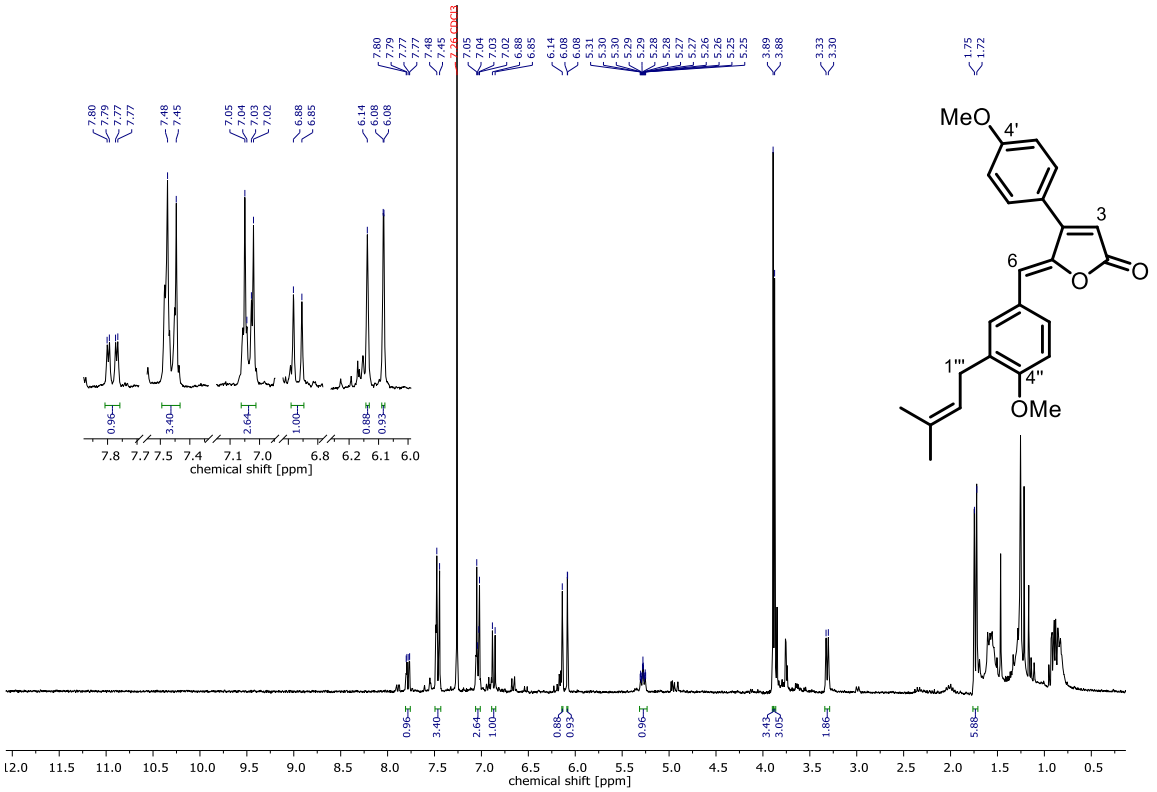

Figure 78: ^{1}H-NMR spectrum (300 MHz, DMSO-d_6, 298 K) of **134**.

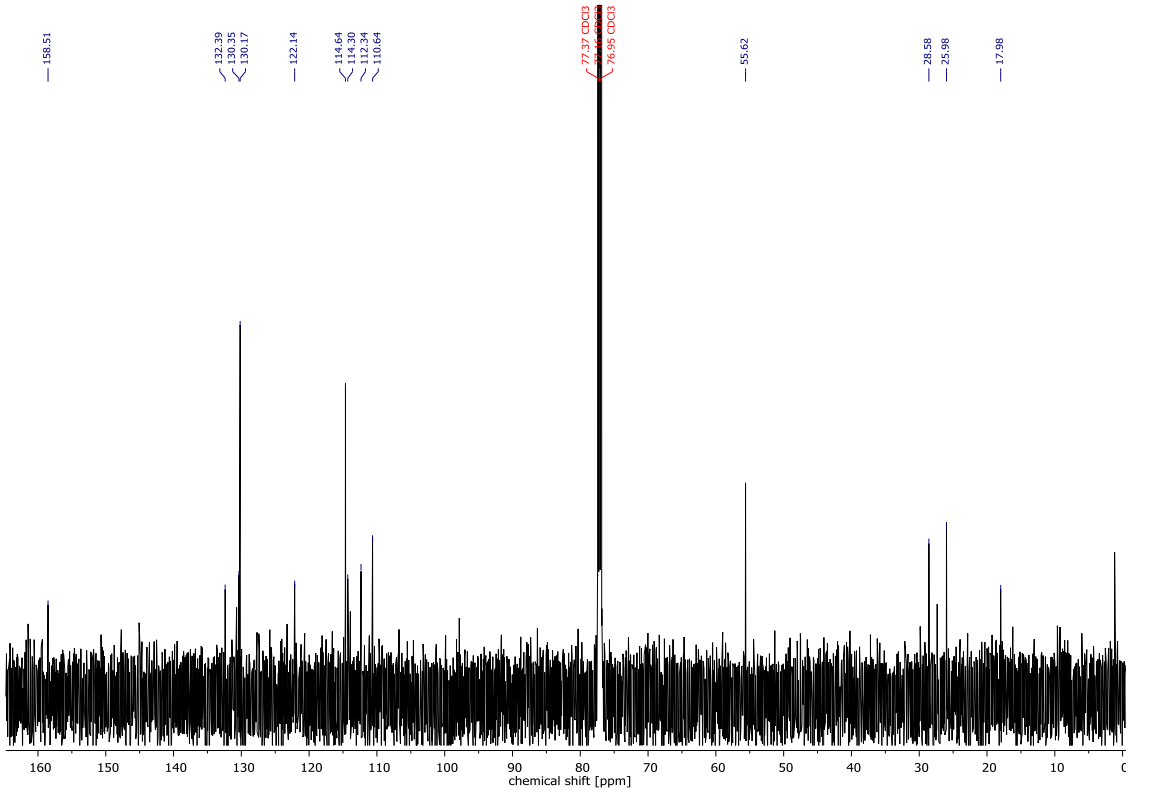

Figure 99: ^{13}C-NMR spectrum (151 MHz, DMSO-d_6, 298 K) of **134**.

Rubrolide R 12

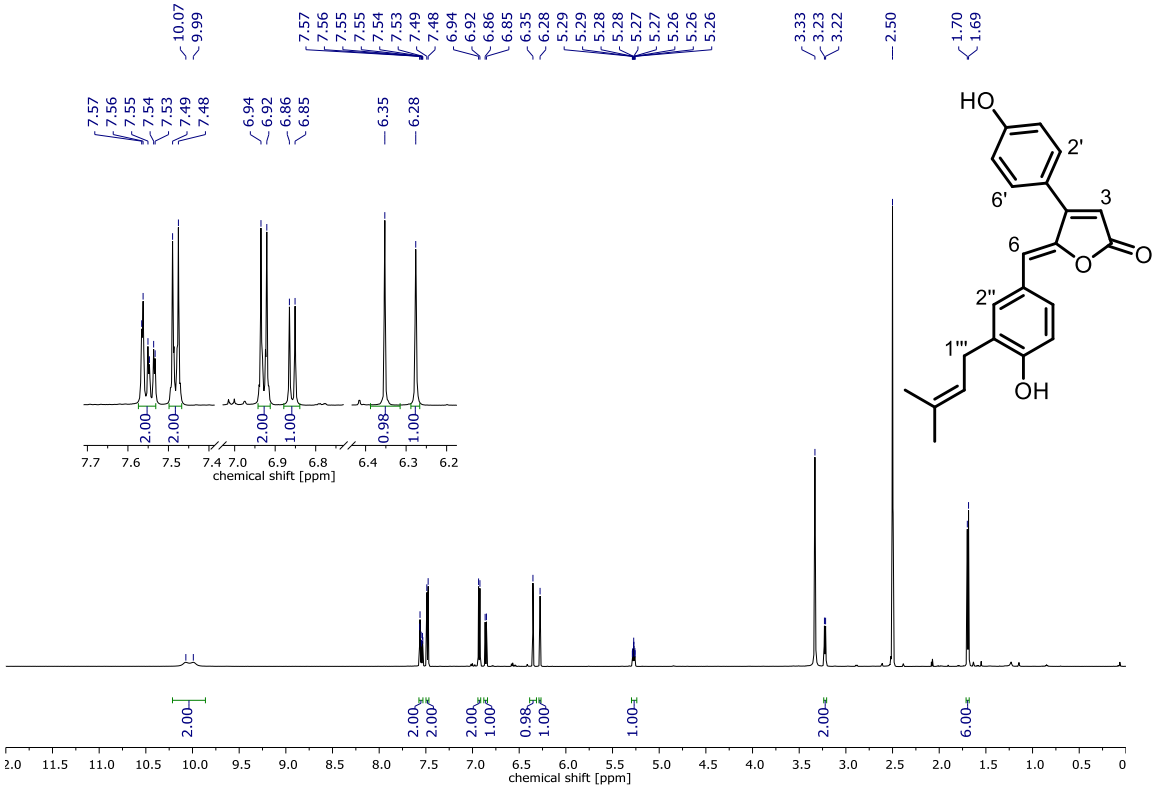

Figure 80: ^{1}H-NMR spectrum (600 MHz, DMSO-d_6, 298 K) of **12**.

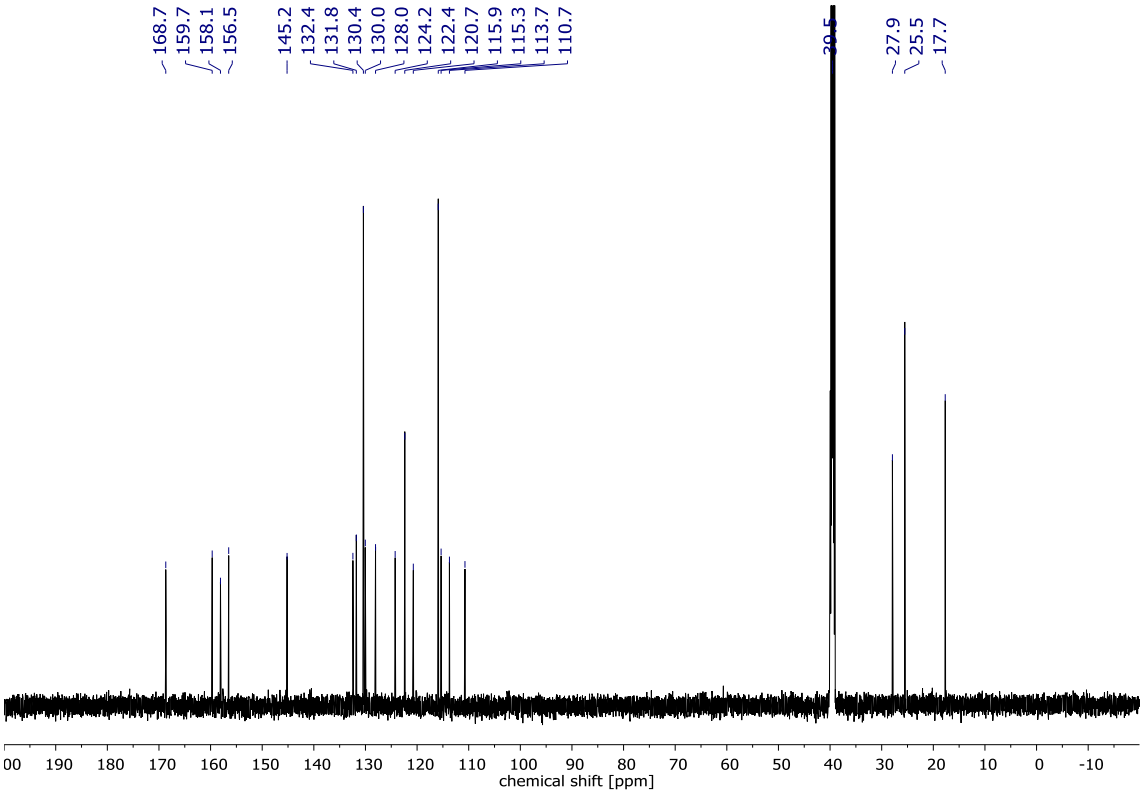

Figure 9: ^{13}C-NMR spectrum (151 MHz, DMSO-d_6, 298 K) of **12**.

Catechol-rubrolide R 174

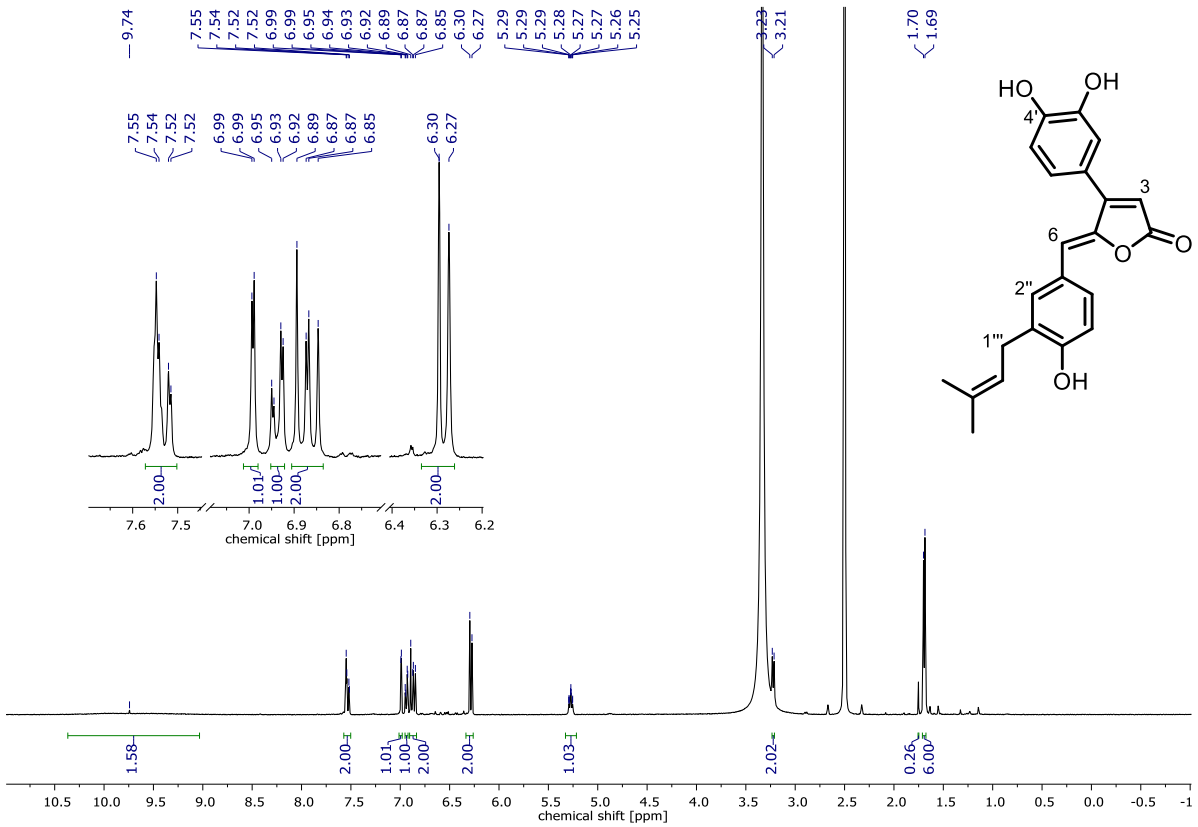

Figure 10: ^{1}H-NMR spectrum (400 MHz, DMSO-d_6, 296 K) of **174**.

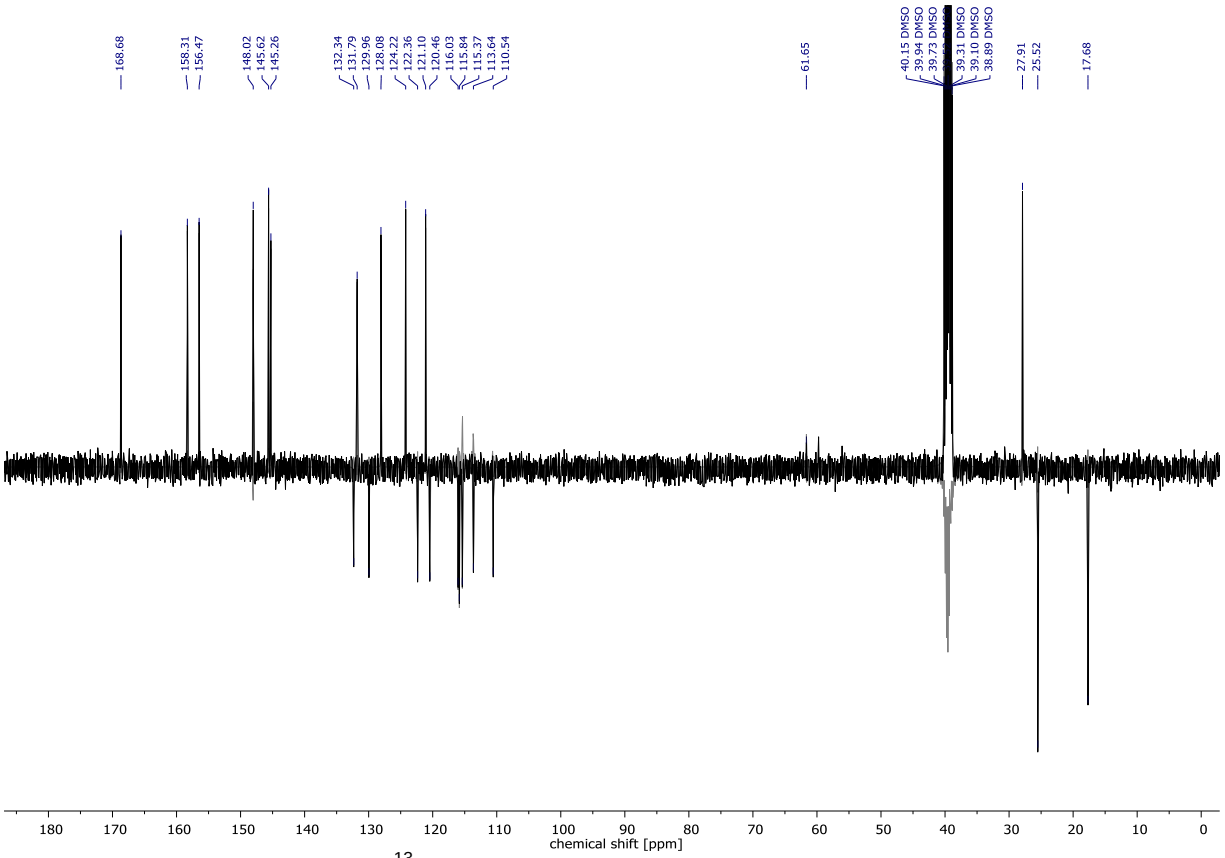

Figure 11: ^{13}C-NMR spectrum (101 MHz, DMSO-d_6, 296 K) of **174**.

Fluoro-rubrolide R 178

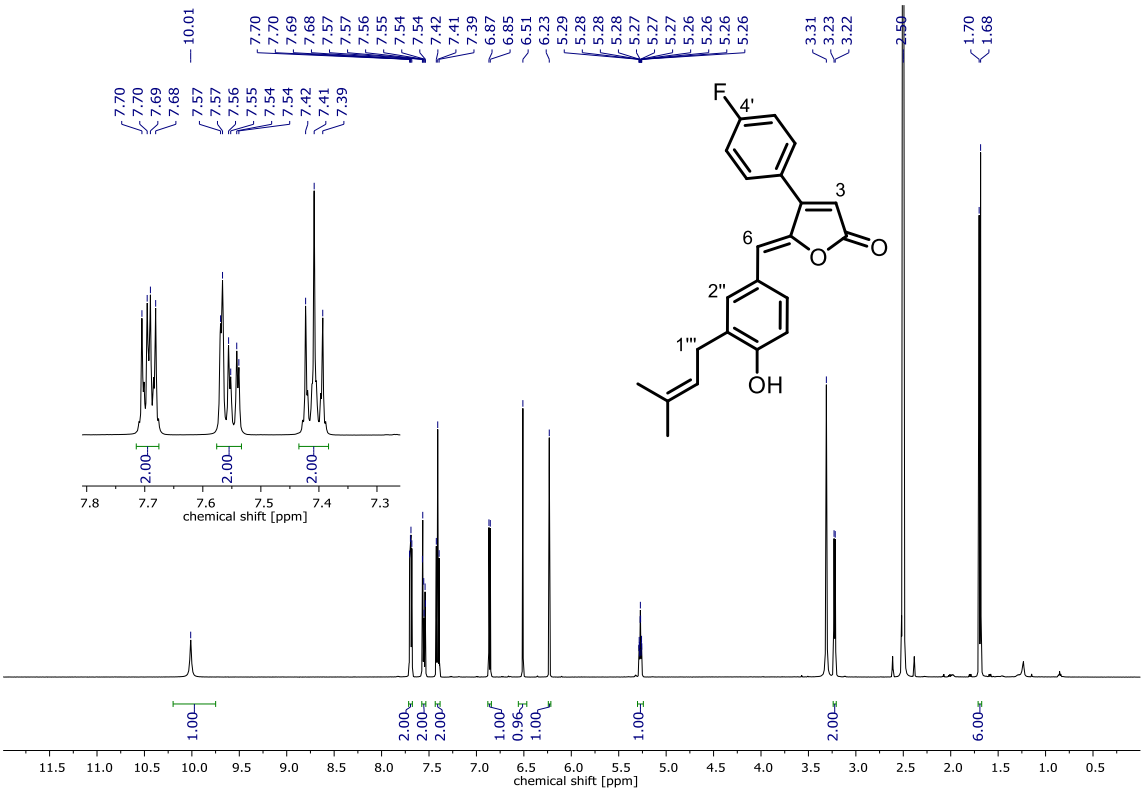

Figure 12: ^{1}H-NMR spectrum (600 MHz, DMSO-d_6, 300 K) of **178.**

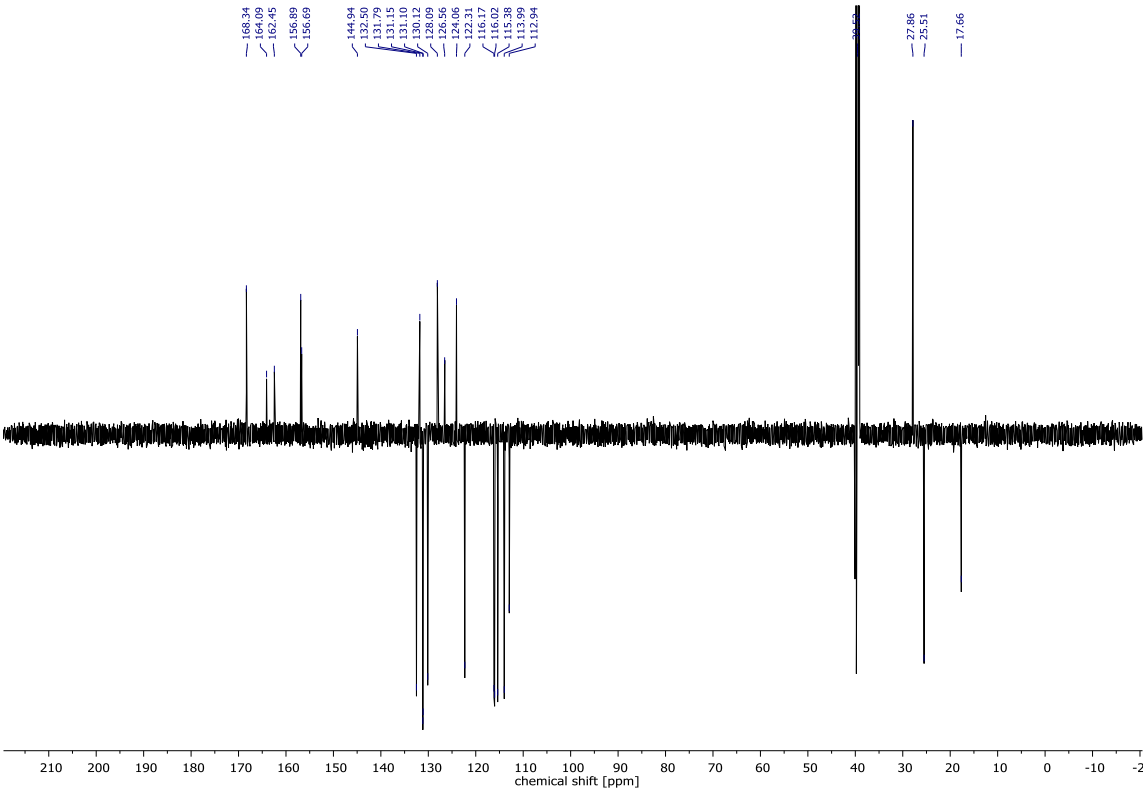

Figure 13: DEPTQ-NMR spectrum (151 MHz, DMSO-d_6, 300 K) of **178**.

N-Acetyl-rubrolide R 176

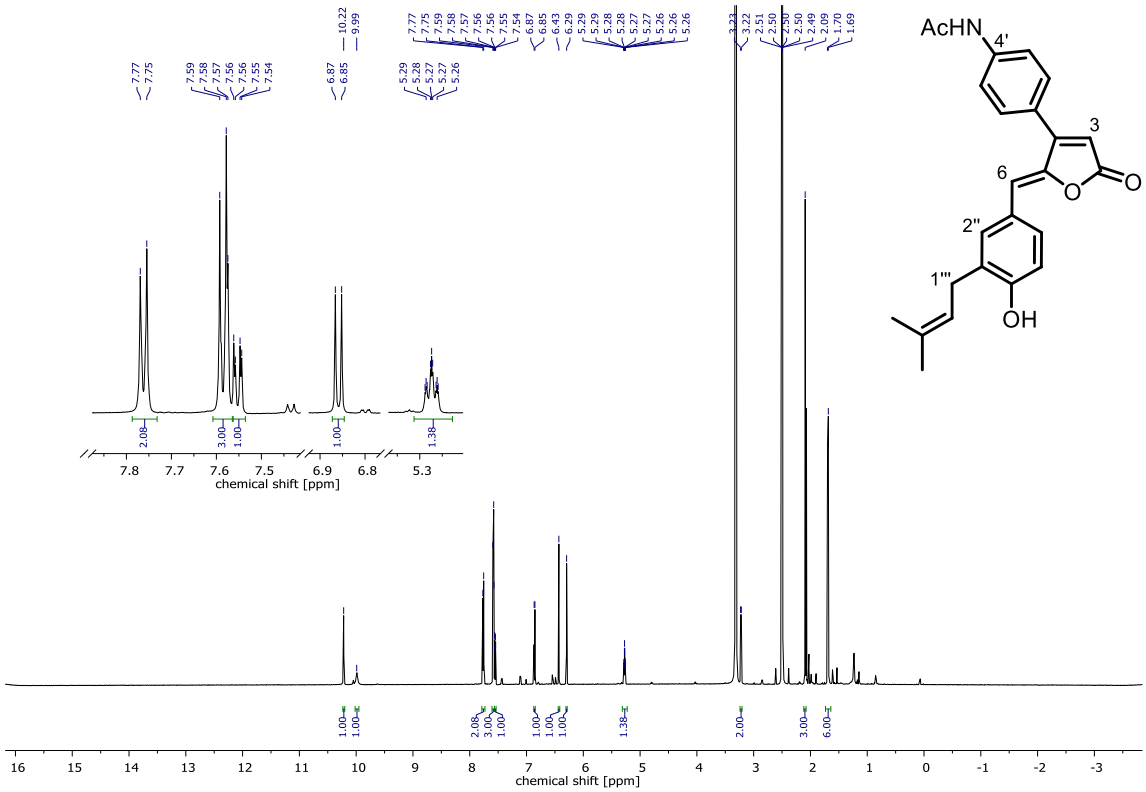

Figure 14: ^{1}H-NMR spectrum (600 MHz, DMSO-d_6, 300 K) of **176**.

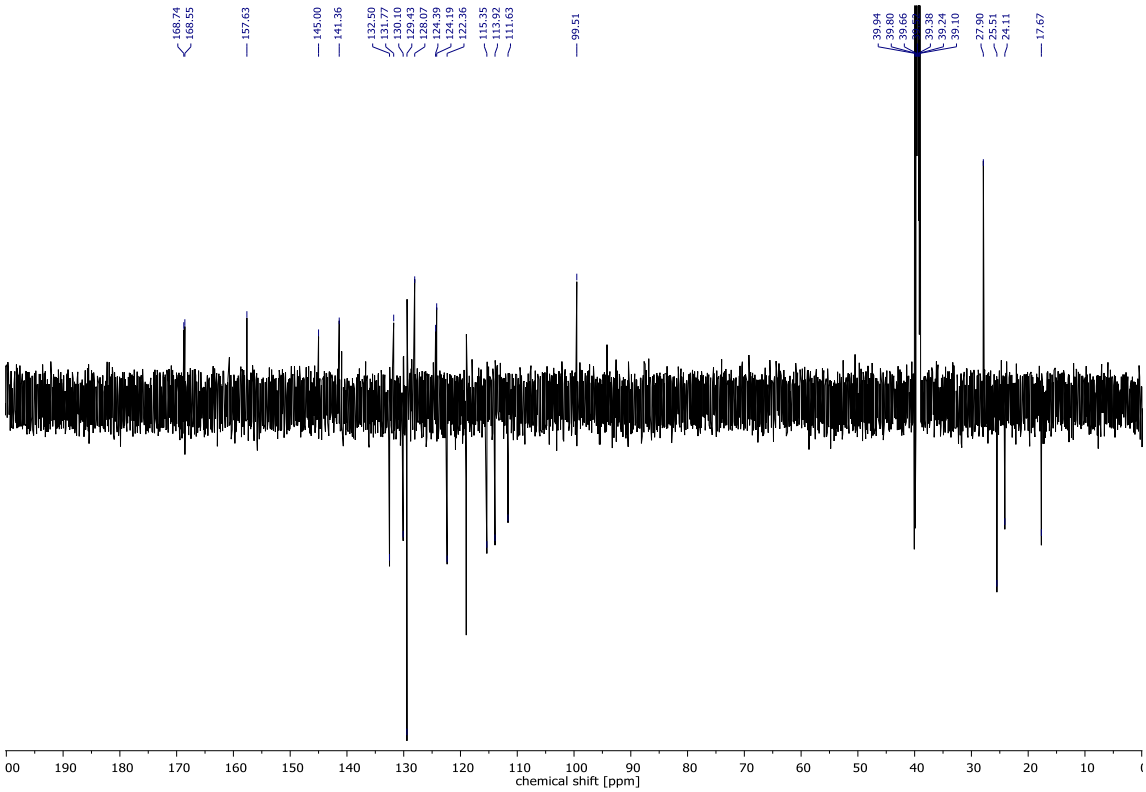

Figure 15: ^{13}C-NMR spectrum (151 MHz, DMSO-d_6, 300 K) of **176**.

Rubrolide S 13

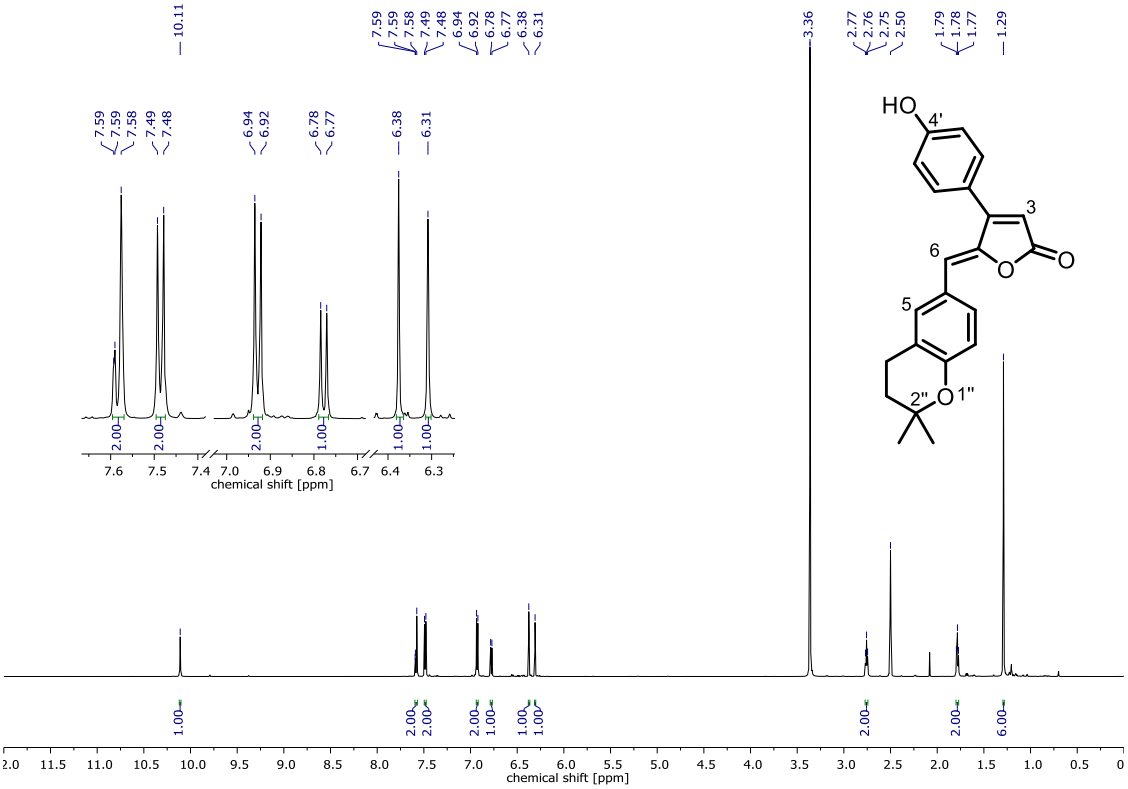

Figure 16: ^{1}H-NMR spectrum (600 MHz, DMSO-d_6, 298 K) of **13**.

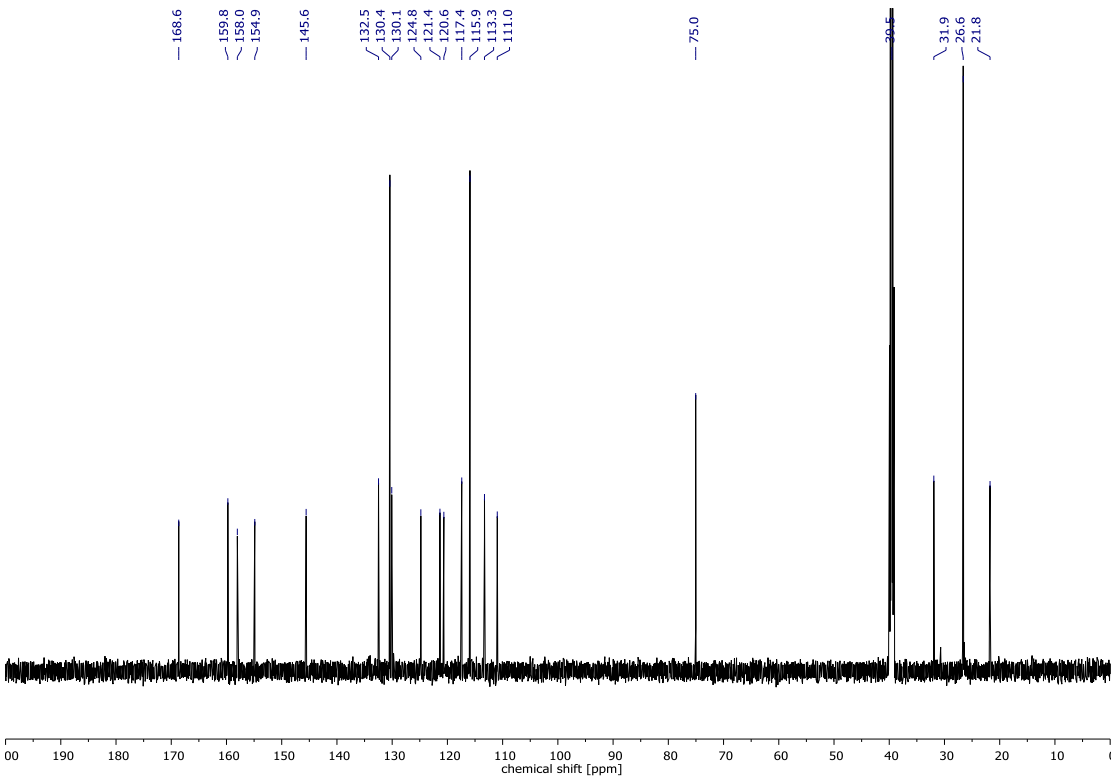

Figure 17: ^{13}C-NMR spectrum (151 MHz, DMSO-d_6, 300 K) of **13**.

Catechol-rubrolide S 175

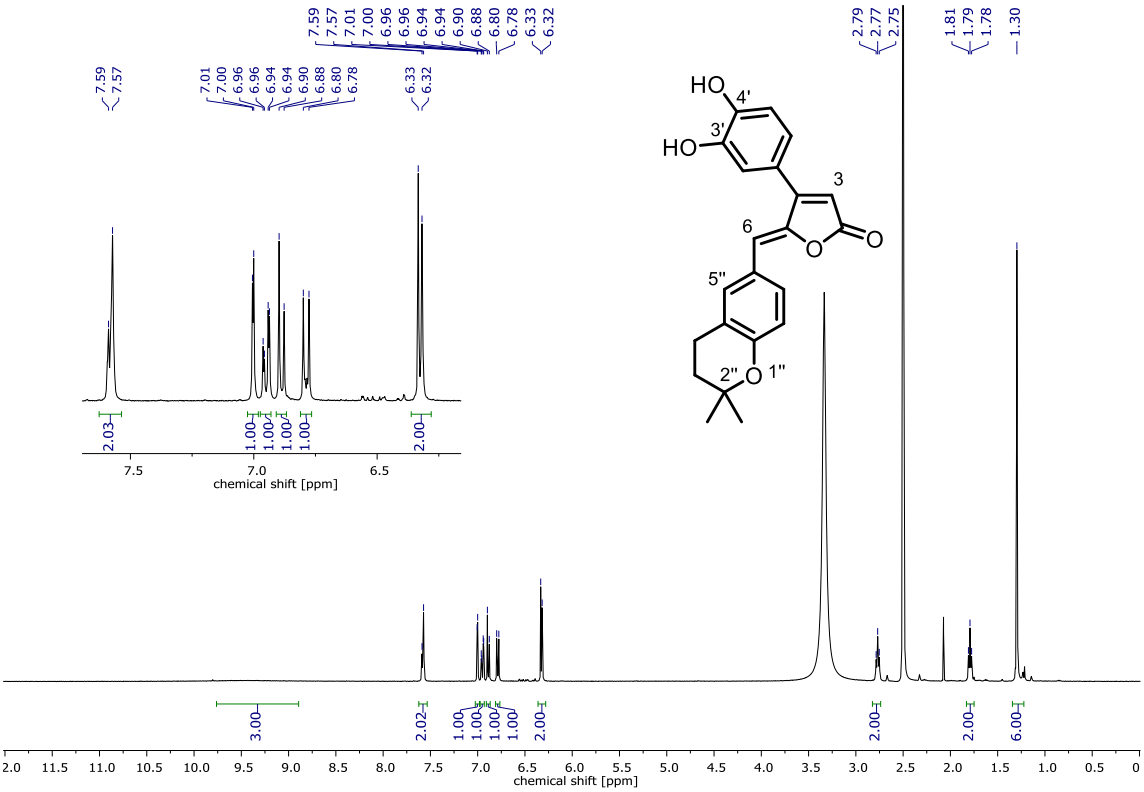

Figure 110: ^{1}H-NMR spectrum (400 MHz, DMSO-d_6, 296 K) of **175**.

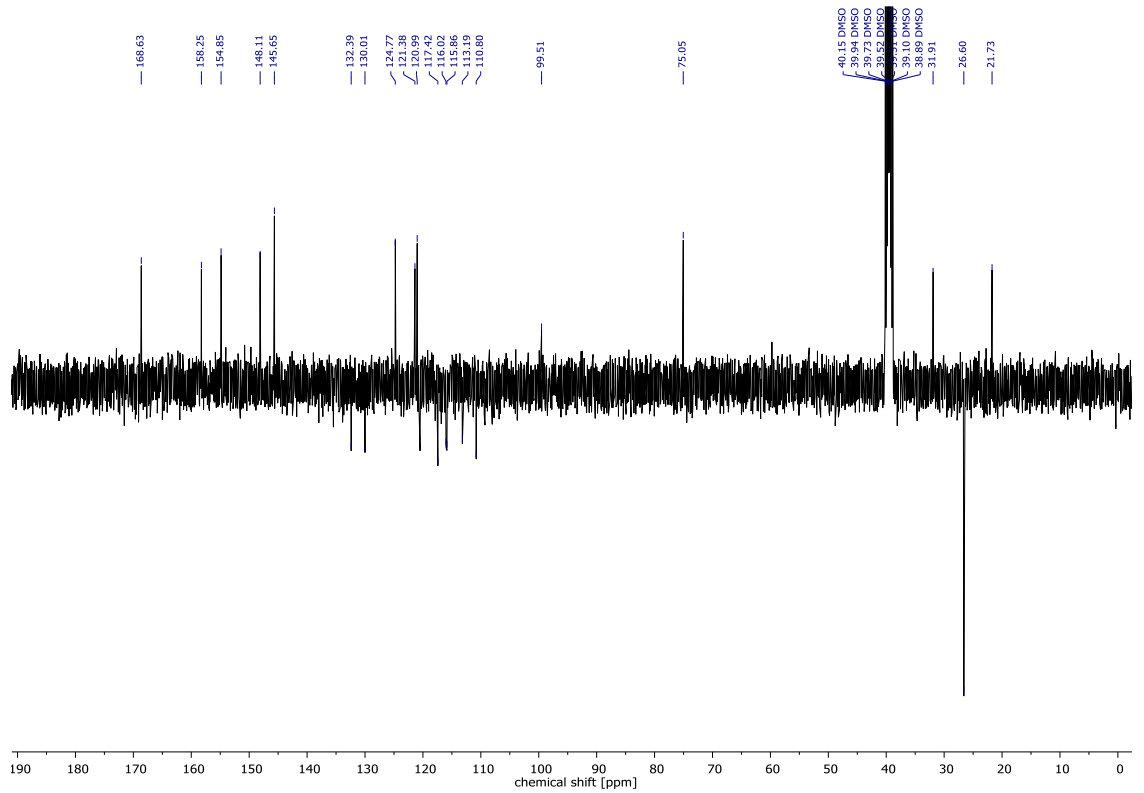

Figure 111: DEPTQ-NMR spectrum (101 MHz, DMSO-d_6, 298 K) of **175**.

Fluoro-rubrolide S 179

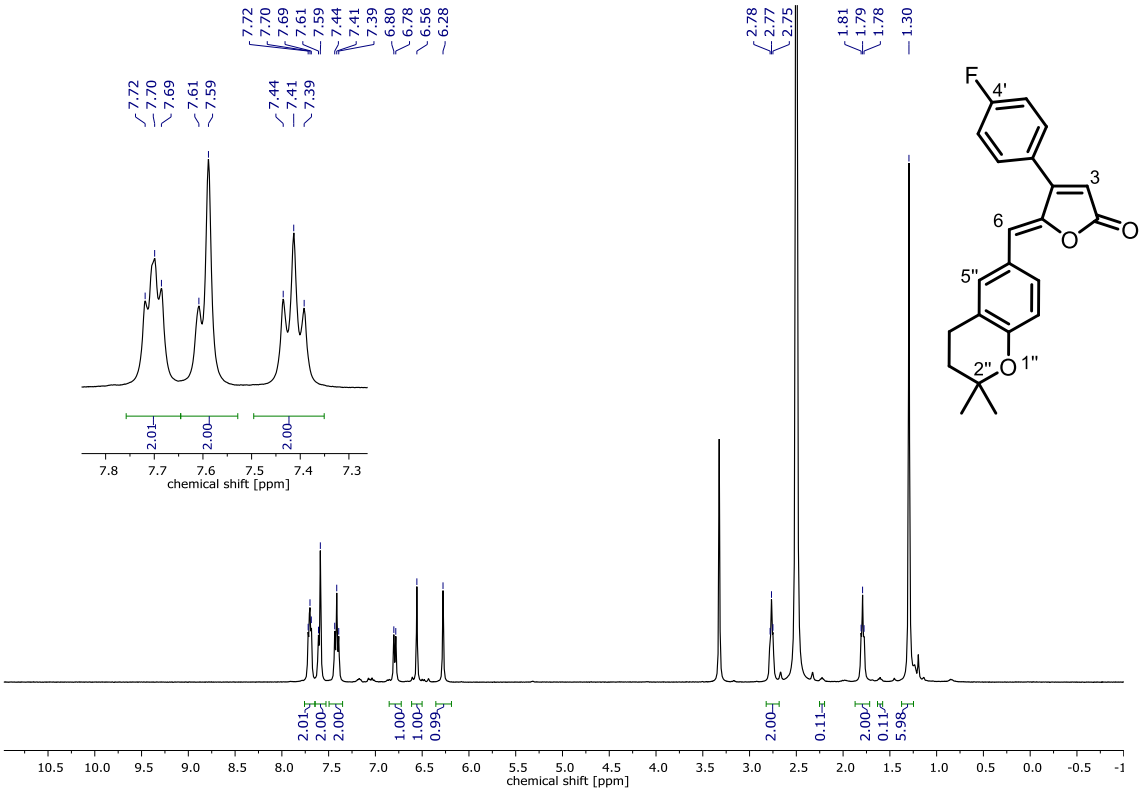

Figure 112: ^{1}H-NMR spectrum (400 MHz, DMSO-d_6, 296 K) of **279**.

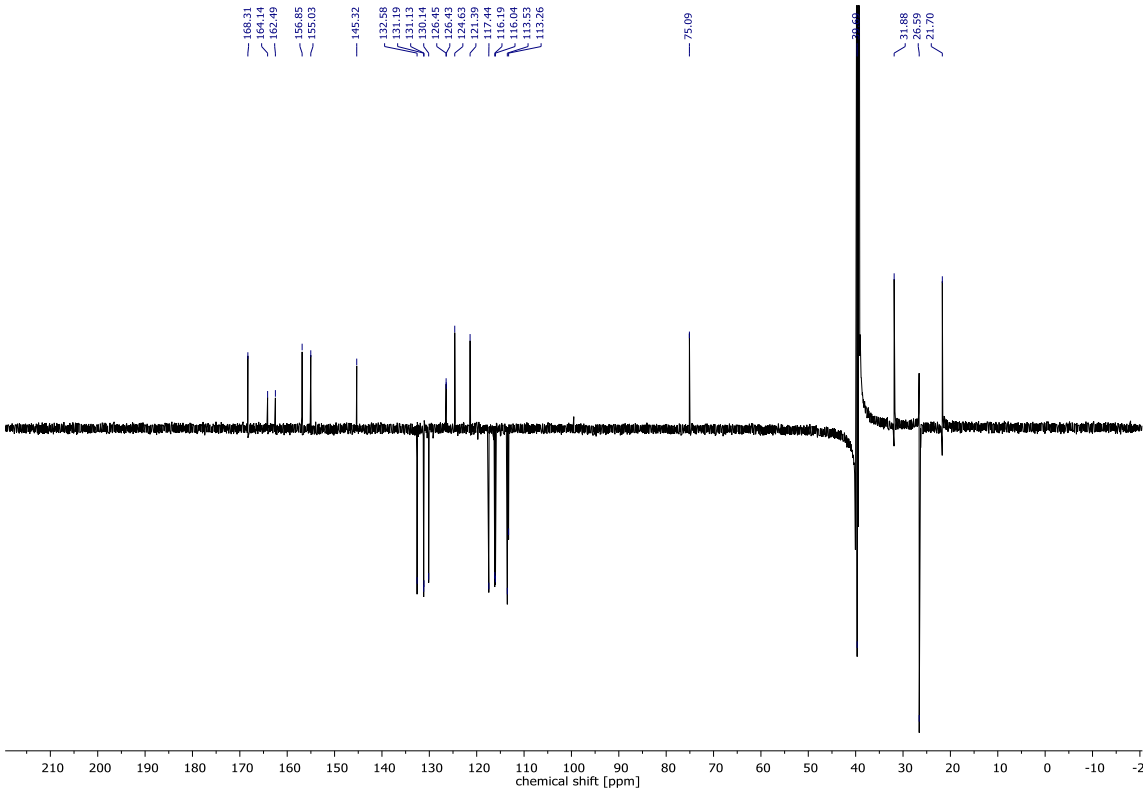

Figure 113: DEPTQ-NMR spectrum (151 MHz, DMSO-d_6, 300 K) of **279**.

N-Acetyl-rubrolide S 177

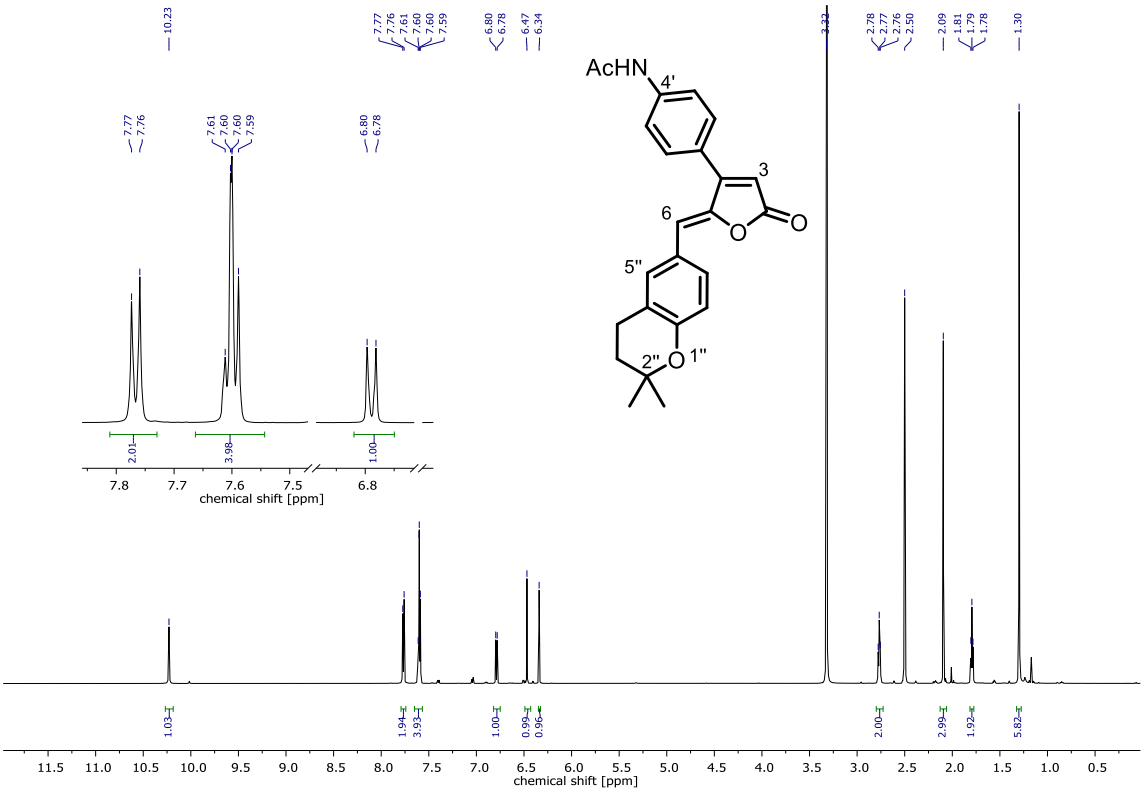

Figure 114: ^{1}H-NMR spectrum (600 MHz, DMSO-d_6, 300 K) of **177**.

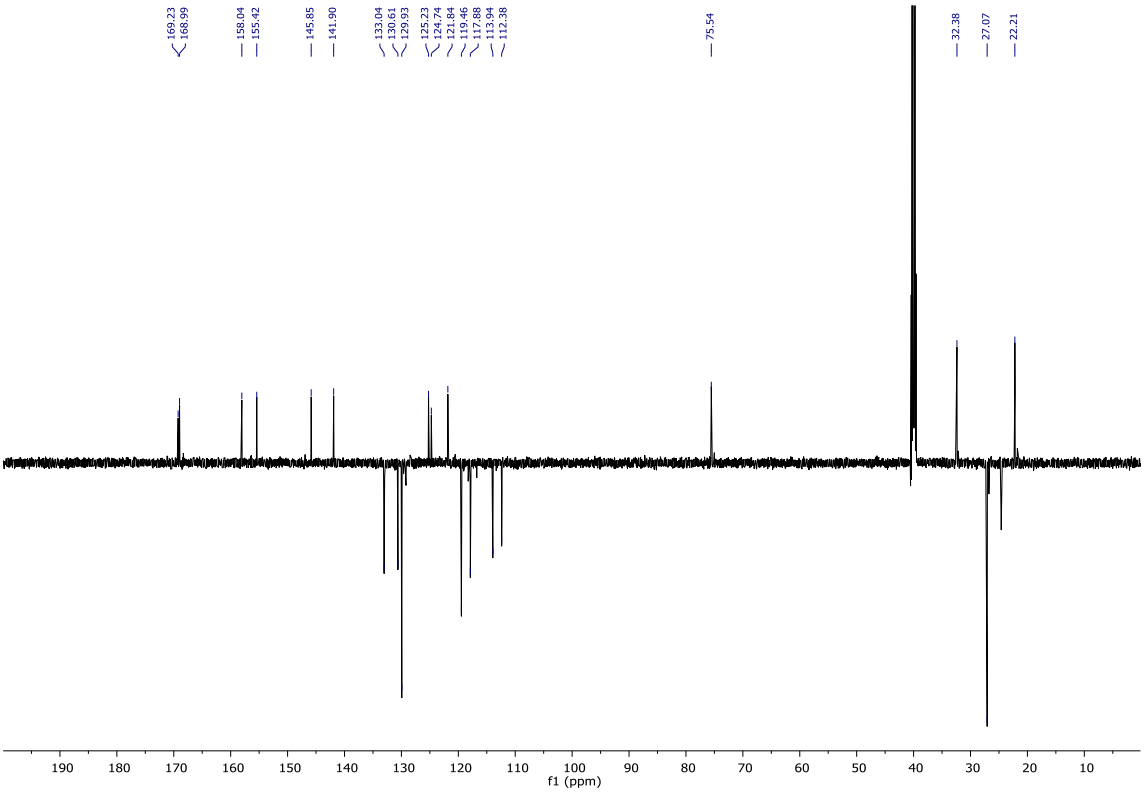

Figure 115: DEPTQ-NMR spectrum (151 MHz, DMSO-d_6, 300 K) of **177**.

Nitro-rubrolide S 181

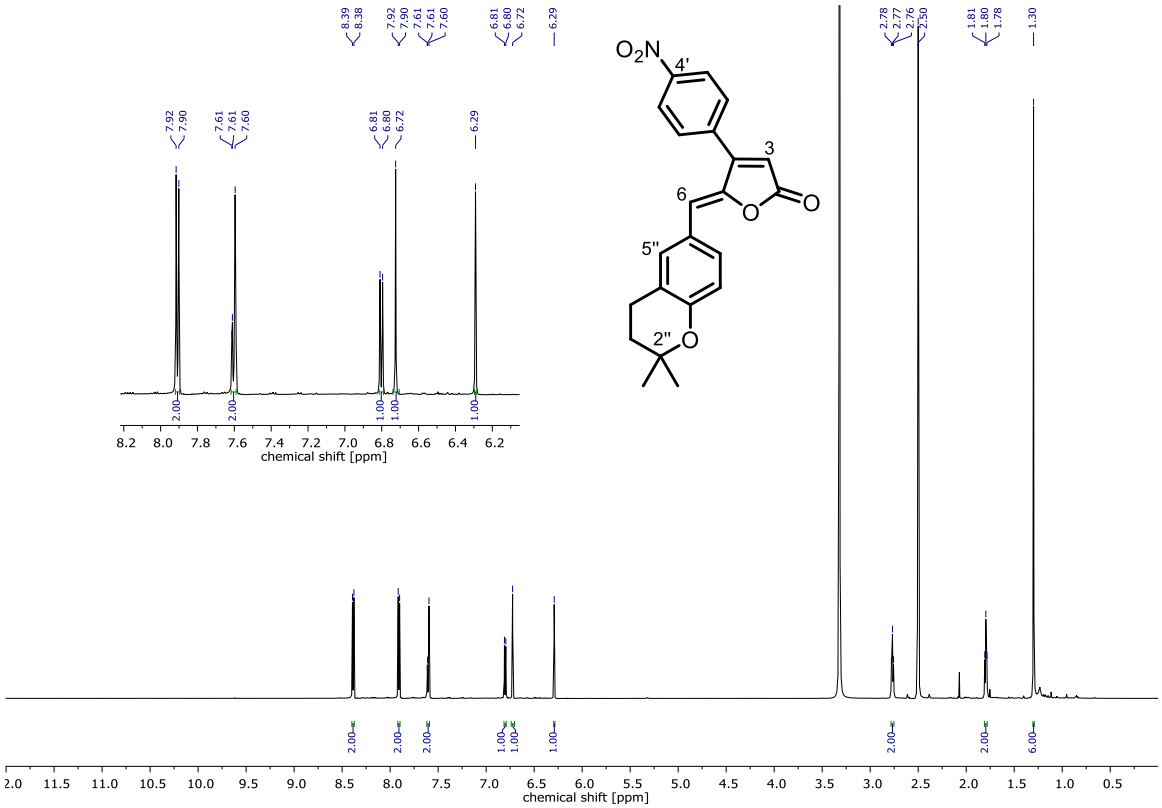

Figure 116: ^{1}H-NMR spectrum (600 MHz, DMSO-d_6, 300 K) of **181**.

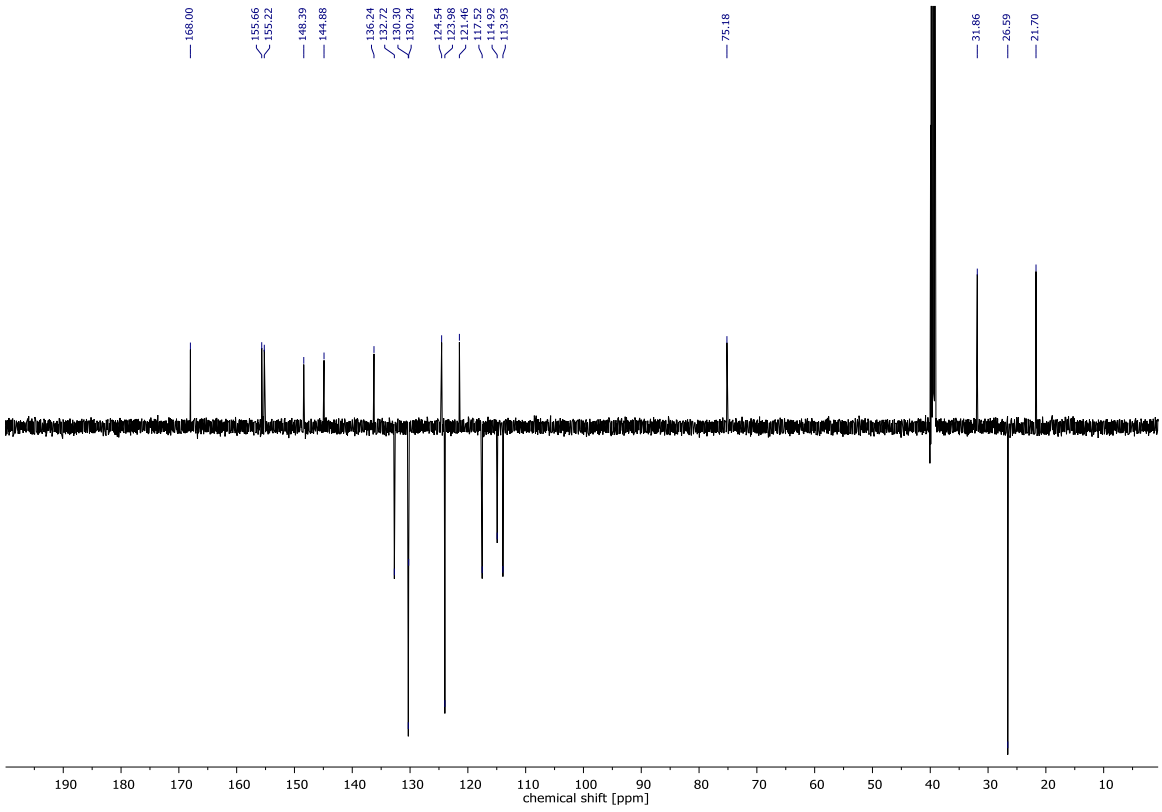

Figure 117: DEPTQ-NMR spectrum (151 MHz, DMSO-d_6, 300 K) of **181**.

Per(OAc)- *α/β*-D-mannosyl- rubrolide S 188

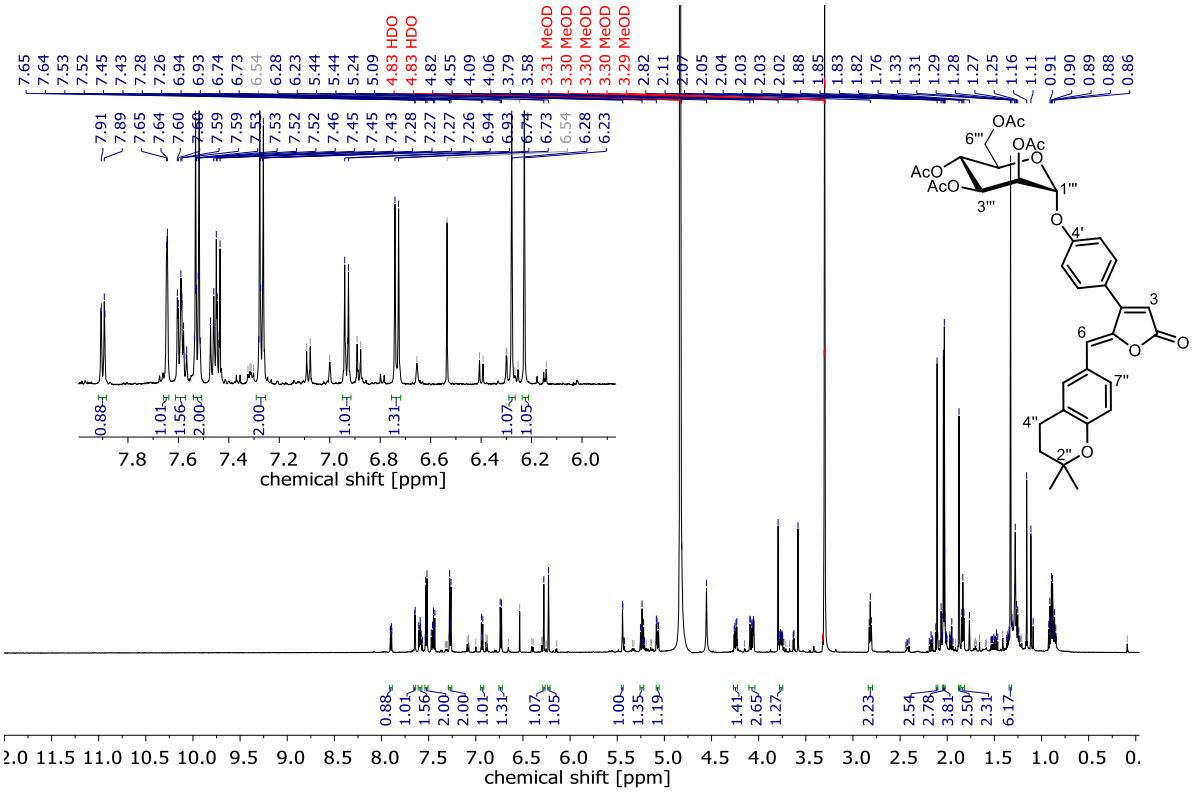

Figure 118: ^{1}H-NMR spectrum (600 MHz, methanol-d_4, 300 K) of **188**.

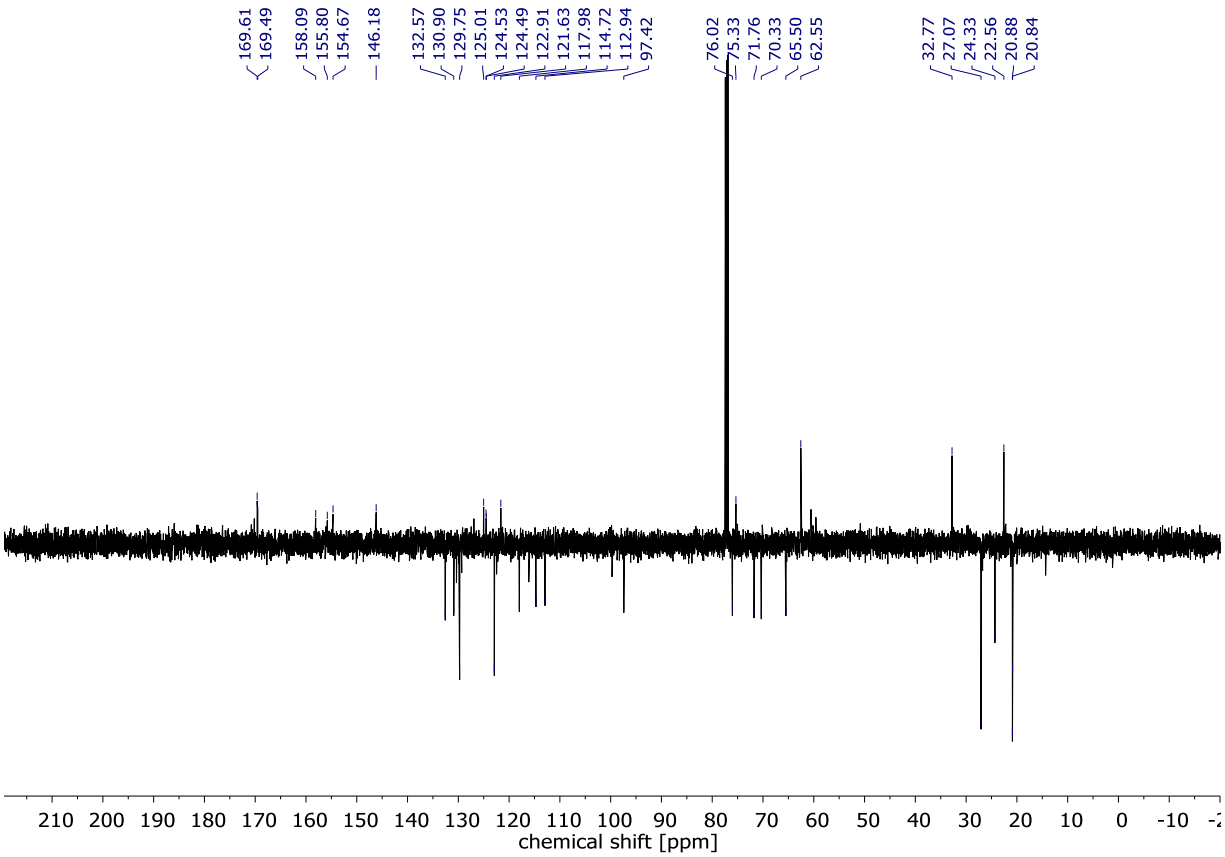

Figure 119: DEPTQ spectrum (126 MHz, $CDCl_3$-d, 296 K) of **188**.

1,2-Diphenylethyne 189

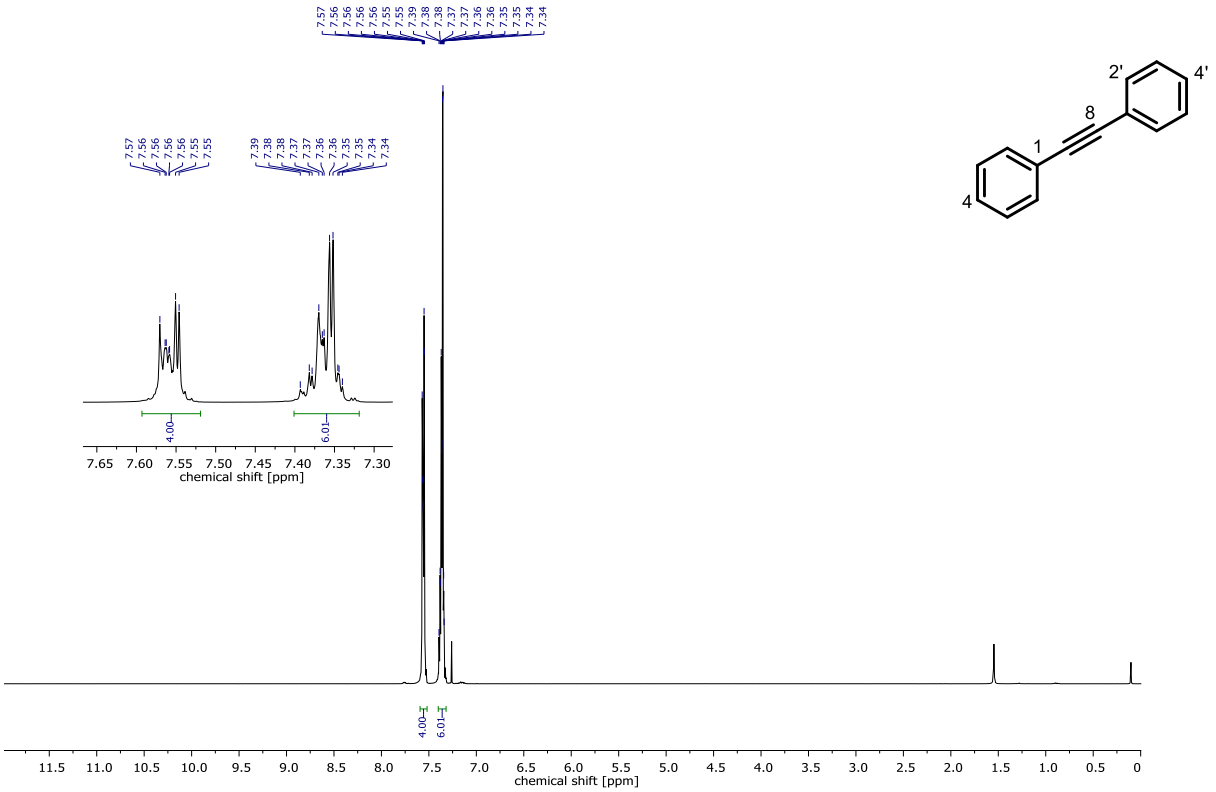

Figure 120: ^{1}H-NMR spectrum (400 MHz, $CDCl_3$, 298K) of **189**.

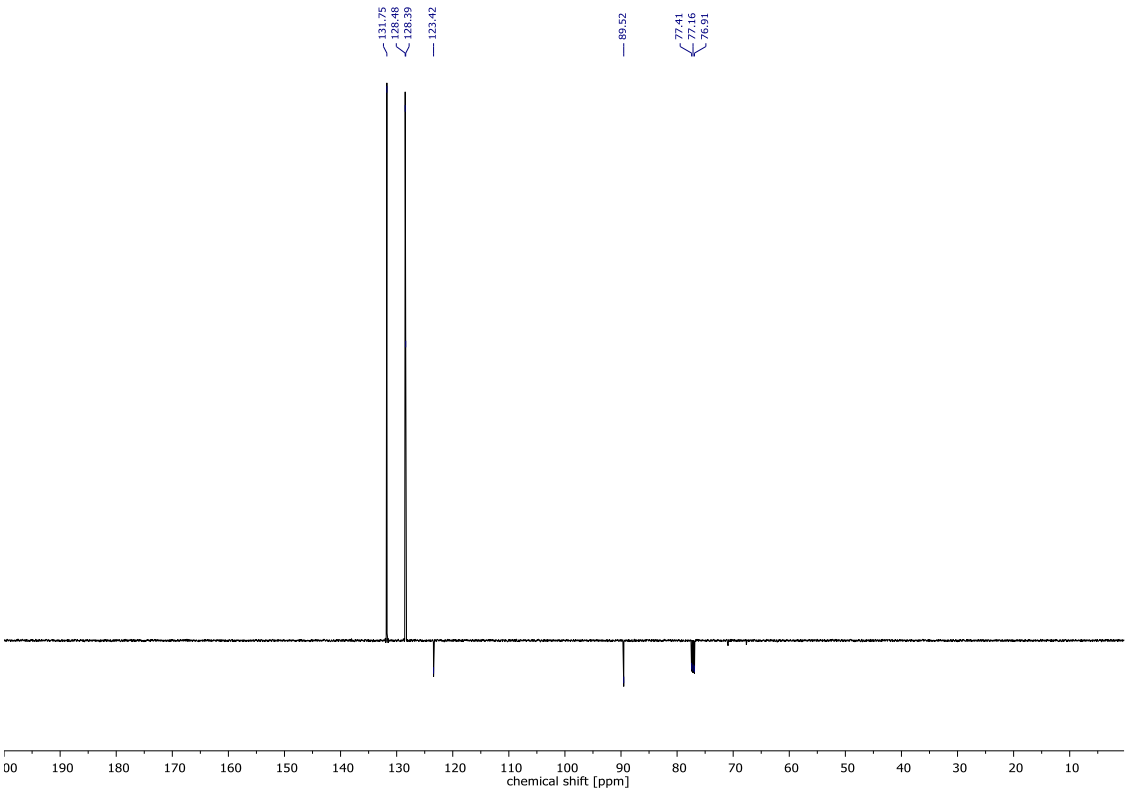

Figure 121: DEPTQ spectrum (126 MHz, $CDCl_3$, 298K) of **189**.

2-Bis(4-methoxyphenyl)ethyne 190

Figure 122: ^{1}H-NMR spectrum (500 MHz, $CDCl_3$, 298K) of **190**.

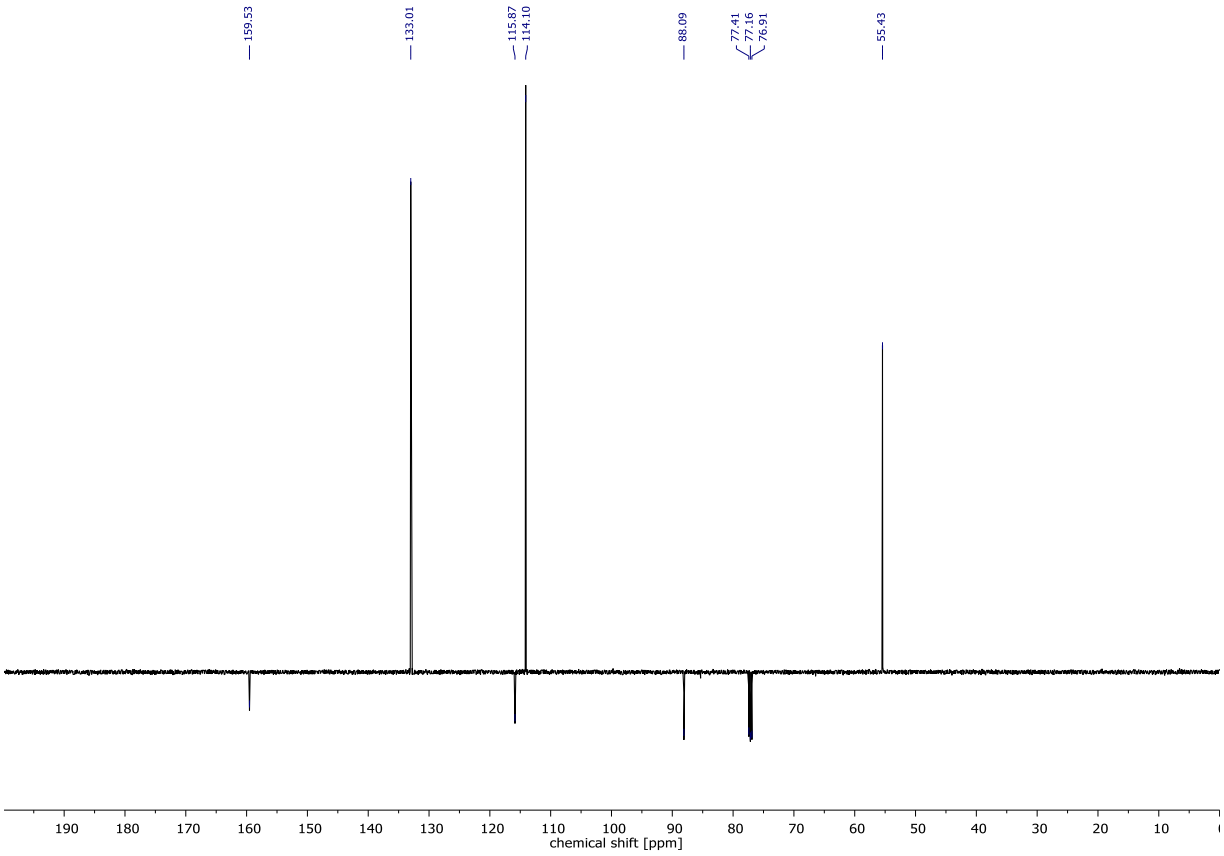

Figure 123: DEPTQ-NMR spectrum (126 MHz, $CDCl_3$, 298K) of **190**.

(*Z*)-1,2-Diphenyl-1,2-bis(4,4,5,5-tetramethyl-1,3,2-dioxaborolan-2-yl)ethane 200

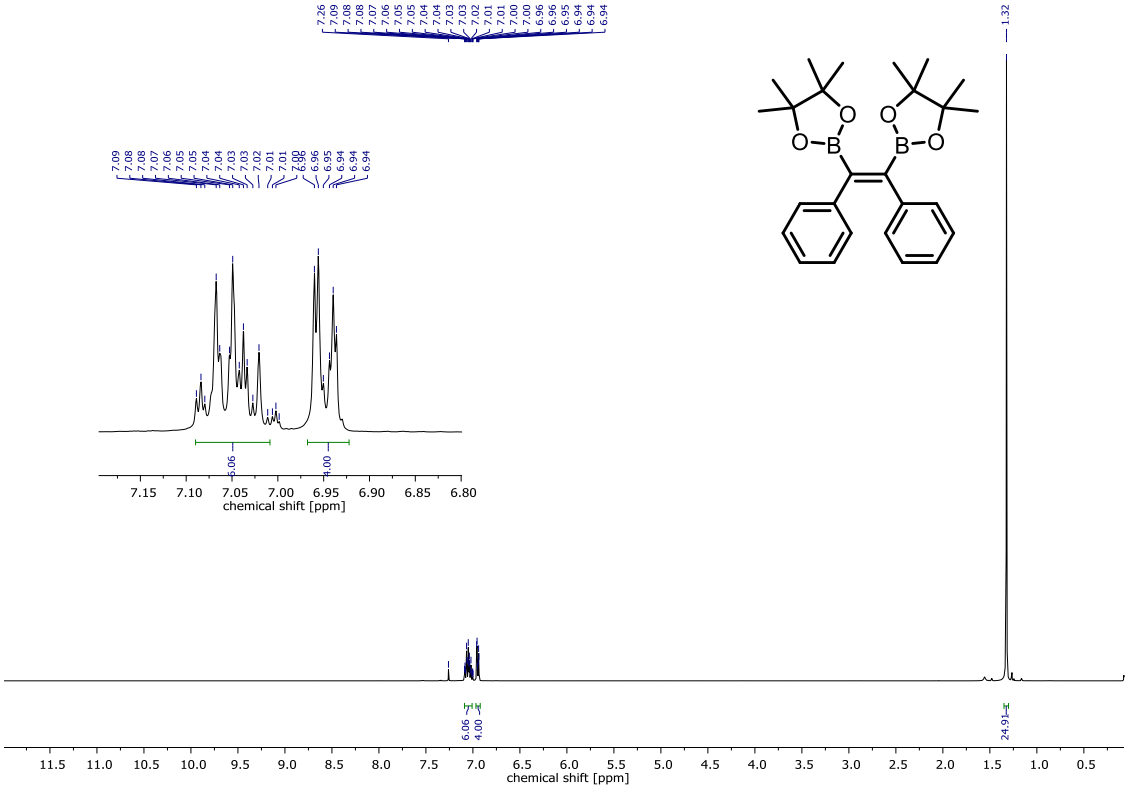

Figure 124: ^{1}H-NMR spectrum (400 MHz, $CDCl_3$-*d*, 298K) of **200**.

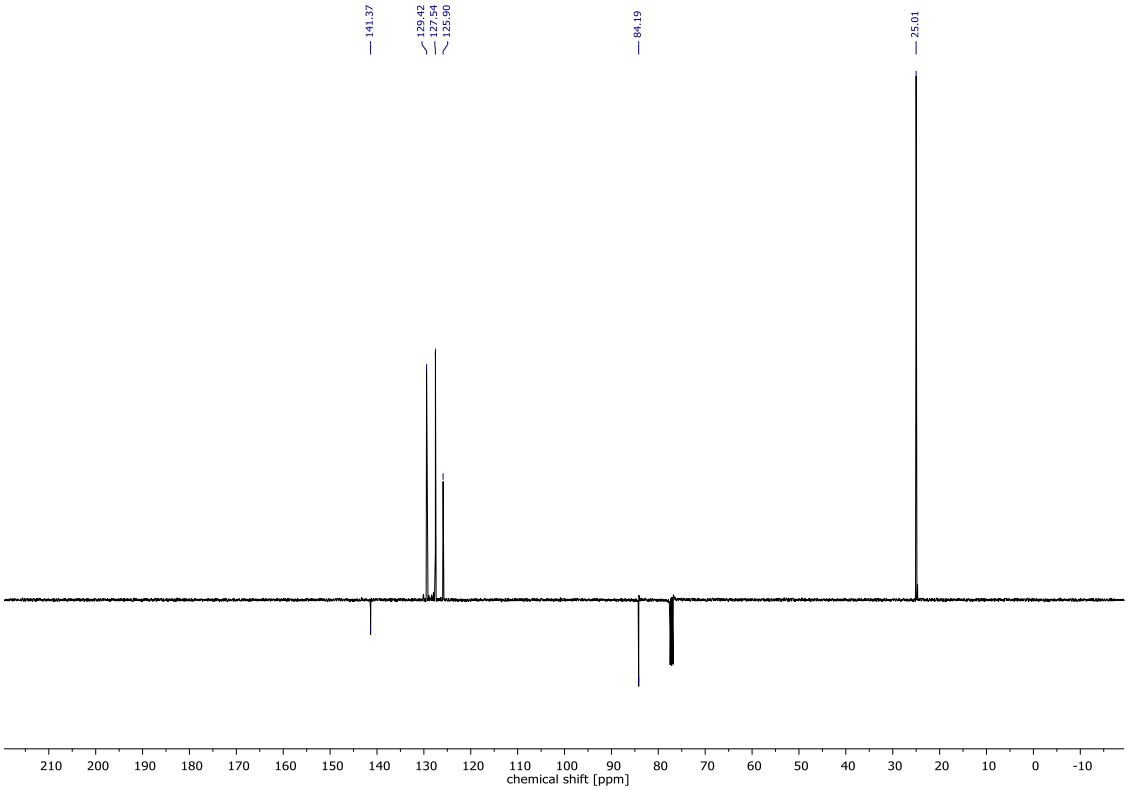

Figure 125: DEPTQ-NMR spectrum (101 MHz, $CDCl_3$-*d*, 294K) of **200**.

(*Z*)-1,2-Diphenyl-1,2-bis(4,4,5,5-tetramethyl-1,3,2-dioxaborolan-2-yl)ethane 125

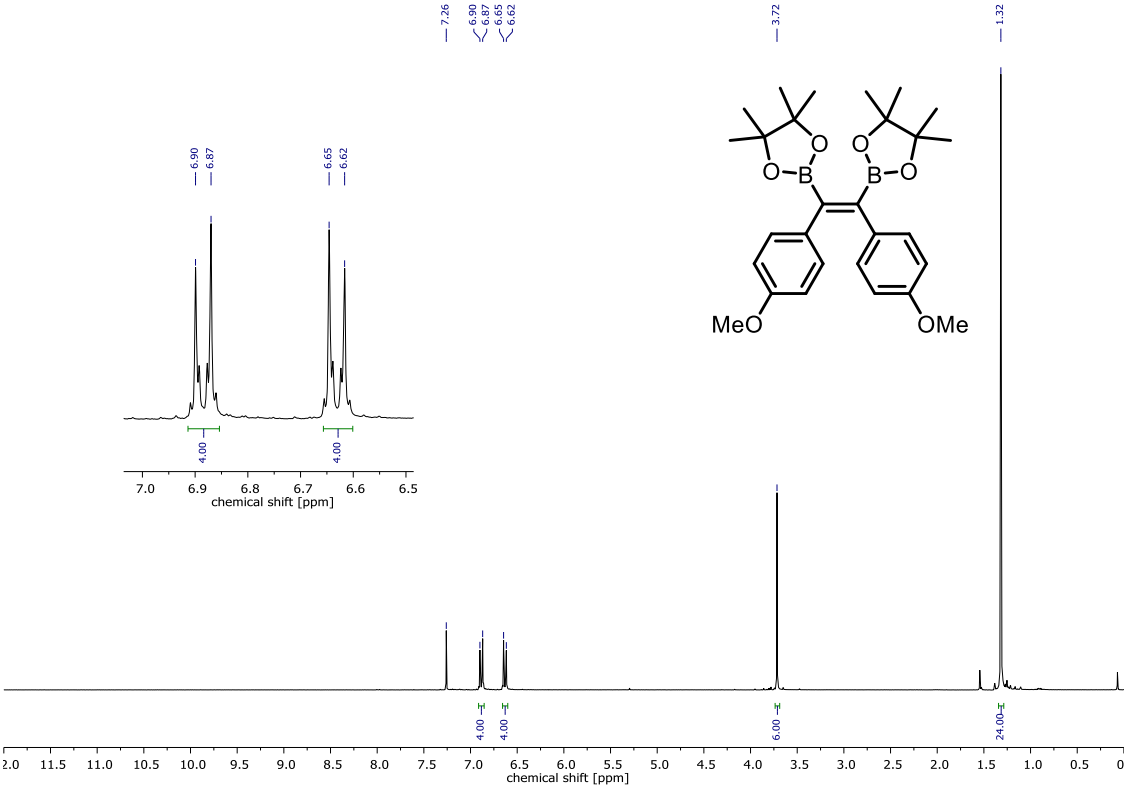

Figure 126: ^{1}H-NMR spectrum (300 MHz, $CDCl_3$-*d*, 298K) of **125**.

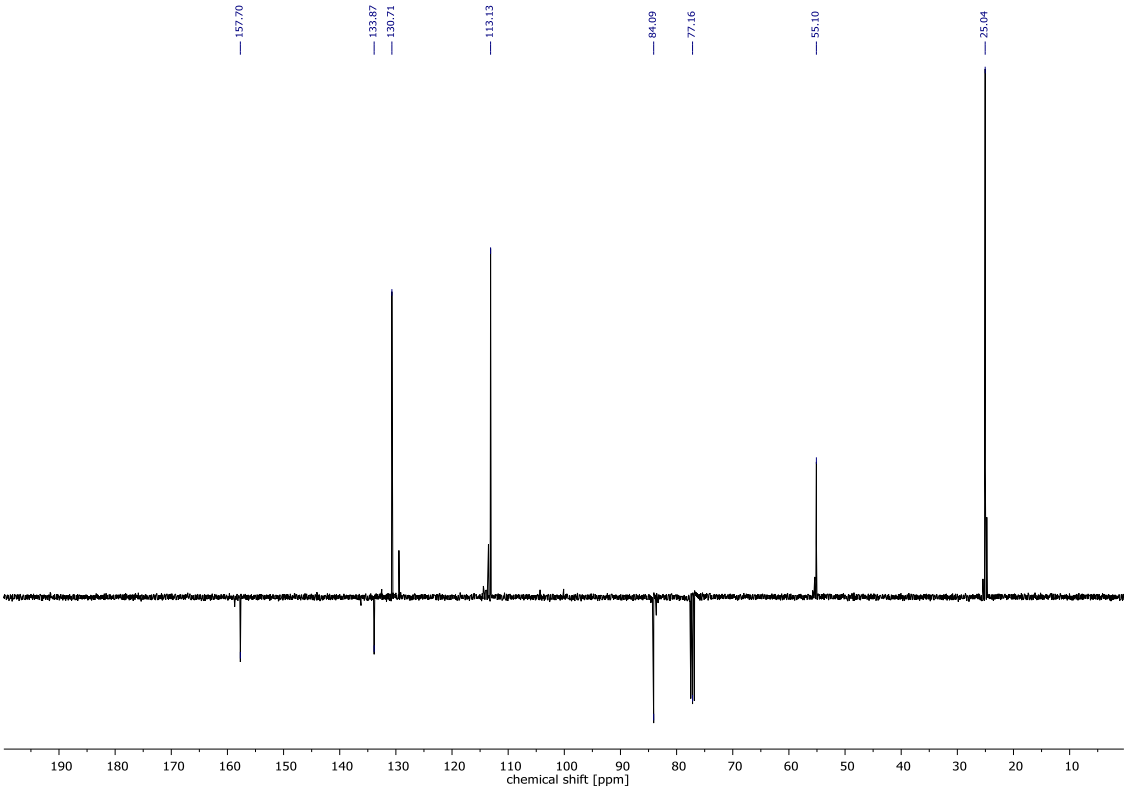

Figure 127: DEPTQ-NMR spectrum (101 MHz, $CDCl_3$-*d*, 295K) of **125**.

(*Z*)-1,2-Bis(5,5-dimethyl-1,3,2-dioxaborinan-2-yl)-1,2-diphenylethene 201

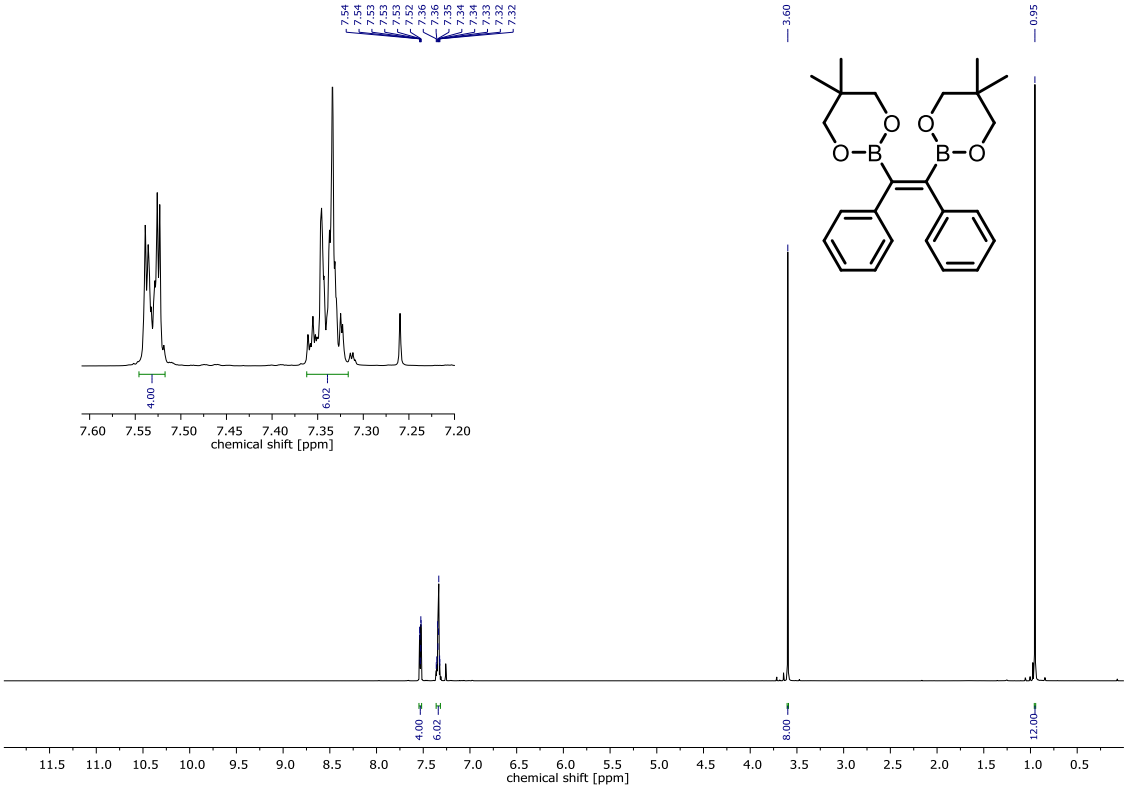

Figure 128: ^{1}H-NMR spectrum (600 MHz, $CDCl_3$, 300K) of **201**.

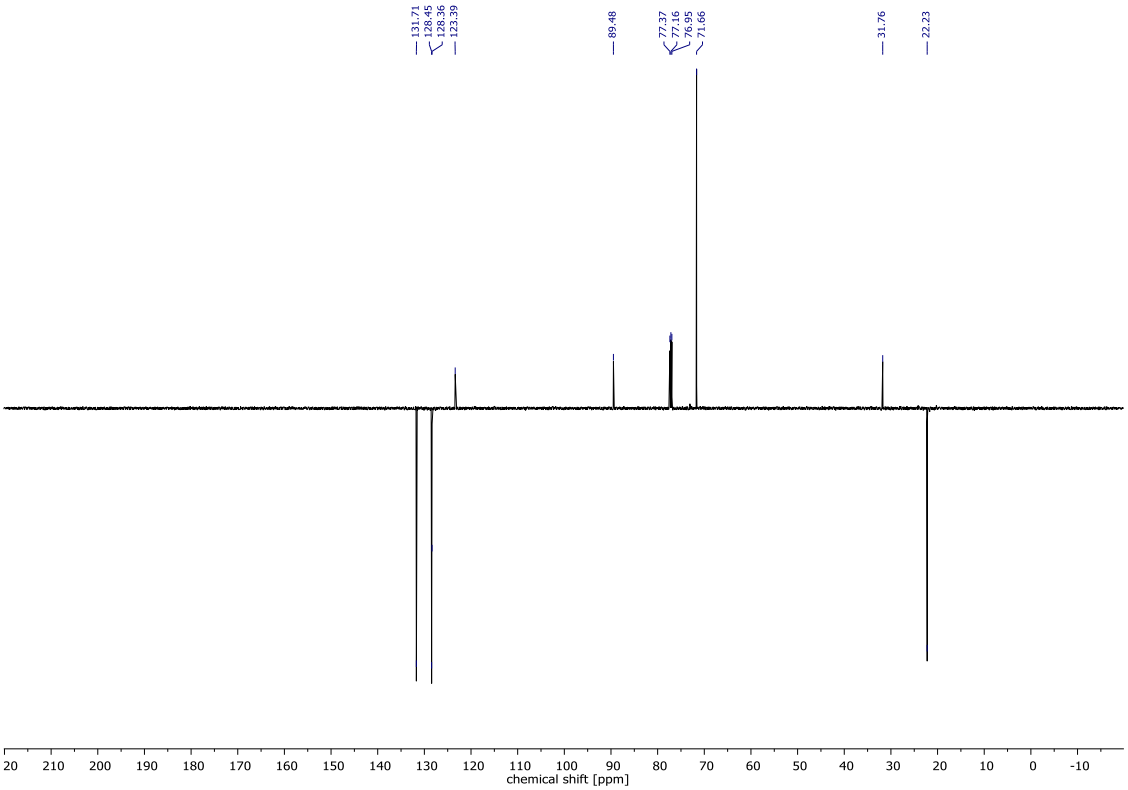

Figure 129: DEPTQ-NMR spectrum (151 MHz, $CDCl_3$, 300K) of **201**.

(*Z*)-1,2-Bis(5,5-dimethyl-1,3,2-dioxaborinan-2-yl)-1,2-bis(4-methoxyphenyl)ethane 202

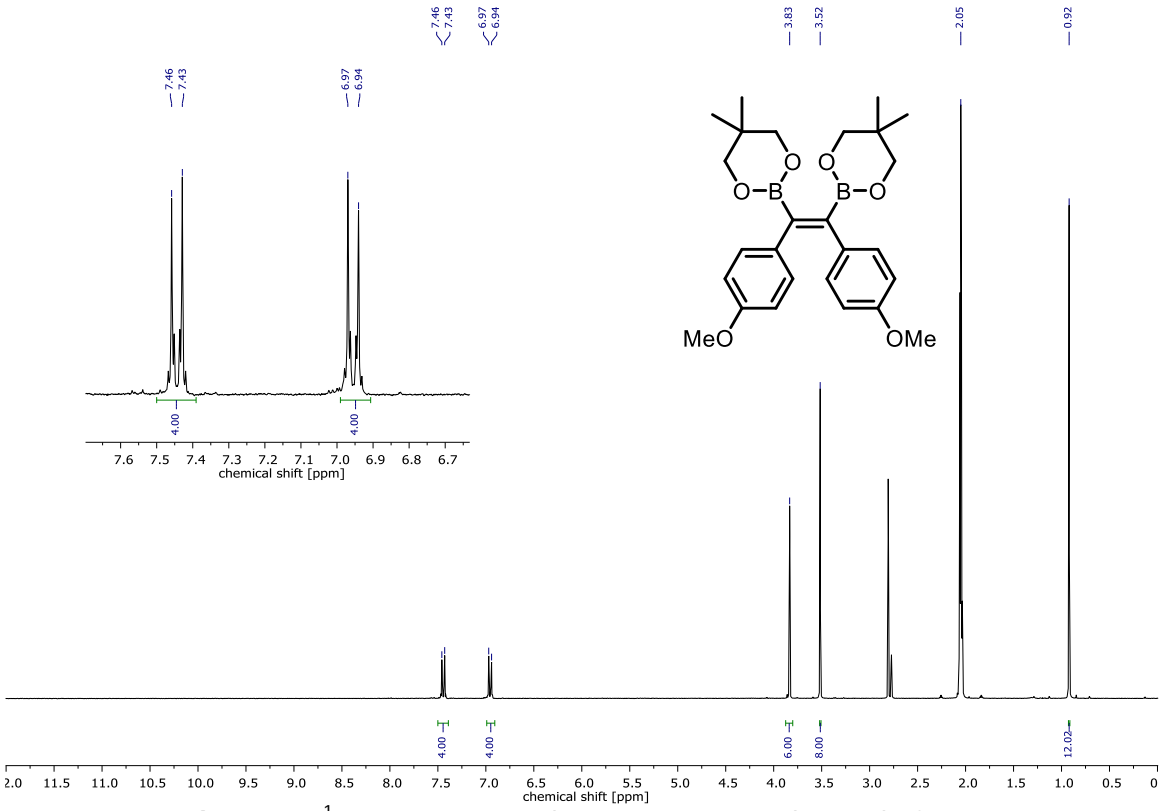

Figure 130: ^{1}H-NMR spectrum (300 MHz, acetone-d_6, 298K) of **202**.

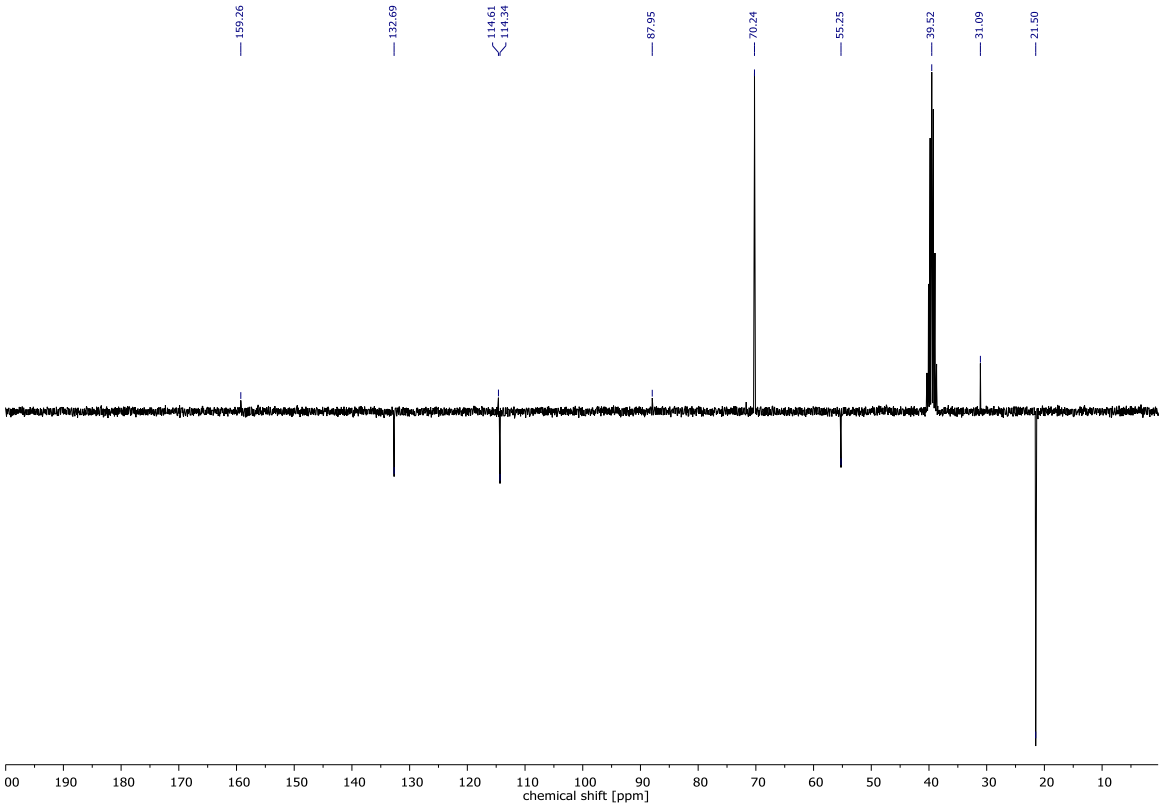

Figure 131: DEPTQ-NMR spectrum (76 MHz, DMSO-d_6, 298K) of **202**.

(*Z*)-3-Bromo-3-(4-methoxyphenyl)acrylaldehyde 128

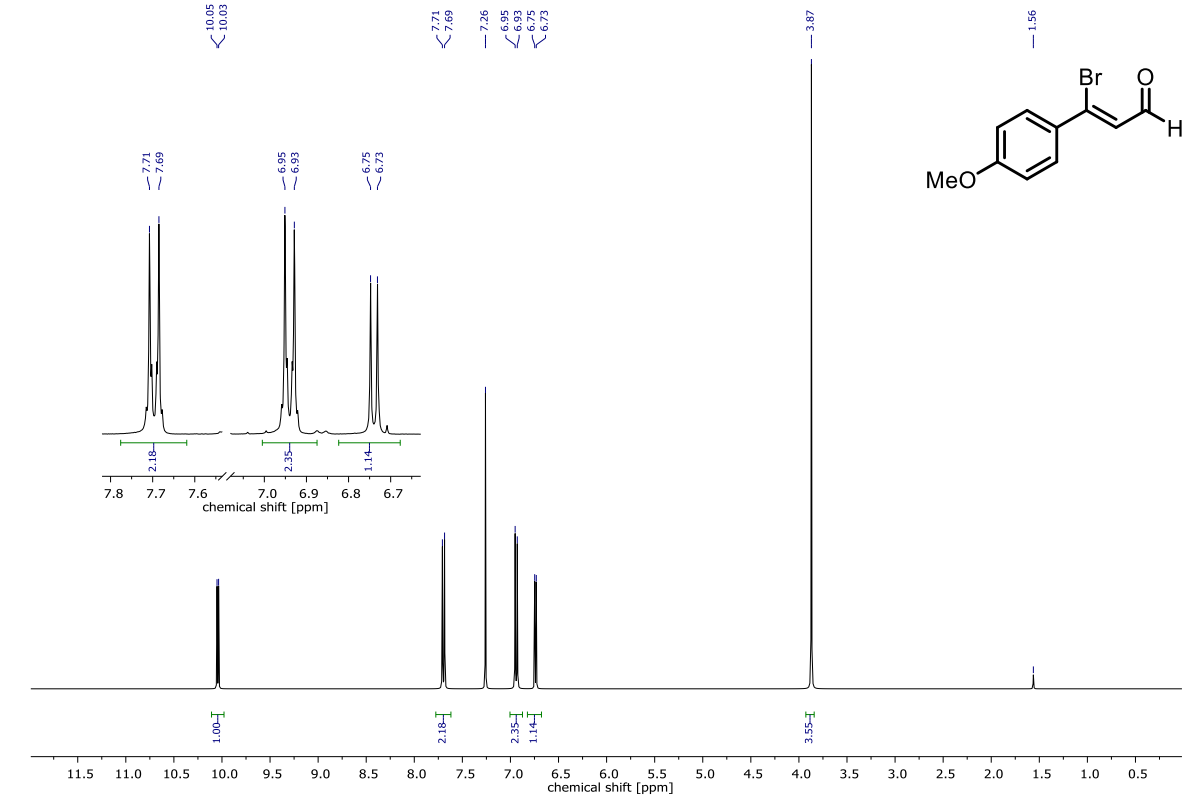

Figure132: ^{1}H-NMR spectrum (400 MHz, $CDCl_3$-*d*, 298K) of **128**.

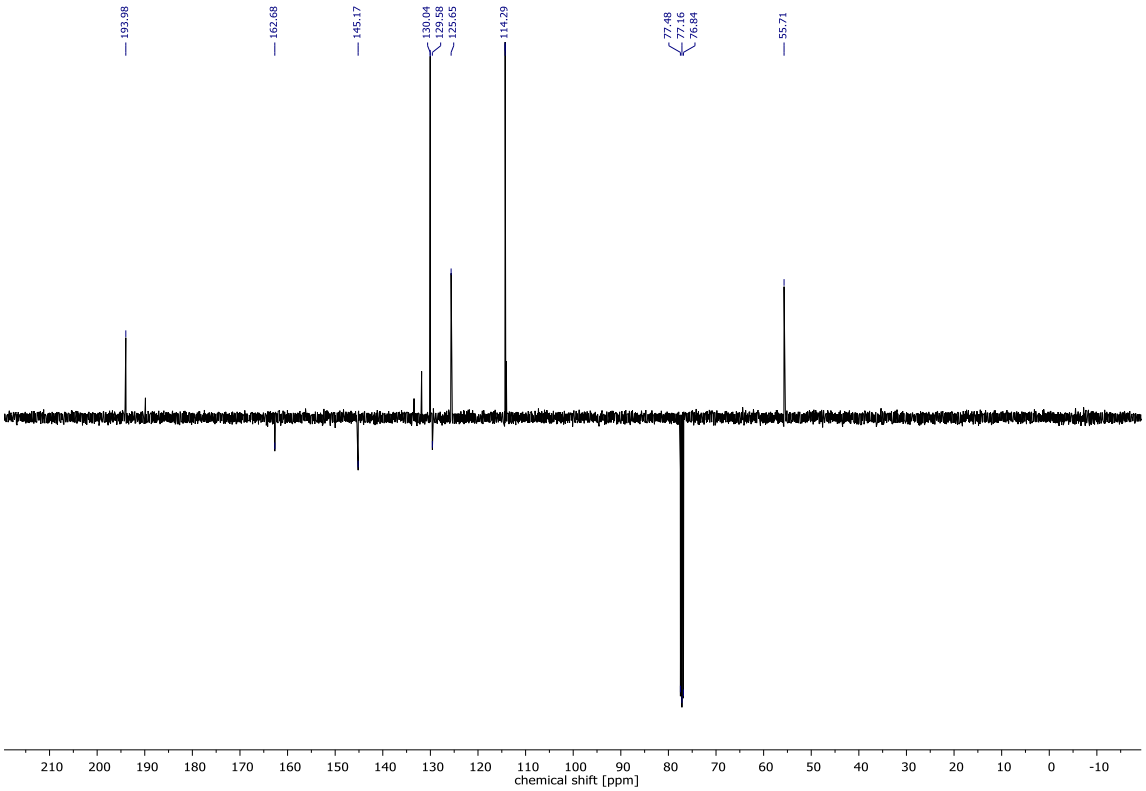

Figure133: DEPTQ-NMR spectrum (101 MHz, $CDCl_3$-*d*, 295K) of **128**.

(*Z*)-3-Bromo-3-(4-methoxyphenyl)acrylic acid 129

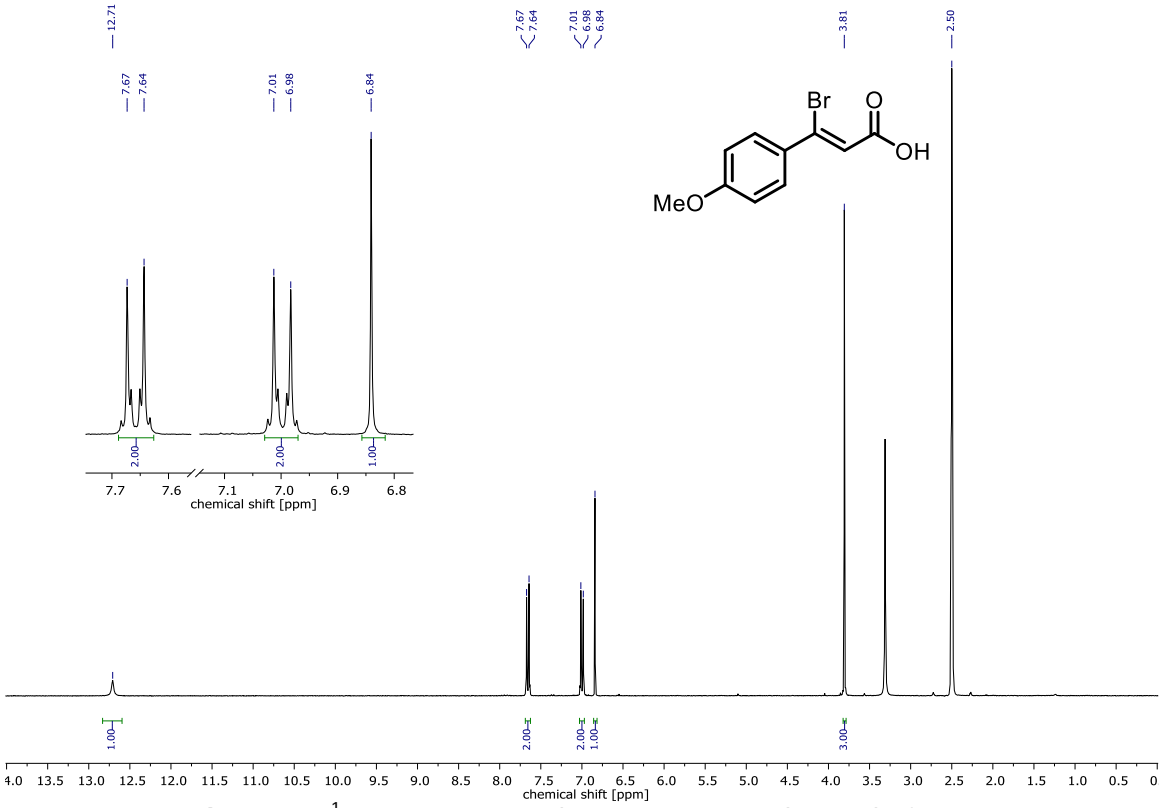

Figure 134: ^{1}H-NMR spectrum (400 MHz, DMSO-d_6, 296K) of **129**.

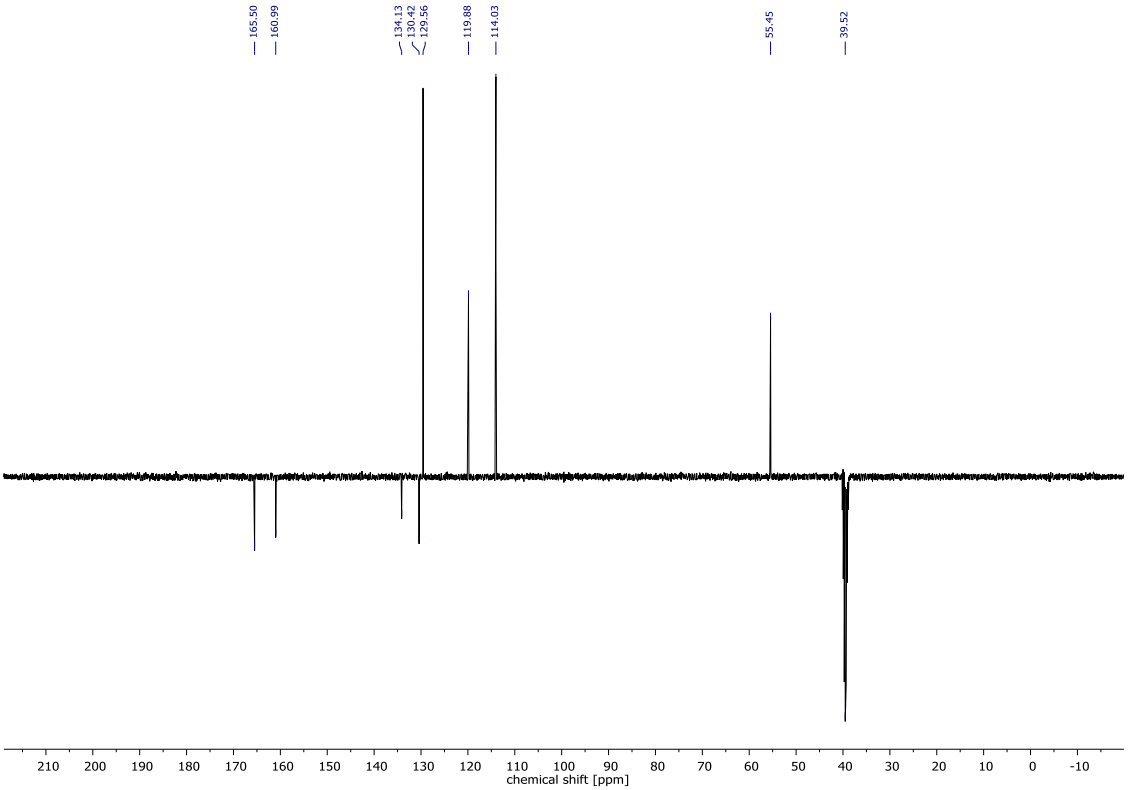

Figure 135: DEPTQ-NMR spectrum (101 MHz, DMSO-d_6, 296K) of **129**.

Methyl (*Z*)-3-bromo-3-(4-methoxyphenyl)acrylate 127

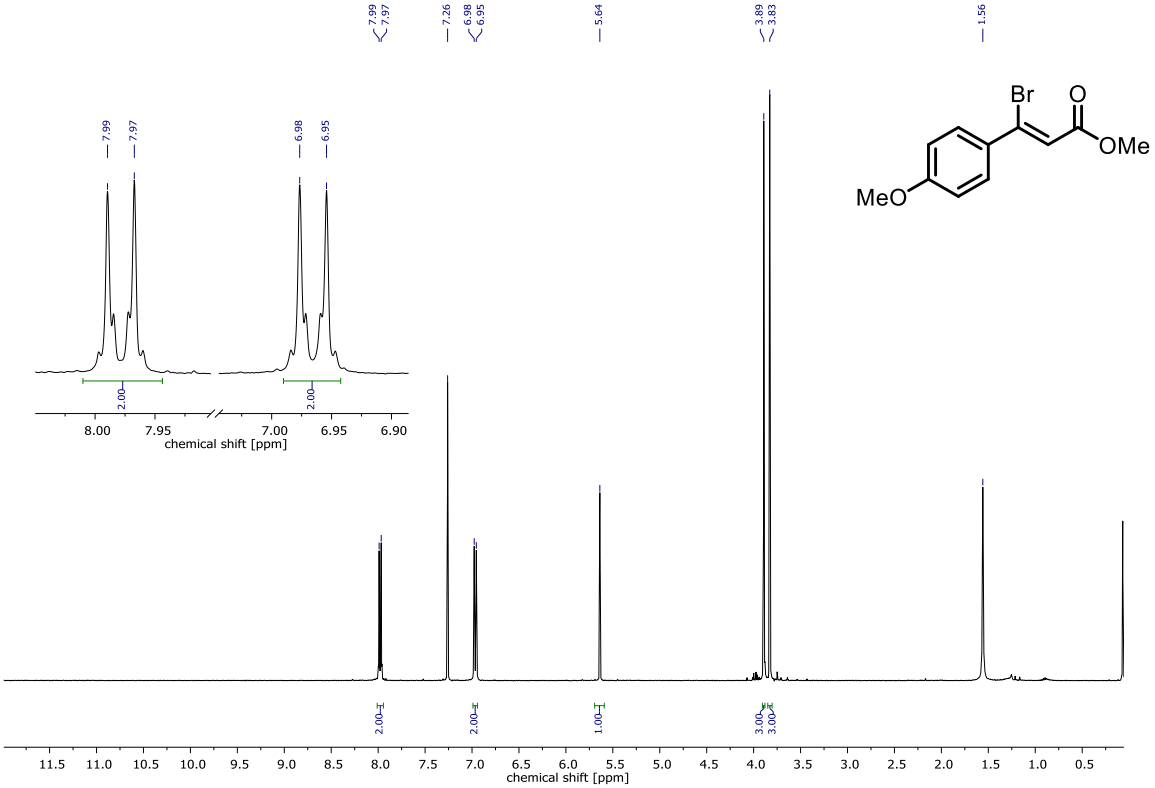

Figure 136: ^{1}H-NMR spectrum (400 MHz, $CDCl_3$-*d*, 298K) of **127**.

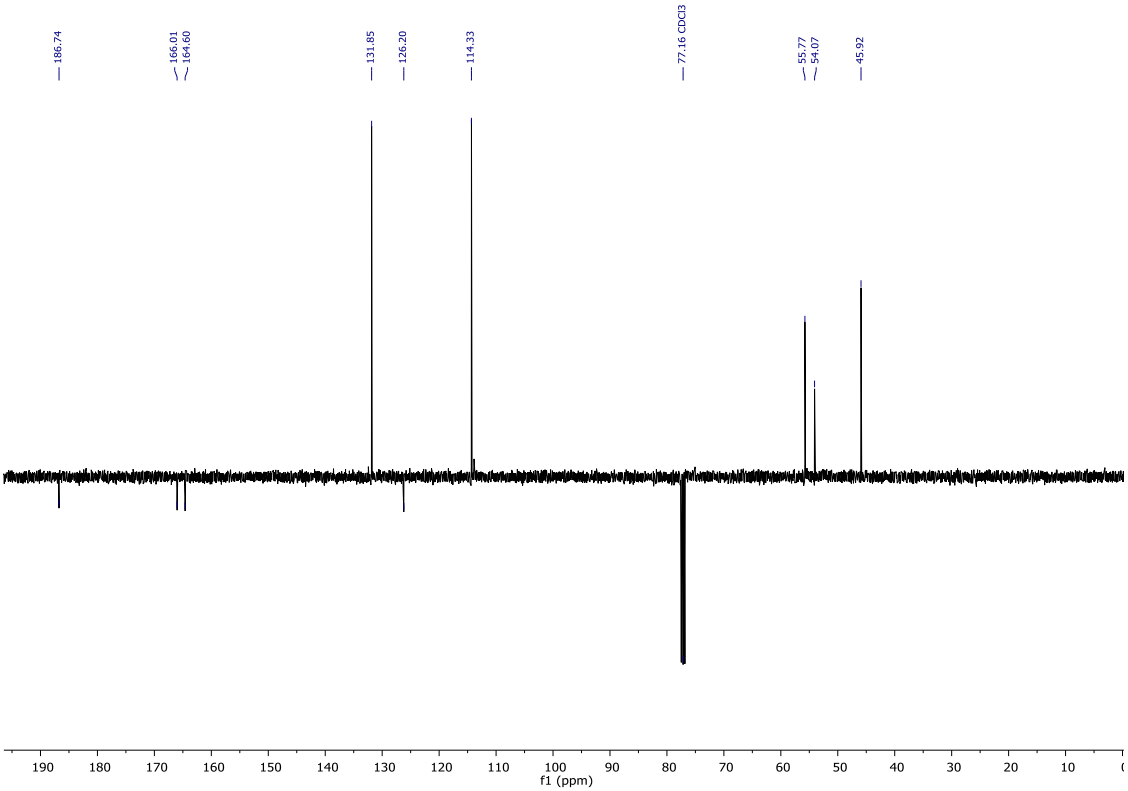

Figure 137: DEPTQ-spectrum (400 MHz, $CDCl_3$-*d*, 295K) of **127**.

Methyl-(*Z*)-3-phenyl-3-(tosyloxy)acrylate 210

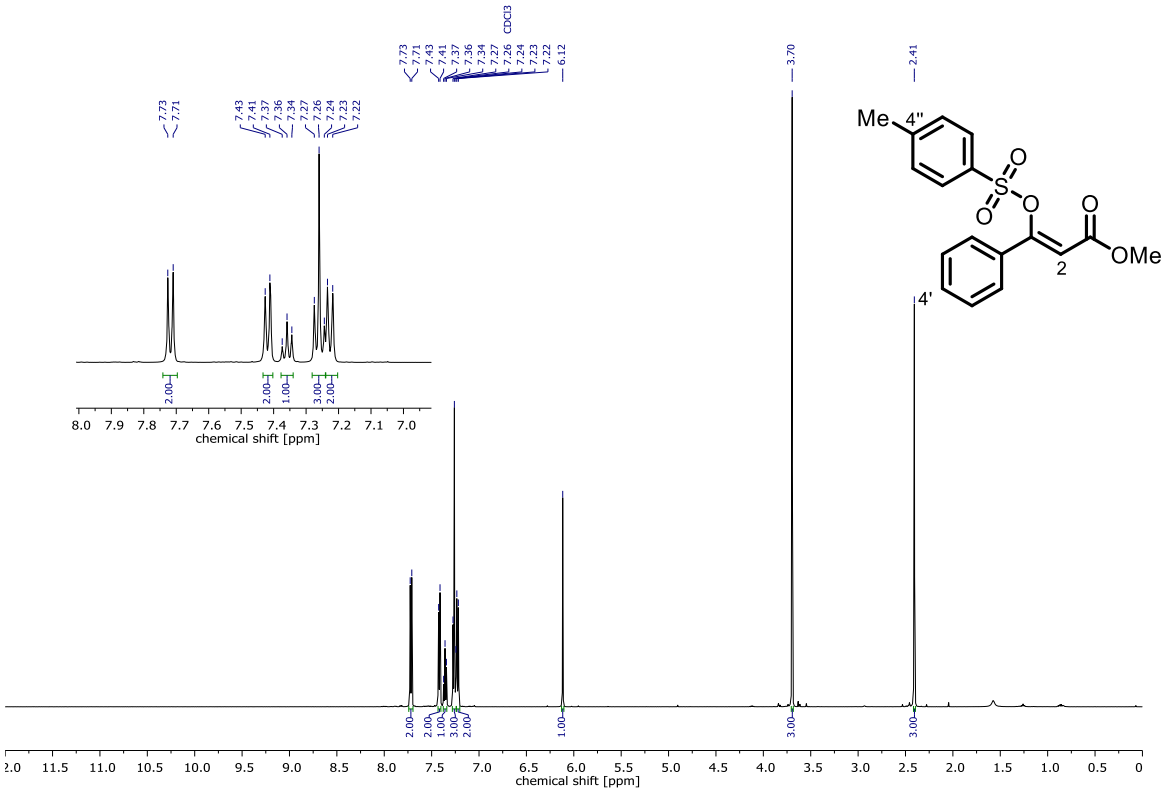

Figure 138: ^{1}H-NMR spectrum (500 MHz, $CDCl_3$, 295 K) of **210**.

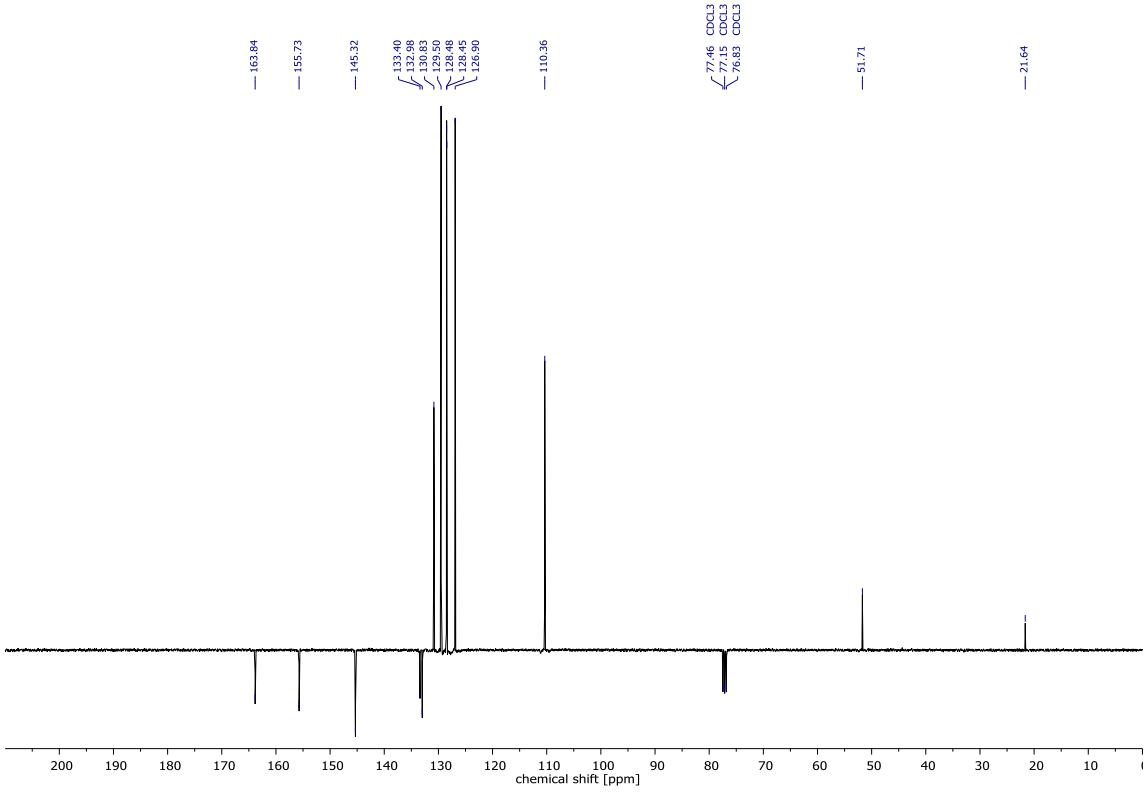

Figure 139: DEPTQ spectrum (101 MHz, $CDCl_3$, 295 K) of **210**.

Methyl-(*Z*)-3-(4-methoxyphenyl)-3-(tosyloxy) acrylate 211

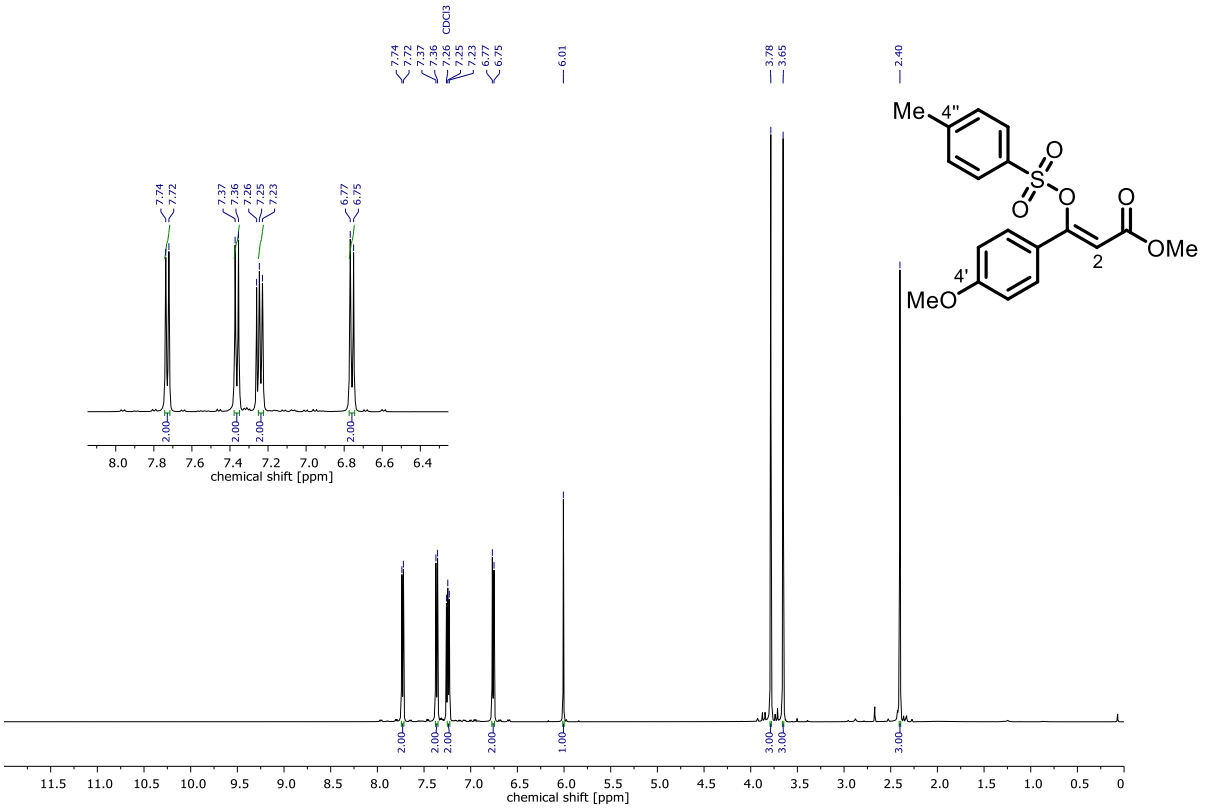

Figure 140: ^{1}H-NMR spectrum (500 MHz, $CDCl_3$, 297 K) of **211**.

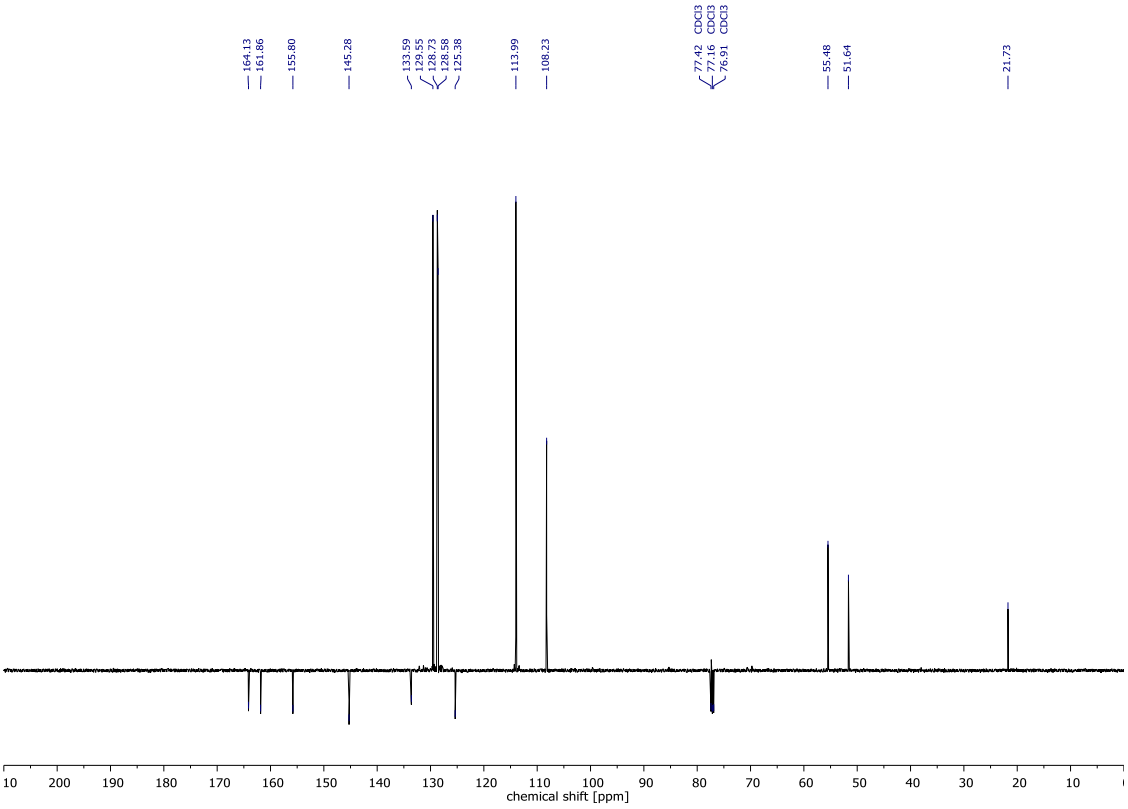

Figure 141: DEPTQ spectrum (126 MHz, $CDCl_3$, 296 K) of **211**.

Methyl-(*Z*)-3-(4-fluorophenyl)-3-(tosyloxy) acrylate 212

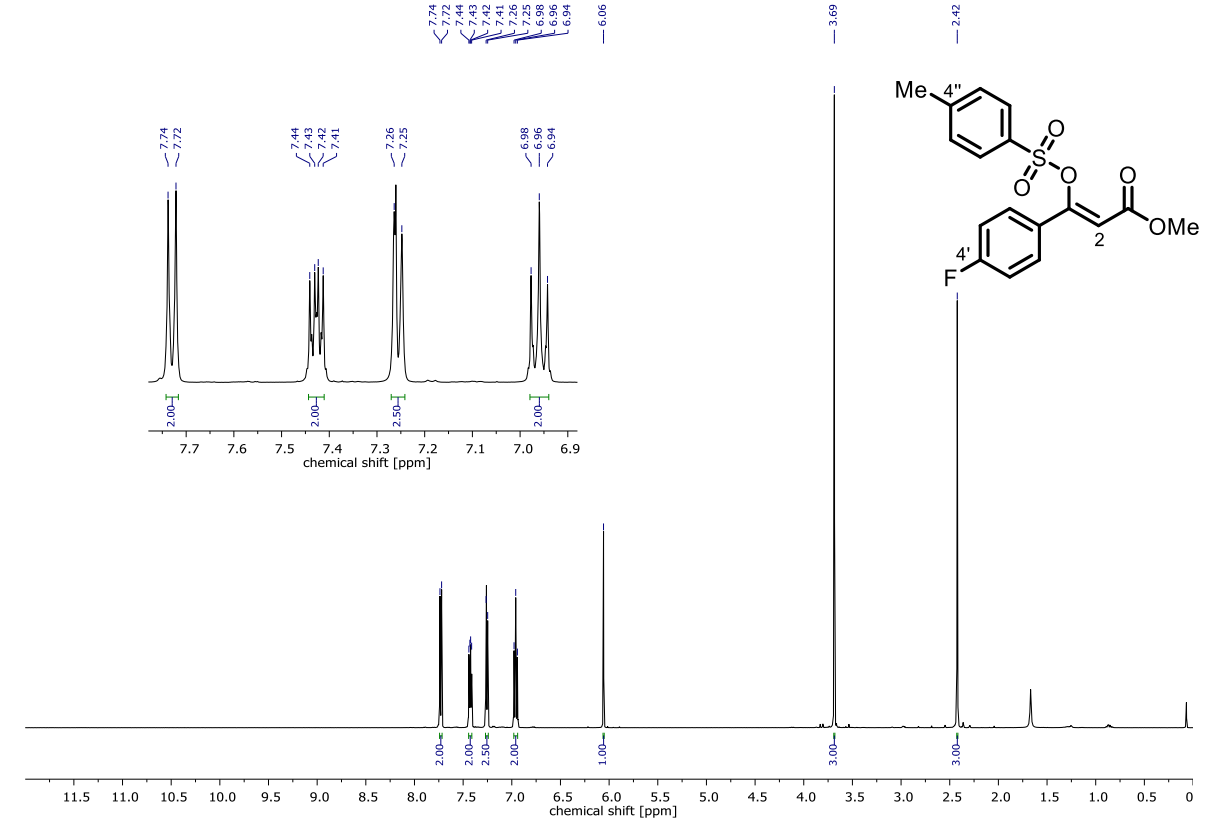

Figure 142: ^{1}H-NMR spectrum (500 MHz, $CDCl_3$, 296 K) of **212**.

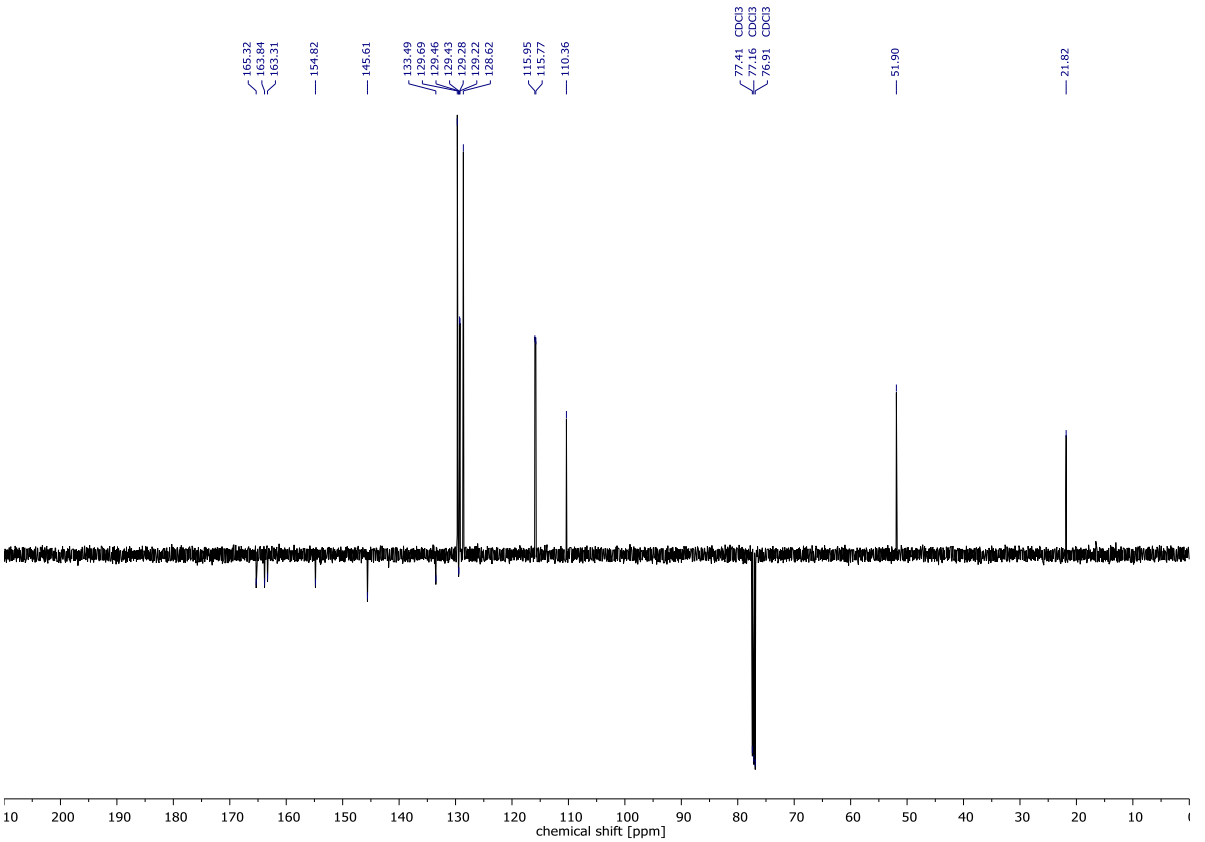

Figure 143: DEPTQ spectrum (126 MHz, $CDCl_3$, 296 K) of **212**.

2,5-Dioxopyrrolidin-1-yl acetate 222

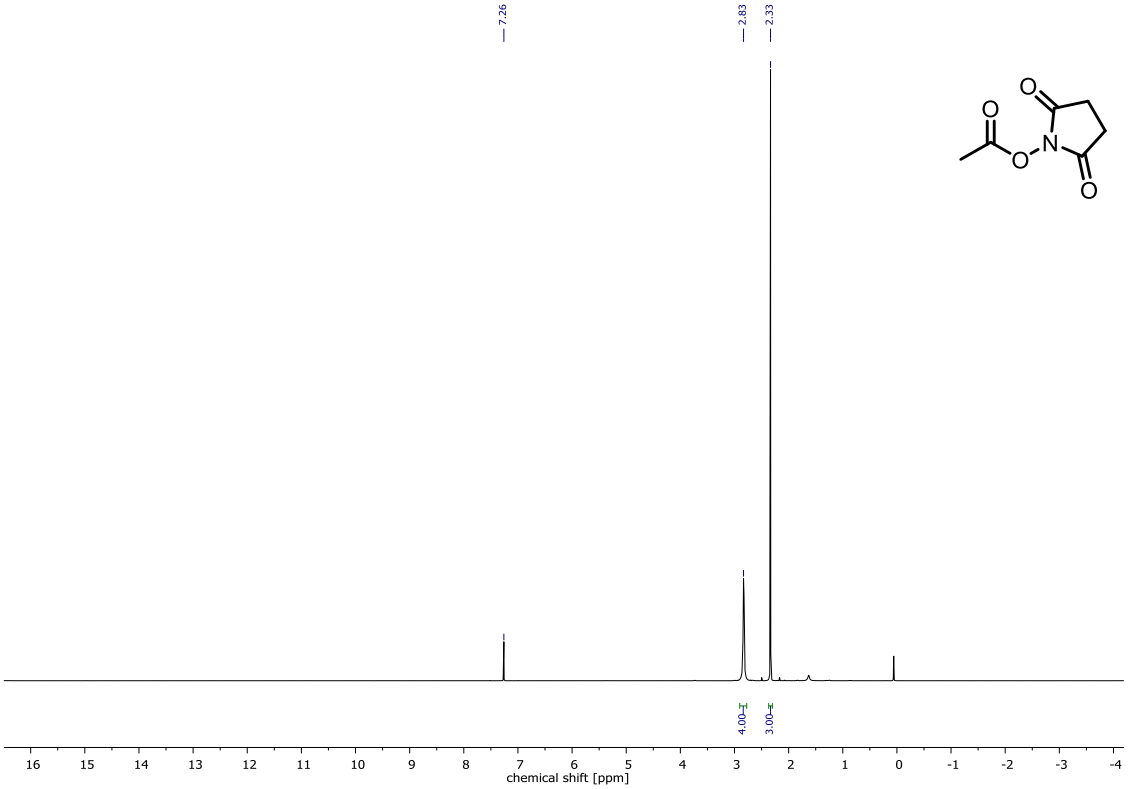

Figure 144: ^{1}H-NMR spectrum (400 MHz, $CDCl_3$-*d*, 298K) of **222**.

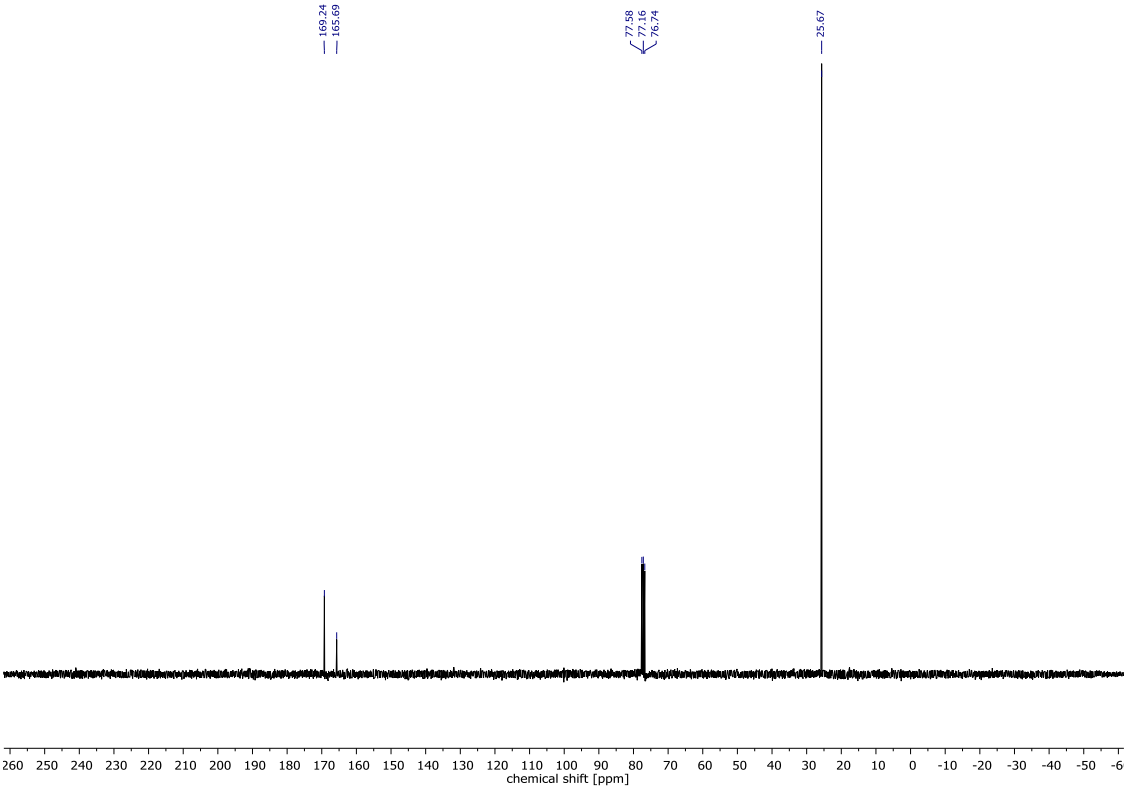

Figure 145: ^{13}C-NMR spectrum (75 MHz, $CDCl_3$-*d*, 298K) of **222**.

2,5-Dioxopyrrolidin-1-yl benzoate 224

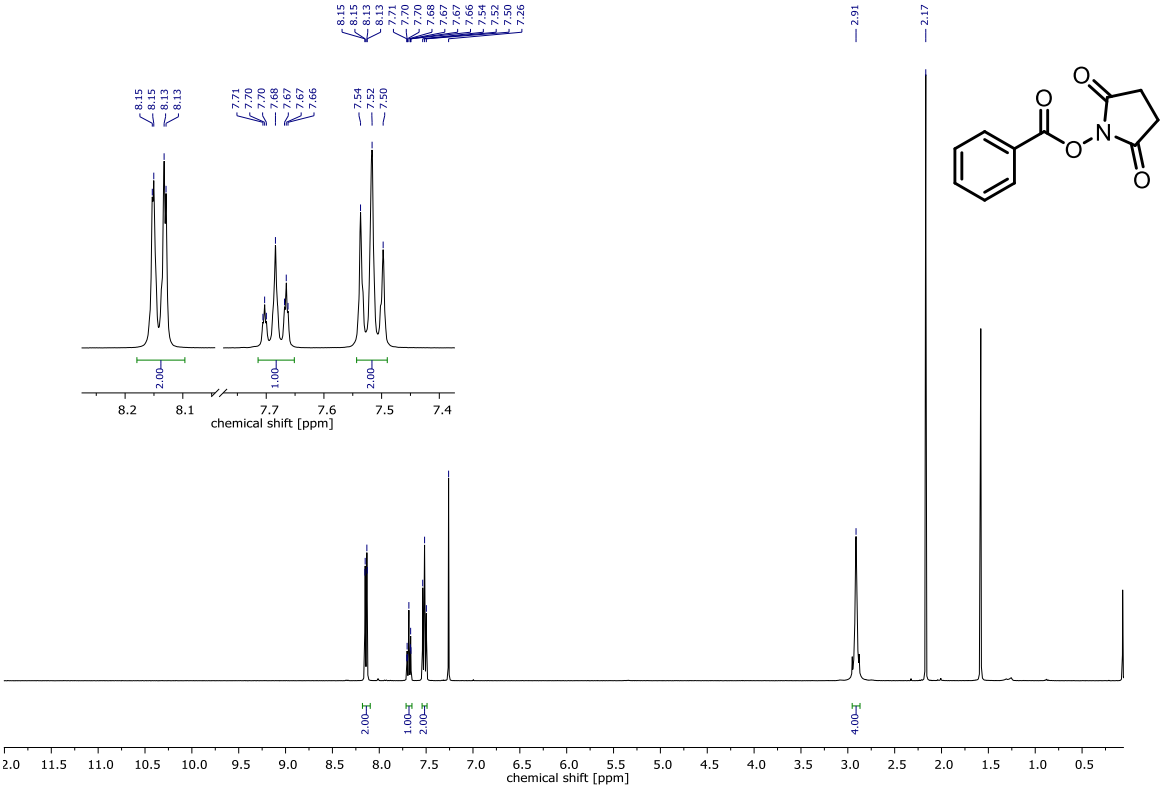

Figure 146: ^{1}H-NMR spectrum (400 MHz, $CDCl_3$-*d*, 298K) of **224**.

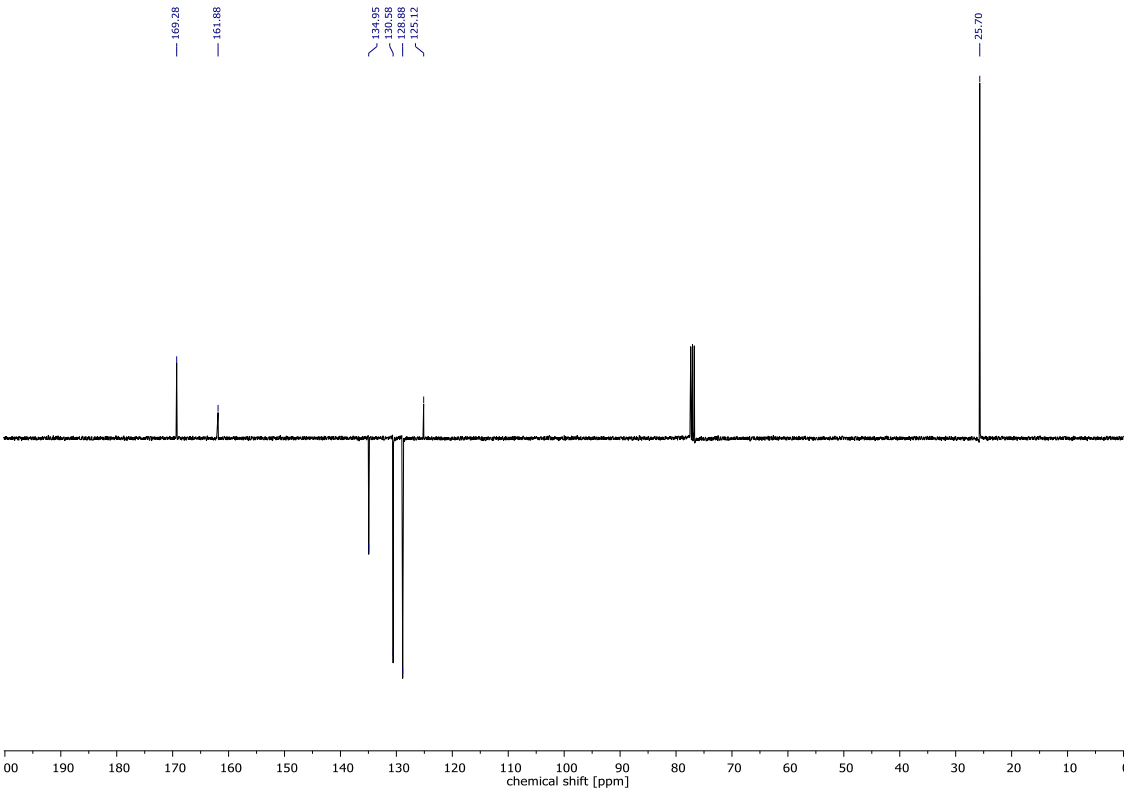

Figure 147: DEPTQ-NMR spectrum (101 MHz, $CDCl_3$-*d*, 295K) of **224**.

Benzophenone 225

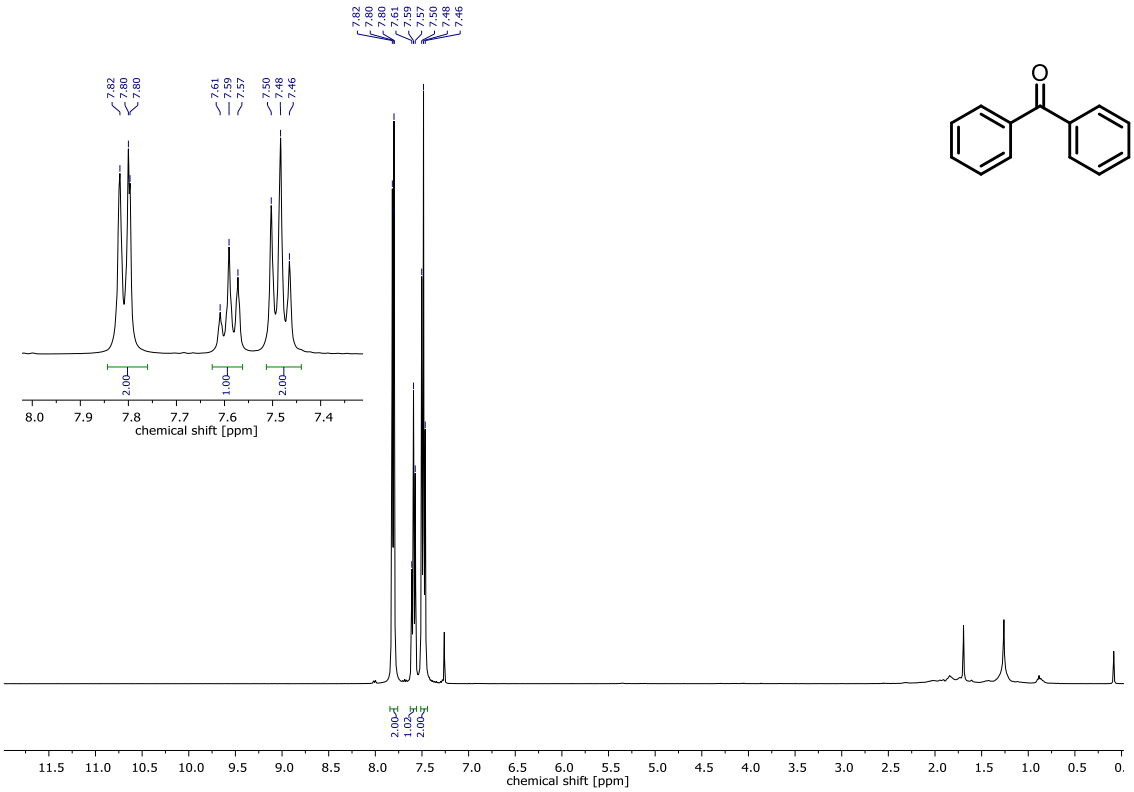

Figure 148: ^{1}H-NMR spectrum (400 MHz, $CDCl_3$-*d*, 298K) of **225**.

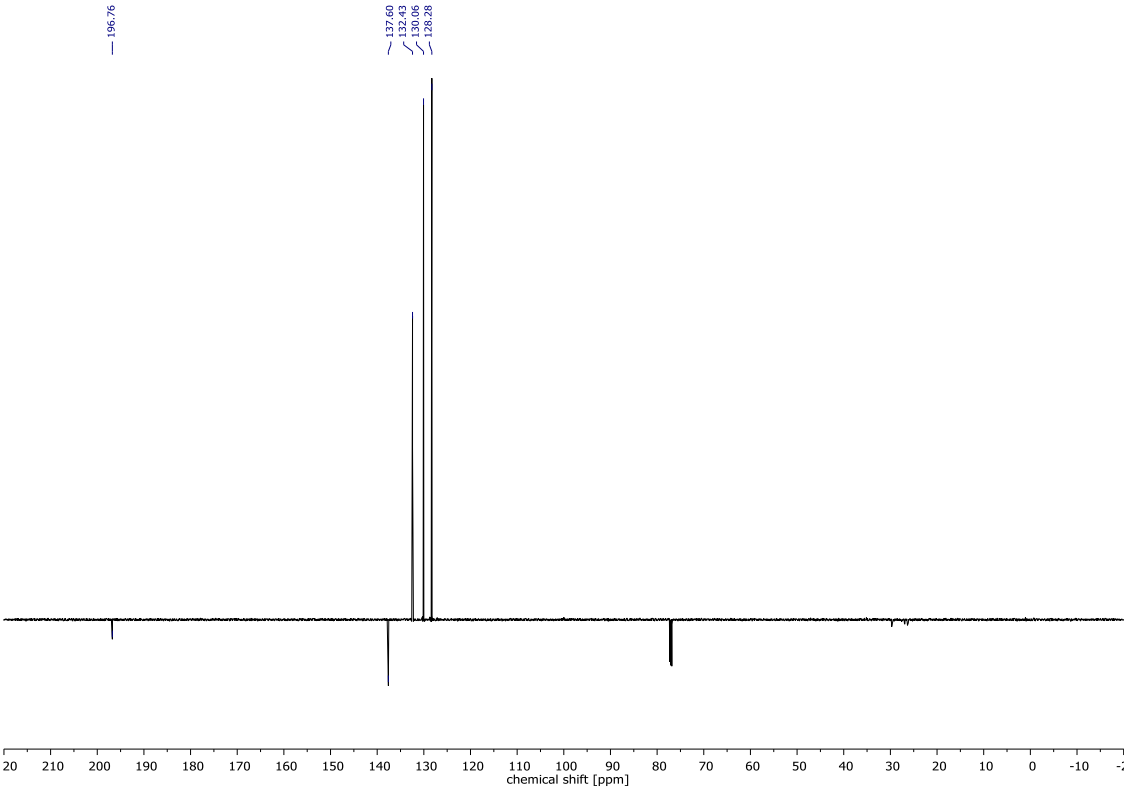

Figure 149: DEPTQ-NMR spectrum (151 MHz, $CDCl_3$-*d*, 298K) of **225**.

4-Methoxybenzophenone 226

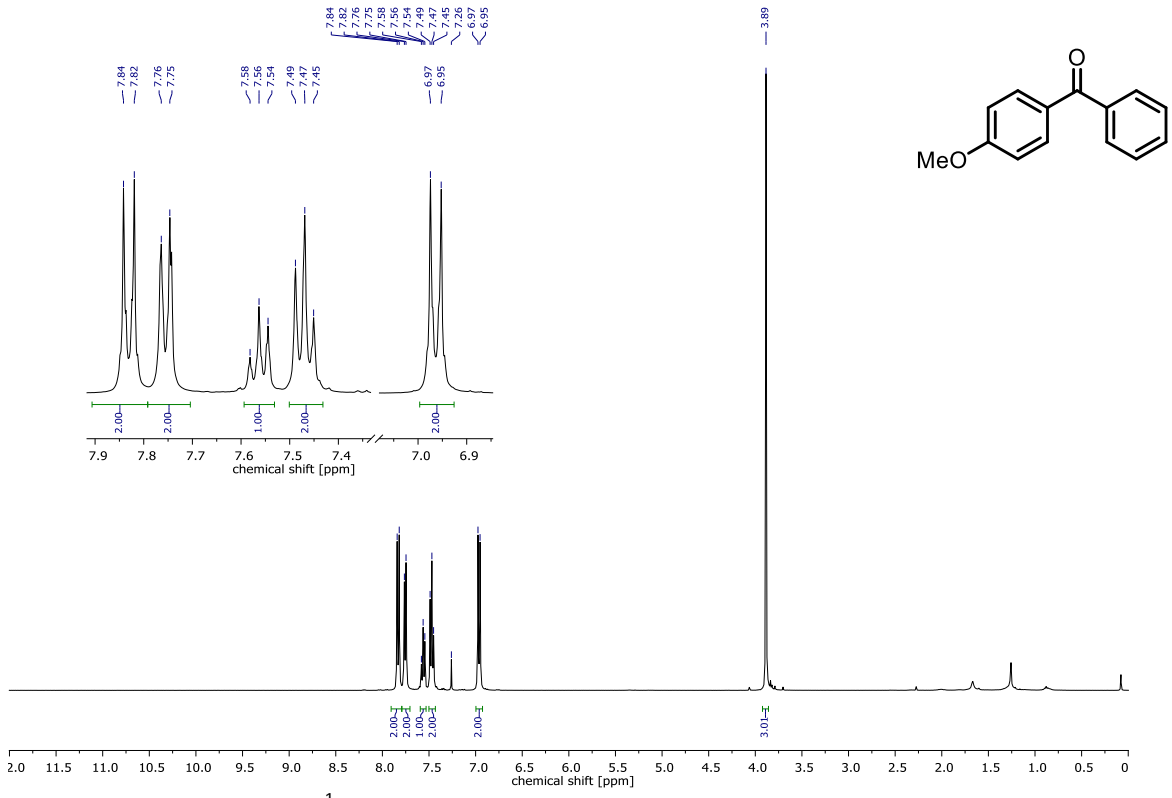

Figure150: ^{1}H-NMR spectrum (400 MHz, $CDCl_3$-*d*, 298K) of **226**.

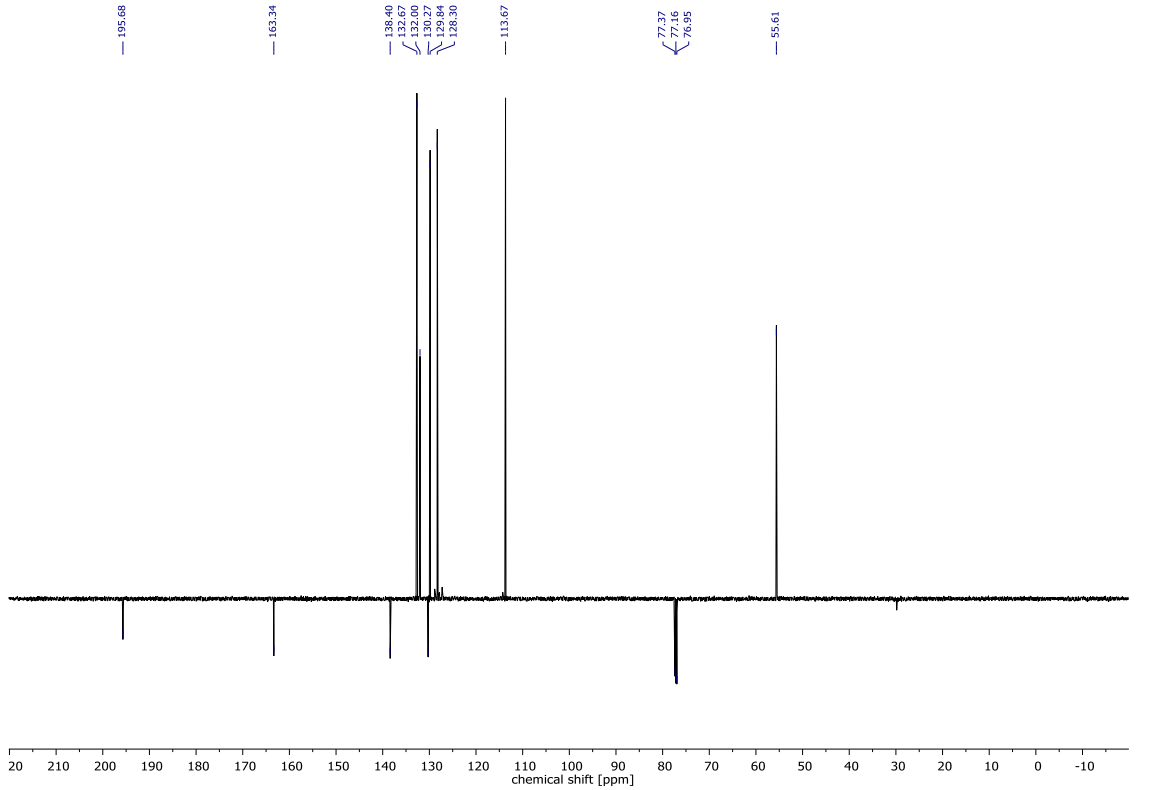

Figure151: ^{1}H-NMR spectrum (151 MHz, $CDCl_3$-*d*, 298K) of **226**.

2,5-Dioxopyrrolidin-1-yl acetate 221

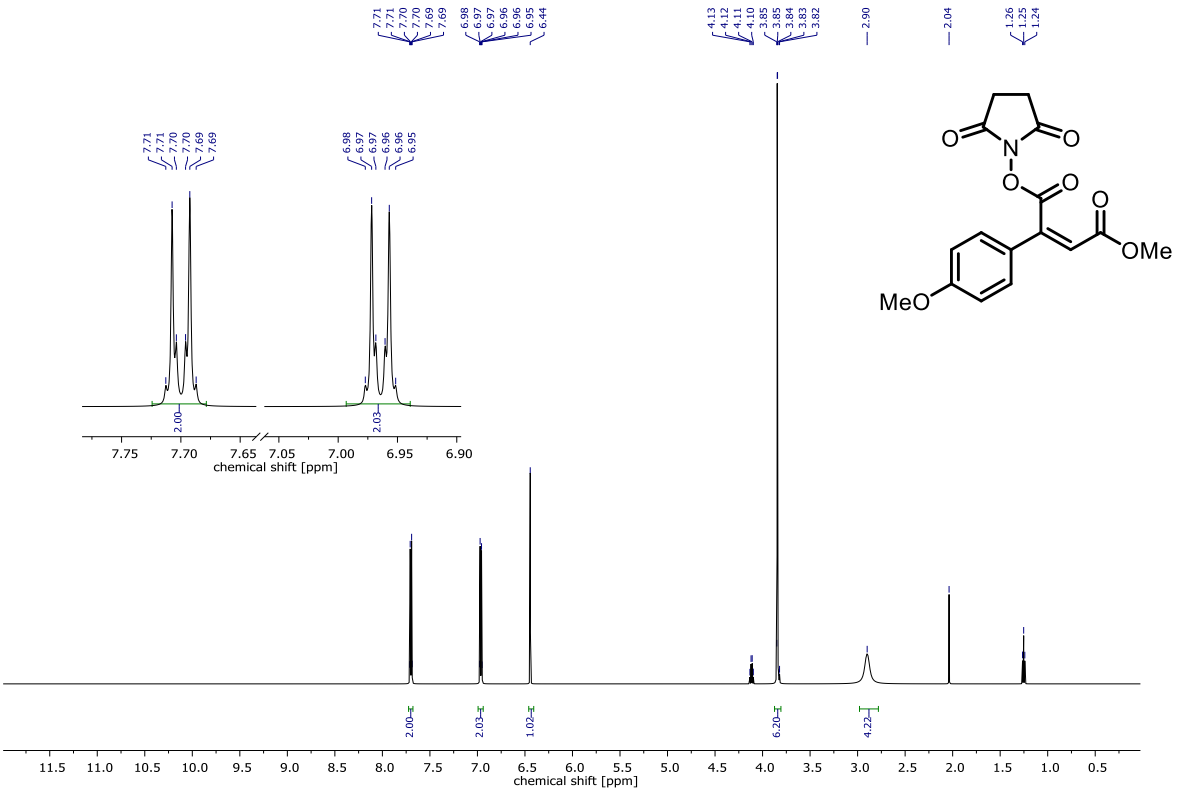

Figure 152: ^{1}H-NMR spectrum (600 MHz, $CDCl_3$-*d*, 300K) of **221**.

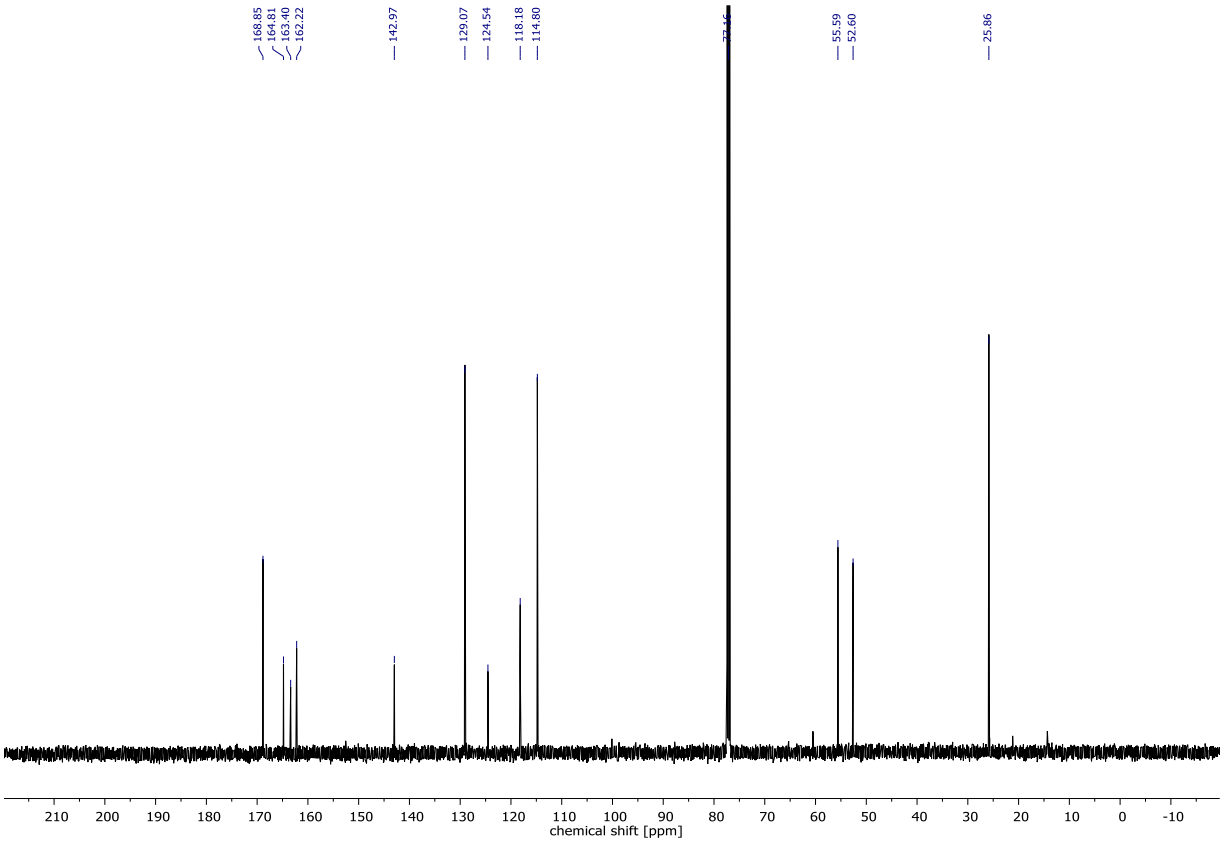

Figure 153: DEPTQ-NMR spectrum (126 MHz, $CDCl_3$-*d*, 298K) of **221**.

Methyl-(*Z*)-4-oxo-3,4-diphenylbut-2-enoate 235

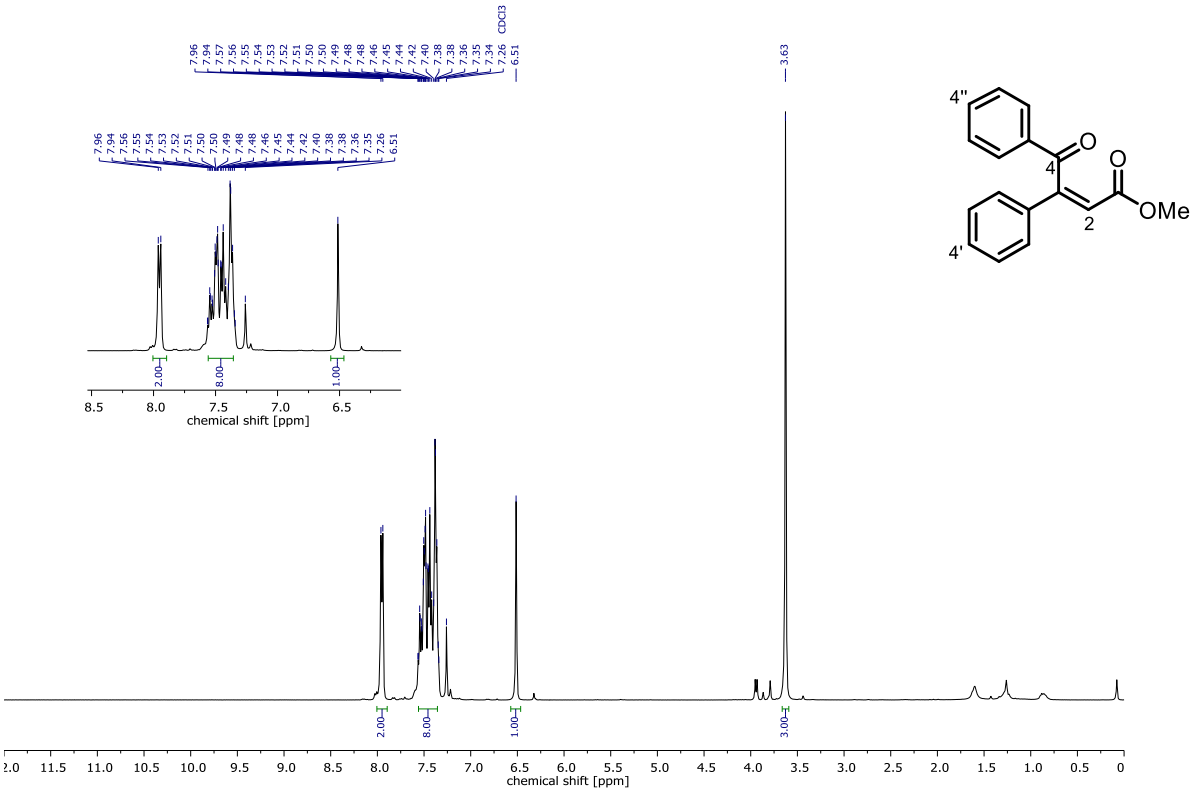

Figure 154: ^{1}H-NMR spectrum (400 MHz, $CDCl_3$, 300 K) of **235**.

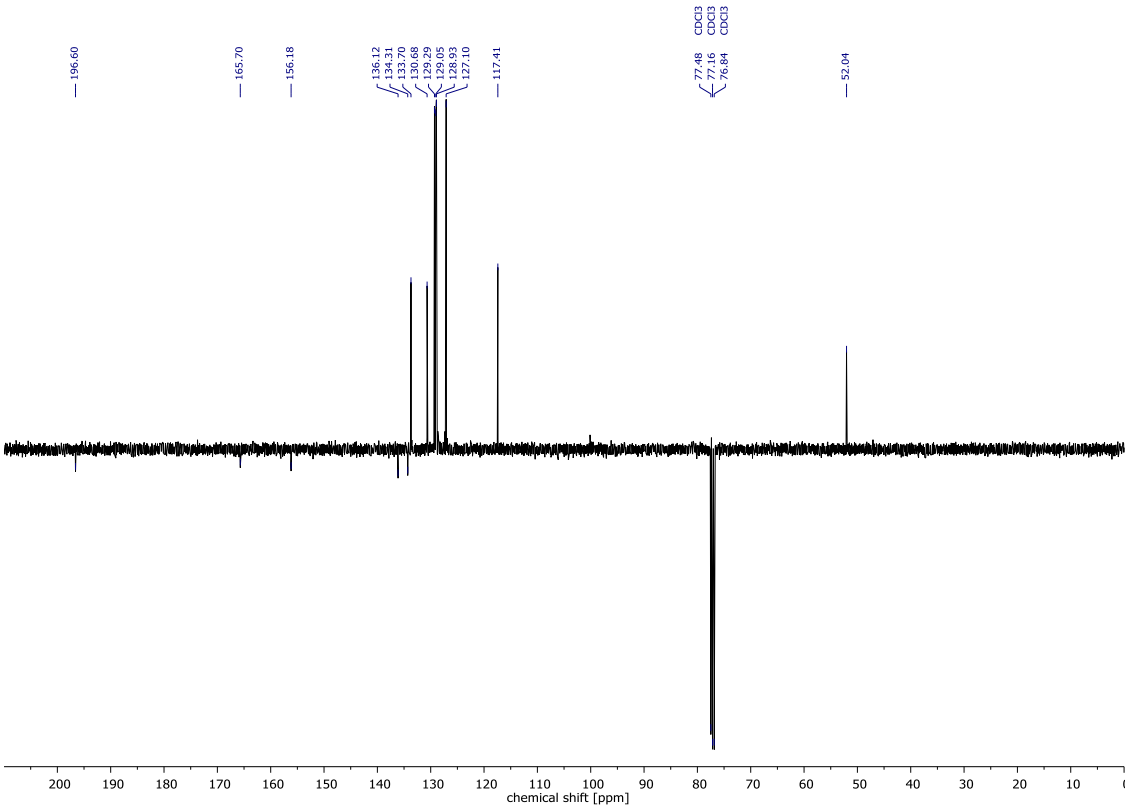

Figure 155: DEPTQ spectrum (101 MHz, $CDCl_3$, 298 K) of **235**.

Methyl-(*Z*)-3-(4-methoxyphenyl)-4-oxo-4-phenylbut-2-enoate 236

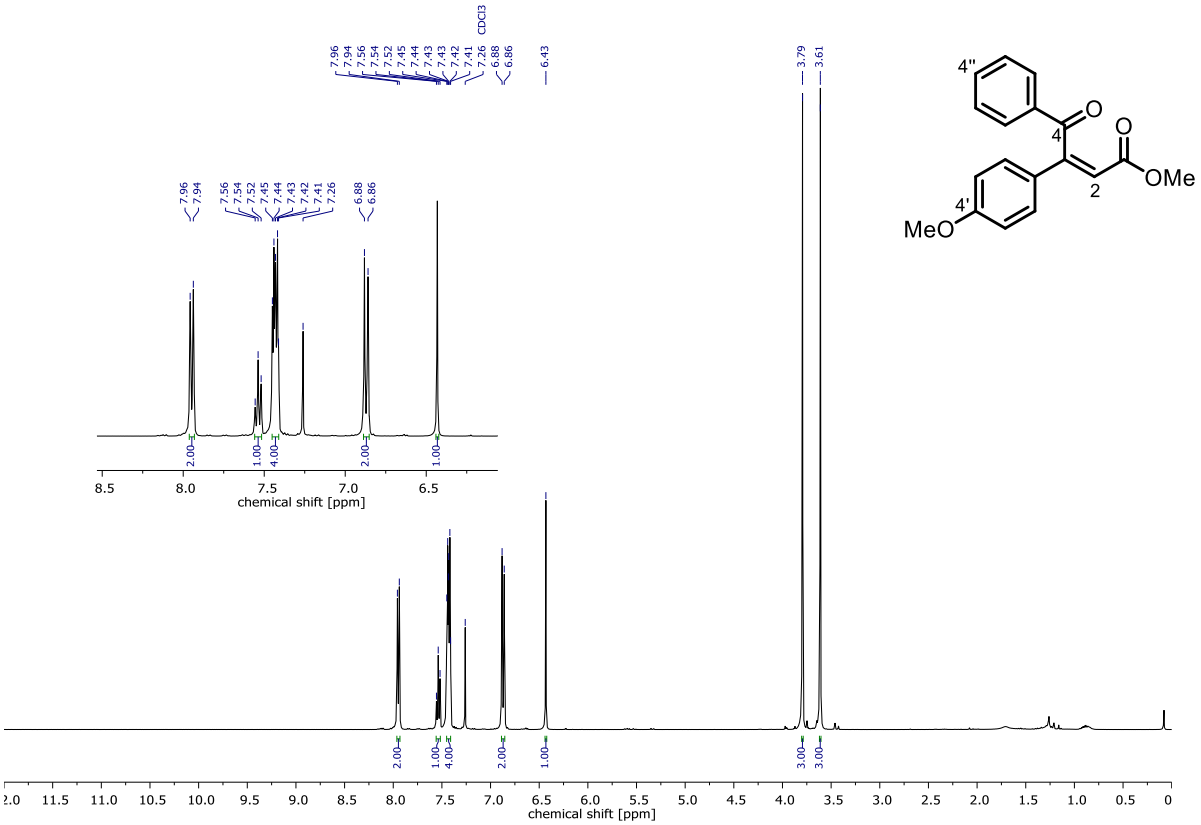

Figure 156: ^{1}H-NMR spectrum (400 MHz, $CDCl_3$, 300 K) of **236**.

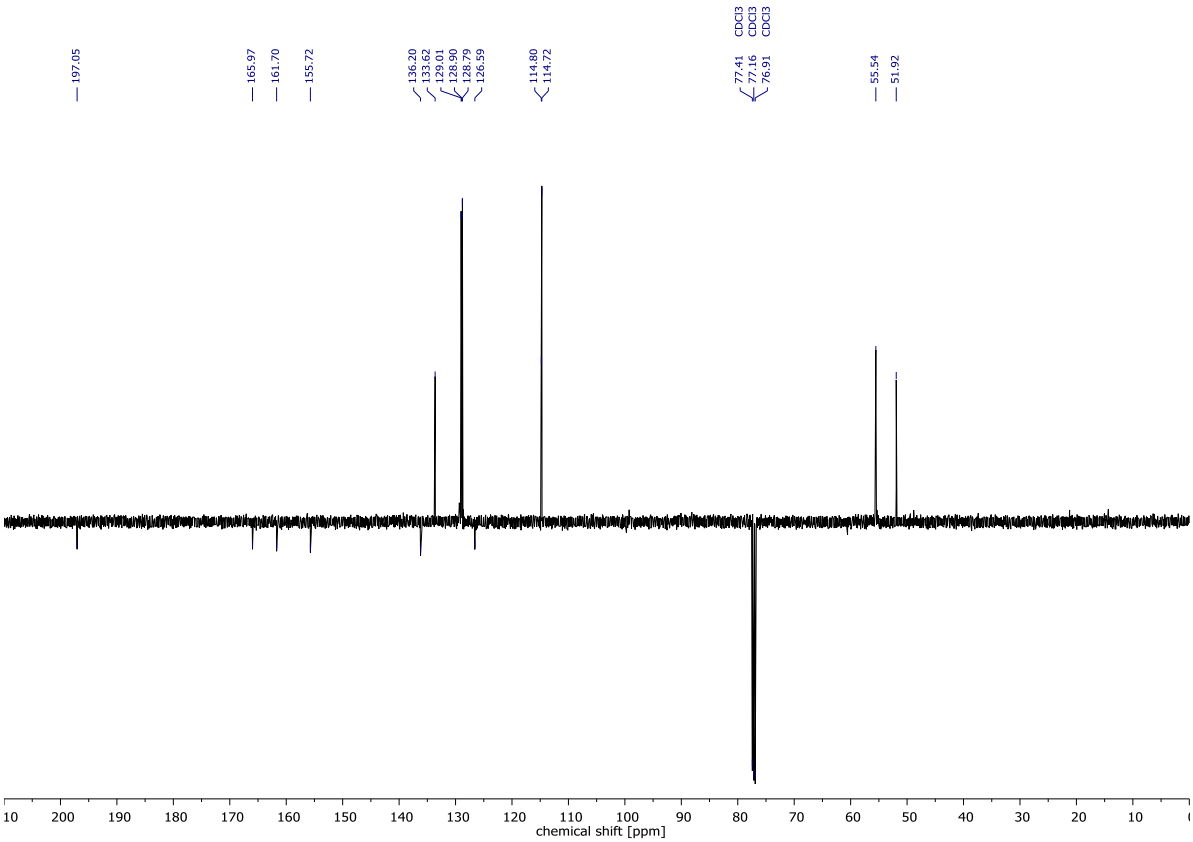

Figure 157: DEPTQ spectrum (126 MHz, $CDCl_3$, 296 K) of **236**.

Methyl-(*Z*)-3-(4-fluorophenyl)-4-oxo-4-phenylbut-2-enoate 237

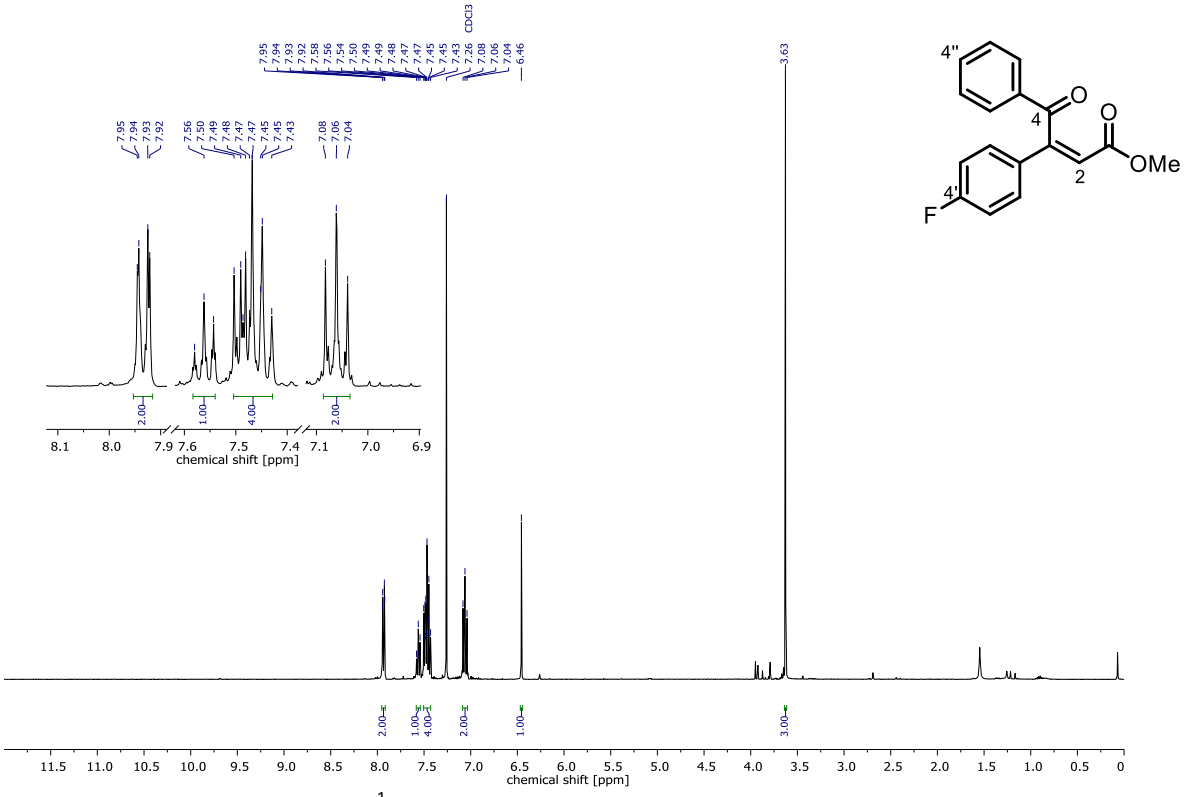

Figure 158: ^{1}H-NMR spectrum (400 MHz, $CDCl_3$, 298 K) of **237**.

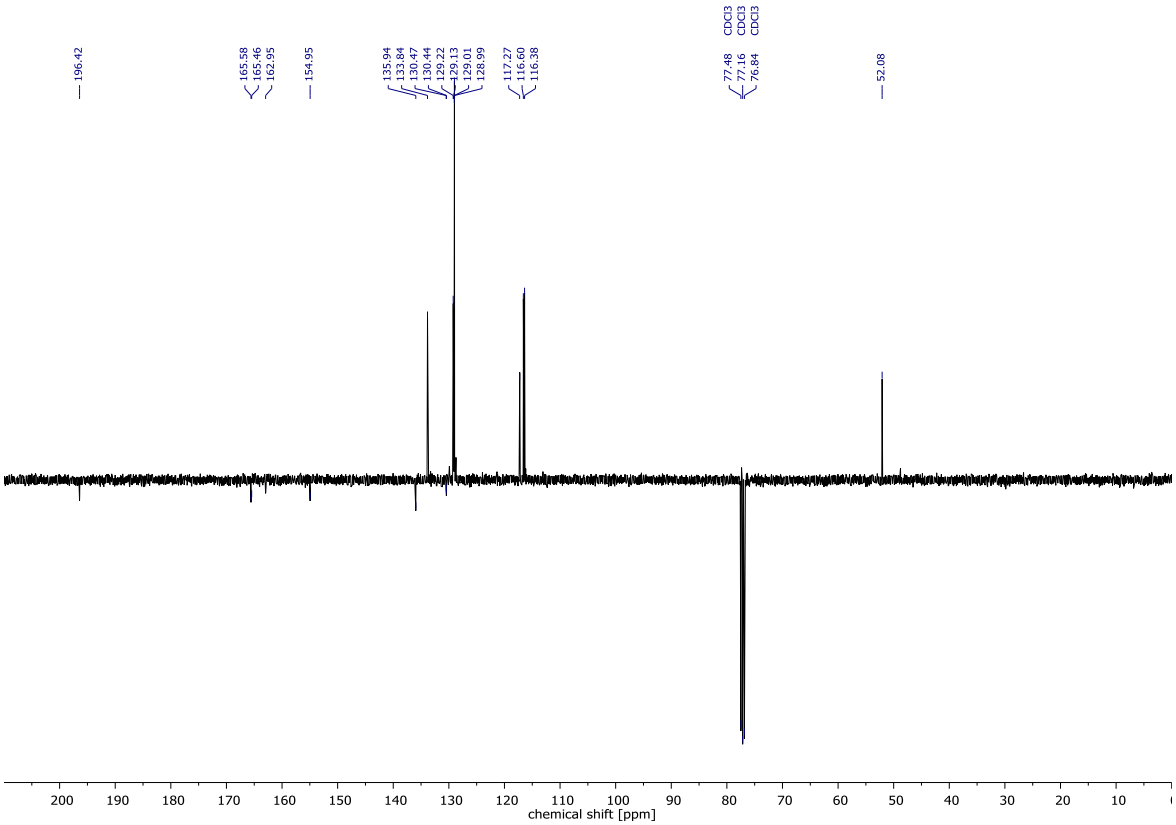

Figure 159: DEPTQ spectrum (101 MHz, $CDCl_3$, 298 K) of **237**.

Methyl-(*Z*)-4-(4-methoxyphenyl)-4-oxo-3-phenylbut-2-enoate 238

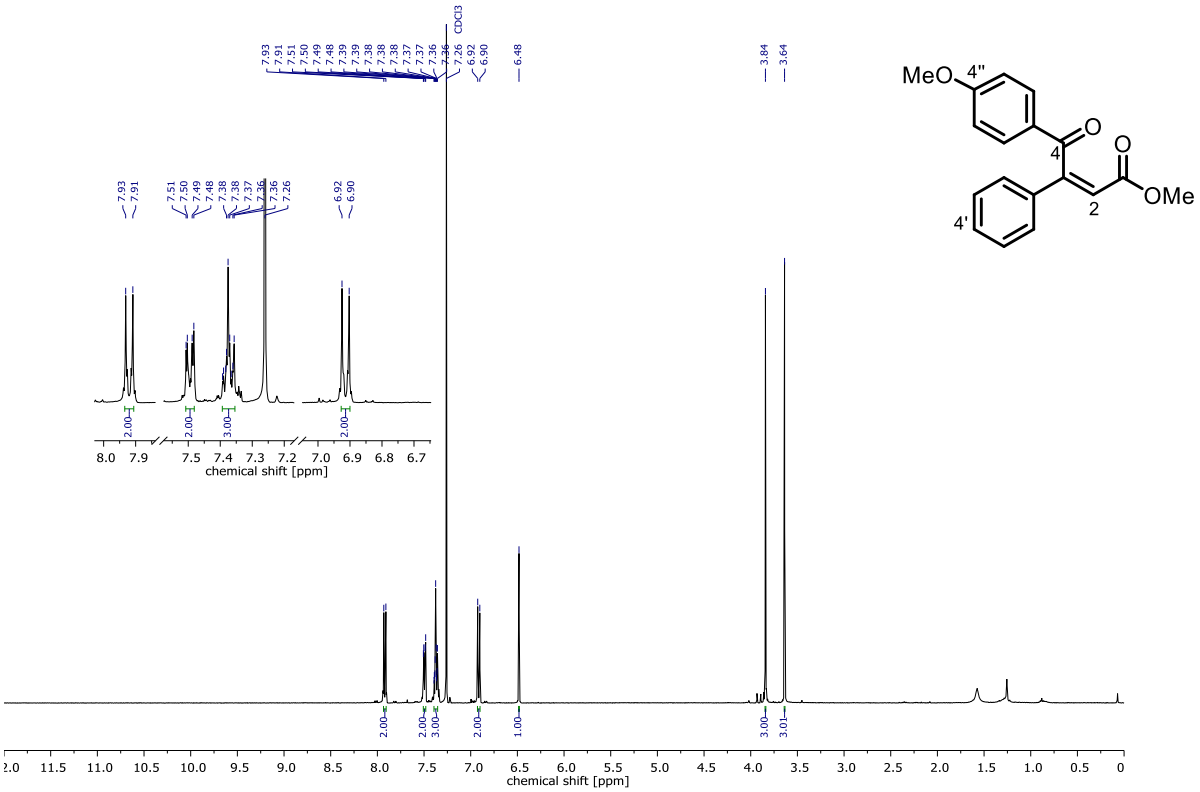

Figure 160: ^{1}H-NMR spectrum (400 MHz, $CDCl_3$, 298 K) of **238**.

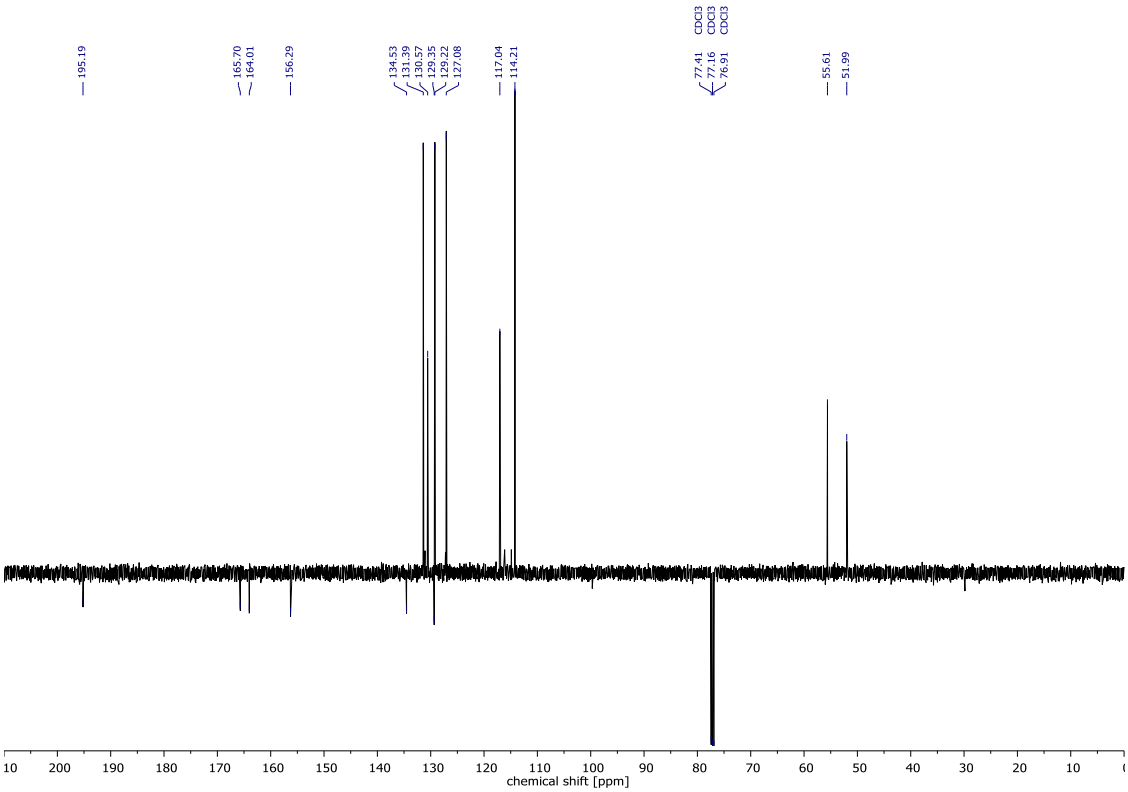

Figure 161: DEPTQ spectrum (126 MHz, $CDCl_3$, 296 K) of **238**.

Methyl-(*Z*)-3,4-di-(4-methoxyphenyl)-4-oxobut-2-enoate 239

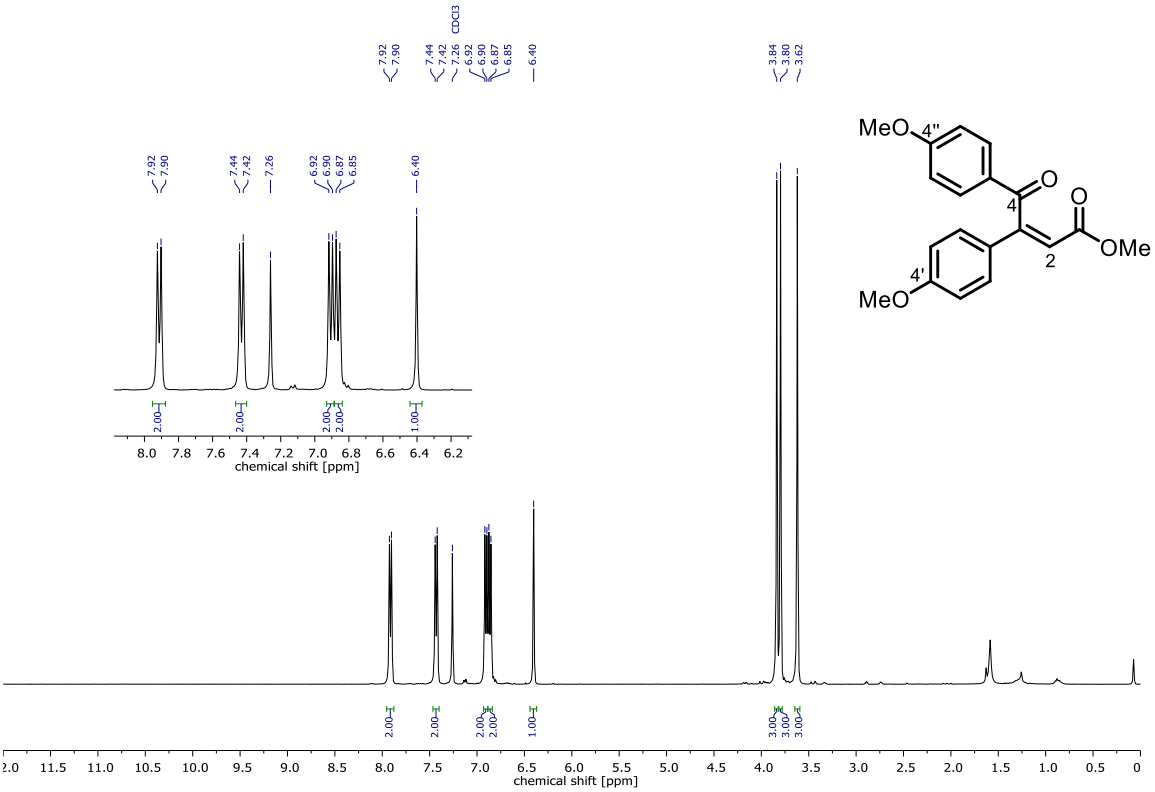

Figure 162: ^{1}H-NMR spectrum (400 MHz, $CDCl_3$, 300 K) of **239**.

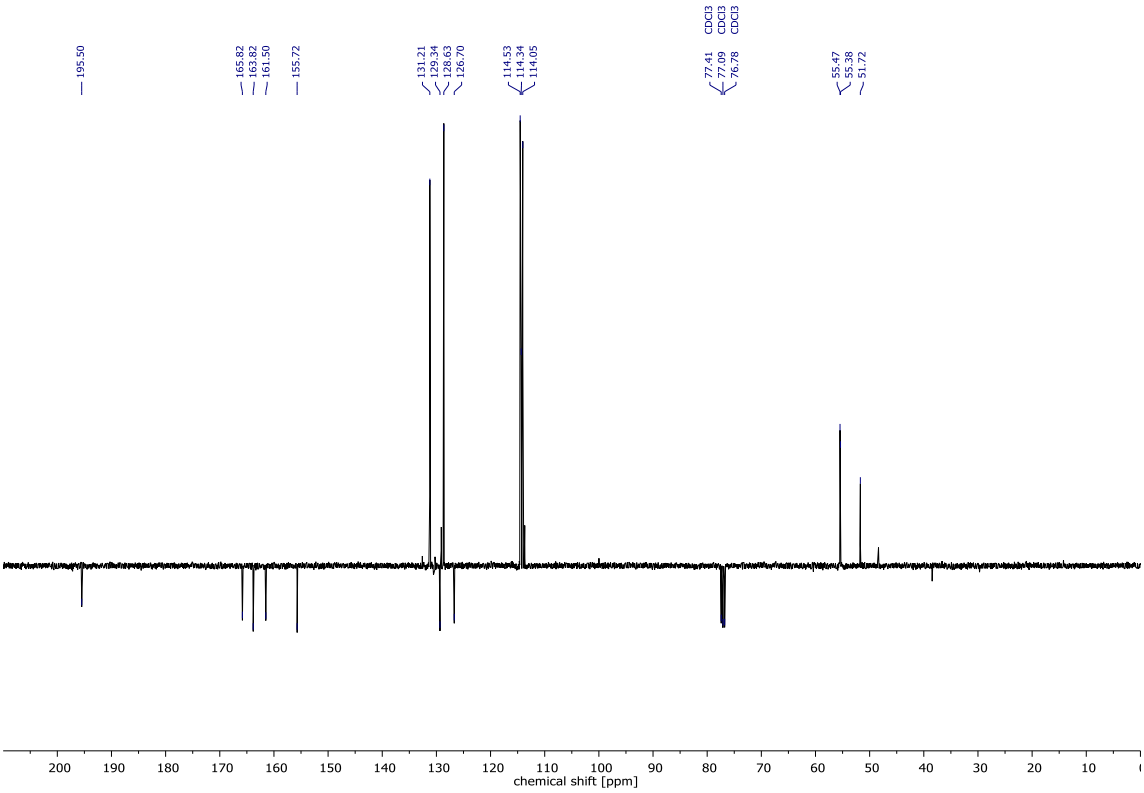

Figure 163: DEPTQ spectrum (101 MHz, $CDCl_3$, 297 K) of **239**.

Methyl-(*Z*)-3-(4-fluorophenyl)-4-(4-methoxyphenyl)-4-oxobut-2-enoate 240

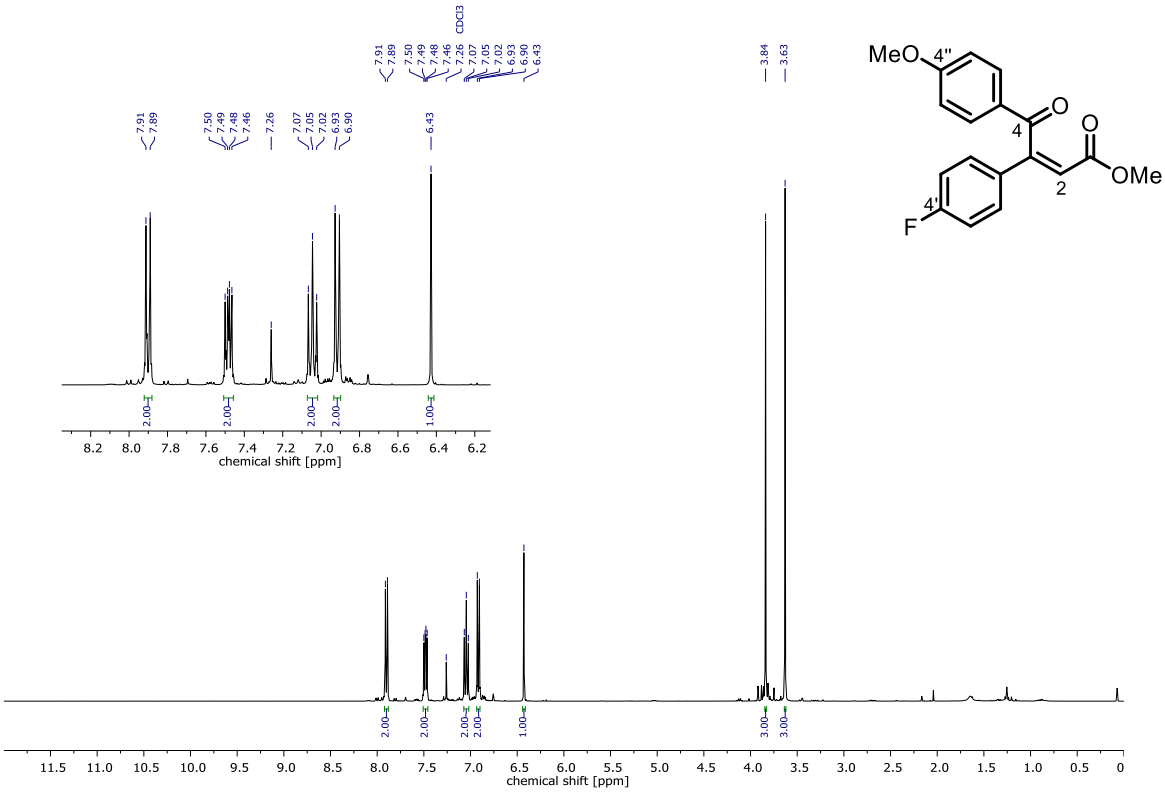

Figure 164: ^{1}H-NMR spectrum (400 MHz, $CDCl_3$, 296 K) of **240**.

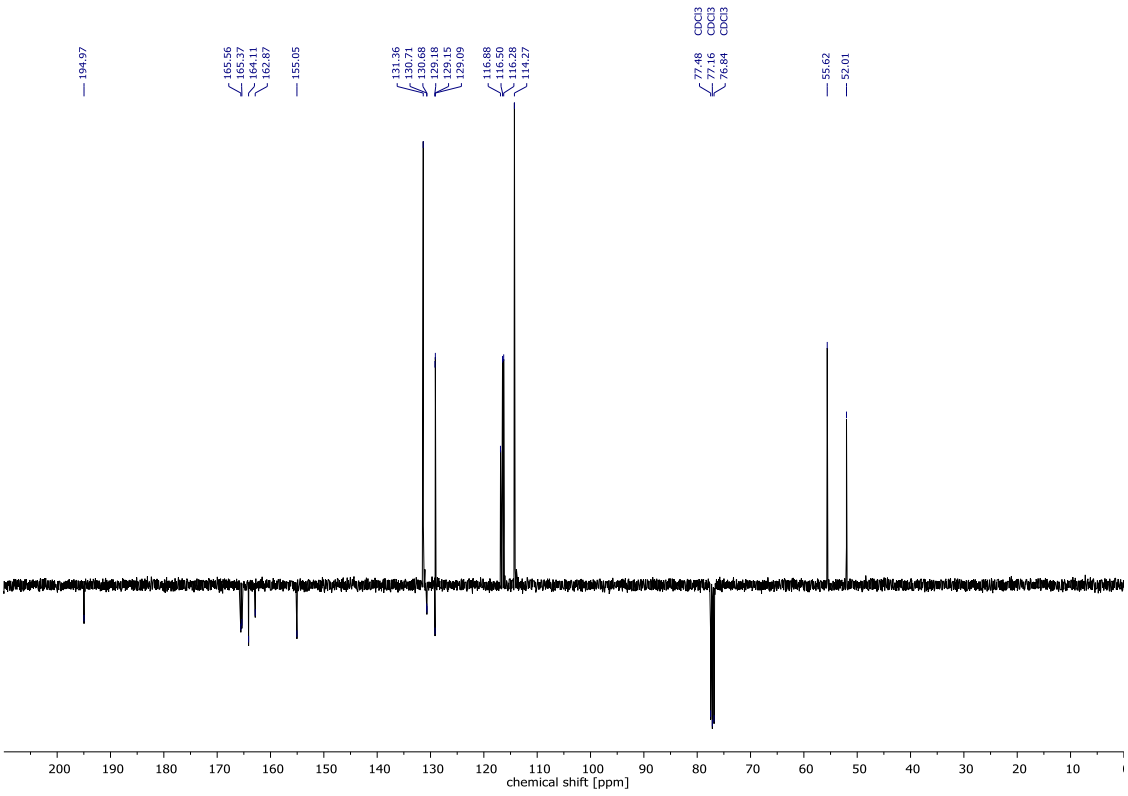

Figure 165: DEPTQ spectrum (101 MHz, $CDCl_3$, 296 K) of **240**.

Methyl-(*Z*)-4-(4-fluorophenyl)-4-oxo-3-phenylbut-2-enoate 241

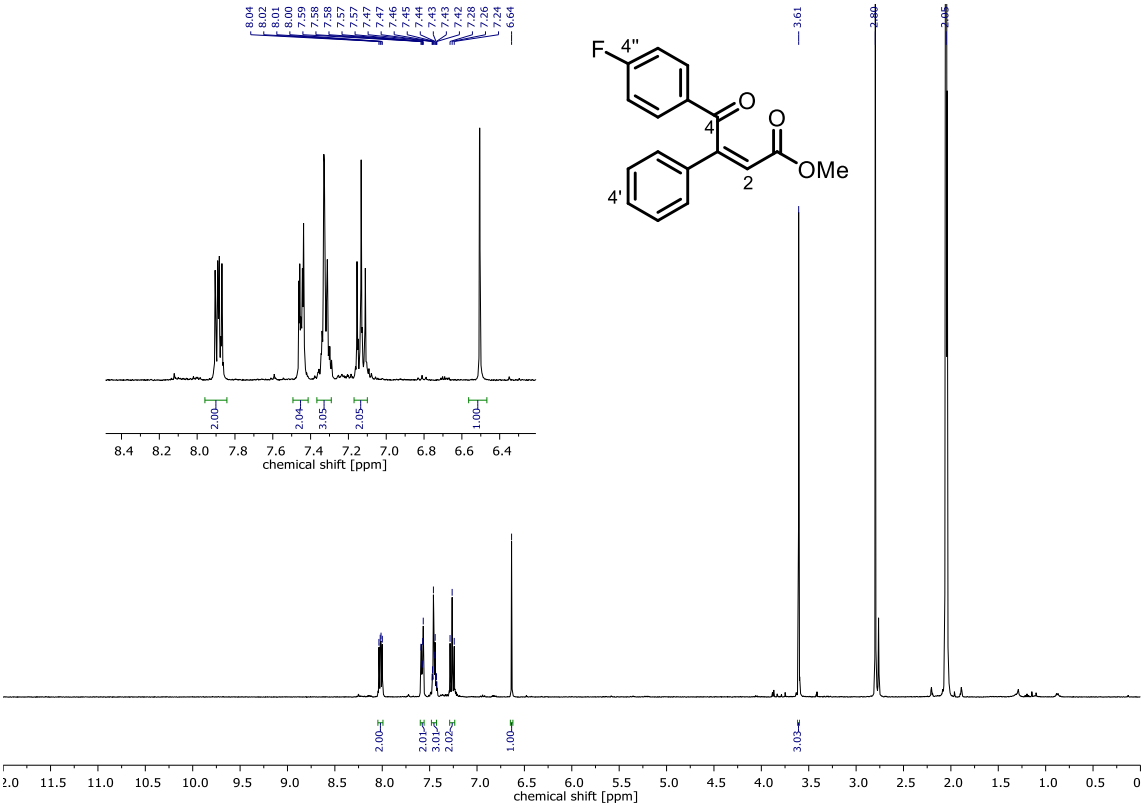

Figure 166: ^{1}H-NMR spectrum (400 MHz, acetone-d_6, 300 K) of **241**.

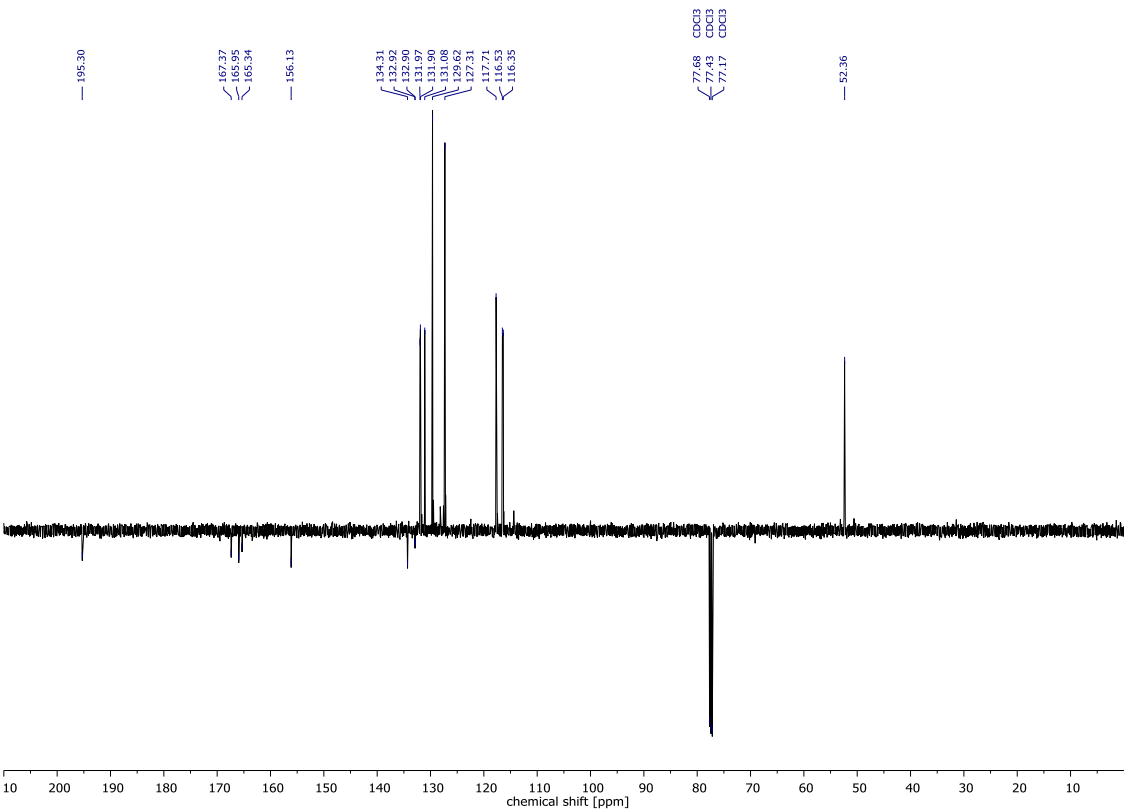

Figure 167: DEPTQ spectrum (126 MHz, $CDCl_3$, 297 K) of **241**.

Methyl-(*Z*)-4-(4-fluorophenyl)-3-(4-methoxyphenyl)-4-oxobut-2-enoate 242

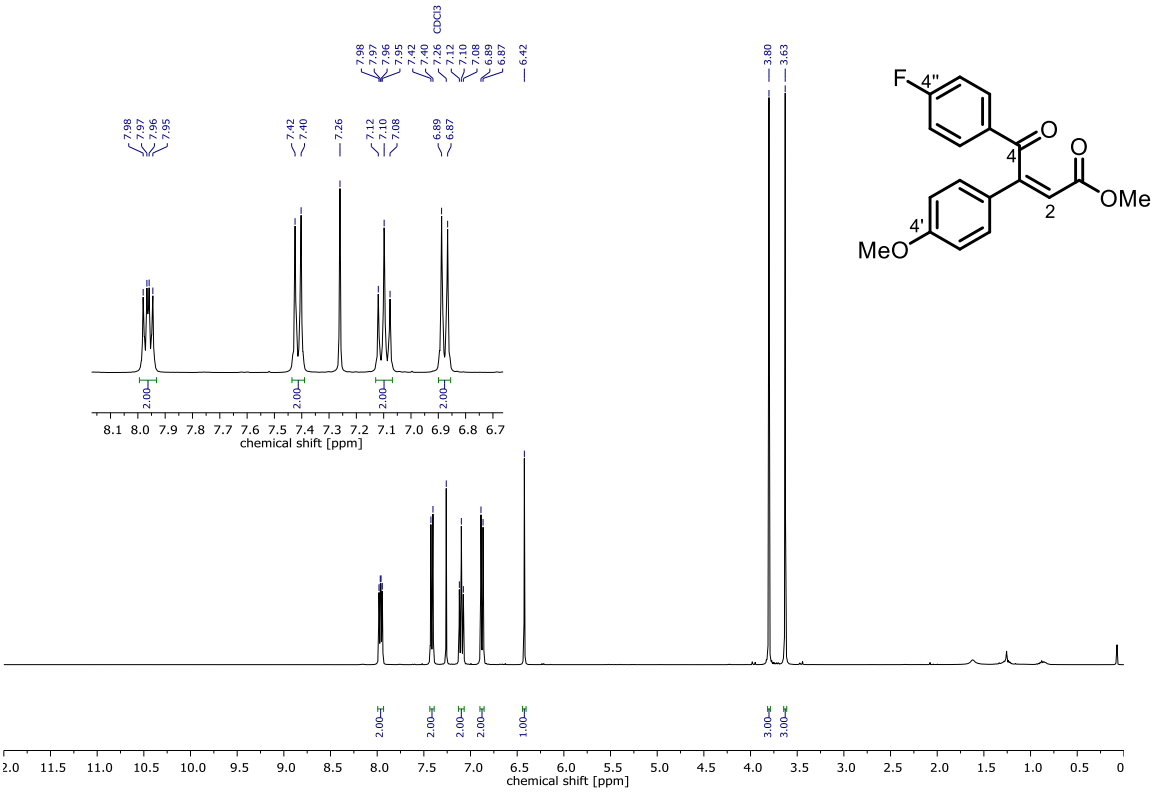

Figure 168: ^{1}H-NMR spectrum (400 MHz, $CDCl_3$, 300 K) of **242**.

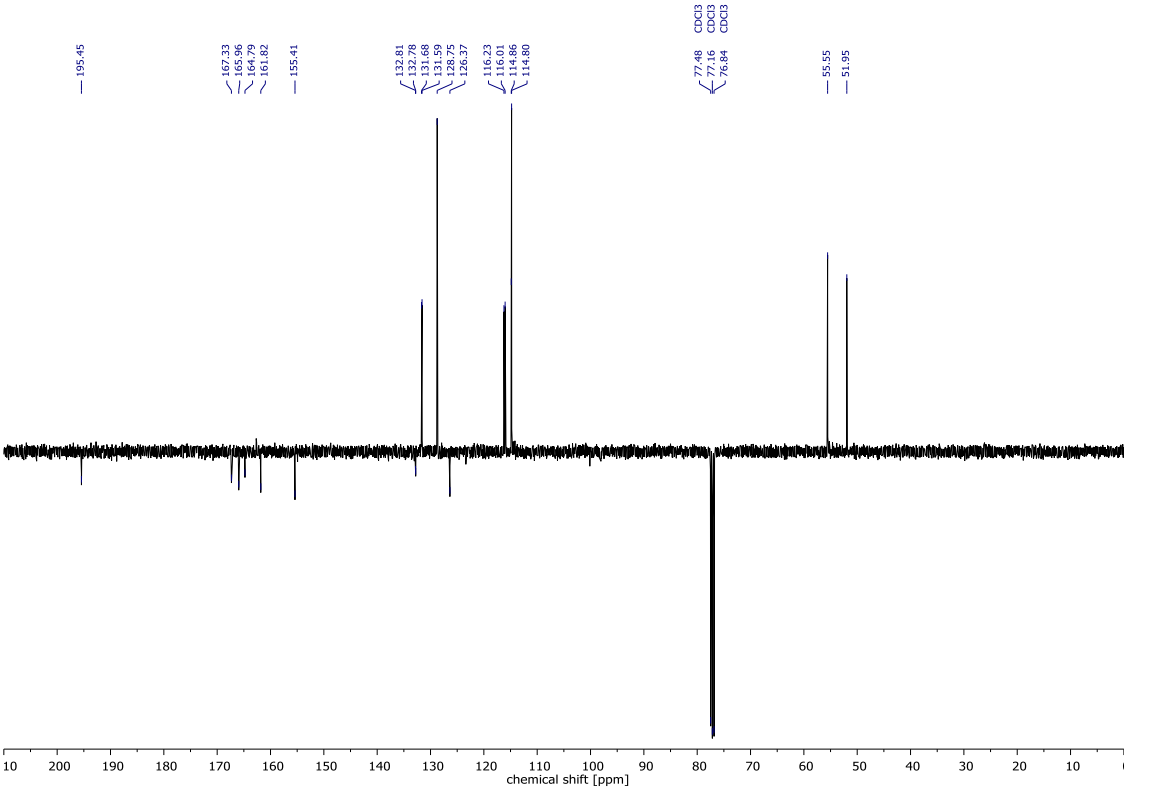

Figure 169: DEPTQ spectrum (101 MHz, $CDCl_3$, 300 K) of **242**.

Methyl-(*Z*)-3,4-di(4-fluorophenyl)-4-oxobut-2-enoate 243

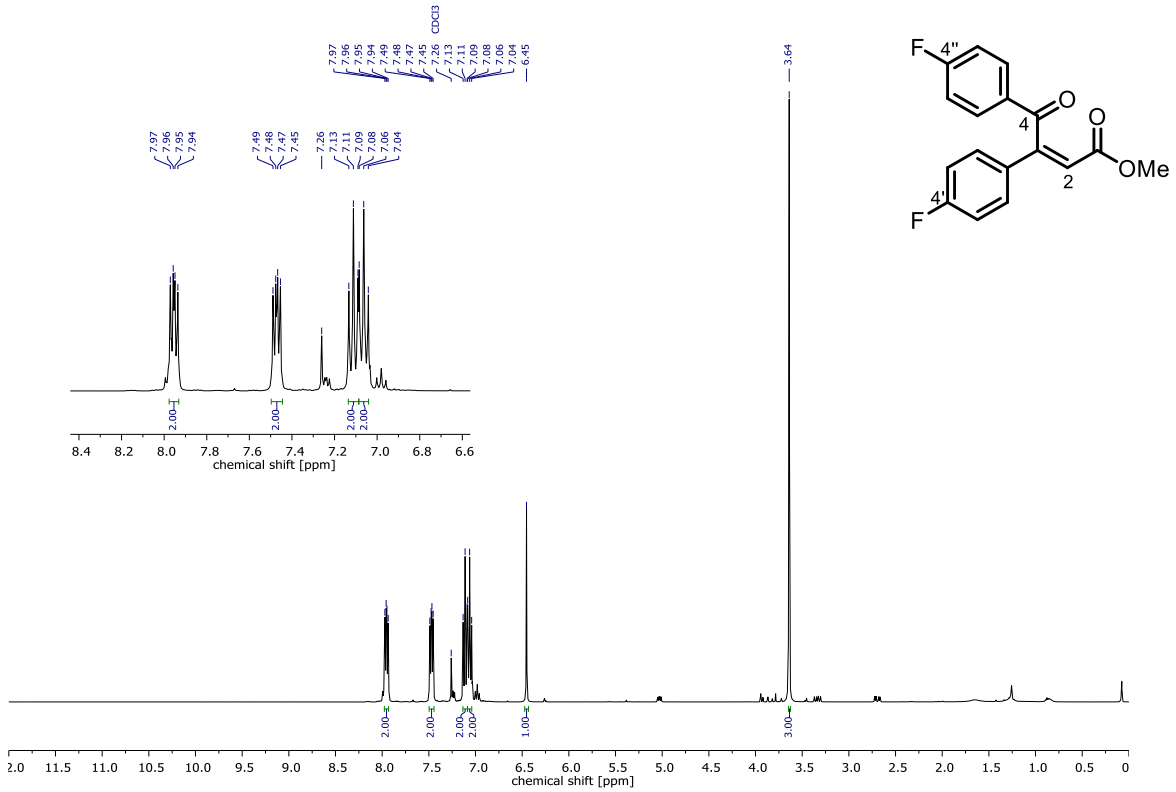

Figure 170: ^{1}H-NMR spectrum (400 MHz, $CDCl_3$, 300 K) of **243**.

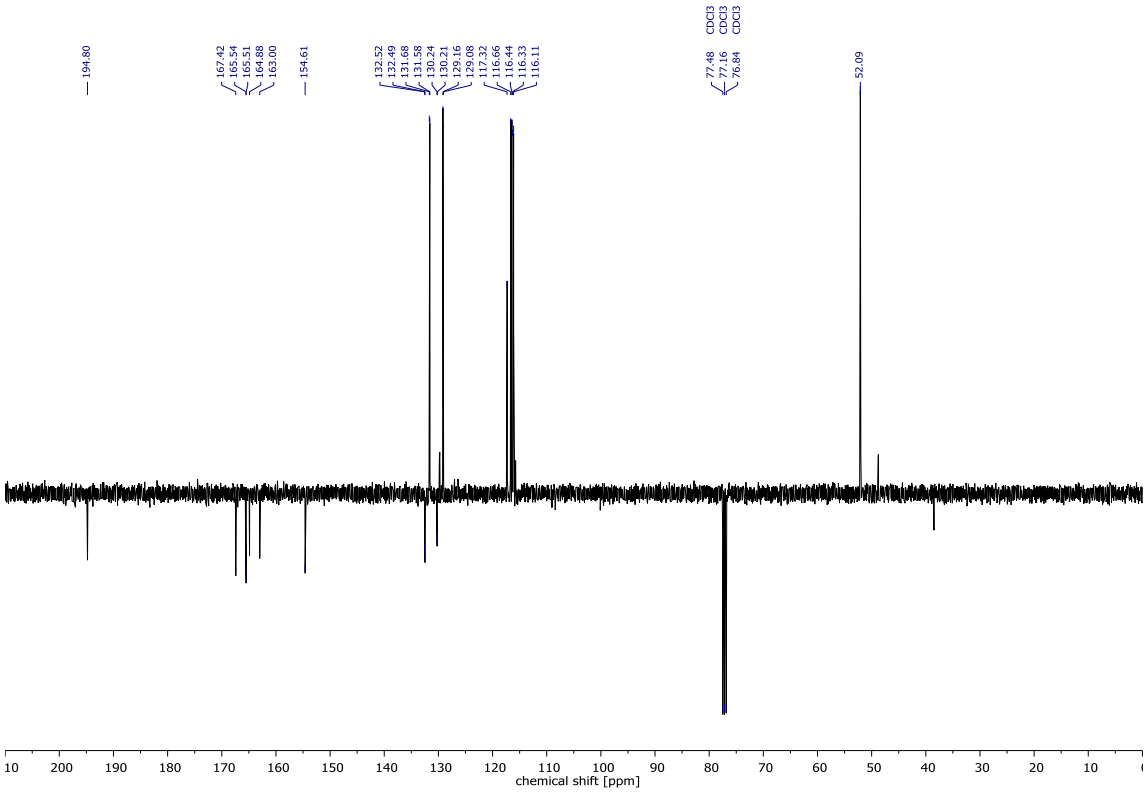

Figure 171: DEPTQ spectrum (101 MHz, $CDCl_3$, 300 K) of **243**.

Methyl-(*Z*)-4-oxo-3-phenyl-4-(*p*-tolyl)but-2-enoate 244.

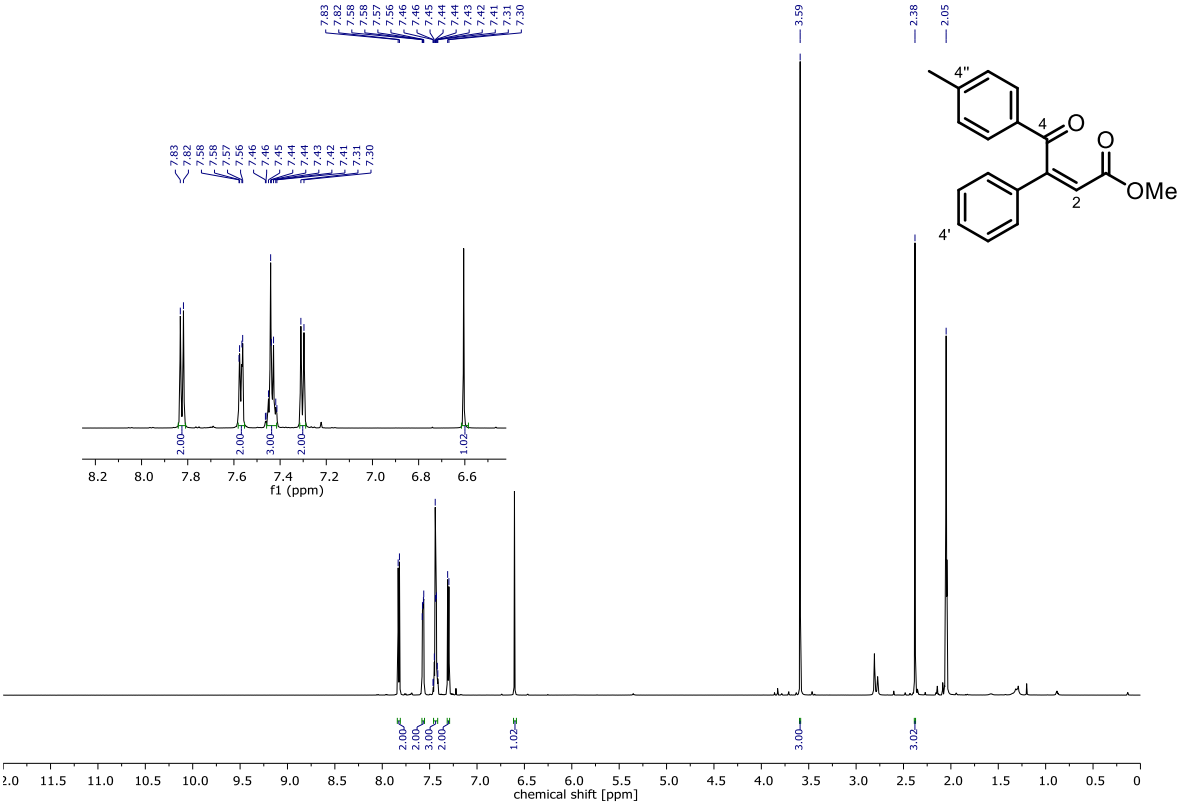

Figure 172: ^{1}H-NMR spectrum (600 MHz, acetone-d_6, 300 K) of **244**.

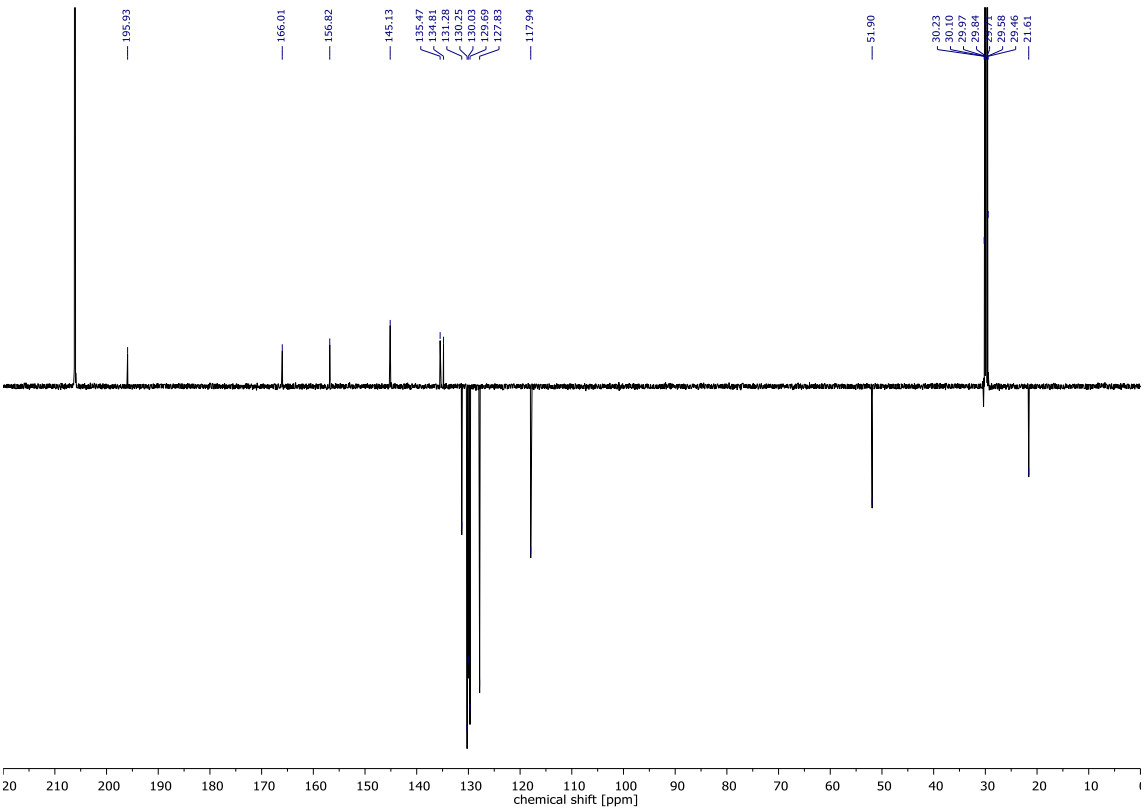

Figure 173: DEPTQ spectrum (151 MHz, acetone-d_6, 300 K) of **244**.

Methyl-(*Z*)-3-(4-methoxyphenyl)-4-oxo-4-(*p*-tolyl)but-2-enoate 245

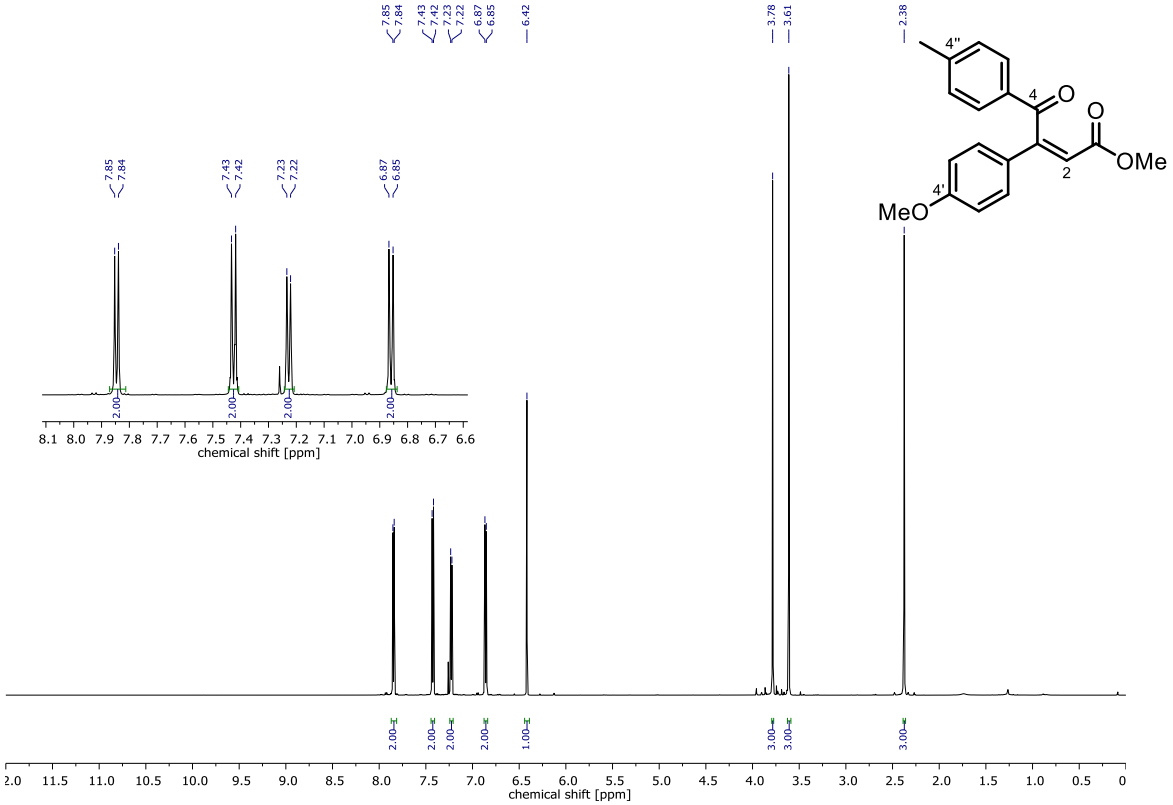

Figure 174: ^{1}H-NMR spectrum (600 MHz, $CDCl_3$, 300 K) of **245**.

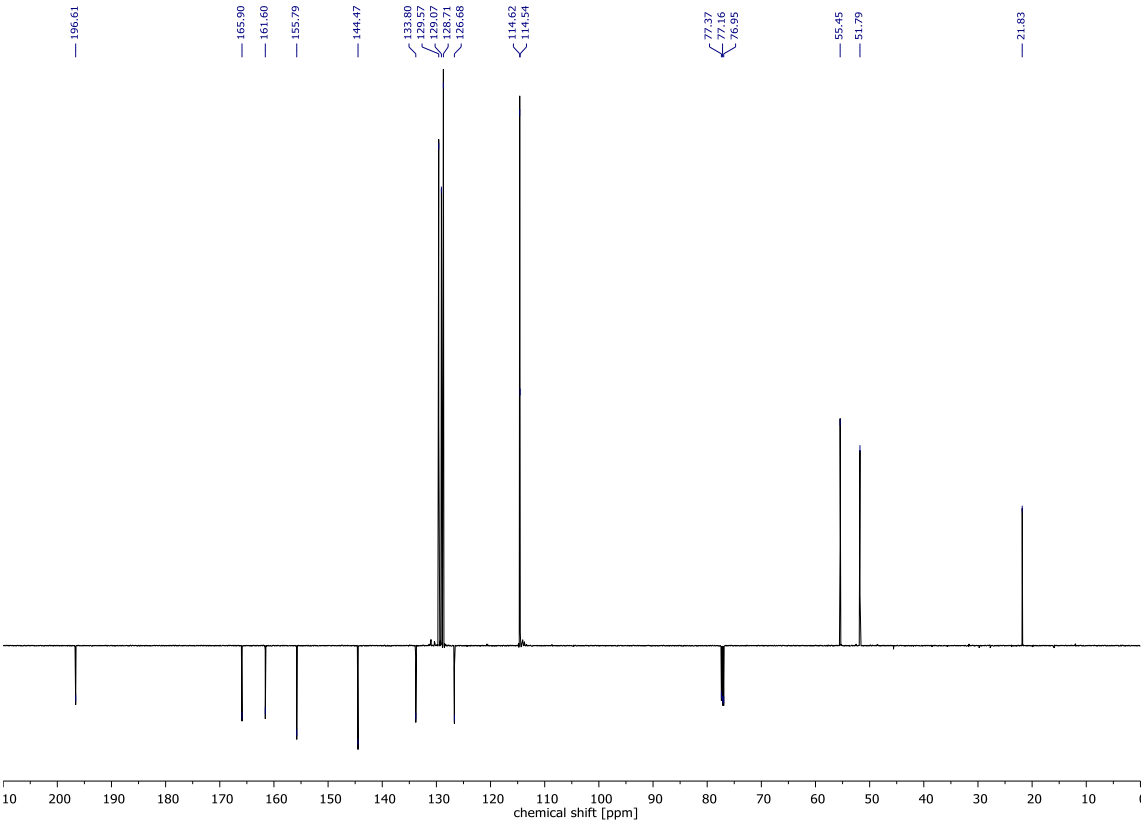

Figure 175: DEPTQ spectrum (151 MHz, $CDCl_3$, 300 K) of **245**.

Methyl-(*Z*)-3-(4-fluorophenyl)-4-oxo-4-(*p*-tolyl)but-2-enoate 246

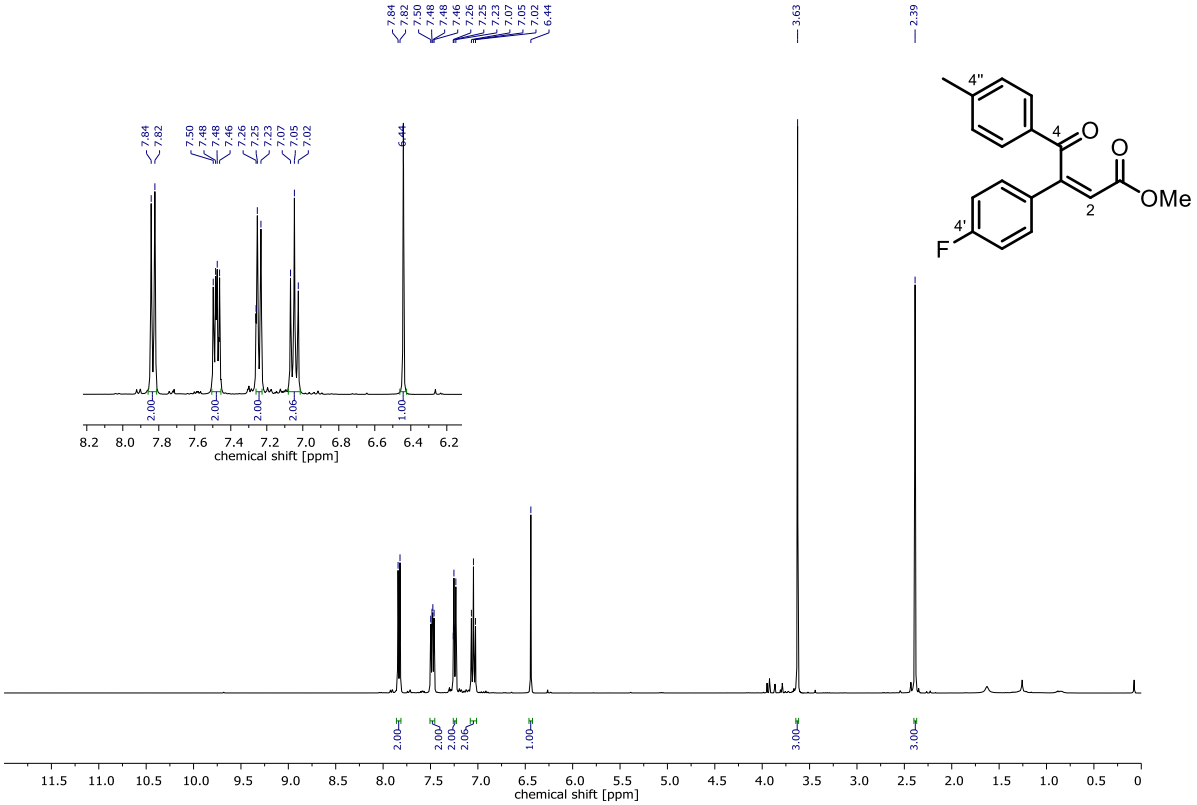

Figure 176: ^{1}H-NMR spectrum (400 MHz, $CDCl_3$, 296 K) of **246**.

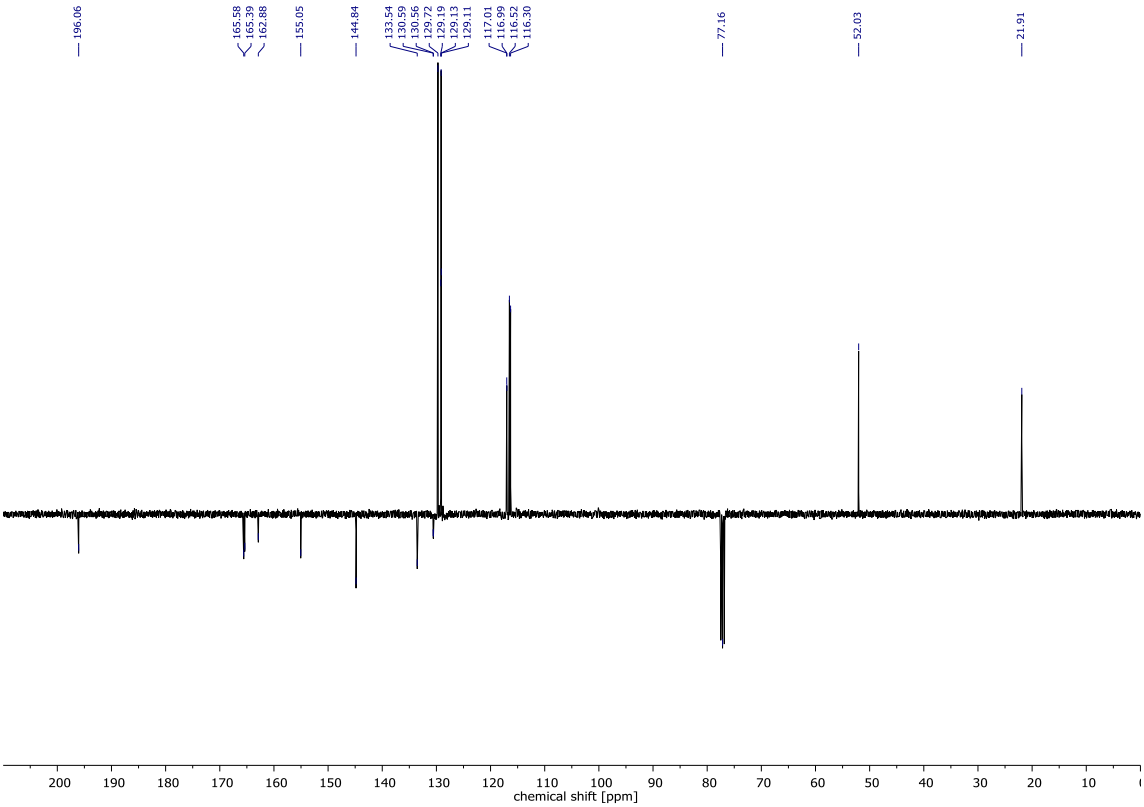

Figure 177: DEPTQ spectrum (101 MHz, $CDCl_3$, 296 K) of **246**.

Methyl-(*Z*)-4-oxo-3-phenyl-4-(*m*-tolyl)but-2-enoate 247

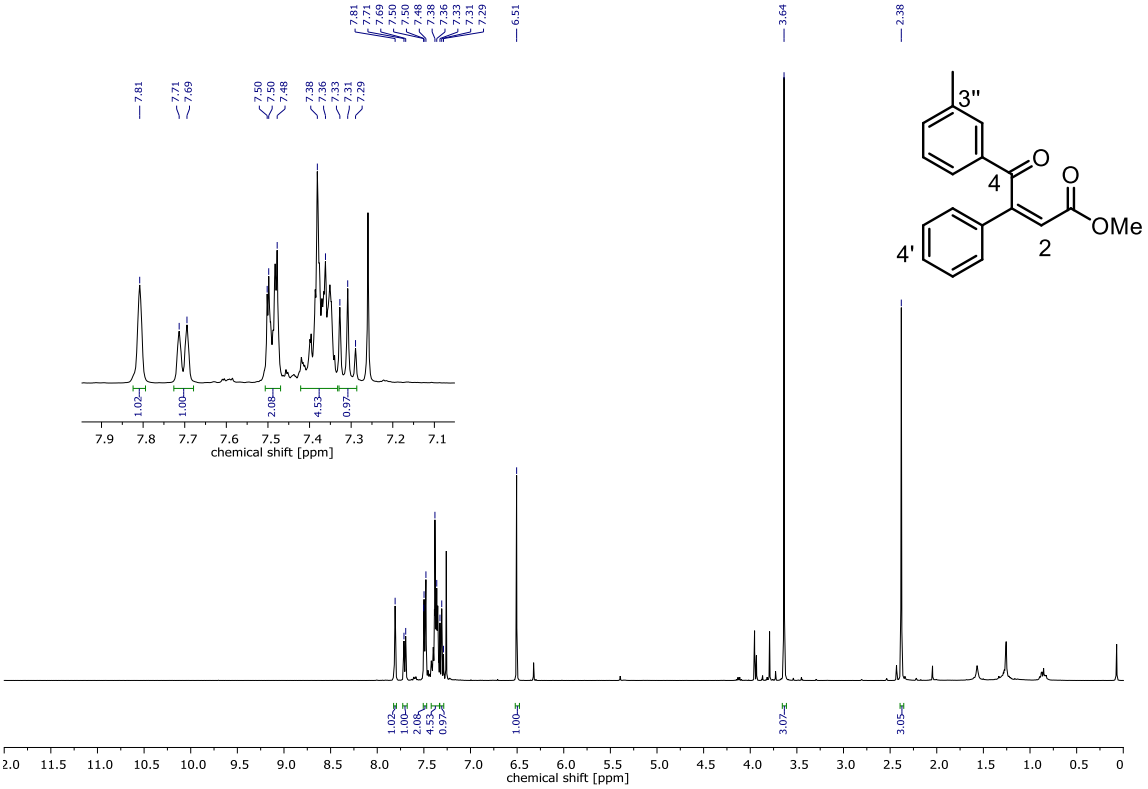

Figure 178: ^{1}H-NMR spectrum (400 MHz, $CDCl_3$, 296 K) of **247**.

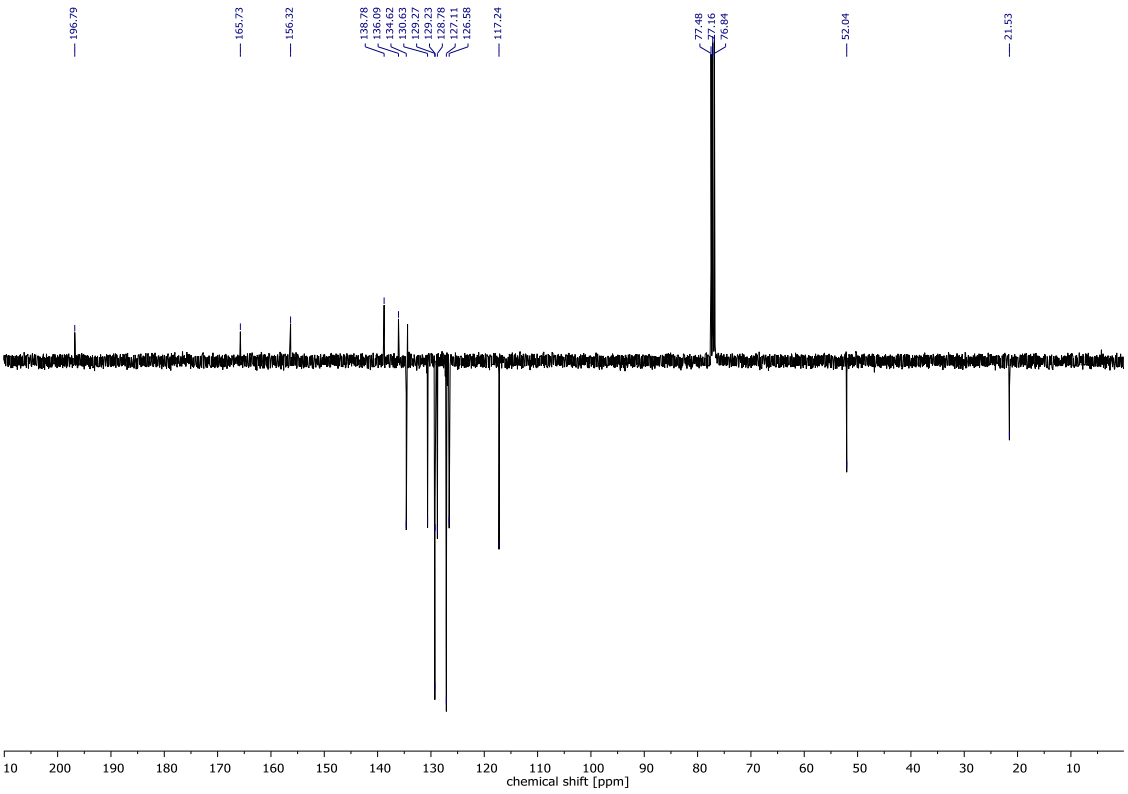

Figure 179: DEPTQ-NMR spectrum (101 MHz, $CDCl_3$, 296 K) of **247**.

Methyl-(Z)-3-(4-methoxyphenyl)-4-oxo-4-(*m*-tolyl)but-2-enoate 248

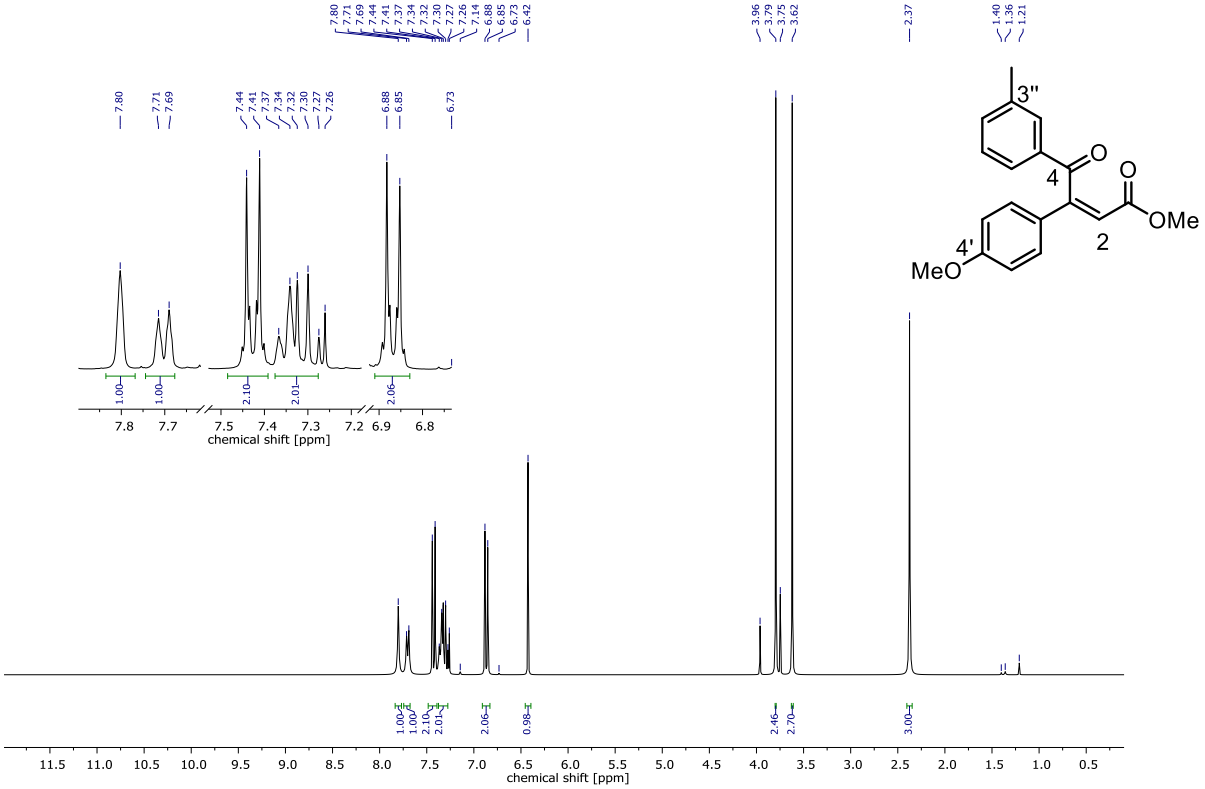

Figure 180: ^{1}H-NMR spectrum (400 MHz, $CDCl_3$, 296 K) of **248**.

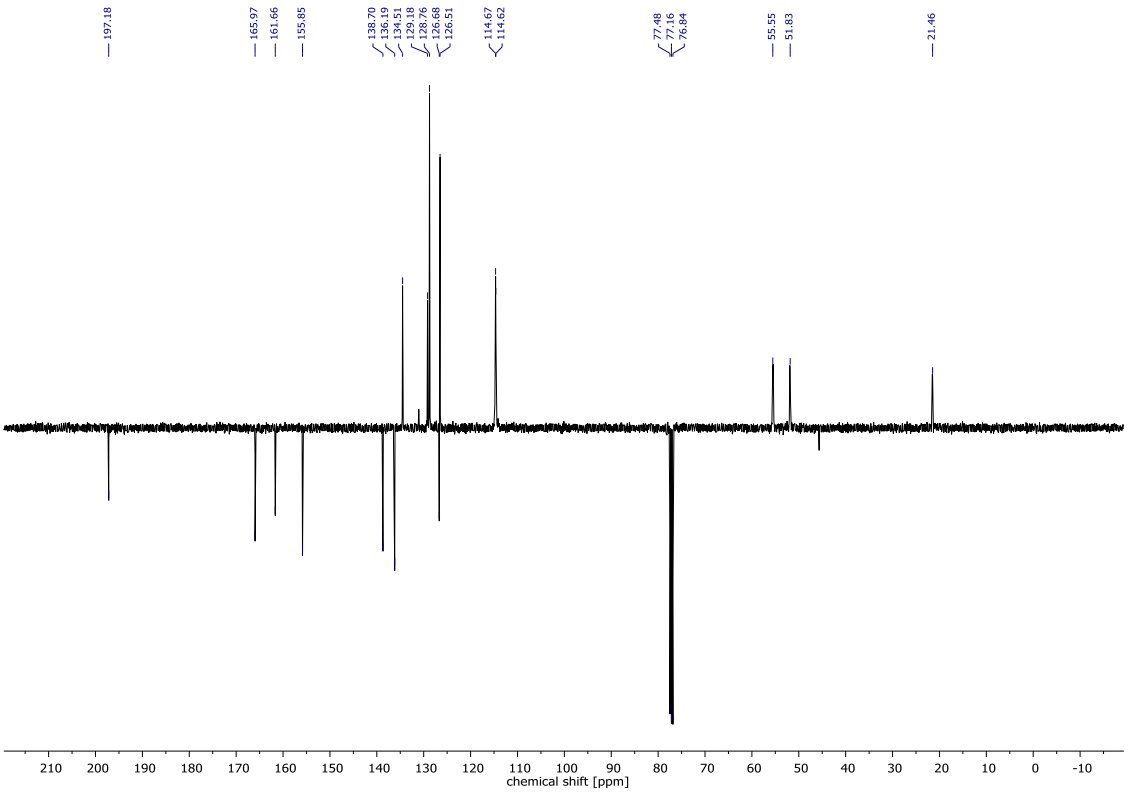

Figure 181: DEPTQ-NMR spectrum (101 MHz, $CDCl_3$, 296 K) of **248**.

Methyl-(*Z*)-3-(4-fluorophenyl)-4-oxo-4-(*m*-tolyl)but-2-enoate 249

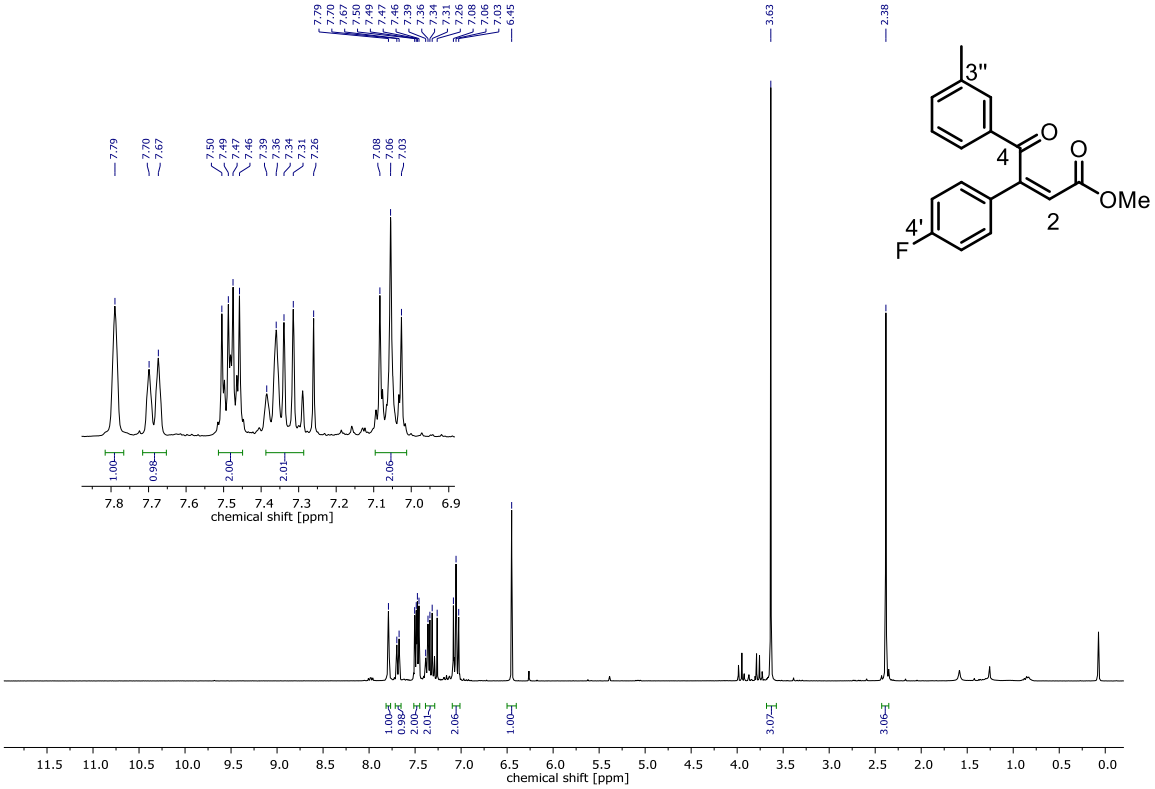

Figure 182: ^{1}H-NMR spectrum (300 MHz, $CDCl_3$, 296 K) of **249**.

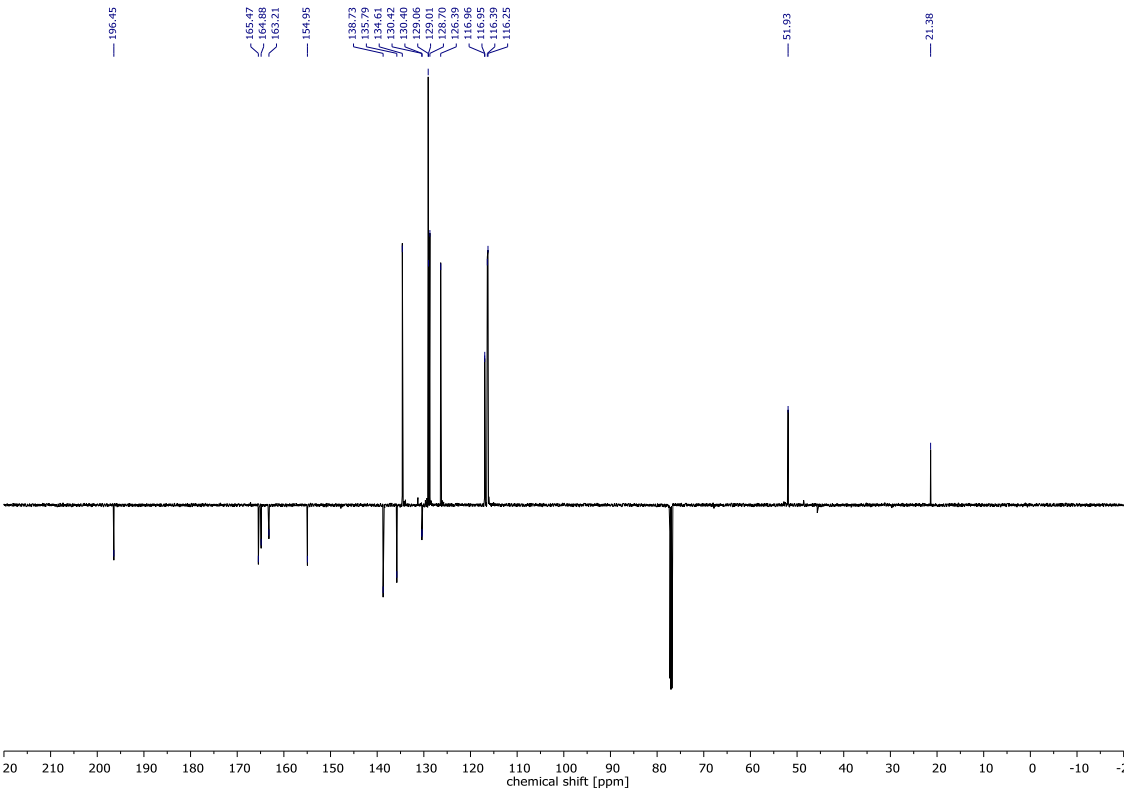

Figure 183: DEPTQ-NMR spectrum (101 MHz, $CDCl_3$, 296 K) of **249**

Methyl-(*Z*)-4-oxo-3-phenyl-4-(*o*-tolyl)but-2-enoate 250

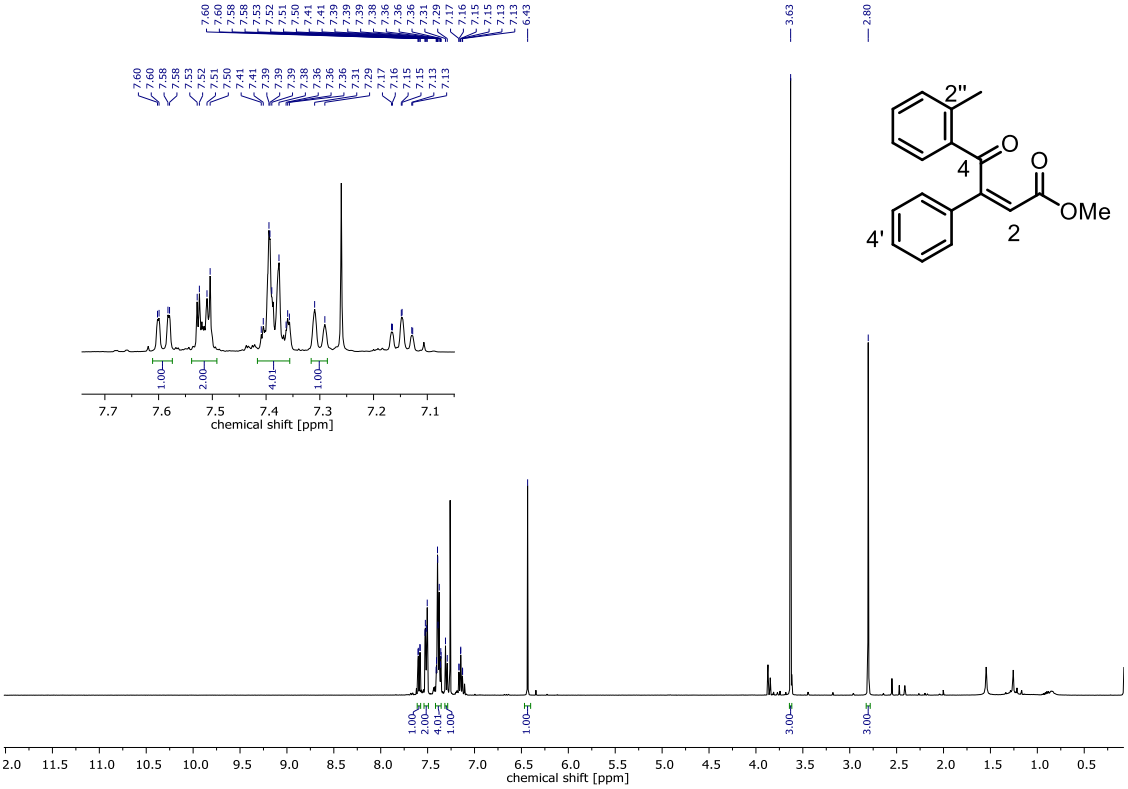

Figure 184: ^{1}H-NMR spectrum (400 MHz, $CDCl_3$, 296 K) of **250**.

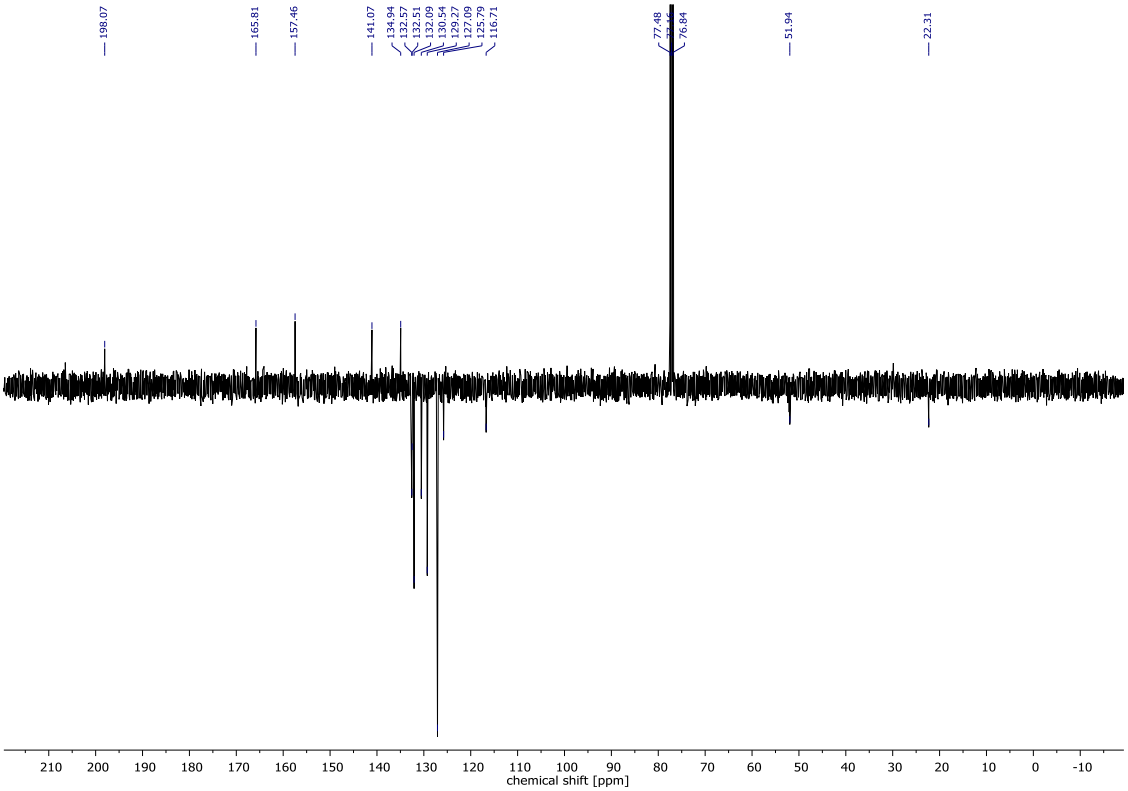

Figure 185: DEPTQ-NMR spectrum (101 MHz, $CDCl_3$, 296 K) of **250**.

Methyl-(*Z*)-3-(4-methoxyphenyl)-4-oxo-4-(*o*-tolyl)but-2-enoate 251

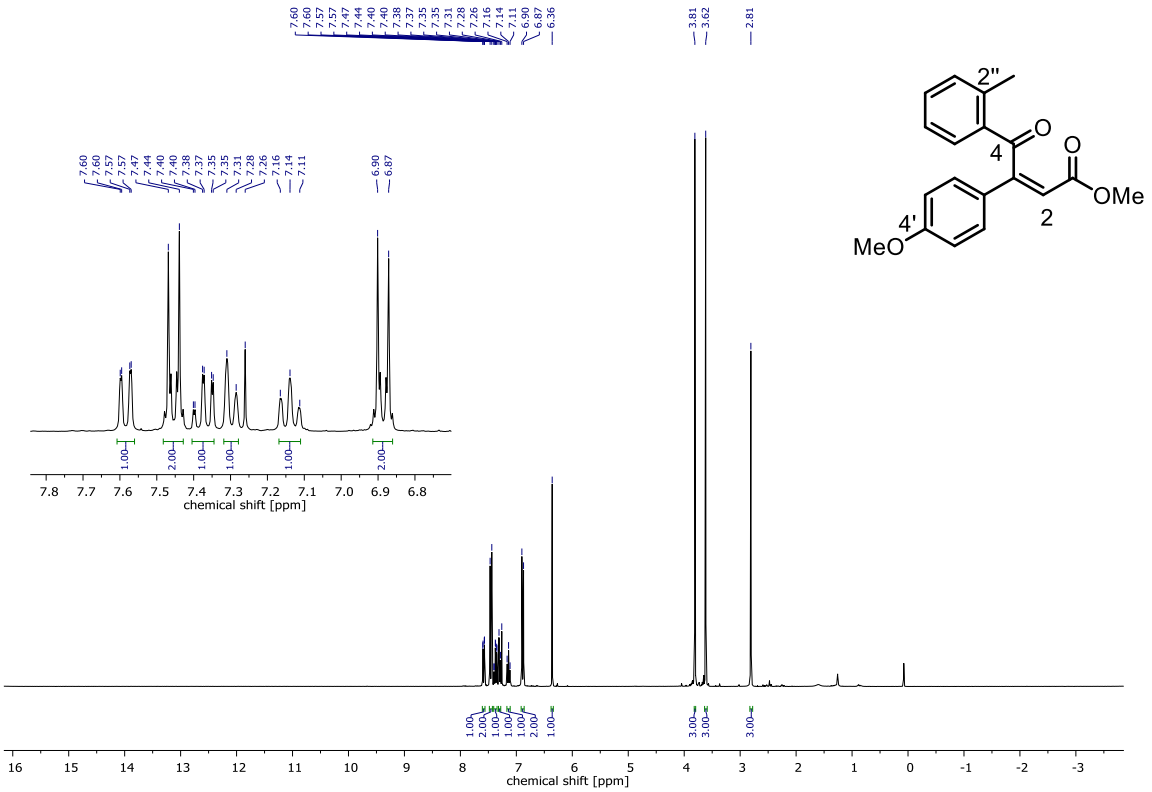

Figure 186: ^{1}H-NMR spectrum (300 MHz, $CDCl_3$, 296 K) of **251**.

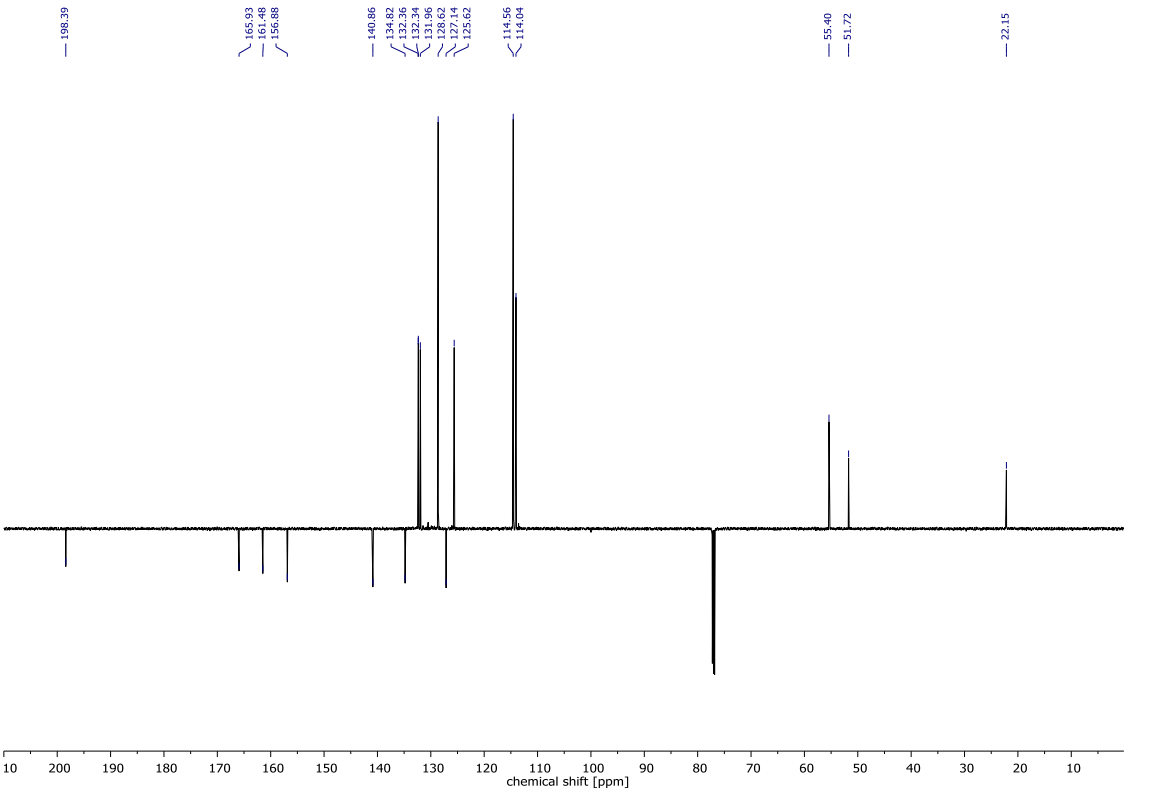

Figure 187: DEPTQ-NMR spectrum (151 MHz, $CDCl_3$, 296 K) of **251**.

Methyl-(*Z*)-3-(4-fluorophenyl)-4-oxo-4-(*o*-tolyl)but-2-enoate 252

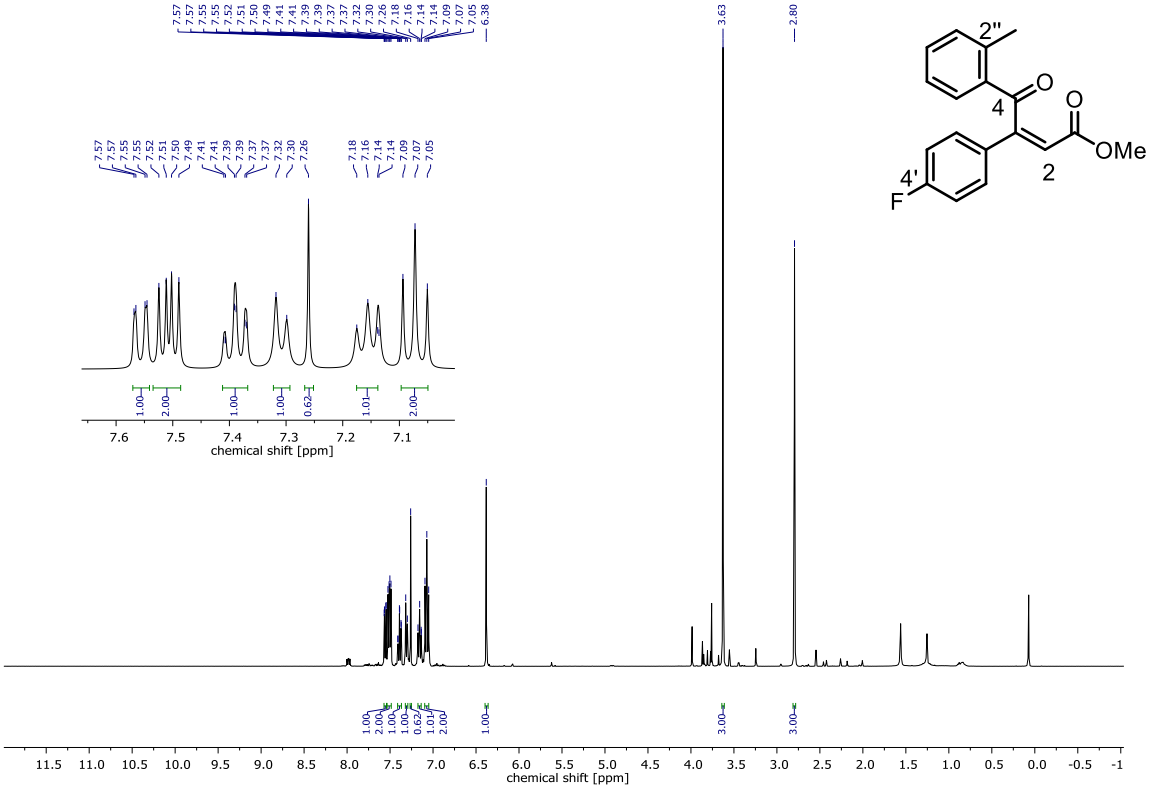

Figure 188: ^{1}H-NMR spectrum (400 MHz, $CDCl_3$, 296 K) of **252**.

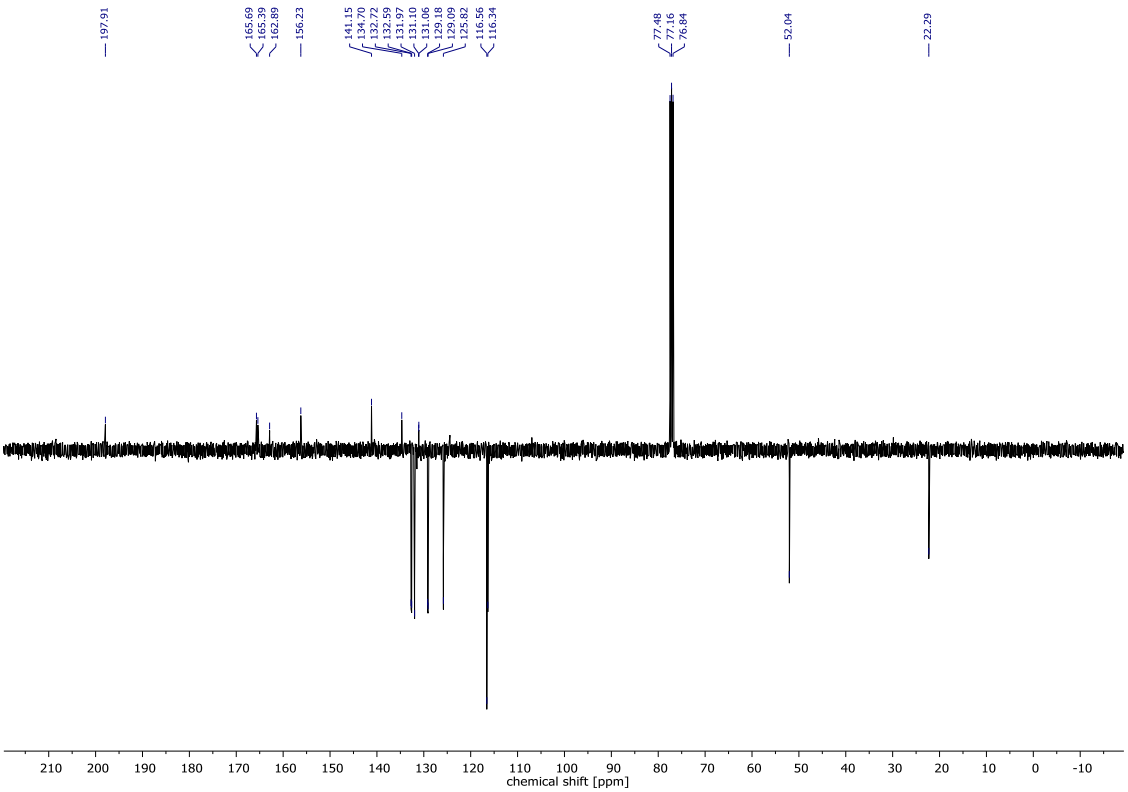

Figure 189: DEPTQ-NMR spectrum (101 MHz, $CDCl_3$, 296 K) of **252**.

Methyl-(*Z*)-4-(naphthalen-2-yl)-4-oxo-3-phenylbut-2-enoate 253

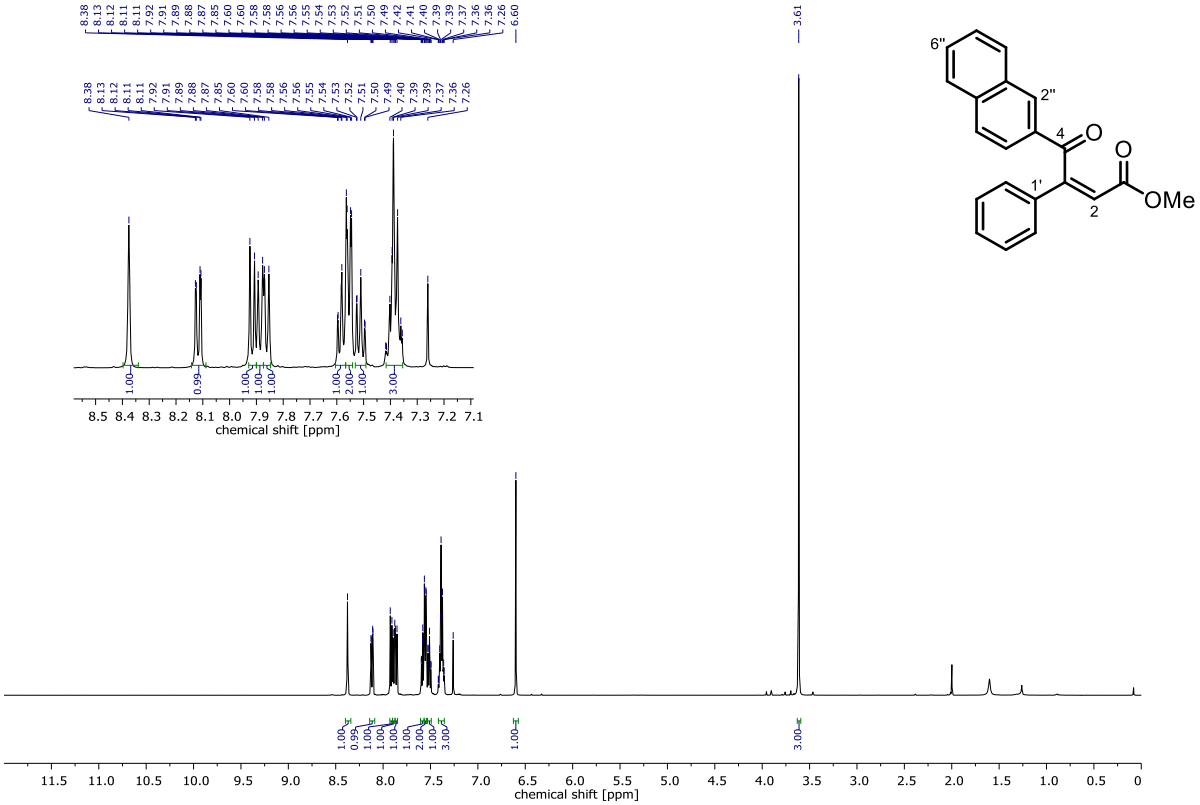

Figure 190: ^{1}H-NMR spectrum (500 MHz, $CDCl_3$, 296 K) of **253**.

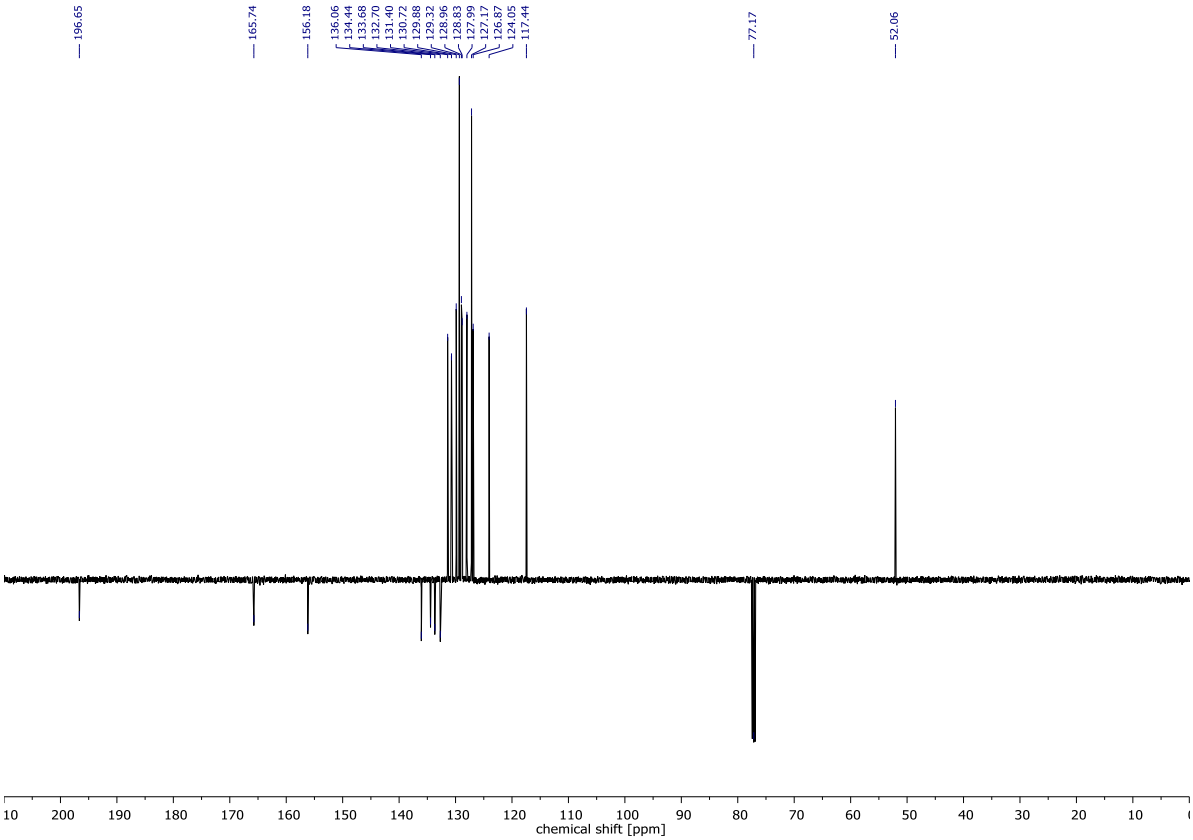

Figure 191: DEPTQ spectrum (126 MHz, $CDCl_3$, 297 K) of **253**.

Methyl-(*Z*)-3-(4-methoxyphenyl)-4-(naphthalen-2-yl)-4-oxobut-2-enoate 254

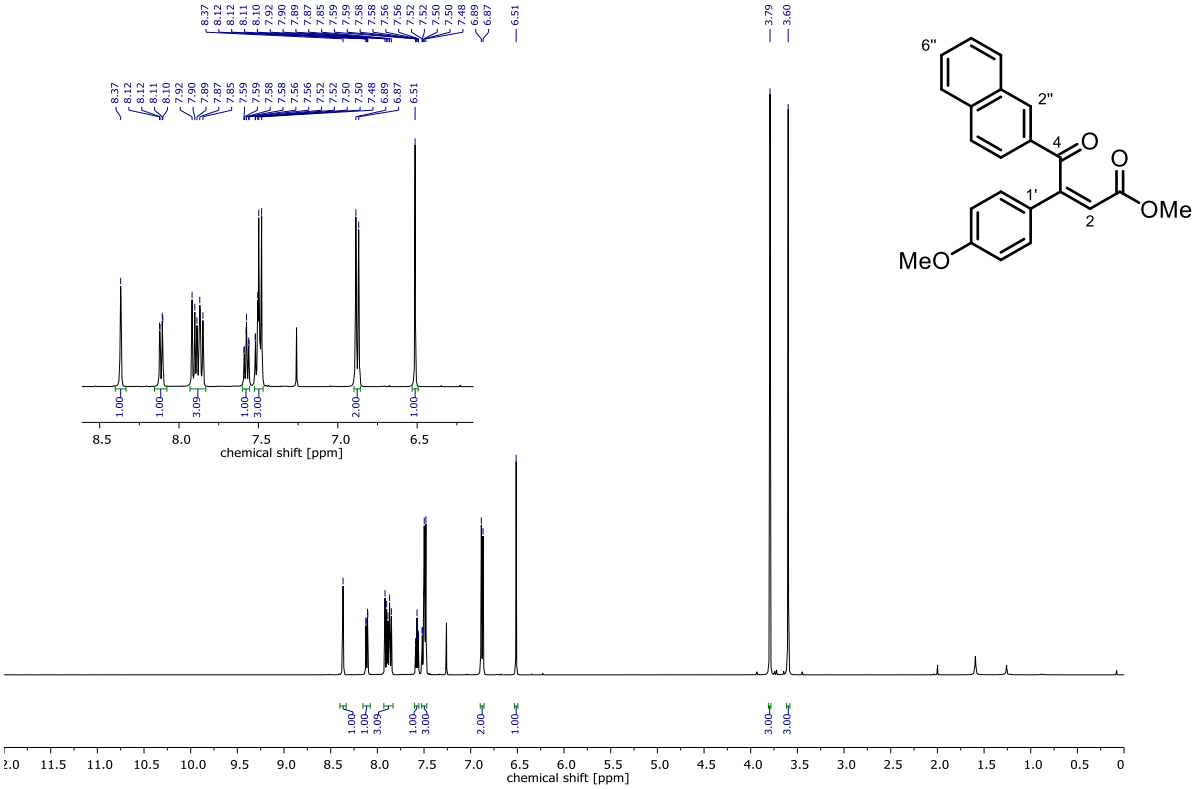

Figure 192: ^{1}H-NMR spectrum (500 MHz, $CDCl_3$, 296 K) of **254**.

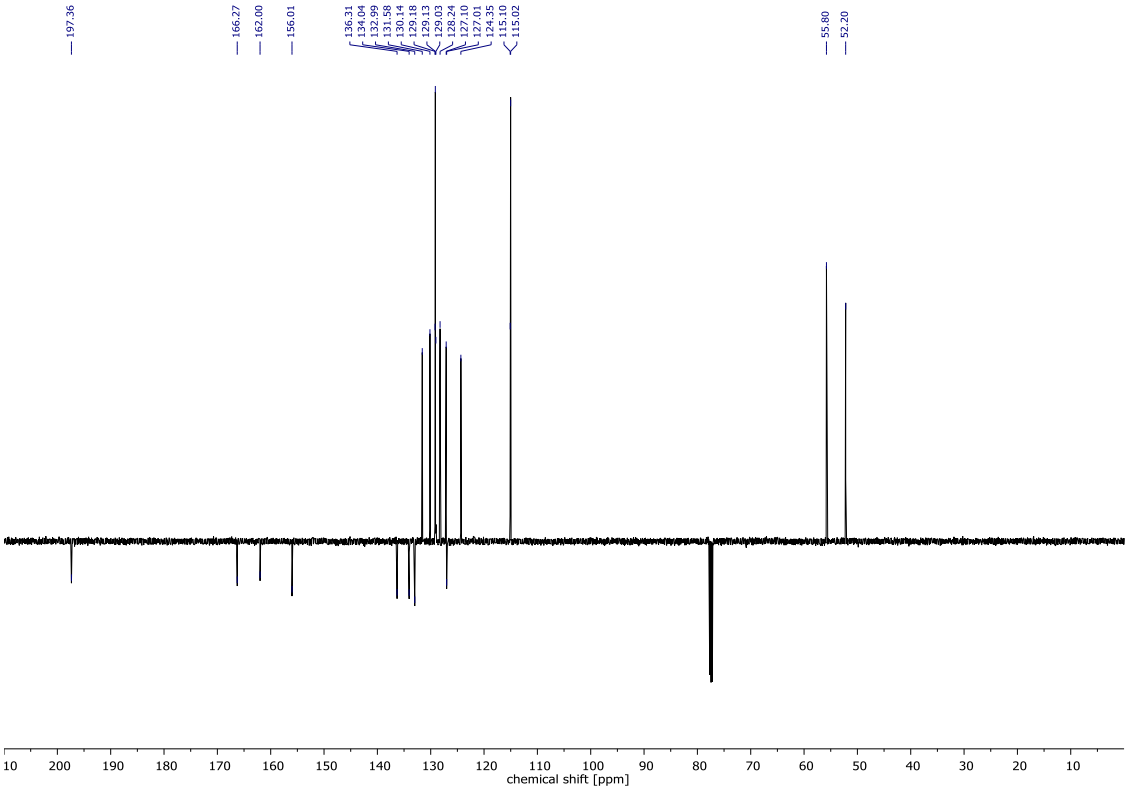

Figure 193: DEPTQ spectrum (126 MHz, $CDCl_3$, 297 K) of **254**.

Methyl-(*Z*)-3-(4-fluorophenyl)-4-(naphthalen-2-yl)-4-oxobut-2-enoate 255

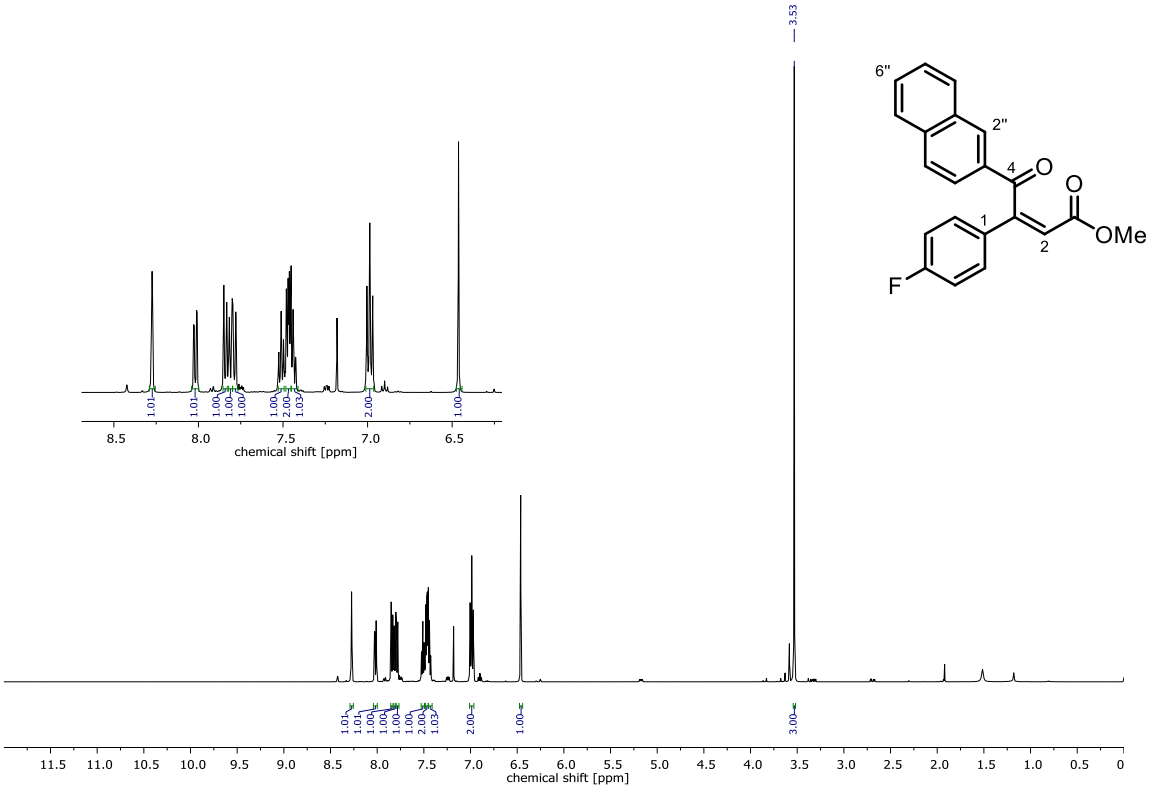

Figure 194: ^{1}H-NMR spectrum (500 MHz, $CDCl_3$, 296 K) of **255**.

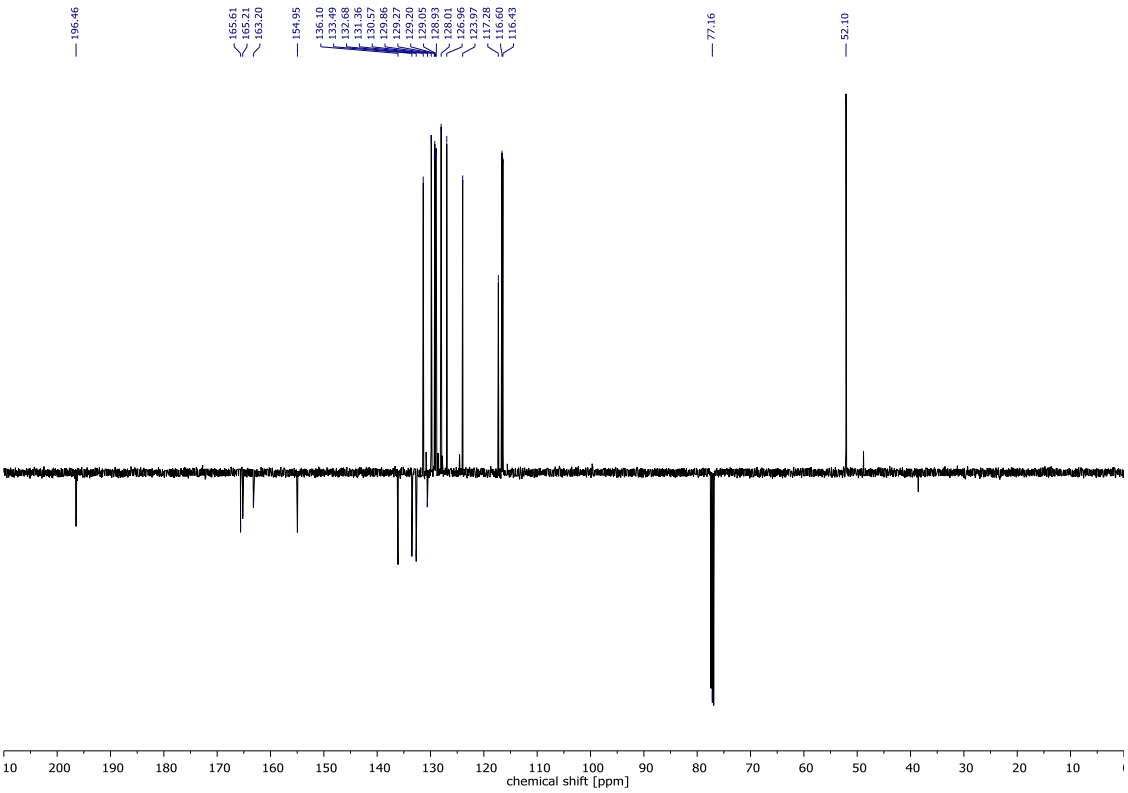

Figure 195: DEPTQ spectrum (126 MHz, $CDCl_3$, 296K) of **255**.

5-Hydroxy-4,5-diphenylfuran-2(5*H*)-one 259

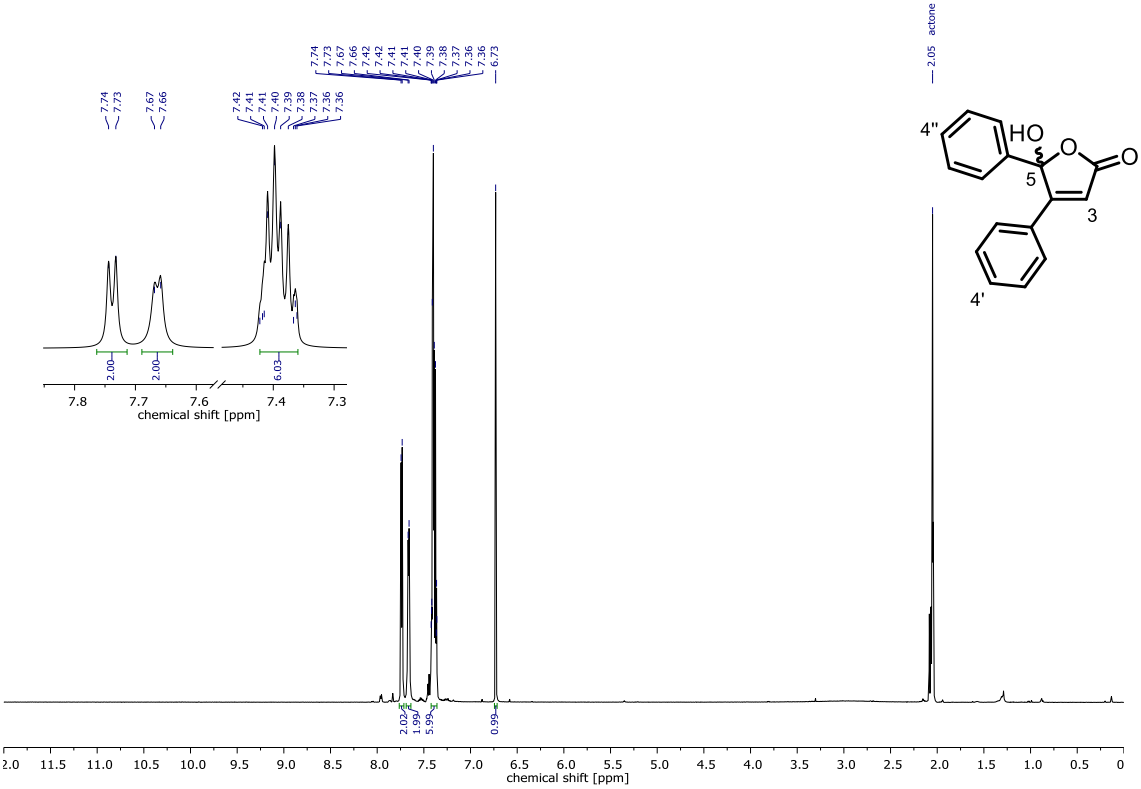

Figure 196: ^{1}H-NMR spectrum (600 MHz, acetone-d_6, 300K) of **259**.

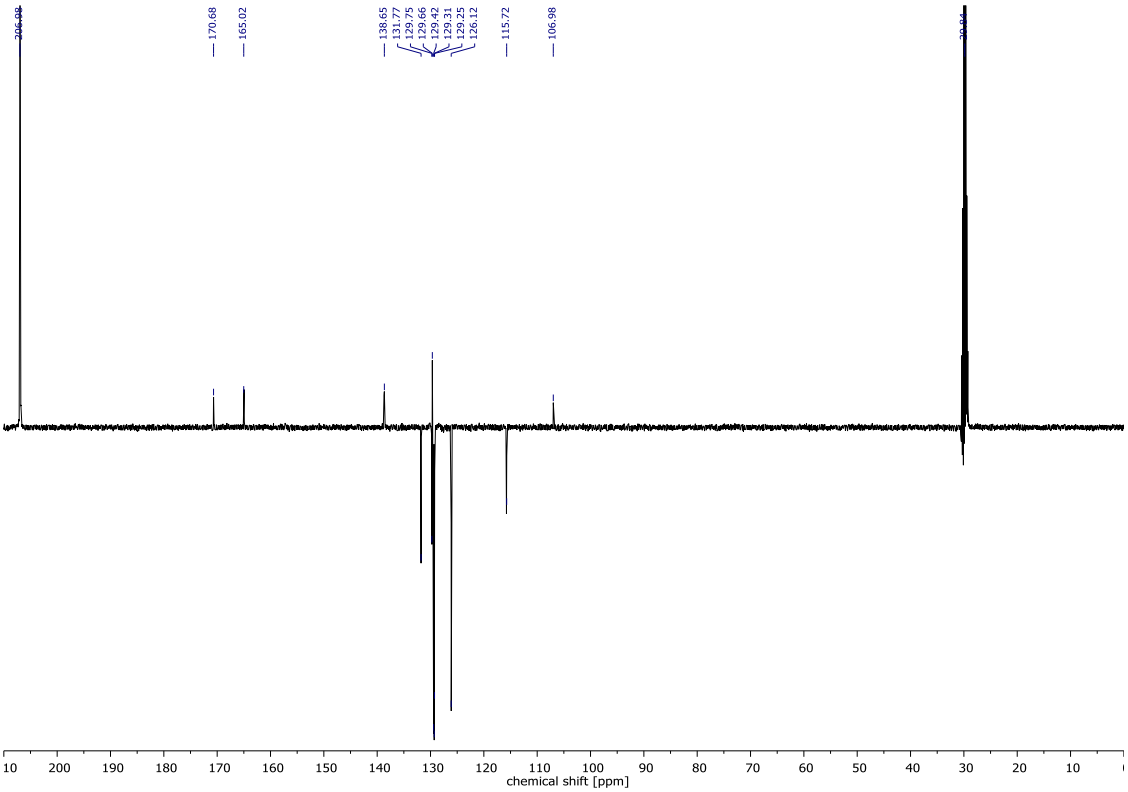

Figure 197: DEPTQ spectrum (101 MHz, acetone-d_6, 223K) of **259**.

5-Hydroxy-4-(4-methoxyphenyl)-5-phenylfuran-2(5*H*)-one 260

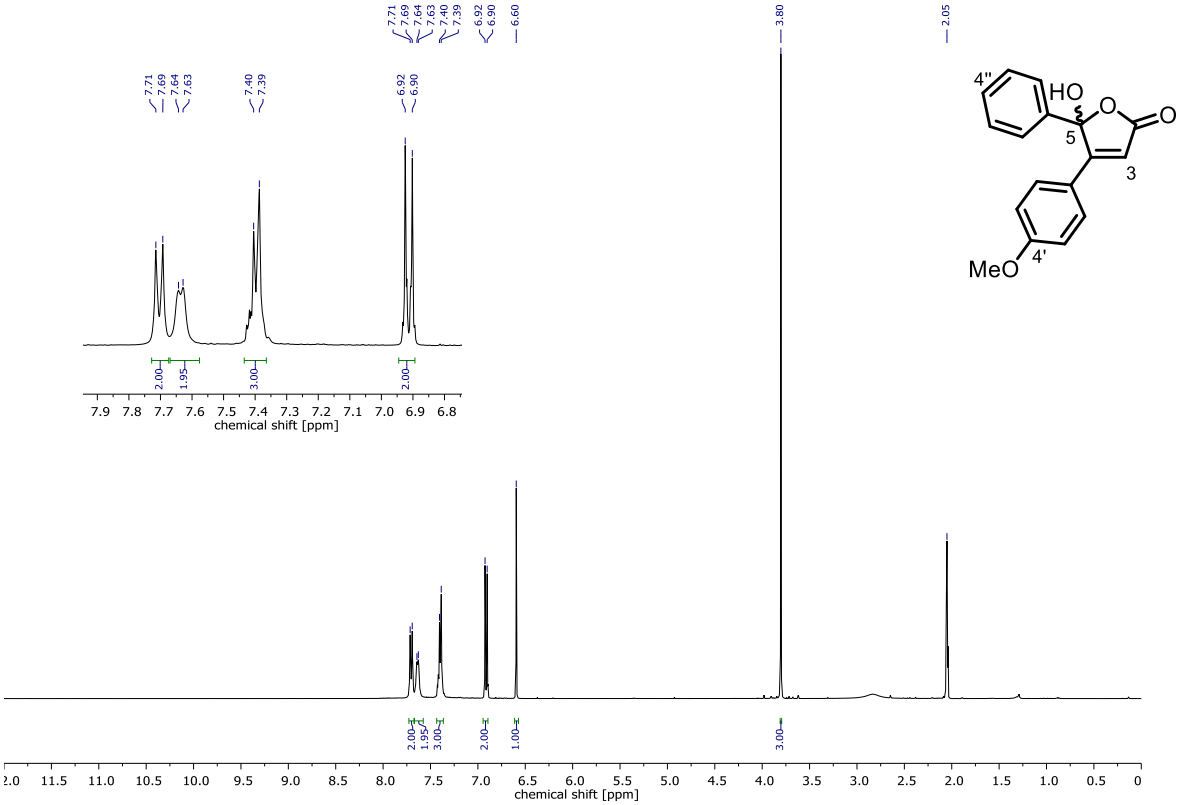

Figure 198: ^{1}H-NMR spectrum (400 MHz, acetone-d_6, 300K) of **260**.

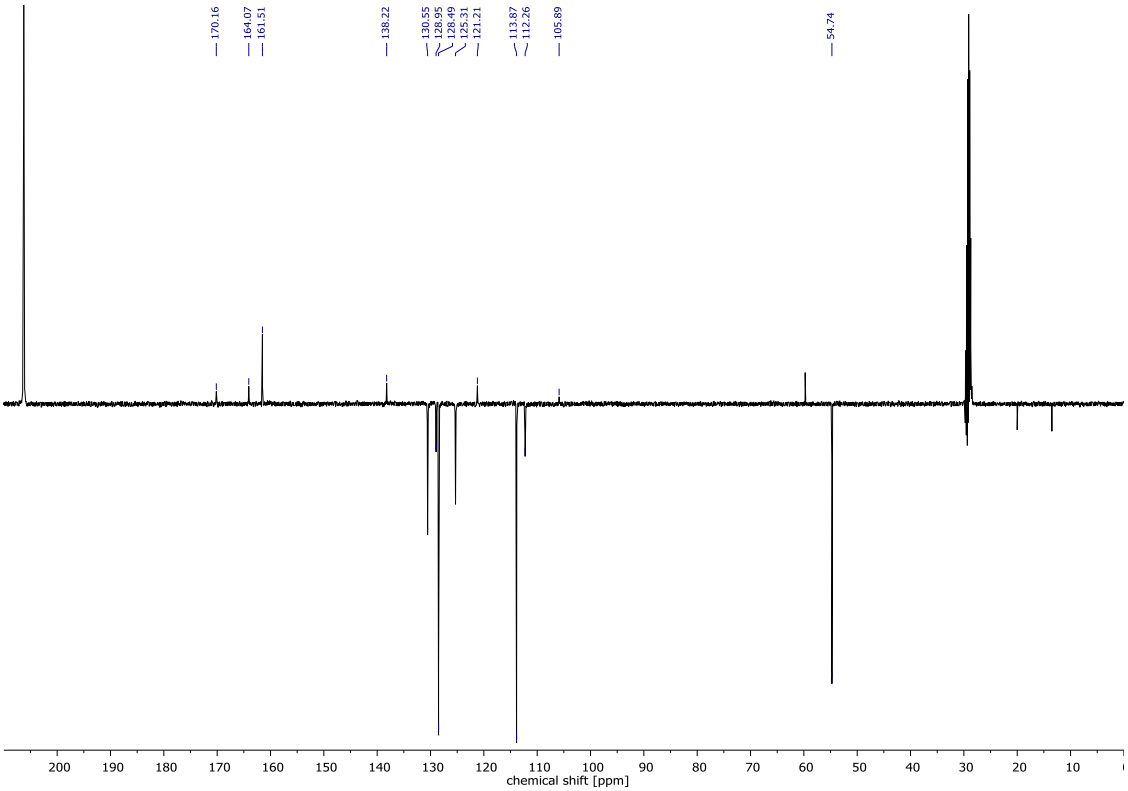

Figure 199: DEPTQ spectrum (101 MHz, acetone-d_6, 223K) of **260**.

4-(4-Fluoroyphenyl)-5-hydroxy-5-phenylfuran-2(5*H*)-one 261

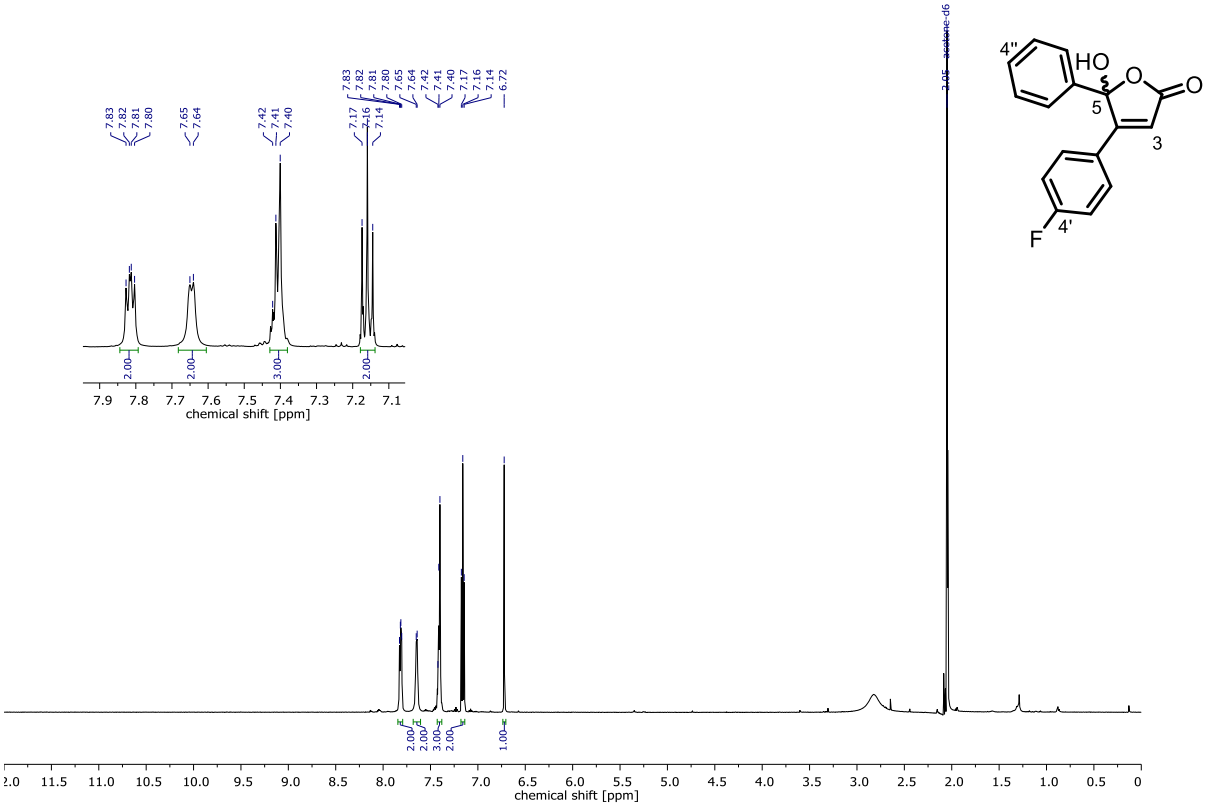

Figure 200: ^{1}H-NMR spectrum (600 MHz, acetone-d_6, 300K) of **261**.

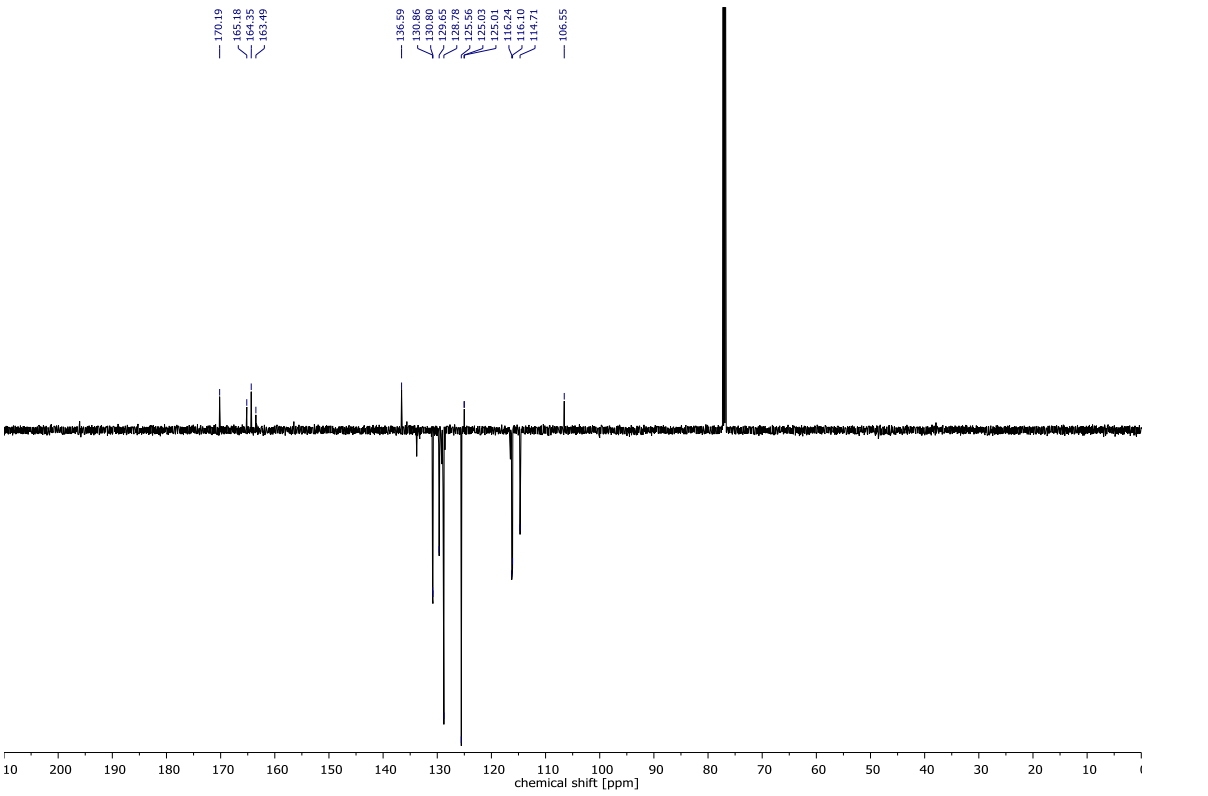

Figure 201: DEPTQ spectrum (150 MHz, $CDCl_3$, 300K) of **261**.

5-Hydroxy-5-(4-methoxyphenyl)-4-phenylfuran-2(5*H*)-one 262

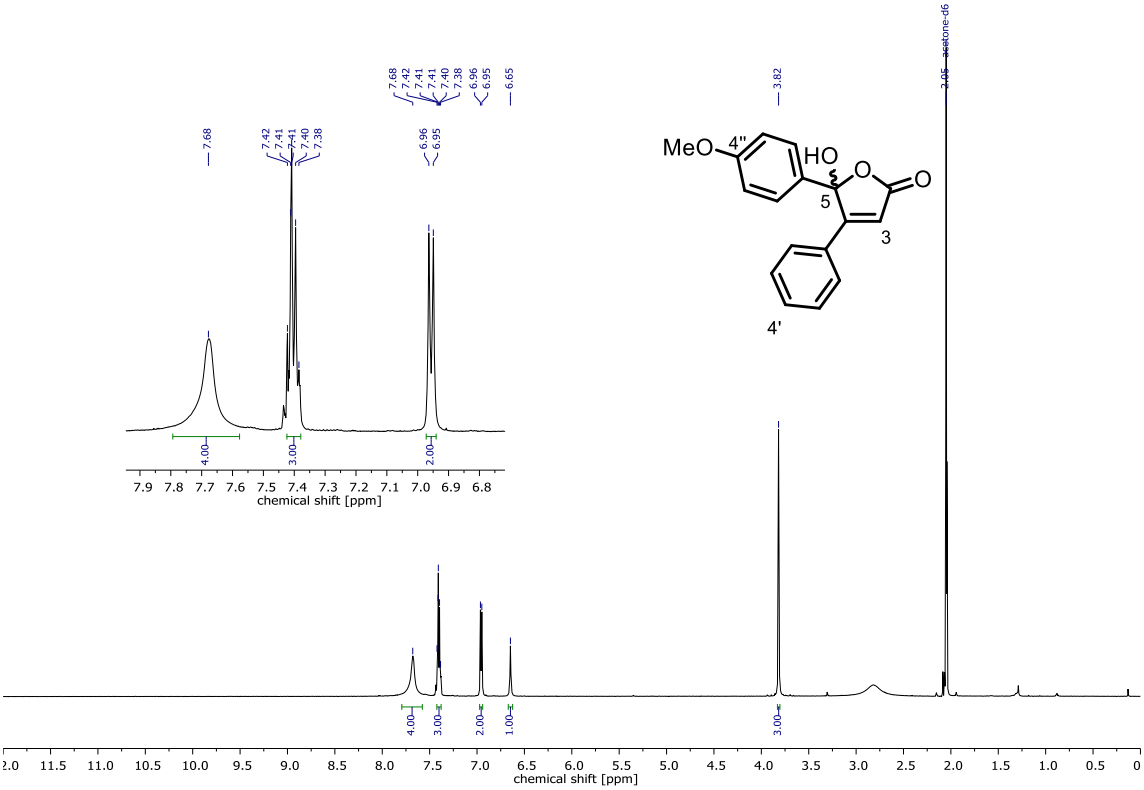

Figure 202: ^{1}H-NMR spectrum (600 MHz, acetone-d_6, 300K) of **262**.

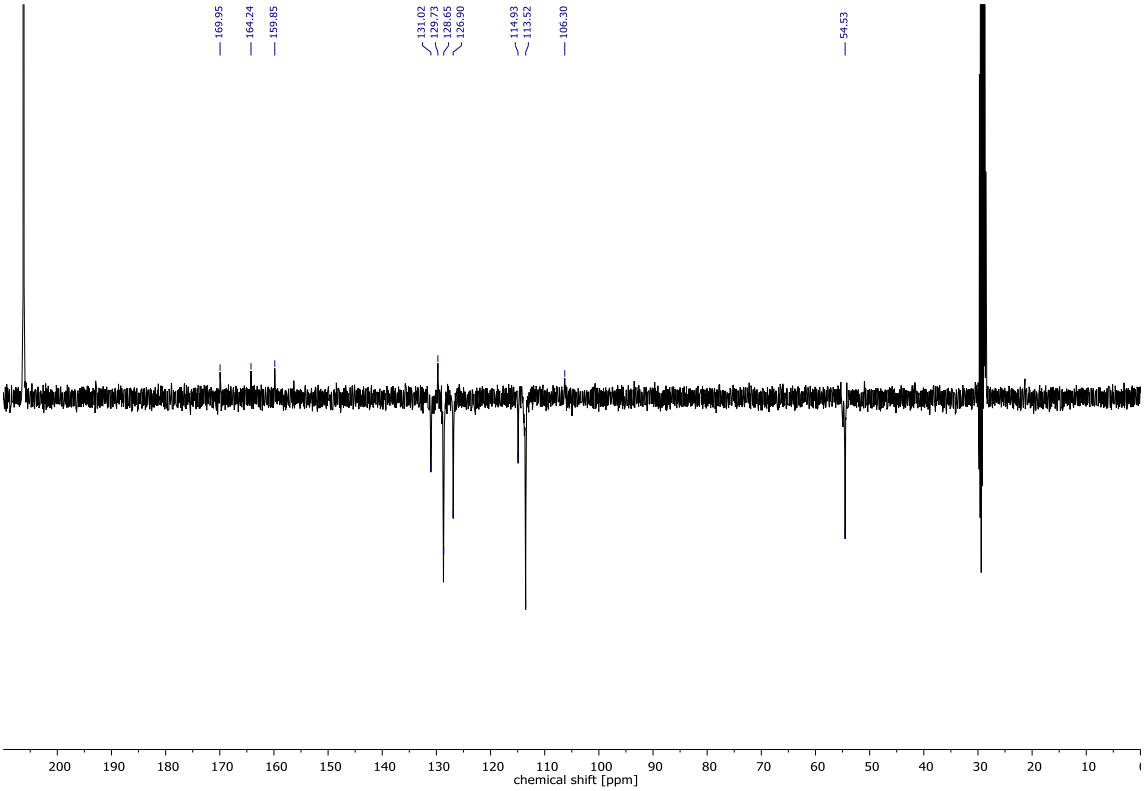

Figure 203: DEPTQ spectrum (101 MHz, acetone-d_6, 223K) of **262**.

5-Hydroxy-4,5-di-(methoxyphenyl)-furan-2(5*H*)-one 263

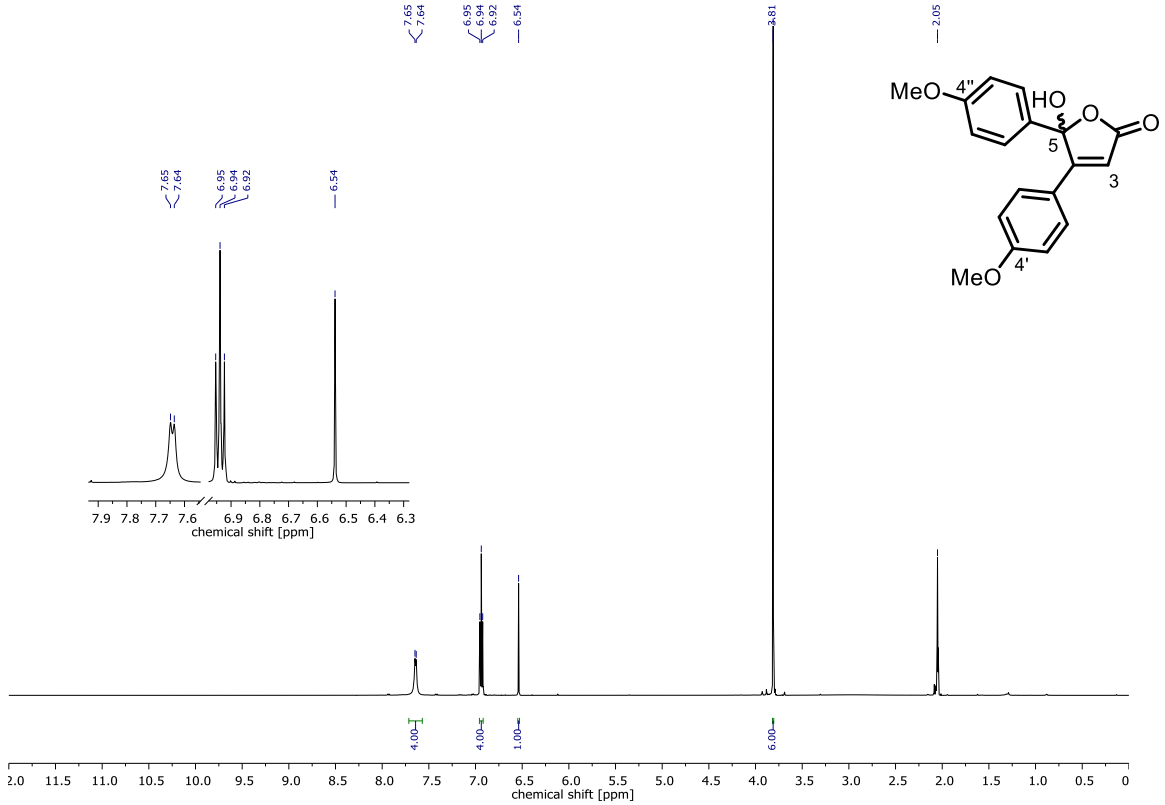

Figure 204: ^{1}H-NMR spectrum (600 MHz, acetone-d_6, 300K) of **263**.

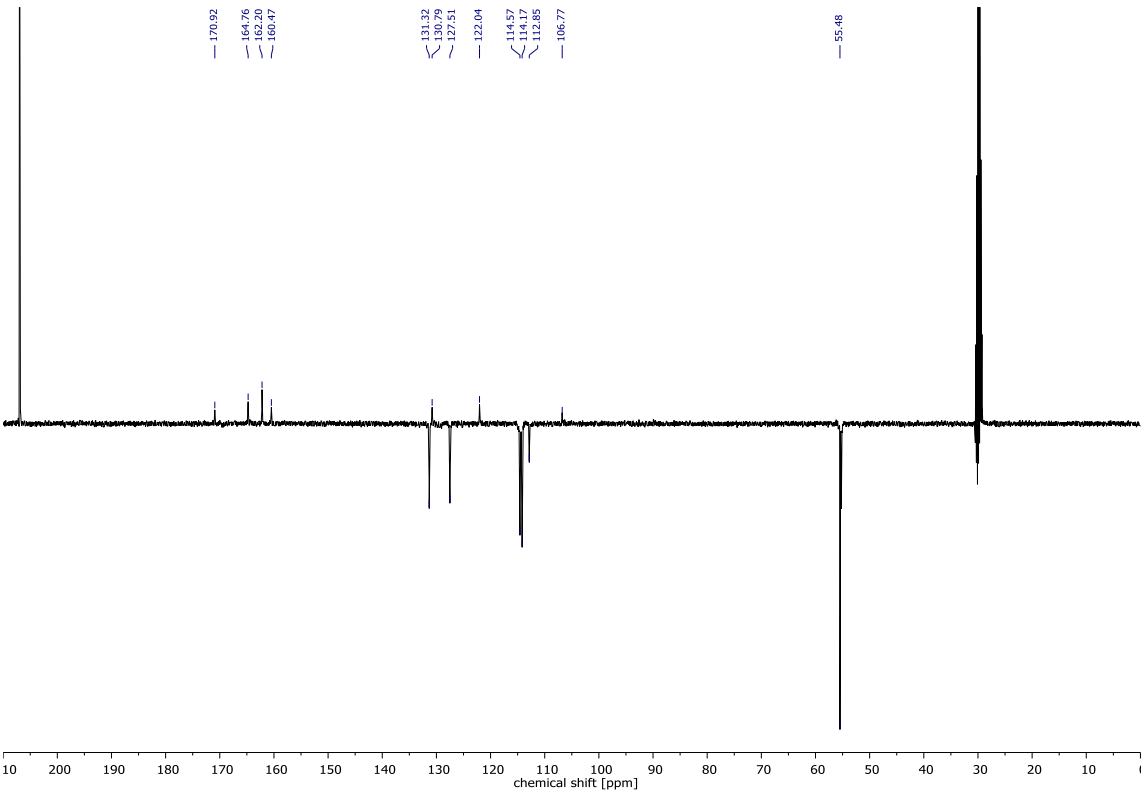

Figure 205: DEPTQ spectrum (101 MHz, acetone-d_6, 223K) of **263**.

4-(4-Fluorophenyl)-5-hydroxy-5-(4-methoxyphenyl)-furan-2(5*H*)-one 264

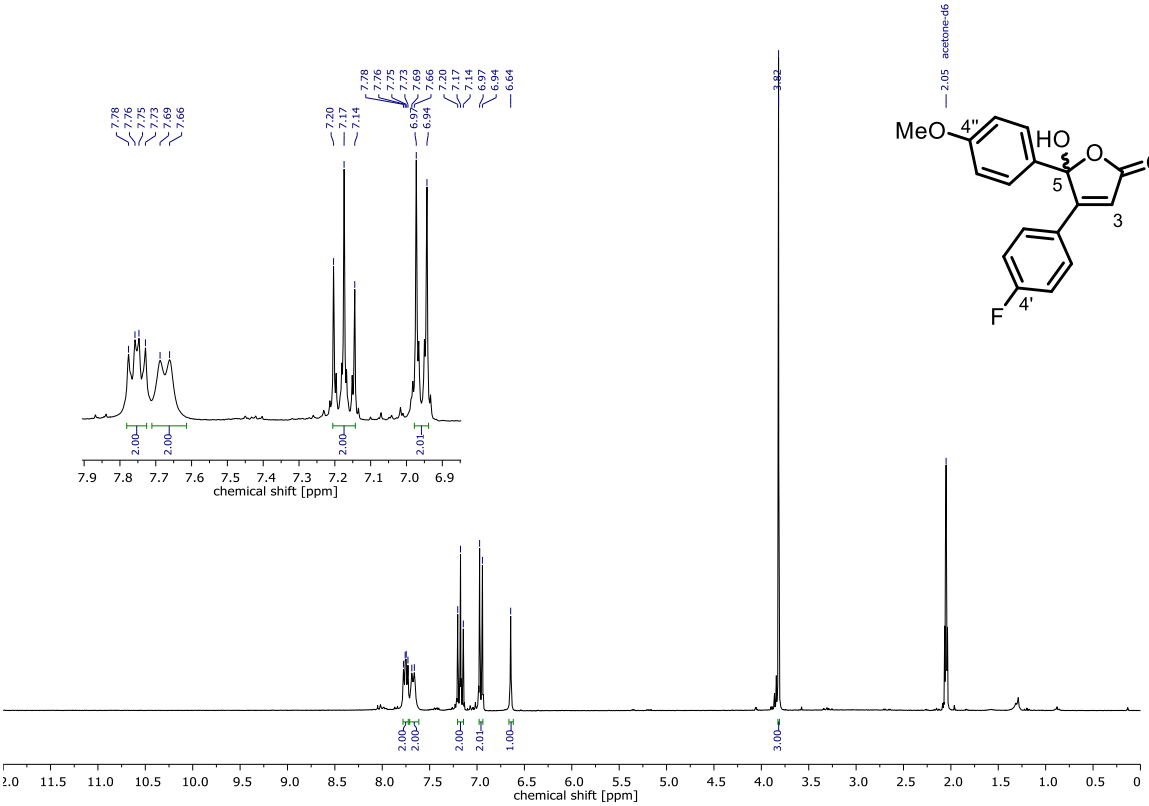

Figure 206: ^{1}H-NMR spectrum (300 MHz, acetone-d_6, 300K) of **264**.

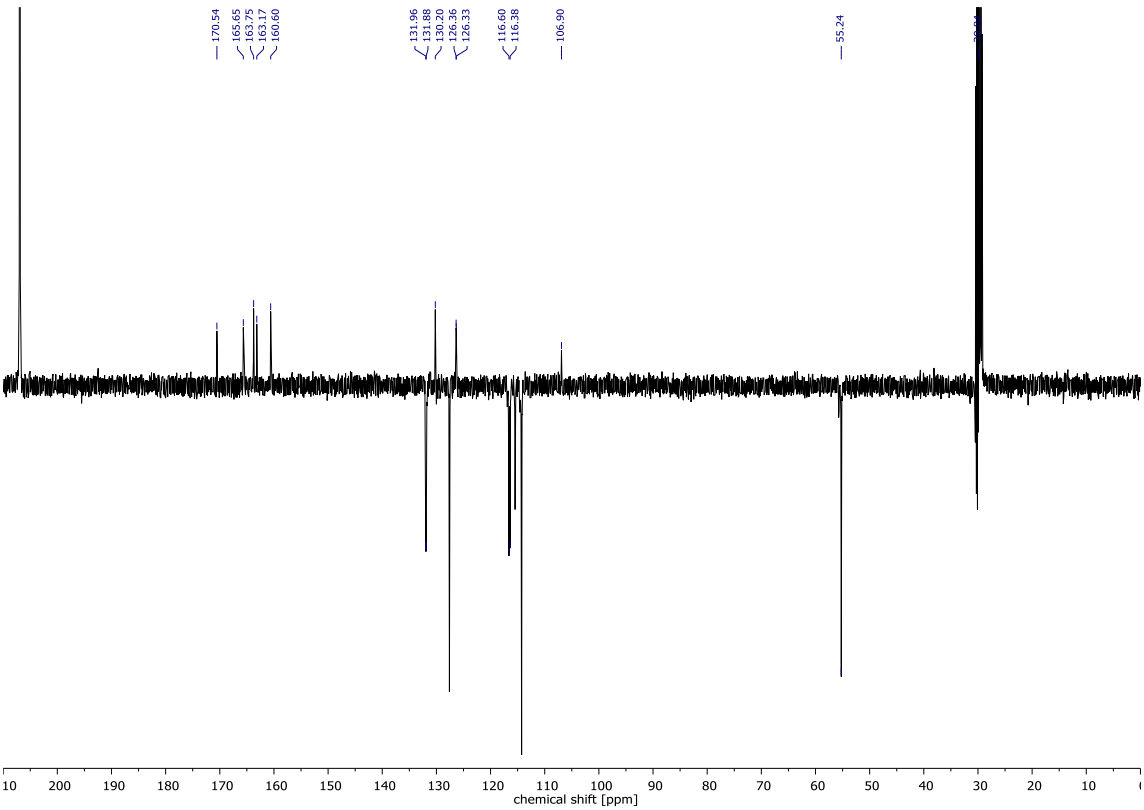

Figure 207: DEPTQ spectrum (101 MHz, acetone-d_6, 223K) of **264**.

5-(4-Fluorophenyl)-5-hydroxy-4-phenylfuran-2(5*H*)-one 265

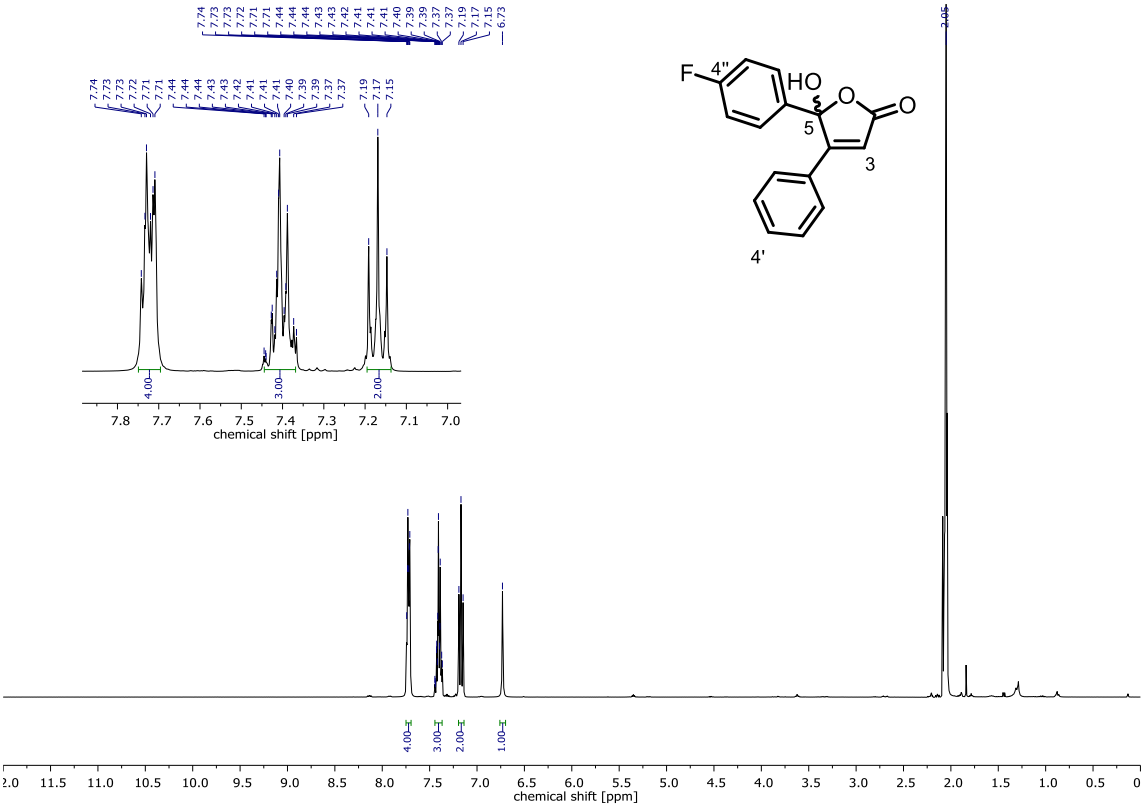

Figure 208: ^{1}H-NMR spectrum (400 MHz, acetone-d_6, 300K) of **265**.

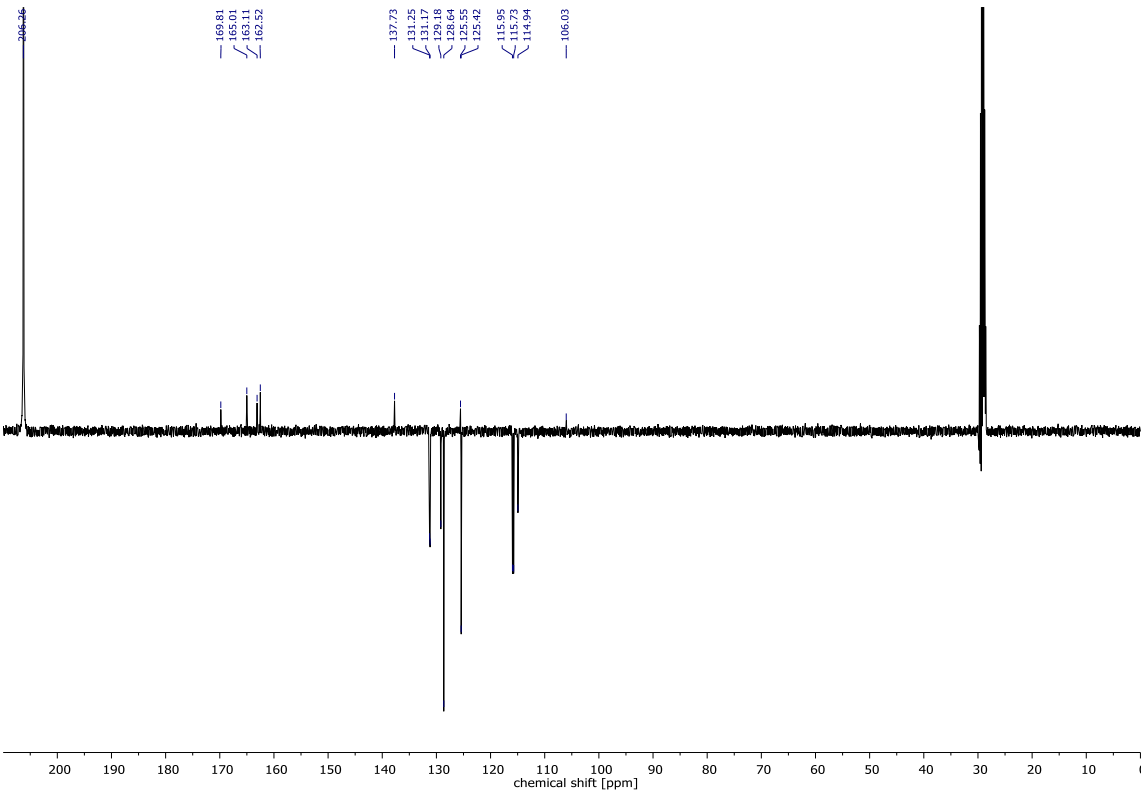

Figure 209: DEPTQ spectrum (101 MHz, acetone-d_6, 223K) of **265**.

5-(4-Fluorophenyl)-5-hydroxy-4-(4-methoxyphenyl)-furan-2(5H)-one 266

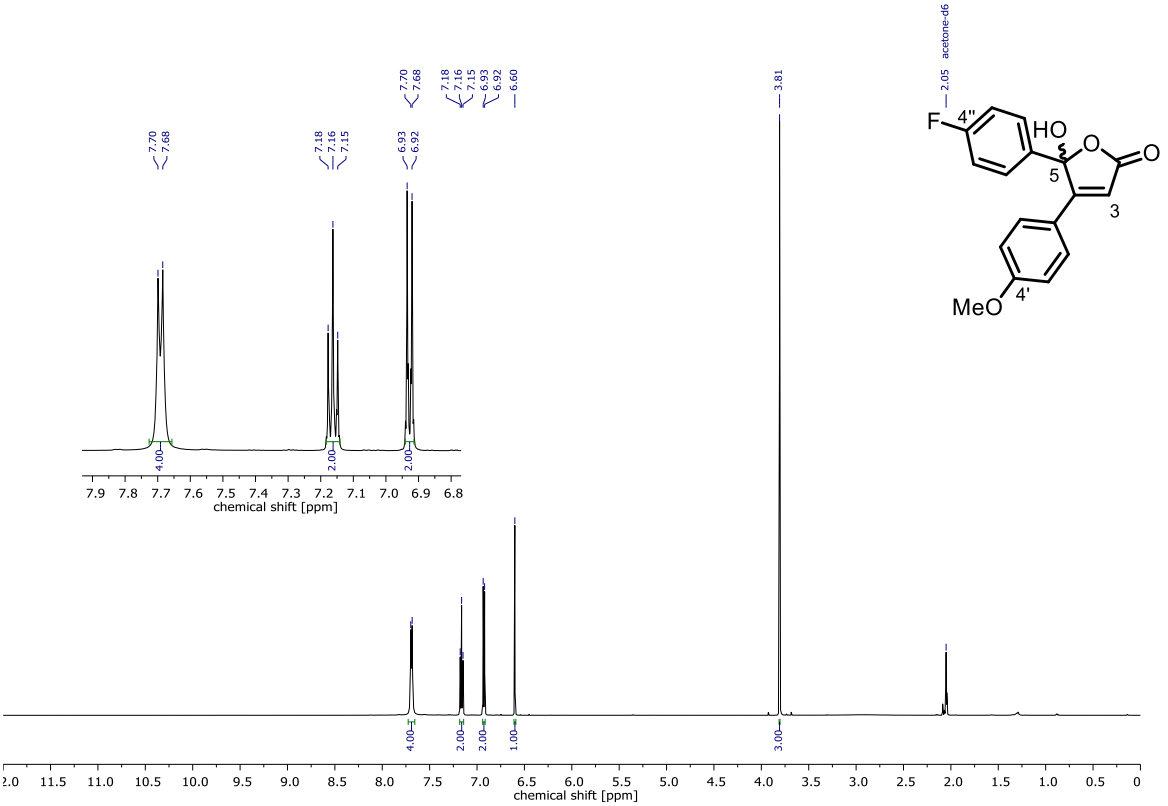

Figure 210: ^{1}H-NMR spectrum (600 MHz, acetone-d_6, 300K) of **266**.

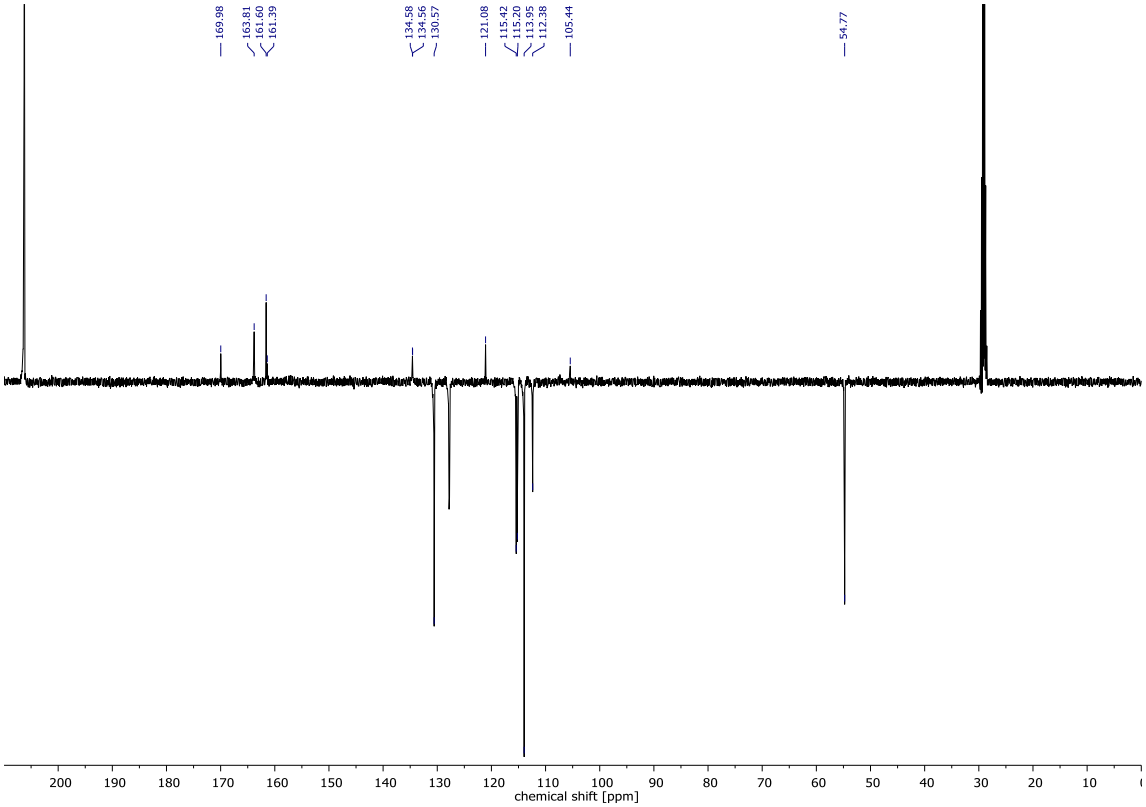

Figure 211: DEPTQ spectrum (101 MHz, acetone-d_6, 223K) of **266**.

4,5-Di-(4-fluorophenyl)-5-hydroxyfuran-2(5*H*)-one 267

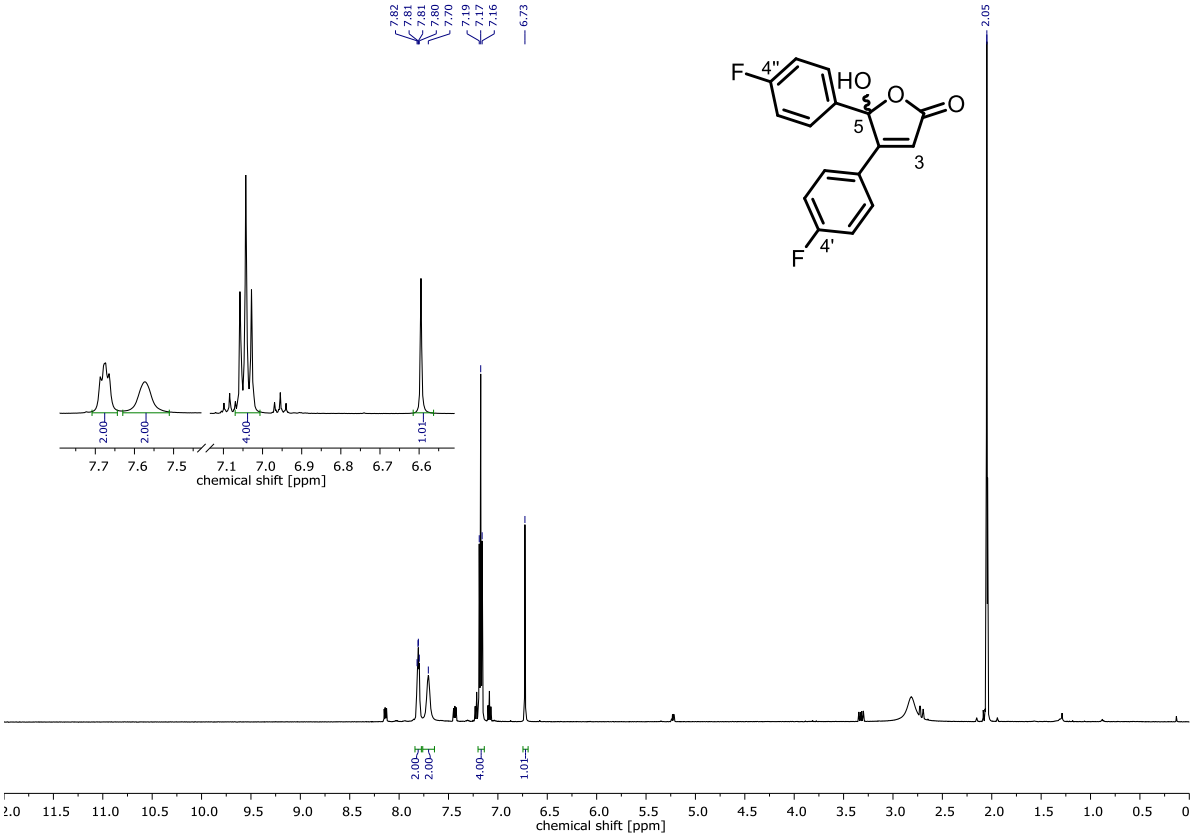

Figure 212: ^{1}H-NMR spectrum (400 MHz, acetone-d_6, 296K) of **267**.

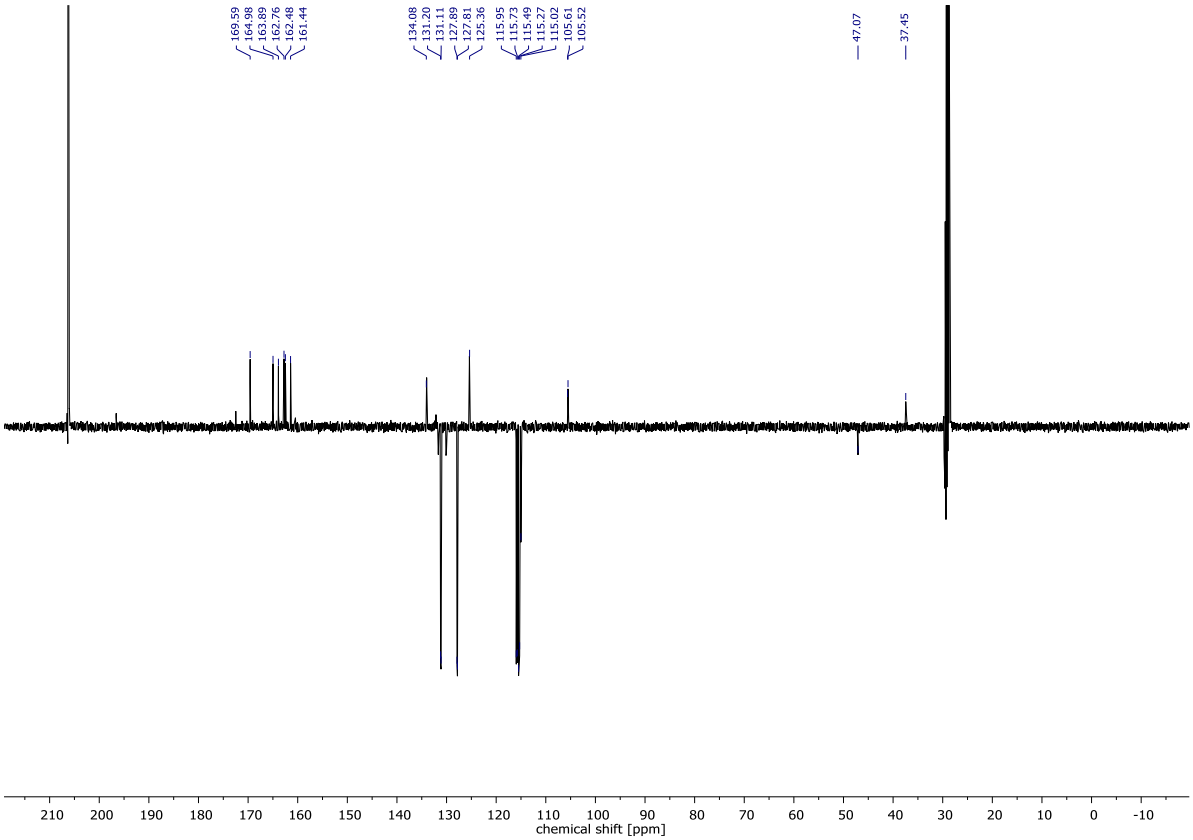

Figure 213: DEPTQ spectrum (101 MHz, acetone-d_6, 223K) of **267**.

5-Hydroxy-4-phenyl-5-(*p*-tolyl)furan-2(5*H*)-one 268

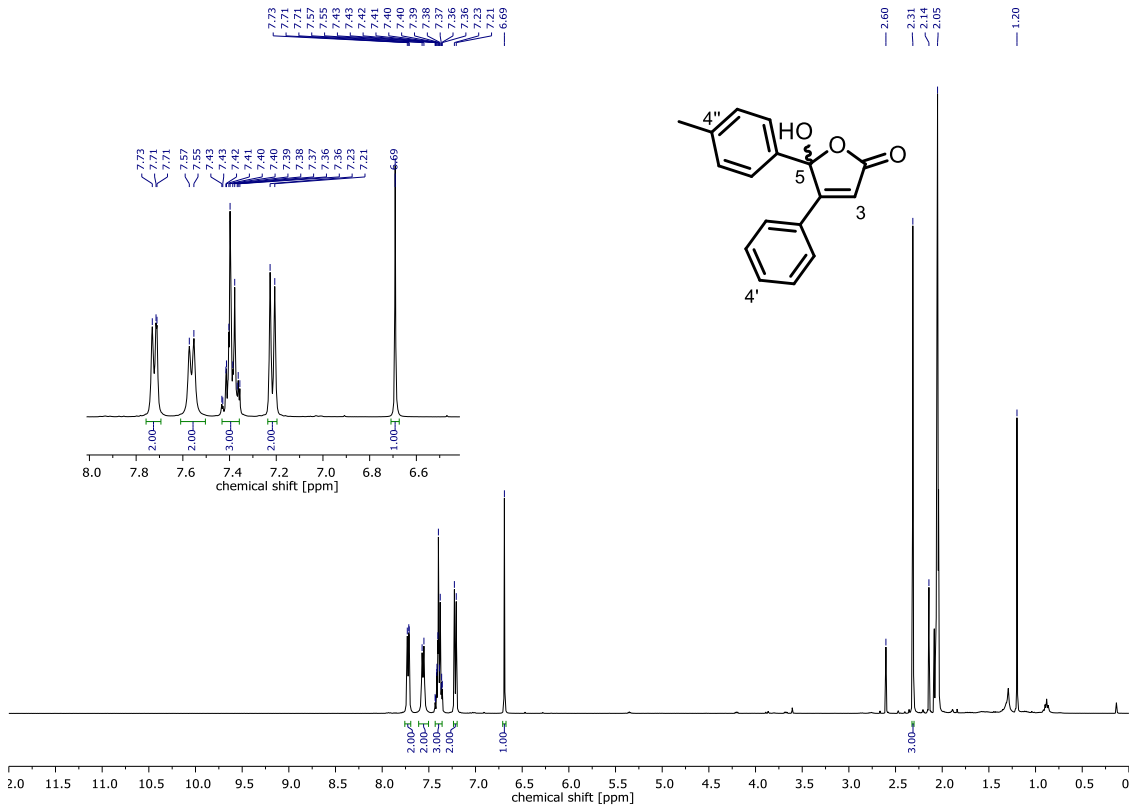

Figure 214: ^{1}H-NMR spectrum (400 MHz, acetone-d_6, 300K) of **268**.

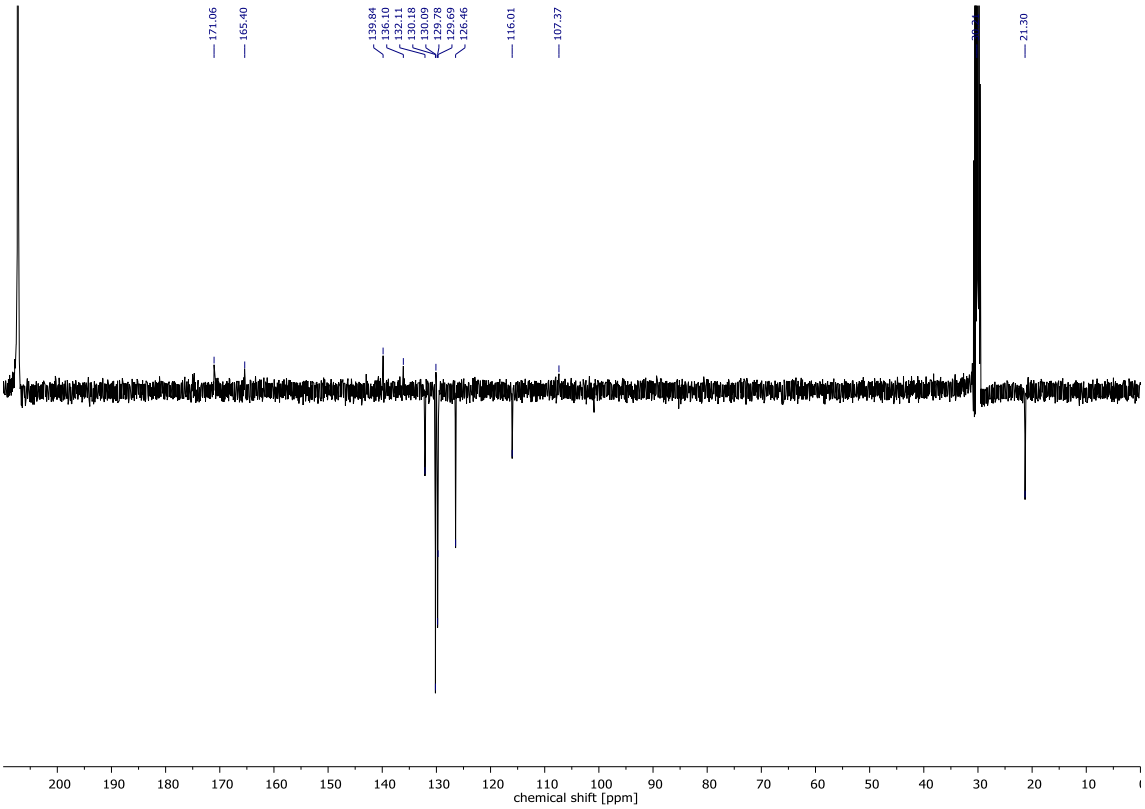

Figure 215: DEPTQ spectrum (101 MHz, acetone-d_6, 223K) of **268**.

5-Hydroxy-4-(4-methoxyphenyl)-5-(*p*-tolyl)furan-2(5*H*)-one 269

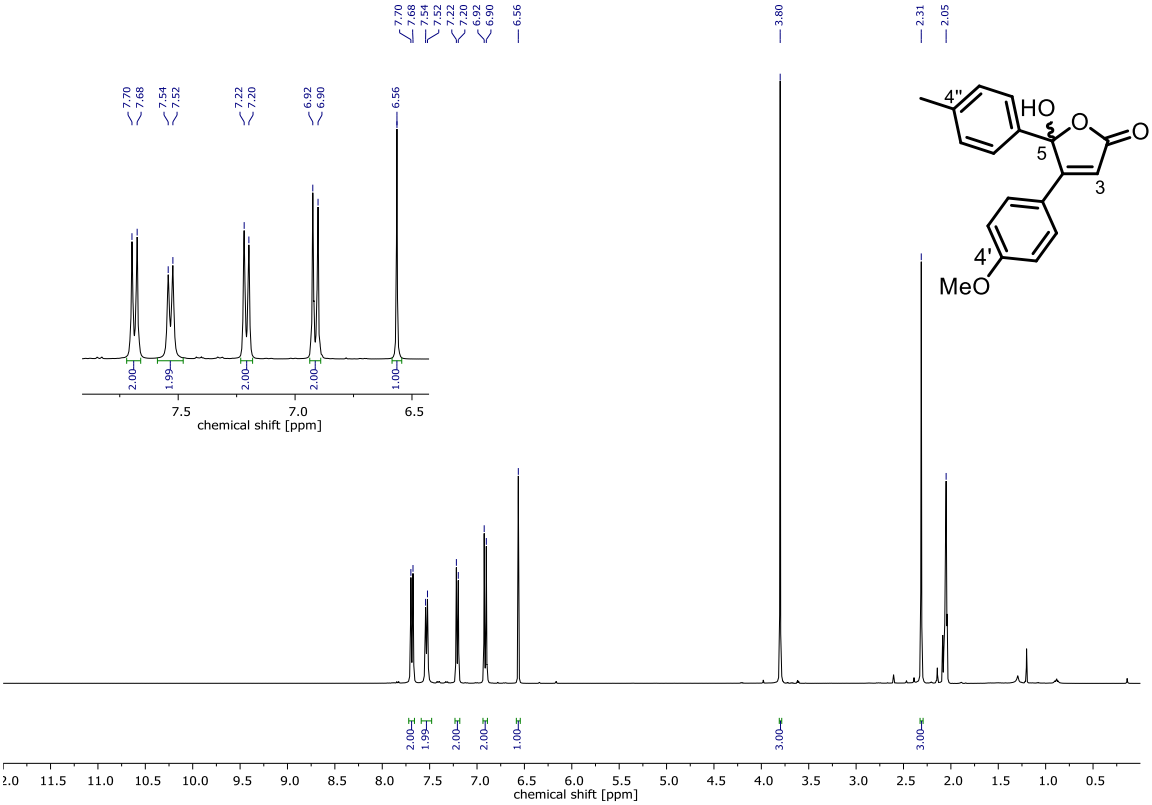

Figure 216: ^{1}H-NMR spectrum (400 MHz, acetone-d_6, 300K) of **269**.

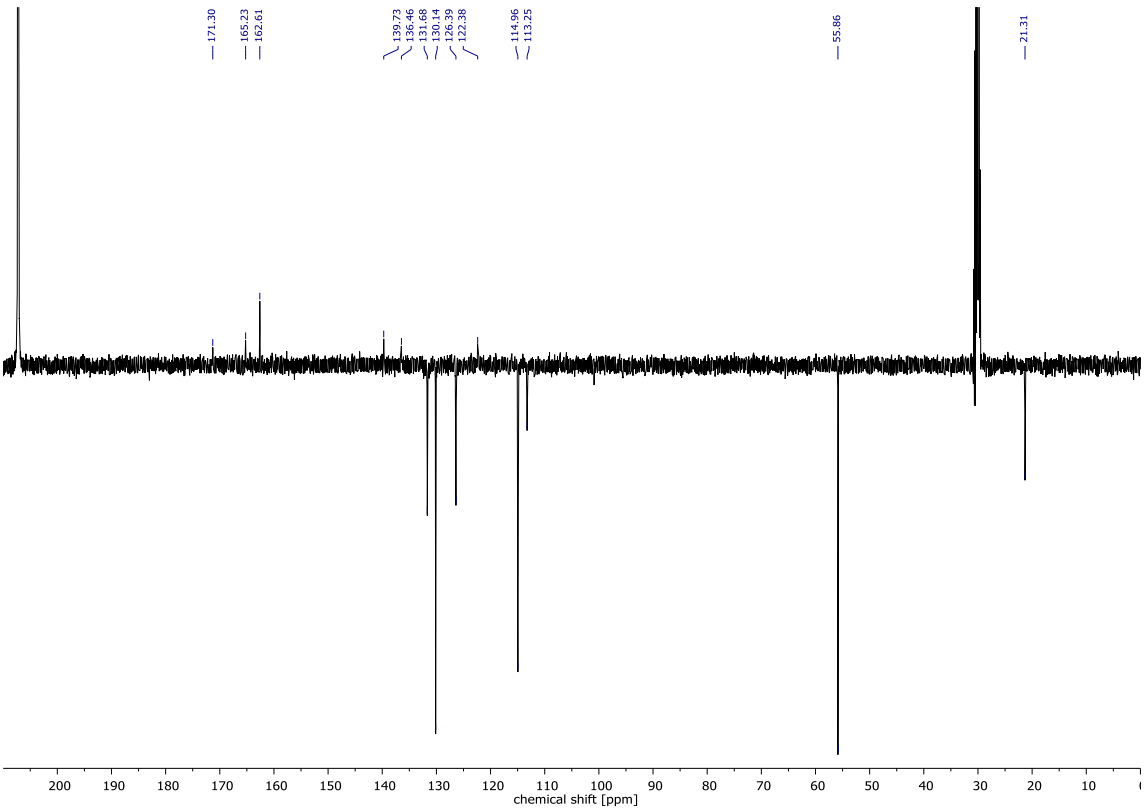

Figure 217: DEPTQ spectrum (101 MHz, acetone-d_6, 226K) of **269**.

4-(4-Fluorophenyl)-5-hydroxy-5-(*p*-tolyl)furan-2(5*H*)-one 270

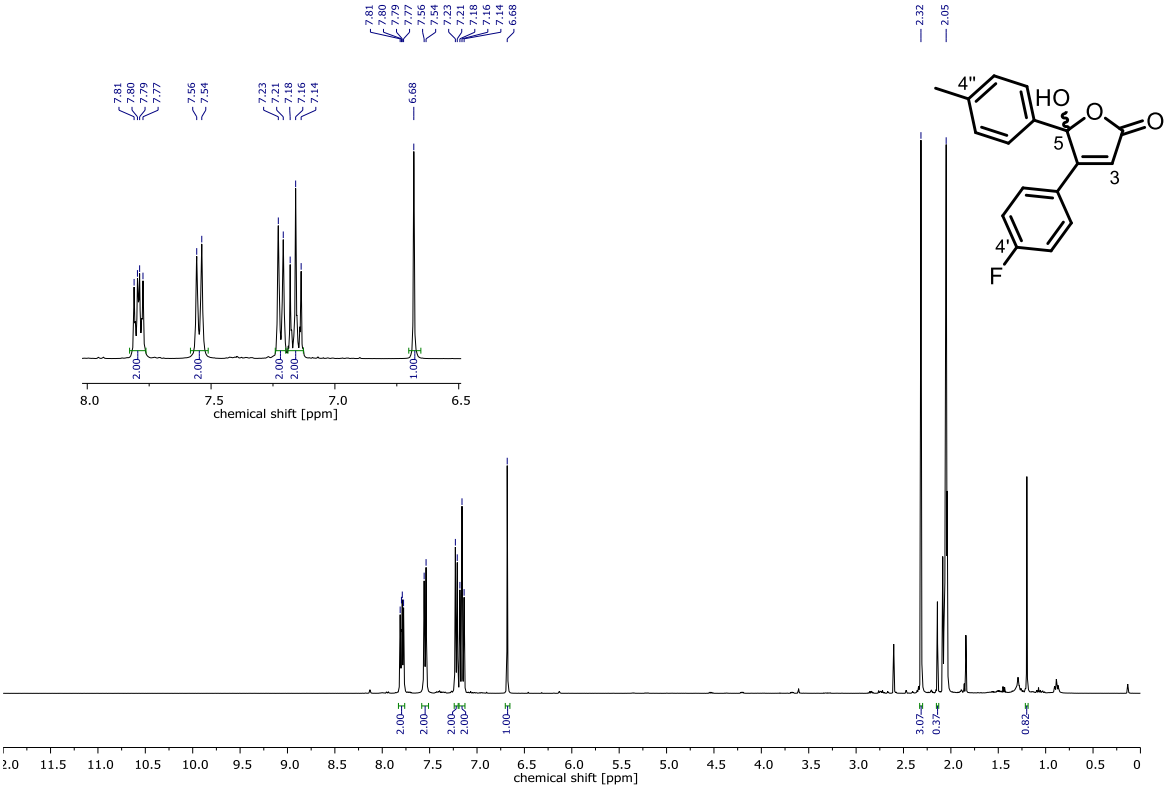

Figure 218: ^{1}H-NMR spectrum (400 MHz, acetone-d_6, 300K) of **270**.

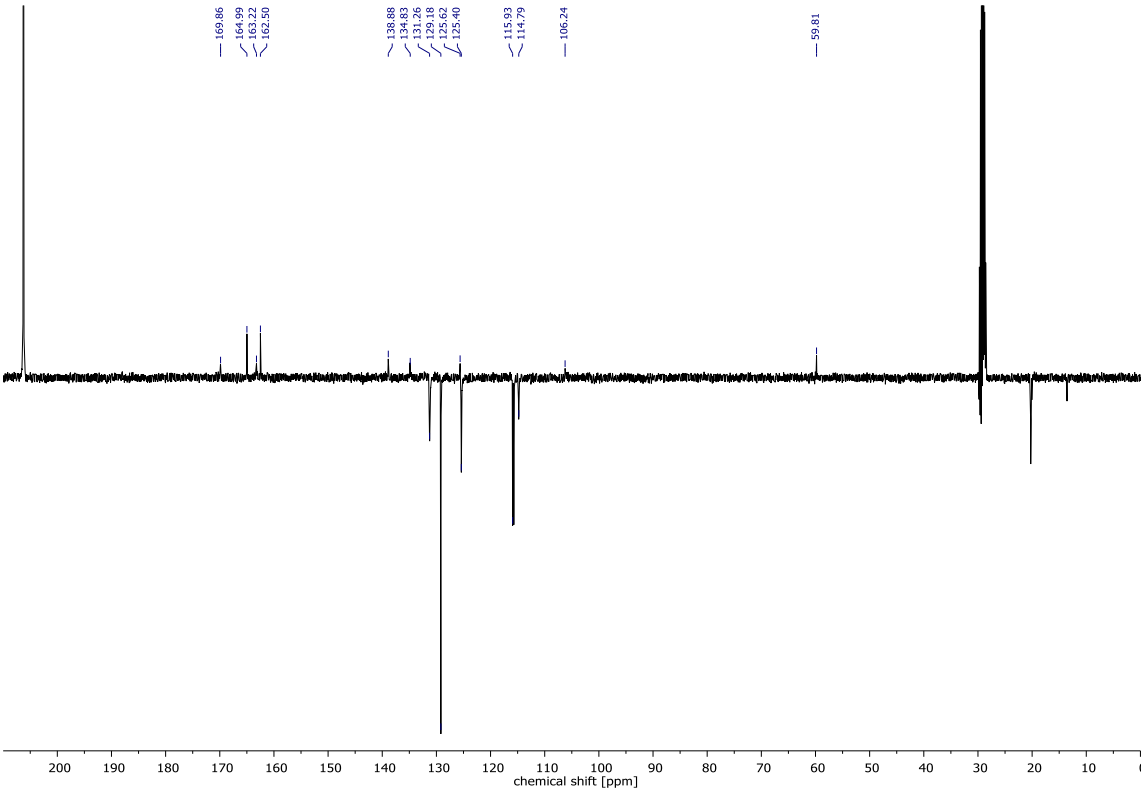

Figure 219: DEPTQ spectrum (101 MHz, acetone-d_6, 223K) of **270**.

5-Hydroxy-4-phenyl-5-(*m*-tolyl)furan-2(5*H*)-one 271

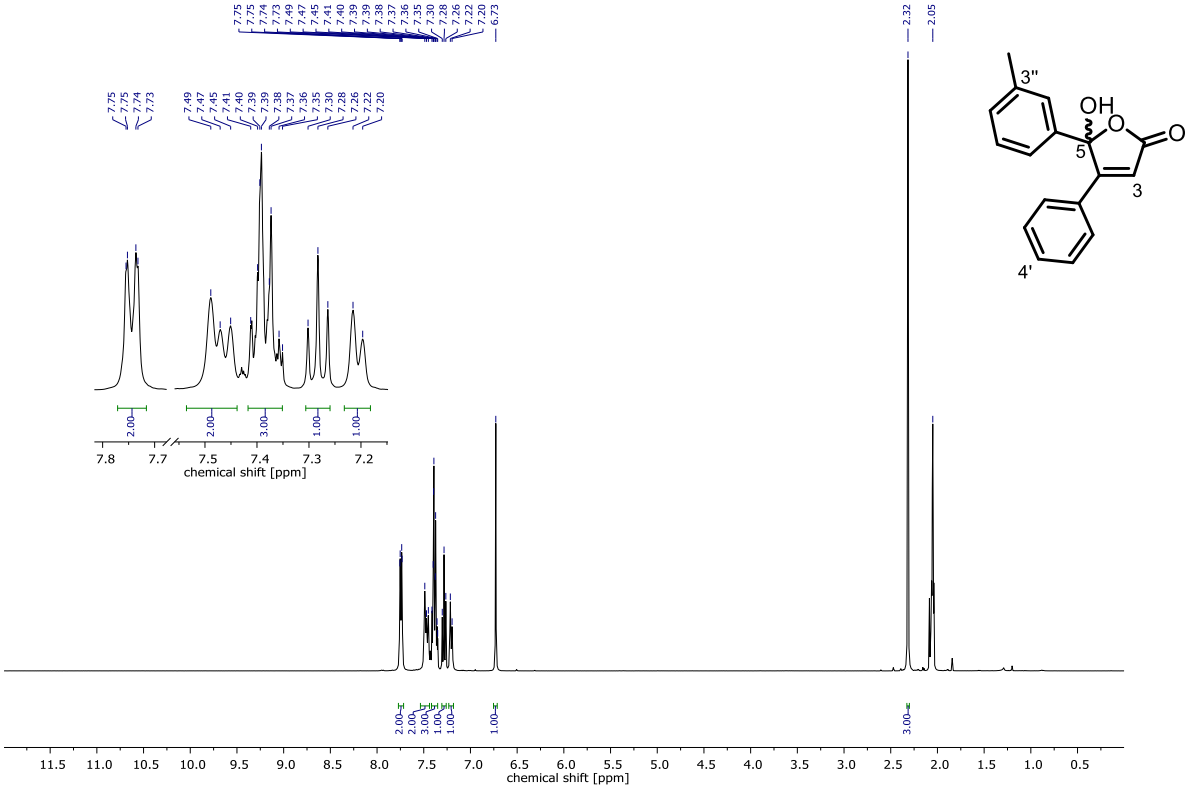

Figure 220: ^{1}H-NMR spectrum (400 MHz, acetone-d_6, 296K) of **271**.

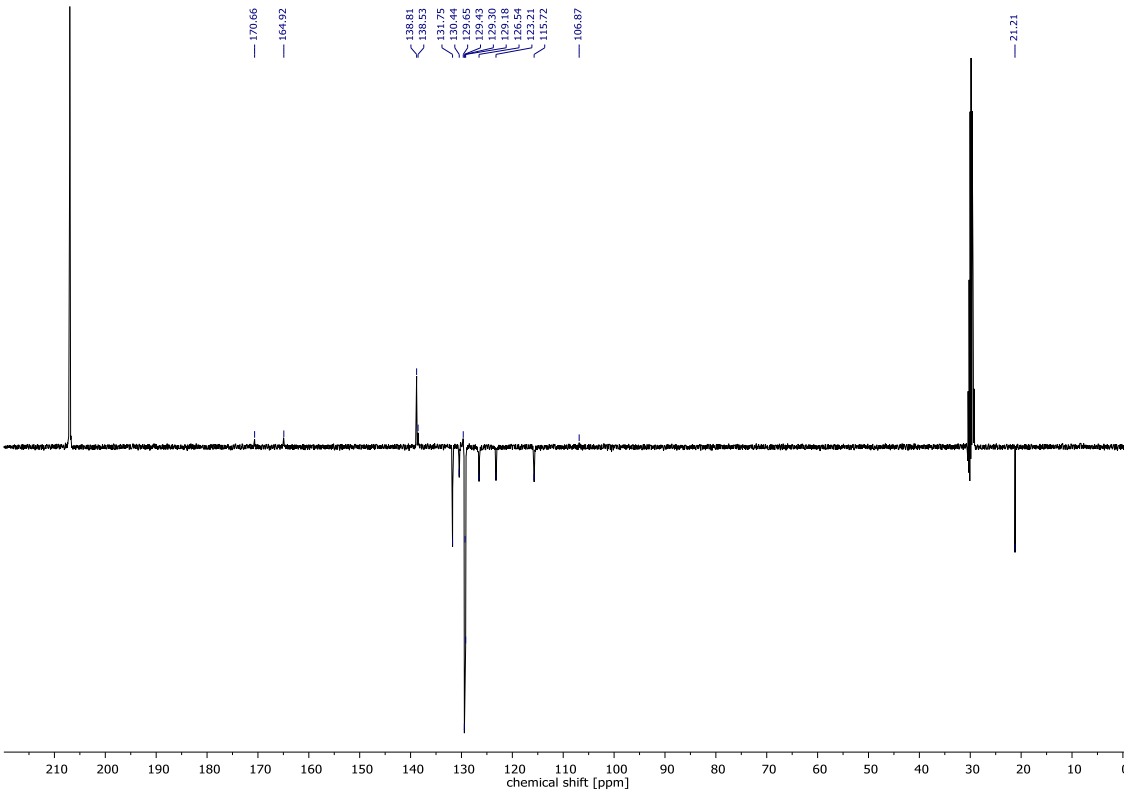

Figure 221: ^{13}C-NMR spectrum (101 MHz, acetone-d_6, 223K) of **271**.

5-Hydroxy-4-(4-methoxyphenyl)-5-(*m*-tolyl)furan-2(5*H*)-one 272

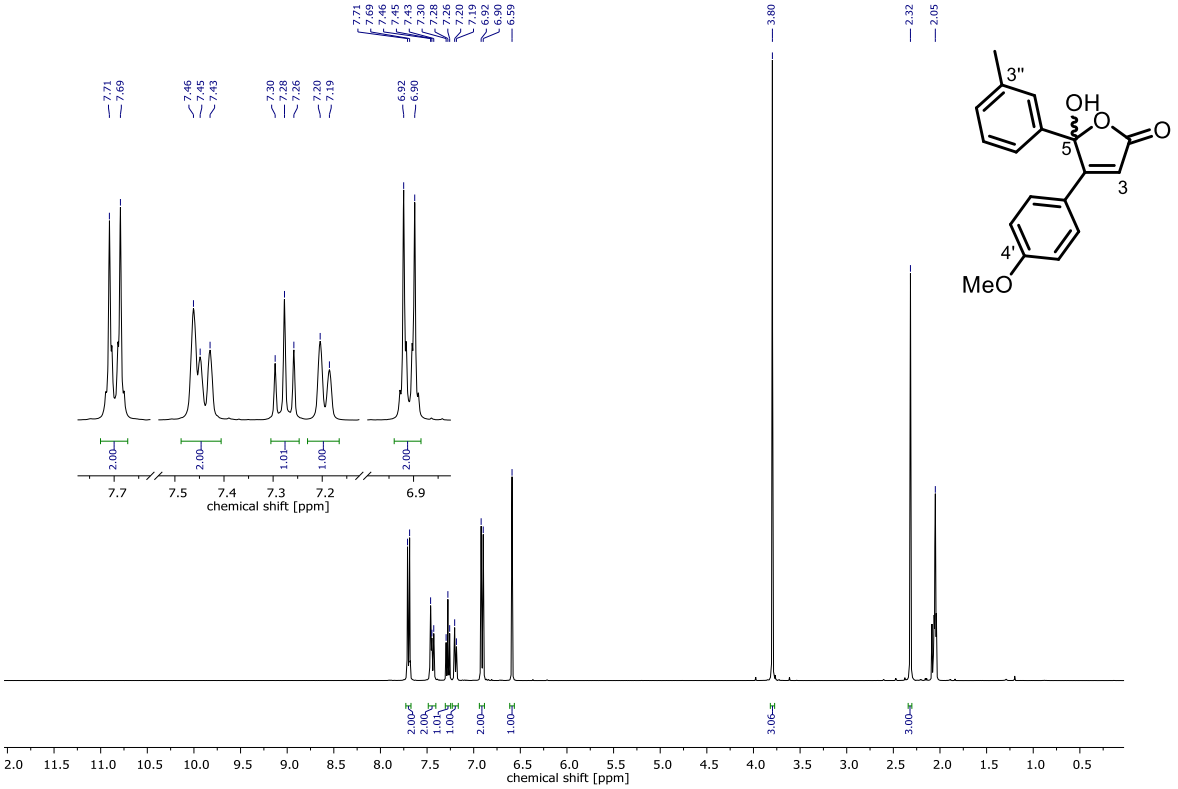

Figure 222 ^{1}H-NMR spectrum (400 MHz, acetone-d_6, 296K) of **272**.

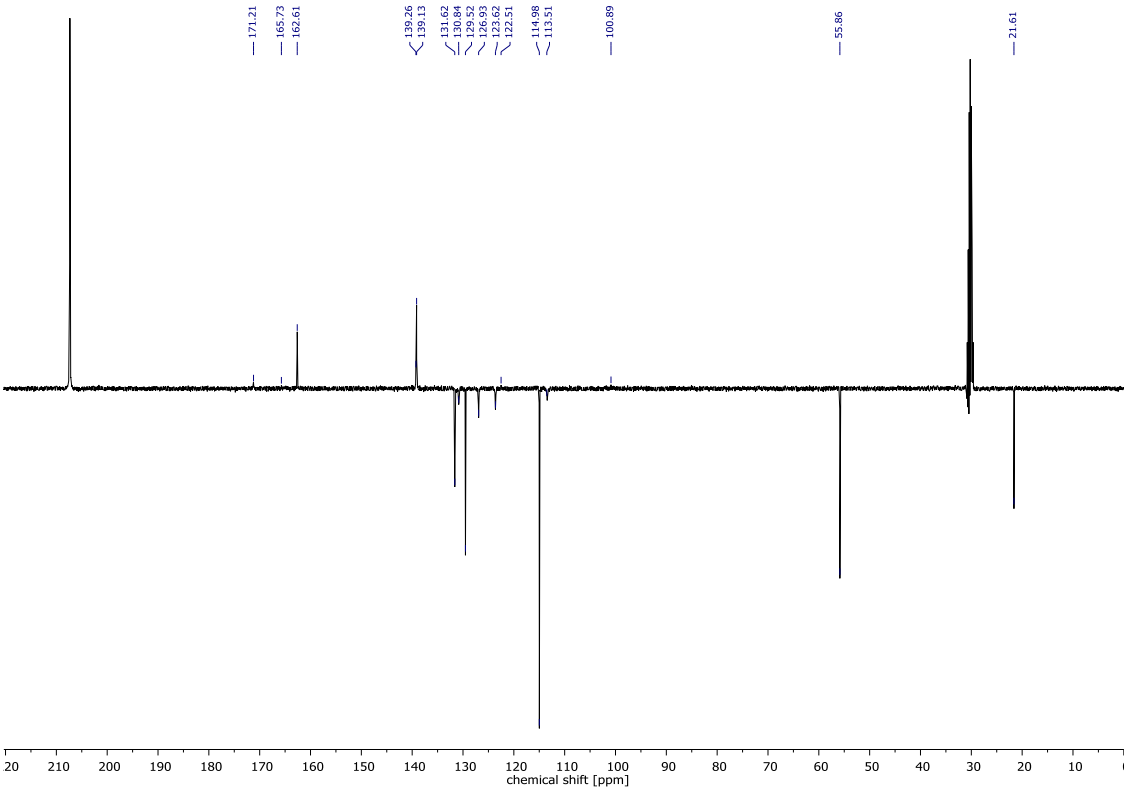

Figure 223: ^{13}C-NMR spectrum (101 MHz, acetone-d_6, 223K) of **272**.

4-(4-Fluorophenyl)-5-hydroxy-5-(*m*-tolyl)furan-2(5*H*)-one 273

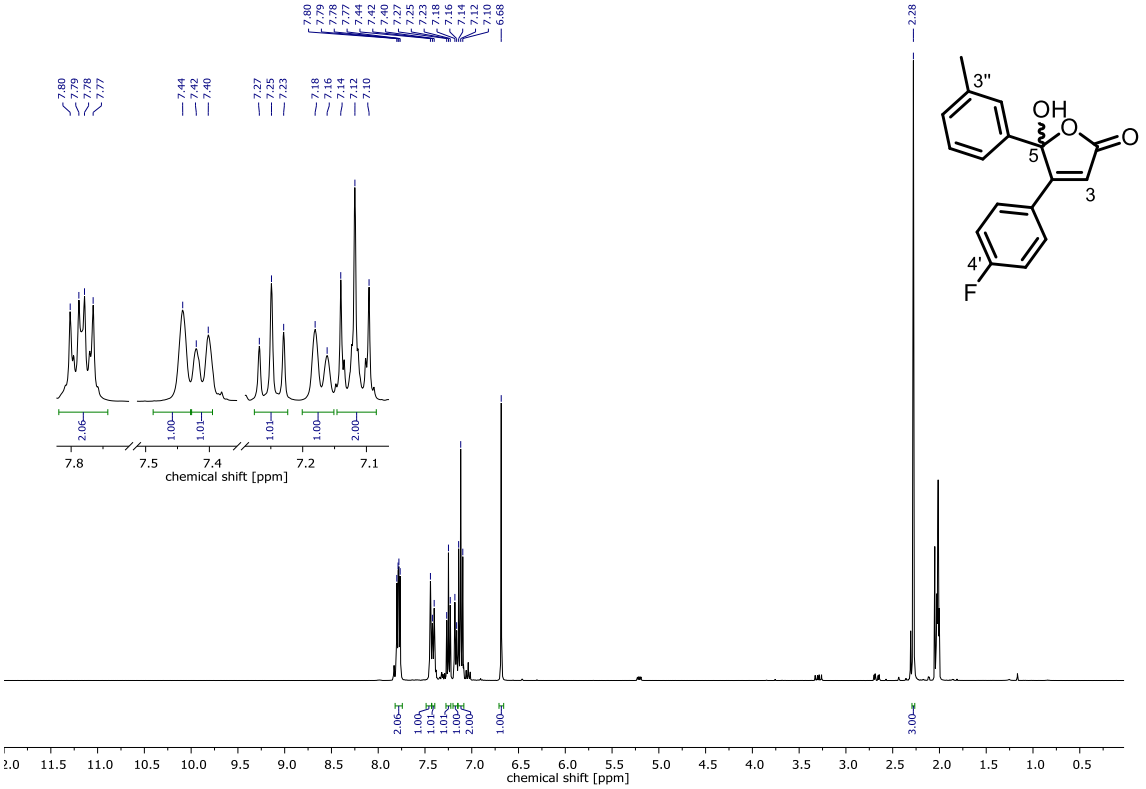

Figure 224: ^{1}H-NMR spectrum (400 MHz, acetone-d_6, 296K) of **273**.

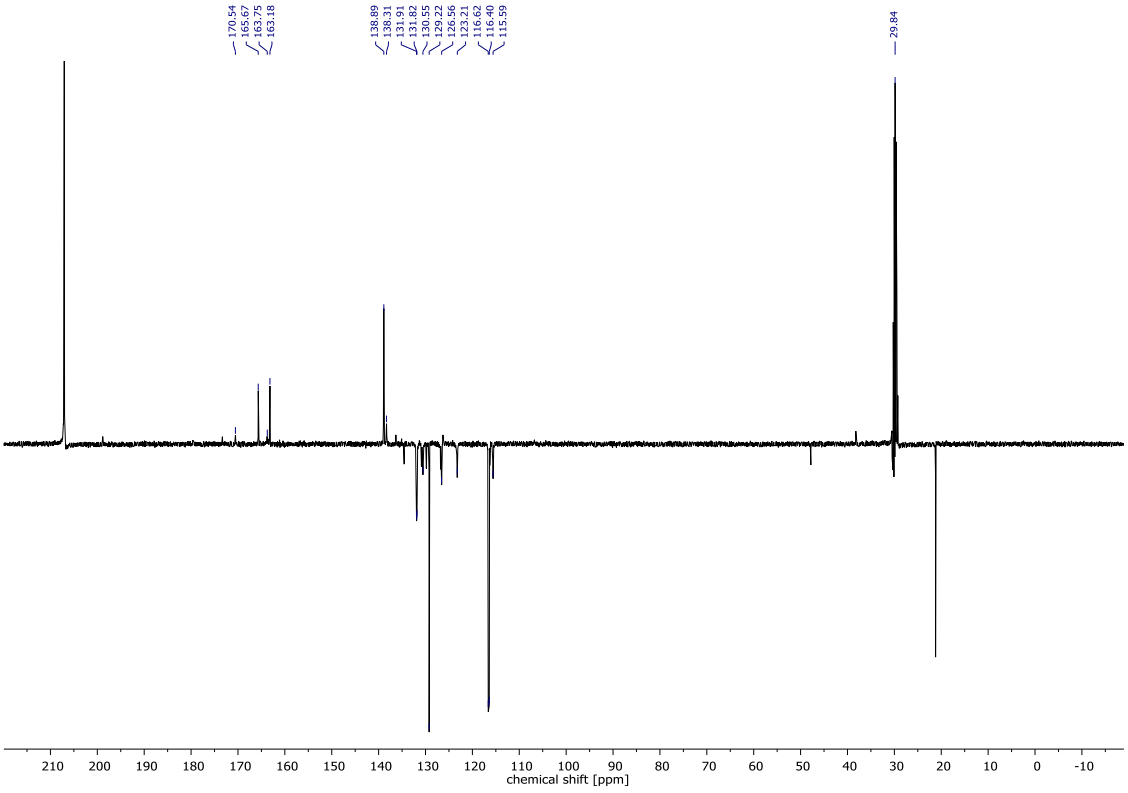

Figure 225: ^{13}C-NMR spectrum (101 MHz, acetone-d_6, 223K) of **273**.

5-Hydroxy-4-phenyl-5-(*o*-tolyl)furan-2(*5H*)-one 274

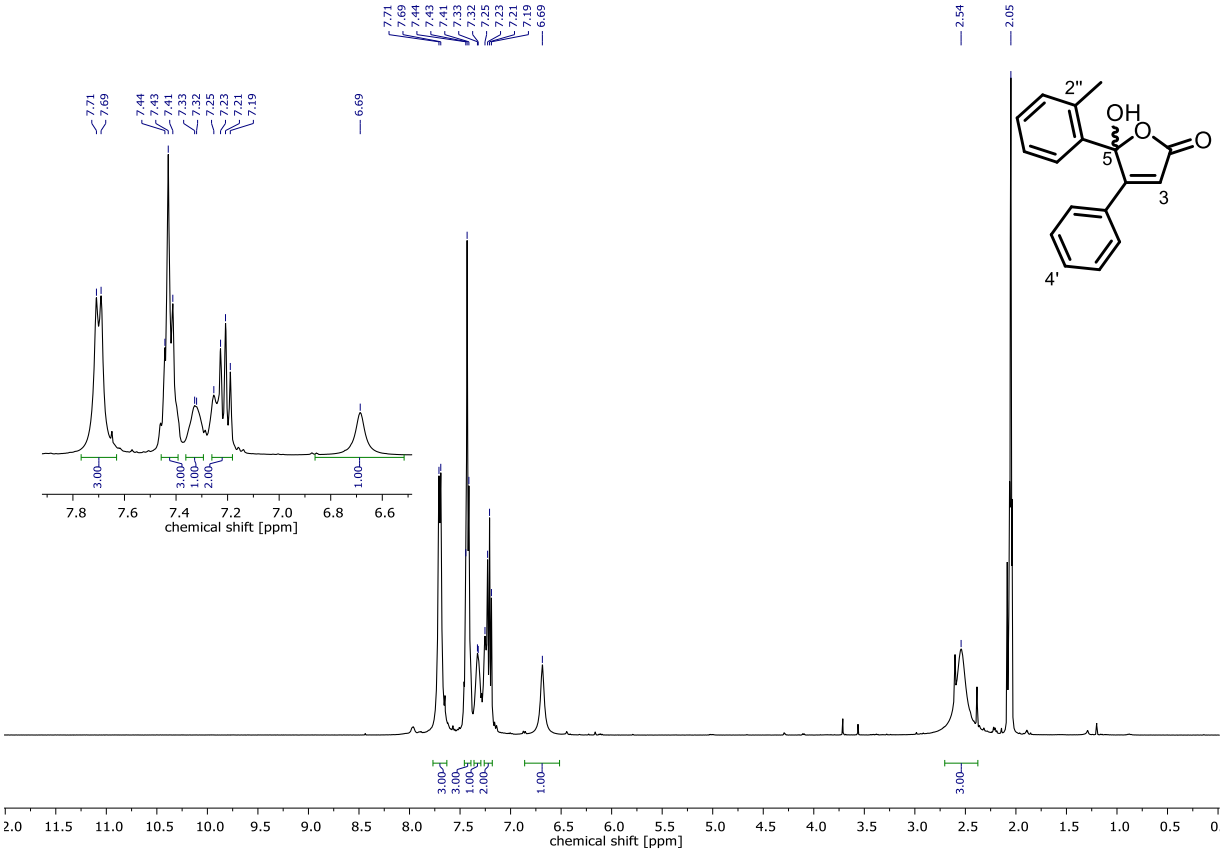

Figure 226: ^{1}H-NMR spectrum (400 MHz, acetone-d_6, 296K) of **274**.

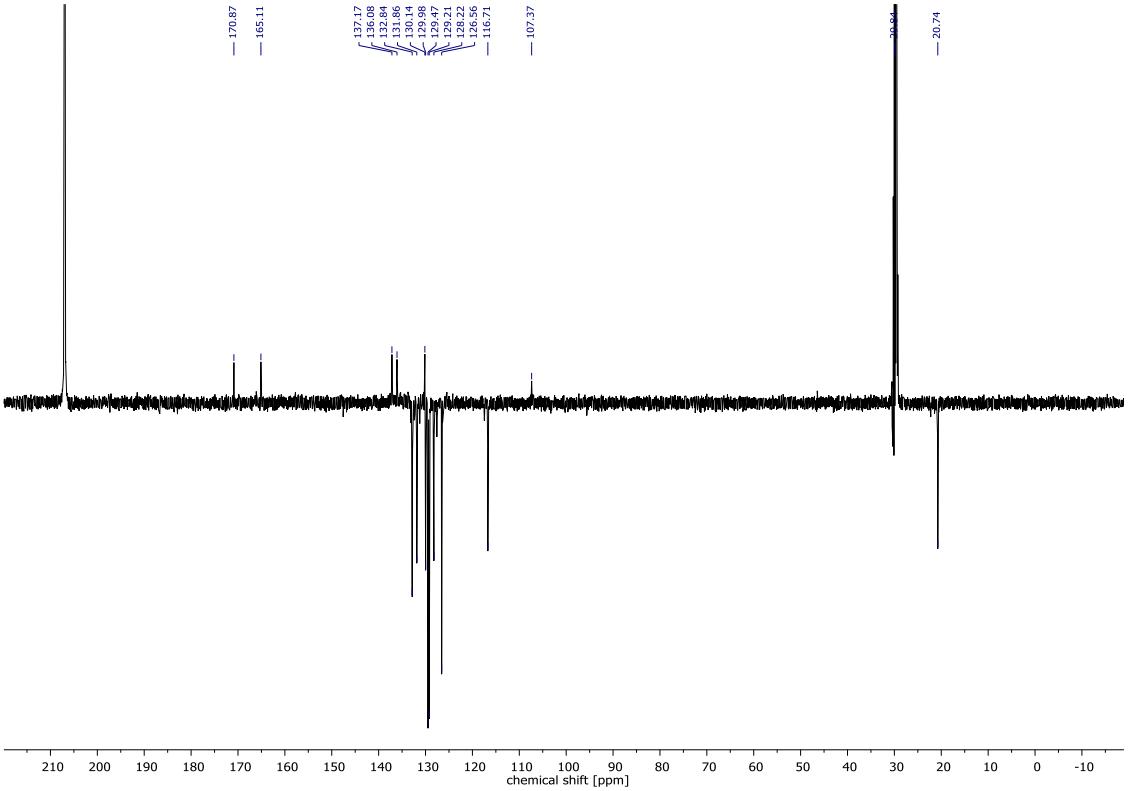

Figure 227: ^{13}C-NMR spectrum (101 MHz, acetone-d_6, 223K) of **274**.

5-Hydroxy-4-(4-methoxyphenyl)-5-(*o*-tolyl)furan-2(*5H*)-one 275

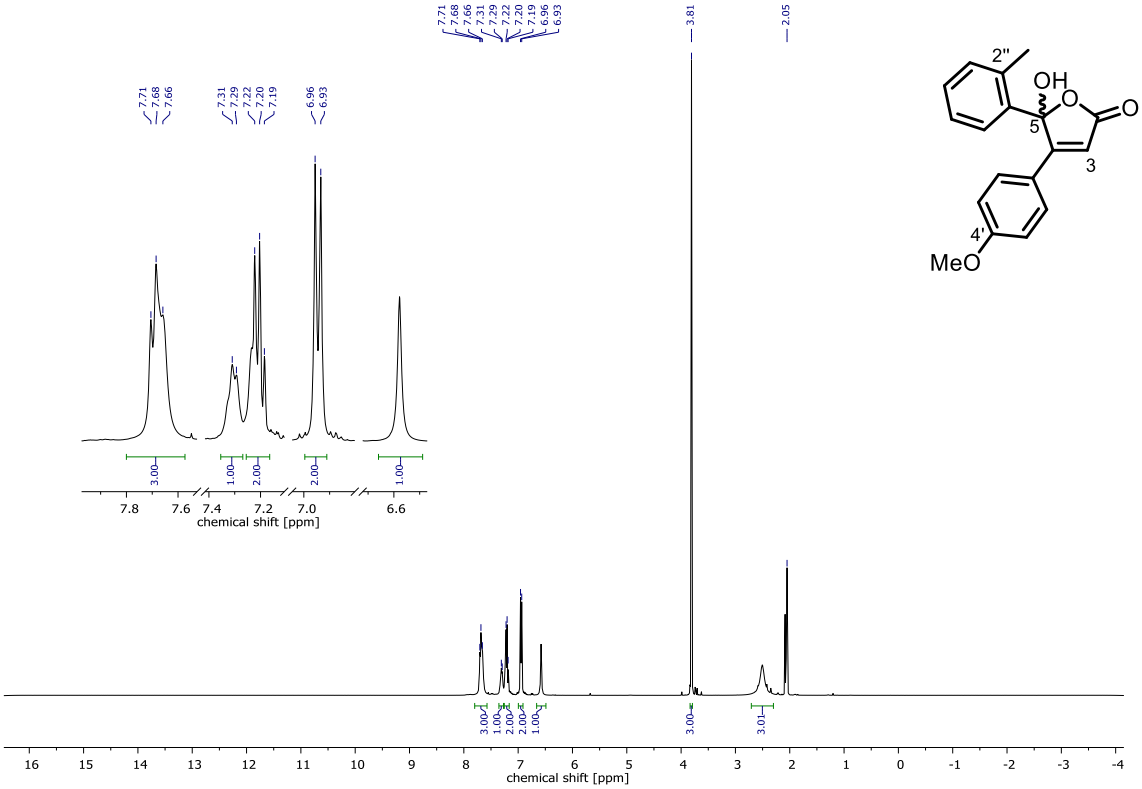

Figure 228: ^{1}H-NMR spectrum (400 MHz, acetone-d_6, 296K) of **275**.

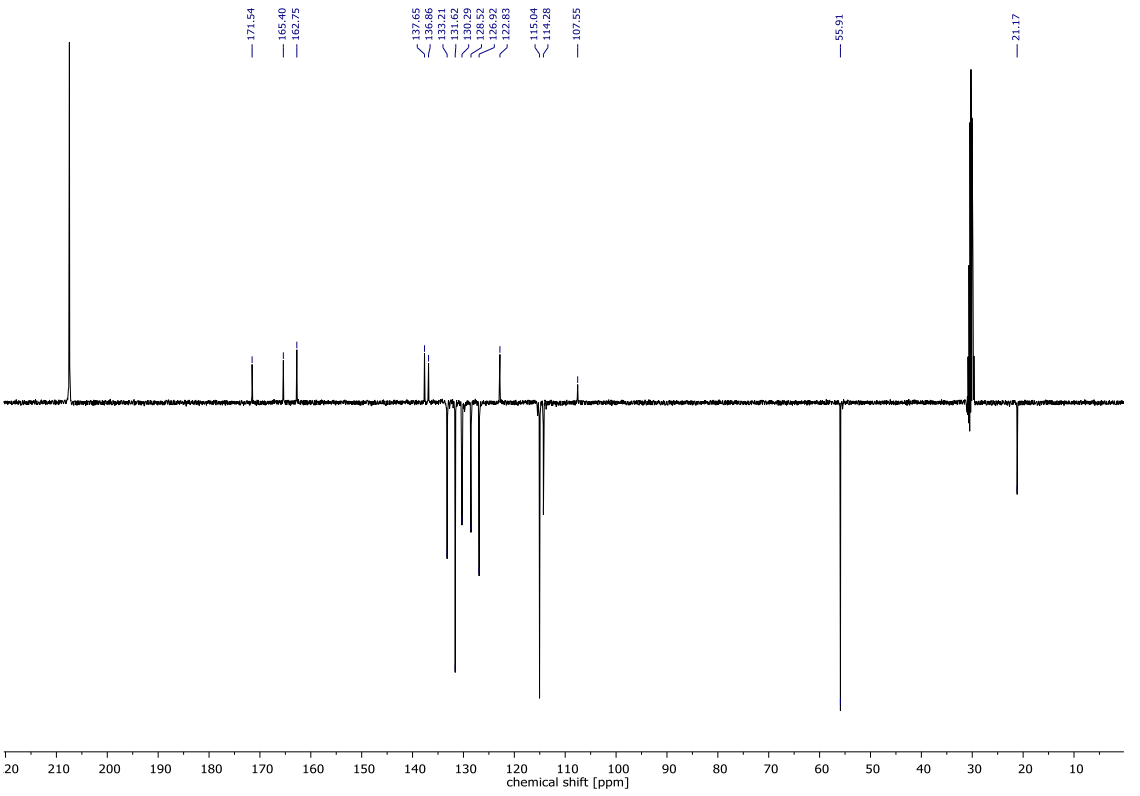

Figure 229: ^{13}C-NMR spectrum (101 MHz, acetone-d_6, 223K) of **275**.

4-(4-Fluorophenyl)-5-hydroxy-5-(*o*-tolyl)furan-2(5*H*)-one 276

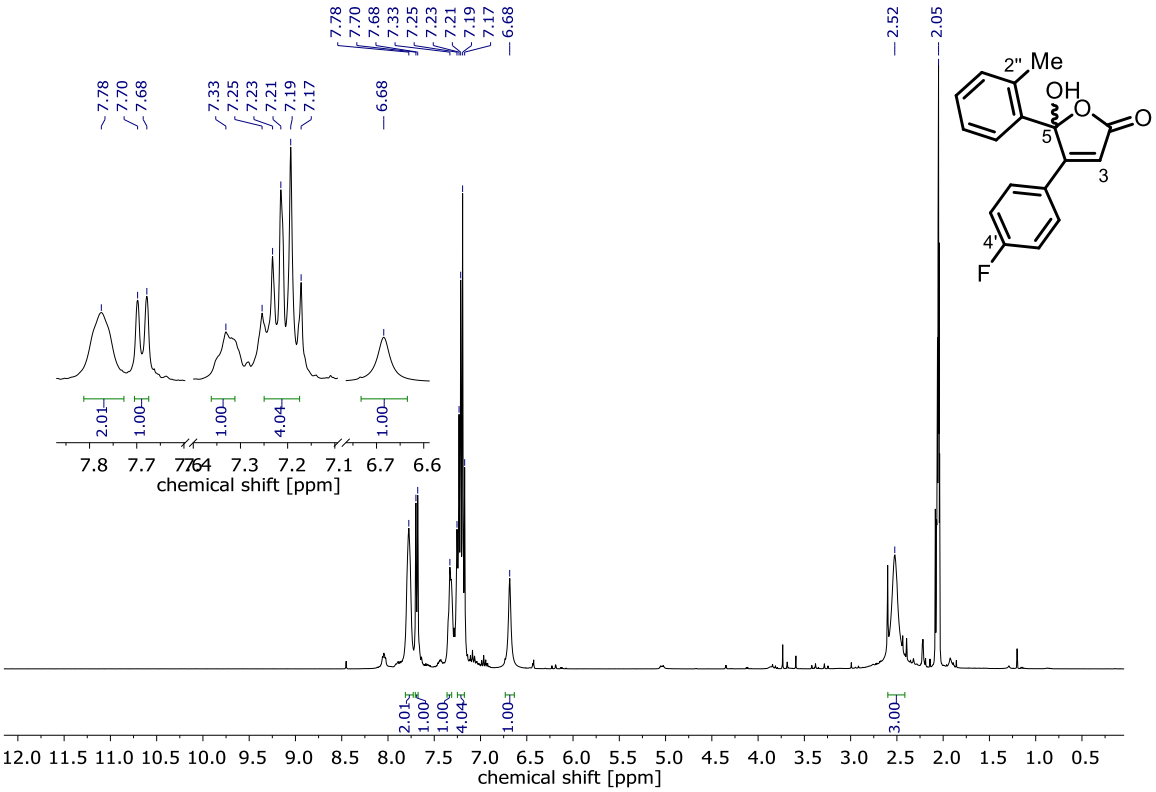

Figure 230: ^{1}H-NMR spectrum (400 MHz, acetone-d_6, 296K) of **276**.

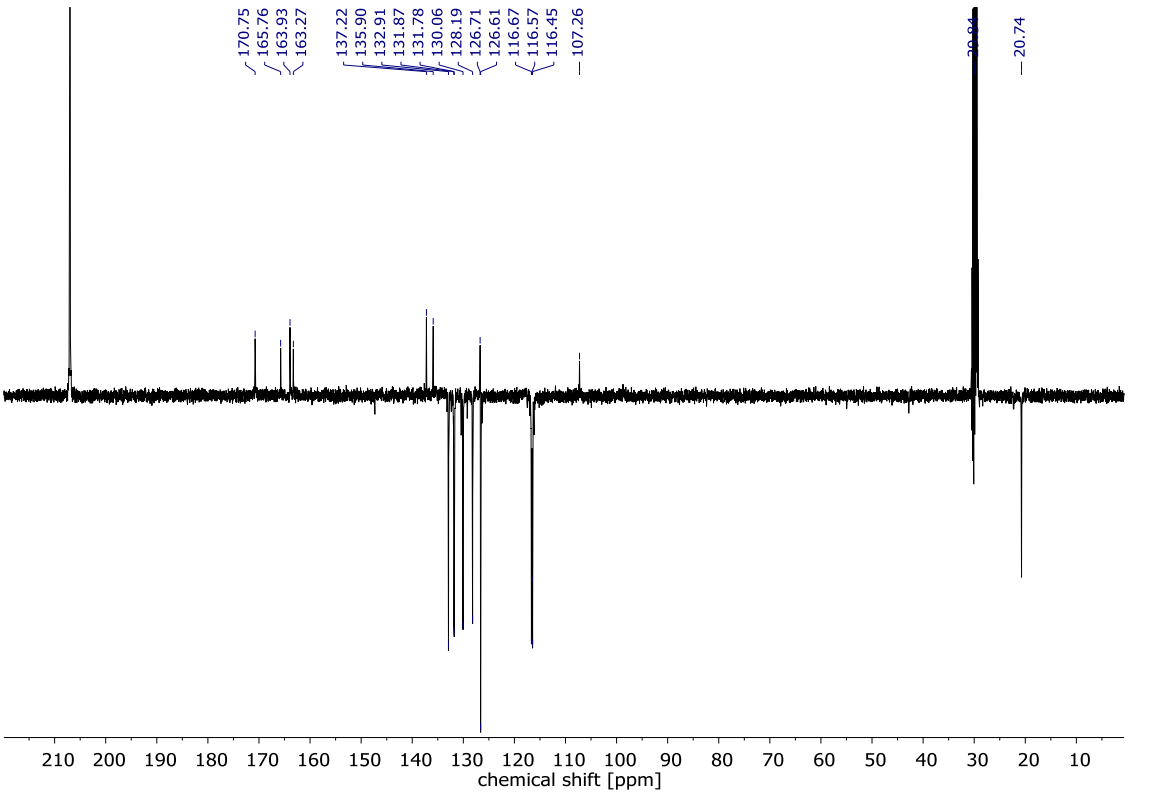

Figure 231: ^{13}C-NMR spectrum (101 MHz, acetone-d_6, 223K) of **276**.

5-Hydroxy-5-(naphthalen-2-yl)-4-phenylfuran-2(5*H*)-one 277

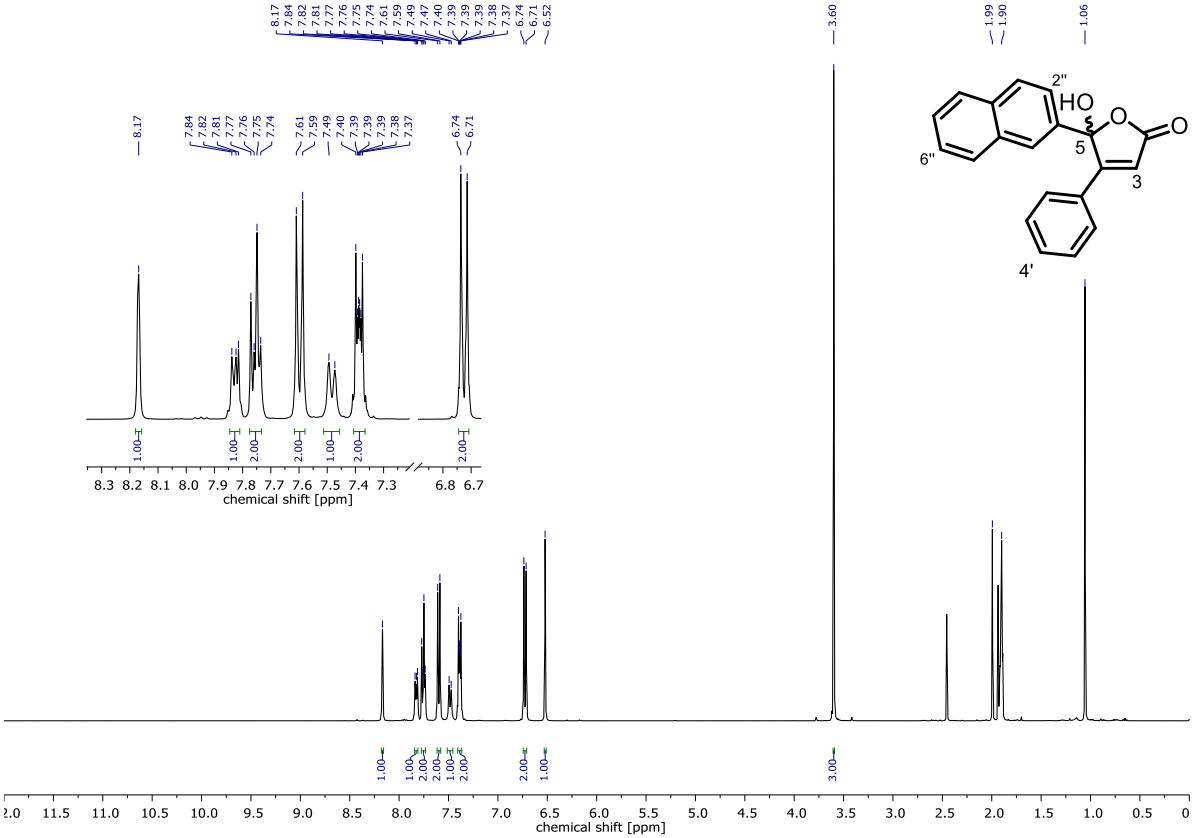

Figure 232: ^{1}H-NMR spectrum (400 MHz, acetone-d_6, 300K) of **277**.

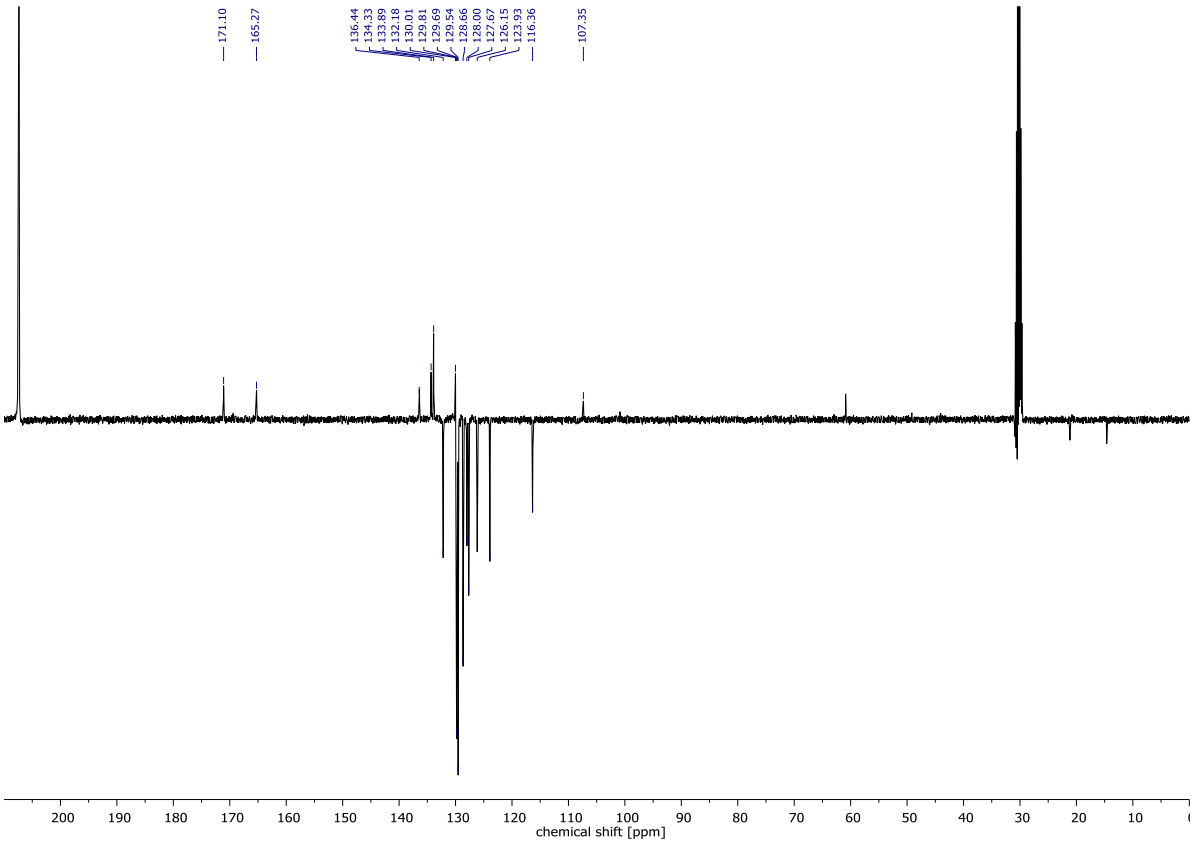

Figure 233: DEPTQ spectrum (101 MHz, acetone-d_6, 223K) of **277**.

5-Hydroxy-4-(4-methoxyphenyl)-5-(naphthalen-2-yl)furan-2(5*H*)-one 278

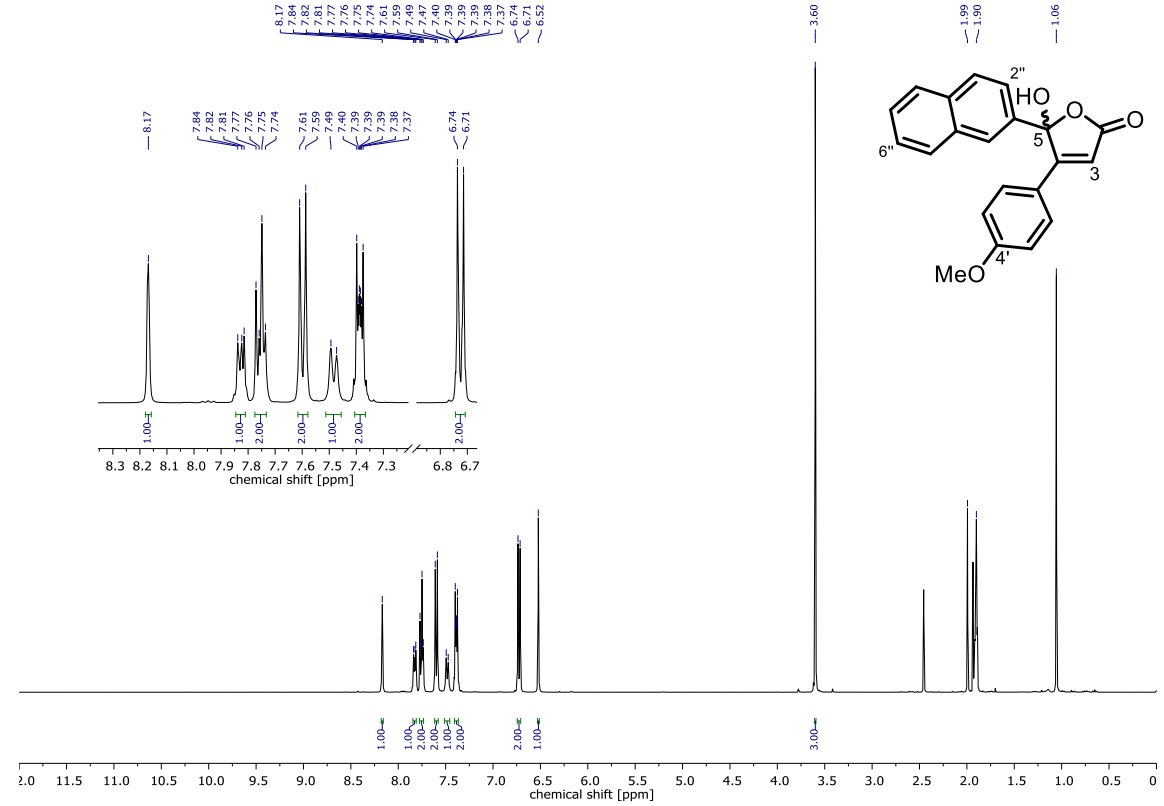

Figure 234: ^{1}H-NMR spectrum (400 MHz, acetone-d_6, 300K) of **278**.

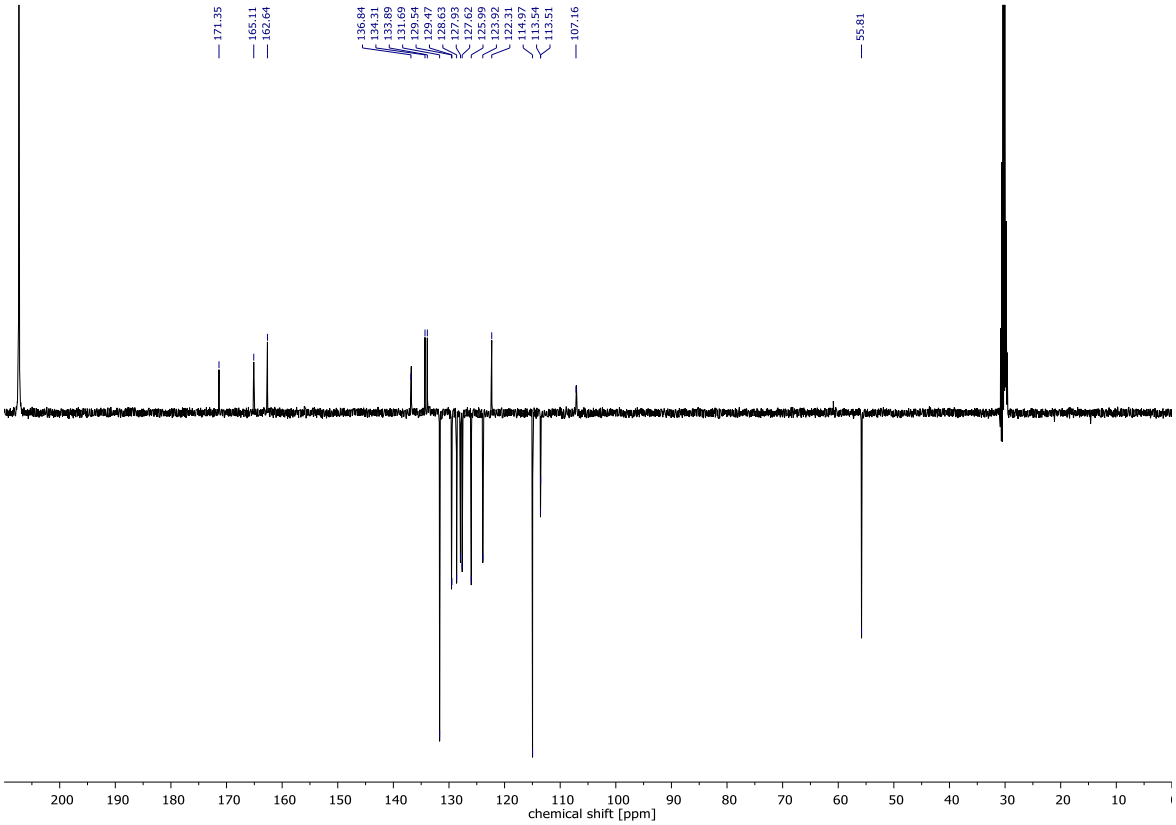

Figure 235: DEPTQ spectrum (101 MHz, acetone-d_6, 223K) of **278**.

4-(4-Fluorophenyl)-5-hydroxy-5-(naphthalen-2-yl)furan-2(5*H*)-one 279

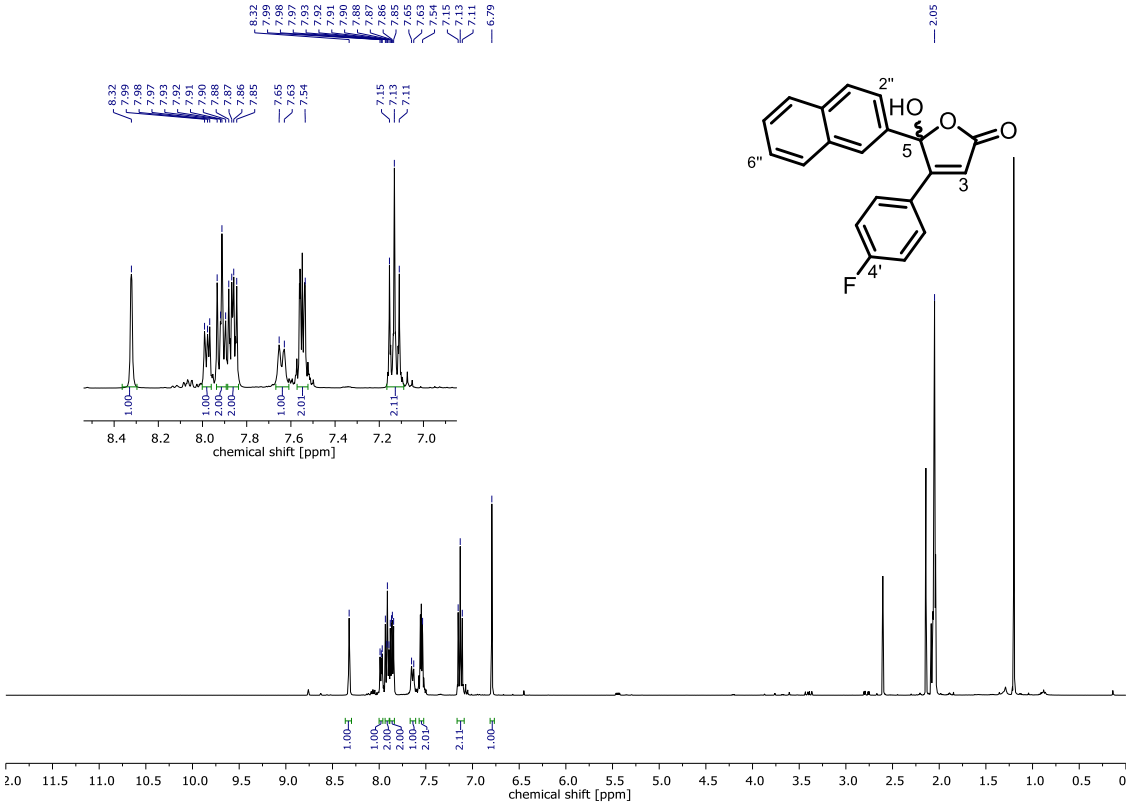

Figure 236: ^{1}H-NMR spectrum (400 MHz, acetone-d_6, 300K) of **279**.

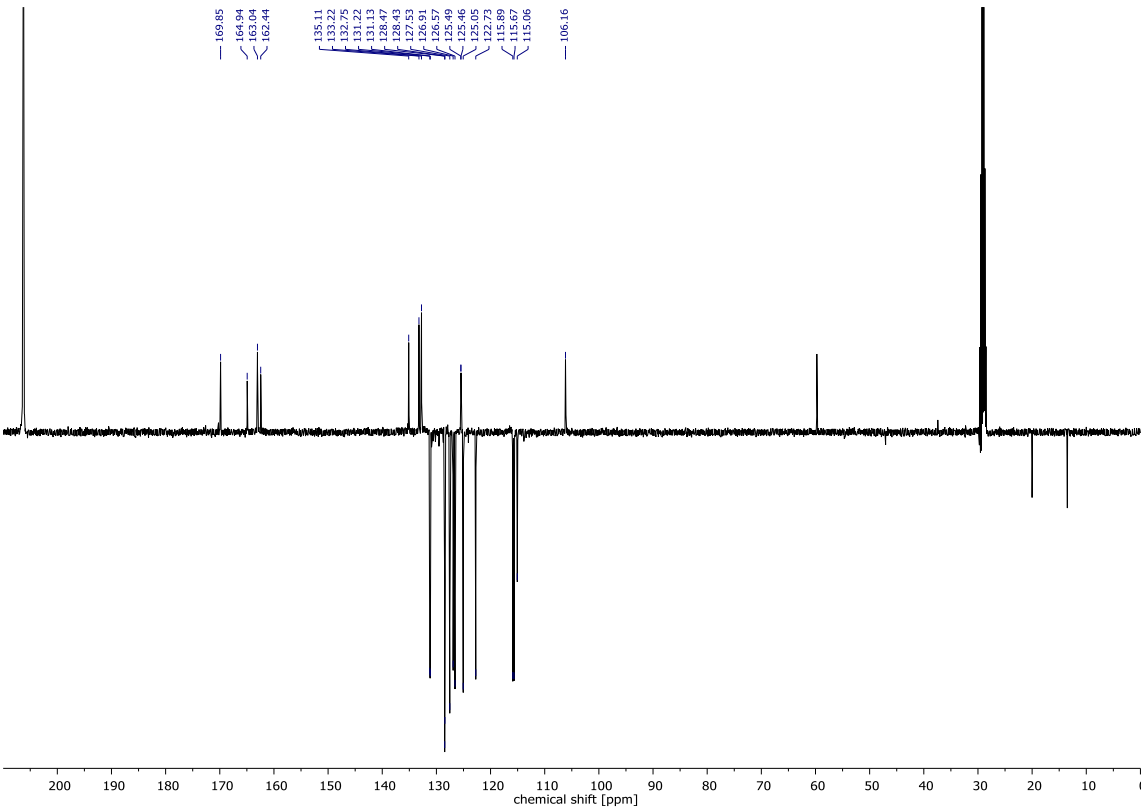

Figure 237: DEPTQ spectrum (101 MHz, acetone-d_6, 223K) of **279**.

Carbon-NMR of 5-Hydroxy-4-(4-methoxyphenyl)-5-phenylfuran-2-(5*H*)one 260 at 298K and 223K

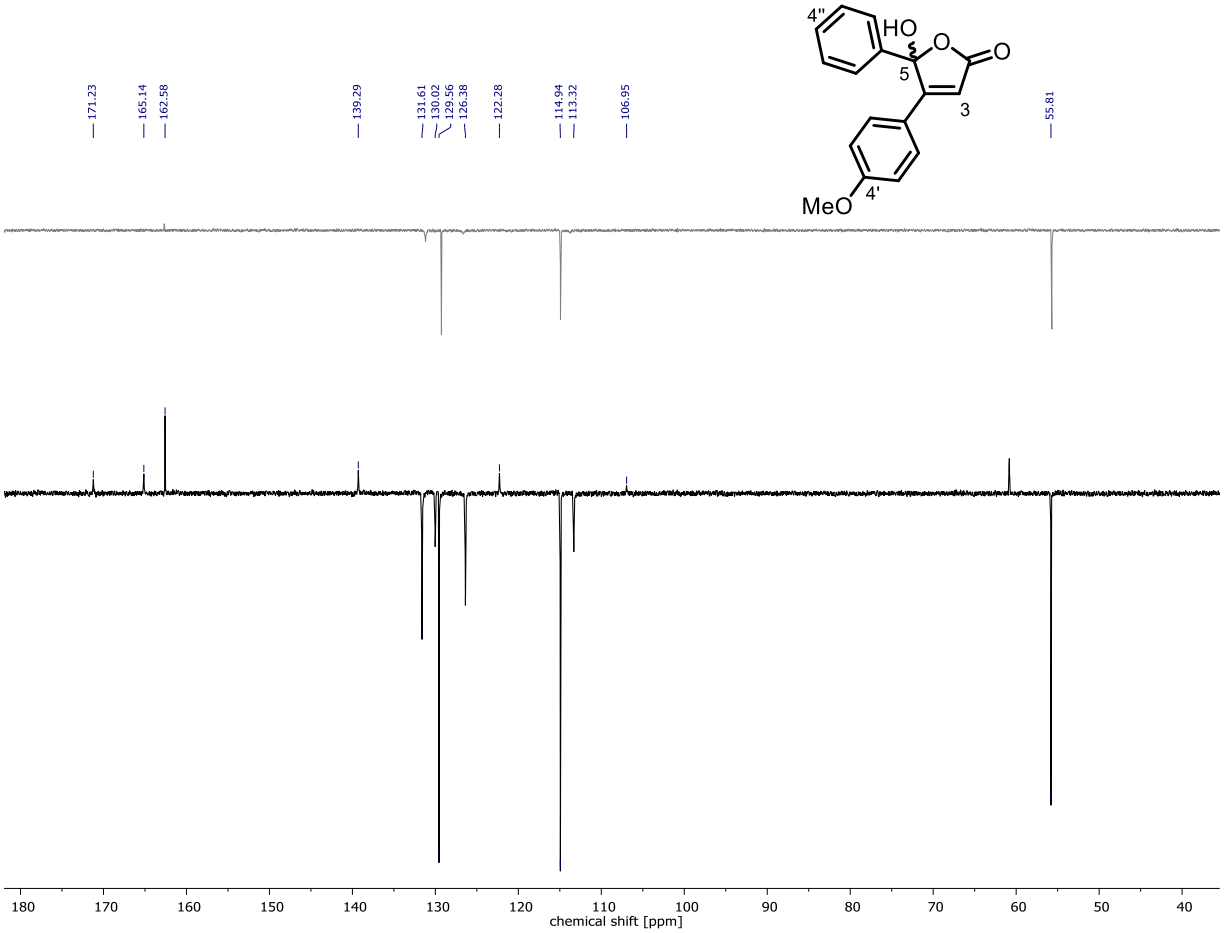

Figure 238: Stacked DEPTQ spectra (101 MHz, acetone-d_6, 298K – top, black; 223K – down, black) of **260**.

7.3. Hazard and precautionary statements

Substance	GHS identification	Hazard statement	Precautionary statements
4 Å molecular sieve[	Warning 07	315, 319, 335	261, 305+351+338
Amberlite	This substance is not classified as dangerous according to Regulation (EC) No 1272/2008		
Acetic acid	Danger 02, 05	226, 314	280, 305+351+338, 310
Acetic anhydride	Danger 02, 05, 06	226, 302, 314, 330	210, 260, 280, 304+340+310, 305+351+338, 370+378
Acetone	Danger 02, 07	225, 319, 336 EUH066	210, 240, 305+351+338, 403+233
Acetonitrile	Danger 02, 07	225, 302+312+332, 319	210, 305+351+338
Acetophenone	Danger 02, 07	225, 302+312+332, 319	210, 280, 305+351+338
Amano Lipase A from Aspergillus niger	This substance is not classified as dangerous according to Regulation (EC) No 1272/2008		
8-Aminoqinoline	Warning 07	315, 319	305+351+338
Ammoniummolybdate	This substance is not classified as dangerous according to Regulation (EC) No 1272/2008.		
Anisole	Danger 02	226	210, 370+378
4-Anisaldehyde	This substance is not classified as dangerous according to Regulation (EC) No 1272/2008.		
Azobis(isobutyrronitrile)	Danger 02, 07	242, 302, 332, 412	210, 280, 273
1,3-Bis(2,6-diisopropylphenyl)-1,3-dihydro-*2H*-imidazol-2-ylidene (SIPr)	This substance is not classified as dangerous according to Regulation (EC) No 1272/2008.		
Bis(neopentyl glycolato)diboron	This substance is not classified as dangerous according to Regulation (EC) No 1272/2008.		
Bis(pinacolato)diboron	This substance is not classified as dangerous according to Directive 67/548/EEC.		
Bis(triphenylphosphine)-palladium(II) dichloride	This substance is not classified as dangerous according to Directive 67/548/EEC.		
Benzene	Danger 02, 07, 08	225, 304, 315, 319, 340, 350, 372, 412	201, 210, 280, 308+313, 370+378, 403+235
p-Benzochinone	Danger 06, 09	301+331, 315, 319, 335, 410	261, 273, 301+310+330, 304+340+312, 403+233, 501
Benzoyl chloride	Danger 05, 07	302+312+332, 314, 317	261, 280, 301+330, 303+361+353, 304+340+310, 305+351+338
Benzylamine	Danger 04, 07	302, 312, 314	280, 305+351+338

Benzyltriethylammonium chloride	Warning 07	315, 319, 335	261, 305+351+338
rac-BINAP	Warning 07	315, 319, 335	280, 305+351+338
Bis(acetonitrile)palladium(II) 4-toluenesulfonate	Danger 06	301, 311, 331	261, 280, 301+310, 311
(2-Biphenyl)di-*tert*-butylphosphine	This substance is not classified as dangerous according to Directive 67/548/EEC.		
Bis(diphenylphosphino)methane	Warning 07	315, 319, 335	261, 302+352, 305+351+338, 321, 405, 501
1,3-Bis(diphenylphosphino)-propane	Warning 07	315, 319, 335	302+352, 304+340, 305+351+338
1,4-Bis(diphenylphosphino)butane	Warning 07	315, 319, 413	305+351+338
Bortribrominde	Danger 05, 06	300+330, 314	260, 264, 280,284, 301+310, 305+351+338
Bromoacetyl bromid	Danger 05	314	280, 305+351+338, 310
3-Bromo-4-hydroxybenzaldehyde	Warning 07	315, 319, 335	261, 305+351+338
5-Bromo-2-hydroxybenzaldehyde	Danger 07, 09	302, 400	273
N-Bromsuccinimide	Danger 05, 07	302, 314	280, 305+351+338, 310
1-Bromo-3-methylbut-2-ene	Danger 02, 06	226, 301	301, 310
n-Butylboronic acid	Warning 07	315, 319, 335	P261, P264, P271, P280, P302+P352, P304+P340, P305+P351+P338, P312, P321, P332+P313, P337+P313, P362, P403+P233, P405, 501
n-Butyllithium solution	Danger 02, 05, 07, 08, 09	225, 250, 261, 304, 314, 336, 361f, 373, 411	210, 222, 231+232, 261, 273, 422
tert-Butyldimethylsilyl trifluoromethane-sulfonate	Danger 02, 05, 07	226, 314, 335	261, 280, 305+351+338, 310
Caesium carbonate	Warning 07	315+319+335	261, 305+351+338
Caesium flouride	Danger 05, 06	301, 311, 314, 331	261, 280, 301+310, 305+351+338, 310
Calcium sulfate (Drierite)	This substance is not classified as dangerous according to Directive 67/548/EEC.		
Carbon monoxide	Danger 02, 06, 08	220, 280, 331, 360D, 372	201, 210, 261, 311, 410+403
Carbon tetrachloride	Danger 06, 08	301+311+331, 317, 351, 372, 412, 420	261, 273, 280, 301+310+330, 403+233, 502
Catecholborane	Danger 02, 05	225, 314	210, 280, 305+351+338, 310
Celite®	Warning 07, 08	319, 335, 373	261, 305+351+338
Cerium(IV)sulfate	Warning 07	315, 319	305+351+338
Chloroform	Danger 05,	302, 315, 319,	261, 281,

	08	331, 336, 351, 361d, 372	305+351+338, 311
Chloro(1,5-cyclooctadiene)-rhodium(I) dimer	Warning 07	319	305+351+338
3-chloro tetronic acid	Warning 07	315, 319, 335	261, 305+351+338
Citrate buffer	Warning 08	351, 373	-
Copper(I)bromide dimethyl sulfide	Warning 07	315, 319, 335	261, 305+351+338
Copper(II) acetate	Danger 05, 07, 09	302, 314, 410	260, 280, 301+312+330, 303+361+353, 304+340+310, 305+351+338
Copper(I) cyanide	Danger 06, 09	300, 310, 330, 410, EUH032	260, 264, 273, 280, 284, 301+310
Copper(I) cyanide di(lithium chloride) complex solution	Danger 02, 06, 08, 09	225, 300+310+330, 315, 319, 335, 351, 410	210, 280, 302+352+310, 304+340+310, 370+378, 403+235
Copper(I) iodide	Warning 07, 09	302, 315, 319, 335, 410	261, 273, 305+351+338, 510
1,8-Diazabicyclo-[5.4.0]undec-7-en	Danger 05, 06	290, 301, 314, 412	273, 280, 301+310, 305+351+338, 310
Cyclopentyl methyl ether	Danger 02, 07	225, 302, 315, 319, 412	210, 301+312+330, 305+351+338, 370+378, 403+235
Dess-Martin Periodane	Warning 07	302, 312, 315, 319, 332, 335	261, 280, 305+351+338
2-Dicyclohexylphosphino-2',6'-dimethoxybiphenyl	This substance is not classified as dangerous according to Regulation (EC) No 1272/2008.		
1,4-Dichlorbenzene	Danger 07, 08, 09	319, 351, 410	273, 280, 305+351+338, 308+313
Dichloromethane	Danger 07, 08	315, 319, 335, 336, 351, 373	260, 280, 305+351+338
Diethyl ether	Danger 02, 07	224, 302, 336, EUH019, EUH066	210, 261
N,*N*-Di*iso*propylethylamine	Danger 02, 05, 06	225, 302, 318, 331, 335	210, 261, 280, 305+351+338, 311
Dimethylamine solution 40wt%	Danger 02, 05, 07	225, 314, 335, 412	210, 280, 303+361+353, 304+340+310, 305+351+338, 370+378
N,*N*-Dimethylaminopyridine	Danger 06	310, 301, 315, 319	302+352, 305+351+338
Dimethyl carbonate	Danger 02	225	210, 403+235
2,2-Dimethyl-chromane-6-carbaldehyde	Warning 07, 09	304, 403	332+313, 305+351+338
N,N-Dimethylacetamide	Danger 07, 08	312, 319, 332, 360	280, 308+313
N,*N*-Dimethylformamide	Danger 02, 07, 08	226, 312+332, 319, 360D	201, 210, 261, 280, 308+313, 370+378
Dibutyl ether	Danger 02,	226, 315, 319,	210, 273,

	07	335, 412	305+351+338, 302+352
Dimethyl sulfoxide	This substance is not classified as dangerous according to Regulation (EC) No 1272/2008.		
1,4-Dioxane	Danger 02, 05, 07	225, 319, 335, 351, EUH019, EUH066	210, 261, 305+351+338,
Diphenylacetylene	This substance is not classified as dangerous according to Regulation (EC) No 1272/2008.		
Di-*tert*-butyl dicarbonate	Danger 02, 05, 06	226, 330, 315, 317, 335	210, 260, 280, 304+340+310, 305+351+338+310, 370+378
Dowex® 50WX8 hydrogen form	Warning 08	319	305+351+338
Esterase from porcine liver	This substance is not classified as dangerous according to Regulation (EC) No 1272/2008.		
Ethanol	Danger 02, 07	225, 319	210, 280, 305+351+338, 337, 313, 403, 235
Ethanolamine	Danger 05, 07	302, 312+332, 314, 335, 412	261, 273, 301+312+330, 303+361+353, 304+340+310, 305+351+338
Ethyl acetate	Danger 02, 07	225, 319, 336, EUH066	210, 361, 305+351+338
1-Ethyl-3-(3-dimethyl-aminopropyl)carbodiimid × HCl	Danger 05, 07	315, 318, 335	261, 280, 305+351+338
1,1′-Ferrocenediyl-bis(diphenylphosphine) (dppf)	This substance is not classified as dangerous according to Regulation (EC) No 1272/2008.		
4-Fluoroacetophenone	Warning 07	315, 319, 335	261, 280, 305+351+338, 304+340, 405, 501
Fluorobenzene	Danger 02, 07	225, 319, 412	210, 273, 305+351+338
4-Fluorophenyl-boronic acid	Warning 07	315, 319, 335	261, 280, 305+351+338, 304+340, 405, 501
Formic acid	Danger 02, 05, 07	226, 302, 314, 331	210, 260, 280, 304+340+310, 305+351+338, 370+378
4-Formylphenyl-boronic acid	Danger 05, 07	314, 317	280, 305+351+338, 310
5-Formyl-2 methoxy-phenyl boronic acid	Warning 07	315, 319	280, 302, 352, 332, 313, 362, 364
2-Furanylboronic acid	This substance is not classified as dangerous according to Regulation (EC) No 1272/2008.		
Hydrobromic acid	Danger 05, 07	314, 335	260, 280, 303+361+353, 304+340+310, 305+351+338
Hydrochloric acid	Danger 05, 07	290, 314, 335	261, 280, 305+351+338, 310
Hydrogen peroxide solution	Danger 05,	302, 318	290, 305+351+338

	07		
4-Hydroxy-benzaldehyde	This substance is not classified as dangerous according to Regulation (EC) No 1272/2008.		
4-Hydroxyphenyl-boronic acid	Warning 07	315, 319	305+351+338
Imidazol	Danger 02, 08, 09	224, 341, 350, 411	201, 210, 280, 308+313, 370+378, 403+235
Iodine	Danger 07, 08, 09	312, 332, 315, 319, 335, 372, 400	273, 302+352, 305+351+338, 314
4-Iodoanisole	This substance is not classified as dangerous according to Regulation (EC) No 1272/2008		
Isoprene	Danger 02, 08, 09	224, 341, 350, 411	201, 210, 280, 308+313, 370+378, 403+235
Lithium chloride	Warning 07	301, 315, 319	301+312+330, 305+351+338
Magnesium sulfate	This substance is not classified as dangerous according to Regulation (EC) No 1272/2008.		
Manganese(IV) dioxide	Danger 07, 08	302+332+373	314
D-(+)-Mannose	This substance is not classified as dangerous according to Regulation (EC) No 1272/2008.		
Methanol	Danger 02, 06, 07	225, 301+311+331, 370	210, 260, 280, 301+310, 311
2-Methylbut-3-en-2-ol	Danger 02, 06, 09	225, 301+311+331, 315, 319, 335, 400	210, 261, 273, 280, 301+310+330, 403+233
4-Methoxyacetophenone	Warning 07	302	301+312+330
4-Methoxyphenylboronic acid	Warning 07	315, 319, 335	261, 305+351+338
Methyl iodide	Danger 06, 08	351, 312, 331, 301, 335, 315	261, 280, 301+310+311
N-Methyl-2-pyrrolidone	Danger 07, 08	315, 319, 335, 360D	201, 308+313, 305+351+338, 302+350
2-Methyltetrahydrofurane	This substance is not classified as dangerous according to Regulation (EC) No 1272/2008.		
Molybdenum-hexacarbonyl	Danger 06	300+310+330	260, 264, 280, 284, 301+310, 302+350
4-(Morpholine-4-carbonyl)-phenylboronic acid pinacol ester	This substance is not classified as dangerous according to Regulation (EC) No 1272/2008.		
2-naphtylboronic acid	Warning 07	315, 319, 335	P261, P264, P271, P280, P302+P352, P304+P340, P305+P351+P338, P312, P321, P332+P313, P337+P313, P362, P403+P233, P405, 501
Nickel(II)acetate tetrahydrate	Danger 07, 08, 09	302+332, 317, 334, 341, 350i, 360, 372, 410	201, 261, 273, 280, 308+313, 501

Nickel(II)chloride	Danger 06, 08, 09	350i, 360D, 341, 301+331, 372, 315, 317, 334, 410	273, 281, 302+352, 304+340, 309+310
Nickel(II) chloride ethylene glycol dimethyl ether complex	Danger 02, 06, 08,09	261, 301, 315, 319, 334, 350, 400	201, 231+232, 261, 273, 280, 301+310+330, 302+335+334, 304+340, 308+313, 370+378, 391
4-nitrophenylboronic acid	Warning 07	302	-
Palladium (II) acetate	Danger 05	318	280, 305+351+338
Palladium(II) chloride	Danger 06	301-317	280, 301+310+330, 333+313
Palladium(II)trifluoroacetate	Warning 07	315, 319, 335	261, 305+351,338
Pentane	Danger 02, 07, 08, 09	225, 304, 336, 411, EUH066	210, 261, 273, 301+310, 331
Petroleum ether	Danger 02, 07, 08, 09	224, 304, 336, 411	210, 261, 273, 301+310, 331
Phenylboronic acid	Warning 07	302	-
Phosphortribromide	Danger 05, 07	314, 335	261, 280, 305+351+338, 310
Piperidine	Danger 02, 05, 06	225, 331, 311, 314	210, 280, 302+352, 301+330+331, 305+351+338, 309+310
Potassium acetate	This substance is not classified as dangerous according to Regulation (EC) No 1272/2008.		
Potassium carbonate	Warning 07	302, 315, 319, 335	261, 305+351+338
Potassium ferrocyanide trihydrate	This substance is not classified as dangerous according to Regulation (EC) No 1272/2008.		
Potassium fluoride	Danger 06	301+311+331	261, 280, 302+352+312, 304+340+312, 403+233
Potassium hydrogendfluoride	Danger 05, 06	301, 314	260, 280, 303+361+353, 304+340+310, 305+351+338
Potassium hydroxide	Danger 05, 07	290, 302, 314	280, 301+312+330, 303+361+353, 304+340+310, 305+351+338
Potassium iodide	Danger 08	372	260, 264, 270, 314, 501
Potassium permanganate	Danger 03, 05, 07, 09	272, 302, 314, 410	211, 273, 280, 301+330+331, 305+351+338, 308+310
ortho-Phosphoric acid	Warning 07	290, 314	280, 303+361+353, 304+340+310, 305+351+338
2-Propanol	Warning 02, 07	225, 319, 336	210, 233, 305+351+338

Pyridine	Danger 02, 07	225, 302+312+332, 315, 319	210, 280, 305+351+338
Silica	This substance is not classified as dangerous according to Regulation (EC) No 1272/2008.		
Silver(I)carbonate	Warning 07	315, 319, 335	361, 305+351+338
Silver(I)oxide	Danger 03, 05, 09	271, 318, 410	220, 273, 280, 305+351+338, 501
Sodiu acetate trihydrate	This substance is not classified as dangerous according to Regulation (EC) No 1272/2008.		
Sodium carbonate	Warning 07	319	305+351+338
Sodium chloride	This substance is not classified as dangerous according to Regulation (EC) No 1272/2008.		
Sodium chlorite	Danger 03, 05, 06, 08, 09	271, 301, 310, 314, 373, 410	210, 280, 303+361+353, 305+351+338, 370+378
Sodium fluoride	Danger 06	301, 315, 319, EUH032	302+352, 305+351+338, 308+310
Sodium hydride (60% suspension)	Danger 02	260	223, 231,232, 370+378+422
Sodium dihydrogen phosphate	This substance is not classified as dangerous according to Regulation (EC) No 1272/2008.		
Sodium methanolate	Danger 02, 05, 07	251, 302, 314	235, 410, 280, 305+351+338, 310
Sodium hydrogen carbonate	This substance is not classified as dangerous according to Regulation (EC) No 1272/2008.		
Sodium hydroxide	Danger 05	290, 314	280, 303+361+353, 304+340+310, 305+351+338
Sodium periodate	Danger 03, 05, 08, 09r	271, 314, 372, 400	210, 260, 280, 305+351+338, 370+378, 371+380+375
Sodium sulfate	This substance is not classified as dangerous according to Regulation (EC) No 1272/2008.		
Sodium carbonate	Warning 07	319	260, 305+351+338
Succinimide	This substance is not classified as dangerous according to Regulation (EC) No 1272/2008.		
Sulfuric acid	Danger 05	290, 314	260, 305+351+338, 310
Tetra-*n*-butylammonium chlorid	Warning 07	315, 319	305+351+338
Tetra-*n*-butylammonium bromide	Warning 07	302, 319	301, 312+330, 305+351+338
Tetra-*n*-butylammonium tribromide	Warning 07	315, 319, 335	261, 305+350+338
Tert-Butyl isocyanide	Danger 02, 06	225, 330	210, 260, 284, 310
Tert-Butyllithium	Danger 02, 05, 07, 08, 09	225, 250, 260, 304, 314, 336, 411	210, 222, 223, 231+232, 370+378, 422
Tetrahydrofurane	Danger 02, 07, 08	225, 302, 319, 335, 351, EUH019	210, 280, 301+312+330, 305+351+338,

			370+378, 403+235
Tetrahydroxydiboron	Warning 07	302+332, 315, 319, 335	261, 301+312+330, 305+351+338
Tetrakis(triphenylphos-phine)palladium(0)	This substance is not classified as dangerous according to Regulation (EC) No 1272/2008.		
Tetrakis(triphenylphosphine)-platinum(0)	This substance is not classified as dangerous according to Regulation (EC) No 1272/2008.		
Tetronic acid	Warning 07	315, 319, 335	261, 280, 305+351+338, 304+340, 362, 321, 332+313, 403+233, 405, 501
N,*N*,*N´*,*N´*-Tetra-methylethylen diamine	Danger 02, 05, 07	225, 302, 314, 332	210, 280, 305+351+338, 310
2-Thienylboronic acid	This substance is not classified as dangerous according to Regulation (EC) No 1272/2008.		
	Danger 05, 06	302, 331, 314, 335 EUH014, EUH029	280, 301+330+331, 304+340, 305+351+338, 309+310
Toluene	Danger 02, 07, 08	225, 304, 315, 336, 361d, 373	210, 260, 280, 301+310, 370+378, 403+235
2-Tolylboronic acid	Warning 07	315, 319, 335	P261, P264, P271, P280, P302+P352, P304+P340, P305+P351+P338, P312, P321, P332+P313, P337+P313, P362, P403+P233, P405, 501
3-Tolylboronic acid	Warning 07	315, 319, 335	P261, P264, P271, P280, P302+P352, P304+P340, P305+P351+P338, P312, P321, P332+P313, P337+P313, P362, P403+P233, P405, 501
4-Tolylboronic acid	Warning 07	315, 319, 335	P261, P264, P271, P280, P302+P352, P304+P340, P305+P351+P338, P312, P321, P332+P313, P337+P313, P362, P403+P233, P405, 501
4-Toluenesulfonyl chloride	This substance is not classified as dangerous according to Regulation (EC) No 1272/2008		
4-Toluenesulfonic acid	Warning 07	315, 319, 335	302+352, 304+340, 305+351+338

Trichloroacetonitrile	Danger 06, 09	301+311+331, 411	261, 280, 301+330+331+310, 302+352+312, 304+340+311, 403+233
Tricyclohexylphosphine	Warning 07	315, 319, 335	261, 305+351+338
Tri-*n*-butylphosphine	Danger 02, 05, 06	226, 250, 302, 312, 314	222, 231, 280, 305+351+338, 310, 422
Triethylamine	Danger 02, 05, 06	225, 302, 311+331, 314, 335	210, 261, 280, 303+361+353, 305+351+338, 370+378
Triethyl *ortho*-formate	Danger 02	226	210
Trifluoroacetic acid	Danger 05, 07	314, 332, 412	273, 280, 305+351+338, 310
Trifluoromethane-sulfonic acid	Danger 05, 07	290, 302, 314, 335	280, 310, 305+351+338, 303+361+353, 304+340, 301+330+331
Trifluoromethane-sulfonic anhydride	Danger 05, 07	302, 314, EUH014	280, 305+351+338, 310
Trimethylsilylacetylene	Danger 02, 07	225, 319	210, 233, 280, 303+361+353, 337+313, 370+378
Trimetyhlsilyl bromide	Danger 02, 05	225, 314	210, 280, 305+351+338, 310
Trimetyhlsilyl chloride	Danger 02, 05, 06	225, 301+331, 312, 314	210, 261, 280, 301+310, 305+351+338, 310
Trimetyhlsilyl iodide	Danger 02, 05	225, 314	210, 280, 305+351+338, 310
Trimethylsilyl trifluoro-methanesulfonate	Danger 05, 07	226, 314	280, 305+351+338, 310
Tri*iso*propyl borate	Danger 02	225	210
Trimethyl borate	Danger 02, 07, 08	225, 312, 319, 360, 370	201, 210, 260, 302+352+312, 308+311, 337+313
Triphenylphosphine	Warning 07, 08	302, 317, 373	280, 301+312+330, 333+313
Tri(4-tolyl)phosphine	Warning 07	315, 319, 335	261, 305+351+335
Tris(dibenzylideneacetone) dipalladium(0)	This substance is not classified as dangerous according to Regulation (EC) No 1272/2008.		
Tris(triphenylphosphine)rhodium(I) chloride	This substance is not classified as dangerous according to Regulation (EC) No 1272/2008.		
Vanadyl acetylacetonate	Warning 07	302, 315, 319, 335	261, 305+351+338
Vanadium(V)oxide	Danger 05, 07, 08, 09	302+332, 318, 335, 341, 361d, 372, 411	201, 261, 273, 280, 305+351+338+310, 501
Xantphos	This substance is not classified as dangerous according to Regulation (EC) No 1272/2008.		
4-Xylene	Danger 02, 07	226, 304, 312, 315, 332, 319,	210, 280, 305+351+338,

		335, 412	301+330+331
Zinc(II)acetate × 2 H_2O	This substance is not classified as dangerous according to Regulation (EC) No 1272/2008.		
Zinc chloride	Danger 05, 07, 09	302, 314, 410	260, 280, 301+312+330, 303+361+353, 304+340+310, 305+351+338
Zinc	This substance is not classified as dangerous according to Regulation (EC) No 1272/2008.		

GHS pictograms

Exploding bomb
(For explosion or reactivity hazard)

Flame
(for fire hazard)

Flame over circle
(for oxidizing hazards)

Gas cylinder
(for gases under pressure)

Corrosion
(for corrosive damage to metals as well as skin, eyes)

Skulls and Crossbones
(Can cause death or toxicity with short exposure to small amounts)

Exclamation mark
(may cause less serious health effects or damage the ozone layer)

Health hazard
(may cause or suspected of causing serious health effects)

Environment
(may cause damage to the aquatic environment)

8. Literature

[1] World Health Organization. First Comprehensive Global Report on Antimicrobial Resistance, *WHO Library Cataloguing-in-Publication* Data, April **2018**. (http://www.who.int/drugresistance/documents/surveillancereport/en/ last access 28.04.2019)

[2] European Centre for Disease Prevention and Control, *Antimicrobial resistance surveillance in Europe 2015*. Annual Report of the European Antimicrobial Resistance Surveillance Network (EARS-Net), **2014**.

[3] T. F. Molinski, D. S. Dalisay, S. L. Lievens, J. P. Saludes, *Nat. Rev. Drug Discov.* **2009**, *8*, 69–85.

[4] H. Terlau, G. Bach, A. Zeeck, *Internist* **2001**, *42*, 1422–1427.

[5] G. Klebe, *Wirkstoffdesign - Entwurf und Wirkung von Arzneistoffen*, Spektrum Akademischer Verlag, Heidelberg, **2009**.

[6] G. M. Cragg, D. J. Newman, K. M. Snader, *J. Nat. Prod.* **1997**, *60*, 52–60.

[7] I. Paterson, E. Anderson, *Science* **2005**, *310*, 451–453.

[8] C. M. Baldino, *J. Comb. Chem.* **2000**, *2*, 89–103.

[9] R. E. Dolle, *J. Comb. Chem.* **2000**, *2*, 383–433.

[10] F. Wunder, B. Kalthof, T. Muller, J. Huser, *Comb. Chem. High Throughput Screen.* **2008**, *11*, 495–504.

[11] M. Miyashita, F. Taga, F. Iinuma, T. Matsumoto, H. Matsukubo, K. Okamura, K. Hamada, H. Sekiguchi, K. Nishino, *J. Med. Chem.* **1992**, *35*, 2446–2451.

[12] P. Mayer, P. Brunel, C. Chaplain, C. Piedecoq, F. Calmel, P. Schambel, P. Chopin, T. Wurch, P. J. Pauwels, M. Marien, J.L. Vidaluc, T. Imbert, *J. Med. Chem.* **2000**, *43*, 3653–3664.

[13] L. Zhang, W. Xia, B. Wang, Y. Luo, W. Lu, *Synth. Commun.* **2011**, *41*, 3140–3146.

[14] D. J. Newman, G. M. Cragg, *J. Nat. Prod.* **2012**, *75*, 311–335.

[15] R. Montaser, H. Luesch, *Futur. Med. Chem.* **2011**, *3*, 1475–1489.

[16] S. Grabley. G. Kreysa, *Vorbild Natur: Stand und Perspektiven der Naturstoff-Forschung in Deutschland, DECHEMA Gesellschaft für Chem. Tech. und Biotechnol. e.V.*, Frankfurt am Main, **2007**.

[17] W. Bergmann, R. J. Feeney, *J. Org. Chem.* **1951**, *16*, 981–987.

[18] W. Bergmann, D. C. Burke, *J. Org. Chem.* **1956**, *21*, 226–228.

[19] W. Bergmann, M. F. Stempien, *J. Org. Chem.* **1957**, *22*, 1575–1577.

[20] S. Farr-Jones, G. P. Miljanich, L. Nadasdi, J. Ramachandran, V. J. Basus, *J. Mol. Biol.* **1995**, *248*, 106–124.

[21] H. Liu, M. De Waard, V. E. S. Scott, C. A. Gurnett, V. A. Lennon, K. P. Campbell, *J. Biol. Chem.* **1996**, *271*, 13804–13810.

[22] K. L. Rinehart, T. G. Holt, N. L. Fregeau, J. G. Stroh, P. A. Keifer, F. Sun, L. H. Li, D. G. Martin, *J. Org. Chem.* **1995**, *55*, 4512–4515.

[23] A. Kijjoa, P. Sawangwong, *Mar. Drugs* **2004**, *2*, 73–82.

[24] R. A. Raphael, *Nature* **1947**, *160*, 261–262.

[25] B. E. Haynes, H. A. Bessen, W. D. Wightman, *Ann. Emerg. Med.* **1985**, *14*, 350–353.

[26] J. Felth, L. Rickardson, J. Rosén,M. Wickström, M. Fryknäs, M. Lindskog, L. Bohlin, J. Gulbo, *J. Nat. Prod.* **2009**, *72*, 1969–1974.

[27] J. L. W. F. Bergel, A. L. Morrison, A. R. Moss, R. Klein, H. Rinderknecht, *Nature* **1943**, 750–751.

[28] S. Miao, R. J. Andersen, *J. Org. Chem.* **1991**, *56*, 6275–6280.

[29] J. Sikorska, S. Parker-Nance, M. T. Davies-Coleman, O. B. Vining, A. E. Sikora, K. L. McPhail, *J. Nat. Prod.* **2012**, *75*, 1824–1827.

[30] M. J. Ortega, E. Zubía, J. M. Ocaña, S. Naranjo, J. Salvá, *Tetrahedron* **2000**, *56*, 3963–3967.

[31] U. A. Pereira, L. C. A. Barbosa, C. R. A. Maltha, A. J. Demuner, M. A. Masood, A. L. Pimenta, *Eur. J. Med. Chem.* **2014**, *82*, 127–138.

[32] U. A. Pereira,T. A. Moreira, L. C. A. Barbosa, C. R. A. Maltha, I. S. Bomfim, S. S. Maranhão, M. O. Moraes, C. Pessoa, F. W. A. Barros-Nepomuceno, *Medchemcomm* **2016**, *7*, 345–352.
[33] D. Smitha, M. M. K. Kumar, H. Ramana, D. V. Rao, *Nat. Prod. Res.* **2014**, *28*, 12–17.
[34] T. Zhu, Z. Chen, P. Liu, Y. Wang, Z. Xin, W. Zhu, *J. Antibiot.* **2014**, *67*, 315–318.
[35] K. Damodar, J. K. Kim, J. G. Jun, *Tetrahedron Lett.* **2017**, *58*, 50–53.
[36] E. N. Matin Kotora, *Synthesis* **1997**, 121–128.
[37] S. P. Chavan, A. B. Pathak, A. Pandey, U. R. Kalkote, *Synth. Commun.* **2007**, *37*, 4253–4263.
[38] N. P. Tale, A. V. Shelke, G. B. Tiwari, P. B. Thorat, N. N. Karade, *Helv. Chim. Acta* **2012**, *95*, 852–857.
[39] S. Cacchi, G. Fabrizi, A. Goggiamani, A. Sferrazza, *Synlett* **2009**, 1277–1280.
[40] F. Bellina, C. Anselmi, S. Viel, L. Mannina, R. Rossi, *Tetrahedron* **2001**, *57*, 9997–10007.
[41] F. Bellina, C. Anselmi, F. Martina, R. Rossi, *Eur. J. Org. Chem.* **2003**, *2*, 2290–2302.
[42] F. Bellina, C. Anselmi, R. Rossi, *Tetrahedron Lett.* **2002**, *43*, 2023–2027.
[43] R. Rossi, F. Bellina, E. Raugei, *Synlett* **2000,** 1749–1752.
[44] L. C. A. Barbosa, C. R. A. Maltha, M. R. Lage, R. C. Barcelos, A. Donà, J. W. M. Carneiro, G. Forlani, *J. Agric. Food Chem.* **2012**, *60*, 10555–10563.
[45] J. O. S. Varejão, L. C. A. Barbosa, G. Á. Ramos, E. V. V. Varejão, B. King-Díaz, B. Lotina-Hennsen, *J. Photochem. Photobiol. B* **2015**, *145*, 11–18.
[46] U. A. Pereira, L. C. A. Barbosa, A. J. Demuner, A. A. Silva, M. Bertazzini, G. Forlani, *Chem. Biodivers.* **2015**, *12*, 987–1006.
[47] J. Boukouvalas, L. C. McCann, *Tetrahedron Lett.* **2010**, *51*, 4636–4639.
[48] J. Boukouvalas, N. Lachance, M. Ouellet, M. Trudeau, *Tetrahedron Lett.* **1998**, *39*, 7665–7668.
[49] S. Murata, *Tetrahedron* **1988**, *44*, 4259–4275.
[50] C. W. Downey, M. W. Johnson, *Tetrahedron Lett.* **2007**, *48*, 3559–3562.
[51] C. W. Downey, M. W. Johnson, K. J. Tracy, *J. Org. Chem.* **2008**, *73*, 3299–3302.
[52] L. J. Gooßen, *Chem. Commun.* **2001**, *84*, 669–670.
[53] J. Boukouvalas, F. Maltais, *Tetrahedron Lett.* **1995**, *36*, 7175–7176.
[54] A. R. Carroll, P. C. Healy, R. J. Quinn, C. J. Tranter, *J Org Chem* **1999**, *64*, 2680–2682.
[55] I. Margaros, T. Montagnon, M. Tofi, E. Pavlakos, G. Vassilikogiannakis, *Tetrahedron* **2006**, *62*, 5308–5317.
[56] N. Sofikiti, M. Tofi, T. Montagnon, G. Vassilikogiannakis, M. Stratakis, *Org. Lett.* **2005**, *7*, 2357–2359.
[57] S. De Rosa, A. Crispino, A. De Giulio, C. Iodice, R. Pronzato, N. Zavodnik, *J. Nat. Prod.* **1995**, *58*, 1776–1780.
[58] S. De Rosa, S. De Stefano, N. Zavodnik, *J. Org. Chem.* **1988**, *53*, 5020–5023.
[59] S. De Rosa, R. Puliti, A. Crispino, A. De Giulio, C. De Sena, C. Iodice, C. A. Mattia, *Tetrahedron* **1995**, *51*, 10731–10736.
[60] S. De Rosa, A. Crispino, A. De Giulio, C. Iodice, R. Benrezzouk, M. C. Terencio, M. L. Ferrándiz, M. J. Alcaraz, M. Payá, *J. Nat. Prod.* **1998**, *61*, 931–935.
[61] S. De Rosa, A. Crispino, A. De Giulio, C. Iodice, P. Amodeo, T. Tancredi, *J. Nat. Prod.* **1999**, *62*, 1316–1318.
[62] S. P. Gunasekera, P. J. McCarthy, M. Kelly-Borges, *J. Am. Chem. Soc.* **1996**, *118*, 8759–8760.
[63] B. E. Roberts, E. J. Corey, *J. Am. Chem. Soc.* **1997**, *119*, 12425–12431.
[64] M. Takahashi, K. Dodo, Y. Sugimoto, Y. Aoyagi, Y. Yamada, Y. Hashimoto, R. Shirai, *Bioorg. Med. Chem. Lett.* **2000**, *10*, 2571–2574.
[65] J. L. Blanchard, D. M. Epistein, M. D. Boisclair, J. Rudolph, K. Pal., *Bioorg. Med. Chem. Lett.* **1999**, *9*, 2537–2538.
[66] M. S. Majik, D. Shirodkar, C. Rodrigues, L. D'Souza, S. Tilvi, *Bioorg. Med. Chem. Lett.* **2014**, *24*, 2863–2866.

[67] A. Randazzo, C. Debitus, L. Minale, P. G. Pastor, M. J. Alcaraz, M. Payá, L. Gomez-Paloma, *J. Nat. Prod.* **1998**, *61*, 571–575.
[68] B. C. M. Potts, D. J. Faulkner, R. S. Jacobs, *J. Nat. Prod.* **1992**, *55*, 1701–1717.
[69] E. D. de Silva, P. J. Scheuer, *Tetrahedron Lett.* **1980**, *21*, 1611–1614.
[70] G. X. Zhou, T. F. Molinski, *J. Asian Nat. Prod. Res.* **2006**, *8*, 15–20.
[71] A. Schüffler, D. Kautz, J. C. Liermann, T. Opatz, T. Anke, *J. Antibiot.* **2009**, *62*, 119–121.
[72] A. Schüffler, J. C. Liermann, T. Opatz, T. Anke, *ChemBioChem* **2011**, *12*, 148–154.
[73] A. Schüffler, T. Anke, *Nat. Prod. Rep.* **2014**, *31*, 1425–1448.
[74] H. Shi, S. Yu, D. Liu, L. Van Ofwegen, P. Proksch, W. Lin, *Mar. Drugs* **2012**, *10*, 1331–1344.
[75] B. Yang, X. Wei, J. Huang, X. Lin, J. Liu, S. Liao, J. Wang, X. Zhou, L. Wang, Y. Liu, *Mar. Drugs* **2014**, *12*, 5316–5327.
[76] G. Chen, H. F. Wang, Y. H. Pei, *J. Asian Nat. Prod. Res.* **2014**, *16*, 105–122.
[77] W. Yuan, S. Cheng, W. Fu, M. Zhao, X. Li, Y. Cai, J. Dong, K. Huang, K. R. Gustafson, P. Yan, *J. Nat. Prod.* **2016**, *79*, 1124–1131.
[78] A. M. Doherty, W. C. Patt, J. J. Edmunds, K. A. Berryman, B. R. Reisdorph, M. S. Plummer, A. Shahripour, C. Lee, X.-M. Cheng, D. M. Walker, S. J. Haleen, J. A. Keiser, M. A. Flynn, K. M. Welch, H. Hallak, D. G. Taylor, E. E. Reynolds, *J. Med. Chem.* **1995**, *38*, 1259–1263.
[79] W. C. Patt, J. J. Edmunds, J. T. Repine, K. A. Berryman, B. R. Reisdorph, C. Lee, M. S. Plummer, A. Shahripour, S. J. Haleen, J. A. Keiser, M. A. Flynn, K. M. Welch, E. E. Reyn- olds, R. Rubin, B. Tobias, H. Hallak, A. M. Doherty, *J. Med. Chem.* **1997**, *40*, 1063–1074.
[80] M. R. Kernan, D. J. Faulkner, *J. Org. Chem.* **1988**, *53*, 2773–2776.
[81] S. I. Shigeo Katsumura, S. Fujiwara, S. Isoe, *Tetrahedron Lett.* **1985**, *26*, 5827–5830.
[82] J. Coombs, E. Lattmann, H. M. R. Hoffmann, *Synthesis* **1998**, 1367–1371.
[83] A. Soriente, M. De Rosa, A. Apicella, A. Scettri, G. Sodano, *Tetrahedron Asymmetry* **1999**, *10*, 4481–4484.
[84] A. K. Cheung, R. Murelli, M. L. Snapper, *J. Org. Chem.* **2004**, *69*, 5712–5719.
[85] K. H. Kim, H. S. Lee, S. H. Kim, K. Y. Lee, J. E. Lee, J. N. Kim, *Bull. Korean Chem. Soc.* **2009**, *30*, 1012–1020.
[86] J.-W. Lim, K.-H. Kim, S.-H. Kim, J.-N. Kim, *Bull. Korean Chem. Soc.* **2012**, *33*, 1781–1784.
[87] A. K. Cheung, M. L. Snapper, *J. Am. Chem. Soc.* **2002**, *124*, 11584–11585.
[88] S. J. D. Steven. R. Magnuson, L. Sepp-Lorenzino, N. Rosen, S. J. Danishefsky, *J. Am. Chem. Soc.* **1998**, *120*, 1615–1616.
[89] I. S. Marcos, A. Diego, P. Basabe, S. Delgado, M. de Román, F. Sanz, J. G. Urones, *Tetrahedron* **2007**, *63*, 8939–8948.
[90] P. Basabe, S. Delgado, I. S. Marcos, D. Diez, A. Diego, M. de Román, J. G. Urones, *J. Org. Chem.* **2005**, *70*, 9480–9485.
[91] H. Miura, K. Takeuchi, T. Shishido, *Angew. Chem. Int. Ed.* **2016**, *55*, 278–282.
[92] W. Mao, C. Zhu, *Chem. Commun.* **2016**, *52*, 5269–5272.
[93] D. Milstein, J. K. Stille, *J. Am. Chem. Soc.* **1978**, *100*, 3636–3638.
[94] K. Tamao, K. Sumitani, M. Kumada, *J. Am. Chem. Soc.* **1972**, *94*, 4374–4376.
[95] E. Negishi, A. O. King, N. Okukado, *J. Org. Chem.* **1977**, *42*, 1821–1823.
[96] K. Sonogashira, Y. Tohda, N. Hagihara, *Tetrahedron Lett.* **1975**, *16*, 4467–4470.
[97] N. Miyaura, K. Yamada, A. Suzuki, *Tetrahedron Lett.* **1979**, *20*, 3437–3440.
[98] N. Miyaura, A. Suzuki. *J. Chem. Soc. Chem. Comm.* **1979**, 866–867.
[99] A. A. Thomas, S. E. Denmark, *Science* **2016**, *352*, 329–332.
[100] C. Amatore, A. Jutand, M. A. M'Barki, *Organometallics* **1992**, *11*, 3009–3013.
[101] C. Amatore, A. Jutand, *J. Organomet. Chem.* **1999**, *576*, 254–278.
[102] C. Amatore, A. Jutand, *Acc. Chem. Res.* **2000**, *33*, 314–321.
[103] F. Ozawa, A. Kubo, T. Hayashi, *Chem. Lett.* **1992**, *21*, 2177–2180.
[104] T. Hayashi, A. Kubo, F. Ozawa, *Pure Appl. Chem.* **1992**, *64*, 421–427.

[105] F. E. Goodson, T. I. Wallow, B. M. Novak, *Org. Synth.* **1998**, *75*, 61–68.
[106] Y. Deng, L. Gong, A. Mi, H. Liu, Y. Jiang, *Synthesis* **2003**, 337–339.
[107] M. Toshihiko, N. Tohru, K. Kazuhiko, K. Masanori, *Bull. Chem. Soc. Jpn.* **1983**, *56*, 2869–2870.
[108] W. A. Herrmann, C. Brosmer, T. Priermeier, K. Ofele *J. Organomet. Chem.* **1994**, *481*, 97–108.
[109] S. Saito, M. Sakai, N. Miyaura, *Tetrahedron Lett.* **1996**, *37*, 2993–2996.
[110] S. Saito, S. Oh-tani, N. Miyaura, *J. Org. Chem.* **1997**, *62*, 8024–8030.
[111] J. Han, Y. Liu, R. Guo, *J. Am. Chem. Soc.* **2009**, *131*, 2060–2061.
[112] A. F. Indolese, *Tetrahedron Lett.* **1997**, *38*, 3513–3516.
[113] J.-C. Galland, M. Savignac, J.-P. Genet, *Tetrahedron Lett.* **1999**, *40*, 2323–2326.
[114] K. Inada, N. Miyaura, *Tetrahedron* **2000**, *56*, 8657–8660.
[115] V. Percec, G. M. Golding, J. Smidrkal, O. Weichold, *J. Org. Chem.* **2004**, *69*, 3447–3452.
[116] B. M. Rosen, C. Huang, V. Percec, *Org. Lett.* **2008**, *10*, 2597–2600.
[117] P. Garcia, M. Malacria, C. Aubert, V. Gandon,L. Fensterbank, *ChemCatChem* **2010**, *2*, 493–497.
[118] N. Dwadnia, J. Roger, N. Pirio, H. Cattey, R. Ben Salem, J. C. Hierso, *Chem. Asian J.* **2017**, *12*, 459–464.
[119] M. Barbero, S. Dughera, *Tetrahedron* **2018**, *74*, 5758–5769.
[120] N. Miyaura, A. Suzuki, *Chem. Rev.* **1995**, *95*, 2457–2483.
[121] I. P. Beletskaya, A. V. Cheprakov, *Chem. Rev.* **2000**, *100*, 3009–3066.
[122] A. H. Roy, J. F. Hartwig, *Organometallics* **2004**, *23*, 194–202.
[123] L. Zhang, T. Meng, J. Wu, *J. Org. Chem.* **2007**, *72*, 9346–9349.
[124] H. N. Nguyen, X. Huang, S. L. Buchwald, *J. Am. Chem. Soc.* **2003**, *125*, 11818–11819.
[125] S. Li, Y. Lin, J. Cao, S. Zhang, *J. Org. Chem.* **2007**, *72*, 4067–4072.
[126] S. D. Dreher, S.-E. Lim, D. L. Sandrock, G. A. Molander, *J. Org. Chem.* **2009**, *74*, 3626–3631.
[127] Z. J. Jiang, Z. H. Li, J. B. Yu, W. K. Su, *J. Org. Chem.* **2016**, *81*, 10049–10055.
[128] A. I. Lansakara, S. V. S. Mariappan, F. C. Pigge, *J. Org. Chem.* **2016**, *81*, 10266–10278.
[129] N. Alnafta, J. P. Schmidt, C. L. Nesbitt, C. S. P. McErlean, *Org. Lett.* **2016**, *18*, 6520–6522.
[130] J. Rajaram, R. G. Pearson, J. A. Ibers, *J. Am. Chem. Soc.* **1974**, *96*, 2103–2108.
[131] J. K. Stille, K. S. Y. Lau, *Acc. Chem. Res.* **1977**, *10*, 434–442.
[132] P. Fitton, E.A. Rick, *J. Organomet. Chem.* **1971**, *28*, 287–291.
[133] A. Gillie, J. K. Stille, *J. Am. Chem. Soc.* **1980**, *102*, 4933–4941.
[134] B. P. Carrow, J. F. Hartwig, *J. Am. Chem. Soc.* **2011**, *133*, 2116–2119.
[135] A. T. K. Koshvandi, M. M. Heravi, T. Momeni, *Appl. Organometal. Chem.* **2018**, *32*, 1–59.
[136] T. Ishiyama, N. Miyaura, A. Suzuki, *Tetrahedron Lett.* **1991**, *32*, 6923–6926.
[137] T. Ishiyama, H. Kizaki, T. Hayashi, A. Suzuki, N. Miyaura, *J. Org. Chem.* **1998**, *63*, 4726–4731.
[138] M. Schacht, D. Mohammadi, N. Schützenmeister, *Eur. J. Org. Chem.* **2019**, 2587-2591.
[139] X. Qi, L. B. Jiang, H. P. Li, X. F. Wu, *Chem. Eur. J.* **2015**, *21*, 17650–17656.
[140] P. Sharma, S. Rohilla, N. Jain, *J. Org. Chem.* **2017**, *82*, 1105–1113.
[141] Y. Li, D. H. Tu, B. Wang, J. Y. Lu, Y. Y. Wang, Z. T. Liu, Z. W. Liu, J. Lu, *Org. Chem. Front.*, **2017**, *4*, 569-572.
[142] K. Yamazaki, Y. Kondo, *J. Comb. Chem.* **2004**, *6*, 121–125.
[143] M. Iizuka, Y. Kondo, *Eur. J. Org. Chem.* **2007**, 5180–5182.
[144] N. Sun, Q. Sun, W. Zhao, L. Jin, B. Hu. Z. Shen, X. Hu, *Adv. Synth. Catal*. **2019**, *361*, 2117-2123.
[145] A. Pyo, A. Park, H. Jung, S. Lee, *Synthesis* **2012**, *44*, 2885–2888.
[146] L. R. Odell, F. Russo, M. Larhed, *Synlett* **2012**, *23*, 685–698.

[147] H. V. Motwani, M. Larhed, *Eur. J. Org. Chem.* **2013**, 4729–4733.
[148] L. Åkerbladh, P. Nordeman, M. Wejdemar, L. R. Odell, M. Larhed, *J. Org. Chem.* **2015**, *80*, 1464–1471.
[149] S. Roslin, L. R. Odell, *Chem. Commun.* **2017**, *53*, 6895–6898.
[150] J. Lindh, A. Fardost, M. Almeida, P. Nilsson, *Tetrahedron Lett.* **2010**, *51*, 2470–2472.
[151] J. Sävmarker, J. Lindh, P. Nilsson, *Tetrahedron Lett.* **2010**, *51*, 6886–6889.
[152] F. Jafarpour, P. Rashidi-Ranjbar, A. O. Kashani, *Eur. J. Org. Chem.* **2011**, 2128–2132.
[153] V. V. Bykov, D. N. Korolev, N. A. Bumagin, *Russ. Chem. Bull.* **1997**, *46*, 1631–1632.
[154] D. N. K. Nikolay A. Bumagin, *Tetrahedron Lett.* **1999**, *40*, 3057–3060.
[155] Y. Urawa, K. Ogura, *Tetrahedron Lett.* **2003**, *44*, 271–273.
[156] S. Eddarir, N. Cotelle, Y. Bakkour, C. Rolando, *Tetrahedron Lett.* **2003**, *44*, 5359–5363.
[157] B. P. Bandgar, A. V. Patil, *Tetrahedron Lett.* **2005**, *46*, 7627–7630.
[158] Y. Nishihara, Y. Inoue, M. Fujisawa, K. Takagi, *Synlett* **2005**, 2309–2312.
[159] V. Poláčková, Š. Toma, I. Augustínová, *Tetrahedron* **2006**, *62*, 11675–11678.
[160] M. Haddach, J. R. McCarthy, *Tetrahedron Lett.* **1999**, *40*, 3109–3112.
[161] K. Ekoue-Kovi, H. Xu, C. Wolf, *Tetrahedron Lett.* **2008**, *49*, 5773–5776.
[162] L. Zhang, J. Wu, L. Shi, C. Xia, F. Li, *Tetrahedron Lett.* **2011**, *52*, 3897–3901.
[163] G. Meng, M. Szostak, *Org. Lett.* **2015**, *17*, 4364–4367.
[164] N. A. Weires, E. L. Baker, N. K. Garg, *Nat. Chem.* **2016**, *8*, 75–79.
[165] R. Kakino, I. Shimizu, A. Yamamoto, *Bull. Chem. Soc. Jpn.* **2001**, *74*, 371–376.
[166] H. Tatamidani, F. Kakiuchi, N. Chatani, *Org. Lett.* **2004**, *6*, 3597–3599.
[167] R. P. Tripathi, S. S. Bisht, V. P. Pandey, S. K. Pandey, S. Singh, S. K. Sinha, V. Chaturvedi, *Med. Chem. Res.* **2011**, *20*, 1515–1522.
[168] S. R. Bheemireddy, P. C. Ubaldo, P. W. Rose, A. D. Finke, J. Zhuang, L. Wang, K. N. Plunkett, *Angew. Chem. Int. Ed.* **2015**, *54*, 15762–15766.
[169] T. Ishiyama, N. Matsuda, M. Murata, F. Ozawa, A. Suzuki, N. Miyaura, *Organometallics* **1996**, *15*, 713–720.
[170] T. Ishiyama, N. Matsuda, N. Miyaura, A. Suzuki, *J. Am. Chem. Soc.* **1993**, *115*, 11018–11019.
[171] H. Prokopcová, J. Ramírez, E. Fernández, C. O. Kappe, *Tetrahedron Lett.* **2008**, *49*, 4831–4835.
[172] G. Wang, X. Chen, G. Miao, W. Yao, C. Ma, *J. Org. Chem.* **2013**, *78*, 6223–6232.
[173] D. Prim, A. Fuss, G. Kirsch, A. M. S. Silva, *J. Chem. Soc. Perkin Trans. 2* **1999**, 1175–1180.
[174] R. Grigg, V. Savic, M. Thornton-Pett, *Tetrahedron* **1997**, *53*, 10633–10642.
[175] G. J. Boehlich, Synthesis of rubrolide S, *Bachelor Thesis* **2015**, Universität Hamburg.
[176] R. Gopinath, S. J. Haque, B. K. Patel, *J. Org. Chem.* **2002**, *67*, 5842–5845.
[177] J. De Vries, Synthesis of Rubrolide R by Palladium Catalysis, *Bachelor Thesis* **2016**, Universität Hamburg.
[178] A. Speicher, T. Backes, S. Grosse, *Tetrahedron* **2005**, *61*, 11692–11696.
[179] A. Speicher, J. Kolz, R. P. Sambanje, *Synthesis.* **2002**, 2503–2512.
[180] A. Speicher, T. Backes, K. Hesidens, J. Kolz, *Beilstein J. Org. Chem.* **2009**, *5*, 1–9.
[181] P. A. Cox, A. G. Leach, A. D. Campbell, G. C. Lloyd-Jones, *J. Am. Chem. Soc.* **2016**, *138*, 9145–9157.
[182] A. Maiti, M. Cuendet, V. L. Croy, D. C. Endringer, J. M. Pezzuto, M. Cushman, *J. Med. Chem.* **2007**, *50*, 2799–2806.
[183] V. K. Ahluwalia, K. K. Arora, *Tetrahedron* **1981**, *37*, 1437–1439.
[184] G. I. Feutrill, R. N. Mirrington, *Tetrahedron Lett.* **1970**, *16*, 1327–1328.
[185] M. Schacht, G. J. Boehlich, J. de Vries, S. Bertram, G. Gabriel, P. Zimmermann, P. Heisig, N. Schützenmeister, *Eur. J. Org. Chem.* **2017**, 1745–1748.
[186] J. Ruchti, E. M. Carreira, *J. Am. Chem. Soc.* **2014**, *136*, 16756–16759.
[187] G. Bartoli, M. Bosco, A. Carlone, R. Dalpozzo, M. Locatelli, P. Melchiorre, P. Palazzi, L. Sambri, *Synlett* **2006**, 2104–2108.
[188] B. M. Trost, T. J. Fullerton, *J. Am. Chem. Soc.* **1973**, *95*, 292–294.

[189] B. M. Trost, D. A. Thaisrivongs, *J. Am. Chem. Soc.* **2008**, *130*, 14092–14093.
[190] A. N. Pearce, E. W. Chia, M. V. Berridge, E. W. Maas, M. J. Page, V. L. Webb, J. L. Harper, B. R. Copp, *J. Nat. Prod.* **2007**, *70*, 111–113.
[191] S. Manzanaro, J. Salva, J. A. J. A. de la Fuente, *J. Nat. Prod.* **2006**, *69*, 1485–1487.
[192] M. Karak, J. A. M. Acosta, L. C. A. Barbosa, J. Boukouvalas, *Eur. J. Org. Chem.* **2016**, 3780–3787.
[193] A. F. Littke, C. Dai, G. C. Fu, *J. Am. Chem. Soc.* **2000**, *122*, 4020-4028.
[194] J. Zhang, P. G. Blazecka, D. Belmont, J. G. Davidson, *Org. Lett.* **2002**, *4*, 4559–4561.
[195] W. Wang, H. Kim, S.-J. Nam, B. J. Rho, H. Kang, *J. Nat. Prod.* **2012**, *75*, 2049–2054.
[196] T. D. Porter, M. J. Coon, *J. Biol. Chem.* **1991**, *266*, 13469–13472.
[197] H. Y. Neujahr, A. Gaal, *Eur. J. Biochem.* **1975**, *58*, 351–357.
[198] K. Nepali, H. Y. Lee, J. P. Liou, *J. Med. Chem.* **2019**, *62*, 2851-2893.
[199] J. Janneschütz, Synthesis of catechol-Rubrolide derivatives, *Bachelor Thesis* **2017**, Universität Hamburg.
[200] K. Q. Zhao, Y. Gao, W. H. Yu, P. Hu, B. Q. Wang, B. Heinrich, B. Donnio, *Eur. J. Org. Chem.* **2016**, *2016*, 2802–2814.
[201] R. Meißner, Studies towards the synthesis of Rubrolide-Mannosides, *Bachelor Thesis* **2017**, Universität Hamburg.
[202] S. A. Abbas, C. F. Pskorz, K. L. Matta, *Carbohydr. Res.* **1987**, *167*, 131–141.
[203] M. Tosin, P. V. Murphy, *J. Org. Chem.* **2005**, *70*, 4107–4117.
[204] W. Dullenkopf, J. C. Castro-Palomino, L. Manzoni, R. R. Schmidt, *Carbohydr. Res.* **1996**, *296*, 135–147.
[205] F. T. Ferse, K. Floeder, L. Hennig, M. Findeisen, P. Welzel, D. Müller, J. Van Heijenoort, *Tetrahedron* **1999**, *55*, 3749–3766.
[206] R. R. Kale, C. M. McGannon, C. Fuller-Schaefer, D. M. Hatch, M. J. Flagler, S. D. Gamage, A. A. Weiss, S. S. Iyer, *Angew. Chem. Int. Ed.* **2008**, *47*, 1265–1268.
[207] K. Ágoston, A. Dobó, J. Rákó, J. Kerékgyártó, Z. Szurmai, *Carbohydr. Res.* **2001**, *330*, 183–190.
[208] J. Huchting, C. Meier, *Eur. J. Org. Chem.* **2014**, 3423–3429.
[209] L. Poncini, G. N. Richards, *Carbohydr. Res.* **1978**, *65*, 209–217.
[210] A. G. González, I. Brouard, F. León, J. I. Padrón, J. Bermejo, *Tetrahedron Lett.* **2001**, *42*, 3187–3188.
[211] A. Baba, T. Yoshioka, *Org. Biomol. Chem.* **2006**, *4*, 3303–3310.
[212] J. T. Gupton, N. Telang, E. J. Banner, E. J. Kluball, K. E. Hall, K. L. Finzel, X. Jia, S. R. Bates, R. S. Welden, B. C. Giglio, J. E. Eaton, P.J. Barell, J. A. Stafford, M. B. Coppock, E. F. Worrall, R. P. Kanters, K. Keertikar, R. Ostermann, *Tetrahedron* **2010**, *66*, 9113–9122.
[213] E. Dalcanale, F. Montanari, *J. Org. Chem.* **1986**, *51*, 567–569.
[214] B. S. Bal, W. E. Childers, H. W. Pinnick, *Tetrahedron* **1981**, *37*, 2091–2096.
[215] T. Takemoto, K. Yasuda, S. V. Ley, *Synlett* **2001**, 1555–1556.
[216] D. Talukdar, K. Sharma, S. K. Bharadwaj, A. J. Thakur, *Synlett* **2013**, *24*, 963–966.
[217] R. Gopinath, B. Barkakaty, B. Talukdar, B. K. Patel, *J. Org. Chem.* **2003**, *68*, 2944–2947.
[218] R. Gopinath, B. K. Patel, *Org. Lett.* **2000**, *2*, 577-579.
[219] Y. Ashida, Y. Sato, T. Suzuki, K. Ueno, K. I. Kai, H. Nakatsuji, Y. Tanabe, *Chem. Eur. J.* **2015**, *21*, 5934–5945.
[220] Y. Sato, Y. Ashida, D. Yoshitake, M. Hoshino, T. Takemoto, Y. Tanabe, *Synthesis* **2018**, 4659–4667.
[221] Y. Ashida, Y. Sato, A. Honda, H. Nakatsuji, Y. Tanabe, *Synthesis.* **2016**, 4072–4080.
[222] Y. Ashida, A. Honda, Y. Sato, H. Nakatsuji, Y. Tanabe, *ChemistryOpen* **2017**, *6*, 73–89.
[223] H. Nakatsuji, H. Nishikado, K. Ueno, Y. Tanabe, *Org. Lett.* **2009**, *11*, 4258–4261.
[224] H. Nishikado, H. Nakatsuji, K. Ueno, R. Nagase, Y. Tanabe, *Synlett* **2010**, 2087–2092.

[225] M. E. Kavanagh, A. G. Coyne, K. J. McLean, G. G. James, C. W. Levy, L. B. Marino, L. P. S. de Carvalho, D. S. H. Chan, S. A. Hudson, S. Surade, D. Leys, A. W. Munro, C. Abell, *J. Med. Chem.* **2016**, *59*, 3272–3302.
[226] D. Mohammadi, Synthesis of 5-Hydroxybutenolides, *Bachelor Thesis* **2018**, Universität Hamburg.
[227] A. J. J. Lennox, G. C. Lloyd-Jones, *Angew. Chem. Int. Ed.* **2012**, *51*, 9385–9388.
[228] A. J. J. Lennox, G. C. Lloyd-Jones, *Chem. Soc. Rev.* **2014**, *43*, 412–443.
[229] S. Shi, M. Szostak, *Org. Lett.* **2016**, *18*, 5872–5875.
[230] K. A. Jacobson, K. L. Kirk, W. L. Padgett, J. W. Daly, *J. Med. Chem.* **1985**, *28*, 1341–1346.
[231] C. Amatore, E. Carre, A. Jutand, M. A. M'Barki, G. Meyer, *Organometallics* **1995**, *14*, 5605–5614.
[232] M. A. Sparks, K. W. Williams, C. Lukacs, A. Schrell, G. Priebe, A. Spaltenstein, G. M. Whitesides, *Tetrahedron* **1993**, *49*, 1–12.
[233] L. Gooßen, K. Ghosh, *Chem. Commun.* **2001**, 2084–2085.
[234] T. B. Halima, W. Zhang, I. Yalaoui, X. Hong, Y.-F. Yang, K. N. Houk, S. G. Newman, *J. Am. Chem. Soc.* **2017**, *139*, 1311–1318.
[235] A. M. Forbes, G. P. Meier, E. Jones-Mensah, J. Magolan, *Eur. J. Org. Chem.* **2016**, , 2983–2987.
[236] T. Ishiyama, H. Kizaki, N. Miyaura, A. Suzuki, *Tetrahedron Lett.* **1993**, *34*, 7595–7598.
[237] T. Ishiyama, H. Kizaki, T. Hayashi, A. Suzuki, N. Miyaura, *J. Org. Chem.* **1998**, *63*, 4726–4731.
[238] L. Bartali, A. Guarna, P. Larini, E. G. Occhiato, *Eur. J. Org. Chem.* **2007**, 2152–2163.
[239] J. H. Kim, S. Kim, *RSC Adv.* **2014**, *4*, 26516–26523.
[240] B.M. O'Keefe, N. Simmons, S.F. Martin, *Org. Lett.* **2008**, *10*, 5301-5304.
[241] T. Hayashi, J. Tang, K. Kato, *Org. Lett.* **1999**, *1*, 1487–1489.
[242] C. Y. Hao, D. Wang, Y. W. Li, L. L. Dong, Y. Jin, X. R. Zhang, H. Y. Zhu, S. Chang, *RSC Adv.* **2016**, *6*, 86502–86509.
[243] V. Yadav, V. Srivastava, L. Yadav, *Synlett* **2016**, 2826-2830.
[244] M. Harrold, R. Zavod, *Basic Concepts Med. Chem.*, ASHP, *Bethesda*, **2013.**
[245] A. Kar, N. P. Argade, *Synthesis* **2005**, 2995-3022.
[246] E. R. Marshall, J. A. Kuck, R. C. Elderfield, *J. Org. Chem.* **1942**, *7*, 444–456.
[247] P. Thombare, J. Desai, A. Argade, S. Gite, K. Shah, L. Pavase, P. Patel, *Synth. Commun.* **2009**, *39*, 2423–2429.
[248] B. Schmidt, M. Riemer, U. Schilde, *Eur. J. Org. Chem.* **2015**, 7602–7611.
[249] G. V. Rao, B. N. Swamy, V. Chandregowda, G. C. Reddy, *Eur. J. Med. Chem.* **2009**, *44*, 2239–2245.
[250] J.-E. Lee, J. Kwon, J. Yun, *Chem. Commun.* **2008**, 733–734.
[251] S. Wan, S. R. Wang, W. Lu, *J. Org. Chem.* **2006**, *71*, 4349–4352.

Eidesstaatliche Versicherung

Hiermit versichere ich an Eides statt, die vorliegende Dissertation mit dem Titel:

“Synthesis of Natural Abundant Butenolides and Analogues”

selbst verfasst und keine anderen als die angegebenen Hilfsmittel benutzt zu haben. Die eingereichte schriftliche Fassung entspricht der auf dem elektronischen Speichermedium. Ich versichere, dass diese Dissertation nicht in einem früheren Promotionsverfahren eingereicht wurde.

Hamburg, den 30.06.2019 Unterschrift